

# **ncasi**

---

NATIONAL COUNCIL FOR AIR AND STREAM IMPROVEMENT

**SCALE CONSIDERATIONS AND  
THE DETECTABILITY OF SEDIMENTARY  
CUMULATIVE WATERSHED EFFECTS**

**TECHNICAL BULLETIN NO. 776**

**JANUARY 1999**

**For more information about this research, contact:**

Walter F. Megahan, Ph.D.  
Principal Research Scientist  
NCASI  
615 W Street  
Port Townsend, WA 98368  
(360) 379-9915  
wmegahan@ncasi.org

**For information about NCASI publications, contact:**

Publications Coordinator  
NCASI  
P.O. Box 13318  
Research Triangle Park, NC 27709-3318  
(919) 558-1999  
publications@ncasi.org

National Council of the Paper Industry for Air and Stream Improvement, Inc. (NCASI). 1999. *Scale considerations and the detectability of sedimentary cumulative watershed effects*. Technical Bulletin No. 776. Research Triangle Park, N.C.: National Council of the Paper Industry for Air and Stream Improvement, Inc.

© 1999 by the National Council of the Paper Industry for Air and Stream Improvement, Inc.



*servicing the environmental research needs of the forest products industry since 1943*

## **PRESIDENT'S NOTE**

The concept of "cumulative effects" was introduced in U.S. environmental law through the National Environmental Policy Act and defined by the Council of Environmental Quality as "The impact on the environment which results from the incremental impact of the action when added to other past, present, and reasonable foreseeable future actions..." Cumulative effects continue to be a concern in dealing with issues arising from the subsequent legislation including the Clean Water Act and the Endangered Species Act.

Sediment from watershed disturbances is often cited as one of the most important cumulative effects because the downstream routing and accumulation of sediment can cause a variety of downstream damages, especially to aquatic habit. Such damages have often led to severe constraints on land use.

In 1991, NCASI initiated a Cumulative Watershed Effects (CWE) Program to deal with cumulative effects issues. One important research project generated by the program was a comprehensive study of the effects of temporal and spatial scale on cumulative sedimentation effects. This work was done under the direction of Drs. Kristen Bunte and Lee MacDonald from Colorado State University. In addition to Colorado State University, the study was a cooperative effort between NCASI and three U.S. Forest Service units, including the Southern Research Station, the Stream Systems Technology Center and the Pacific Southwest Forest and Range Experiment Station.

This report was written by Drs. Kristen Bunte and Lee MacDonald. It provides a comprehensive evaluation of the three factors influencing sediment: CWE assessment, temporal and spatial scale, and measurement uncertainty. Temporal scale factors considered range from instantaneous sediment transport to characterization of annual sediment yields. Spatial scale discussions span the differences in sediment transport rates across a given stream location to differences in sediment production within and between basins. Finally, the difficulty of detecting sedimentary CWEs is discussed in light of the uncertainty inherent in measurements of sediment transport. Given the high spatial and temporal variability and the uncertainties of measuring sediment transport, the authors conclude with a discussion of how much change in sediment production would be needed to show an effect and how much information would be needed to verify the change.

A handwritten signature in black ink, appearing to read "Ron Yeske", is written in a cursive style.

Ronald A. Yeske

January 1999



## **Abstract**

Cumulative watershed effects (CWEs) result from the overlapping effects of management activities in time or space. The routing and downstream accumulation of sediment from forest management activities is of particular concern because it directly affects key aquatic resources, and these sedimentary CWEs are often the most severe constraints on forest management activities. The prediction and detection of sedimentary CWEs is particularly difficult because of the complex interactions among temporal scale, spatial scale, and measurement uncertainty. The goal of this project was to evaluate the extent to which sedimentary CWEs are dependent on the spatial scale of the analysis. In reality, the effects of spatial scale cannot be separated from the temporal scale or measurement uncertainty. Thus this report evaluates each of these factors as a guide to developing more effective monitoring programs, improving the predictability of sedimentary CWEs, and identifying avenues for future research.

Temporal scale considerations range from the short-term variability of sediment transport rates to the variability in annual sediment loads within a single basin. Short-term fluctuations in bedload transport rates commonly extend over one order of magnitude, and high-intensity sequential samples had an average coefficient of variation of 79% for near constant flow, and 95% when samples were taken during a high flow event. An analysis of existing data indicated that 13-95% of the variation in sediment transport rates could be explained by discharge.

At the interannual scale, the coefficient of variation for annual sediment loads is typically at least 70-100%. There was a weak tendency for the interannual variability to increase with increasing annual sediment yields, but there was no indication that interannual variability decreased with increasing basin size. The distribution of annual sediment yields tended to be lognormal, although basins with lower annual sediment yields were often normally distributed. Given this variability, almost a decade of measurements are needed to determine the annual sediment yield to within 100% of the true value at the 95% confidence level.

The effects of spatial scale range from the variability in sediment loads within a cross-section, to the variation in the amount of sediment transport along a downstream gradient, and the interbasin variability in annual sediment loads. Temporal and spatial scales are not easily separated, and a knowledge of both spatial and temporal variability is necessary to efficiently allocate sampling effort. The short-term and small-scale variability problems tend to be more severe for bedload transport than suspended sediment.

Spatial scale issues are particularly important in terms of the downstream delivery of sediment and the reliability of interbasin comparisons. Sediment delivery ratios are not appropriate for routing different-sized particles through a sequence of varying stream types. An analysis of tracer data suggested that mean annual transport distances increase with gradient in braided or aggrading streams, but decline with gradient in steep, hydraulically-rough streams. Although there are a series of problems with extrapolating from tracer studies, typical annual transport distances are estimated to be approximately 10, 2, and 0.1 km for suspended sediment, sand, and coarse particles, respectively. These rates indicate that there will often be a substantial lag in the occurrence of a sedimentary CWE, and the timing and location of a sedimentary CWE is highly dependent on key factors such as the particle size of the sediment being introduced, the sequence of stream types, and the sedimentary state of the streams through which the sediment must pass.

A series of interbasin comparisons indicated considerable variability in the strength of the correlation in annual sediment yields between adjacent undisturbed basins. Of particular concern was the observation that a slight shift in the years of comparison could greatly alter the strength and slope of the relationship between basins. This instability also extended to the relationship between various flow parameters (e.g., annual water yield) and annual sediment yields on a given basin.

The uncertainty in detecting sedimentary CWEs is further compounded by the problems of accurately measuring sediment transport rates over a range of temporal scales. Since any sampler disturbs the flow lines in the stream, there is an inherent bias in the data and this varies as a function of particle size. Since we typically sample much less than one percent of the possible samples in time and space, sediment yield estimates require considerable extrapolation. Both summation and rating curve techniques are subject to bias, and a change in the calculation or bias-adjustment procedure can alter the estimated sediment yields by more than a factor of two. Unfortunately, sediment transport equations are even less accurate, and calculated sediment transport rates extremely sensitive to which equation is used and the value of the key input parameters.

Taken together, these factors suggest that we should not expect to detect less than a twofold change in sediment transport rates or sediment yields. Changes in measurement techniques, calculation procedures, or the period of comparison can create the appearance of a sedimentary CWE when none actually exists. The inherent spatial and temporal variability suggests that at least 5-10 years of both pre- and post-monitoring are likely to be necessary to reliably detect a sedimentary CWE. Since management decisions often cannot be delayed and longer-term monitoring projects cannot be implemented on all reaches of concern, alternative approaches are necessary. A geomorphic analysis of the current sedimentary state of the stream network is an essential first step towards any CWE analysis or monitoring effort. Modified sediment delivery ratios can be developed by considering, at a minimum, the sizes of the particles being introduced, as well as the sequence and condition of stream types. This basin-specific understanding is essential for determining the appropriate temporal and spatial scales for analysis and monitoring. A universal sedimentary CWE model is simply not realistic given the diversity and complexity of sediment production, transport, and delivery processes.

## **Acknowledgments**

This work was conducted under Cooperative Research Agreement 19-82-087 between Colorado State University and the U.S.D.A. Southern Research Station. We are extremely grateful to Dan Marion of the Southern Research Station and Walt Megahan and the National Council for Air and Stream Improvement for their assistance in initiating this project and their financial support. Additional financial support came from the U.S.D.A. Forest Service Stream Systems Technology Center and the Pacific Southwest Forest and Range Experiment Station. None of these institutions are faceless, and we would like to explicitly acknowledge the support of Larry Schmidt, John Potyondy, and Neil Berg. Most of these individuals also provided their time and advice at informal advisory meetings as the project evolved, and we greatly appreciate their commitment and advice. Special thanks are also due to George Ice of NCASI, as he provided enthusiastic support for the initial ideas that then evolved into this project.

A number of friends and colleagues were most helpful in terms of providing data sets for analysis under the auspices of this project. Randy Dinehart, Ian Reid, Roger Kuhnle, Tom Lisle, Bill Emmett, Rob Ferguson, John Stednick, Jim Nankervis, and Jonathan Swift all provided data and information beyond what was available in the literature, and we appreciate their efforts in doing so. Others helped guide our search for data, and we would like to particularly thank Alex Sutherland, Bob Ziemer, and Terry Cundy. Pepe Salas contributed his statistical expertise to the project, and we appreciate his contribution.

Finally, we would like to thank all of the sponsors and administrators for continuing their patience until this report could be completed. One characteristic that is common to both streams and research is that what initially appears complex is even more so upon further investigation. Thus this report does not provide a single "answer" with regard to the scale considerations associated with cumulative watershed effects. Nevertheless, the information presented here should help evaluate spatial and temporal effects on a particular basin according to key factors such as the sources and type of sediment, sedimentary state of the basin, sequence of stream types, and measurement techniques being applied. The results and synthesis presented in this report should also point the way towards more effective monitoring, more realistic evaluations of sedimentary cumulative effects, and an increased recognition of the interacting factors that govern stream response to management activities. This report should also help guide additional work on this topic. Most importantly, we hope that this report will improve our capability to manage cumulative watershed effects and help protect our aquatic resources.



## **Table of contents**

---

Abstract .....	ii
Acknowledgments.....	iv
List of Figures.....	x
List of Tables.....	xix
Metric and English Units .....	xxiv

### **Part A: Introduction, objectives, and considerations of cumulative watershed effects and scale** ..... **1**

<b>1. Introduction.....</b>	<b>1</b>
<b>2. Objectives and structure of the report .....</b>	<b>3</b>
<b>3. Cumulative watershed effects and scale .....</b>	<b>5</b>
<b>3.1 Definition of cumulative watershed effects .....</b>	<b>5</b>
<b>3.2 Stream channel responses to cumulative watershed effects .....</b>	<b>5</b>
<b>3.2 Prediction of CWE.....</b>	<b>7</b>
3.2.1 Prediction of CWE by models.....	7
3.2.1.1 Short-term effects on water and sediment yield .....	7
3.2.1.2 Long-term CWEs .....	8
3.2.2 Prediction of sedimentary CWE by stream monitoring.....	10
3.2.2.1 Detectability of sedimentary CWEs: effects of spatial scale .....	11
3.2.2.2 Simplistic models indicating the importance of spatial scale.....	11
3.2.2.3 Scale effects in the specific locations where sedimentary CWE might occur .....	12
3.2.3 Stream types and locations susceptible to sedimentary CWE.....	13
3.2.3.1 Steep mountain rivers .....	13
3.2.3.2 Response reaches in gravel-bed streams .....	14
3.2.3.3 Sand- and silt-bed rivers .....	14
<b>3.3 Summary.....</b>	<b>18</b>

### **Part B: Processes, measurability, and variability of sediment transport** ..... **19**

<b>1. Physical processes and the temporal and spatial variability of sediment transport .....</b>	<b>19</b>
<b>1.1 Introduction .....</b>	<b>19</b>
<b>1.2 Processes causing variability of bedload transport .....</b>	<b>20</b>
1.2.1 Temporal variability of bedload transport .....	20
1.2.1.1 Short-term fluctuations of bedload transport rates.....	21
1.2.1.2 Intra-event variability of bedload transport.....	27
1.2.1.3 Between storm and seasonal variation.....	42
1.2.1.4 Summary and implication for measuring and sampling .....	42

1.2.2	Spatial variability of bedload transport.....	43
1.2.2.1	Longitudinal variability.....	43
1.2.2.2	Cross-sectional variability	49
<b>1.3</b>	<b>Variability of suspended sediment concentration .....</b>	<b>52</b>
1.3.1	Temporal variability .....	53
1.3.1.1	Short-term variability.....	53
1.3.1.1	Intra-event variability.....	54
1.3.1.2	Inter-event variability of Cs .....	58
1.3.2	Spatial variability of suspended sediment concentration.....	59
1.3.2.1	Vertical variation .....	59
1.3.2.2	Lateral variability .....	64
1.3.2.3	Longitudinal variation .....	71
<b>1.4</b>	<b>Implications for sediment sampling for CWE analyses .....</b>	<b>73</b>
<b>2.</b>	<b>Statistical Analysis of Bedload Transport Variability and Sampling</b>	
<b>Uncertainty .....</b>		<b>75</b>
<b>2.1</b>	<b>Testing the statistical distribution of bedload transport rates.....</b>	<b>77</b>
2.1.1	Schleyer-test for goodness-of-fit to normality and lognormality .....	77
2.1.2	Test for goodness-of-fit to a Hamamori distribution.....	79
2.1.3	W-Test for normality and lognormality.....	79
2.1.4	Test Results .....	80
2.1.5	Distribution parameters: mean, sorting, skewness.....	88
2.1.6	Shape of the cumulative distribution curves .....	91
2.1.7	Summary of the test results.....	94
<b>2.2</b>	<b>Effects on the statistical distribution type.....</b>	<b>95</b>
2.2.1	Short-term and intra-event variability .....	97
2.2.2	Sampling intensity and performance.....	97
2.2.3	Continuous and sequential sampling .....	100
<b>2.3</b>	<b>Variability of bedload transport: coefficient of variation (CV).....</b>	<b>101</b>
2.3.1	Effects of bedload particle-size.....	102
2.3.2	Effects of the type of flow event and the respective bedload transport patterns .....	105
<b>2.4</b>	<b>Empirical sampling schemes and number of samples needed for preset levels of accuracy.....</b>	<b>106</b>
2.4.1	Empirical sampling schemes.....	106
2.4.2	Number of samples needed.....	112
2.4.3	Total sampling time and sampling performance needed.....	117
<b>2.5</b>	<b>Summary.....</b>	<b>119</b>
<b>3.</b>	<b>Measurement Techniques and Uncertainty .....</b>	<b>122</b>
<b>3.1</b>	<b>Introduction .....</b>	<b>122</b>
<b>3.2</b>	<b>Measurement techniques and uncertainties of bedload sampling .....</b>	<b>123</b>
3.2.1	Helley-Smith-type samplers: effects on sampling efficiency .....	123
3.2.1.1	Orifice size and large particles .....	128
3.2.1.2	Area ratio and hydraulic efficiency .....	129
3.2.1.3	Bedload transport rates .....	132
3.2.1.4	Bedload particle size .....	133
3.2.1.5	Bag size, mesh width, and sampling duration.....	135
3.2.1.6	Contact with the river bed .....	138
3.2.1.7	Poor operating .....	141
3.2.1.8	Summary .....	142

3.2.2	Basket and net samplers .....	142
3.2.3	Annual surveying or excavation of bedload traps or debris basins .....	145
3.2.4	Continuously recording bedload traps.....	146
3.2.5	Indirect methods of bedload transport measurements .....	150
3.3.6	Measuring bedload transport using tracer techniques .....	150
3.3.6.1	Techniques and recovery rates .....	150
3.3.6.2	Transport rates and continuous transport records.....	152
3.2.7	Summary: measurement uncertainties of bedload sampling .....	154
<b>3.3</b>	<b>Measurement techniques and uncertainty of suspended sediment sampling .....</b>	<b>156</b>
3.3.1	One-point bottle sampling.....	156
3.3.2	DH-48 width and depth integrated sampling.....	157
3.3.3	One-point pump samplers.....	157
3.3.4	One-point continuous turbidity monitoring and calibration with episodic, instantaneous measurements of Cs .....	158
3.3.5	Reservoirs or stilling ponds, annual survey or excavation .....	158
3.3.6	Summary: measurement uncertainties of suspended sediment sampling.....	158

#### **4. Sampling Schemes for Rating Curves and Annual Load Estimates:**

<b>Do we know or are we guessing? .....</b>	<b>160</b>
<b>4.1 Introduction .....</b>	<b>160</b>
<b>4.2 Accuracy and precision of suspended sediment load estimates.....</b>	<b>160</b>
4.2.1 Rating curve problems for sediment load estimates .....	161
4.2.1.1 Effects of sampling schemes .....	161
4.2.1.2 Accounting for hysteresis and rating curve variability.....	165
4.2.1.3 First-time rating curve: general sedimentary state of the river, its tributaries and the basin: .....	166
4.2.1.4 Effects of bias correction.....	166
4.2.2 Summation of daily sediment loads.....	169
4.2.3 Rating curves or summation procedures?.....	173
4.2.4 Summary: Suspended sediment load estimates.....	173
<b>4.3 Uncertainties in annual load estimates of bedload transport .....</b>	<b>176</b>
4.3.1 Differences in rating curves of suspended sediment and bedload transport.....	176
4.3.2 Effects of sampling on rating curve correlations.....	178
4.3.2.1 Range and variability of sediment transport, range of flows and sample size.....	178
4.3.2.2 Effect of sample size and bias correction on the prediction of total load .....	182
4.3.2.3 The effect of time of day on the representativeness of bedload sampling: favorable measuring times in a snowmelt regime.....	187
4.3.3 Sediment transport equations .....	189
4.3.4 Summary: Uncertainty of estimates of annual bedload transport.....	193

#### **5. Annual Variability of Sediment Yield (Total Load) .....**

<b>5.1 Extent and evaluation of natural variability.....</b>	<b>195</b>
<b>5.2 The Data set .....</b>	<b>196</b>
<b>5.3 Annual variability of sediment yield: mean values and extreme values .....</b>	<b>198</b>

<b>5.4 Inter- and intra-basin variability in undisturbed basins within one experimental forest</b> .....	<b>199</b>
5.4.1 Hubbard Brook Experimental Forest .....	199
5.4.2 Fraser Experimental Forest .....	205
<b>5.5 Comparison of variability of sediment yields in disturbed and undisturbed basins</b> .....	<b>209</b>
5.5.1 Difference in mean and coefficient of variation in disturbed and undisturbed basins .....	209
5.5.2 Amount and duration of sedimentary effects in disturbed basins .....	210
5.5.3 Predictability of annual sediment yield from interbasin comparisons.....	217
<b>5.6 Variability: years of record needed and downstream change</b> .....	<b>218</b>
5.6.1 Coefficient of variation.....	218
5.6.2 Distribution type and number of samples needed .....	218
5.6.3 Downstream decrease of annual variability in sediment load .....	220
<b>5.7. Sedimentary response in the years following the large event</b> .....	<b>223</b>
5.7.1 Cumulative sediment yield .....	223
5.7.2 Time until first response occurs.....	225
<b>5.8 Summary</b> .....	<b>226</b>

**Part C: Downstream Transport of Sediment ..... 227**

**1. Introduction.....227**

**2. Sediment Delivery Ratios .....229**

**2.1 Definition and development**..... **229**

**2.2 General applicability of DR curves** .....

        2.2.1 Interbasin and temporal variability of sediment delivery ratios .....

        2.2.2 Downstream variability of sediment delivery ratios .....

**2.3 Modified DR curves to detect changes in sediment yield**..... **233**

        2.3.1 Differentiation according to sediment production and delivery processes .....

        2.3.2 Differentiation of DR according to grain sizes and sediment transport processes .....

        2.3.3 Differentiation of DR according to sediment storage dynamics .....

        2.3.4 Stream Type and Grain-size Selective Stream Delivery Ratios .....

        2.3.5 Summary .....

**3. Modeling the effect of dilution on the downstream decrease of sediment concentration**..... **243**

**3.1 Applicability of a dilution model** .....

**3.2 The dilution model** .....

        3.1.1 Modelled scenarios.....

**3.2 Results**.....

        3.2.1 Sediment concentration from impaired basin and background .....

        3.2.1 Different scenarios of stream flow .....

**4. Travel distance and travel velocity of downstream sediment transport**..... **252**

**4.1 Introduction** .....

<b>4.2</b>	<b>Suspended sediment transport.....</b>	<b>253</b>
4.2.1	Fingerprinting sources of fine sediment, its travel paths and sinks .....	254
4.2.2	Estimating transport distances by comparing downstream loads .....	255
4.2.1.1	Data sets and methodology.....	255
4.2.1.2	Scour and storage in the reaches between the stations .....	257
4.2.3	Review of data on the downstream travel distance of turbidity .....	261
<b>4.3</b>	<b>Processes affecting the downstream travel distance of bedload sediment ....</b>	<b>262</b>
4.3.1	Information needed for long-term mean annual travel distances ....	262
4.3.2	Studies addressing the dispersion of bedload sediment.....	263
4.3.2.1	Longitudinal dispersion: travel distances .....	263
4.3.2.2	Statistical distribution of longitudinal dispersion .....	264
4.3.2.3	Vertical dispersion: processes and effects on travel distances .....	266
4.3.2.4	Lateral dispersion .....	267
4.3.3	Effects of particle size and shape, bedforms, and stream morphology on the downstream travel distance .....	268
4.3.3.1	Particle size and shape .....	268
4.3.3.3	Magnitude and duration of flow.....	270
4.3.3.4	Bedforms and micromorphology.....	272
4.3.3.5	Channel and Valley Morphology.....	273
4.3.3.6	Long-term sediment storage .....	276
4.3.3.7	Summary .....	277
4.3.4	Extrapolation of short-term and medium term tracer experiments? .....	278
<b>4.4</b>	<b>Extrapolation of mean annual travel distances from medium- and short-term studies .....</b>	<b>282</b>
4.4.1	Downstream movement of sands and fine gravels.....	283
4.4.2	Single particle tracers of pebbles and cobbles.....	284
4.4.3	Predictability of mean annual travel distances by stream type and gradient? .....	286
4.4.4	Annual travel distances as a function of grain-size .....	289

**Part D: Conclusions and Recommendations..... 291**

1.	The issue of spatial scale in sedimentary cumulative watershed effects.....	291
2.	Detectability of CWEs .....	292
3.	Measurement uncertainty .....	292
4.	Determination of annual sediment loads.....	295
5.	Interannual and interbasin variability in sediment loads .....	296
6.	Downstream travel velocity .....	297
7.	Detecting a sedimentary cumulative watershed effect.....	299

**Part E: References..... 301**



## List of Figures

### Chapter A-1

**Fig. A-3; 1:** Schematic diagram showing how the interplay between management activities in different basins at different times can interact with background conditions to cause a cumulative watershed effect (after Lawrence and Ice, 1986). Sediment transport rate in the center graphs is monitored at a location in close proximity to the management activities, while the bottom graphs depict sediment transport rate measured further downstream.

**Fig. A-3; 2:** Six-stage model of channel evolution following channelization (from Hupp and Simons 1991).

### Chapter B-1

**Fig. B-1; 1:** Time-distance diagram showing the position of individual radio-tagged cobbles of different sizes during a flood event at the Lainbach, an Alpine step-pool river in Bavaria, Germany. Between 3 p.m. and 7 p.m., cobble positions were recorded about every half hour. Cobbles spend longer time periods resting than moving. The last position record was after midnight. The smallest particle only moved after 7 p.m. The dashed line indicates a mean travel speed of 800 m /11 hours (from Ergenzinger et al. 1989).

**Fig. B-1; 2:** Short-term variability at Goodwin Creek, a sand-gravel stream in Mississippi, caused by migration of dunes between 6:00 and 8:15, and possibly bedload sheets between 8:15 and 9:45. Flow was about 21 m<sup>3</sup>/s during the first phase, and 16.5 m<sup>3</sup>/s during the latter (after Kuhnle et al., 1989; and Kuhnle, pers. comm., 1993).

**Fig. B-1; 3:** Various forms of intra-event variability in bedload transport rates during a single high-flow event. Q indicates the hydrograph, and Q<sub>b</sub> the temporal variation of bedload transport rates.

1. Sudden, isolated pulses or unsystematic increases of bedload transport at a specific time during a flood event. These bedload pulses are often caused by a sudden increase in sediment supply from a bursting log jam, bank collapse, etc.
2. Bedload pulses with a discernible return period, but which may not be associated with the highest flows. Recurring storage and deposition of bedload associated with a riffle-pool morphology may be responsible for this pulsed nature of bedload transport as well as local interactions between flow and the channel bottom.
3. A lagged or accelerated response of sediment transport in relation to the timing of the flow event (i.e., hysteresis). This can be caused by several processes including river bed consolidation that delays armor layer break-up, an easily accessible sediment storage that becomes depleted, or vortex erosion.
4. Systematically increasing or decreasing bedload transport rates without any significant change in discharge may be the result of increasing supply from undercut, unstable banks, progressive armoring, or exhaustion of sediment supply.

**Fig. B-1; 4:** Sudden increase of bedload transport during a small flood event at Goodwin Creek during almost constant flow (R. Kuhnle, pers. comm., 1993).

**Fig. B-1; 5:** Intra-event variability of bedload transport during a storm at Prairie Creek, a coastal stream in northern California. In addition to the fluctuations in transport rates, bedload transport lags behind discharge by about 5 hours, and produces high peaks on the falling limb of flow (after Lisle, 1989; and Lisle, pers. comm., 1993).

**Fig. B-1; 6:** Bedload pulses recurring over approximately 20-minute intervals following peak discharge at the Erlenbach torrent in the Swiss Alps. Start of the event is May 31, 1987, 5:57 p.m. (from Bänzinger and Burch, 1990).

**Fig. B-1; 7:** Bedload pulses recurring in 10-15 minute intervals at the Erlenbach torrent in the Swiss Alps (from Rickenmann, 1994).

**Fig. B-1; 8:** Bedload pulses recurring in about 2-hour intervals during a high flow event at Goodwin Creek (R. Kuhnle, pers. comm., 1993).

**Fig. B-1; 9:** Bedload pulses occurring at various frequencies. Most distinguishable are frequencies of 1.5, 4-6, and 24 hours. Bedload pulses recurring at 4-6 hours are marked with arrows. Bedload measurements were made in 5-minute intervals using the magnetic tracer technique over a 3-day period during a snowmelt high flow at Squaw Creek, a mountain stream in Montana (Bunte 1991; 1996).

**Fig. B-1; 10:** Bedload waves observed on the rising and falling limb, respectively, at Squaw Creek in the middle of snowmelt high flow (after Ergenzinger and De Jong, 1995).

**Fig. B-1; 11:** Examples of lead and lag in bedload transport (submerged weight) during consecutive flood events in 1978 and 1979 at Turkey Brook, a gravel-bed river in Great Britain. Plots for consecutive events follow the columns down. Axes scales are the same for all plots (slightly altered, from Reid et al. 1985).

**Fig. B-1; 12:** Increasing lag in bedload transport rates during a flood event with multiple peaks at the Erlenbach torrent in the Swiss Alps. The number of impulses/min. recorded at hydrophone 3 is smoothed by a moving average over 5 minutes of hydrophone impulses (H3 (5' mean)) (from Rickenmann, 1994).

**Fig. B-1; 13:** Vortex erosion around an obstacle embedded in erodible sediment: profile view - moderate flow intensity (top); plane view - moderate flow intensity (center); plan view - high flow intensity (bottom) (from Bunte and Poesen, 1994).

**Fig. B-1; 14:** Fluctuations of bedload transport measured at 1-hour intervals over a 15-day period during a snowmelt high flow at Squaw Creek (from Bunte, 1991; 1996). The relative amount of sediment transported by primary and tertiary daily bedload wave shifts from primary waves at the beginning of the snowmelt period to tertiary waves at the end of the high flow period.

**Fig. B-1; 15:** Schematic diagram indicating general magnitude of bedload transport rates (top) and fluctuations of bedload transport rates on a riffle and in a pool (bottom) during a high flow event.

**Fig. B-1; 16:** Hypothetical examples of sediment volumes stored behind LWD of various sizes.

**Fig. B-1; 17:** Cross-sectional variability of coarse bedload transport in Turkey Brook, a cobble-gravel stream in UK (from Reid et al. 1985).

- Fig. B-1; 18:** Travel paths of coarse and fine bedload through a meander bend and lateral sorting of bedload grain sizes in riffle areas (after Bridge and Jarvis 1982; Anthony and Harvey 1991).
- Fig. B-1; 19:** Schematic diagram indicating the interplay between flow cells, bed material topography, channel roughness, and the lateral variability of bedload transport (after Ergenzinger et al. 1993; Ergenzinger et al. 1994; De Jong 1995).
- Fig. B-1; 20:** Hjulström's curve indicating threshold velocities for erosion, transport, and deposition of different grain sizes based on a flow depth of 1 m, and uniform grain-size distributions (from Morisawa 1968).
- Fig. B-1; 21:** Correspondence between turbidity (OBS output) and turbulent flow velocity in vertical (v) and horizontal (u) direction at the Fraser River, British Columbia (from Lapointe, 1992).
- Fig. B-1; 22:**  $C_s$  (solid line), turbidity (dashed line), and stage (dotted line) during a reservoir release at Llyn Celyn, about 8 km downstream from the reservoir (from Gilvear and Petts 1985).
- Fig. B-1; 23:** Different shapes of hysteresis loops in Australian rivers (from Rieger and Olive 1986).
- Fig. B-1; 24a:** Theoretical vertical distribution of relative suspended sediment concentration in a flow profile. The numbers on the curves express the ratio  $z = w/\kappa v^*$  where  $w$  = particle fall velocity,  $v^*$  = shear velocity, and  $\kappa$  = the von Karman constant (from Raudkivi 1976).
- Fig. B-1; 24b:** Theoretical vertical distribution of relative suspended sediment concentration in a flow profile. For a given flow, the value of  $z$  increases with particle size. Clay has an almost homogeneous vertical distribution, while sand is concentrated near the bottom of the stream (from Beschta 1987).
- Fig. B-1; 25:** Measured vertical distributions of suspended sediment at the Mississippi River at St. Louis (from Colby 1963) (top), and the Missouri River at Kansas City (from Guy 1970) bottom).
- Fig. B-1; 26:** Effect of flow depth and velocity on the vertical distribution of  $C_s$  in slow (curves 1 and 3) and fast (curves 2 and 4) flow of deep (curves 1 and 2) and shallow (curves 3 and 4) water (from Colby 1961; 1964).
- Fig. B-1; 27:** Effect of velocity profile (parabolic, logarithmic, and linear) on the vertical  $C_s$  distributions (from Nordin and McQuivey 1971). Velocity profiles (left), vertical  $C_s$  distributions (right).
- Fig. B-1; 28:** Effect of water temperature on mean  $C_s$  in a vertical profile (top); on the bottom sediment concentration  $C_b$  (center); and the ratio of  $C_b/C_s$  (bottom) (replotted from Hong et al., 1984).
- Fig. B-1; 29:** Lateral distribution of suspended sediment concentration (top), stream flow velocity (center), and flow depth (bottom) at section C in the Middle Loup River in Nebraska (from Hubbell and Matejka, 1959).

**Fig. B-1; 30:** Lateral distribution of depth, stream velocity, and  $C_s$  at the Niobrara River near Valentine, Nebraska (from Colby 1963).

**Fig. B-1; 31:** Cross-sectional variation of coarse (0.062-2 mm) (top), and fine (<0.062 mm) (bottom) suspended sediment concentrations at the Rio Grande near Bernardo, NM (from Culbertson, 1977).

**Fig. B-1; 32:** Temporal variability of the lateral distribution of  $C_s$  over six 20-minute intervals in the Arkansas River at Portland, CO, during steady flow: depth-integrated  $C_s$  per equal discharge increment (top); and percent of total  $C_s$  finer than 0.063 mm (silt and clay) (bottom). Flow increased during the sixth measurement at 100 minutes (data from Horowitz et al., 1989).

**Fig. B-1; 33:** Temporal variability of the lateral distribution of  $C_s$  over six measurements over six 20-minute intervals in the Cowlitz River at Kelso, WA, during steady flow: depth-integrated  $C_s$  per equal discharge increment (top); and percent of total  $C_s$  finer than 0.063 mm (silt and clay) (bottom) (data from Horowitz et al., 1989).

**Fig. B-1; 34:** Comparison of longitudinal mixing lengths in terms of stream width for different stream scenarios: For equal discharge and width-depth ratios, mixing lengths increase as gradient decreases (top); For equal stream power ( $Q \cdot S$ ) and stream width, mixing length increases for steep, high-energy streams (bottom).

## **Chapter B-2**

**Fig. B-2; 1a and b:** Percent goodness-of-fit of relative transport rates for lognormal distributions versus percent goodness-of-fit for Gaussian distributions (top). Percent goodness-of-fit of relative transport rates to lognormal distribution versus goodness-of-fit to Hamamori distribution (bottom).

**Fig. B-2; 2:** Percent goodness-of-fit of relative transport rates  $qb_r$  for Gaussian and lognormal distributions versus the mean (top), sorting (center), and skewness (bottom) of relative transport rates  $qb_r$ .

**Fig. B-2; 3:** Percent goodness-of-fit of relative transport rates  $qb_r$  for Gaussian and lognormal distributions versus the 5th (top), and 95th (bottom) percentile of the cumulative distribution functions  $qb_r$ .

**Fig. B-2; 4:** Average cumulative distribution functions of relative transport rates  $qb_r$  for those data sets found to be normal or lognormal using the  $W$ -test, and the ideal Hamamori function (top). Average cumulative distribution functions for  $qb_r$ -data sets with better-than-average percentages of goodness-of-fit to Gaussian and lognormal distributions according to the Schleyer-test, and better-than-average percentage goodness-of-fit to the Hamamori distribution (bottom).

**Fig. B-2; 5:** Average frequency distribution of relative bedload transport rates for Gaussian and lognormal distributions (as determined by the  $W$ -test), and the ideal Hamamori distribution.

**Fig. B-2; 6:** Relationship between the goodness-of-fit of relative transport rates to a Hamamori distribution and the absolute difference between the sorting of relative transport rates and the value for sorting obtained from the ideal Hamamori distribution.

**Fig. B-2; 7:** Relationship between goodness-of-fit of relative transport rates to Gaussian and lognormal distributions and sample size (top), sampling intensity (center), and sampling performance (bottom).

**Fig. B-2; 8:** Coefficient of variation in fractional bedload transport rates taken during different periods of snowmelt highflow at Squaw Creek, Montana. Bedload samples were taken with a large frame sampler. Size of the opening was 0.3 m by 1.5 m, and netting mesh width was 10 mm.

**Fig. B-2; 9:** Lateral distribution of bedload transport rates assumed in the transport models of Hubbell and Stevens (1986), and Hubbell (1987).

**Fig. B-2; 10:** Maximum percent error associated with two sampling schemes, different levels of variability in transport rates at individual locations (left-hand plots), and different spatial distribution of lateral variability within the cross-section (right-hand plots). Open symbols of  $\Delta$ ,  $\circ$ , and  $\square$  in the left-side plots represent narrow, equal, and wide distribution of large transport rates over the cross-section as shown in Figure B-2; 9. The closed symbols of  $\blacktriangle$ ,  $\bullet$ , and  $\blacksquare$  in the right-hand plots represent ratios of mean high to low transport rates of 1.5:1, 7:1, and 25:1, respectively. Heavy lines show the error associated with taking samples at only four cross-section locations, while thin lines represent the error associated with 20 cross-section locations. Boxes contain the maximum probable percent error for a sample size of 40. (Data plotted from Hubbell 1987).

**Fig. B-2; 11:** Maximum probable percent error versus sample size for moderately nonuniform transport (ratio of high to low mean transport rates of 1.5:1, and equal widths of large and small transport rates), and extremely non-uniform transport (ratio of high to low mean transport rates of 25:1, and 80% of the stream width covered by transport rates) (From Hubbell 1987).

**Fig. B-2; 12:** Variation in the percent error (Eq. 22) of an estimate of the mean relative at-a-point bedload transport rate that can be expected not to be exceeded at the 99, 95, 90, and 50% confidence levels, with number of random samples. The relations are based on the Hamamori probability distribution function (Eq. 6) (from Gomez et al. 1990).

**Fig. B-2; 13:** Exponential increase in sample size with increasing accuracy of estimating the population mean with 95% confidence interval; lines represent CV values between 50 and 125 percent.

**Fig. B-2; 14:** Number of samples needed to estimate the median transport rate with 95% confidence as a function of percent relative error in lognormally distributed data. The top figure shows sample size to be a function of variance ( $s^2$ ) and the potential number of samples ( $M$ ), with the heavy lines representing a lower variance than the thinner lines. The bottom figure shows the variation in sample size required to estimate the mean and median transport rates for Gaussian and lognormally distributed data sets, respectively. The gray band represents Gaussian-distributed data sets with a CV between 50 and 100%; the broken line in the center indicates a CV of 75%. The three upper lines without symbols represent the number of samples required for lognormally distributed data with the indicated variance.

### **Chapter B-3**

**Fig. B-3; 1:** 3 x 3 inch standard Helley-Smith bedload sampler (7.6 cm by 7.6 cm). Oblique (top), plan and side elevation views of (a) the entire sampler, and (b) the sampler nozzle. All dimensions in cm (from Emmett 1981).

**Fig. B-3; 2:** Zone of converging streamlines in front of the standard Helley-Smith sampler after Druffel et al. (1976) (from DVWK 1992).

**Fig. B-3; 3:** Velocity profile in front of and within the sampler orifice (top); Increase of hydraulic efficiency ( $v_{mv}/v_{mf}$ ) with curvature of the velocity profile ( $v_2/v_1$ ) within the sampler orifice (bottom) (from DVWK 1992).

**Fig. B-3; 4:** Calibration curves for sampling efficiency of various Helley-Smith-type samplers for well-sorted bed material with a  $D_{50}$  of 6.5 mm (after Hubbell and Stevens 1986; Hubbell 1987).

**Fig. B-3; 5:** Comparison between bedload transport rates sampled with the standard Helley-Smith sampler and the BL-86-3 at the Colorado River near Supai, AZ, during low flows. Top: dotted line represents perfect agreement and the solid line is the observed regression given by Gray et al. (1991). Bottom: percent difference between bedload transport rates sampled with the standard Helley-Smith sampler and the BL-86-3.

**Fig. B-3; 6:** Calibration curves for adjusting sampled rates of various size fractions of material collected with the standard Helley-Smith sampler (left) and the BL-84 (right). The diagonal is the line of perfect agreement (from Hubbell and Stevens, 1986; Hubbell, 1987).

**Fig. B-3; 7:** Measured values of sampling efficiency for the standard Helley-Smith sampler and resulting interpolated curve (after DVWK 1992).

**Fig. B-3; 8:** Conceptual model demonstrating the combined effects of particle sizes and bedload transport rates on sampling efficiency for three differently-shaped 3 x 3-inch Helley-Smith samplers (area ratios of 1.1, 1.4, and 3.22) and the standard 6 x 6-inch Helley-Smith sampler with an area ratio of 3.22 for low bedload transport rates (top) and high bedload transport rates (bottom)..

**Fig. B-3; 9:** Effects of bag size and mesh width on sampled mean bedload transport rates by grain-size. The thin line in each graph represents the bedload captured with a 6000 cm<sup>2</sup> bag with a 0.2-mm mesh (data from Johnson et al. 1977).

**Fig. B-3; 10:** Effects of bag size and sampling duration on weight of sandy bedload sampled with a standard 3 x 3 inch Helley-Smith sampler. Sampled weight does not increase linearly with time for small bags (top). This effect is more pronounced for higher transport rates (bottom), and sampling efficiency (thin line) decreases strongly within the first minute of sampling (data replotted from Beschta 1981).

**Fig. B-3; 11:** Comparison of grain-size distributions sampled at three gravel-bed streams with a 3 x 3-inch Helley-Smith sampler directly on the stream bottom (solid line) and at a sill (bars) (data from Wilcox et al. 1996).

**Fig. B-3; 12:** Percent sampling efficiency (%E) as a function of the ratio of sampling duration  $t^*$  times shear velocity  $u^*$  and sampler size  $L_s$ . The three values of  $L_s/D_{50} = 80, 106,$  and  $160$  plot on one curve (top). A different curve is obtained for a smaller ratio of  $L_s/D_{50} = 27$ . Stippled curve is curve from the plot above (bottom) (from Engel and Lau 1981).

**Fig. B-3; 13:** (a) Percent sampling efficiency as a function of particle size for two basket-type samplers (Y-64 and Y-80), and two pressure-difference-type samplers (TR-2 and 6 x 6 inch HS) in flume experiments (upper left); (b) Factor by which 6 x 6-inch Helley-Smith sampler oversampled Y-64, Y-80, and TR-2 sampler in flume experiments (center left); (c) Relative sampling efficiency of Y-80 sampler in flume experiments (lower left); (d) Factor by which 6 x 6 inch Helley-Smith sampler oversampled Y-64, Y-80, and TR-2 sampler in field measurements (center right); (e) Relative sampling efficiency of Y-80 sampler in field experiments (lower right) (Data from Gao 1991; Xiang and Zhou 1992).

**Fig. B-3; 14:** Comparison of grain-size distributions sampled at three gravel-bed streams with a 3 x 3 inch Helley-Smith sampler at a sill (solid line), and the grain-size distributions of bedload accumulated in debris basins (bars) (data from Wilcox et al. 1996).

**Fig. B-3; 15:** Schematic diagram of a vortex sampler (top); Elevation of streamline dividing between sediment that goes into the sampler and sediment that passes over it (bottom) (from Atkinson 1994).

#### **Chapter B-4**

**Fig. B-4; 1:** Effect of sampling type (as defined in Table B-4; 1) and the temporal resolution of the flow series (i.e., hourly and daily values) on the accuracy of the total load estimates in terms of absolute values (top), percentage values (center), and variability (i.e., the CV of 50 replicate load estimations) (bottom).

**Fig. B-4; 2:** Effect of sampling interval and summation procedures (as defined in Table B-4; 3) on the accuracy in terms of total values (top), percentage values (center), and variability (i.e., the CV of 50 replicate load estimations) (bottom).

**Fig. B-4; 3:** Number of repetitions of 50 replicate sediment load analyses needed for the estimated sediment load to be within 20% (top), and 5% (bottom) of the indicated accuracy (i.e., the percentage of total load averaged from 50 replicate analyses). Full symbols refer to summation procedures SP, and the corresponding numbers indicate the sampling interval in days. Open symbols indicate rating curve load estimates based on 7 years of weekly (w) sampling (Sampling Type 1); w + = weekly sampling plus 200 high flow samples (Sampling Type 3), w + + = weekly sampling plus 1000 high flow samples (Sampling Type 4). These sampling types were applied to hourly (hrl.), and daily (dl.) flow series; and hourly samples with separate rating curves for summer and winter, rising and falling limb (hrl., sep.) (Sampling Types 3a and 4a, respectively).

**Fig. B-4; 4:** Effects of range of flows, range of sediment transport rates, variability in sediment transport, and sample size of sediment transport on rating curve  $r^2$  and regression functions. Shaded areas depict the data ranges.

**Fig. B-4; 5:** Relation between bedload transport signal rates and discharge at Squaw Creek, a gravel-bed mountain stream for various levels of temporal resolution: 5 minutes (top), 1 hour (center), and 1 day (bottom).

**Fig. B-4; 6:** Mean (top), and standard deviation (bottom) of the total signal load as a function on the sample size  $N$  obtained from actual data based on the rating curve estimators QMLE, FOA, MVUE for Squaw Creek, Montana (data from Bunte 1991).

**Fig. B-4; 7:** Mean (top), and standard deviation (bottom) of the total sediment load as a function on the sample size  $N$  obtained from actual data based on the rating curve estimators QMLE, FOA, MVUE for the East Fork River, Wyoming (data from Emmett 1980).

**Fig. B-4; 8:** Mean (top), and standard deviation (bottom) of the total sediment load as a function on the sample size  $N$  obtained from actual data based on the rating curve estimators QMLE, FOA, MVUE for Prairie Creek (data from Lisle 1989, and Lisle pers. com.).

**Fig. B-4; 9:** Mean (top), and standard deviation (bottom) of the total sediment load as a function on the sample size  $N$  obtained from actual data based on the rating curve estimators QMLE, FOA, MVUE for Goodwin Creek, Mississippi (data from Kuhnle, pers. com.).

#### **Chapter B-5**

**Fig. B-5; 1:** Annual bedload yields from three undisturbed control watersheds (WS 1, 3, and 6) at the Hubbard Brook Experimental Forest for 1975 to 1990.

**Fig. B-5; 2:** Annual streamflows in the three undisturbed control watersheds (WS 1, 3, and 6) at the Hubbard Brook Experimental Forest from 1975 to 1990.

**Fig. B-5; 3:** Annual streamflows in the two disturbed watersheds (WS 2 and 5) at the Hubbard Brook Experimental Forest from 1975 to 1990.

**Fig. B-5; 4:** Highest instantaneous annual streamflow at WS 3, 1975-1988.

**Fig. B-5; 5:** Seasonal streamflows (April -September) from two control watersheds (Lexen Creek and East St. Louis Creek) at Fraser Experimental Forest, 1965-1991.

**Fig. B-5; 6:** Annual sediment yields from two control watersheds (Lexen Creek and East St. Louis Creek) at Fraser Experimental Forest, 1965-1991.

**Fig. B-5; 7:** Annual sediment yields from the undisturbed WS 6 and the disturbed WS 2 at the Hubbard Brook Experimental Forest from 1966 to 1990.

**Fig. B-5; 8:** Annual bedload yields from the undisturbed WS 6 and the disturbed WS 5 at the Hubbard Brook Experimental Forest from 1966 to 1990.

**Fig. B-5; 9:** Annual bedload yields from three disturbed watersheds (Deadhorse Creek - Main, Deadhorse Creek - North, and Deadhorse Creek - South) at Fraser Experimental Forest, 1965-1991.

**Fig. B-5; 10:** Coefficient of variation versus mean annual sediment yield for 38 basins.

**Fig. B-5; 11:** The coefficient of variation of annual suspended sediment yield for Piceance Creek in northwestern Colorado and its tributaries as a function of basin area. Data were calculated from values measured from 1975 to 1981, inclusive.

**Fig. B-5; 12:** Coefficient of variation of annual sediment yield versus watershed area for 38 basins.

**Fig. B-5; 13:** Three different responses of watersheds to management impacts at the H.J. Andrews Experimental Forest, 1958-1988 (after Grant and Wolff 1991).

### **Chapter C-2**

**Fig. C-2; 1:** Relationship between sediment delivery ratio and drainage basin area for different regions based on data from Roehl (1962), Sokolovskii (1968), Piest et al. (1975), Renfro (1975), A.S.C.E. (1975), Williams (1977), and Mou and Meng (1980) (from Walling 1983).

**Fig. C-2; 2:** Conceptual downstream sequence of channel types (Montgomery and Buffington, 1993, 1997), bedload grain-size distributions, and expected unit bedload transport rates.

**Fig. C-2; 3:** Conceptual grain-size sediment delivery curves, assuming a constant stream type.

### **Chapter C-3**

**Fig. C-3; 1a to 1c:** (a) The effects of dilution (background suspended sediment concentration,  $(Cs_d)$ ) on downstream total sediment concentration ( $Cs_{tot}$ ) for different increases in suspended sediment concentration from an impaired watershed ( $Cs_i$ ). (b) Size of the impaired basin ( $A_i$ ) is increased from 5 to 50 ha. (c) Size of the impaired basin ( $A_i$ ) is increased from 5 to 400 ha.

**Fig. C-3; 1d to 1f:** (d) The effects of dilution (background suspended sediment concentration,  $(Cs_d)$ ) on downstream total sediment concentration ( $Cs_{tot}$ ) for different increases in suspended sediment concentration from an impaired watershed ( $Cs_i$ ). Water yield ( $qA_i$ ) is increased from 0.1 l/s·ha to 0.2 l/s·ha. (e) Size of the impaired basin ( $A_i$ ) is increased from 5 to 50 ha, and water yield ( $qA_i$ ) is increased from 0.1 l/s·ha to 0.2 l/s·ha. (f) Size of the impaired basin ( $A_i$ ) is increased from 5 to 400 ha, and water yield ( $qA_i$ ) is increased from 0.1 l/s·ha to 0.2 l/s·ha.

**Fig. C-3; 1g:** Generalized model of dilution effects on suspended sediment concentrations in a fourth-order basin as a function of the sediment concentrations from an impaired (disturbed) basin, the proportion of the basin that is disturbed, and the background concentration of suspended sediment from the unimpaired portions of the fourth-order basin.

**Fig. C-3; 1h:** Effects of dilution on suspended sediment concentrations in a fourth-order basin under different runoff conditions as a function of the sediment concentrations from an impaired (disturbed) basin, the proportion of the basin that is disturbed, and the background concentration of suspended sediment from the unimpaired portions of the fourth-order basin.

**Fig. C-4; 1:** Map of the Piceance Creek basin in northwestern Colorado. Scale is 1:500,000.

**Fig. C-4; 2:** Mean daily suspended sediment load for four stations (P1 to P4) along Piceance Creek in northwestern Colorado, 1975 - 1981.

**Fig. C-4; 3:** Mean daily suspended sediment load for three tributaries to Piceance Creek, 1975 - 1981.

**Fig. C-4; 4:** Annual deviation (in percent) of the mean daily suspended sediment loads at a downstream station relative to the mean increase between the two stations over the period of record.

**Fig. C-4; 5:** Cumulative distributions of relative travel distances ( $l/l_m$ ) for a negative exponential distribution (straight line) and a gamma distribution (curved graph) (after Kirkby 1991). Note that the y-axis is a logarithmic scale so that the negative exponential distribution plots as a straight line.

**Fig. C-4; 6:** Mean transport distance (m) of pebble and cobble tracers versus excess stream power ( $\Omega_{max} - \Omega_{crit}$  in  $\text{kg/m}\cdot\text{s}$ ) of peak flows for various flood events at the Lainbach, a step-pool stream in Bavaria (Gintz 1994). The dashed line represents the data from Hassan et al. (1992) for less steep streams that do not have a step-pool morphology.

**Fig. C-4; 7:** Mean travel velocity (m/h) of pebble and cobble tracers versus excess stream power ( $\Omega_{max} - \Omega_{crit}$  in  $\text{kg/m}\cdot\text{s}$ ) of peak flows for various flood events at the Lainbach, a step-pool stream in Bavaria (from Gintz 1994). The dashed line represents data from Hassan et al. (1992) for less steep streams that do not have a step-pool morphology.

**Fig. C-4; 8:** Daily transport velocities as the ratio of displacement distance and dispersion time for modes and means of displacement distances at North Loup River (data from Sayre and Hubbell 1965).

**Fig. C-4; 9:** Mean annual travel distance of bedload transport as a function of stream type and gradient. All data sets (top); data from braided, and steep, aggrading streams (center), and data from streams classified as step-pool, pool-riffle, mountain, alternate bars, ephemeral, large streams, and sand-bedded streams.

## List of Tables

### Chapter A-1

**Table A-3; 1:** Four stages of stream channel change due to variations in the ratio of sediment supply to conveyance capacity (Phillips 1987).

**Table A-3; 2:** Stages of channel evolution in a degrading environment causing an upstream migration of headcuts and downstream variation in bank stability ( $h$  is the bank height, and  $h_{crit}$  is the maximum stable bank height) (Watson et al. 1986, 1988).

**Table A-3; 3:** Stages of channel evolution in a meandering stream following stream canalization (Hupp and Simons 1991).

**Table A-3; 4:** Channel evolution following reduced flows (Everitt 1993).

## **Chapter B-1**

**Table B-1; 1:** Varying time scales for the temporal variability of sediment transport

**Table B-1; 2:** Short-term bedload transport fluctuations observed in various streams and laboratory experiments.

**Table B-1; 3:** Observed sources and timing of intra-event variability in bedload transport rates in gravel-bed streams.

**Table B-1; 4:** Hystereses shapes and temporal variability of  $C_s$  in relation to discharge (after Rieger and Olive (1986)).

**Table B-1; 5:** Various hystereses shapes in the relation between suspended sediment concentration and discharge (after Williams 1989).

## **Chapter B-2**

**Table B-2; 1:** Description of the 40 data sets used for analyses of sediment transport event variability: sampling schemes and statistical results.

**Tables B-2; 2a - d:** Percentiles of cumulative frequency of relative transport rates, distribution parameters, percentage goodness-of-fit to ideal normal and lognormal distributions, and to the Hamamori distribution, sample size, sampling intensity and sampling performance. Data sets are sorted according to their goodness-of-fit to

- a **lognormal distribution** (Schleyer-test) (Table 2a),
- a **Gaussian distribution** (Schleyer-test) (Table 2b),
- **Hamamori distribution** (Table 2c), and
- to the results of the  $W$ -Test:  $x$  indicates a fit to a lognormal or Gaussian distribution with a 95% probability level (Table 2d).

**Table B-2; 3:** Mean, standard deviation and range of the calculated goodness-of-fit (%) of all bedload data sets to Gaussian and lognormal distributions (Schleyer-test), and to the Hamamori distribution.

**Table B-2; 4:** Average percentage goodness-of-fit (%) of data sets that have the highest percent goodness-of-fit for a Gaussian, lognormal, or for the Hamamori distribution, and the corresponding percent goodness-of-fit to the respective other distributions.

**Table B-2; 5:** Percentage goodness-of-fit to normal and lognormal distributions according to the Schleyer-test, and to the Hamamori distribution, of data sets for which normality and lognormality was approved or rejected by the  $W$ -test.

**Table B-2; 6:** Distribution parameters for Gaussian, lognormal, and Hamamori distributions, as established by different techniques.

**Table B-2; 7:** Percentiles of relative transport rates by distribution type (Gaussian, lognormal, neither of the two, and Hamamori distributions, as determined by different procedures).

**Table B-2; 8:** Percentage of small, medium, and large relative transport rates ( $qb_r$ ) in each of the three distribution types as determined by the  $W$ -test.

**Table B-2; 9:** Relation between temporal scale of bedload transport variability (constant and unsteady discharge) and distribution type. Normal and lognormal distributions were determined by positive *W*-tests. The top 50% goodness-of-fit for a Hamamori distribution were then separated by constant and unsteady discharge.

**Table B-2; 10:** Relation between sampling schemes and the probability distribution of samples.

**Table B-2; 11a:** Number of data sets falling into various sampling categories, and the distribution of those data sets by type of distribution.

**Table B-2; 11b:** Percentage of all lognormal, Gaussian, or Hamamori-distributed data sets falling into one of the three sampling types.

**Table B-2; 12:** Preferential associations of stream and sampling parameters with a statistical distribution type.

**Table B-2; 13:** Variation of *CV* with grain-size class at Oak Creek (from Beschta 1983).

**Table B-2; 14:** Bedload sampling with a large net bedload sampler at Squaw Creek, 1991: transport rates and number of samples and sampling days.

**Table B-2; 15:** Coefficients of variation (*CV*) for measured and predicted bedload transport rates for constant and unsteady flows in flumes and streams.

**Table B-2; 16:** Average maximum percent errors in bedload transport for 40 subsamples taken under two different sampling schemes for differing amounts and spatial distributions of high bedload transport rates.

**Table B-2; 17:** Median values of sampling parameters associated with different sampling accuracies.

**Table B-2; 18:** Average values of selected distribution parameters of relative bedload transport rates  $qb_r$ , by type of distribution.

### **Chapter B-3**

**Table B-3; 1:** Mean daily values of bedload transport rates and suspended sediment load during a typical snowmelt highflow season at Squaw Creek, a gravel-bed mountain stream in Montana (drainage area of 105 km<sup>2</sup>) (data from Bunte et al. 1987; Bunte 1996).

**Table B-3; 2:** Pressure difference samplers and their dimensions (after Hubbell et al. 1985).

**Table B-3; 3:** Mean bedload transport rates during high flow events in various streams.

**Table B-3; 4:** Bedload grain-size distributions (mm) sampled with a 3 x 3 inch Helley-Smith sampler on a wooden sill, in a stream cross-section, and excavated from a debris basin (data from Wilcox et al. 1996).

**Table B-3; 5:** Characteristics of bedload samplers compared by Gao (1991) and Xiang and Zhou (1992).

**Table B-3; 6:** Percentage of original tracer particles recovered after consecutive floods for low (50%) and high (90%) tracer recovery rates.

**Table B-3; 7:** Mean quadratic error in percent for single-point suspended sediment sampling using the Polish 2-liter bottle sampler (from Branski 1981).

#### **Chapter B-4**

**Table B-4; 1:** Various sampling strategies used by Walling and Webb (1981) to compute the annual load using a rating curve approach.

**Table B-4; 2:** Percentage of true sediment load and coefficient of variation (CV) obtained for uncorrected rating curve load estimates, and for corrected rating curve estimates of sediment load for three rivers and 50 replicates of two different sampling schemes: regular weekly sampling (weekly) and regular weekly sampling plus flood period sampling ( $w + \hat{Q}$ ). (Data from Walling and Webb 1988).

**Table B-4; 3:** Sediment load summation procedures (from Walling and Webb 1981).

**Table B-4; 4:** Sediment transport range (arbitrary unit), factor of scatter, discharge range (arbitrary unit), and sample size used for regression analysis, and the resulting rating curve  $r^2$ , exponents, and coefficients.

**Table B-4; 5:** Relative signal rates normalized by the mean signal rate of the entire high flow period.

**Table B-4; 6:** Relative signal rates normalized by the mean signal rate of a calendar day.

**Table B-4; 7:** Relative signal rates normalized by the mean signal rate of a discharge day.

#### **Chapter B-5**

**Table B-5; 1:** Data base for the calculation of the variability of annual sediment yield.

**Table B-5; 2:** Linear regressions between annual sediment yields of undisturbed (WS 1, 3, 6) and disturbed watersheds (WS 2 and 5) at Hubbard Brook Experimental Forest for the entire period of 1975 (or 1976) - 1990, the period of high sediment yield 1975 (or 1976)- 1982, and the period of low sediment yield 1983-1990. For each regression,  $a$  is the slope,  $b$  is the y-intercept,  $r^2$  is the coefficient of determination, and StD of  $y$  is the standard error of the regression.

**Table B-5; 3:** Mean annual bedload yields ( $Q_{ba}$ , t/km<sup>2</sup>) and mean annual streamflow ( $Q_a$ , mm) over various times periods for three undisturbed watersheds at the Hubbard Brook Experimental Forest.

**Table B-5; 4:** Correlation coefficients ( $r^2$ ) of linear regressions of annual sediment yields versus seasonal flow for various time periods for the undisturbed basins East St. Louis Creek and Lexen Creek, Fraser Experimental Forest, Colorado.

**Table B-5; 5:** Mean annual sediment yields and seasonal stream flow for various time periods at East St. Louis Creek and Lexen Creek, Fraser Experimental Forest, Colorado, and coefficients of determination ( $r^2$ ) for linear regressions between annual sediment yields of the two watersheds.

**Table B-5; 6:** Coefficient of determination ( $r^2$ ) between the duration of various flow levels and annual sediment yields for two control basins at Fraser Experimental Forest (from Troendle, 1993).

**Table B-5; 7:** Coefficient of variation (in percent) for various time periods for undisturbed watersheds at Hubbard Brook and Fraser Experimental Forest. Time periods in the left-hand column are for Hubbard Brook; time periods in the extreme right-hand column are for Fraser.

**Table B-5; 8:** Mean annual bedload yields ( $t/km^2$ ) for disturbed basins at Hubbard Brook and Fraser Experimental Forest for various time periods.

**Table B-5; 9:** Coefficient of variation (in percent) of mean annual bedload yields ( $t/km^2$ ) for disturbed basins at Hubbard Brook and Fraser Experimental Forest for various time periods.

**Table B-5; 10:** Percent difference in mean and CV of annual sediment yields between a wet (1975-1982) and dry (1983-1990) period at Hubbard Brook, and a dry (1975-1982) and wet (1983-1991) period at Fraser Experimental Forest.

**Table B-5; 11:** Regression equations for annual sediment yields between undisturbed (Lexen and East St. Louis Creek) and disturbed watersheds (Deadhorse Creek North, South, and Main) at Fraser Experimental Forest for the entire period of 1975-1990, the period of high sediment yield (1975-1982), and the period of low sediment yield (1983-1990)\*. ( $a$  is the slope,  $b$  is the y-intercept, and  $StE$  represents the standard error of the regression.)

**Table B-5; 12:** Number of years of record for annual sediment yields needed for the sample mean to be within 10, 20, 30, 50 and 100% of the population mean for Gaussian distributed time series of annual sediment yields.

## **Chapter C-2**

**Table C-2; 1:** Reported values for the exponent ( $b$ ) and variability in the range of  $DRs$  (in percent) for various drainage basin areas in published collections of  $DRs$  and  $DR$  curves.

## **Chapter C-4**

**Table C-4; 1:** Area, mean daily suspended sediment load, years of record, and location of mainstem and tributary stations with suspended sediment data along a 40-km reach of Piceance Creek.

**Table C-4; 2:** Transport distances by size class over a larger than normal snowmelt highflow in North St. Vrain Creek (from Thompson 1994).

**Table C-4; 3:** Effects of channel morphology and micromorphology on entrainment probability, transport distances, and deposition probability of 480 artificial 1.0 kg tracers. Data were obtained after either one or two consecutive summer flood events in a mountain stream (from Gintz and Schmidt 1991; Schmidt and Ergenzinger 1992).

**Table C-4; 4:** Seasonal transport distances and dispersion ranges (m) of "pink" tracers of various grain-size classes during snowmelt highflow at East Fork River in 1979 (data from Emmett and Myrick (1985)).

**Table C-4; 5:** Travel velocities (m/d) of "pink" tracers of various grain-size classes during snowmelt highflow at East Fork River in 1979 (data from Emmett and Myrick, 1985).

**Table C-4; 6:** Flood events, mobility, and transport distances between 1989 -1992 at the Lainbach (from Gintz, 1994).

**Table C-4; 7:** Basin area, stream characteristics, sediment residence time, and mean annual transport distances for five steep mountain rivers in Japan (from Nakamura et al., (1987).

**Table C-4; 8:** Estimated mean annual bedload travel distances (m) based on individual studies and predicted mean annual travel distances based on regression functions (Eqs. 6 and 7).

**Table C-4; 9:** Range and mean of annual transport distances (km/year) for suspended sediment, predominantly sand-sized bedload, and single pebbles or cobbles.

## Conversion of units

g	gram	= 0.001 kg	= 0.0353 ounces
kg	kilogram	= 1000 g	= 2.205 pounds
t	metric tonne	= 1,000 kg	= 1.103 tons
mm	millimeter	= 0.001 m	= 0.0394 inches
m	meter	= 3.281 feet	= 1.094 yards
km	kilometer	= 1,000 m	= 0.621 miles
m <sup>2</sup>	square meter	= 10.76 sq.ft.	= 1.197 square yards
ha	hectare	= 10,000 m <sup>2</sup>	= 2.471 acres
km <sup>2</sup>	square km	= 100 ha	= 0.386 square miles
l	liter	= 0.001 m <sup>3</sup>	= 0.0353 cubic feet
m <sup>3</sup>	cubic meter	= 1000 l	= 35.316 cubic feet
°C	degree Celsius	= degree Fahrenheit · (9/5) + 32	

## **Part A: Introduction, objectives, and considerations of cumulative watershed effects and scale**

### **1. Introduction**

Federal regulations under the 1969 National Environmental Policy Act (NEPA) require federal agencies to determine whether a proposed action, in conjunction with past, present, and reasonably foreseeable future actions, will result in a cumulative effect. A cumulative effect is defined as:

"...the impact on the environment which results from the incremental impact of the actions when added to other past, present, and reasonably foreseeable future actions regardless of what agency or person undertakes such actions. Cumulative impacts can result from individually minor but collectively significant actions taking place over a period of time." (CEQ 1978).

Many states have enacted parallel legislation to require state agencies to consider cumulative effects in their environmental assessments and environmental impact statements. The Clean Water Act and its amendments require protection of the designated beneficial uses of water and restricts the degradation of waters that meet or exceed existing water quality standards. In many forested areas the designated beneficial use of greatest concern is coldwater and warmwater fisheries.

The combination of NEPA and the Clean Water Act means that forest managers must explicitly address the likely effects of their activities on basin-scale runoff, sediment production, sediment transport, and sediment deposition. A limited number of previous studies (e.g., MacDonald, 1989; Harr, 1989) have suggested that the results of such analyses may be highly dependent on spatial scale. Current methodologies suggest that the analysis of cumulative effects be conducted on the scale of 50-500 km<sup>2</sup>, but there has been little explicit work on how spatial scale affects our ability to detect changes in runoff and sediment. The focus in this report is on cumulative sedimentary effects, as the downstream routing of runoff has long been a topic of concern. However, the complexity of the issues means that even a report of this magnitude cannot completely cover all aspects and scenarios.

It is logistically and financially impossible to measure all on-site changes in runoff and sediment production over time at each location where they occur. Thus most measurements are focussed in the stream network because the effects of watershed disturbance are integrated and expressed in terms of altered stream flow, sediment yield, and channel change. These changes can then be more directly related to the designated beneficial uses of coldwater fisheries, municipal water supply, reservoir storage, etc. The basic problem is that the conceptual advantage of making measurements within the stream channel may be offset by the additional complications of sediment storage, dilution, measurement accuracy, and the varying sensitivity of different sections of the stream network to a given set of management actions. Cumulative watershed effects are particularly difficult to predict and identify because the individual water and sediment inputs are delivered to the stream system at different points in time and space, and these interact with the water and sediment already in the stream.

If changes in sediment transport are to be used to detect sedimentary cumulative effects, sediment transport needs to be closely monitored. Again the complexity of monitoring

sediment is such that guidelines are needed to maximize the effectiveness and likelihood of detecting change. The detectability of a change in sediment transport is greatly influenced by three factors:

- the distance between the sediment input(s) and the measuring site,
- the accuracy and precision of the sediment transport and sediment load estimates, and
- the natural variability of sediment transport across a wide range of spatial and temporal scales.

Spatial scale considerations come into play for each of these components, but these have not been explicitly analyzed despite their potential for affecting a particular monitoring effort or cumulative effects assessment. Spatial scale also cannot be separated from temporal scale, as the detectability of a sediment pulse moving downstream is a function of both time and distance. Similarly, the uncertainty associated with a single sediment transport measurement is affected by both the short-term temporal variation in sediment transport and the spatial variability of sediment transport with depth and across a stream cross-section. Monitoring results can be improved by locating the measuring site within the reach where a sediment wave will pass during the measuring period, by allocating sampling effort to minimize the uncertainty in sediment transport rates and sediment loads, by using techniques appropriate to the stream and sediment load of primary concern, and by adjusting sample size according to the inherent variability. The purpose of this report is to collect and analyze the heretofore scattered information on each of these topics, and to help guide managers and technical staff in their efforts to cumulative sedimentary effects.

## 2. Objectives and structure of the report

The goal of this report was to assess how the detectability of sedimentary cumulative watershed effects is affected by spatial scale. However, we also recognize that the effects of spatial scale cannot be separated from the underlying measurement uncertainty and the natural variability across temporal and spatial scales, the specific objectives of the project were to evaluate the:

- Natural variability of sediment transport in time and space;
- Accuracy and precision of sediment transport measurements and sediment load estimates;
- Variability of annual sediment yields in and between basins; and
- Amount and distance of downstream transport of different particle sizes.

These issues are closely interrelated and affected by a variety of other factors such as the grain size of the sediment, the desired level of accuracy, and the temporal scale (short-term, event, or interannual).

This report begins with an introduction to sedimentary cumulative effects. This is immediately followed by a discussion of sediment transport processes because this understanding is basic to all other aspects of the report. An understanding of sediment transport processes is also critical to an evaluation of the uncertainties associated with standard measurement techniques. This uncertainty then affects the accuracy and precision of the individual sediment transport rates as well as the estimates of sediment loads over all time scales. Sediment transport processes also control the natural variability of sediment transport over the short-term, intra-event, and inter-event time scales. Quantifying the variability and underlying statistical distribution of sediment transport rates is necessary to estimate the uncertainty associated with a given sample size and the sample size needed to determine the sediment transport rate with a given degree of uncertainty.

Understanding the relative variability over time and space is necessary to optimize sampling strategy and determine the amount of change that might be detected under different sampling schemes. Since many monitoring schemes are directed at detecting a change in annual sediment loads, it is also necessary to evaluate the techniques used to extrapolate from a limited number of measurements to annual loads, as well as the variability in annual loads within and between basins. About two-thirds of this report is therefore devoted to the following topics:

### **Part B: Processes, measurability, and variability of sediment transport**

- Processes of sediment transport
  - short-term
  - event
- Statistical analyses of the variability of sediment transport
  - short-term
  - event
- Measurement techniques and uncertainties of individual measurements
  - short-term
  - event

- Sampling schemes and load estimates of sediment transport events
  - rating curves
  - summation of loads
- Statistical analyses of the variability of annual sediment yield
  - disturbed and undisturbed watersheds
  - years of records needed to quantify yields and assess change, and
  - persistence of response to increased sediment yields.

Each of these topics is discussed for both bedload and suspended sediment, although the former tends to be emphasized because it is more commonly regarded as a serious constraint on management.

Critical to the evaluation of spatial scale is an understanding of the rate of storage and downstream transport of sediments of various grain sizes. This affects both the selection of the proper measurement site as well as the likelihood and location of a possible sedimentary cumulative effect. To detect a cumulative sedimentary effect, measurements must be made at the location where the sediments of concern will appear or pass within the monitoring period. Part C addresses this downstream transport of sediment as a function of stream type, particle size, sedimentary status of the stream, and the discharge regime.

#### **Part C: Downstream transport of sediment transport**

- Dilution of fines (for clayey material only),
- Delivery ratios, and
- Tracer studies.

The dilution of suspended sediment is clearly a function of spatial scale, and the detection of a given input can be evaluated if each input of water and sediment is known. Such calculations implicitly assume that there is no settling or storage of the suspended particles, and this is rarely, if ever, the case in natural stream systems. The storage of sediment in the downstream direction is generally a much more important process than dilution. Delivery ratios were originally developed to predict reservoir infilling in agricultural lands, and they have been widely used to estimate the downstream transport of sediment. Again there is a critical and erroneous implicit assumption in the use of sediment delivery ratios, namely that there is a consistency in stream types and sediment transport rates with increasing basin area. This problem is particularly severe for topographically diverse basins and for mountain streams where sediment transport rates are not easily predicted. The alternative adopted in this study is to review and summarize the tracer studies that have analyzed the downstream travel velocity of sand, pebbles and cobbles. The results of these studies, when interpreted in the context of sediment transport processes, is believed to provide a better means for predicting mean annual travel distances in different stream types. From this data we can then better predict the relative likelihood, location, and detectability of a sedimentary cumulative effect.

The last part of this report (Part D) summarizes the results of the study. This section also provides guidelines and recommendations for detecting sedimentary CWEs and for future work on this topic.

### 3. Cumulative watershed effects and scale

#### 3.1 Definition of cumulative watershed effects

Swanson (1986) defined cumulative watershed effects as off-site, downstream changes in hydrology, sediment production, transport, and temporary storage in response to forest and other land management practices within a drainage basin. However, the integrated response of a stream system cannot necessarily be traced back to a particular activity or site within a catchment. The often nebulous relation between management activities and stream response has even resulted in CWEs being called the UFOs of hydrology (Rice and Thomas 1986). This difficulty in determining the specific cause(s) of a stream system response is built into the definition of CWEs (e.g., Ice, 1984) as being caused by:

- two or more management activities separated in space and/or time,
- activities that are simultaneous or take place at the same location but are persistent over time.

One concept of CWEs is illustrated in **Fig. A-3; 1**. Another example would be the sequential and additive compaction of soil due to repeated activities over time spans shorter than the recovery rate. However, work by Phillips (1987) and Grant and Wolff (1991) suggest there may not necessarily have to be multiple occurrences or different lag times.

#### 3.2 Stream channel responses to cumulative watershed effects

All of the above definitions of CWE imply that fluvial systems operate on a simple cause-and-response mechanism, and that the cause-and-response relationship only becomes complicated when two or more different impacts interact to cause a CWE. However, fluvial systems usually do not operate in a simple manner (Phillips, 1987; Grant and Wolff, 1991). The number and timing of processes that generate and transport sediment (e.g., upslope erosion, channel erosion, fluvial transport, and fluvial storage) cause the fluvial response to be highly complex.

This means that the simple cause-effect mechanism for sedimentary CWEs has to be replaced by complex response mechanisms. Interactions between current stream conditions and management effects may enhance or reduce a specific disturbance (e.g., Phillips, 1987), or result in a sequence of responses at different locations. Negative feedbacks reduce the response and generally result in a more stable system, and are generally the rule. For example, the sediment introduced by a debris flow into a high energy stream with a large transport capacity will typically cause an initial aggradation, and the stream will usually scour these sediments in subsequent years until pre-impact conditions are generally restored. Positive feedbacks can generate temporally and spatially varied responses that exceed the effects of the original perturbation. Returning to the debris flow example, a positive feedback could result if the newly aggraded stream channel starts to widen substantially in response to the initial sediment input. This would then generate more sediment than was provided by the debris flow alone. Regaining equilibrium conditions may then take much longer. It should also be noted that the additional sediment from bank erosion will eventually arrive in the downstream reaches, and this may in turn trigger additional bank erosion. This latter example indicates that a single impact may result in an

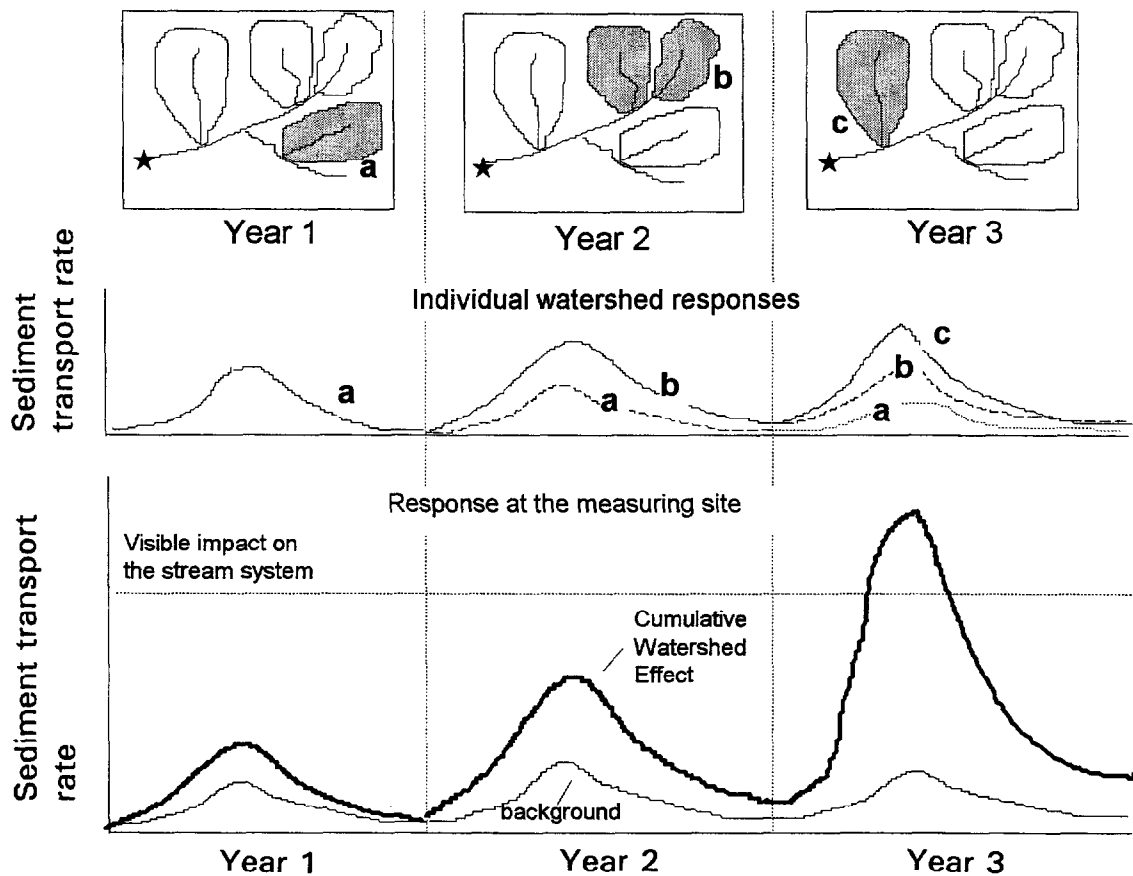


**Fig. A-3; 1:** Schematic diagram showing how the interplay between management activities in different basins at different times can interact with background conditions to cause a cumulative watershed effect (after Lawrence and Ice, 1986). Sediment transport rate in the center graphs is monitored at a location in close proximity to the management activities, while the bottom graphs depict sediment transport rate measured further downstream.

unstable stream system by provoking a difficult-to-predict series of spatially and temporally varying responses. While this sequence of events may not necessarily meet the legal definition of a CWE, the net effect on the channel and the designated beneficial uses is similar. Hence it may not be appropriate to *a priori* limit the consideration of CWEs to the case of spatially and temporally overlapping impacts.

Prediction of whether logging-related impacts will generate a simple or a complex response can only be done by careful investigation of the possible interactions between the various catchment and stream system components. The change in the definition of CWE from interference between several forestry-related impacts (Ice 1984) to interference between "...management impacts and natural environmental processes..." (Sidle and Hornbeck 1991) suggests that the complexity of the response patterns and the importance of existing conditions have probably been underestimated in earlier discussions and definitions of CWEs.

## 3.2 Prediction of CWE

To accurately predict sedimentary CWEs we have to answer questions such as:

- What is the likelihood of downstream CWEs due to the interaction of temporally and spatially varied sediment inputs of varying grain sizes from different sources (roads, gullies, and mass movements), coupled with a change in discharge, in a stream system with various stream types and budgetary states?
- Will one or more disturbances trigger a complex sequence of changes, such as aggradation, widening and flooding at one place or point in time, to be followed by degradation, scour, and entrenchment?
- How will the channel type and existing channel condition affect the likelihood, type, and magnitude of CWEs?
- Will the stream channel return to its pre-existing condition, or will there be longer-term changes persisting well beyond the usual period of analysis?

Few researchers have begun to tackle this complex web of causes, effects, interactions, and sequential changes (Grant 1987). We believe that the information in this report should provide a solid basis for additional progress. However, we still don't have an effective predictive model or definitive answers to all the issues associated with the problems of predicting and detecting sedimentary CWEs.

### 3.2.1 Prediction of CWE by models

Intensive research has been conducted over the last twenty years on the effects of various logging and forestry practices on water and sediment yields. This has helped to formulate watershed models to predict the short-term effects of forestry practices on runoff and sediment yields. However, both instream observations and longer-term models indicate that there may be a substantial time delay in the occurrence of CWEs and that CWEs can persist over time periods ranging from decades to centuries.

#### 3.2.1.1 Short-term effects on water and sediment yield

A variety of models have been developed for predicting sedimentary CWEs, or the relative susceptibility to sedimentary CWEs. These include WRENSS (U.S.F.S. 1980), the R1-R4 sediment model (U.S.F.S. 1981), a modified version of Universal Soil Loss Equation for forest lands (Dissmeyer and Foster 1984), BOISED (Potyondy et al. 1991), and the R1-WATSED model (U.S.F.S. 1992). These models explicitly recognize some or most of the key erosion and sediment transport processes within a drainage basin, but it is extremely difficult to incorporate our understanding of all the various processes into a model that is to be used over a wide area with very limited input data. Water and sediment yields are calculated from general assumptions, a limited number of input variables and indices, and possibly a field survey combined with remote sensing data. None of these models have any algorithm or explicit procedure for addressing the likely lags in sediment transport and delivery, although they do typically consider the recovery of different sources over time. Thus these models cannot predict longer-term sedimentary CWEs.

Model makers repeatedly emphasize the need to gather a good data set that encompasses the interplay among site conditions, hydrologic regime, and stream channel processes. In

most cases the models have not been fully calibrated, much less validated. The models are generally much more able to predict management-induced increases in water yield than increases in sediment yields. These models have even more difficulty in predicting sedimentary CWEs. Much of this rather poor predictive performance can probably be attributed to the nonlinear, interacting fluvial processes associated with CWEs, even though the prediction of CWEs was often the primary rationale for developing these models.

### 3.2.1.2 Long-term CWEs

Many studies have shown that the response of a river system to anthropogenic or natural disturbance can extend over a long time period or exhibit a long lag between the initial disturbance and the subsequent stream impact. For example, certain streams in California were subjected to hydraulic gold mining in the 1800s, and the stream network has continued to respond for over 100 years (James 1991). Another mining-related example is the delayed response in the downstream progression of mining waste in New Zealand (Pickup et al. 1983; Pickup 1988). Riefenberger and Baird (1991) showed that 40 years of mitigation efforts were not effective in stabilizing a stream reach that was disturbed by a mining-related water diversion that ran out of control almost a century ago.

Because CWEs can be long-lasting, or have long lag times until the onset of a response, the prediction of CWEs should not be limited to just the short-term increases in water and sediment yields. To predict CWEs over a longer time scale it is necessary to determine when, and for how long, sedimentary CWEs might be expected. The initial answers to these questions then govern the duration of a proposed monitoring effort as well as the type and time scale of any modeling effort.

Both the duration and the potential lag in expressing a CWE are complicated by the closely-linked issue of spatial scale. Often it is not possible to completely separate the temporal and spatial scales, as both water and sediment travel downstream over time, and thus time and space are interconnected. For water yield and peak flows the downstream travel velocity of water can be predicted relatively easily. Both Harr (1981; 1989) and King (1989) have made use of this interdependence and give examples of how the temporal and spatial scheduling of management activities might be used to desynchronize high flows and avoid downstream flooding. The prediction of when, where, and for how long a sedimentary CWE will occur is much more complicated, since sediment will generally not travel through the fluvial system at an even rate, and will not behave the same or cause the same degree of adverse effects at every location within the stream system.

For example, a newly-constructed road may generate an initial pulse of sand and suspended sediment. Although much of this sediment might be temporarily deposited in a kilometer-long downstream step-pool reach, a substantial proportion of this sediment is likely to travel beyond this reach during the next high flow season. A meandering gravel-bed reach that is five kilometers downstream might not be affected by the increase in sand-sized material until a couple of years later. If a pulse of gravel is supplied to this same step-pool reach, it might take several years for this material to be transmitted downstream. Depending on the rate of transport, the downstream meandering reach might receive these gravels over a number of years. The initial sediment input might then be attenuated to the point that there is little or no detectable change in either the bedload transport rates or the channel morphology in the downstream meandering reach. However, if the upstream gravel source continued to generate sediment, severe aggradation might develop over time. The resultant change in channel morphology and behavior could then persist for decades or even centuries.

This discussion indicates that the appropriate temporal and spatial scale depends on several factors, including the:

- Amount and grain-size distribution of the sediment supplied to the stream system;
- Location of the sediment sources within the stream network;
- Duration of sediment inputs;
- Travel speed of the various sediment sizes supplied to the river system, which is partly a function of the available storage in the sequence of downstream reaches;
- Discharge regime; and
- Downstream succession of river types with their characteristic budgetary state and their sensitivity to sediment inputs.

Several modeling studies have attempted to assess long-term CWEs, and these have indicated that a stream may develop a sedimentary CWE some decades after logging. In one case the temporal variation of slope stability was due to the decay rate of dead roots from logged areas and the growth rate of new roots from forest regeneration (Ziemer 1981). Slope stability was predicted to be at a minimum about 10 years after logging, indicating that the largest potential for slope failure will be delayed until about a decade after logging. As noted above, there will probably be another delay while the sediment is transported to the reach of interest.

Sidle (1991) also modeled the temporal changes in root cohesion over the course of many management cycles and under different forest practices. If the time between clearcuts is less than the time required for the roots to regrow to their maximum strength, the net rooting strength decreases over several rotations, and this can cause an adverse cumulative effect.

In another model Ziemer et al. (1991a and b) combined temporal and spatial aspects to model channel bed elevations for twelve one-kilometer stream sections at the downstream end of a 100 km<sup>2</sup> watershed. Sediment yield was increased under various logging scenarios, and the effects were simulated along a fifth-order mainstem stream with fourth-order tributaries joining at the end of reaches 3, 7, and 9. The Muskingum procedure was used to route stream flows, and bedload transport rates for each reach were calculated using the Meyer-Peter and Müller equation. The model was set up so that aggradation led to a decrease in the  $D_{50}$  of the bed material. Since this decrease in bed material size then increased transport rates, the model had a built-in negative feedback loop. The model assumed that 80% of the eroded headwater sediment was stored in tributaries, with only 20% reaching the fifth-order mainstem.

The results showed that stream width increased from 20 to 28 m over the 12-km reach, and there was an overall decline in gradient from 0.0055 to 0.004. However, the reach-scale bed profiles varied from an even longitudinal profile by up to 20%. Aggradation of more than 10 cm occurred most frequently in the second century after logging. This lag between the initial forest harvest and the main channel response was due to the time needed for sediment eroded from the slopes to be transported into and through the tributaries to the main channel. Reaches below tributary confluences experienced more frequent aggradation, and this was most pronounced in and adjacent to segment 9 (nearest the mouth of the basin). Possible reasons for this susceptibility to aggradation include lower stream gradients

relative to upstream segments, and an accumulation of sediment from upstream reaches and the fourth-order tributary that was furthest downstream.

This study is an important step towards predicting where, when, and to what degree a particular downstream location might be affected by a CWE. However, an accurate, deterministic prediction of sediment transport and channel response in real stream networks is still beyond our current capabilities. This is due to the difficulty of accurately predicting bedload transport rates in gravel-bed rivers, as well as key processes such as overbank storage, bank erosion, and sediment travel time.

Specific physically-based modeling and sediment routing techniques are needed to model each individual case, and there is an abundance of literature that applies sediment transport or sediment routing models to a particular reach. It is not, however, the purpose of this study to discuss the general performance of sediment routing models. Sources such as *Sediment Transport Modeling* (Wang 1989) and the *Proceedings of the Fifth* (FISP, 1991) and *Sixth* (FISP, 1996) *Federal Interagency Sedimentation Conferences* provide an initial introduction to these topics. Overall, it seems that the modeling success in each case is related to how well a particular model can be adapted or matched to the specific conditions, the quality of the input data, and the consistency between the resolution and the spatial scale of the model. Sediment transport modeling appears to be most successful at small spatial and temporal scales, such as the prediction of scour around bridge piers. Larger-scale modeling--e.g., to predict the response of a 10-km river reach to altered flow or sediment supply--is still a major challenge for researchers and land managers.

The persistence of stream channel response over periods ranging from decades to millennia also means that future responses may be greatly affected by the current state of a channel and its response to previous events. Benda and Dunne (1987) note that the present behavior of rivers in coastal Oregon (e.g., aggrading, degrading, and armoring) may be a response to past debris flows that routed large amounts of sediments into these alluvial streams over time intervals of 100 to 1000 years. Heede (1991) posits a much longer time span between an action and geomorphologic response, as he suggests that some rivers are still expressing their Pleistocene (10,000 to 100,000 years) heritage and adjusting to Holocene conditions. A similar view is expressed by Slaymaker (1990), when he states that present-day rivers in British Columbia are still nourished by sediment deposited by their Pleistocene ancestors.

The implication is that CWEs may result from a series of superimposed effects over different time scales, and that some of these may stem from past events unrelated to current management activities. Thus the likelihood of adverse sedimentary CWEs must be evaluated with respect to the current geomorphic and sediment balance of the stream.

### **3.2.2 Prediction of sedimentary CWEs by stream monitoring**

The evaluation of sedimentary CWEs by instream monitoring can be done by measuring sediment transport rates and sediment yields, or by evaluating channel condition through methods such as the Pfankuch channel stability rating (Pfankuch 1978), the Riffle Stability Index (Kappesser 1995), or the change in percent fines (e.g., King and Potyondy 1993; Potyondy and Hardy 1994; Bevenger and King 1995). But in many cases, the required monitoring results are not sufficiently accurate or precise to detect small changes. From both a management and a resource protection standpoint, there is a need to increase the sensitivity of our monitoring techniques. A greater sensitivity to detect change would allow a more rapid adjustment of management activities, and this would reduce the likelihood of more persistent adverse changes in stream channel condition and aquatic resources. In

order to provide this sensitivity, the accuracy of monitoring results and thus the detectability of CWEs has to be increased.

### 3.2.2.1 Detectability of sedimentary CWEs: effects of spatial scale

#### ***Analogy to water flow***

The spatial scale issue in detecting cumulative watershed effects is relatively straightforward in the case of discharge. Once water enters the channel network, most of this flow is rapidly routed on through the channels as a flood wave. Considerable research has been done on the effect of tributaries and the attenuation of the flood wave in the downstream direction. Thus the shape of the flood wave is modified by the channel morphology and by the flood waves that join the main river from the tributaries. Several flow routing models are described in Maidment (1993), and these range from the simple and well-known Muskingum model to much more complex, physically-based models using the St. Venant equations.

If changes in streamflow is the cumulative effect of interest, the downstream development of the flood wave should ideally be measured in a series of nested stream gages (Harr 1989). The high costs of establishing and maintaining nested gages are likely to preclude this approach. For the Oregon Coast Range, Harr (1989) suggests that the ideal size for detecting change is a second-order stream. Both Harr and MacDonald (1989) posit a steady decrease in the relative ease of detecting cumulative effects from a second-order basin to a fourth-order basin for water yield, and MacDonald (1989) extended this argument to sediment using a very simple dilution model. Both of these studies suggested that the likelihood of detecting cumulative effects decreases drastically in basins larger than fourth order. Given practical measurement constraints, Harr (1989) suggests that measurements to detect hydrologic cumulative effects should focus on third- to fourth-order basins. The question that led to the present study is whether there also is a particular stream order or spatial scale where sedimentary cumulative effects can most easily be detected.

Gessler (1976) recommended that sedimentary CWEs be measured directly in the headwaters where logging impacts lead to increased sediment inputs. This should not only eliminate the difficulties of following the sediment on its downstream path or of trying to detect it at some downstream location, but it should also help to relate observed downstream increases to upstream sources and processes. However, it would require a tremendous effort to monitor all headwater streams potentially affected by management, and it is also not clear that the headwater streams have the highest value for key uses such as coldwater fisheries. To optimize monitoring efforts in terms of cost efficiency, the spatial scale of the monitoring should be as large as possible while still allowing the detection of cumulative watershed effects. Another issue is the relative cost of measuring large streams versus smaller headwater streams. Again the question is whether there is a spatial range in which sedimentary CWE can be best detected, but in this case the question is couched in terms of cost efficiency rather than absolute detectability.

### 3.2.2.2 Simplistic models indicating the importance of spatial scale

The simplest modeling scenario is to neglect the transport of sediment already in the stream bed and presume that an anthropogenic sediment input travels downstream as a wave of bedload transport or a cloud of suspended sediment. The difference between faster and slower moving particles will tend to disperse this sediment wave as it moves downstream. This dispersion will attenuate the peak and partially mask both the initial increase and the tail end of the sediment wave. If one further assumes some loss to storage, then

somewhere along the way sufficient sediment will have been deposited such that the amount of sediment still in transport will no longer be detectable using typical field techniques. The third component is dilution, and we would expect that a cloud of suspended sediment will eventually be diluted beyond detectability as it proceeds in the downstream direction.

The two simplest and most commonly used models for downstream sediment transport are the delivery ratio (DR) curve and the dilution model. Both support the idea that sediment yields and sediment concentrations decrease in the downstream direction (e.g., Walling, 1983), and thus the importance of spatial scale.

DR curves generally use basin area to define the ratio of sediment yield at a specific point to basinwide sediment production above that point. In almost every case this ratio decreases downstream according to a power function with a negative exponent. This decrease is due mainly to continuing sediment deposition.

DR curves would be a valid means to predict downstream deposition if:

- channel types and gradients followed an absolute and consistent pattern along the river course so that sediment deposition in a reach was a constant proportion of the sediment entering that reach;
- there was only one grain-size class; and
- flow patterns were consistent for the time period of interest (e.g., between years).

The dilution model calculates how the concentration of fine suspended sediment from a muddy tributary is diluted by inputs from other tributaries. This dilution will cause a sediment input from a tributary basin to be undetectable at some point downstream. To distinguish dilution from storage, the working assumption is that no material is deposited in the stream channels (i.e., the delivery ratio is 1). For clarity it is also assumed that inflows from the rest of the basin have a lower sediment concentration; relaxing this assumption will simply make the sediment pulse harder to detect and push the detectability limit further upstream.

Part C of this report evaluates the use of delivery ratio curves and a dilution model to predict the occurrence of sedimentary CWEs. Their limited usefulness means that they cannot help define the specific spatial range in which sedimentary CWE are detectable at a particular level of uncertainty. Relatively simple suggestions to improve the usefulness of these type of procedures are made in the latter part of Section C.

### 3.2.2.3 Scale effects in the specific locations where sedimentary CWE might occur

Section 3.2.1.2 identified several factors that control where sedimentary CWEs might occur, and these include:

- Sediment supplied to the stream system (particularly the amount, grain size distribution, and duration),
- Travel speed of the various sediment sizes through the fluvial system,
- Current sediment balance of the different reaches within the network of concern, and
- Susceptibility of downstream reaches to sedimentary CWEs.

All of these factors vary with the type of management activities, the sequence of stream types within the fluvial system, and the runoff during the period of interest. Those stream

reaches closer to the sediment sources are obviously subject to the highest input rates, but CWEs may be unlikely if the local stream gradient is high relative to the size or amount of sediment being supplied. As the sediment is dispersed in the downstream direction the sediment input to a downstream reach generally decreases, but the potential for a CWE might increase if the stream gradient decreases or if several tributaries each contribute an increased sediment load. The implication is that the likelihood of a certain stream reach to experience a sedimentary CWE must be assessed on a case-by-case basis. Such assessments require, at a minimum, some knowledge of the amount and size distribution of the sediment being introduced, and the succession of stream types. Only with this information can one hope to predict whether a particular downstream reach is likely to be affected by a sedimentary CWE within the time frame of interest.

### **3.2.3 Stream types and locations susceptible to sedimentary CWE**

Streams in mountainous areas often have uneven longitudinal profiles with a mixture of steeper and lower gradient reaches. Rarely is there a fixed longitudinal succession of stream types beyond the general observation that supply-limited, steeper streams are more frequent in the headwaters, while lower-gradient, transport-limited streams occur more frequently further downstream. Thus it is very difficult to set out the relative likelihood of sedimentary CWEs as a function of scale for all combinations of sediment sources (amount, type, and location) and stream types. The following sections therefore provide only a few examples of susceptibility to sedimentary CWEs as a function of stream type and current sediment balances.

Although CWEs by definition stem from various combinations of changes in discharge and sediment supply, the following discussion will assume a moderately increased supply of sand, gravels, and cobbles, combined with a moderate increase in peak flows in mountain streams and alluvial gravel-bed rivers. An increased in suspended sediment is not explicitly discussed as this is likely to have a smaller effect in these types of streams, and the pattern of CWEs will generally be a less distinct version of the patterns discussed under each stream type.

#### **3.2.3.1 Steep mountain rivers**

The susceptibility of mountain streams to sedimentary CWEs increases with decreasing stream gradient and decreasing sediment transport capacity, as these both increase the potential for sediment storage. Thus aggrading streams are more likely to exhibit CWEs than degrading streams. CWEs are quite likely where there is an abrupt transition in gradient or budgetary state. For example, a CWE might be expected where an upstream degrading reach turns into a downstream depositional reach, such as on an alluvial fan. Alternatively, a CWE might be expected just downstream of the transition from a steep step-pool morphology to meadow meanders, especially if several sediment-carrying tributaries come together.

Within the Montgomery and Buffington (1993, 1997) stream classification for mountain rivers, the susceptibility to sedimentary cumulative watershed effects increases as one progresses from cascades to step-pool, plane-bed, riffle-pool, and finally regime-type streams. Cascade and step-pool streams, which are roughly equivalent to A and B-type streams in the alphanumeric Rosgen (1994, 1996) stream classification, can often transport nearly all of the sediment supplied to them, and are therefore less susceptible to sedimentary CWEs. The effects of additional sediment supply are likely to be confined to

local depositional sites, such as plunge pools, sediment traps around large woody debris (LWD), backwater eddies, or side channels.

Other locations for sediment entrapment are areas with very coarse and uneven beds, such as boulder-rich reaches. Pebbles and cobbles can be caught in the wake of boulders, or fine gravels may accumulate in pockets between the boulders. The stream-bed itself can also entrap fine gravels and sand that can then be worked into the cobble bed.

As an example of a gravel-carrying river in a drier environment, Laird and Harvey (1986) identified three channel types along a 5-km long reach of El Oso Creek in Arizona. The severely supply-limited bedrock channel should be able to convey most of an increase in sediment supply, but a CWE is more likely in the reaches that experience periodic storage and flushing, or those that are always transport-limited.

### 3.2.3.2 Response reaches in gravel-bed streams

Within the Montgomery and Buffington (1993, 1997) sequence of stream types, the cascade and step-pool stream types are followed by plane-bed, riffle-pool, and regime-type streams as gradient decreases. The latter three types are designated as "response reaches" because of the presumed shift from supply-limited to transport-limited (Montgomery and Buffington, 1993, 1997). In the Rosgen (1994, 1996) classification these last three stream types would most likely fall into stream types B, C and E, and D and possibly F, respectively. As suggested by the term "response reach", the susceptibility of these stream types to sedimentary CWEs is greater due to the decreasing stream gradient, decreasing transport capacity, and the increased potential for instream sediment storage.

In contrast to the steep mountain streams, where the sedimentary response was confined primarily to those locations with low flow velocities, one would expect a temporally and spatially greater response in gravel-bed rivers. In riffle-pool reaches the pools might fill in and this would be accompanied by an increase in pool spacing. In plan view, a decrease in the number of pools would also lead to a decrease in stream sinuosity. With a further increase in sediment supply, a pool-riffle stream might eventually be altered into a stream with alternate bars. Aggradation in this stream type increases the number, size, and mobility of lateral gravel bars. Stream widening and bank erosion is often associated with the development and shifting of mid-channel bars, and this in turn supplies more sediment to the stream. This mechanism can lead to a positive feedback loop of channel aggradation and widening, and this might lead to a braided stream pattern that could migrate downstream.

### 3.2.3.3 Sand- and silt-bed rivers

The previous two sections indicated an increasingly complex response as one goes from steep mountain streams to low-gradient response reaches in gravel-bed streams. The possible responses of sand and silt-bed rivers to changes in water and sediment yield are likely to be even more complex, as the channels might go through several stages of adjustment before a quasi-equilibrium state is regained. One factor that contributes to this complexity is that present day sand and silt-bedded streams in anthropogenically altered landscapes are often leveed or entrenched due to prior cycles of erosion and deposition. Any channel widening is then associated with bank failure, with higher banks leading to larger amounts of sediment being supplied to the stream. The following four case studies show some of the possible sequences of channel adjustment due to disturbance by aggradation, degradation, canalization, and reduced flows.

In the first example Phillips (1987) observed four stages of channel evolution following an increase in sediment yield relative to the conveyance capacity. The successive budgetary states and corresponding channel changes are summarized in **Table A-3; 1**.

**Table A-3; 1:** Four stages of stream channel change due to variations in the ratio of sediment supply to conveyance capacity (Phillips 1987).

Stage	Budgetary state	Observed channel change
1	supply > conveyance capacity	Alluvial storage, deposition, aggradation
2	supply < conveyance capacity	Remobilization of alluvial storage, degradation
3	supply < conveyance capacity	Bed scour after alluvial storage has been emptied
4	supply = conveyance capacity	Quasi-steady state

Stage 1 developed from about 1830 to 1940 as a result of downslope rowcropping, as this caused severe soil erosion and excessive sediment inputs. After soil conservation measures were instituted in the 1940s the supply of sediment to the river decreased, and the rivers moved sequentially through stages 2, 3, and 4. These stages of development were observed to migrate downstream over time. Similar historical changes in the fluvial sediment budget were reported earlier by Trimble (1983) and Dissmeyer (1976).

An example of channel evolution in a degrading environment was presented by Watson et al. (1986, 1988) in a modeling study. This showed that a lowering of the stream channel at some distance downstream caused channel degradation and the formation of headcuts that migrated upstream. Similar results could be expected from a decrease in sediment supply. The evolving channel stages were defined largely on the basis of bank stability, as the channel changed from stable bank conditions to a new quasi-equilibrium via total disequilibrium (**Table A-3; 2**). Since the headcuts migrated upstream, stages 1 to 5 would be sequentially observed as the headcut moved past an observer, or in a downstream direction at one point in time.

**Table A-3; 2:** Stages of channel evolution in a degrading environment causing an upstream migration of headcuts and downstream variation in bank stability.  $h$  is the bank height, and  $h_{crit}$  is the maximum stable bank height (Watson et al. 1986, 1988).

Stage	Location	Channel processes	Bank condition
1	upstream of headcut	Slow degradation, no bank failures	stable ( $h < h_{crit}$ )
2	downstream of headcut	Rapid degradation, beginning basal erosion	unstable ( $h > h_{crit}$ )
3	downstream of stage 2	Aggradation, widening due to basal erosion	unstable ( $h > h_{crit}$ )
4	downstream of stage 3	Aggradation, widening due to bank slumping	unstable ( $h = h_{crit}$ )
5	downstream of stage 4	Slow aggradation, no bank failures	stable ( $h < h_{crit}$ )

In the third case study Simon and Hupp (1990) and Hupp and Simons (1991) studied channel evolution in a generally aggrading stream with sandy-silty bed material. The stream was leveed but not entrenched. Following major channel dredging and straightening six evolutionary stages were identified (**Table A-3; 4**). The first change after straightening was

that the channel incised and became steeper, and this led to aggradation and stream widening (Fig. A-3; 2). Hupp and Simons (1991) provide an extensive table listing the dominant fluvial and hillslope processes, characteristic fluvial geomorphology, and geobotanical evidence for each stage. An abbreviated version of this table is presented as Table A-3; 4. Note that these stages show many reveal similarities to the model results of Watson et al. (1986, 1988).

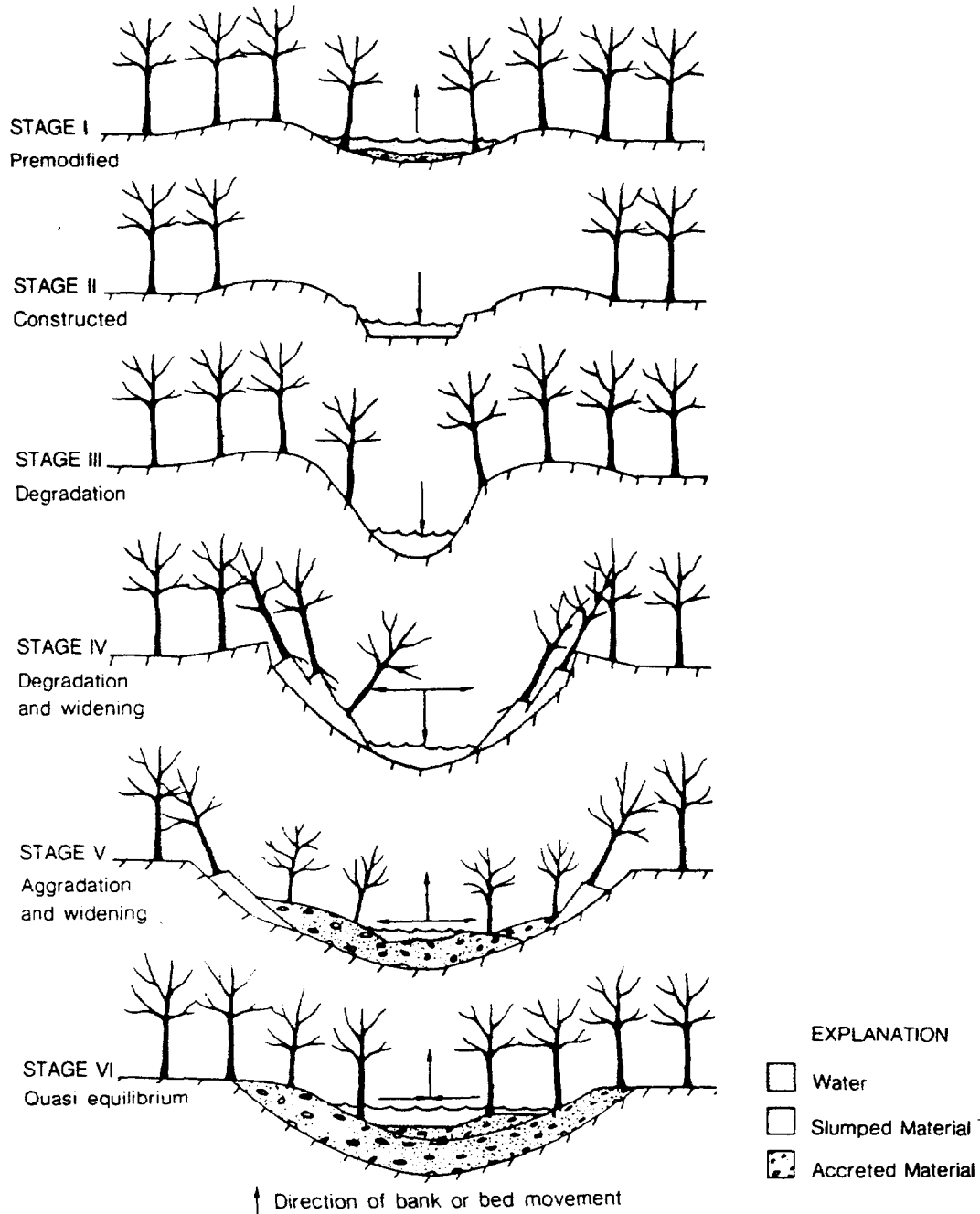


**Fig. A-3; 2:** Six-stage model of channel evolution following channelization (from Hupp and Simons 1991).

**Table A-3; 4:** Stages of channel evolution in a meandering stream following stream canalization (Hupp and Simons 1991).

Stage	Channel state	Dominant fluvial processes
1	Premodified	Mild aggradation, sustained meandering
2	Construction	Imposed dredging and straightening
3	Degradation	Downcutting and basal bank erosion
4	Degradation and widening	Basal bank erosion and bank slumping
5	Aggradation and widening	Bank slumping, develop meandering thalweg and alternate bars
6	Restabilization	Further development of meandering thalweg, alternate bars

In the final case study Everitt (1993) defined three stages of channel development as a consequence of the reduced flows and reduced bedload transport in the Rio Grande in Texas (Table A-3; 5). In this example tributary deposits are the primary control of stream gradient in the aggrading main stream.

**Table A-3; 5:** Channel evolution following reduced flows (Everitt 1993).

Stage	Channel state	Dominant fluvial processes
1	Stream aggradation	Decreasing cross-sectional area
2	Valley aggradation	Overbank flow deposits on levees and floodplains
3	Steepening below the tributary, with flattening and ponding upstream	Deposits at tributaries locally re-grade the valley

These four examples of channel evolution following different types of disturbance have several implications for CWE analyses:

- 1) The examples provide some insight into the possible sequences of channel changes;
- 2) The spatial and temporal sequence of channel changes may affect the response time between disturbance and a particular effect at a specific location. The delivery of additional sediment to a specific reach may be expedited or delayed, depending on the upstream budgetary condition.
- 3) The spatial sequence of channel changes will also affect both the location and magnitude of channel response. The CWE response at a location of concern may be absent, moderate, or severe, depending on whether a change in sediment load will be absorbed further upstream, or if the channel response in upstream reaches is damped through negative feedback.
- 4) Stream response to disturbance might not always be straightforward and predictable. For example, what will be the immediate response when additional sediment is supplied to a degrading stream that already is in the process of replenishing its sediment supply through bank erosion? In such a case will bank erosion and stream widening stop, or will it proceed

at a faster or slower rate than before? The answer will probably be controlled by the degree of degradation the stream was experiencing, the stage it has reached in its adjustment, and the amount of new sediment supplied to the stream. To make reliable predictions of channel response to changes in water and sediment yields, the river condition (e.g., bank stability, budgetary state) and the expected duration of that condition has to be carefully assessed. An assessment of the river's condition through geomorphic assessments is therefore of major importance in predicting and detecting CWEs.

### **3.3 Summary**

The cause-and-response mechanisms of CWEs are complex and often nebulous, and it is therefore difficult to develop a precise definition of a CWE. The development of a CWE stems from multiple watershed disturbances, with potentially different durations and lag times, and an interaction with the stream type and current stream condition.

Typically we attempt to predict and evaluate CWEs through a combination of models and instream monitoring. Most models, however, have not been adequately tested and have a relatively poor predictive capability. Stream observations and large-scale models indicate that CWEs might occur in stream reaches tens of kilometers downstream from impacted watersheds, and decades or even centuries after the initial disturbance. Such models are important in terms of identifying the likely location and timing of possible CWEs, but their accuracy cannot be validated at this time.

The other alternative, detecting CWEs by stream monitoring, is affected by spatial scale and constrained by the accuracy of our measurements. The scale problem is partly a function of the distance between the sediment input and the measuring site. Due to the dispersion of sediment within the fluvial system during downstream travel, an increase in sediment yield should be less detectable as one moves further away from the impact site, but the rate of downstream travel and dispersion is irregular and difficult to predict. Thus, choosing the right time and place for monitoring becomes more problematic as one moves further from the input locations. Monitoring high in the catchment may not be a feasible solution because of the very large number of potential monitoring sites, the lower sensitivity of headwater channels, and the fact that the most critical areas may be in the lower-gradient reaches further downstream.

The susceptibility of a particular reach to CWEs is a function of stream type, its budgetary state, and the budgetary states of the upstream reaches upstream. Current budgetary states may be the result of conditions or watershed disturbances in past decades, centuries, or even millennia.

## Part B: Processes, measurability, and variability of sediment transport

### 1. Physical processes and the temporal and spatial variability of sediment transport

This chapter has two primary objectives:

- Identify and discuss the various processes that control the natural variability in bedload and suspended sediment transport rates; and
- Show--initially in a qualitative manner--how this variability affects sampling techniques and the calculation of sediment yields.

The following sections summarize the main processes that cause the observed temporal and spatial variability in bedload transport rates and suspended sediment concentrations. We then discuss the implications of these processes for measuring bedload and suspended sediment. The variability and measurement uncertainty must be quantified in order to evaluate our ability to estimate sediment transport rates and directly detect cumulative watershed effects. We anticipate that the development of statistical models to quantify the uncertainty associated with stream order, sampling intensity, and time scale will be a primary objective in a future project. Hence this literature review represents a first and essential step towards the development of more complete quantitative models and guidelines.

#### 1.1 Introduction

Before starting the review of bedload transport processes it is important to review the somewhat arbitrary distinction between *bedload* and *suspended load*. Sediment transport comprises particles that range in size from clay to boulders. Particles sand-sized and larger are mostly transported as bedload in close contact to the river bottom, while particles finer than sand are mainly transported in suspension. There is no threshold grain-size diameter that strictly separates bedload transport from suspended sediment transport. Even boulders become suspended in a waterfall. However, the distinction between bedload and suspended load is necessary because, in most cases, bedload transport and suspended sediment transport are governed by different processes. Friction with the river bed is an important factor in bedload transport, while the amount and location of suspended sediment in the water column is mostly affected by the turbulence of flow. These different transport processes lead to different patterns in the temporal and spatial variability of bedload transport and suspended load, and different sampling schemes should therefore be employed for each transport mode. The distinction between bedload and suspended load is also necessary because different techniques are used to sample each of these components. A combination of sampling results from different techniques can be difficult due to unsampled zones and different sampling schemes. The only technique that can capture all sediment sizes is a large sediment trap such as a reservoir, and this is impractical in most cases. Thus there are no practical measuring devices to sample all transported particle sizes, particularly for mountain streams.

The problems of measurement accuracy and sampling intensity would be greatly ameliorated if measured bedload transport rates or suspended sediment concentrations were evenly

distributed within the cross-section and vertical profile, and if sediment transport was strictly a function of discharge. However, such situations are rarely, if ever, the case. A variety of processes cause systematic and unsystematic temporal fluctuations and spatial variability of bedload transport and suspended sediment concentrations. The following sections will discuss the causes and document the variability observed at different spatial and temporal scales. To the extent that our understanding and the data permit, this section will also quantify the controlling variables.

## 1.2 Processes causing variability of bedload transport

### 1.2.1 Temporal variability of bedload transport

Temporal variation of bedload transport rates has been observed since the 1930s in gravel bed rivers by Ehrenberger (1931) in the Danube, by Mühlhofer (1933) in the Inn, by Nesper (1937) in the Rhein, and in laboratory flumes by Shields (1936) and Einstein (1937). However, little was known about the processes that caused the observed variability. During the next 50 years a multitude of individual studies on sediment transport processes and variability of transport rates appeared. Church (1985) was one of the first to summarize and review many of these studies. The more recent review by Gomez et al. (1989) focused on the different frequencies of bedload fluctuations, while the various processes of bedload transport that cause temporal variations were exhaustively discussed by Gomez (1991). Parker's (1992) review concentrated on those bedload transport phenomena that produce a temporal and spatial variability of the transported grain-size distribution. Oliver and Rieger (1985) and Williams (1989) review the temporal and spatial variation in suspended sediment concentrations discussed in Section 1.3.

The documented temporal variability of sediment transport and sediment yield occurs across time scales ranging from seconds to several years (**Table B-1; 1**). In all time scales variability is caused by the same basic mechanisms, such as sediment availability, incipient motion, the transport action, and the temporary storage of sediment, but the importance of the roles played by each of these mechanisms usually differs according to process and time scale. Fluctuations of consecutive measurements of bedload transport may be referred to as *short-term*, if the fluctuations are much faster than changes in flow. If the temporal patterns of bedload transport during a high flow event differ from the fluctuations of the hydrograph, *intra-event* variability occurs. Intra-event variability can be different in each event, thus causing *inter-event*, or seasonal variability.

**Table B-1; 1:** Varying time scales for the temporal variability in sediment transport.

Time scale	Time range	Discharge range	Measuring and sampling problems
short-term	seconds - hours	almost constant flow	fluctuating transport rates
intra-event	hours - days	storm hydrograph	variable transport rates & hysteresis effects
inter-event	days - months	several flood events	variable transp. & variable hyster. effects
inter-annual	several years	annual discharge cycles	variable runoff-sediment load responses

The time scales at which these processes occur are intimately linked with the respective spatial scales. Short-term fluctuations are usually the result of rather local actions (e.g.,

within a few meters), while intra- and inter-event variations of sediment transport result from processes that may extend up to the reach scale, or even to the entire drainage system. The interplay between temporally and spatially varying processes is such that a distinction between temporal and spatial variation can become somewhat arbitrary in a specific situation. For example, the fluctuations in bedload transport at a specific location within a cross-section can be due to shifts in both transport rates and the paths of particles as different portions of the bed become unstable due to the successive movement of other particles.

The variation in consecutive measurements of bedload transport rates and suspended sediment concentrations often reach about an order of magnitude in the short-term time scale, and up to three orders of order of magnitude for a given discharge at the intra- and inter-event scale. Given such magnitudes of variability, it is essential to employ the best possible sampling schemes and accurate measurement procedures. This is necessary to both characterize the magnitude of the variability in a particular situation and to identify the most likely underlying processes. This knowledge can then be used to select the most appropriate measurement techniques and sampling schemes for the main phase of a monitoring project. The use of poor measuring and sampling techniques will only exacerbate the inherent variability and greatly reduce the likelihood of detecting significant differences or changes.

The following sections describe sediment transport processes and the measured temporal variability at the short-term, intra-event, and inter-event time scale. The annual variability of sediment transport will be characterized and discussed in chapter B-5.

#### 1.2.1.1 Short-term fluctuations of bedload transport rates

We define short-term fluctuations of bedload transport rates as those fluctuations that occur over time spans of seconds, minutes, or perhaps hours, depending on the size of the stream. They differ from intra-event variability, in that the observed short-term bedload transport fluctuations occur over relatively constant flows and often have an element of regularity. This periodicity is then overlain by non-periodic fluctuations. In contrast, intra-event variability features fluctuations that are mostly non-periodic, extend over longer time periods, and are usually related to changes in flow. The distinction between short-term variability, with its periodic and non-periodic bedload transport fluctuations, and intra-event variability with its *large-scale fluctuations* and transport variability not in phase with the hydrograph, has important implications for sediment sampling. The distribution of the periodic bedload transport fluctuations can be described by the Hamamori (1962) distribution, but other functions have been proposed as well to describe the distribution of bedload transport data. A knowledge of the underlying statistical distribution of consecutive transport rates is necessary to determine the best sampling scheme. This topic will be discussed in much more detail in the next chapter (B-2).

It should be noted that the observed periodicities of transport fluctuations are affected by the sampling scheme. In general, a higher temporal resolution of bedload measurements reveals yet finer-scale periodicities in transport rates. For example, a 5-minute resolution of bedload transport rates at the East Fork River revealed periodicities of 10-15 and 70-90 minutes (Gomez et al. 1989; Gomez and Emmett 1990; Gomez et al. 1991). Simultaneous sampling with a 1-minute resolution showed an additional periodicity of 2-3 minutes. Similar examples of double sampling are provided by Gomez et al. (1989) and Gomez (1991) for flume experiments, and by Bunte (1991, 1996) and Ergenzinger et al. (1994) for bedload transport measurements in a gravel-bed stream. The temporal resolution of the measurements needs to be at least three times, or better five times, higher than the

periodicity that one is hoping to detect. Short-term fluctuations have been observed for several bedload transport processes in streams and flumes with different grain-size distributions. These processes and the conditions under which they occur are discussed below. An overview is provided in **Table B-1; 2**.

### ***Step-wise motion of bedload transport***

Individual bedload particles often travel in an intermittent, stepwise motion in which a particle is entrained, moves a certain distance, and comes to rest before it again takes another step forward. This kind of bedload motion has been observed in flume experiments (Einstein 1937) and under natural conditions (Drake et al. 1988; Ergenzinger et al. 1989; Schmidt et al. 1989; Buskamp and Ergenzinger 1991, Schmidt and Ergenzinger 1992; Buskamp 1993, 1994) (**Fig. B-1; 1**). During the steps bedload particles often move a distance of approximately 200 particle diameters before coming to rest again. The rest

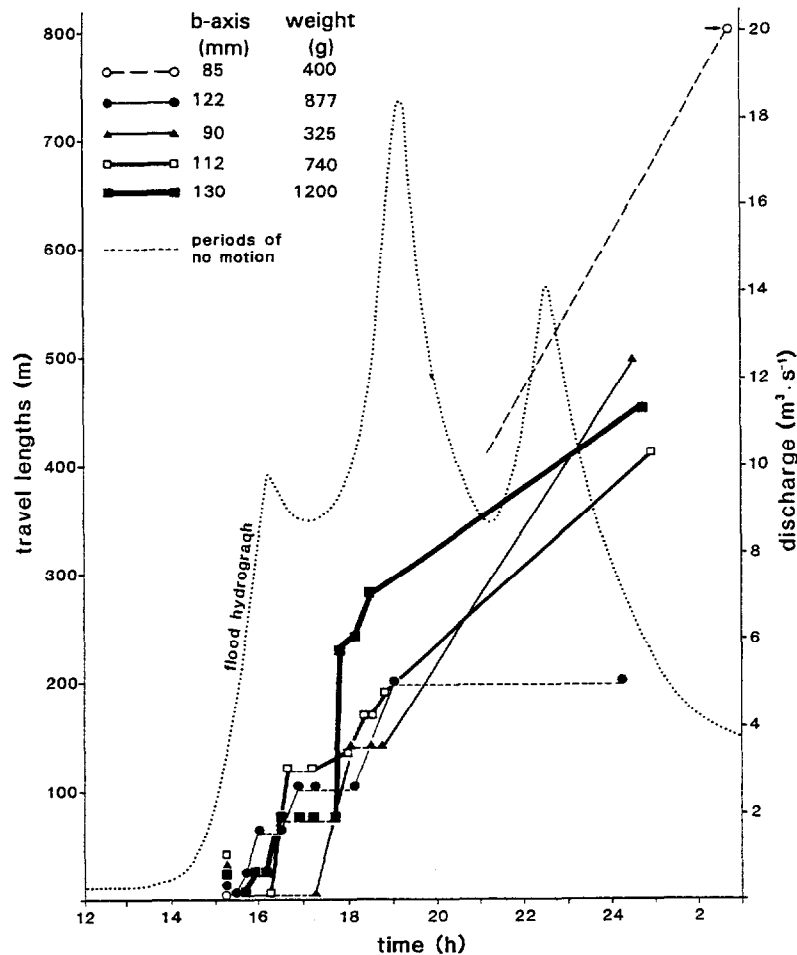


**Fig. B-1; 1:** Time-distance diagram showing the position of individual radio-tagged cobbles of different sizes during a flood event at the Lainbach, an Alpine step-pool river in Bavaria, Germany. Between 3 p.m. and 7 p.m., cobble positions were recorded about every half hour. Cobbles spend longer time periods resting than moving. The last position record was after midnight. The smallest particle only moved after 7 p.m. The dashed line indicates a mean travel speed of 800 m/11 hours (from Ergenzinger et al. 1989).

periods are usually much longer than the transport phases, so that bedload transport comprises a series of steps interrupted by relatively long periods of rest. Step-wise motion may affect all, or only the largest particles, depending on stream hydraulics and channel roughness. Transport rates associated with step-wise motion are usually rather small. Since few particles are in motion at any given time, the chance of catching moving particles in a small bedload sampler are rather slim. Samples are therefore likely to be inaccurate, in that transport rates are overestimated if a large particle happens to be caught, and underestimated if this is not the case. In order to increase the representativeness of the measured bedload transport rate, the sampling intensity needs to be increased. This can be achieved by using a large sampler opening, or increasing the sampling time, or both.

The effects of single-step motion on the temporal variability of bedload transport was quantitatively assessed by Naden (1987a, b, 1988). This study generated a temporal record of bedload transport based on modeled single-step motion during the passage of a flood wave. Modeled transport rates for a given discharge were found to vary by more than one order of magnitude. But since the periodicity of these fluctuations were a function of the model structure and parameters rather than observed fluctuations in bedload transport, this example is not included in **Table B-1; 2**.

**Table B-1; 2:** Short-term bedload transport fluctuations observed in various streams and laboratory experiments.

Reference	Stream /flume	bed mater. $D_{50}$ (mm) or descript. of dom. size	avg. flow velocity (m/s)	avg. bed-load transport rate (kg/m·s)	Period. or duration of pulses (min)	Sampling duration/sampling interval
<u>Bedload sheets and longitudinal sorting</u>						
Iseya & Ikeda 1987	flume (sev.)	fine gr./sand	0.4	0.04	2.5-5	10 s / 10 s
Kuhnle & Southard 1988	flume (sev.)	fine gr.	0.7-1.0	0.03-1.1	6-14; 25	30 s / 30 s
Whiting et al. 1988	Duck Creek	fine gr.	0.6-0.9	0.04	6-14	? / 2 min
<u>Dunes with superimposed riffles</u>						
Dinehart 1992	NF Toutle R.	coarse gr.	2.2-2.5	2.7-4.2	3*; 10-15	10 s / 2-3 min
Kuhnle et al. 1989a	Goodwin Cr.	fine gr.	0.9-1	0.4-0.8	10-45	variable / 4 min
Gomez 1991 Gomez et al. 1989 Gomez & Emmett 1990	Fall River	sand/gr.	~1.3	0.4	25-55	30 s / 5 min
Gomez et al. 1991 Gomez & Emmett 1990	East Fork R.	sand/gr.	~0.9	0.1	10-15; 70-90	30 s / 5 min
Gomez et al. 1989	East Fork R.	sand/gr.	~0.9	0.1	3; 10-15	60 s / 60 s
Carey 1983; 1985	SF Obion	sand	1.4	0.4	10-30	30 s / 3 min
Carey & Hubbell 1986	flume	2.1	1.1	0.1	10-40	2 min / 2 min

**Table B-1; 2 (continued):** Short-term bedload transport fluctuations observed in various streams and laboratory experiments.

Reference	Stream /flume	bed mater. $D_{50}$ (mm) or descript. of dom. size	avg. flow velocity (m/s)	avg. bed-load transport rate (kg/m <sup>2</sup> s)	Period. or duration of pulses (min)	Sampling duration/ sampling interval
Hubbell & Stevens 1986	flume	6.5	1.2	0.1	10; 80	2 min / 2 min
Hubbell et al. 1987	flume	6.5	1.6	0.7	15	2 min / 2 min
Hubbell 1987						
Gomez et al. 1989	flume	23.5	2.3	1.4	2; 10; 100	18 s / 18 s
Gomez 1991	flume	23.5	2.3	1.4	0.5; 2	6 s / 6 s
<u>Particle exchange with bed material or no specific process indicated</u>						
Custer et al. 1987	Squaw Cr.	coarse gr.	1.3	-	0.1-6	2 s / 2 s
Ergenzinger et al. 1993	Squaw Cr.	coarse gr.	1.6	0.002-0.2	1.5	10 s / 10 s
Bunte 1991, 1996	Squaw Cr.	coarse gr.	1.6	-	0.5-5	10 s / 10 s
Bänzinger & Burch 1990	Erlenbach	coarse	-	-	5; 30	1 min / 1min
Rickenmann 1993	torrent	gravel			5-15	1 min / 1min
Schlatter 1984	Möll	coarse gr.	3-4	-	5-15; 45-90	1.5min/1.5min
Tacconi & Billi 1987	Virginio Cr.	coarse gr.	-	0.3	30	5 min / 5 min
Bunte 1991; 1996	Squaw Cr.	coarse gr.	1.6	0.002-0.2	90	5 min / 5 min
Nesper 1937 after Gomez 1991	Rhein	coarse gravel	-	0.2	20-80	2 min / 3-4 min
Mühlhofer 1933 after Hubbell 1964	Inn	coarse gravel	-	~1	7	? / 3 min
Ehrenberger 1931 after Gomez 1991	Danube	coarse gravel	-	0.2	18	1.7-5min/5-6min
Hayward & Sutherland 1974	Torless St.	med. gr.	-	0.02-0.2	20-30	~2min / 7.5min
Emmett 1975**	Slate Cr.	med. gr.	1.8	0.2-2	20-60	few s / 4-5min
Ergenzinger & De Jong '95	Squaw Cr.	coarse gr.	1.6	0.01-0.3	30-90	10 min / 10 min

gr = gravel; \*the 3 minute periodicity in data by Dinehart (1992) was determined from high resolution sonar measurements of the stream bed elevation.

\*\* Emmett (1975) did not indicate any bedload transport process, but the very high bedload transport rate and increase in bed surface with an increase in transport rates indicate the migration of a bedform.

***Turbulence of flow***

The response of small bedload particles to the turbulent action of water flow has been observed by several researchers (Brayshaw 1985; Heathershaw and Thorne 1985; Williams et al. 1989a and 1989b, Apperley and Raudkivi 1989; Thorne et al. 1989; Nelson et al. 1993). Of the four directions of turbulent movements in 2-dimensional flow (forwards, backwards, upwards, and downwards), the "sweep", a combination of a downward and a fast forward component, and the "burst" or "ejection", which has a strong upward but low forward speed, generally produce high localized rates of bedload transport. Heathershaw and Thorne (1985) provide high resolution data on sediment transport rates as affected by turbulent flow, and the observed transport rates also have periodic fluctuations. These records are not included in **Table B-1; 2** because they were measured in an estuary with a large ratio of flow depth to particle size, a condition that is not commonly found in lower-order montane channels.

Nevertheless, flow turbulence has also been observed to affect bedload transport in gravel-bed rivers. Drake et al. (1988) filmed the bottom of Duck Creek, a river with fine gravels in Wyoming, during a bankfull flow event. Turbulent fluctuations in the bed shear stress caused abrupt bedload transport that could be characterized as brief, localized, and apparently random waves of very high entrainment. Bedload material was transported over a small distance and then deposited. The bedload waves moved downstream faster than the average near-bed water velocity until their excess momentum was dissipated. Transport rates of small gravels transported during these "random sweep events" were approximately 10 times greater than the background rate, and appear to be comparable to what Heathershaw and Thorne (1985) named "sweep and ejection". Although these "sweep transports" lasted only 1 to 2 seconds and occurred only 9% of the total time, they transported about 70% of the bedload and were the most important transport mode at low excess shear stresses. The implications of these brief, localized and apparently random transport waves for measuring and sampling are a need for larger bedload sampler openings and sampling times sufficient to accurately capture the relative frequency and variability of both sweep and non-sweep transport.

***Passage of bedforms: bedload sheets and dunes***

Short-term fluctuations of bedload transport rates due to the passage of bedforms have been observed in laboratory flumes and natural rivers (e.g., Dietrich et al. 1989, Kuhnle and Southard 1988, Kuhnle et al. 1989a, Whiting et al. 1988). The passage of bedforms in gravel-bed rivers appears to be associated with gravelly-sandy sediment mixtures, bedload supply rates that exceed transport capacity, and the process of longitudinal sorting described by Iseya and Ikeda (1987). The latter process results in the formation of sequential transverse strips of coarse, medium and fine gravels that extend across much of the channel. Coarse gravels form the ascending slope of these bedforms, while the medium and fine gravels form the gentler descending slope. High transport rates of coarse gravels indicate the passage of the coarse stoss (ascending slope) side of the bedload sheet. The passage of the tail of the bedload sheet is characterized by declining transport rates of medium and fine gravels.

Iseya and Ikeda (1987) showed that the development of migrating bedload sheets depends on the proportion between sand and fine gravels. Their experiments showed that the sand content needed to be between 25 and 50% to develop bedload sheets. If the sand content increased to more than 50%, bedload transport occurred in the form of migrating dunes, often with superimposed ripples.

The downstream migration of dunes with superimposed ripples is a common phenomenon that has been observed in sand-bed streams, flume experiments with uniform gravels ranging in size from 2.1 to 23.5 mm, and in gravel-bed rivers that transport mostly sand (Table B-1; 2). Given a sufficiently large sediment supply, large-scale dunes with superimposed ripples can even form in rather uniform pebble- and cobble-sized material, as observed by Dinehart (1992) in the North Fork of the Toutle River in Washington, where much of the 736 km<sup>2</sup> basin area was devastated in the eruption of Mt. St. Helens. Like migrating bedload sheets, migrating dunes with superimposed ripples also cause a rather well-defined periodicity in bedload transport.

The periodicity of bedload waves associated with the passage of bedload sheets or dunes is usually quite well defined and commonly lies in the range of a few minutes to about one hour (Table B-1, 2). Transport rates typically extend over an order of magnitude (Fig. B-1; 2). The amplitude (height of the bedform) and frequency (spacing of the bedforms) of bedload sheets is controlled by the rate of sediment supply and discharge. For bedload sheets, the oscillations become faster and amplitudes decrease with increasing bedload supply. When supply becomes limited the occurrence of bedload sheets ceases, and transport is confined to the central part of the channel (Dietrich et al. 1989; Ferguson et al. 1989).

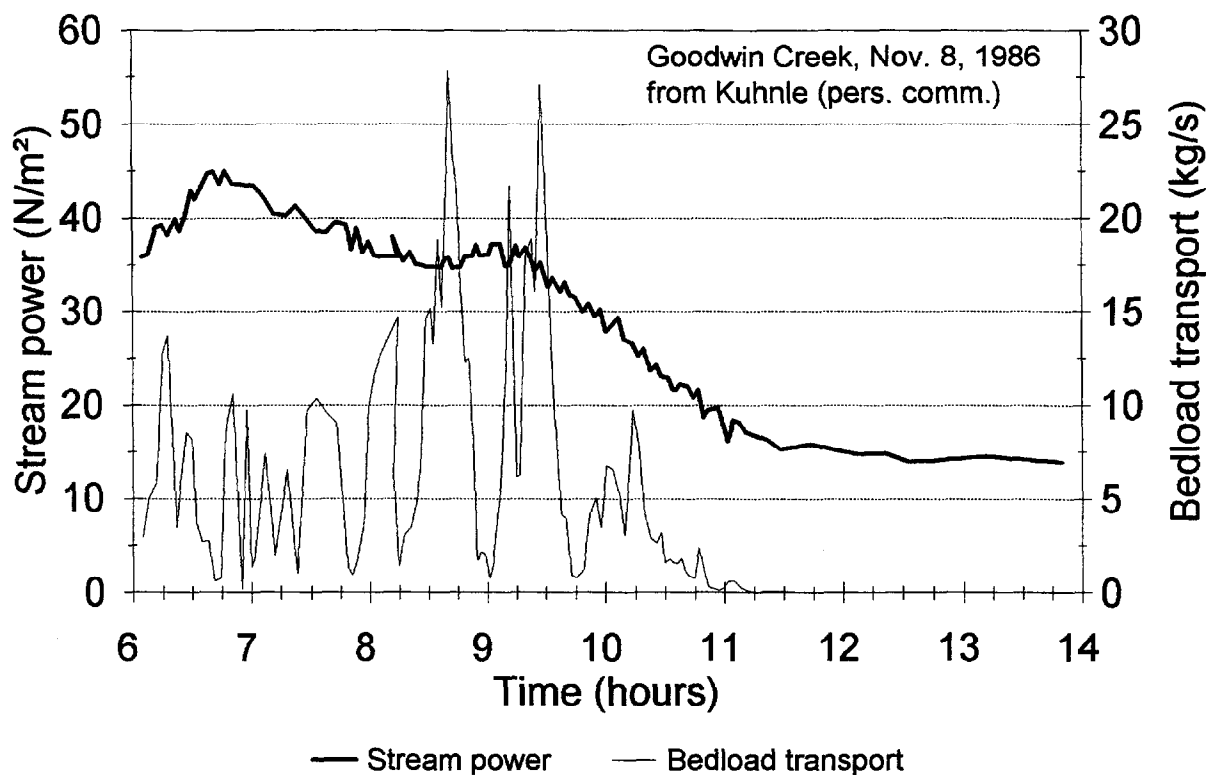


**Fig. B-1; 2:** Short-term variability at Goodwin Creek, a sand-gravel stream in Mississippi, caused by a) migration of dunes between 6:00 and 8:15, and b) possibly bedload sheets between 8:15 and 9:45. Flow was about 21 m<sup>3</sup>/s during the first phase, and 16.5 m<sup>3</sup>/s during the latter (after Kuhnle et al., 1989; and Kuhnle, pers. comm., 1993).

The passage of bedload sheets and the migration of dunes results in a higher temporal variability of bedload transport rates and bedload grain-size distributions. This again means that an accurate estimate of bedload transport rates, even at constant discharge, will require a high sampling intensity. This sampling intensity will usually have to be gained by high frequency sampling, as the high bedload transport rates associated with these transport processes may quickly fill the sampler.

***Fluctuating transport rates due to interactions between bedload and the channel bottom***

Many records of bedload transport in coarse gravel-bed rivers also show short-term fluctuations. Periodic fluctuations commonly are in the range of 30-90 minutes. Besides these fluctuations, almost all high resolution records of bedload transport contain more frequent, smaller periodicities of 5-15 minutes. Thus, the temporal variability is quite similar to the time scale of the periodicities observed for migrating bedload sheets or dunes with superimposed ripples (Table B-1; 2). But conditions in most gravel-bed rivers are different from those necessary for the passage of bedforms (i.e., high rates of sandy-gravelly bedload supply), and the observed bedload waves do not show the typical characteristics for bedload sheets (i.e., that coarse material precedes finer material, a well-defined periodicity, and that fluctuations increase in frequency and decrease in magnitude with increasing sediment supply).

Bunte (1991, 1996) assumed discontinuously operating interactions between bedload and the bed material were one reason for these bedload transport fluctuations in coarse supply-limited gravel-bed rivers. Consecutive samples of coarse bedload (1-25 cm in diameter) taken at 2-hour-intervals with a 30 by 155 cm net-sampler during snowmelt high-flow yielded transport rates that were highly fluctuating (3.25 to 72.2 g/m<sup>2</sup>·s) while flow varied by less than three percent (5.58 to 5.73 m<sup>3</sup>/s (0.053 - 0.054 m<sup>3</sup>/km<sup>2</sup>)). The grain-size distributions of consecutive samples varied between predominantly fine gravels, predominantly coarse gravels, or complete grain-size spectra (i.e., all grain sizes being transported). These observations are best explained by the interaction of local hydraulics and channel-bed conditions, and exchange processes between moving bedload and particles of the river bottom. Local, momentary flow either selectively winnows out the fine gravels, or transports subsequently exposed large clasts. If the local, momentary shear stress is high enough, almost all particle sizes in the local stream can be entrained.

If bedload transport alternates between low transport rates with truncated grain-size spectra and high transport rates with complete grain-size spectra, accurate sediment sampling requires both a sampler opening that can accommodate the larger particles and a high sampling intensity. The high sampling intensity can be achieved either by frequent repetition or long sampling durations, depending on the magnitude of transport rates and the amount of sediment that the sampler can hold.

**1.2.1.2 Intra-event variability of bedload transport**

The preceding discussion of short-term fluctuations in bedload sediment transport presumed relatively constant discharge. The intra-event variability is still greater because changes in discharge affect the sediment transport capacity and sediment availability. The magnitude and timing of the changes in flow will also affect the sediment transport rate for a given discharge at different points in the runoff hydrograph. Thus the intra-event variability incorporates both the effects of changes in discharge and the hysteresis effect for a given discharge. Since the processes governing short-term variability also apply within an event, it is very difficult to associate a specific cause with an observed change in bedload transport.

Bedload transport fluctuations within an event can be seen in many records of bedload transport. Fluctuations often range over one order of magnitude for a given discharge, and the periodicities of bedload transport rates are frequently on the order of 1 to 2 hours (Table B-1; 3). Usually the causative process is not specified. Depending on the length of the high flow event, and the temporal resolution of the bedload measurements, these fluctuations are a combination of short-term and intra-event variability, and overlap in the references are therefore unavoidable.

The intra-event variability of bedload transport can take many different forms. Since a given phenomenon can be caused by different processes, a sorting by pattern may be as appropriate as a sorting by process. Common observations of intra-event bedload transport in mountain or small streams are included in Fig. B-1; 3.

The phenomena shown in Fig. B-1;3 can occur individually or in any combination. Examples for these phenomena will be discussed below. Table B-1; 3 lists observed intra-event variability of bedload transport rates in gravel-bed streams.

#### ***Sudden waves of upstream sediment supply***

Hayward and Sutherland (1974) and Hayward (1980) used a vortex-tube to measure bedload transport continuously at the Torlesse Stream, which drains a steep 3.9-ha basin in New Zealand. Supply-limited conditions were inferred because several bedload formulas predicted higher than measured transport rates. Occasionally, however, bank failures, the breakdown of the armored layer, or the sudden movement of boulders supplied an abundance of sediment during snow-melt high-flow. Such events triggered sediment waves, during which transport rates were highly fluctuating. The fluctuations had a frequency of less than half an hour and bedload transport rates extended over more than one order of magnitude during a 3-hour period with a nearly constant discharge of 0.4 m<sup>3</sup>/s (9.6 m<sup>3</sup>/s·km<sup>2</sup>).

Extra sediment supply can cause sediment transport rates to increase drastically above values previously observed at similar discharges. Sources of sudden sediment supply can be material from debris flows that enter the stream (Pitlick and Thorne 1987), readily available sediment from in-channel sources, and washload from bare gorge walls (Bathurst et al. 1986), collapse of undercut banks (Thorne 1981, 1991), check-dam bursts (Ruby 1976; Schmidt 1993), or log jam bursts. Bugosh and Custer (1989) found bedload transport rates increased by 2 to 3 times after a log-jam burst during a bankfull highflow. Nolan and Janda (1981) observed unusually high bedload transport rates during large storms because sediments stored in tributaries during previous small storms were being released. Sudden peaks in sediment transport are not confined to large floods or special events that provide sediment, but can occur during unspectacular high flows as well, as observed by Kuhnle (pers. comm. 1993) at Goodwin Creek in northern Mississippi (Fig. B-1; 4).

The effect of a sudden, nearby sediment input on transport rates depends not only on the amount and grain sizes of the surplus sediment, but also on the transport capacity of the respective stream during high flow. Thus, a sudden input of sediment supply can lead to different consequences in different stream types. Supply-limited steep mountain rivers can experience a substantial increase in transport rates before transport capacity is reached and channel change becomes visible. But when sediment supply exceeds transport capacity, deposition can initiate drastic channel change. Then as this sediment supply is exhausted, the river starts to scour a new channel into these new deposits. Consequently, higher than average transport rates can prevail during the falling limb of flow, and perhaps during subsequent high flow events as well.

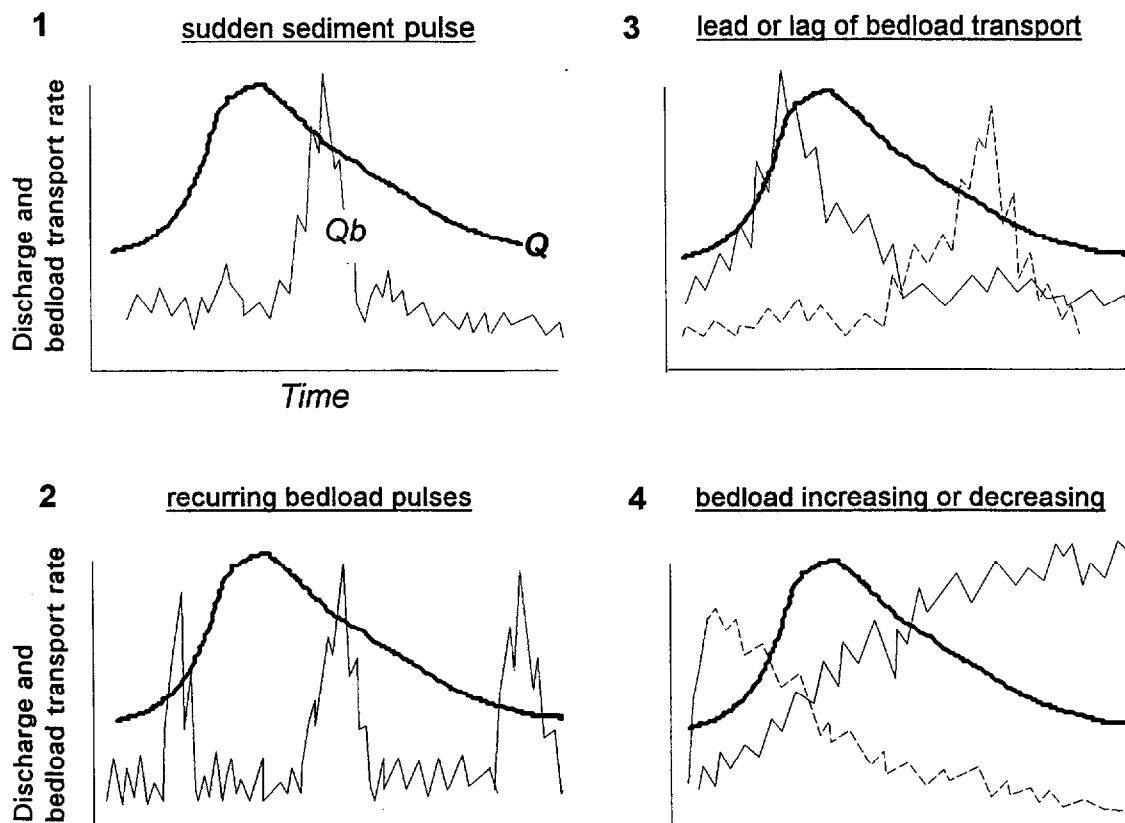


**Fig. B-1; 3:** Various forms of intra-event variability in bedload transport rates during a single high-flow event. Q indicates the hydrograph, and Qb the temporal variation of bedload transport rates.

1. Sudden, isolated pulses or unsystematic increases of bedload transport at a specific time during a flood event. These bedload pulses are often caused by a sudden increase in sediment supply from a bursting log jam, bank collapse, etc.
2. Bedload pulses with a discernible return period, but which may not be associated with the highest flows. Recurring storage and deposition of bedload associated with a riffle-pool morphology may be responsible for this pulsed nature of bedload transport as well as local interactions between flow and the channel bottom.
3. A lagged or accelerated response of sediment transport in relation to the timing of the flow event (i.e., hysteresis). This can be caused by several processes including river bed consolidation that delays armor layer break-up, an easily accessible sediment storage that becomes depleted, or vortex erosion.
4. Systematically increasing or decreasing bedload transport rates without any significant change in discharge may be the result of increasing supply from undercut, unstable banks, progressive armoring, or exhaustion of sediment supply.

Sediment transport rates in rivers with a naturally high sediment supply, such as braided rivers or rivers with alternate bars, will show a less dramatic increase after an additional sediment input because these rivers are already transporting close to their maximum capacity. Aggradation and lateral channel migration will be the more probable response.

**Table B-1; 3:** Observed sources and timing of intra-event variability in bedload transport rates in gravel-bed streams.

Reference	Observed phenomena	Timing* (hours)	Process observed or inferred	Sampling duration/int'vl
Bänzinger & Burch 1990	-fluctuations		-	1 min / 1 min
	-sudden bursts	-	-	
	-lead/lag	few min.	-	
Rickenmann 1994	-recurring pulses	0.2	-	1 min / 1 min
	-sudden bursts		-	
	-lead/lag	few min.	-	
Schlatte 1984	-fluctuations	0.7-1.5	-	1.5min/1.5min
	-lag	1	-	
Bunte 1991, 1996	-recurring pulses	4-6	-storage on riffle	5 min / 5 min
	-lag	5		
Ergenzinger et al. 1994	-recurring pulses	6-7	-absence of flow cells	10 min/10 min
Reid & Frostick 1986b	-fluctuations	1.5-2	-traction carpet	30 min/30 min
	-lag	1-2	-particle interlock	
	-lead	1-7	-erodible bed	
	-sudden bursts	-		
Ergenzinger & Custer 1983	fluctuations	2-4	-	1 hr / 1 hr
Ergenzinger 1988	-sustained high rates		-armor torn up	1 hr / 1 hr
Bunte 1991, 1996	-lead ->lag	2	-availability	1 hr / 1 hr
Tacconi & Billi 1987	-fluctuations	-	-	1 hr / 1 hr
	-lead/lag	-	-	
D'Agostino et al. 1993	-fluctuations	1-3	-	1 hr / 1 hr
Lisle 1989	-fluctuations	0.7-1.5	-	15 s / 15 min
Hayward & Sutherl. 1974	-fluctuations	0.5		~2 min/10-20min
	-sudden bursts	-	-sed. supply	
Campbell & Sidle 1985	-fluctuations	0.5-2	-	~30 s / ~ 30 min
Kuhnle pers. comm. 1993	-recurring pulses	2	-	few min / 18 min
	-individual peak		-	
Bathurst et al. 1986	-fluctuations			
Jackson & Beschta 1982	-fluctuations		-channel change	

**Table B-1; 3 (continued):** Observed sources and timing of intra-event variability in bedload transport rates in gravel-bed streams.

Reference	Observed phenomena	Timing* (hours)	Process observed or inferred	Sampling duration/int'vl
Gomez 1983	-decreasing rates		-armoring	
Pitlick & Thorne 1987	sudden bursts lag/lead		-high sediment supply	

\* Timing either refers the time difference between lead or lag of sediment transport and peaks in the hydrograph, or to the periodicity of sediment transport fluctuations and recurring pulses.

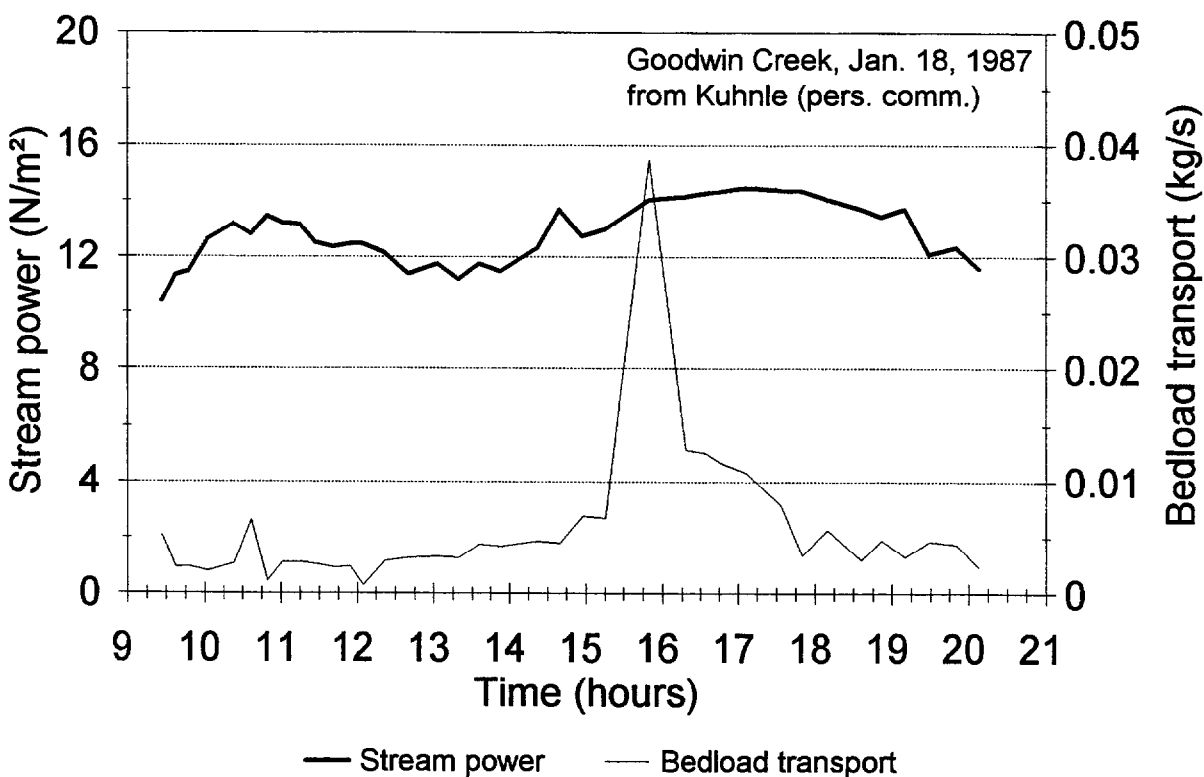


**Fig. B-1; 4:** Sudden increase of bedload transport during a small flood event at Goodwin Creek during almost constant flow (R. Kuhnle, pers. comm., 1993).

***Non-periodic fluctuations***

Non-periodic fluctuations of bedload transport are frequently reported in the literature (Table B-1; 2 and 3), but information on the causative processes is rare. A plot of bedload transport from Prairie Creek shows a great deal of temporal variability across different time scales with much of the bedload transport occurring lower on the recession limb (Lisle, 1989) (Fig. B-1; 5).

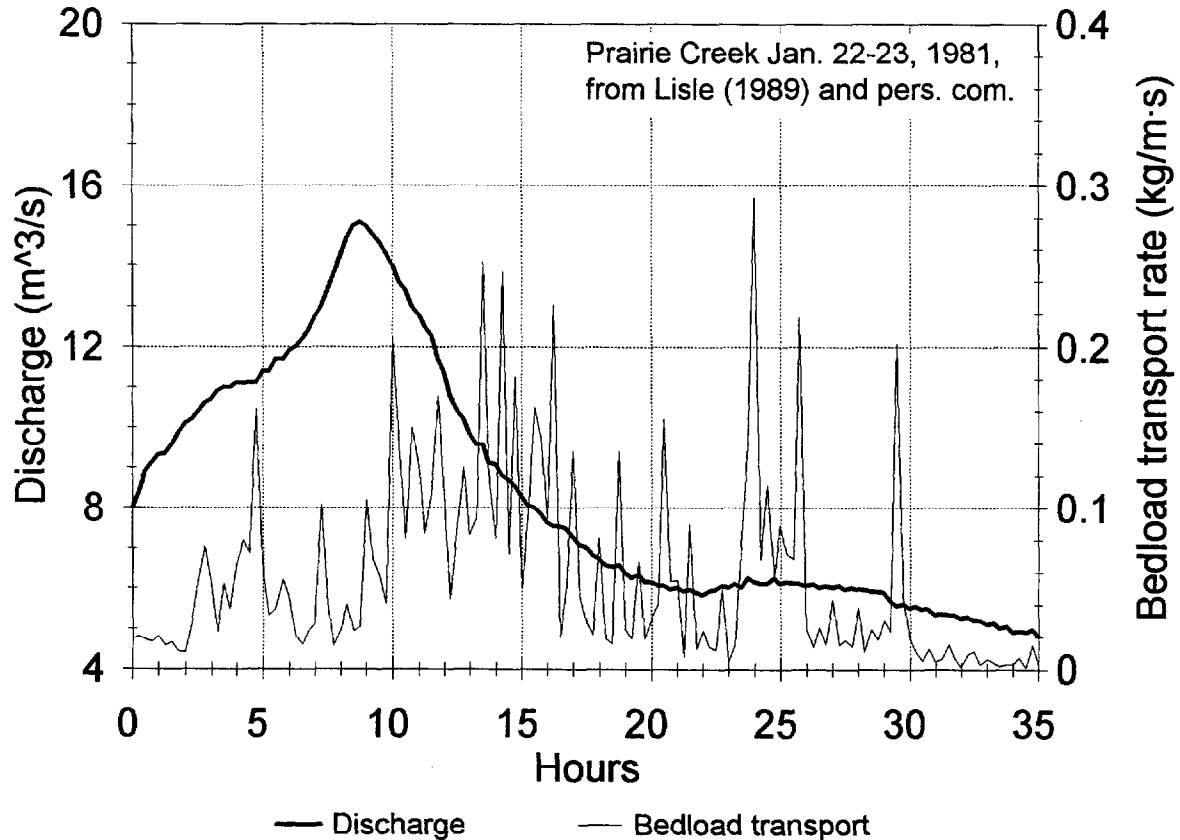


**Fig. B-1; 5:** Intra-event variability of bedload transport during a storm at Prairie Creek, a coastal stream in northern California. In addition to the fluctuations in transport rates, bedload transport lags behind discharge by about 5 hours, and produces high peaks on the falling limb of flow (after Lisle, 1989; and Lisle, pers. comm., 1993).

***Recurring bedload pulses***

Bedload pulses can recur in regular intervals. Rather short intervals of 15-20 minutes were reported from the Erlenbach torrent by the Swiss studies of Bänzinger and Burch (1990) (Fig. B-1; 6), and Rickenmann (1994) (Fig. B-1; 7). In these two studies a hydrophone was used to obtain a continuous record of bedload transport, and the results again showed why the distinction between temporal scales is difficult. The 1-minute temporal resolution detected rapid fluctuations that might normally be associated with short-term variability, but the flashy nature of the recorded flood events (1-3 hours) mean that these fluctuations might also be considered as intra-event variability. Fluctuations with a recurrence interval of about 2 hours are reported by Kuhnle (pers. comm. 1993) from the sandy-gravelly Goodwin Creek (Fig. B-1; 8). None of the above studies give any cause for the recurring fluctuations.

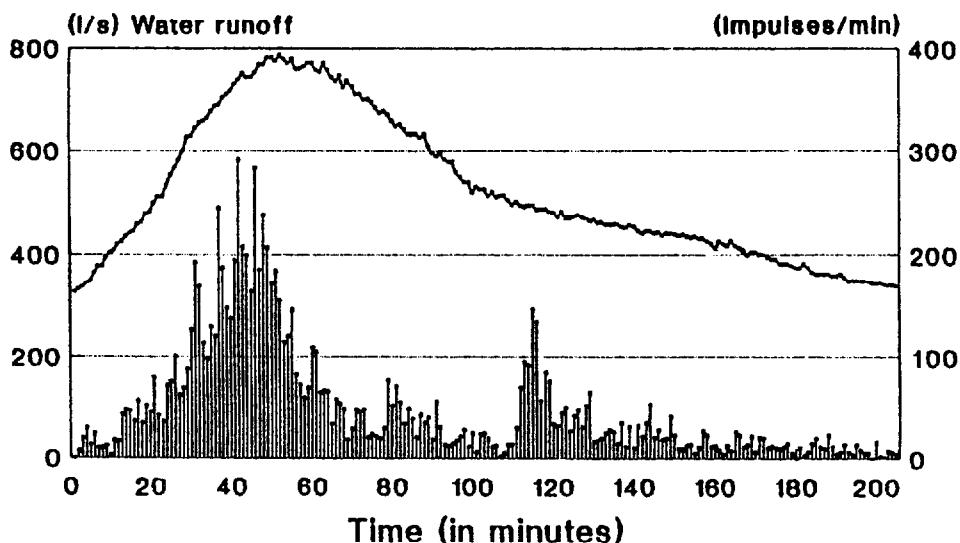


**Fig. B-1; 6:** Bedload pulses recurring over approximately 20-minute intervals following peak discharge at the Erlenbach torrent in the Swiss Alps. Start of the event is May 31, 1987, 5:57 p.m. (from Bänzinger and Burch, 1990).

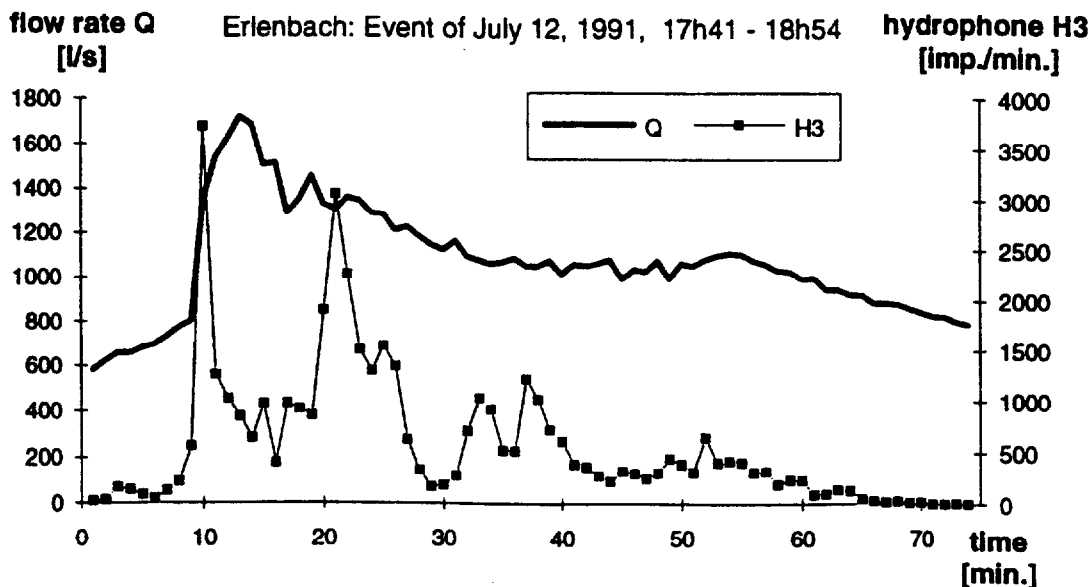


**Fig. B-1; 7:** Bedload pulses recurring in 10-15 minute intervals at the Erlenbach torrent in the Swiss Alps (from Rickenmann, 1994).

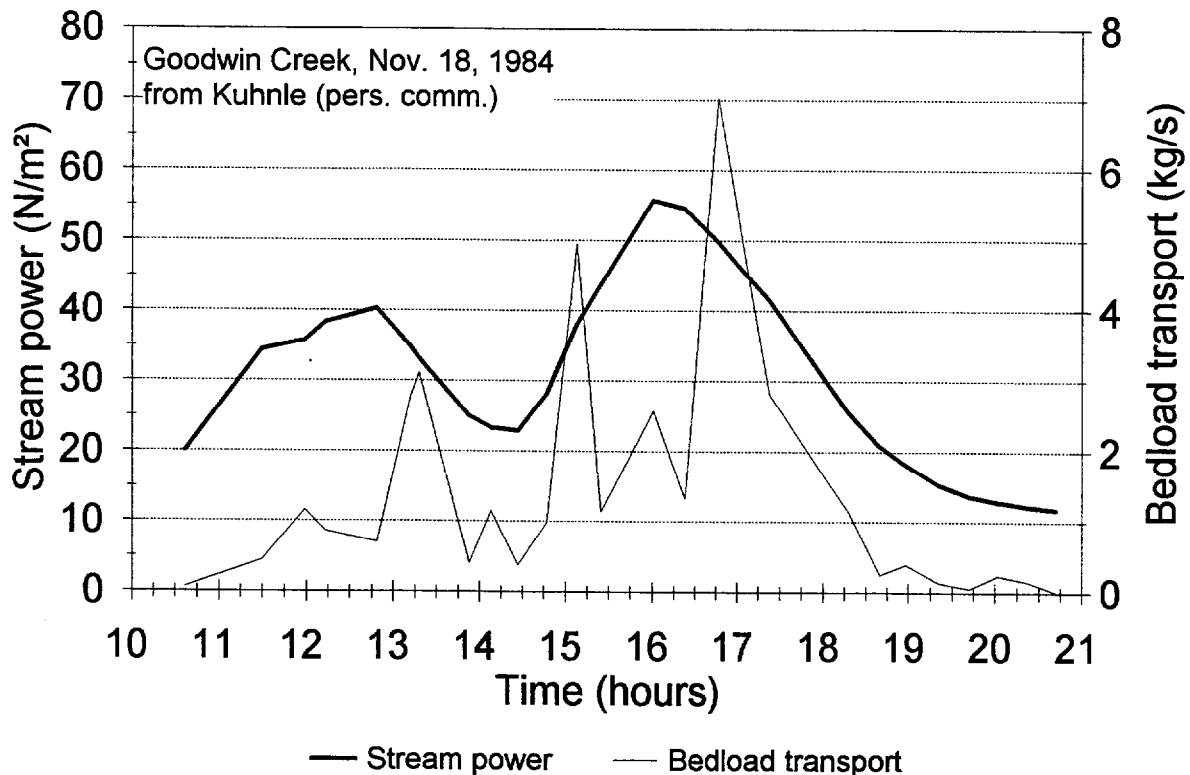
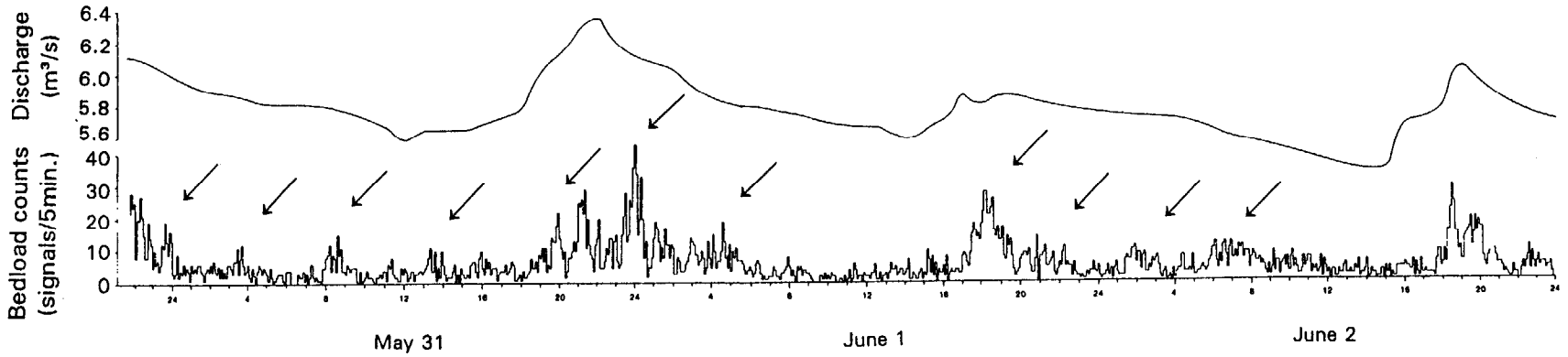


Fig. B-1; 8: Bedload pulses recurring in about 2-hour intervals during a high flow event at Goodwin Creek (R. Kuhnle, pers. comm., 1993).

Recurring pulses of bedload transport with a periodicity of 5-6 hours were evident in a continuous, 3-day record with a 5-minute resolution by recorded passage of magnetic pebbles and cobbles over a detector log (Bunte, 1991; 1996). These recurring bedload waves were especially prominent during the falling limbs of the diurnal fluctuations during snowmelt (Fig. B-1; 9). Simultaneous records of the water surface slope over an adjacent riffle were found not to be in phase with the diurnal fluctuations of flow. The temporal patterns of the water surface fluctuations suggested that sediment was accumulated on the riffle for a few hours before being eroded in one batch. Jackson and Beschta (1982) also attributed similar patterns in bedload transport to channel change.

These discontinuous adjustments of the river bed happen within a time frame of several hours. The resulting bedload transport waves often cause hysteresis effects because many high flow events only last for a day or have daily peaks, such as snowmelt high flows. A one-day record of coarse bedload transport during snowmelt high flow (Ergenzinger and De Jong, 1995) showed two major bedload waves: one on the rising limb and one on the falling limb with little transport at the time of peak flow (Fig. B-1; 10). This example shows that elevated flow magnitude is a necessary but not sufficient agent of bedload transport. Thus the relation between water discharge and sediment transport can be very complex.



**Fig. B-1; 9:** Bedload pulses occurring at various frequencies. Most distinguishable are frequencies of 1.5, 4-6, and 24 hours. Bedload pulses recurring at 4-6 hours are marked with arrows. Bedload measurements were made in 5-minute intervals using the magnetic tracer technique over a 3-day period during a snowmelt high flow at Squaw Creek, a mountain stream in Montana (Bunte 1991; 1996).

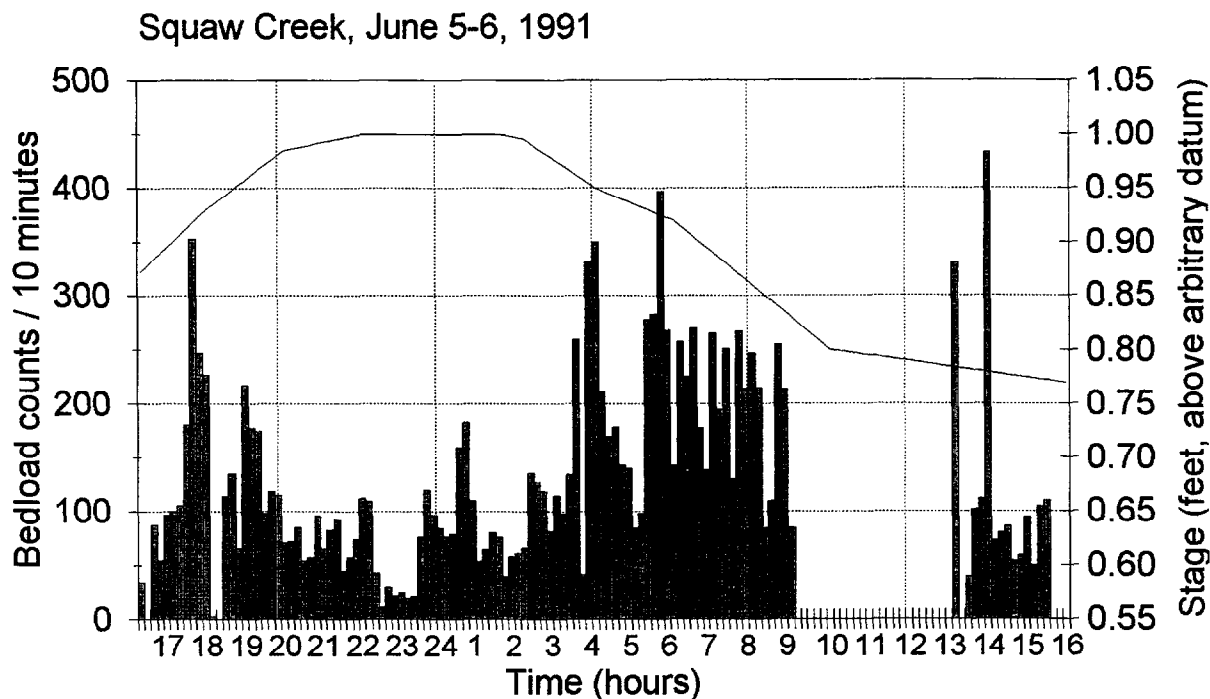


**Fig. B-1; 10:** Bedload waves observed on the rising and falling limb, respectively, at Squaw Creek in the middle of snowmelt high flow (after Ergenzinger and De Jong, 1995).

***Hysteresis effects: lead and lag of sediment transport***

When consecutive pairs of discharge and sediment transport measurements for a single-peak high-flow event are plotted and serially connected, the data usually do not fall on a single line, but form a hysteresis loop. Transport rates that are larger on the rising limb of the hydrograph than on the falling limb (lead of sediment) plot as a clockwise loop, while a counter-clockwise loop indicates higher transport rates on the falling limb (lag of sediment).

A lead of sediment transport during a high-flow event is caused by nearby sediment that is readily available for transport as flow increases. A lag is often caused when local sediments are not immediately available or when it takes some time for sediment from further away to arrive at the measuring stations. Both local availability and upstream supply of sediment are influenced by the antecedent history of flow.

***Lag of sediment transport***

Reid et al. (1985) observed for Turkey Brook, a gravel-bed river in Great Britain, that long periods between floods consolidate the gravel bed by particle interlock. During the first flood in the season bedload is only generated on the receding limb after flows during the rising limb have loosened the channel bottom structure and winnowed out the fines (Fig. B-1; 11: see floods of 10-11 Dec. 1978, 28-29 Dec 1978, 26 May 1979, and 9-10 Dec. 1979). Higher bedload transport rates during the falling limb of the hydrograph have also been reported by Klingeman and Emmett (1982) and O'Leary and Beschta (1981). In these cases the availability and mobility of bed material in these cases was controlled by the armor layer which was not broken up until the receding flow. Transport rates for similar flows on the rising and falling limbs of the hydrograph differed by an order of magnitude. Increasing lag periods of sediment transport during a high flow

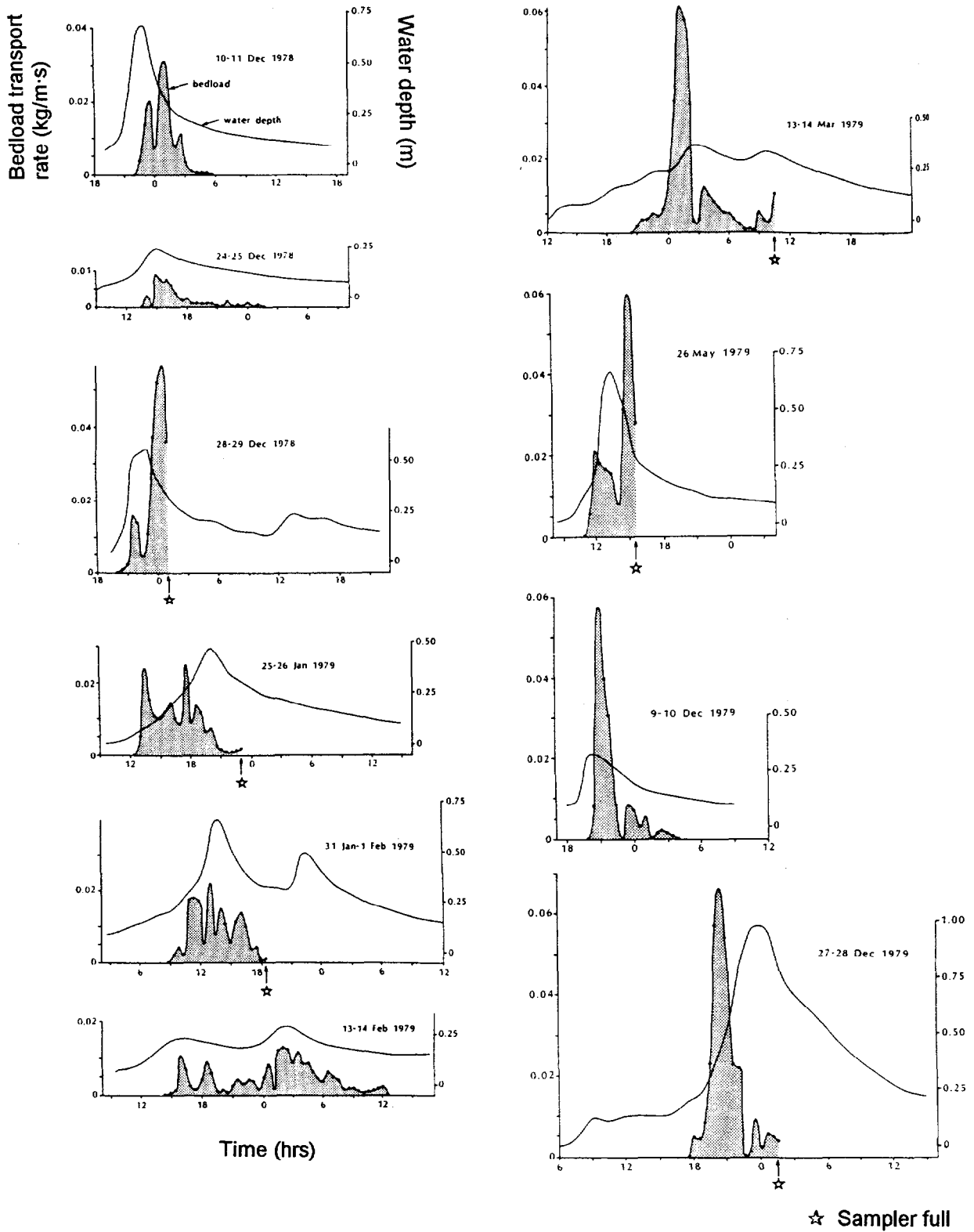
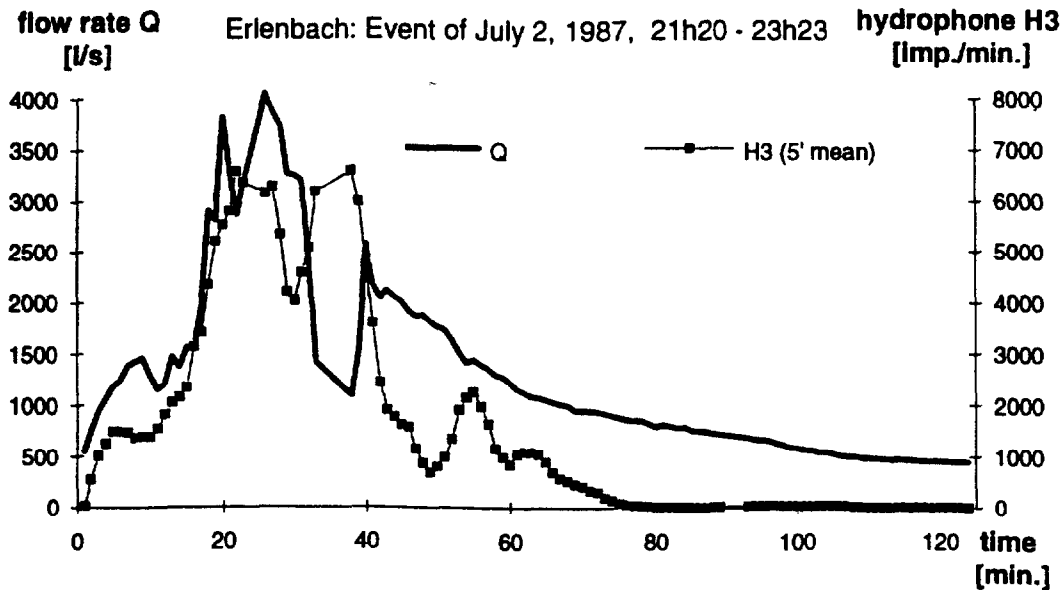


Fig. B-1; 11: Examples of lead and lag in bedload transport (submerged weight) during consecutive flood events in 1978 and 1979 at Turkey Brook, a gravel-bed river in Great Britain. Plots for consecutive events follow the columns down. Axes scales are the same for all plots (slightly altered, from Reid et al. 1985).

event with multiple peaks were evident in the data provided by Rickenmann (1994) for the Erlenbach (Fig. B-1; 12).



**Fig. B-1; 12:** Increasing lag in bedload transport rates during a flood event with multiple peaks at the Erlenbach torrent in the Swiss Alps. The number of impulses/min. recorded at hydrophone 3 is smoothed by a moving average over 5 minutes of hydrophone impulses (H3 (5' mean)) (from Rickenmann, 1994).

#### ***Lead of sediment transport***

Reid et al. (1985) observed that a partly consolidated river bed provides a readily available supply of coarse sediment and thus allowed a fast response of bedload transport to increasing flow (Fig. B-1; 11, e.g., 25-26 Jan. 1979). In subsequent event, supply soon become exhausted which resulted in substantially lower transport rates on the falling limb (see Fig. B-1; 11, 13-14 Mar. 1979, and 27-28 Dec. 1979). Similar clockwise hysteresis loops were reported by Nanson (1974) and Klingeman and Emmett (1982).

An extreme lead in sediment transport during a flood event can be caused by vortex erosion that forms scour holes at the stoss side of flow obstructions imbedded into finer sediment (e.g., Karcz 1968; Bunte and Poesen 1993a, b and 1994) (Fig. B-1; 13). The same scour holes can form in gravel-bed rivers with isolated cobbles or boulders. Transport rates are very high at the onset of vortex erosion and decrease by about an order of magnitude as the development of the scour holes becomes completed. The magnitude and shape of this sediment transport wave depends on the size and shape of the flow obstructions, the size of the sediment around the obstacles, and on the flow itself. The dynamics of this vortex erosion are described in the literature on scour around bridge piers (e.g., Laursen 1963; Raudkivi 1986; Yanmaz and Altmbilek 1991). Vortex erosion can be quite effective in relatively small events when flows normally would not have the capacity or competence for sediment entrainment if obstructions were not present on the stream bed.

#### ***Change from sediment lead to sediment lag during multiple peak high flows***

A three-week continuous record of bedload transport during a snowmelt high flow at Squaw Creek, a mountain river in Montana, provided a good opportunity to analyze the temporal

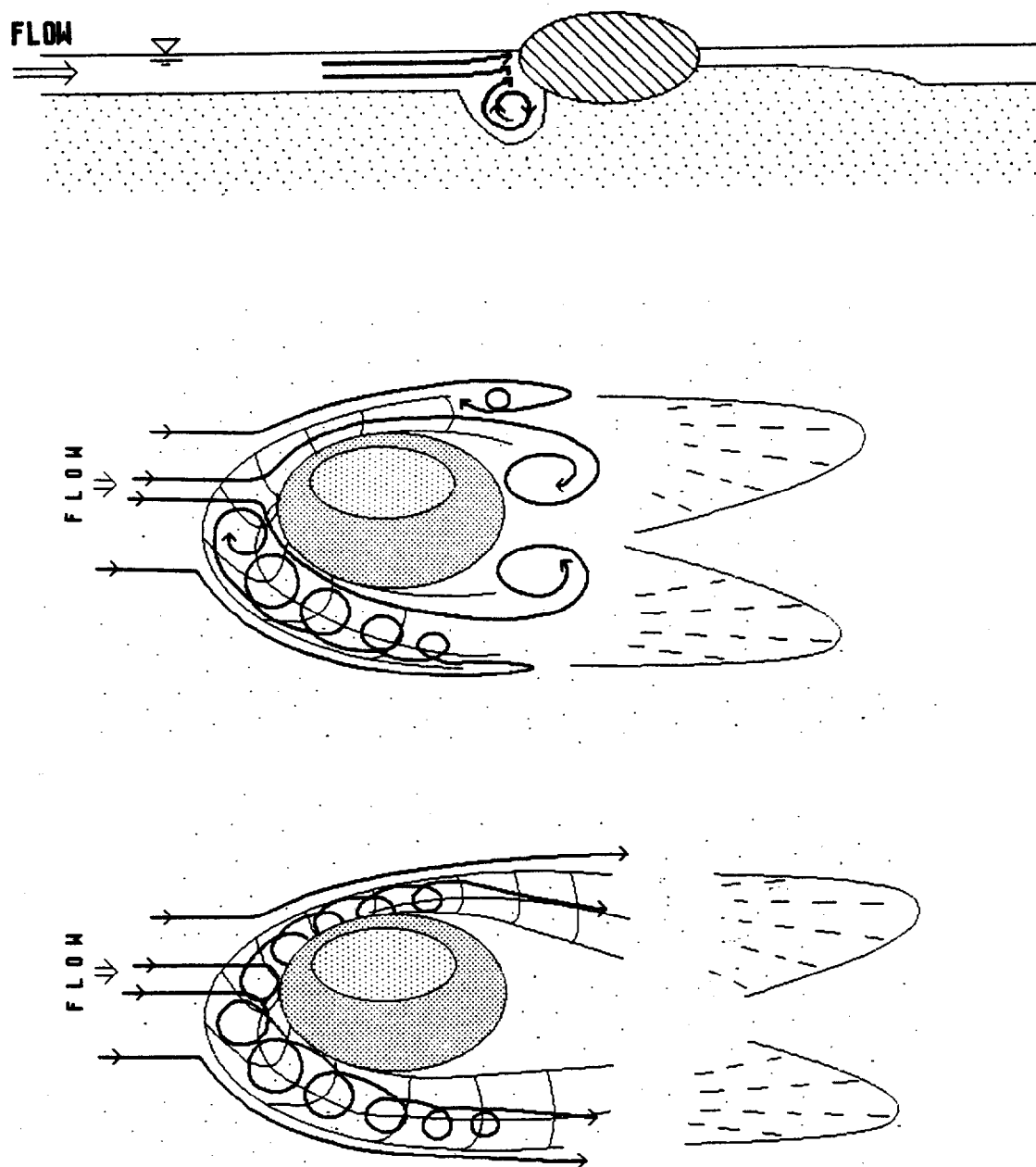


**Fig. B-1; 13:** Vortex erosion around an obstacle embedded in erodible sediment: profile view - moderate flow intensity (top); plane view - moderate flow intensity (center); plan view - high flow intensity (bottom) (from Bunte and Poesen, 1994).

variation of the daily hysteresis effects between bedload transport rates (quantified by number of signals/hour) and discharge (Bunte et al. 1987; Bunte 1991, 1996). Three major peaks of bedload transport occurred during the diurnal fluctuations in flow; the first peak (primary wave) was on the rising limb or around peak flow, the peak of the second wave was about 4-6 hours later on the falling limb, and a third bedload wave was observed another 4-6 hours later (**Fig. B-1; 14**).

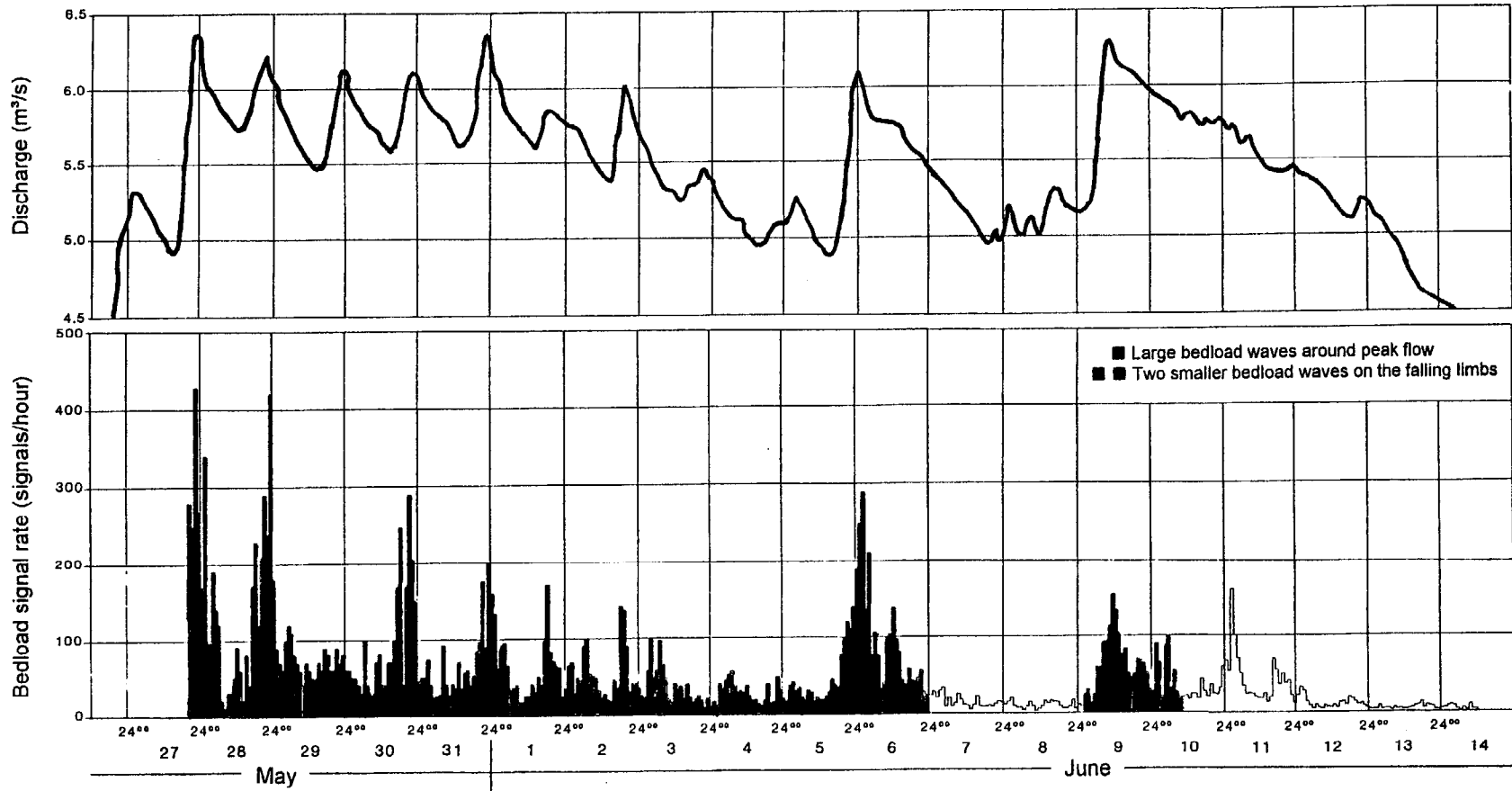


**Fig. B-1; 14:** Fluctuations of bedload transport measured at 1-hour intervals over a 15-day period during a snowmelt high flow at Squaw Creek (from Bunte, 1991; 1996). The relative amount of sediment transported by primary and tertiary daily bedload waves shifts from primary waves at the beginning of the snowmelt period to tertiary waves at the end of the high flow period.

These waves were attributed to the discontinuous transport of sediment through a riffle-pool unit, in which bedload was stored on a riffle until local hydraulics were sufficient to erode the fresh deposit. The total amount of bedload signals per day (from low flow to next day's low flow) correlated strongly with the total amount of daily runoff, indicating a generally balanced relationship between runoff volume and sediment volume. However, the proportion of sediment transported by the respective bedload waves changed as daily runoff volumes declined. In particular the proportion of sediment transported by primary waves became smaller, while the amount of sediment transported by the third wave increased. This change in the daily patterns of bedload transport brings about a systematic change in the hysteresis effect over the course of the hydrograph. The hysteresis loop changed from a clockwise direction with a lead in sediment at the beginning of snowmelt to a counter-clockwise direction with a lag in sediment.

***Sustained high or rapidly decreasing bedload transport rates***

Once a large volume of sediment is introduced into a stream system, transport rates can remain high on the receding limb of flow. Sustained high sediment transport rates on the receding limb of a high flow event were observed by Lisle (1989) at Jacobi Creek, a coastal stream in northern California. Ergenzinger (1988) reported that bedload transport in a snowmelt stream continued into late summer flows after an enormous rain-on-snow event in late May had torn up the armor layer and thus provided a continuous sediment supply. Months of high sand transport rates resulted from an artificial sediment input into a groundwater-fed gravel-bed river in Michigan (Hansen and Alexander, 1976). Episodically recurring high bedload transport rates were observed by Roberts and Church (1986) and attributed to the downstream migration of sediment waves in severely disturbed catchments in British Columbia. High transport rates out of phase with flow were reported by Pitlick and Thorne (1987) after a debris flow supplied an abundance of sediment into the Fall River in Rocky Mountain National Park.

A disproportionate decrease of transport rates during receding flows was observed by Gomez (1983) as a result of progressive armoring in a gravel-bed stream. Similarly, Mantz and Emmett (1986) showed that an increase in channel roughness is concomitant with an decrease of bedload transport rates.

The grain-size distribution of bedload transport often follows the general patterns of the hydrograph, coarsening as the flow increases, and fining on the falling limb. Part of this systematic variation of grain sizes over the course of the hydrograph is due to the changes in flow competence. However, the availability of sediment also plays a part, and the combined effects of temporal variation of flow competence and the temporal variation of the availability of sediment sizes can lead to unpredictable sediment responses with respect to flow. Sustained transport of sand and fine gravels during the first days of a high flow periods may indicate that the flow is still clearing out interstitial fines or washload (Phase 1 transport as defined by Beschta 1987). Coarsening of bedload over the course of the high flow event may be due to a tear up of the armor layer (Phase 2 transport as defined by Beschta 1987), or a depletion of fine material on the receding flow when the fines are trapped under the developing armor layer (Emmett 1976). An exhaustion of interstitial fines after the first few days of a snowmelt high flow was also believed to cause a coarsening of the bedload in Squaw Creek, Montana (Bunte 1991, 1996).

The complex processes that interact in time and space during a high-flow event in a gravel-bed river can also lead to a high temporal variability in the transport of sediment sizes (Beschta 1987). This notion, that not only the amount of bedload, but also its grain-size composition can be quite variable over time, is also of great importance for accurate measurements and sampling of bedload, since different bedload particle sizes should be

sampled with different samplers to increase the sampling success. Periodically recurring fining and coarsening of transport rates within less than an hour may be associated with migrating bedload sheets (Iseya and Ikeda 1987; Kuhnle and Southard 1988), or with a particle exchange between bedload and channel bottom (Bunte 1991, 1996). Another alternation between times of coarser and times of finer bedload transport during a flood event was observed by Emmett et al. (1983a and b) at the East Fork River. This was attributed to the spatial variation of flow hydraulics, grain-size sorting, and channel roughness through the riffle-pool reaches.

### 1.2.1.3 Between storm and seasonal variation

The variability of bedload transport between storms or during a high flow season can be due to the same mechanisms (river bed consolidation, depletion of upstream sources, and the availability of extra sediment supply) that control intra-event variability. However, a further effect on the variability in the relation of sediment transport and flow is due to a seasonal variability of the shape of the hydrographs.

#### ***Length of time period between floods***

Reid et al. (1985) provided examples of how the length of time between high flow events controls the sediment transport during the flood. Floods following closely to each other had higher bedload transport rates than floods that occurred several weeks or months apart, as in the latter case the river bed has had time to consolidate, and particles are less easily detached once they have interlocked (see Fig. B-1; 11).

#### ***Seasonal variation in erodibility and sediment availability***

Bänzinger and Burch (1990) found that it was not the length of time between floods, but the seasonal variation in river bed erodibility and sediment availability that caused seasonally different sediment responses at the Erlenbach, a steep (0.2 m/m) Alpine stream. Late summer to early winter floods required 2-3 times more runoff to initiate bedload motion than floods later in winter and spring. The lower entrainment threshold of winter floods is attributed to several seasonally variable processes including: (1) winter frost heaving during frequent freeze-thaw cycles loosens the stream bed to provide transportable sediment; (2) higher sediment input from landslides during the rainy winter season; (3) high summer floods that scour the river bed and leave less material for subsequent floods.

#### ***Seasonal variation of hydrographs, entrainment thresholds, and sediment load***

The seasonal shape of flood hydrographs naturally depends on the respective hydrologic regime. Pluvial regimes in central Europe, for example, typically feature flashy summer floods from more intense localized storms than winter floods caused by prolonged rain. Although entrainment thresholds ( $Q_{crit}$ ) were lower in winter (Bänzinger and Burch 1990), the sediment load for a given volume of excess flow ( $Q < Q_{crit}$ ) was generally smaller because the prolonged winter floods barely exceed the threshold of motion (Rickenmann 1993), while summer floods typically peaked at a flow of roughly twice the critical discharge.

### 1.2.1.4 Summary and implications for measuring and sampling

Fluctuations of bedload transport can occur in any time scale, in any stream type, and any flood event. Bedload transport fluctuations are due to a variety of processes, but detailed descriptions of the process mechanisms and the resulting effects on bedload transport

fluctuations are rare, and become scarcer as temporal and spatial scales increase beyond laboratory scales which are usually in the temporal range of minutes to hours and a spatial range of centimeters to meters. When measuring and sampling bedload transport for comparing annual load estimates as part of CWE analyses, highly fluctuating transport rates have to be assumed for almost every case. Unless general bedload transport patterns of a stream are well known from prior detailed temporal records, this variability in bedload transport necessitates that transport rates be measured and sampled intensively. Intensive measurements refer to collecting bedload samples that are representative for the average bedload transport rate and its grain-size distributions within a time span over which flow can be assumed to be relatively constant. This problem is further discussed in chapters B-2 and B-3.

Intensive sampling also refers to the problem that bedload transport in almost all streams experiences some kind of hysteresis effects, and these vary for events with multiple peaks, for consecutive events, and over the course of the high flow season. Hysteresis effects are usually quite large, resulting in a one- to two-order of magnitude variation in bedload transport rates for a given rate of flow (Reid and Frostick 1986a). The omnipresent but difficult to predict hysteresis effects require bedload measurements to be continued through the entire duration of the high flow. This problem will be further discussed in chapter B-3 and B-4.

## 1.2.2 Spatial variability of bedload transport

Both instantaneous bedload transport rates and annual sediment loads usually differ by locations in the stream, and this variation can be caused by other factors than varying contributions of water and sediment from tributaries. This spatial variability can occur longitudinally (i.e., in the direction of flow), or within the cross-section. If transport rates and annual loads are spatially variable, this is of major importance for selecting measuring sites and for measuring and sampling bedload transport.

### 1.2.2.1 Longitudinal variability

Longitudinal variability of bedload transport occurs in different spatial scales and in regular as well as irregular intervals. The following section addresses three factors:

- Riffle-pool sequences,
- Proximity to sites of local sediment supply (e.g., gullies), and storage (e.g., log jams),
- Control of downstream sediment conveyance by storage and release function of LWD and log jams, and
- longitudinal variability of stream budgetary states.

#### ***Bedload sampling in gravel-bed rivers: sampling in pools or on riffles?***

Variation of bedload transport due to *riffle-pool sequences* occurs at *regular* intervals of about five channel widths, the average spacing between consecutive riffles (Keller and Melhorn 1978). This spacing is somewhat larger for streams with high sediment supply, and smaller as riffle-pool morphologies approach step-pool sequences in steeper streams. Assuming stream widths in the range of 2 - 20 m for mountain streams, riffles tend to be between 10 and 100 m apart.

A riffle-pool sequence is maintained by scour and fill of riffles and pools at alternating stages of high flow. This mechanism is explained by the *velocity reversal* theory. Consequence

of this different timing of scour and fill on riffles and pools is that transport rates measured in pools at a given time are different from those measured on riffles.

Since Keller's (1971) publication of the velocity reversal theory, which was first noted by Gilbert (1914), many studies have confirmed that bottom flow velocity and shear stress are higher on riffles than in pools during low flows, strongly increase in pools during rising flows, and often exceed the riffle shear stress at bankfull and higher flows. The zones of highest shear stress shift back to riffles as flow recedes (e.g., Lisle 1979; Emmett et al. 1983 a and b; Lisle and Madej 1992; Lisle and Hilton 1992; Keller and Florsheim 1993; Carling and Wood 1994). Thus, pools are the storage sites for bedload sediment during low flows, while bedload is scoured from and transported through the pools at high flows. Conversely, sediment is deposited onto the riffles during high flows, and scoured from riffles during waning flows. Extensive studies by Gintz (1990), Gintz and Schmidt (1991), Schmidt and Ergenzinger (1992), Gintz (1995) and Gintz and Schmidt (1995) on the movement of traced cobble particles through a step-pool mountain stream confirm the relatively undelayed sediment conveyance through pools, while particles rest for relatively long times during a high flow event on steps.

This velocity reversal and the corresponding patterns of scour and fill should affect bedload transport through a riffle-pool reach during a high flow event. This is confirmed by results from Meade et al. (1981, 1982) and Meade (1985) who performed cross-section measurements at East Fork River on a daily schedule over a period of two months during spring high flow. The difference between cross-section area during consecutive high flow waves indicates that sediment is deposited on riffles during high flows, and eroded from riffles during low flows and deposited in pools.

Another study analyzed the temporal variation of the water level between two points 17 m apart at the upstream and downstream side of a riffle over several days during a snowmelt hydrograph with diurnal fluctuations of flow (Bunte 1991; 1996). Over a period of several hours around peak flow, water levels first increased disproportionately high on the upstream point, then on the downstream point as well. High water levels then first dropped on the upstream side, and a little later on the downstream side. The temporal pattern of this water surface change could not be explained by the passage of a high flow wave alone. However, the completion of this "pumping" motion was always followed by increased bedload transport rates. This coincidence lead to the conclusion that the water surface change modeled the passage of a bedload wave over a riffle with initial deposition and subsequent scour.

Based on these general patterns of scour and fill in riffle-pool sequences, bedload transport rates during flow around bankfull should be lower in pools than on riffles during rising and falling limbs of the flow, and be highest in pools around peak flow. This is shown schematically in **Fig. B-1; 15 (top)**. Since sediment cannot be continuously deposited on riffles or scoured from pools without fresh sediment supply, sediment needs to be episodically transported off the riffle, and this may bring about fluctuations in bedload transport rates. Pools, on the other hand, can probably convey the supplied sediment at all times during the peak flow, but since the sediment comes in waves, some of the wavy patterns will probably be maintained during the passage through the pools (Beschta 1987). The resulting sediment transport patterns are shown schematically in **Fig. B-1; 15 (bottom)**.

Assuming that the sediment transport patterns of **Fig. B-1; 15 (bottom)** are correct, and that there is no net channel change after the high flow, riffles are the more preferable sediment sampling sites because transport rates are generally lower on riffles than in pools during peak flows and larger than in pools during waxing and waning flows. A smaller range of transport rates over the entire course of a high flow should make bedload measurements easier since sampling times would not have to be as frequently or as drastically adjusted

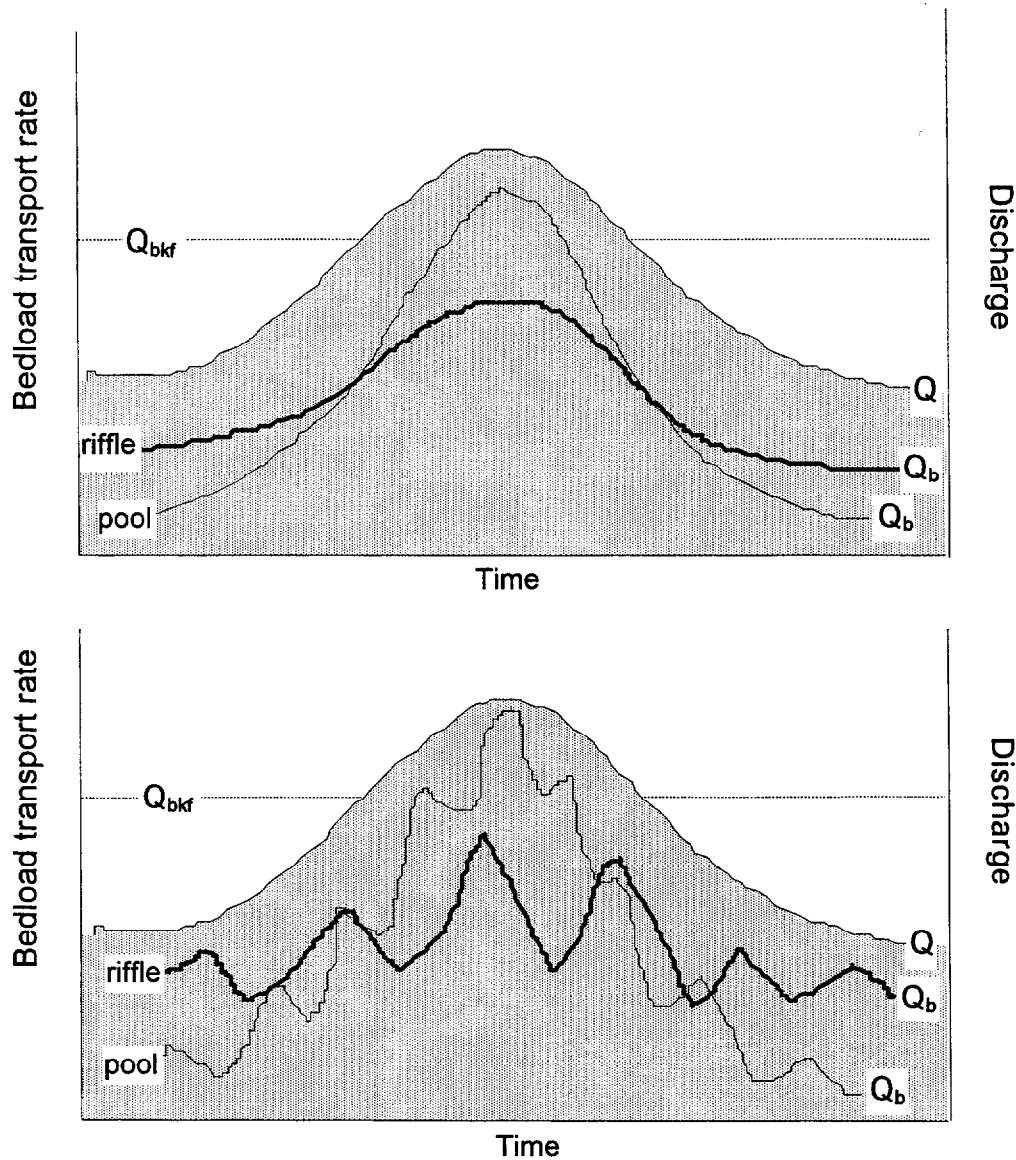


**Fig. B-1; 15:** Schematic diagram indicating general magnitude of bedload transport rates (top) and fluctuations of bedload transport rates on a riffle and in a pool (bottom) during a high flow event.

to transport rates. Note that a reduced range between minimum and maximum transport rates results in a decreased slope of a bedload transport rating curve.

However, while absolute differences between minimum and maximum transport rates might be lower on riffles than in pool, fluctuations between consecutive measurements might be larger on riffles than in pools where particles have a better chance of continuous transport than on riffles. The sampling problem posed by the presumably high fluctuations of bedload transport on a riffle due to the repeated deposition and scour of sediment may be reduced by locating the measuring site at the upstream end of the riffle above the riffle crest, or at the pool exit slope where these fluctuations may still be somewhat small. The fact that riffles may be the only wadable sections of a stream during high flow, and that pools may

be too deep and fast to safely sample further contributes to a preference for riffles as sampling sites.

The general pattern of scour in pools during rising flow and deposition during recession cannot be taken for granted in all cases. As already observed by Keller (1972) and others (e.g., Carling 1991), a velocity reversal may only occur at other, usually higher, discharges than bankfull, may require certain roughness of the riffle or pool, or may not occur at all. Silverston and Laursen (1976) found scour and deposition in a pool to depend on both the amount of upstream sediment supply to the pool and the morphology of the receiving pool. Therefore, a pool in a downstream sequence of riffle-pool reaches can either fill or scour as the flow increases. This irregularity disturbs the regular downstream patterns of sediment sources and sinks, and the patterns of longitudinal variability of transport rates associated with riffle-pool sections. And since the conveyance of bedload through a riffle-pool section depends on the particular flow hydraulics and bed-material characteristics, transport rates can even be different between consecutive riffles (Campbell and Sidle 1985). Foley (1976) observed scour and fill along the stream to be very local phenomena, not necessarily tied to riffle-pool structures.

***Distance from sites of local sediment supply and storage***

*Irregular* spatial variability in bedload transport can be associated with *sediment supply* such as from gullies, debris flows, undercut banks, and the release of sediment formerly stored behind large woody debris and log jams (see below). Sites of local sediment supply are irregularly spaced, and the spatial scale addressed here is in the range of 100 m to a few km.

If a stream receives sediment in quantities and sizes generally transportable by commonly occurring flows, this sediment passes through downstream reaches in a wave that becomes attenuated during its downstream travel. Consequently, transport rates measured in close proximity to the site of sediment supply quickly increase above average values during the next high flows, and since the wave will have passed the reach quickly, transport rates will drop to predisturbance levels quickly as well. At measuring sites further away from the sediment input site, an increase in bedload transport rates will occur later, due to the time it takes for the introduced bedload to be transported down the stream. In order to better estimate the timing of an increase in bedload transport rates at a distant site, the travel speed of bedload needs to be known which for coarse bedload in mountain gravel-bed rivers tends to be of the range of 20 - 500 m per year (see Chapter C-4). Transport rates at a measuring site further downstream will increase to a lesser degree than at a location just below the input site, but elevated transport rates will sustain over longer periods.

*Irregular* spatial variability in bedload transport can also be associated with *sediment storage* behind naturally occurring dams of large woody debris (LWD), log jams, beaver dams, and artificial check dams. After the conveyance of bedload is completely blocked by a newly formed log jam or check dam, bedload transport rates shortly below the blockage decline over time until the channel bottom develops an erosion resistant pavement that prevents further particle pick-up from the bed. The larger the distance between the measuring site and the blockage, the longer the time period until transport rates start to decrease.

Measured bedload transport rates are not only controlled by the proximity to log jams and LWD. The entire downstream conveyance of sediment can be controlled by storage and release of sediment by LWD and log jams, so that bedload transport measured at a certain location may be more dependent on the dynamics of the storage components than on discharge. The extent of this sediment storage, its transient nature, and the effects resulting from sudden sediment release behind LWD are described in more detail below.

***Control of downstream sediment conveyance by storage and release function of LWD and log jams***

In forested terrain, large woody debris (LWD) can cause a partial or total blockage of bedload transport and store large amounts of sediment, especially coarse gravels (Megahan 1982; Pearce and Watson 1983; Ketcheson 1986). Factors that promote LWD include the presence of a mature riparian forest, the riparian disturbance history and, in some cases, beaver activity. The actual sediment storage volume depends on the amount of LWD in the stream, stream size, stream gradient, and hillslope as well as valley morphology (Keller and Swanson 1979). Using the example of a mountain stream 10 m wide, **Fig. B-1; 16** provides estimates of the sediment volumes that may be stored behind LWD of different dimensions.

LWD and log jams only store sediment temporarily. LWD can either shift annually (Megahan and Nowlin (1976), or be artificially removed from the channel (Bilby 1981). The sediment storage can overflow, logs can rot away, or blow out in a sudden log jam burst. The residence time of sediments stored behind large woody debris depends on the rate of LWD deterioration or removal, which is controlled by factors such as time, submergence frequency, the resistance of wood towards rotting, occurrence of large high flows that can move or blow out log jams, and the amount of storage relative to the rate of incoming sediment. Streams with high bedload transport rates may fill all of the available storage, and LWD will then lose its ability to reduce the downstream transport of sediment. The net downstream conveyance of sediments stored behind large woody debris depends on the ratio of deteriorating log jams to developing log jams.

The removal of LWD from a reach can have pronounced effects of bedload transport rates. Beschta (1979) calculated that scour depths averaged 0.9 m after large woody debris was taken out of a small stream in the Oregon Coast Range. This scour produced 21 m<sup>3</sup> of sediments per meter stream length, or more than 5000 m<sup>3</sup> in a 250 m reach. An increase in bedload transport rates by a factor of 2-3 was observed by Bugosh and Custer (1989) for the rest of the snowmelt season after a log jam burst. A long-term effect on annual sediment yields that lasted for six years was observed at Hubbard Brook, an experimental station in New Hampshire, after trees in the catchment were felled, and revegetation was delayed by spraying herbicides. In this case the rotting of LWD without a new supply of logs caused a four-fold increase in annual sediment yields (Bilby 1981, 1984; Federer et al. 1990). The effect of LWD on bedload transport also varies with particle size. Coarse bed material is more subject to storage than sand sized particles as the latter can be flushed away more easily. These storage dynamics around LWD can cause severe problems for monitoring annual sediment yields and this topic will be picked again in chapter B-5.

***Selection of measuring sites in the presence of sediment sources and sinks***

A preferred measuring site for annual comparisons of bedload transport would be away from obvious upstream sediment sources or sinks, in order to obtain the most even distribution of bedload transport throughout a high flow and to keep hysteresis effects to a minimum. However, the problem is that sites of sediment storage and scour in a stream are spatially and temporally variable. Storage sites induced by LWD can form and disintegrate quickly during a high flow, especially during log jam bursts. Thus, former storage sites can suddenly become scour sites that supply large amounts of sediment for transport, and vice versa.

***Budgetary state of stream reaches between site of sediment supply and measuring site***

The above considerations about the effect of distance between a measuring site and locations of sediment supply or storage assumed that there was no genuine difference in sediment transport capacity over that stretch of stream. However, that assumption cannot

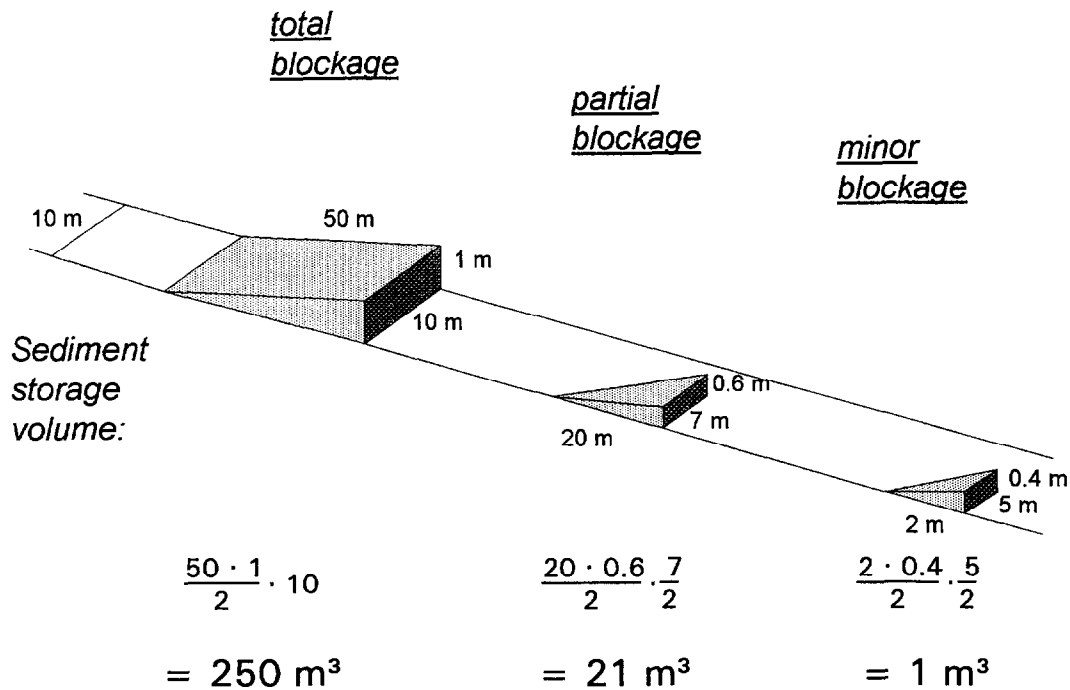


**Fig. B-1; 16:** Hypothetical examples of sediment volumes stored behind LWD of various sizes.

be made for mountain streams which often have a stepped longitudinal profile in which reaches of steeper gradient (through-transport) alternate with reaches of more gentle gradient (deposition), or reaches with degradation or sediment scour (e.g., cutting into erodible sediment). Sediment transport rates are likely to vary between reaches of different stream morphology and different sedimentary budgetary states. The spatial scale addressed is in the range of 100 m to a few km.

If bedload sediment in similar sizes as the main stream is supplied to a steep and armored reach in which no sediment is stored, this introduced sediment will pass through the reach rather quickly with relatively little attenuation of the sediment wave. In this case, distance to the sediment input site is not a particularly crucial factor. If sediment is supplied to a rather low gradient reach, flow capacity<sup>1</sup> might not suffice to move the newly introduced sediment, and aggradation occurs. Much of the supplied sediment will be stored in the stream bed and on bars, and can remain there for years or decades. No significant increase in transport rates is likely to be measurable downstream from an aggrading reach.

#### ***Sediment storage and storage dynamics associated with gravel bars***

As direct measurements of bedload transport may be difficult during high flows in wide streams with high sediment supply and multi-channel shifting flow, an analysis of sediment storage dynamics may be an alternative (Martin and Church 1995; Lane et al. 1995; Lane and Richards 1995). Another approach is to determine the residence time of bedload on gravel bars which is affected on how frequently flows are able to erode sediments from the surface or sides of the bar. The vegetation on the bar surface and erosion marks along the

<sup>1</sup> Flow (or transport) capacity refers to the amount of sediment transportable by flow, while flow competence refers to the largest movable sediment size.

bankline can give some indication of the stability or activity of the gravel bar, and how long gravels might have been stored. Residence times of bedload particles on gravel bars often range from years to decades. Residence times tend to increase with distance away from the channel as it will take another high flow event of similar size to reentrain these deposits. Floodplain and terrace deposits are respectively much less dynamic, and it may take centuries to millennia for lateral scour to reentrain these sediments.

Thus, an analysis of the spatial variation of stream morphology, and the spatial distribution of storage sites should provide the first insight into the spatial variability of bedload transport, and whether this variability recurs regularly or irregularly. The longitudinal variability of bedload supply, entrainment, and transport causes hysteresis effects, influences the site selection for measurements, and affect the sampling regime.

### 1.2.2.2 Cross-sectional variability

Bedload transport across the cross-section is often concentrated in one or a few narrow transport paths that may shift their locations during the high flow event. This cross-sectional variability was recorded in cobble-gravel-bed streams (Reid et al. 1985 (Fig. B-1; 17); Bunte et al. 1987; Bunte 1991, 1996; Ergenzinger et al. 1994; Powell et al. 1995), in

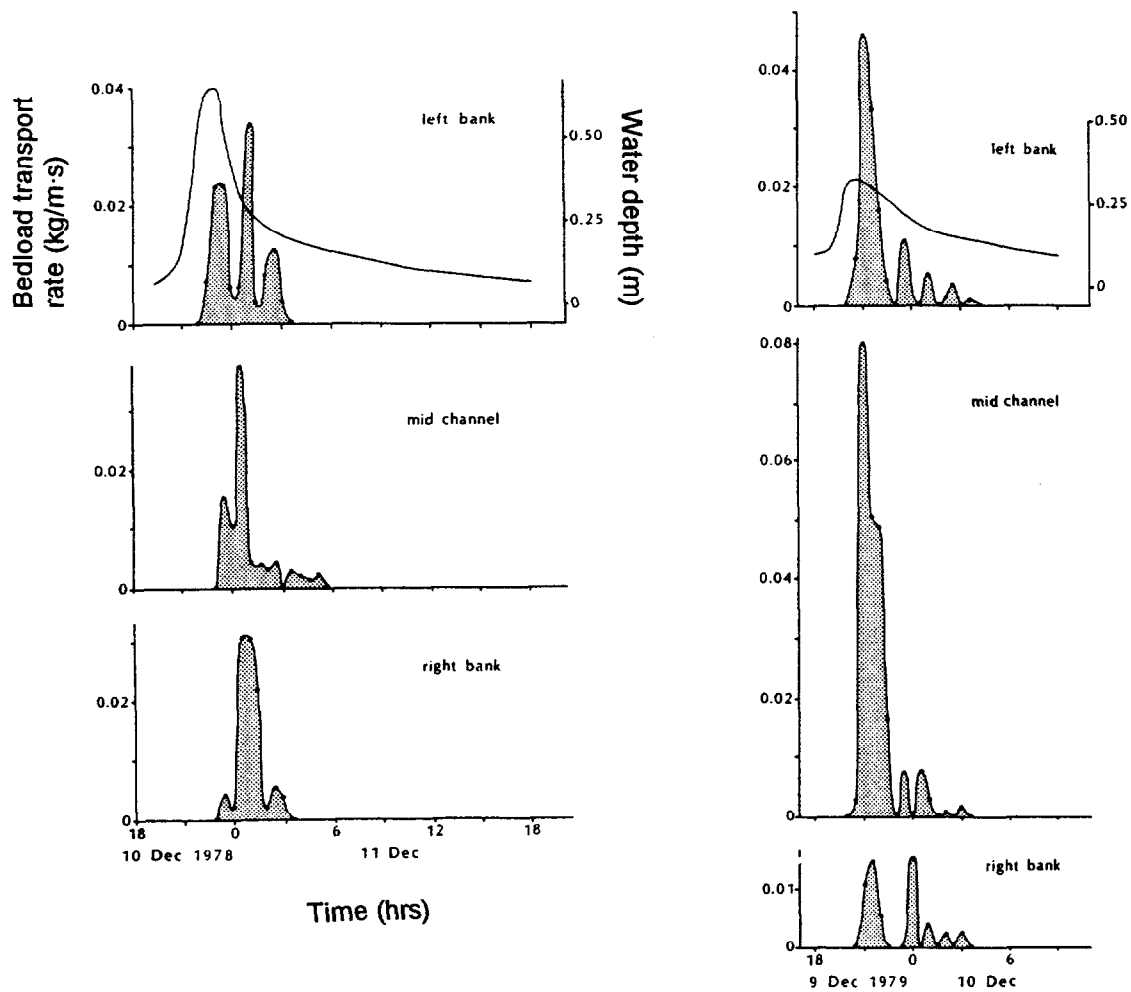


**Fig. B-1; 17:** Cross-sectional variability of coarse bedload transport for two flood events at Turkey Brook, a cobble-gravel stream in UK. Axes are the same for all individual plots (from Reid et al. 1985).

gravel-bed rivers that transport mainly sand (Pitlick 1987; Emmett et al. 1996), and in sand-bedded rivers (Mahmood and Mehrdad 1991). The lateral variation of bedload transport is not necessarily directly related to the cross-sectional channel morphology. The cross-sectional variability has implications for bedload sampling. It not only requires that bedload be measured over the entire cross-section, but it also means that some cross-sectional samples will be unmeasurably small, while others are very large. This in turn means that the duration of sampling is a compromise between sampling too much at some locations and not sampling enough at other locations (Section B-2.4.1).

***Different paths for fines and coarse particles in meander bends***

In addition to variation in the mass of bedload, the grain-size spectrum will also vary across the channel. One reason for this variability is the helical motion of secondary currents through a meander bend. This causes coarse bedload transport to shift from the inside of a bend at the upstream end of a point bar to the center of the channel a little upstream from the bend apex and then to the outside bank at the bend exit. The fine material behaves just the opposite way: from the outside bend it crosses the preferential path of the coarse material in mid stream at the bend apex to the lower end of the point bar at the bend exit (Dietrich and Smith, 1984; Anthony and Harvey, 1991; and Bridge and Jarvis, 1976; 1982) (Fig. B-1; 18). With respect to bedload transport measurements, this systematic lateral variation of coarse and fine sediments within a meandering reach means that even on riffles, the recommended sites for bedload transport measurements, bedload will be coarser on one side than on the other. This factor will have to be taken into account when choosing sampling equipment and determining appropriate sample times.

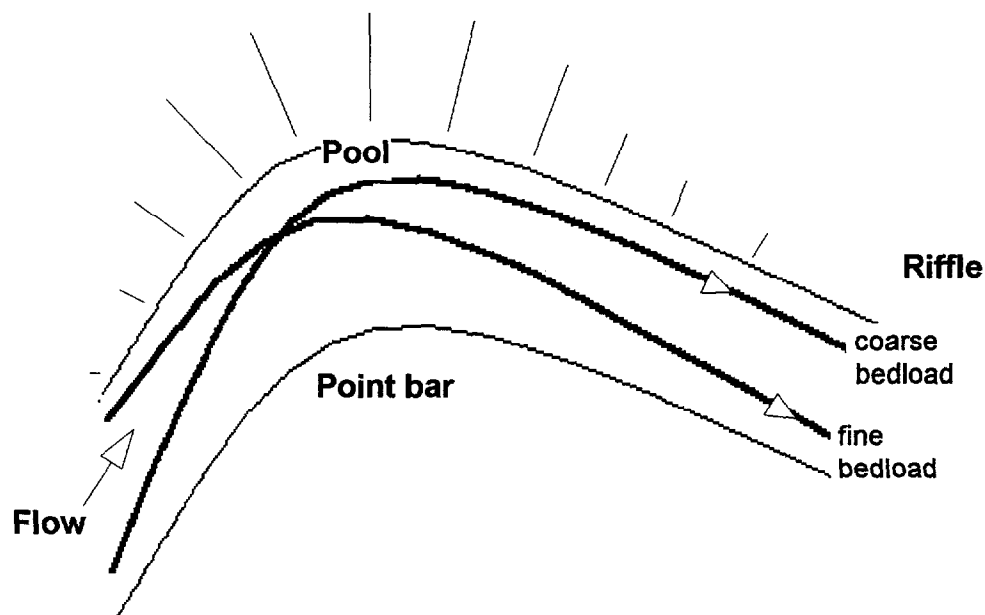


**Fig. B-1; 18:** Travel paths of coarse and fine bedload through a meander bend and possible lateral sorting of bedload grain sizes in riffle areas (after Bridge and Jarvis 1982; Anthony and Harvey 1991).

This systematic lateral variation of coarse and fine sediments within a meandering reach is also stage dependent. The cross-sectional sorting of grain size distributions is most apparent during high flows when the asymmetrical cross-sectional channel shape is best developed. During low flows, the meandering reach loses some of its asymmetrical characteristics and bedload transport becomes more evenly distributed across the channel width.

**Longitudinal streaks**

The cross-sectional variability of bedload transport rates in straight reaches is also due to longitudinal streaks of finer and coarser bed material (Parker 1992). These stem from the formation of several secondary flow cells across the channel (Nezu and Nakagawa 1984) and a concentration of bedload in the streaks with the finer sediment. Flows in neighboring flow cells swirl in opposite directions, causing either upward flow or downward flow where two flow cells meet. Downward flow diverges on the channel bottom, causing a trough and high bedload transport rates. Upward flow results from flow that converges over a longitudinal mound of coarse bed material (Ergenzinger et al. 1993, 1994; De Jong (1995), and little transport happens here (Fig. B-1; 19). As the presence of the flow cells is reflected in the cross-sectional waviness of the water surface, the water surface topography might be used as an indication of the current locations of bedload transport.

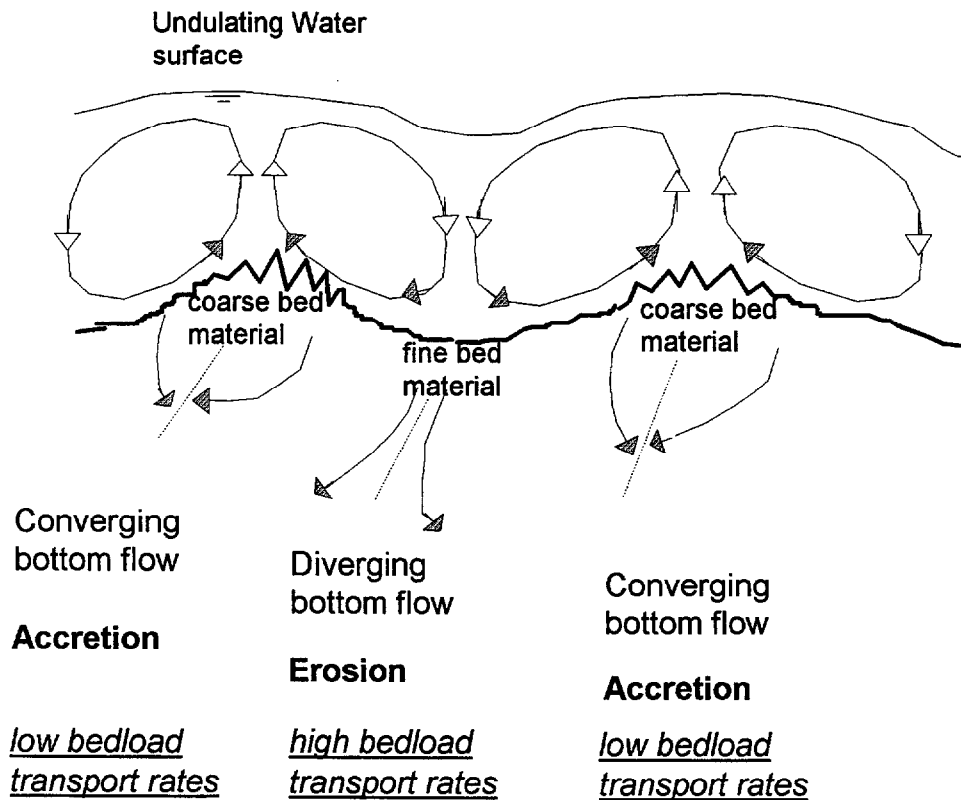


**Fig. B-1; 19:** Schematic diagram indicating the interplay between flow cells, bed material topography, channel roughness, and the lateral variability of bedload transport (after Ergenzinger et al. 1993; Ergenzinger et al. 1994; De Jong 1995).

### 1.3 Variability of suspended sediment concentration

Contrary to bedload transport, fine sediment travels mostly suspended within the water column and has little or no contact with the channel. Suspended sediment is therefore measured as part of the water flow and quantified as a concentration of solids in g/l, or as parts per million (ppm; mg/l; g/m<sup>3</sup>) if concentration values are small.

Suspended sediment is usually limited to clays (< 0.002 mm), silts (< 0.063 mm), and sands (< 2 mm). This three order of magnitude variability in transported sediment sizes causes much of the temporal and spatial variability that is usually encountered when sampling suspended sediment. Different grain sizes are mobilized from different sources at different times or flood stages, and different grain sizes have different erodibility and transportability. Hjulström's (1935) diagram (Fig. B-1; 20) depicts quite graphically that clay-sized particles require high flow velocities for entrainment, but once in motion clay may be transported over long distances before an almost zero flow velocity allows deposition. Sand, in turn, is much more responsive to flow, requiring relatively low flow velocities for entrainment. But sand also settles easily when flow velocity drops beyond a threshold value, which may readily occur in backwater or other areas.

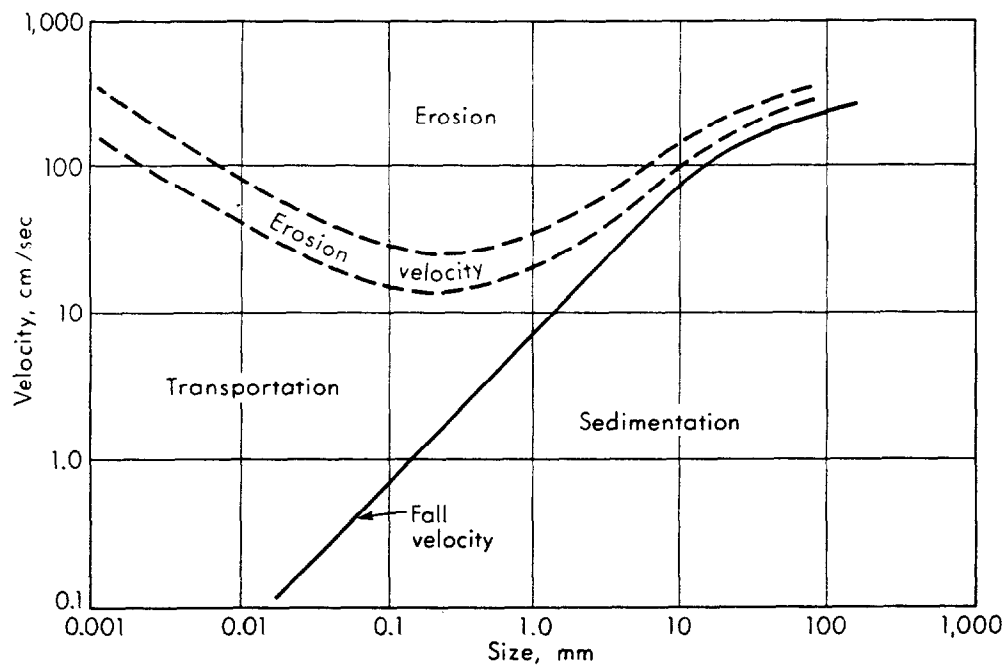


**Fig. B-1; 20:** Hjulström's curve indicating threshold velocities for erosion, transport, and deposition of different grain sizes based on a flow depth of 1 m, and uniform grain-size distributions (from Morisawa 1968).

Suspended sediment concentrations are not evenly distributed in the cross-section. Vertical distribution profiles are grain-size dependent, and concentrations tend to be highest near the bottom and towards the middle of the stream. Suspended sediment concentrations also vary in flow direction. As with bedload, consecutive measurements of suspended sediment concentration show fluctuations at constant discharge. Consecutive sampling also shows

that as discharge varies, the temporal patterns of the sedigraph do not follow the temporal patterns of the hydrograph. This temporal and spatial variability of suspended sediment causes sampling and measurement problems similar to bedload transport. In order to adjust the measurement techniques and sampling strategies to this variability both the underlying processes and the extent of this variability needs to be known. These topics will be described below. A more quantitative analysis of the accuracy of sediment loads is in chapter B-4.

The somewhat lengthy wording "suspended sediment concentration" will be abbreviated as *C<sub>s</sub>* during the remainder of this chapter.

### 1.3.1 Temporal variability

Temporal variability of *C<sub>s</sub>* can occur at different temporal scales. Fluctuations of consecutive measurements of *C<sub>s</sub>* may be referred to as *short-term*, if the fluctuations are much faster than changes in flow. If the temporal patterns of *C<sub>s</sub>* during a high flow event are different from that of the hydrograph, *intra-event* variability occurs. Intra-event variability can be different in each event, thus causing *inter-event*, or seasonal variability. The following chapters will discuss the variability of *C<sub>s</sub>* in these three temporal scales. There is also *inter-annual* variability of suspended sediment load between individual years, but this will be discussed separately in chapter B-5.

#### 1.3.1.1 Short-term variability

##### ***Turbulence and flow dynamics***

The interplay between longitudinal forces of flow, helical secondary currents, and turbulent pulsations affects the spatial and temporal distribution of fine suspended sediment within a river reach (Nemenyi 1946). The development of fast and automated measurement methods have made it possible to record discharge-independent fluctuations of *C<sub>s</sub>* within seconds, minutes (Lapointe 1992; Darbyshire and West 1993), and hours (Al-Ansari and Al-Sinawi 1988) in various flow environments, and to show the close correspondence of *C<sub>s</sub>* to the three dimensional turbulence patterns in flow velocity and other factors. These short-term fluctuations commonly extend over a factor of three or more (Fig. B-1; 21). Thus, any *C<sub>s</sub>* sampling program needs to have sufficiently long sampling times or enough repetitions to cover these fluctuations.

##### ***Instantaneous response in flashy floods***

Short-term variability can also be brought about by the abrupt onset of *C<sub>s</sub>* in a flood event. If sediments on the stream bottom are easily erodible, or if the stream receives sediment laden overland flow *C<sub>s</sub>* can increase almost instantaneously at the onset of a flood. Peak *C<sub>s</sub>* may be reached after only a few minutes and thus may occur on the rising limb of flow. Beschta (1987) showed that the peak value of *C<sub>s</sub>* may be related to the steepness of the slope of the rising limb of a storm hydrograph. A steep rise in discharge increases *C<sub>s</sub>* much more than a slow increase in discharge. Since peak *C<sub>s</sub>* values may be so large that the majority of the sediment load is transported during a relatively short period on the rising limb, it is important to start high temporal resolution sampling at the onset of a high flow event. This means that the sampling of *C<sub>s</sub>* is usually a compromise between the longer sampling necessary to capture the short term variability, and the high resolution sampling necessary to capture the rapid rise and possible early peak in *C<sub>s</sub>*.

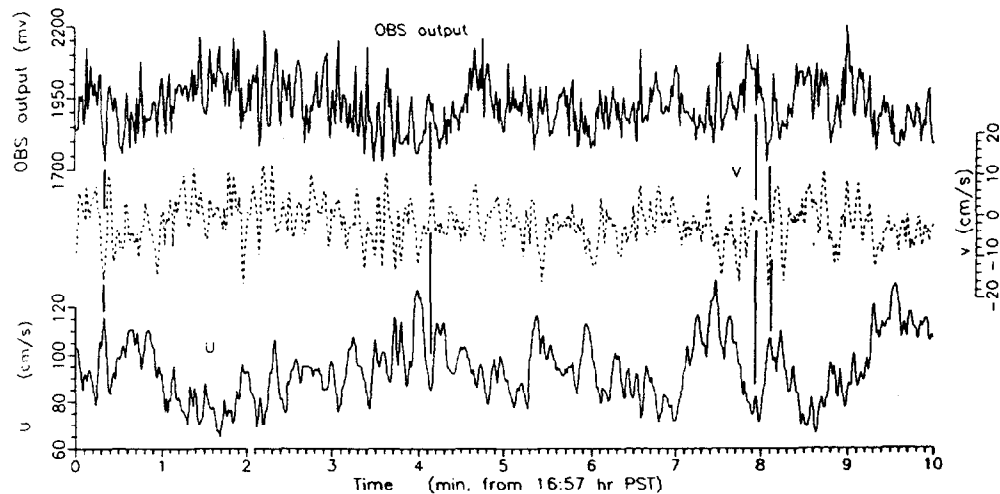


**Fig. B-1; 21:** Correspondence between turbidity (OSB output) and turbulent fluctuations of flow velocity in vertical (v) and horizontal (u) direction at the Fraser River, British Columbia (from Lapointe, 1992).

### 1.3.1.1 Intra-event variability

The intra-event variability further complicates the sampling of  $C_s$  over a high flow event, as the temporal variability of  $C_s$  may not correspond to the rising and falling of the hydrograph. There is an abundance of literature documenting the various kinds of temporal variability of  $C_s$  during high flow events. The multitude of observed phenomena, and the variety of processes to which the phenomena are attributed are too numerous to be individually discussed and reviewed in this report. This study will therefore mostly refer to summary reports on the temporal variability of  $C_s$  and focus on the most commonly observed temporal patterns.

#### ***Lead and lag in $C_s$***

In many studies peak  $C_s$  occurs prior to peak discharge (e.g., Walling 1977a; Walling and Webb 1987, 1988; Goodwin and Denton 1991). This lead in  $C_s$  over discharge is usually attributed to readily available sediment either from instream or from near-stream sources. Often  $C_s$  not only increases abruptly, but also decreases rather quickly. Besides the depletion of sediment sources, a decrease in  $C_s$  during a flood event can result from clear water inputs from tributaries and subsurface flow (Walling and Webb 1987).

A lag in  $C_s$  over discharge is less commonly observed than a lead. Lags in  $C_s$  are encountered when a rather high threshold discharge has to be exceeded to initiate sediment transport. This may be the case in clayey lowland streams with a relatively low sediment erodibility. In gravel-bed rivers, a delayed response of  $C_s$  could be due to the breaking up of the armor layer, as this usually takes some time to develop. Other reasons for the belated onset of  $C_s$  can be a long distance between the sediment source (e.g., sediment laden tributary) and the measuring site.

**Several peaks in Cs**

During a high flow event suspended sediment will usually be produced by several processes active at different times and locations in the stream and in the watershed. This temporal and spatial variability in sediment production may cause several peaks in *Cs* during a flood event. Gilvear and Petts (1985), and Petts (1987) reported the successive response of *Cs* to various instream factors during a controlled reservoir release, in which case the usual spatially and temporally varying processes within the drainage basin can be ignored (Fig. B-1; 22). In this study the arrival of the flood wave immediately brought easily detachable sediments into suspension. The resulting peak in *Cs* was followed by another peak generated by scour in local storage zones. A third peak in *Cs* resulted from the arrival of suspended sediment from upstream, because the propagation of the floodwave was faster than the mean velocity of the flow. Such individual responses are often difficult to distinguish in a temporal record, as individual waves of *Cs* may blend into each other, creating a seemingly random variation of *Cs* during relatively steady flow. A distinction between sediment from different sources requires a qualitative analysis of the suspended sediment properties, such as its grain-size distributions, mineralogy, and the organic matter content. Other processes, such as bank collapse or the breakage of a debris dam, can also cause pulses in *Cs* during relatively steady flows. For these reasons suspended sediment sampling needs to be continued throughout a high flow event, since any decrease in *Cs* may only be temporary.

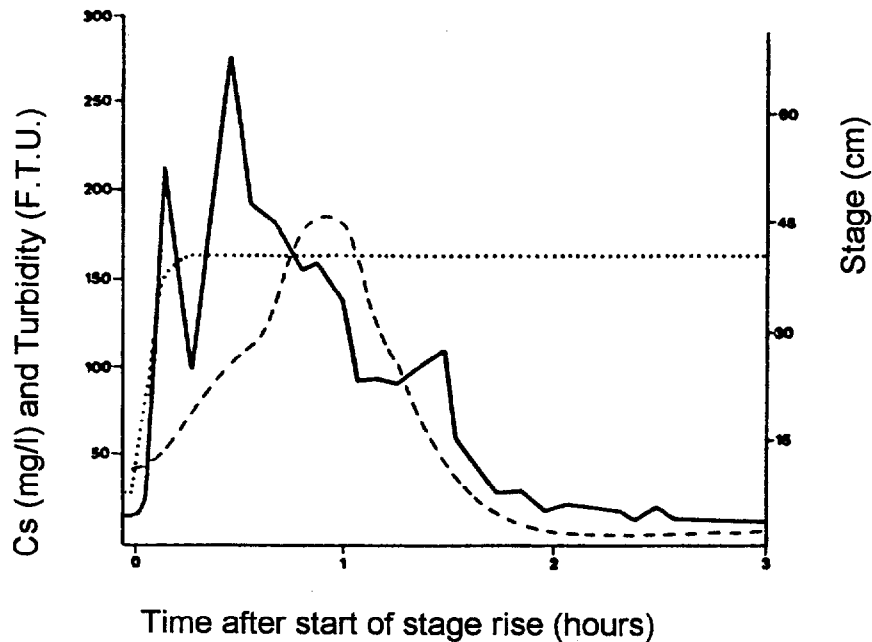


**Fig. B-1; 22:** *Cs* (solid line), turbidity (dashed line), and stage (dotted line) during a reservoir release at Llyn Celyn, about 8 km downstream from the reservoir (from Gilvear and Petts 1985).

**Hysteresis shapes**

To calculate the event sediment load, *Cs* is commonly plotted over discharge to obtain a rating curve. Time-increment discharge values from the hydrograph are then multiplied by the respective *Cs* values from the rating curve and summed (see chapter B-4 for different methods of using a rating curve). A close correspondence between *Cs* and discharge leads to a power function relationship that plots as a straight line on log-log paper. But if *Cs* and

discharge do not rise and fall concurrently, which is usually the case, the serially connected data points of the rating curve deviate from a straight line, plotting as a bent curve or a hysteresis loop. The graphical shape of the rating curve is therefore often used as a means to describe the temporal relationship between  $C_s$  and the hydrograph.

Olive and Rieger (1984) (cited after Pickup 1988), Olive and Rieger (1985), and Rieger and Olive (1986) identified seven different types of responses of  $C_s$  during 39 storm events monitored in five catchments of the Wallagaraugh River in New South Wales, Australia (Fig. B-1; 23). The  $C_s$  responses are summarized in Table B-1: 3.

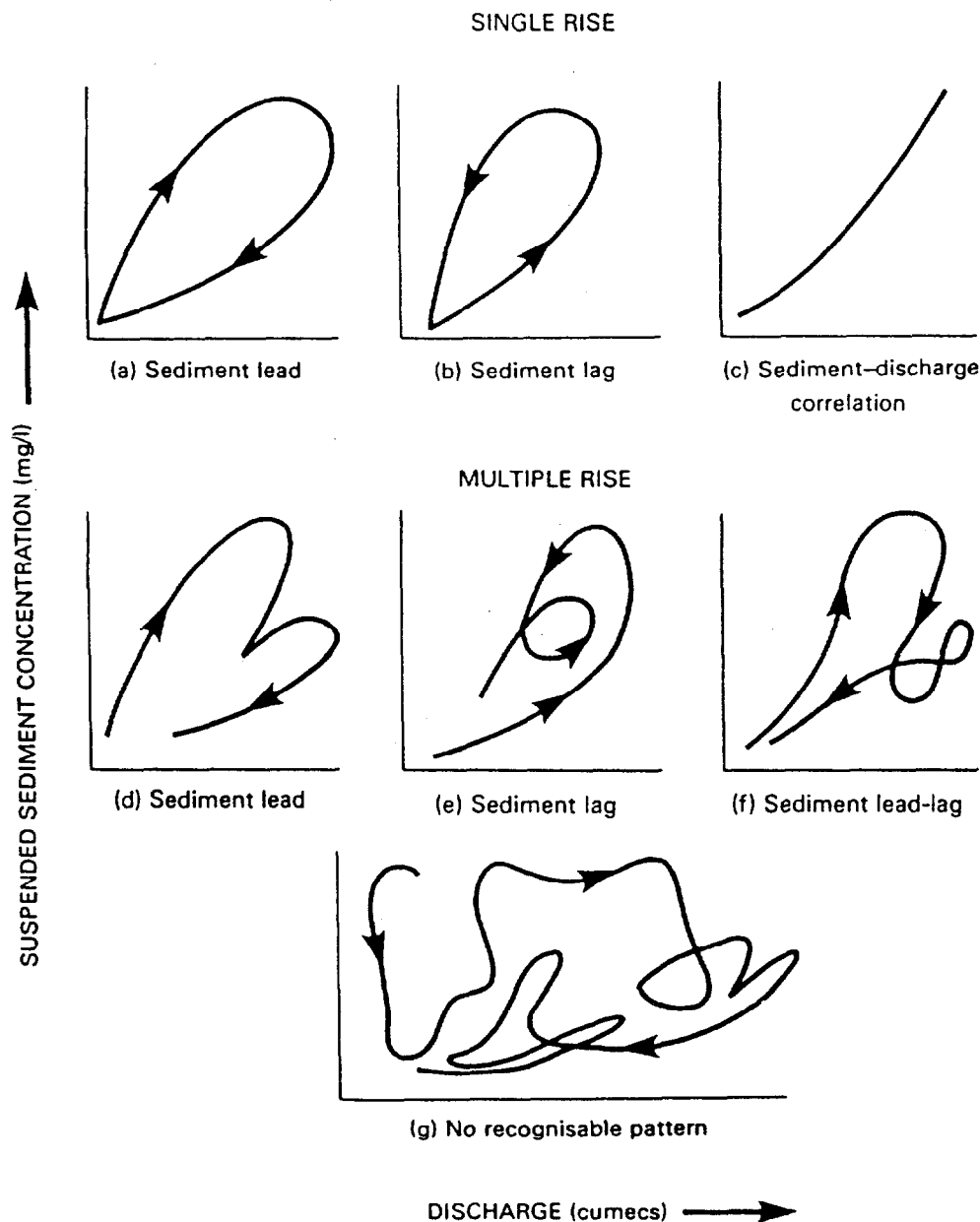


Fig. B-1; 23: Different shapes of hysteresis loops in Australian rivers (from Rieger and Olive 1986).

**Table B-1; 4:** Hysteresis shapes and temporal variability of  $C_s$  in relation to discharge (after Rieger and Olive (1986)).

Hysteresis shape	Temporal relation between $C_s$ and discharge
<ul style="list-style-type: none"> <li>• single rise with</li> </ul>	<ul style="list-style-type: none"> <li>- sediment lead</li> <li>- discharge and sediment correlation</li> <li>- sediment lag</li> </ul>
<ul style="list-style-type: none"> <li>• multiple rise with</li> </ul>	<ul style="list-style-type: none"> <li>- sediment lead</li> <li>- sediment lag</li> <li>- both lead and lag response</li> </ul>
<ul style="list-style-type: none"> <li>• random</li> </ul>	

None of these streams maintained a consistent pattern in the response of  $C_s$  throughout the study period, except for a threshold storm size that had to be exceeded in order to initiate a  $C_s$  response. However, the threshold storm size varied between catchments and storms, and was only vaguely related to a combination of rainfall intensity, antecedent moisture conditions and total rainfall. Within individual events  $C_s$  could vary by a factor of 2-10 times for a given discharge.

An even more substantial catalogue with examples of any imaginable relationship between  $C_s$  and discharge was assembled by Williams (1989). A shortened and simplified version of his table is given in **Table B-1; 5**.

**Table B-1; 5:** Various hystereses shapes in the relation between suspended sediment concentration and discharge (after Williams 1989).

Class	Relation between suspended sediment and discharge
I	Single-valued line (i.e., no hysteresis) <ul style="list-style-type: none"> <li>- Straight line</li> <li>- Curve with increasing slope for high values of Q</li> <li>- Curve with decreasing slope for high values of Q</li> </ul>
II	Clockwise loop
III	Counterclockwise loop
IV	Single line plus loop
V	Figure eight

These two collections of data indicating the lack of correspondence between  $C_s$  and the hydrograph emphasize the need to sample suspended sediment with a high temporal resolution throughout each high flow event. A fixed-interval, weekly, or perhaps even daily sediment sampling scheme may be sufficient to indicate a long-term trend, but low intensity, fixed-term  $C_s$  measurements do not provide the basis for accurate event and annual sediment load computations. The accuracy of sediment load estimates is critical for detecting CWEs and this will be discussed in greater detail in chapter B-4.

### 1.3.1.2 Inter-event variability of $C_s$

As already indicated by Rieger and Olive (1986), the temporal patterns of  $C_s$  are often different for each high flow event at a given stream site. Apart from the magnitude of the high flow, this inter-event variability may be attributed to several factors, such as the:

- time since the last flood,
- magnitude of the previous flood,
- seasonal variability in sediment erodibility,
- seasonal variability in sediment sources, and
- seasonal variability in the erosivity of high flow events.

A long time between events may allow a build up of sediment supply during small events, while sediment supply can be exhausted if floods follow in quick succession. Thus the first flood in the Sacramento River (California) after the dry summer period had a markedly higher  $C_s$  than later storms (Goodwin and Denton, 1991).

The magnitude of the previous flood often affects the  $C_s$  of a following flood. Supply depletion can lead to lower  $C_s$  when the flow event occurred after annual peak discharge as Beschta (1987) found for three undisturbed rivers in the Oregon Coastal Range. A similar effect was observed over a 10-day period during a snowmelt high flow in southwest Montana (Bunte et al. 1987). Peak sediment concentrations during consecutive high-flow days with similar peak discharges decreased strongly, until a somewhat higher discharge peak introduced another source of sediment.

Seasonal changes in the sediment erodibility may also lead to seasonal changes in the response patterns of  $C_s$ . A vegetation cover protects off-stream sediment sources from erosion and transport (Walling 1977a), while soil crusting and sealing reduce infiltration, and thus increase runoff and erosion.

A seasonal variation of sediment sources and sediment loads was documented by Bathurst et al. (1986) at the Roaring River in Rocky Mountain National Park. The onset of snowmelt highflow flushed fine sediments from instream locations, and the finest sediments were transported in suspension. A further increase in flow provided a high sediment input from the channel margin and slumping gorge walls. As snowmelt flows receded, the gorge wall stabilized. Mean and peak suspended sediment discharge decreased to about 60% and 12 to 25%, respectively, of the comparable values for similar flows on the rising limb. Summer storms caused heavy rill erosion on the bare sides of the gorge, increasing mean and peak suspended discharge by almost two and one order of magnitude, respectively, compared to similar discharges during the rising limb of snowmelt.

Seasonal changes in the erosivity of the flow may be caused by the seasonal change of the hydrograph shape, and this again can lead to seasonally different  $C_s$  responses (Walling 1977a). Prolonged winter rain from frontal systems, for example, mainly leads to groundwater inflow into the stream. The rather low erosivity of those slowly increasing floods, and the small sediment transport capacity of the low peak flows result in low  $C_s$ . Rapidly increasing flashy summer floods from thunderstorms have higher peak flows and steeper water surface slopes, and are thus more erosive than slowly increasing flows.

The natural inter-event variability may be so large that it becomes difficult to detect a change in sediment loads as a result of watershed impacts. Olive and Rieger (1991) found that suspended sediment concentrations following disturbance were frequently within the

observed range prior to disturbance so the natural variability of the system was greater than the magnitude of any increase associated with basin disturbance.

### ***Rating curve variability***

Inter-event changes in the  $C_s$  response to flow necessarily lead to different rating curves for each event. While a rating curve for an individual high flow event can already have an order of magnitude variation in  $C_s$  for a given flow, rating curves for combined events can have even more variability, according to the number and magnitude of the events. The combined rating curve for a sequence of six storms which each had a different rating curve had  $C_s$  values varying over 1.5 orders of magnitude (Beschta 1987). Walling and Webb (1988) obtained a scatter of three orders of magnitude when they combined all floods at the river Dart in GB over a 10-year period.

Since the  $C_s$  response may be different in each flood event, rating curves are usually not interchangeable between floods. This means that if an accurate sediment load estimate is desired each flood event has to be monitored, and sediment loads have to be calculated for each flood. Annual or long-term sediment loads can be very inaccurate when based on a single rating curve. The accuracy of sediment load estimates based on rating curves for different time intervals will be discussed in detail in chapter B-4.

## **1.3.2 Spatial variability of suspended sediment concentration**

Suspended sediment concentrations vary throughout the depth of the water column, across the stream, and longitudinally along the stream channel. While the temporal variability of  $C_s$  has implications for the duration and scheduling of the sampling, the spatial variability has implications for the number of vertical and lateral measurements as well for the location of the measurements within the stream network.

### **1.3.2.1 Vertical variation**

#### ***Effects of sediment size and energy of flow***

The vertical distribution of  $C_s$  is usually described by diffusion theory (Rouse 1937). The other models described in Raudkivi (1976) are less commonly employed, and will therefore not be discussed here. In the diffusion theory, the vertical distribution of  $C_s$  is dependent on particle size and flow. Fine particles with low fall velocities in fully turbulent flow are kept in suspension by dispersion processes, resulting in an even vertical distribution. The same turbulence intensity of flow may not be large enough to keep coarse particles with high fall velocities evenly suspended throughout the water column. Thus, the concentration of coarse particles increases towards the bottom of the stream.

Assuming a logarithmic velocity profile, Rouse (1937) quantified the vertical distribution of  $C_s$  as follows: if flow depth is normalized by the ratio of  $y$  (observation height above ground) to  $d$  (total depth), and  $C_s$  is normalized by the ratio of  $C_y$  (concentration at a height  $y$ ) to  $C_a$  (concentration at a known reference height  $a$  close to the stream bottom where  $a$  equals  $0.05 d$ , concentration profiles will vary according to the value of  $z$  (which is basically the ratio of particle size to flow intensity).  $z$ , also called the Rouse number, is dimensionless and defined as

$$z = \frac{w}{\kappa \cdot v^*} \quad (1)$$

where  $w$  is particle fall velocity,  $v^*$  is shear velocity ( $\sqrt{g \cdot d \cdot S}$ ), where  $g$  is acceleration due to gravity and  $S$  is water surface slope.  $\kappa$  is the von Karman constant (and this has a value of 0.4 for clear water flows). Fall velocity for fine sediment of nearly spherical shape can be computed from the Stokes' equation:

$$w = \frac{2g \cdot D^2 \cdot (\rho_s - \rho_f)}{18\nu}$$

where  $D$  is particle size,  $\rho_s$  and  $\rho_f$  are sediment and water density,  $\nu$  is kinematic water viscosity). Finally, the concentration profiles are given by

$$\frac{C_y}{C_a} = \left[ \left( \frac{d-y}{d-a} \right) \frac{a}{y} \right]^z \quad (2)$$

A group of concentration profiles for different values of the exponent  $z$  is shown in **Fig. B-1; 24a**. Steep concentration profiles with small values of  $z$  are either obtained by high energy flow, or by fine sediment. For a given flow intensity, **Fig. B-1; 24b** shows the grain-size dependent vertical distribution of  $C_s$ . Vertical concentration profiles for different grain-size fractions measured in various streams (e.g., Hubbell and Matejka 1959; Colby 1963; Guy 1970) approach the theoretical distributions, but do not give a perfect match (**Fig. B-1; 25**).

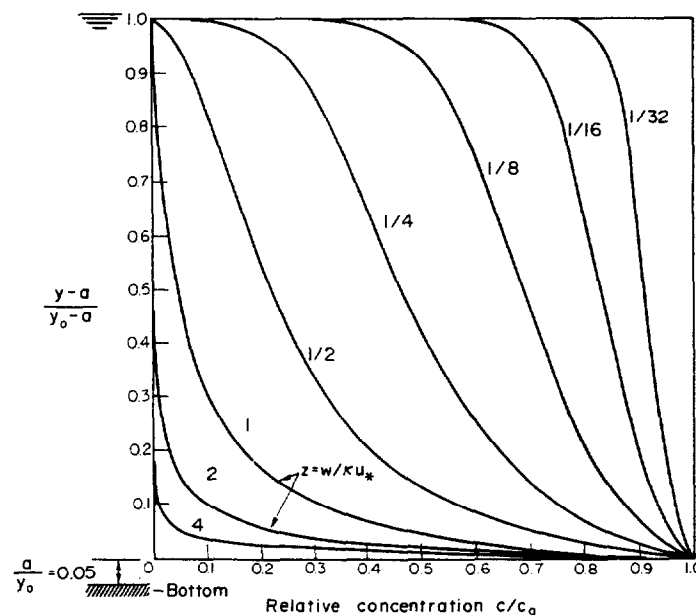


**Fig. B-1; 24a:** Theoretical vertical distribution of relative suspended sediment concentration in a flow profile. Numbers on the curves express the ratio  $z = w/k \cdot v^*$  where  $w$  = particle fall velocity,  $v^*$  = shear velocity, and  $k$  = the von Karman constant (from Raudkivi 1976).

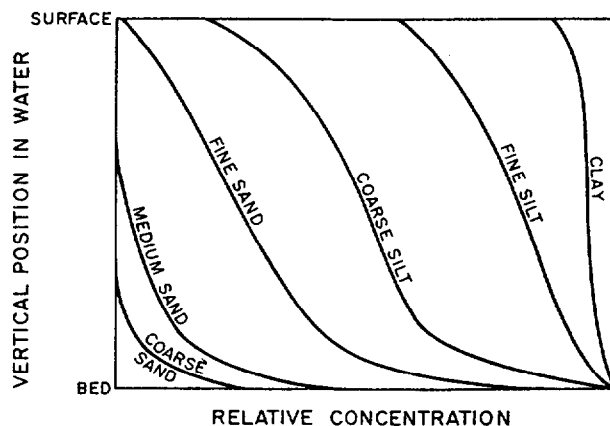


**Fig. B-1; 24b:** Theoretical vertical distribution of relative suspended sediment concentration in a flow profile. For a given flow, the value of  $z$  increases with particle size. Clay has an almost homogeneous vertical distribution, while sand is concentrated near the bottom of the stream (from Beschta 1987).

Several reasons are stated for the deviation between measured and predicted vertical concentration profiles. Colby (1961) noted that concentration profiles differ for high and low flow velocities, and for deep and shallow flows (Fig. B-1; 26). Nordin and Demster (1963) pointed out that the vertical distribution of  $C_s$  is similar to that predicted by Rouse (1937) only when flow is at the lower flow regimes featuring a dune bed, but that the vertical distribution of  $C_s$  is more uniform than predicted when flow is at the upper regime producing a plane bed. Nordin and McQuivey (1971) indicated that the vertical distribution of  $C_s$  is determined not only by the mean flow velocity, but also by the shape of the velocity profile. Not all streams exhibit a logarithmic velocity profile and this is particularly true for coarse bedded mountain streams (Marchand et al. 1984). Given the same mean flow velocity for a logarithmic, parabolic, and linear velocity profile, Nordin and McQuivey (1971) calculated the respective  $C_s$ - profiles (Fig. B-1; 27). Setting the calculated sediment load for a logarithmic velocity profile as 1, parabolic and linear velocity profiles increase the depth-integrated sediment load by factors of 1.3 and 1.7, respectively.

Raudkivi (1976) summarized additional evidence that vertical  $C_s$  profiles deviate from the model proposed by Rouse (1937). In particular, the velocity profiles are usually not logarithmic in real stream situations; that the velocity profile itself is affected by  $C_s$ , causing flow to slow at the bottom and increase near the water surface as the  $C_s$  concentration increases; the value of the von Karman constant  $\kappa$  decreases with  $C_s$  because  $C_s$  dampens the turbulence; and the effects of secondary currents on  $C_s$  is not fully understood. The interplay between local turbulence or hydraulics and  $C_s$  is still being analyzed using high resolution measurement techniques. Results of this research are discussed in Bechteler (1986) and Clifford et al. (1993).

Since the vertical distribution of  $C_s$  cannot be well predicted, it is necessary to sample  $C_s$  over the entire flow depth. This can be done by taking samples at several vertical locations or by using depth-integrated sampling. Another alternative is to select sample sites where complete vertical mixing occurs, such as at a free overfall.

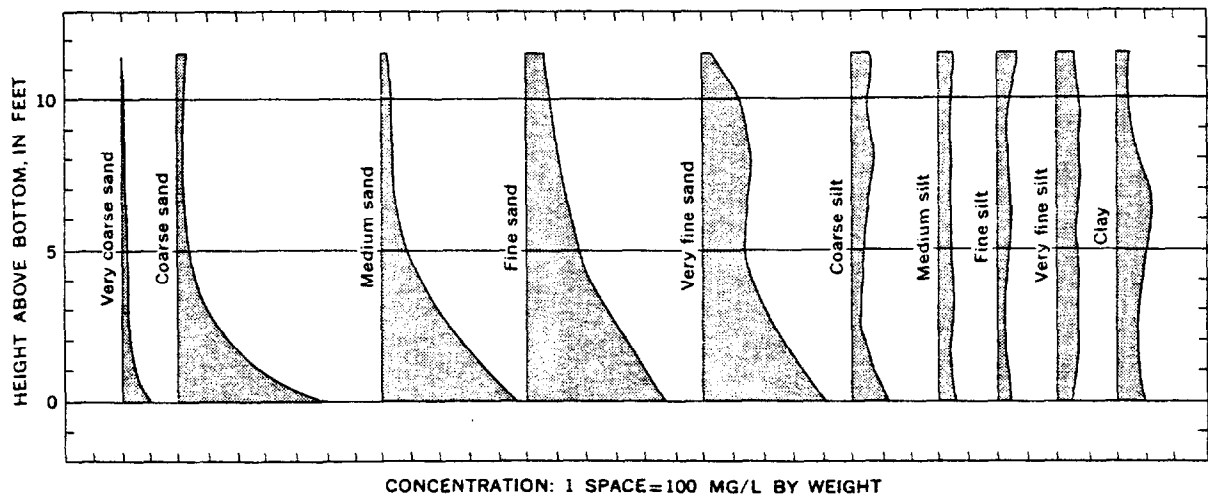
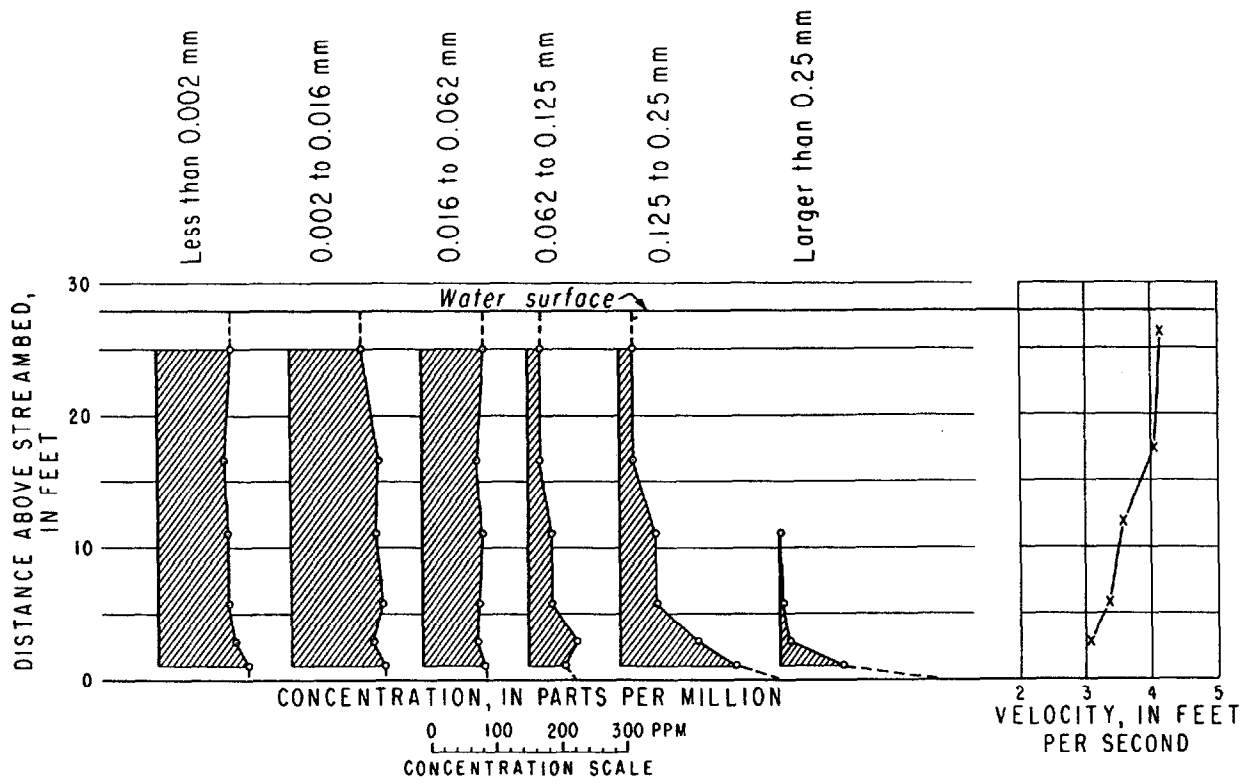


**Fig. B-1; 25:** Measured vertical distributions of suspended sediment at the Mississippi River at St. Louis (from Colby 1963) (top), and the Missouri River at Kansas City (from Guy 1970) (bottom).

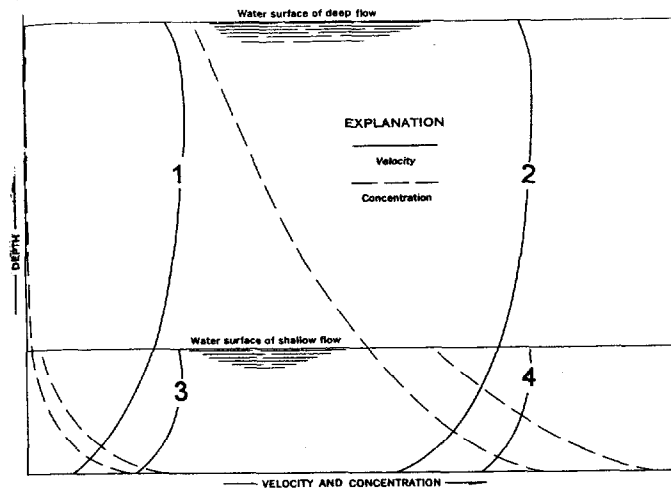


**Fig. B-1; 26:** Effect of flow depth and velocity on the vertical distribution of  $C_s$  in slow (curves 1 and 3) and fast (curves 2 and 4) flow of deep (curves 1 and 2) and shallow (curves 3 and 4) water (from Colby 1961; 1964).

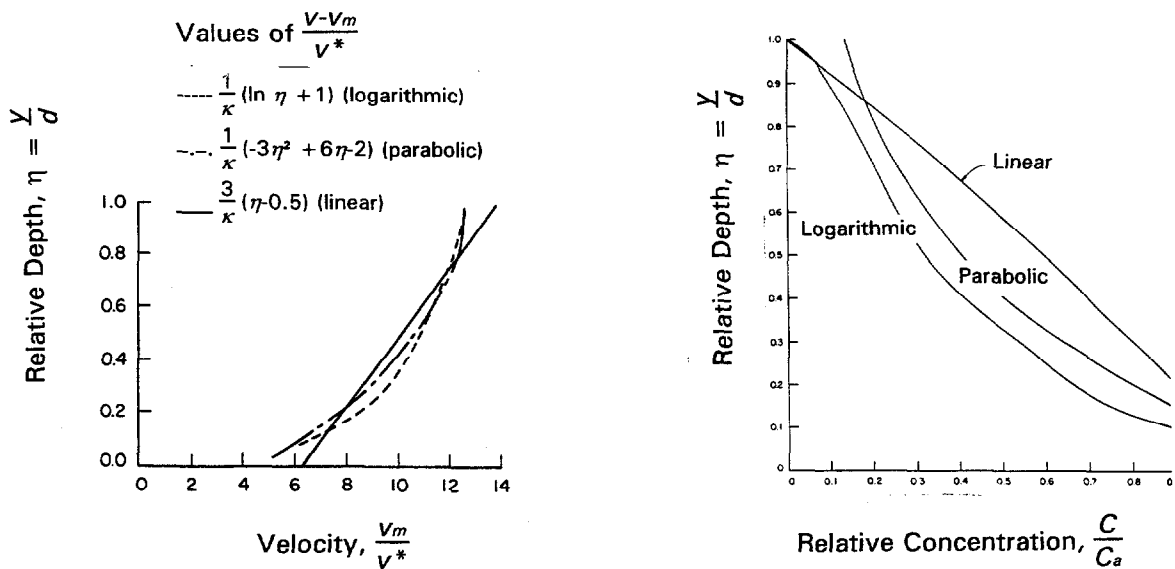


**Fig. B-1; 27:** Effect of velocity profile (parabolic, logarithmic, and linear) on the vertical  $C_s$  distributions (from Nordin and McQuivey 1971). Velocity profiles (left), vertical  $C_s$  distributions (right).

#### ***Effect of water temperature on the vertical distribution of suspended sediment***

Water temperature also affects the vertical distribution of  $C_s$ , because cold water temperatures increase water viscosity which, in turn, reduces the particle fall velocity (Colby 1964; Colby and Scott 1965; Hong et al. 1984). The results of the analyses by Hong et al. (1984) are replotted in Fig. B-1; 28. Depending on the energy of the flow, a temperature drop from 30°C to 0.4°C increases the vertically-averaged mean  $C_s$  by a factor of 7 for moderate flows with a Froude number ( $Fr = v^2/g \cdot d$ ) of 0.5, and by an order of magnitude for  $Fr = 0.85$ . Bottom sediment concentration  $C_b$  was increased by a factor of 2.6 for  $Fr = 0.5$ , and a factor of 4.1 for  $Fr = 0.85$ . Temperature did not have any significant effect on  $C_s$  for flows with  $Fr = 0.3$ , as bottom sediment concentrations were very low.

#### **1.3.2.2 Lateral variability**

According to the model by Rouse (1937) the vertically-averaged  $C_s$  for a given grain size should be at a maximum at the *deepest* location in the cross-section, and decline as depth becomes shallower. Several measurements of the lateral distribution of  $C_s$  have confirmed that  $C_s$  is generally lower near shallow stream banks. However the lateral distribution of  $C_s$  across the stream has been shown to deviate from the Rouse model and vary between individual cross-sections, between streams, between floods, and with stage. Flow velocity, bed topography, and the source of the suspended sediment all seem to play a major role.

#### ***Effects of bed morphology and flow hydraulics***

An analysis of the detailed measurements of stream bed topography, flow velocity and  $C_s$  (Hubbell and Matejka, 1959) at the Nebraska Middle Loup River, a sand-bedded river, suggests that the locations of *peak*  $C_s$  usually correspond with bar faces where flow depths and velocities are relatively low. Secondary peaks in  $C_s$  mainly coincide with locations of high flow velocity (Fig. B-1; 29) Colby's (1963) measurements at the sand-bed Niobrara River indicated that peak  $C_s$  coincides with both the bar face and the highest flow velocities in the cross-section (Fig. B-1; 30). In this case the local maximum in  $C_s$  results from an increase in coarse suspended particles, while the concentration of silt is evenly distributed over the cross-section.

Culbertson (1977) documented the cross-sectional variation of coarse and fine  $C_s$  for the sand-bedded Rio Grande near Bernardo, NM, a stream about 23 m wide and 1.3 to 1.8 m deep. While the  $C_s$  of sand generally followed the expected vertical distribution and showed little lateral variation the  $C_s$  of silt and clay seemed to follow secondary flow patterns (Fig. B-1; 31). However, as values for  $C_s$  of sand range from 350 to 3000 mg/l for different cross-sectional locations, suspended sand has a much greater potential for causing sampling errors than the chaotic, but in terms of magnitude almost negligible variation of fines within a range of less than 10%.

#### ***Effects of total $C_s$ and tributary influence***

Tributaries may carry the same or a different  $C_s$  as the main stream, and the ratio of tributary  $C_s$  to main stream  $C_s$  may vary within a flood and between floods. Thus, the longitudinal distribution of  $C_s$  within a stream network changes with stage, between floods, and over time, and is consequently not very predictable by models. Martens (1995) presents four instantaneous pictures of the vertical and lateral variability of  $C_s$  and its grain-size distribution in the Lainbach, an Alpine gravel-bed stream in Bavaria, Germany, with a stream width of 10-15 m, and a mean flow depth of 0.4 to 0.6 m. The measurement site is

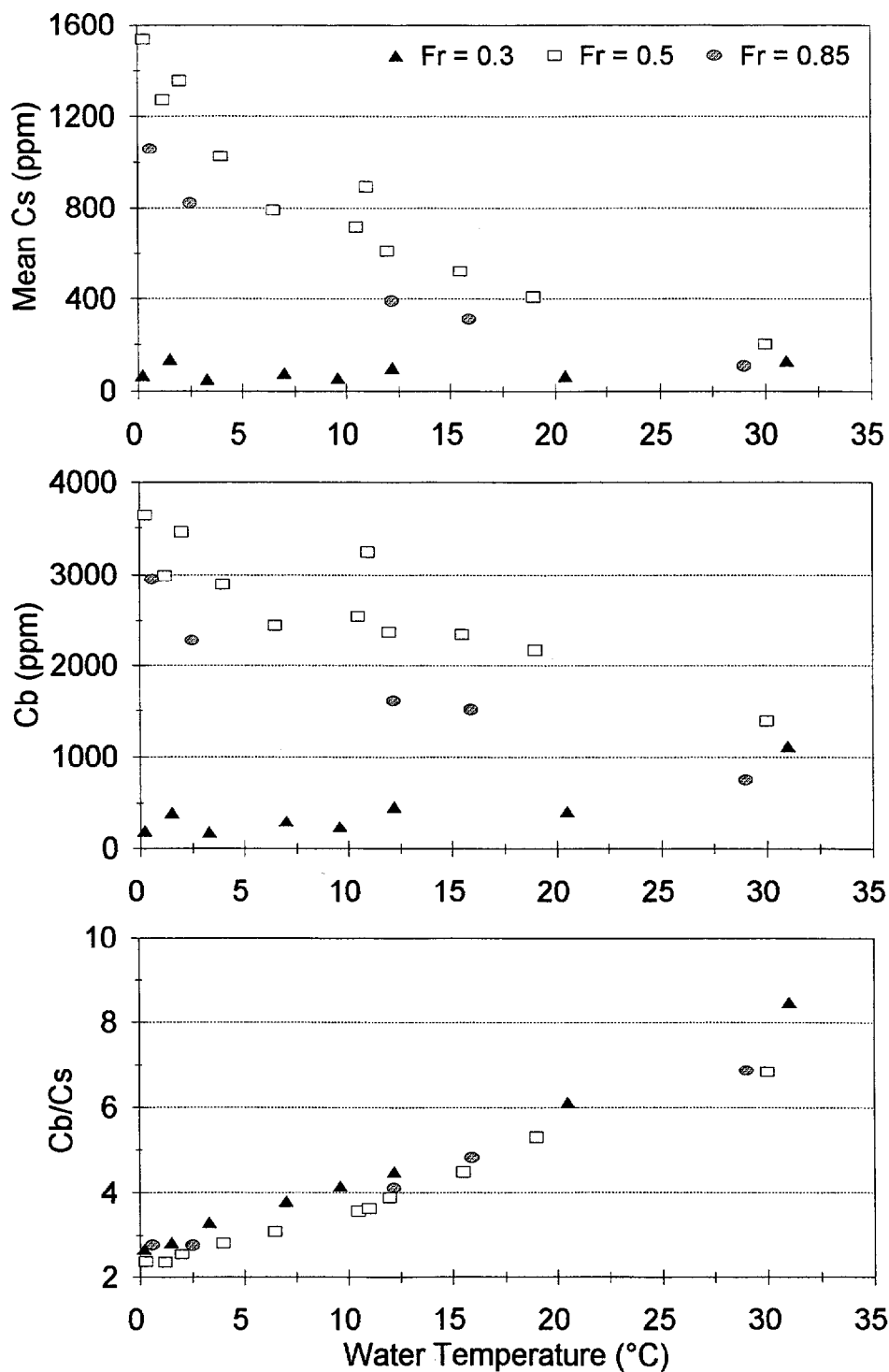


**Fig. B-1; 28:** Effect of water temperature on mean  $C_s$  in a vertical profile (top); on the bottom sediment concentration  $C_b$  (center); and the ratio of  $C_b/C_s$  (bottom) (replotted from Hong et al., 1984).

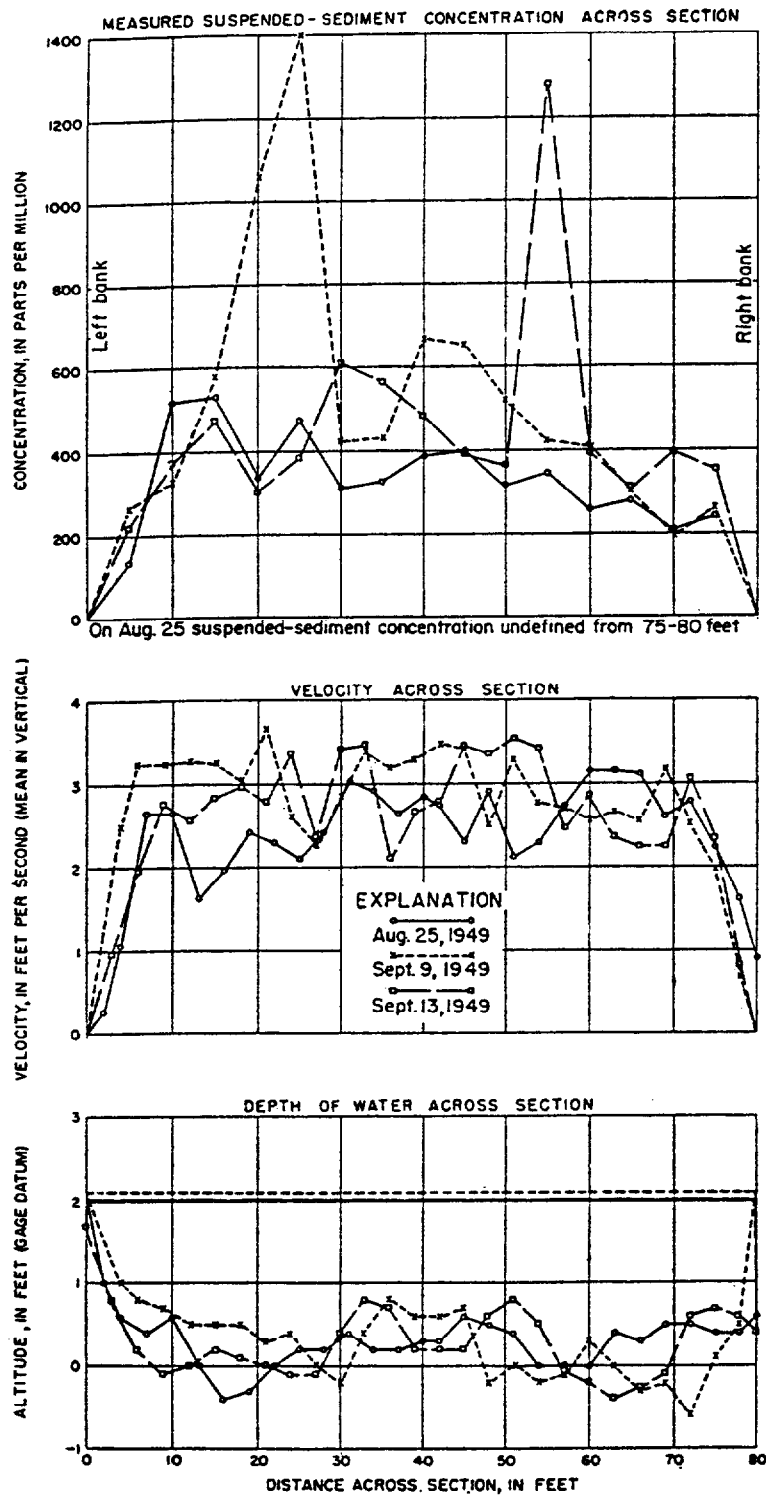
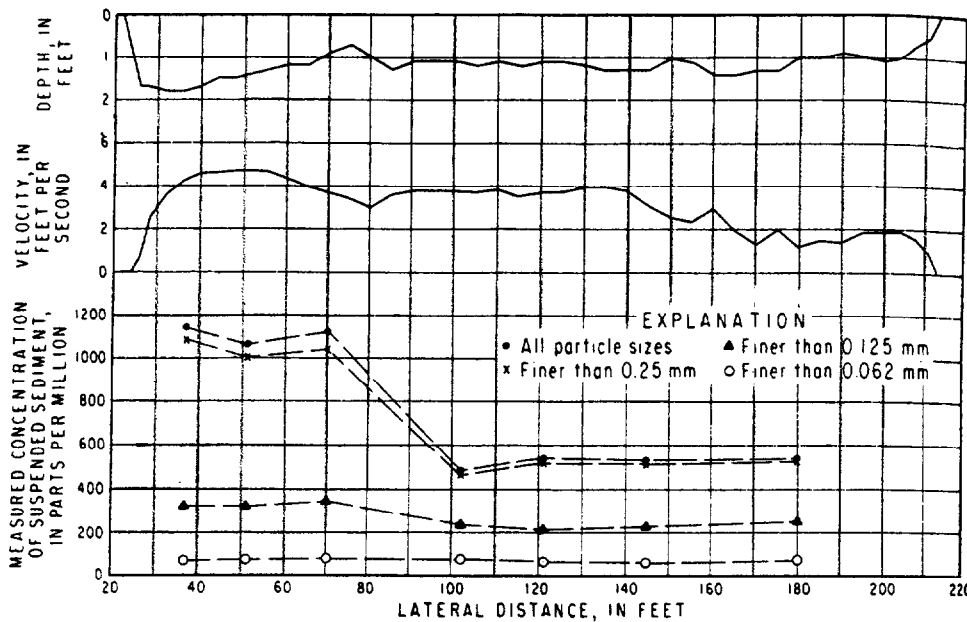


Fig. B-1; 29: Lateral distribution of suspended sediment concentration (top), stream flow velocity (center), and flow depth (bottom) at section C in the Middle Loup River in Nebraska (from Hubbell and Matejka, 1959).



**Fig. B-1; 30:** Lateral distribution of depth, stream velocity, and  $C_s$  at the Niobrara River near Valentine, Nebraska (from Colby 1963).

about 300 m downstream from a major confluence. Each picture was derived from about 20 samples, and samples were taken in three storm events with different total  $C_s$ . In floods with low and medium  $C_s$ , the cross-sectional distributions of  $C_s$  basically followed the Rouse diffusion model.  $C_s$  was highest in the deepest portion of the stream. The percent sand was highest near the bottom in the center of the stream, while the maximum concentration of silt and clay was near the stream surface. Thus the vertically-averaged percentage sand is highest in the center of the stream, while the vertically-averaged percentage silt and clay is lowest near the center of the stream.

As total  $C_s$  increased during other floods, the cross-sectional distribution of  $C_s$  shifted from horizontal stratification to diagonal and lateral stratification. During a small flood with high total  $C_s$  the percent sand was highest at one side of the stream. On the other hand, the silt and clay became concentrated in the center of the stream when total  $C_s$  was high.

Some of this variation in cross-sectional distribution of  $C_s$  may reflect a tributary influence. The joint flow length of roughly 300 m was probably not enough for complete mixing of the water from the two tributaries with different  $C_s$  and different grain-sizes. Other reasons for deviations from the expected pattern of  $C_s$  may include bank collapse, or local scour.

The inability to accurately predict the lateral variability in  $C_s$  for the stream just discussed makes it necessary to sample suspended sediment over the entire cross-section. Martens (1995) determined that the cross-sectionally averaged  $C_s$  would be underpredicted by almost 50% if samples were only taken close to the left bank; taking only one sample in the center of the stream would overpredict  $C_s$  by almost 50%.

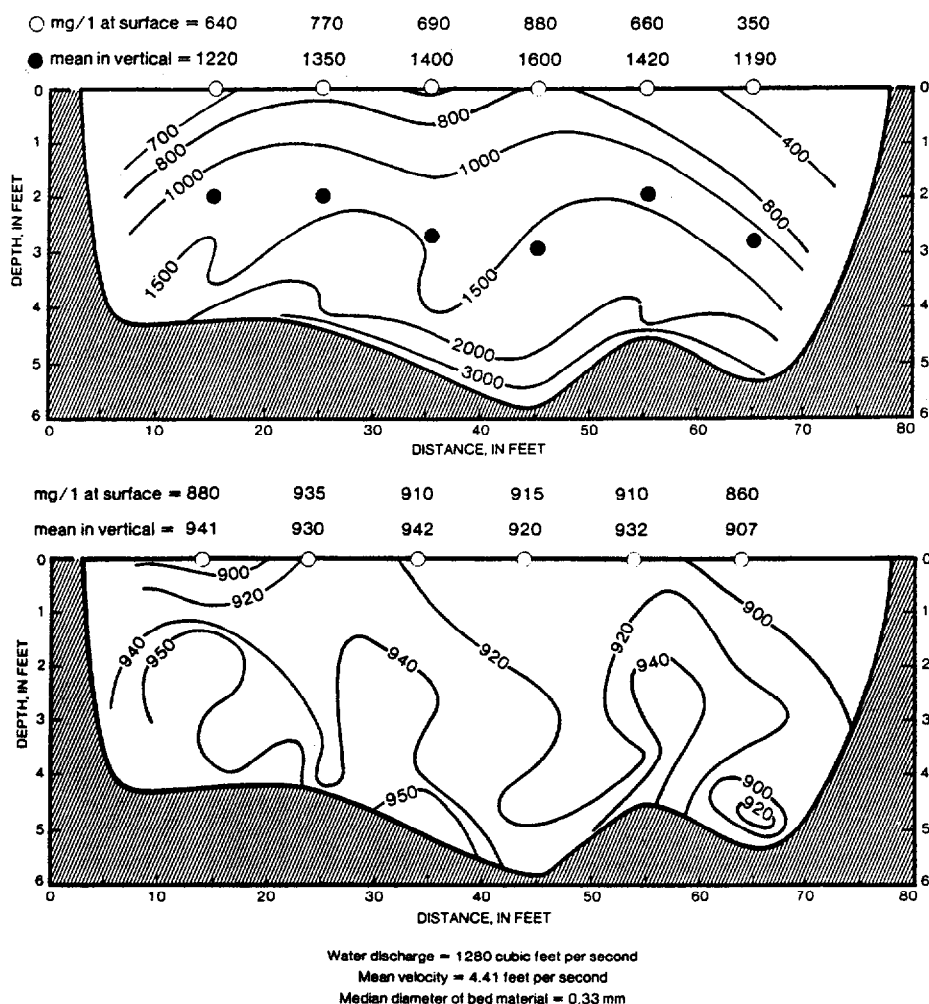
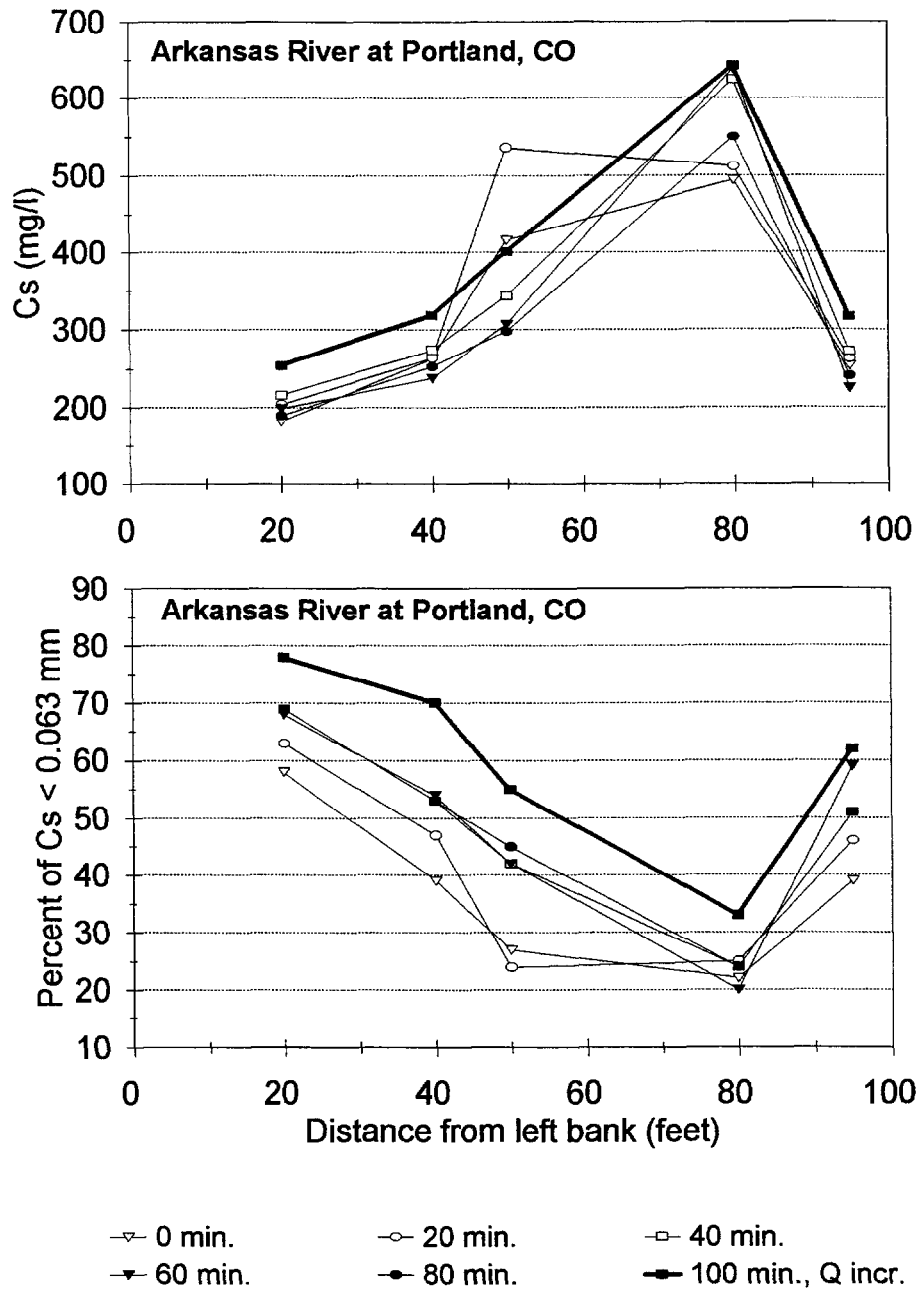


Fig. B-1: 31: Cross-sectional variation of coarse (0.062-2 mm) (top), and fine (<0.062 mm) (bottom) suspended sediment concentrations at the Rio Grande near Bernardo, NM (from Culbertson, 1977).

#### ***Temporal variability of the lateral distribution of $C_s$***

The lateral distribution of the vertically-averaged  $C_s$  is temporally variable even if discharge is constant. The measurements by Horowitz et al. (1989) at the Arkansas River at Portland (CO) (Figs. B-1; 32) and the Cowlitz River at Kelso (WA) (Figs. B-1; 33) indicate that the location of peak  $C_s$  changes over time, and that  $C_s$  at a given location is quite variable over time. The coefficient of variation (CV) of five consecutive  $C_s$  measurements taken at 20-minute intervals ranged from 1-7% near the banks to 12-26% in the central part of the two streams. The temporal variability of the lateral distribution of the suspended sediment grain sizes is slightly higher. The variability of the ratio of silt and clay (< 0.63 mm) to percent sand (> 0.63 mm) had coefficients of variation of 13-30% in the central areas of the stream.



**Fig. B-1; 32:** Temporal variability of the lateral distribution of  $C_s$  over six 20-minute intervals in the Arkansas River at Portland, CO, during steady flow: depth-integrated  $C_s$  per equal discharge increment (top); and percent of total  $C_s$  finer than 0.063 mm (silt and clay) (bottom). Flow increased during the sixth measurement at 100 minutes (data from Horowitz et al., 1989).

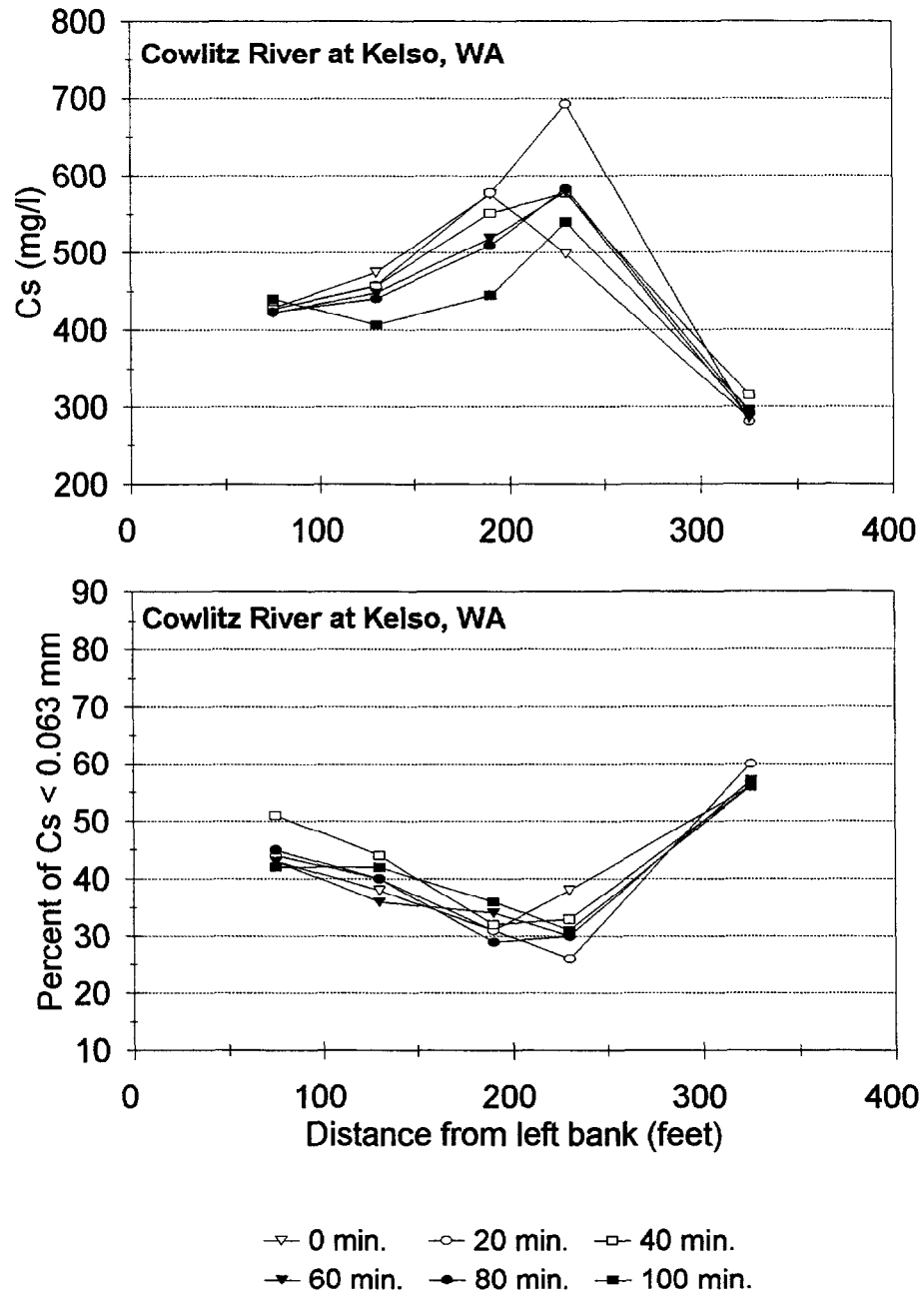


**Fig. B-1; 33:** Temporal variability of the lateral distribution of  $C_s$  over six measurements over six 20-minute intervals in the Cowlitz River at Kelso, WA, during steady flow: depth-integrated  $C_s$  per equal discharge increment (top); and percent of total  $C_s$  finer than 0.063 mm (silt and clay) (bottom) (data from Horowitz et al., 1989).

#### **Longitudinal mixing length**

Point sources of high  $C_s$  (e.g., sediment-laden tributaries or a bank collapse) affect the cross-sectional distribution of  $C_s$  because it takes some distance before there is complete mixing. Sanders (1996) gives the distance for complete lateral mixing ( $L_y$ ) as:

$$L_y = \frac{l^2 \cdot v}{2 E_y} \quad (3)$$

where  $l$  is the distance between the point source and the most distant point in the cross-section (i.e., the stream width),  $v$  is the average flow velocity, and  $E_y$  is a lateral diffusion coefficient that can be estimated by

$$E_y = 0.23 \cdot d \cdot \sqrt{g \cdot d \cdot S} \quad (4)$$

**Fig. B-1; 34** show calculated mixing lengths for different conditions and stream types. The dependency of the mixing length on the width-depth ratio of the stream is clearly visible in both figures.

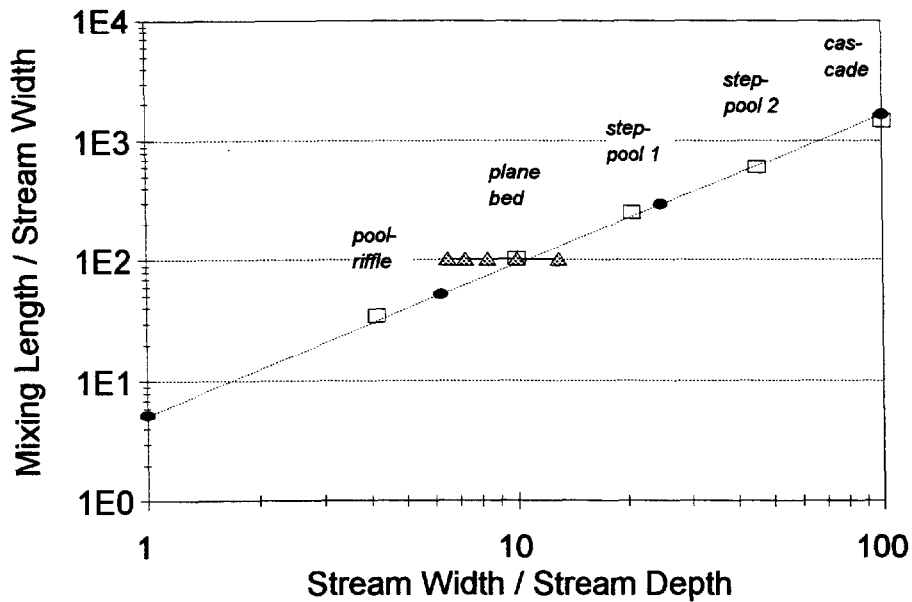
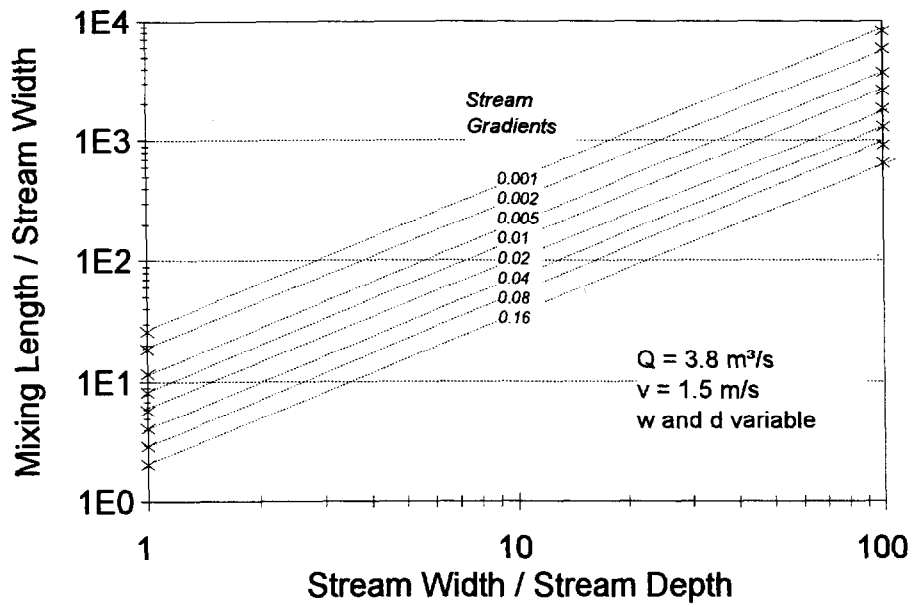
There is no a priori determination of the effects of stream types on mixing lengths. If one only varies gradient, mixing lengths decrease with increasing gradient. For example, a stream with a 2% gradient and a width-depth ratio of 10, requires a downstream distance of about 100 stream widths for complete mixing. Only 50 channel widths are required for complete mixing in an 8% gradient stream while a 0.1% gradient with a width-depth ratio of 10 has a mixing length of about 500 channel widths (**Fig. B-1; 34** (top)). Comparing different types of mountain streams for *constant width and stream power* which, for this purpose can be taken as the product of discharge and slope, varying stream gradient and geometry gives the opposite result. Mixing lengths are longest in high energy streams like steep step-pool systems or cascades, and shortest in pool-riffle streams (**Fig. B-1; 34** (bottom)).

This analysis together with the examples of cross-sectional variability (e.g., Martens, 1995), indicate that tributaries or other local sediment sources can affect the cross-sectional distribution of  $C_s$  for a substantial distance downstream.

### 1.3.2.3 Longitudinal variation

Rosgen (1976) found several incidences of longitudinal variability of  $C_s$  using color infrared photography in the West Fork of the Madison in SW Montana. Fine sand, eroded in meander bends, was redeposited within the next 400 yards downstream. Headwater streams had high sediment input from overland flow, rilling, and gullyng during snowmelt, but this sediment was quickly deposited in the channel. In those parts of the river system where sediment erodibility was high,  $C_s$  increased downstream of the tributary confluences, indicating that the increase in flow caused instream erosion. This increase in instream erosion was not observed in more erosion-resistant channels with coarse and angular bed material.

The above example emphasizes the importance of selecting the proper measurement locations for detecting sedimentary CWE. An appropriate sampling location should not only have a suitable cross-section with little lateral inhomogeneity in sediment transport patterns, but it should also be in close proximity to where sediment enters a stream. Several



□ Effect of Strm. Typ: Const. Strm. Powr.    ● Effect of Channel Shape: Q=6 m<sup>3</sup>/s  
 ▲ Effect of Discharge

**Fig. B-1; 34:** Comparison of longitudinal mixing lengths in terms of stream width for different stream scenarios: For equal discharge and width-depth ratios, mixing lengths increase as gradient decreases (top); For equal stream power ( $Q \cdot S$ ) and stream width, mixing length increases for steep, high-energy streams (bottom).

sampling locations may have to be set up if there is substantial disturbance over a long stream reach, or if the travel speed or conveyance of sediment through the stream system is of concern. Since an observed increase in  $C_s$  could be generated by upstream sources or some local source such as a bank collapse or local scour, sediment monitoring may need to track the sediment movement at various locations in order to identify the likely source(s). "Finger-printing" methods can also be used to relate measured  $C_s$  to upstream sources using either the natural mineralogical qualities of the sediment or artificial tracers. The problem of identifying sources will be discussed in further detail in chapter C-4.

#### **1.4 Implications for sediment sampling for CWE analyses**

The above chapters have introduced the different processes, phenomena, and variability encountered in sediment transport measurements. Such an understanding is essential to understanding why commonly employed sampling strategies in a specific location may provide only a rough estimate of the sediment load. As management practices continue to be modified to minimize adverse impacts, the detection of CWEs will require higher intensity sampling.

The physical processes discussed in this chapter clearly indicate that sampling intensity and sampling location need to be tailored to the sediment transport processes and the resultant variability at each site over the flows of interest. Sediment transport processes and patterns differ between streams, between locations within streams, and between individual events at a given site. In order to detect a sedimentary CWE, one needs to determine that the post-impact event or annual sediment load has changed relative to pre-management conditions. In order to determine the event or annual sediment load, the sediment sampling must represent the entire sediment load that is transported through the measurement site. In statistical terms, the distribution of the sample population(s) should approach the distribution of the target population(s).

Sampling recommendations usually focus on whether the sampling method is appropriate to accurately determine the mean and the variance of the population of interest. However, the problem for CWEs is that instantaneous bedload transport rates and suspended sediment concentrations are highly variable, and this limits their comparability. In the absence of intensive and longer-term sampling, the magnitude and pattern of temporal variability at different scales is unknown, and thus the uncertainty is unknown. Similarly, intensive sampling within the cross-section is needed to evaluate the accuracy of samples taken at selected locations. The interplay of spatial and temporal variability cannot be ignored, and the short-term measurement problem is generally more severe in bedload sampling than suspended sediment sampling.

We also know that cross-sectional measurements of bedload transport rates or  $C_s$  can vary by an order of magnitude for a given flow within a single event. Later chapters will discuss the longer-term variability and the fact that the variation in sediment transport around the rating curve is typically an order of magnitude.

In many cases the sampling period for detecting CWEs is likely to be rather short because results are needed quickly in order to mitigate problems and modify management practices. The intensity and duration of sampling is often limited by personnel and budgetary constraints, and both of these factors affect the likelihood of detecting a CWE at any spatial or temporal scale. These issues are discussed at successively larger scales in the following chapters, but an understanding of these issues must stem from an appreciation for the basic processes reviewed here. Unfortunately the variation in processes between locations and

over time means that it is difficult to provide very specific guidelines, or to provide a definitive answer to the problem of detecting CWEs.

## 2. Statistical Analysis of Bedload Transport Variability and Sampling Uncertainty

The previous chapter discussed the phenomena and underlying processes of sediment transport, and indicated the large temporal and spatial variability encountered for both bedload transport and suspended sediment concentration. This variability causes sampling problems. In particular, it is usually not known how many cross-sectionally-averaged samples are needed to accurately determine a mean bedload transport rate for a given discharge and a time interval. This problem can be resolved if the underlying distribution of consecutive bedload transport samples is known. Thus a first step is to compare the observed frequency distributions of relative transport rates with theoretical probability density functions. One can then select an appropriate distribution and use this to estimate how long the sampling has to continue until a sufficiently low degree of deviation is obtained. Second, the degree to which a distributions of bedload transport rates fits a theoretical distribution can be used as a statistical measure by itself. Therefore, this chapter will statistically analyze the temporal variability of bedload transport, focussing on the short-term variability.

Unfortunately, there is no systematic study in the literature that analyzes the statistical distributions of bedload transport rates under various discharge and transport conditions, and under various sampling schemes. The literature reports a variety of different statistical distributions, owing to the fact that bedload transport measurements show different degrees of variability, depending on both the discharge variation and the variability of the upstream sediment supply. Several authors (Carey and Hubbell 1986; Hubbell and Stevens 1986; Hubbell et al. 1987; Hubbell 1987; McLean and Tassone 1987, and Gomez et al. 1989) have shown that cumulative frequency distributions of relative bedload transport rates from different environments qualitatively fit the theoretical *Hamamori* distribution (Hamamori 1962) and the Einstein (1937) distribution, although no measure was provided with which to quantify the goodness-of-fit. Others found consecutive bedload transport rates to be *lognormal* (Shuyou et al. 1988), or Gaussian (*normal*) (Kuhnle and Southard 1988). A complete investigation of this entire topic is beyond the scope of this study, but some aspects of the effects of sediment transport and sampling intensity on the statistical distribution type were examined in the present study.

An extensive literature review found 40 data sets with high-resolution, consecutive bedload transport measurements<sup>1</sup>. Sampling conditions are quite varied, in that sampling was carried out at different flow intensities, during both constant and unsteady flow, in streams and in laboratory flumes, and with different sizes of bed material. Sampling techniques, sampling equipment, sampling times, and time between samples differed among data sets. All measured transport rates were transformed into the same unit of kg/m·s, and mean bedload transport rates were found to range over three orders of magnitude (Table B-2; 1)<sup>2</sup>.

---

<sup>1</sup> As the study progressed we found several other data sets, but time restrictions precluded us from carrying out the same detailed analysis on these additional data sets.

<sup>2</sup> except for two sets of 1986 data from Squaw Creek, when coarse bedload transport was measured in terms of pebble counts per unit width and time. The pebble transport rates from these two data sets are comparable to the 1991 data, when the pebble data were supplemented with data from a large net sampler (Bunte 1991).



## 2.1 Testing the statistical distribution of bedload transport rates

To test and compare the distributions of bedload transport rates, the data were expressed as cumulative frequencies of normalized bedload transport rates. Normalized data were obtained by dividing each measured bedload transport rate ( $qb_i$ ) by the mean bedload transport rate of the respective data set ( $qb_m$ ) (eq. 1a):

$$qb_r = \frac{qb_i}{qb_m} \tag{1a}$$

where

$$qb_m = \frac{1}{n} \sum_{i=1}^n qb_i \tag{1b}$$

The goodness-of-fit of the normalized transport rates for all 40 data sets were then compared to a normal (Gaussian), lognormal, and Hamamori distribution. Two different tests were employed to test for normality and lognormality, the methodology of Schleyer (1987) and the *W*-test after Shapiro-Wilk and D'Agostino (Gilbert 1987).

### 2.1.1 Schleyer-test for goodness-of-fit to normality and lognormality

Schleyer (1987) developed his goodness-of-fit methodology to characterize the downstream change in grain-size distributions from the weathered rock source to surf-transported beach sediments. He found that the goodness-of-fit of the grain-size distributions to a lognormal distribution improved with transport distance. The goodness-of-fit of a frequency distribution to a Gaussian and lognormal distribution can be calculated by analyzing how well the cumulative frequency distribution of the original or log-transformed data, respectively, fit the cumulative frequency of a standard normal distribution.

Because Schleyer's test is based on sieve classes, the consecutive bedload transport rates had to be sorted into classes. For the test of *normal distribution*, classes of  $0.25 qb_r$  were chosen. With relative transport rates ( $qb_r$ ) commonly ranging between 0 and 4, most data sets had about 16 classes. The number ( $n$ ) of relative, or normalized, transport rates per class was recorded, converted into a percentage ( $n(qb_r)\%$ ) and summed over all classes ( $\sum n(qb_r)\%$ ).

$$\sum_{i=1}^j n(qb_r)\% \tag{2}$$

where  $j$  is the number of classes per data set.

In analogy to Schleyer (1987), the equivalent Gaussian distribution ( $Gn$ ) of relative transport rates ( $qb_r$ ) is given by:

$$Gn(qb_{rc}) = \frac{1}{\sigma\sqrt{2\pi}} \cdot \exp\left(-\frac{(qb_{rc} - \mu)^2}{2\sigma^2}\right) \quad (3a)$$

with  $\sigma = 0.75 \cdot (p75 - p25)$ , where  $p75$  and  $p25$  are the 75th and 25th percentile of the cumulative frequency distribution, and  $\mu$  is the *mode*.  $qb_{rc}$  denotes the center of a class of relative transport rates  $qb_r$ .

For the test of goodness-to-fit to a **lognormal distribution**, the log-transformed relative transport rates  $qb_r$  were sorted into classes of 0.1 log units. The smaller increments were necessary in order to obtain roughly the same number of classes as for the test for normality. Schleyer (1987) gives the standard lognormal distribution as

$$Ln(qb_{rc}) = \frac{1}{\sigma\sqrt{2\pi}} \cdot \exp\left(-\frac{(\log qb_{rc} - \mu)^2}{2\sigma^2}\right) \quad (3b)$$

where  $\log qb_{rc}$  denotes the center of a class of log-transformed relative transport rates  $qb_r$ .

Schleyer (1987) uses the mode  $\mu$  instead of the mean (eqs. 2a and b) in order to account for the fact that bedload samples are generally truncated with regard to their grain-size distribution by the mesh size of the sampler or the size of the sampler opening. Identical grain-size distributions which are truncated differently will still have a common mode, but deviate in their mean. For the same reason Schleyer (1987) focuses on the central part of the frequency distribution when he defines the standard deviation  $\sigma$  as  $0.75 \cdot (p75 - p25)$  rather than using the standard formula for  $\sigma$ . Even though this study does not compare grain-size distributions, a focus on the central part of the data sets seems reasonable, because the tails of the frequency distributions of sampled bedload transport rates are likely to be truncated or not very representative. Large transport rates occur rather rarely, and they are more subject to sampling errors. Sampling accuracy for very small transport rates can be rather low as well.

Another factor that prompted us to try the Schleyer (1987) method was that the calculated goodness-of-fit, when expressed as a percentage value can be used to rank the data sets. Other statistical tests for normality and lognormality like the Kolmogorov-Smirnov-test, or the *W*-test, simply approve or reject normality or lognormality at a predefined level of confidence. In following Schleyer's (1987) procedure, the percent goodness-of-fit to a Gaussian and lognormal distribution was calculated by taking the absolute differences between the observed and the theoretical cumulative frequency distribution ( $\sum n(qb_j) \%$ ) for each class, summing these differences over all classes, dividing by  $j - 1$  classes, and subtracting from 100% (eq. 4a and 4b).

$$\% \text{ Gauss fit} = 100\% - \frac{1}{j-1} \cdot \sum_{i=1}^j \left[ \left| \sum_{i=1}^n n(qb_i) \% - \sum_{i=1}^n Gn(qb_i) \% \right| \right] \quad (4a)$$

$$\% \text{ lognormal fit} = 100\% - \frac{1}{j-1} \cdot \sum_{i=1}^j \left[ \left| \sum_{i=1}^n n(qb_i)\% - \sum_{i=1}^n Ln(qb_i)\% \right| \right]. \quad (4b)$$

### 2.1.2 Test for goodness-of-fit to a Hamamori distribution

The Hamamori distribution was derived from the observations that, during the passage of bedload dunes, individual relative bedload transport rates ( $qb_r$ ) would range from 0 to 4 times the mean transport rate, and that small relative transport rates within the class of 0 to  $0.25 qb_r$  would be the most frequent (Hamamori, 1962). A similar result had been obtained by Einstein (1937), who based his computations on the transport length of individual particles per transport step. Einstein (1937) and Hamamori (1962) both set up probability functions of relative bedload transport rates that indicate the percentage frequency with which a certain relative transport rate occurs. Although the two functions are rather similar, the Hamamori function is mathematically easier and will be used in the following analysis.

For the Hamamori probability function the number of relative transport rates per class of  $0.25 qb_r$  width is given by:

$$Hn(qb_r) = \frac{1}{4} qb_r \left[ 1 + \ln \left( \frac{4qb_m}{qb_i} \right) \right] \cdot 100 \quad (5)$$

The percent goodness-of-fit of a cumulative frequency distribution ( $\sum n(qb_i)\%$ ) to the cumulative distribution of the Hamamori function ( $\sum Hn(qb_i)\%$ ) was calculated in accordance with equation (6):

$$\% \text{ Hamamori fit} = 100\% - \frac{1}{j-1} \cdot \sum_{i=1}^j \left[ \left| \sum_{i=1}^n n(qb_i)\% - \sum_{i=1}^n Hn(qb_i)\% \right| \right]. \quad (6)$$

### 2.1.3 W-Test for normality and lognormality

The bedload transport data sets were also tested for conformity with a Gaussian and lognormal distribution using the *W*-test. This allowed us to determine whether there was a correspondence between the two test methods, and to determine what calculated percentage from the Schleyer-test conforms to a 95% probability of a normal or lognormal distribution according to the *W*-test.

The *W*-test, also called the Shapiro-Wilk test, approves or rejects the null hypothesis of normality or lognormality for data sets with a sample size less than 50. As test results are not altered if data sets are divided by a constant (e.g., by mean transport rates in order to normalize the data), the sorted individual transport rates were used to test for normality.

Likewise, the test for lognormality was performed with the sorted, log-transformed values of the original data. Gilbert (1987) gives the following formula for  $W$ :

$$W = \frac{1}{d} \left[ \sum_{i=1}^k a_i (qb_{[n-i+1]} - qb_{[i]}) \right]^2 \quad (7)$$

where  $k = n/2$  for even and  $k = (n+1)/2$  for odd values of  $n$ ; values of  $a_i$  are tabulated in Gilbert (1987).

The variable  $d$  is calculated by equation 8:

$$d = \sum_{i=1}^n (qb_i - qb_m)^2 = \sum_{i=1}^n x_i^2 - \frac{1}{n} \left( \sum_{i=1}^n qb_i \right)^2 = \text{variance} \cdot n \quad (8)$$

If the calculated value for  $W$  exceeds the values tabulated in Gilbert (1987), the null hypothesis (the tested distribution is normal or lognormal) cannot be rejected at the 95% confidence limit. If sample size is larger than 50, the D'Agostino-test for normal or lognormal distribution can be employed (equation 9a):

$$D = \frac{\sum_{i=1}^n [i - 0.5 \cdot (n+1)] qb_{[i]}}{n^2 \cdot s} \quad (9a)$$

where  $D$  is the test statistic and  $s$  is calculated from equation 9b:

$$s = \left[ \frac{1}{n} \sum_{i=1}^n (qb_i - qb_m)^2 \right]^{0.5} \quad (9b)$$

#### 2.1.4 Test Results

The percent goodness-of-fit to a normal and lognormal distribution, and to the Hamamori distribution, was calculated for all 40 data sets. The theoretical Hamamori distribution was also compared to the normal and lognormal distributions in order to provide a basis for comparison. Results are given in **Tables B-2; 2a, 2b, and 2c**, where data sets are sorted according to their goodness-of-fit to one of the three distributions. **Tables B-2; 3 and 4** summarize the results.

##### ***Percentage goodness-of-fit and distinguishability***

All data sets achieved a goodness-of-fit of at least 90% for one or more of the three distributions. None of the three distributions tested stood out as the best for all data sets.

Table B-2; 2a: Percentiles of cumulative frequency of relative transport rates, distribution parameters, percentage goodness-of-fit to ideal normal and lognormal distributions, and to the Hamamori distribution, sample size, sampling intensity and sampling performance. Data sets are sorted according to their goodness-of-fit to a lognormal distribution (Schleyer-test).

Reference	Percentiles of Cumulative Frequency of qbl/qbm							Distribution Parameters						Goodness-of-Fit			Sampling		
	p.05	p.16	p.25	p.50	p.75	p.84	p.95	"mean"	sorting	skewness				lognl. fit (%)	Gauss fit (%)	% Ham. fit	Size n	Intensity %ws-%ts	Perform. ws-ts-n
										sk.sed.	sk.3rd	sk.quart.	kurtosis						
Reid & Frostick '86, 31.1.79	0.03	0.21	0.40	0.78	1.55	1.86	2.06	0.95	0.72	0.28	0.51	0.33	0.72	84.0	92.9	96.6	20	20	4
Reid & Fro. 13/14.2.79	0.06	0.13	0.22	0.73	1.48	2.00	2.76	0.95	0.88	0.43	0.90	0.28	0.88	84.4	92.9	96.2	43	20	8.6
Camp.&Sidle '85,10-17-81u	0.02	0.03	0.15	0.50	1.22	1.42	2.06	0.65	0.66	0.42	1.16	0.34	0.78	85.4	91.0	91.3	21	0.15	0.03
Lisle '89 Caspar C	0.01	0.04	0.05	0.29	1.34	1.80	3.93	0.71	1.03	0.79	1.57	0.62	1.24	85.6	91.3	89.4	39	0.33	0.13
Lisle '89 Jacoby C	0.01	0.03	0.14	0.60	1.24	2.05	3.08	0.89	0.97	0.53	1.24	0.19	1.14	86.1	90.2	92.0	17	0.18	0.03
Emmett East F R '76 vort.	0.01	0.05	0.32	0.72	1.57	1.85	2.69	0.87	0.85	0.37	1.11	0.36	0.88	86.3	91.1	97.6	52	12.1	6.3
Dinehart 12-6-89	0.21	0.39	0.72	0.92	1.17	1.39	1.95	0.90	0.51	0.06	0.87	0.13	1.57	86.7	93.6	87.9	40	0.034	0.014
Kuhnle 11-8-86 Irg.Q	6.8E-05	0.02	0.13	0.53	1.61	2.14	3.22	0.90	1.02	0.59	5.97	0.46	0.89	87.3	93.0	93.3	125	0.469	0.586
Carey '85, Obion R	0.03	0.11	0.20	0.52	1.66	2.10	2.70	0.91	0.90	0.61	1.08	0.56	0.75	87.6	94.9	95.9	122	0.083	0.102
Camp.&Sidle '85,10-1-80,u	0.01	0.09	0.37	1.09	1.41	1.50	1.63	0.89	0.60	-0.39	-0.74	-0.40	0.64	88.0	90.6	90.6	18	0.212	0.038
Dinehart '92, 4-6-91	0.06	0.19	0.50	0.97	1.46	1.51	1.68	0.89	0.58	-0.15	-0.08	0.02	0.69	88.2	81.7	90.9	20	0.034	0.007
Dinehart '92, 4-9-91	0.05	0.07	0.13	0.71	1.60	1.89	2.64	0.89	0.85	0.39	0.72	0.22	0.73	88.2	94.7	96.8	25	0.028	0.007
Nanson '74, BC	0.02	0.06	0.08	0.15	0.83	1.54	4.09	0.58	0.98	0.91	3.35	0.81	2.23	88.4	91.1	81.8	18	0.473	0.085
Hamamori '61	0.03	0.15	0.27	0.75	1.53	1.97	2.81	0.95	0.87	0.41	0.00	0.25	0.90	89.2	82.1	100.0	100	1	100
Hubbell et al. '87, lab	1.0E-03	0.12	0.31	0.92	1.49	1.76	2.17	0.93	0.74	0.09	0.72	-0.04	0.75	89.3	95.1	95.5	120	14	17
Reid & Fro. '86 28/29.12.78	0.03	0.07	0.13	0.61	1.56	1.90	2.39	0.86	0.82	0.45	0.63	0.33	0.68	89.7	88.7	93.3	10	20	2
Lisle '89, Prairie C	0.03	0.16	0.25	0.54	1.44	1.90	3.18	0.87	0.91	0.62	1.67	0.52	1.67	90.0	94.2	96.6	147	0.01	0.014
Kuhnle & Southard '88, L1	0.47	0.67	0.77	1.01	1.25	1.37	1.56	1.02	0.34	0.01	0.13	0.00	0.13	90.1	93.7	83.1	300	100	300
Kuhnle & Southard '88, H5	0.61	0.76	0.87	1.06	1.19	1.26	1.35	1.03	0.24	-0.21	-0.56	-0.20	0.95	90.1	92.6	80.3	60	100	60
Kuhnle & Southard '88, H1	0.38	0.54	0.62	0.95	1.30	1.52	1.85	1.00	0.47	0.19	0.46	0.04	0.89	90.3	98.2	87.2	300	100	300
Bunte unpubl. Squaw C net	0.05	0.15	0.22	0.60	1.60	2.01	2.19	0.92	0.79	0.51	0.51	0.46	0.64	90.5	91.8	95.0	11	4.1	0.447
Dinehart '92, 12-5-89	0.01	0.10	0.28	0.53	1.65	2.04	2.50	0.89	0.86	0.57	0.90	0.64	0.74	90.6	92.9	99.0	30	0.021	0.006
Gomez'91 East FR 6-5-88	0.02	0.05	0.07	0.62	1.43	1.77	2.86	0.81	0.86	0.46	1.96	0.20	0.85	90.8	94.7	92.9	55	0.058	0.032
Dinehart '92, 4-5-91	0.07	0.29	0.39	0.60	1.58	1.84	2.60	0.91	0.77	0.59	0.91	0.64	0.87	90.9	92.5	95.0	17	0.021	0.004
Hoey & Sutherland '91, #2	0.08	0.17	0.27	0.59	0.76	0.84	0.98	0.54	0.30	-0.20	-0.04	-0.33	0.74	91.0	83.7	86.0	197	100	197
Kuhnle & Southard '88, L2	0.30	0.48	0.61	0.97	1.33	1.51	1.87	0.99	0.50	0.11	0.62	0.00	0.89	91.8	97.5	87.9	300	100	300
Camp.&Sidle '85 10-1-80,lo	0.05	0.07	0.16	0.60	1.60	1.71	2.30	0.79	0.75	0.44	0.82	0.40	0.64	91.8	92.4	95.1	18	0.212	0.038
Emmett '80 East FR '75 vort	0.02	0.07	0.14	0.57	1.27	1.61	2.89	0.75	0.82	0.48	1.50	0.19	1.04	92.9	92.3	94.4	27	5.3	1.4
Hayward & Sutherland '74	0.09	0.31	0.47	0.88	1.39	1.57	1.88	0.92	0.59	0.10	0.50	0.10	0.79	93.2	91.2	91.7	21	28.6	6
Kuhnle & Southard '88, H3	0.34	0.53	0.61	0.95	1.29	1.44	1.97	0.97	0.47	0.17	0.64	0.00	0.98	93.4	96.1	86.7	120	100	120
Reid & Fro. '86 24/25.12.78	1.0E-03	1.0E-03	0.11	0.49	1.24	1.98	3.56	0.82	1.03	0.62	1.56	0.40	1.30	93.5	89.7	90.9	23	20	4.6
Camp&Sidle '85 10-17-81lo	0.08	0.13	0.18	0.96	1.44	1.86	2.30	0.98	0.77	0.12	0.61	-0.24	0.72	93.6	91.9	95.7	22	0.151	0.033
Dinehart '92, 1-11-90	0.03	0.09	0.30	0.79	1.38	1.83	2.59	0.91	0.82	0.31	0.85	0.10	0.97	94.1	92.0	97.6	37	0.034	0.013
Milhouse spring '71	3.7E-05	6.5E-05	1.2E-04	1.3E-03	0.31	0.94	5.02	0.31	1.00	1.00	3.74	0.99	6.55	94.2	93.4	62.7	66	100	66
Carey & Hubbell, '86, lab	1.0E-03	0.16	0.30	0.69	1.63	1.96	2.69	0.94	0.86	0.45	1.26	0.40	0.83	94.3	95.5	98.8	120	14	16.8
Emmett '80 East FR '75 HS	0.07	0.12	0.18	0.51	1.64	1.88	2.65	0.83	0.83	0.61	1.26	0.55	0.72	94.7	93.7	95.0	56	0.014	0.008
Bunte '91Squaw C, 1hr.	0.09	0.18	0.30	0.66	1.28	1.72	3.10	0.85	0.84	0.50	2.46	0.28	1.26	95.4	96.2	95.4	408	20	82
Kuhnle 1-18-87smQ	0.19	0.41	0.47	0.68	1.00	1.25	2.27	0.78	0.53	0.44	4.17	0.51	1.61	95.4	96.2	88.8	37	0.16	0.059
Whiting et al. '88 Duck C	0.23	0.47	0.68	0.89	1.33	1.50	1.96	0.95	0.52	0.22	0.72	0.36	1.08	95.9	96.8	88.8	60	0.023	0.014
Bunte '92 Squaw C, 5min.	0.05	0.34	0.34	0.68	1.37	1.54	2.74	0.86	0.71	0.48	2.27	0.33	1.07	97.1	93.6	94.4	864	173	20
Hoey & Sutherland '91 #1	0.22	0.38	0.41	0.73	1.50	1.88	2.31	1.00	0.69	0.52	0.88	0.41	0.79	98.4	94.7	93.6	176	100	176

Table B-2; 2b: Percentiles of cumulative frequency of relative transport rates, distribution parameters, percentage goodness-of-fit to ideal normal and lognormal distributions, and to the Hamamori distribution, sample size, sampling intensity and sampling performance. Data sets are sorted according to their goodness-of-fit to a Gaussian distribution (Schleyer-test).

Reference	Percentiles of Cumulative Frequency of qbl/qbm							Distribution Parameters						Goodness-of-Fit			Sampling		
	p.05	p.16	p.25	p.50	p.75	p.84	p.95	"mean"	sorting	skewness				lognl. fit (%)	Gauss fit (%)	Hamam fit (%)	Size n	Intensity %ws-%ts	Perform. ws-ts-n
										sk.sec.	sk.3rd	sk.quart.	kurtosis						
Dinehart '92, 4-6-91	0.06	0.19	0.50	0.97	1.46	1.51	1.68	0.89	0.58	-0.15	-0.08	0.02	0.69	88.2	81.7	90.9	20	0.034	0.007
Hamamori '61	0.03	0.15	0.27	0.75	1.53	1.97	2.81	0.95	0.87	0.41	0.00	0.25	0.90	89.2	82.1	100.0	100	1	100
Hoey&Sutherland '91, #2	0.08	0.17	0.27	0.59	0.76	0.84	0.98	0.54	0.30	-0.20	-0.04	-0.33	0.74	91.0	83.7	86.0	197	100	197
Reid & Fro.'86 28/29.12.78	0.03	0.07	0.13	0.61	1.56	1.90	2.39	0.86	0.82	0.45	0.63	0.33	0.68	89.7	88.7	93.3	10	20	2
Reid & Fro.'86 24/25.12.78	1.0E-03	1.0E-03	0.11	0.49	1.24	1.98	3.56	0.82	1.03	0.62	1.56	0.40	1.30	93.5	89.7	90.9	23	20	4.6
Lisle '89 Jacoby C	0.01	0.03	0.14	0.60	1.24	2.05	3.08	0.89	0.97	0.53	1.24	0.19	1.14	86.1	90.2	92.0	17	0.18	0.03
Camp.&Sidle '85 10-1-80,u	0.01	0.09	0.37	1.09	1.41	1.50	1.63	0.89	0.60	-0.39	-0.74	-0.40	0.64	88.0	90.6	90.6	18	0.21	0.038
Camp.&Sidle '85 10-17-81u	0.02	0.03	0.15	0.50	1.22	1.42	2.06	0.65	0.66	0.42	1.16	0.34	0.78	85.4	91.0	91.3	21	0.15	0.032
Emmett '80 East FR '76 vort	0.01	0.05	0.32	0.72	1.57	1.85	2.69	0.87	0.85	0.37	1.11	0.36	0.88	86.3	91.1	97.6	52	12	6.3
Nanson '74 BC	0.02	0.06	0.08	0.15	0.83	1.54	4.09	0.58	0.98	0.91	3.35	0.81	2.23	88.4	91.1	81.8	18	0.47	0.085
Hayward & Sutherland '74	0.09	0.31	0.47	0.88	1.39	1.57	1.88	0.92	0.59	0.10	0.50	0.10	0.79	93.2	91.2	91.7	21	28.6	6
Lisle '89 Caspar C	0.01	0.04	0.05	0.29	1.34	1.80	3.93	0.71	1.03	0.79	1.57	0.62	1.24	85.6	91.3	89.4	39	0.33	0.13
Bunte unpubl. Squaw C, net	0.05	0.15	0.22	0.60	1.60	2.01	2.19	0.92	0.79	0.51	0.51	0.46	0.64	90.5	91.8	95.0	11	4.1	0.447
Camp.&Sidle '85 10-17-81lo	0.08	0.13	0.18	0.96	1.44	1.86	2.30	0.98	0.77	0.12	0.61	-0.24	0.72	93.6	91.9	95.7	22	0.15	0.033
Dinehart '92, 1-11-90	0.03	0.09	0.30	0.79	1.38	1.83	2.59	0.91	0.82	0.31	0.85	0.10	0.97	94.1	92.0	97.6	37	0.034	0.013
Emmett '80 East FR '75,vort	0.02	0.07	0.14	0.57	1.27	1.61	2.89	0.75	0.82	0.48	1.50	0.19	1.04	92.9	92.3	94.4	27	5.3	1.4
Camp.&Sidle '85, 10-1-80,lo	0.05	0.07	0.16	0.60	1.60	1.71	2.30	0.79	0.75	0.44	0.82	0.40	0.64	91.8	92.4	95.1	18	0.21	0.038
Dinehart '92, 4-5-91	0.07	0.29	0.39	0.60	1.58	1.84	2.60	0.91	0.77	0.59	0.91	0.64	0.87	90.9	92.5	95.0	17	0.021	0.004
Kuhnle & Southard '88, H5	0.61	0.76	0.87	1.06	1.19	1.26	1.35	1.03	0.24	-0.21	-0.56	-0.20	0.95	90.1	92.6	80.3	60	100	60
Dinehart '92, 12-5-89	0.01	0.10	0.28	0.53	1.65	2.04	2.50	0.89	0.86	0.57	0.90	0.64	0.74	90.6	92.9	99.0	30	0.021	0.006
Reid & Fro.'86, 13/14.2.79	0.06	0.13	0.22	0.73	1.48	2.00	2.76	0.95	0.88	0.43	0.90	0.28	0.88	84.4	92.9	96.2	43	20	8.6
Reid & Frostick '86, 31.1.79	0.03	0.21	0.40	0.78	1.55	1.86	2.06	0.95	0.72	0.28	0.51	0.33	0.72	84.0	92.9	96.6	20	20	4
Kuhnle 11-8-86 large Q	6.8E-05	0.02	0.13	0.53	1.61	2.14	3.22	0.90	1.02	0.59	5.97	0.46	0.89	87.3	93.0	93.3	125	0.47	0.59
Milhous '73, spring '71	3.7E-05	6.5E-05	1.2E-04	1.3E-03	0.31	0.94	5.02	0.31	1.00	1.00	3.74	0.99	6.55	94.2	93.4	62.7	66	100	66
Dinehart '92, 12-6-89	0.21	0.39	0.72	0.92	1.17	1.39	1.95	0.90	0.51	0.06	0.87	0.13	1.57	86.7	93.6	87.9	40	0.034	0.014
Bunte '92, Squaw C, 5min.	0.05	0.34	0.34	0.68	1.37	1.54	2.74	0.86	0.71	0.48	2.27	0.33	1.07	97.1	93.6	94.4	864	173	20
Kuhnle & Southard '88, L1	0.47	0.67	0.77	1.01	1.25	1.37	1.56	1.02	0.34	0.01	0.13	0.00	0.13	90.1	93.7	83.1	300	100	300
Emmett '80, East FR '75 HS	0.07	0.12	0.18	0.51	1.64	1.88	2.65	0.83	0.83	0.61	1.26	0.55	0.72	94.7	93.7	95.0	56	0.014	0.008
Lisle '89, Prairie C	0.03	0.16	0.25	0.54	1.44	1.90	3.18	0.87	0.91	0.62	1.67	0.52	1.67	90.0	94.2	96.6	147	0.01	0.014
Gomez'91 East FR 6-5-88	0.02	0.05	0.07	0.62	1.43	1.77	2.86	0.81	0.86	0.46	1.96	0.20	0.85	90.8	94.7	92.9	55	0.058	0.032
Hoey & Sutherland '91,#1	0.22	0.38	0.41	0.73	1.50	1.88	2.31	1.00	0.69	0.52	0.88	0.41	0.79	98.4	94.7	93.6	176	100	176
Dinehart '92, 4-9-91	0.05	0.07	0.13	0.71	1.60	1.89	2.64	0.89	0.85	0.39	0.72	0.22	0.73	88.2	94.7	96.8	25	0.028	0.007
Carey '85, Obion R	0.03	0.11	0.20	0.52	1.66	2.10	2.70	0.91	0.90	0.61	1.08	0.56	0.75	87.6	94.9	95.9	122	0.083	0.102
Hubbell et al. '87, lab	1.0E-03	0.12	0.31	0.92	1.49	1.76	2.17	0.93	0.74	0.09	0.72	-0.04	0.75	89.3	95.1	95.5	120	14	17
Carey & Hubbell '86, lab	1.0E-03	0.16	0.30	0.69	1.63	1.96	2.69	0.94	0.86	0.45	1.26	0.40	0.83	94.3	95.5	98.8	120	14	17
Kuhnle & Southard '88, H3	0.34	0.53	0.61	0.95	1.29	1.44	1.97	0.97	0.47	0.17	0.64	0.00	0.98	93.4	96.1	86.7	120	100	120
Kuhnle 1-18-87 small Q	0.19	0.41	0.47	0.68	1.00	1.25	2.27	0.78	0.53	0.44	4.17	0.51	1.61	95.4	96.2	88.8	37	0.16	0.059
Bunte '91, Squaw C, 1hr.	0.09	0.18	0.30	0.66	1.28	1.72	3.10	0.85	0.84	0.50	2.46	0.28	1.26	95.4	96.2	95.4	408	20	82
Whiting et al. '88, Duck C	0.23	0.47	0.68	0.89	1.33	1.50	1.96	0.95	0.52	0.22	0.72	0.36	1.08	95.9	96.8	88.8	60	0.023	0.014
Kuhnle & Southard '88, L2	0.30	0.48	0.61	0.97	1.33	1.51	1.87	0.99	0.50	0.11	0.62	0.00	0.89	91.8	97.5	87.9	300	100	300
Kuhnle & Southard '88, H1	0.38	0.54	0.62	0.95	1.30	1.52	1.85	1.00	0.47	0.19	0.46	0.04	0.89	90.3	98.2	87.2	300	100	300

Table B-2; 2c: Percentiles of cumulative frequency of relative transport rates, distribution parameters, percentage goodness-of-fit to ideal normal and lognormal distributions, and to the Hamamori distribution, sample size, sampling intensity and sampling performance. Data sets are sorted according to their goodness-of-fit to a Hamamori distribution.

Data Set	Percentiles of Cumulative Frequency of qbl/qbm							Distribution Parameters						Goodness-of-Fit			Sampling		
	p.05	p.16	p.25	p.50	p.75	p.84	p.95	"mean"	sorting	skewness			kurtosis	lognorm fit (%)	Gauss fit (%)	% Ham. fit	Size n	Intensity %ws-%ts	Perform. ws-ts-n
										sk.sed.	sk.3rd	m.sk.quart.							
Milhous '73, spring '71	3.7E-05	6.5E-05	1.2E-04	1.3E-03	0.31	0.94	5.02	0.31	1.00	1.00	3.74	0.99	6.55	94.2	93.4	62.7	66	100	66
Kuhnle & Southard '88, H5	0.61	0.76	0.87	1.06	1.19	1.26	1.35	1.03	0.24	-0.21	-0.56	-0.20	0.95	90.1	92.6	80.3	60	100	60
Nanson '74, BC	0.02	0.06	0.08	0.15	0.83	1.54	4.09	0.58	0.98	0.91	3.35	0.81	2.23	88.4	91.1	81.8	18	0.47	0.085
Kuhnle & Southard '88, L1	0.47	0.67	0.77	1.01	1.25	1.37	1.56	1.02	0.34	0.01	0.13	0.00	0.13	90.1	93.7	83.1	300	100	300
Hoey & Sutherland '91, #2	0.08	0.17	0.27	0.59	0.76	0.84	0.98	0.54	0.30	-0.20	-0.04	-0.33	0.74	91.0	83.7	86.0	197	100	197
Kuhnle & Southard '88, H3	0.34	0.53	0.61	0.95	1.29	1.44	1.97	0.97	0.47	0.17	0.64	0.00	0.98	93.4	96.1	86.7	120	100	120
Kuhnle & Southard '88, H1	0.38	0.54	0.62	0.95	1.30	1.52	1.85	1.00	0.47	0.19	0.46	0.04	0.89	90.3	98.2	87.2	300	100	300
Kuhnle & Southard '88, L2	0.30	0.48	0.61	0.97	1.33	1.51	1.87	0.99	0.50	0.11	0.62	0.00	0.89	91.8	97.5	87.9	300	100	300
Dinehart '92, 12-6-89	0.21	0.39	0.72	0.92	1.17	1.39	1.95	0.90	0.51	0.06	0.87	0.13	1.57	86.7	93.6	87.9	40	0.034	0.014
Kuhnle 1-18-87small Q	0.19	0.41	0.47	0.68	1.00	1.25	2.27	0.78	0.53	0.44	4.17	0.51	1.61	95.4	96.2	88.8	37	0.16	0.059
Whiting et al. '88, DC	0.23	0.47	0.68	0.89	1.33	1.50	1.96	0.95	0.52	0.22	0.72	0.36	1.08	95.9	96.8	88.8	60	0.023	0.014
Lisle '89, Caspar C	0.01	0.04	0.05	0.29	1.34	1.80	3.93	0.71	1.03	0.79	1.57	0.62	1.24	85.6	91.3	89.4	39	0.33	0.13
Camp.&Sidle '85,10-1-80,up	0.01	0.09	0.37	1.09	1.41	1.50	1.63	0.89	0.60	-0.39	-0.74	-0.40	0.64	88.0	90.6	90.6	18	0.21	0.038
Dinehart '92, 4-6-91	0.06	0.19	0.50	0.97	1.46	1.51	1.68	0.89	0.58	-0.15	-0.08	0.02	0.69	88.2	81.7	90.9	20	0.034	0.007
Reid & Fro.'86, 24/25.12.78	1.0E-03	1.0E-03	0.11	0.49	1.24	1.98	3.56	0.82	1.03	0.62	1.56	0.40	1.30	93.5	89.7	90.9	23	20	4.6
Camp.&Sidle '85,10-17-81u	0.02	0.03	0.15	0.50	1.22	1.42	2.06	0.65	0.66	0.42	1.16	0.34	0.78	85.4	91.0	91.3	21	0.151	0.032
Hayward & Sutherland '74	0.09	0.31	0.47	0.88	1.39	1.57	1.88	0.92	0.59	0.10	0.50	0.10	0.79	93.2	91.2	91.7	21	29	6.00
Lisle '89, Jacoby C	0.01	0.03	0.14	0.60	1.24	2.05	3.08	0.89	0.97	0.53	1.24	0.19	1.14	86.1	90.2	92.0	17	0.18	0.03
Gomez'91 East FR 6-5-88	0.02	0.05	0.07	0.62	1.43	1.77	2.86	0.81	0.86	0.46	1.96	0.20	0.85	90.8	94.7	92.9	55	0.058	0.032
Kuhnle 11-8-86 large Q	6.8E-05	0.02	0.13	0.53	1.61	2.14	3.22	0.90	1.02	0.59	5.97	0.46	0.89	87.3	93.0	93.3	125	0.47	0.59
Reid & Fro.'86, 28/29.12.78	0.03	0.07	0.13	0.61	1.56	1.90	2.39	0.86	0.82	0.45	0.63	0.33	0.68	89.7	88.7	93.3	10	20	2
Hoey & Sutherland '91, #1	0.22	0.38	0.41	0.73	1.50	1.88	2.31	1.00	0.69	0.52	0.88	0.41	0.79	98.4	94.7	93.6	176	100	176
Emmett '80, East FR '75 vor	0.02	0.07	0.14	0.57	1.27	1.61	2.89	0.75	0.82	0.48	1.50	0.19	1.04	92.9	92.3	94.4	27	5.3	1.4
Bunte '92, Squaw C, 5min.	0.05	0.34	0.34	0.68	1.37	1.54	2.74	0.86	0.71	0.48	2.27	0.33	1.07	97.1	93.6	94.4	864	173	20
Bunte unpubl. Squaw C, net	0.05	0.15	0.22	0.60	1.60	2.01	2.19	0.92	0.79	0.51	0.51	0.46	0.64	90.5	91.8	95.0	11	4.1	0.45
Dinehart '92, 4-5-91	0.07	0.29	0.39	0.60	1.58	1.84	2.60	0.91	0.77	0.59	0.91	0.64	0.87	90.9	92.5	95.0	17	0.021	0.004
Emmett '80, East FR '75,HS	0.07	0.12	0.18	0.51	1.64	1.88	2.65	0.83	0.83	0.61	1.26	0.55	0.72	94.7	93.7	95.0	56	0.014	0.008
Camp.&Sidle '85, 10-1-80,lo	0.05	0.07	0.16	0.60	1.60	1.71	2.30	0.79	0.75	0.44	0.82	0.40	0.64	91.8	92.4	95.1	18	0.21	0.038
Bunte '91, Squaw C, 1hr.	0.09	0.18	0.30	0.66	1.28	1.72	3.10	0.85	0.84	0.50	2.46	0.28	1.26	95.4	96.2	95.4	408	20	82
Hubbell et al. '87, lab	1.0E-03	0.12	0.31	0.92	1.49	1.76	2.17	0.93	0.74	0.09	0.72	-0.04	0.75	89.3	95.1	95.5	120	14	17
Camp.&Sidle '85,10-17-81lo	0.08	0.13	0.18	0.96	1.44	1.86	2.30	0.98	0.77	0.12	0.61	-0.24	0.72	93.6	91.9	95.7	22	0.15	0.033
Carey '85, Obion R	0.03	0.11	0.20	0.52	1.66	2.10	2.70	0.91	0.90	0.61	1.08	0.56	0.75	87.6	94.9	95.9	122	0.083	0.102
Reid & Fro. '86, 13/14.2.79	0.06	0.13	0.22	0.73	1.48	2.00	2.76	0.95	0.88	0.43	0.90	0.28	0.88	84.4	92.9	96.2	43	20	8.6
Lisle '89, Prairie C	0.03	0.16	0.25	0.54	1.44	1.90	3.18	0.87	0.91	0.62	1.67	0.52	1.67	90.0	94.2	96.6	147	0.01	0.014
Reid & Frostick '86, 31.1.79	0.03	0.21	0.40	0.78	1.55	1.86	2.06	0.95	0.72	0.28	0.51	0.33	0.72	84.0	92.9	96.6	20	20	4
Dinehart '92, 4-9-91	0.05	0.07	0.13	0.71	1.60	1.89	2.64	0.89	0.85	0.39	0.72	0.22	0.73	88.2	94.7	96.8	25	0.028	0.007
Emmett '80, East FR '76,vor	0.01	0.05	0.32	0.72	1.57	1.85	2.69	0.87	0.85	0.37	1.11	0.36	0.88	86.3	91.1	97.6	52	12	6.3
Dinehart '92, 1-11-90	0.03	0.09	0.30	0.79	1.38	1.83	2.59	0.91	0.82	0.31	0.85	0.10	0.97	94.1	92.0	97.6	37	0.034	0.013
Carey & Hubbell '86, lab	1.0E-03	0.16	0.30	0.69	1.63	1.96	2.69	0.94	0.86	0.45	1.26	0.40	0.83	94.3	95.5	98.8	120	14	17
Dinehart '92, 12-5-89	0.01	0.10	0.28	0.53	1.65	2.04	2.50	0.89	0.86	0.57	0.90	0.64	0.74	90.6	92.9	99.0	30	0.021	0.006
Hamamori '61	0.03	0.15	0.27	0.75	1.53	1.97	2.81	0.95	0.87	0.41	0.00	0.25	0.90	89.2	82.1	100.0	100	1	100

Table B-2; 2d: Percentiles of cumulative frequency of relative transport rates, distribution parameters, percentage goodness-of-fit to ideal normal and lognormal distributions, and to the Hamamori distribution, sample size, sampling intensity and sampling performance. Data sets are sorted according to the results from the W-test: x = tested positive on a 95% confidence level for a Gaussian, or a lognormal distribution

Data Set	Percentiles of Cumulative Frequency of qbi/qbm								Distribution Parameters					Fits distrib. on 95% signif. level			Goodn. of fit (%)	Sampling		
	p.05	p.16	p.25	p.50	p.75	p.84	p.95	"mean"	sorting	skewness			kurtosis	lognl.	Gauss	Hamam		n	Intensity	Perform.
										sk.sed.	sk.3rd	m.sk.quart.								
Dinehart '92, 4-6-91	0.06	0.19	0.50	0.97	1.46	1.51	1.68	0.89	0.58	-0.15	-0.08	0.02	0.69		x		90.9	20	0.034	0.007
Whiting et al. '88, Duck C	0.23	0.47	0.68	0.89	1.33	1.50	1.96	0.95	0.52	0.22	0.72	0.36	1.08		x		88.8	60	0.023	0.014
Camp.&Sidle '85,10-17-81lo	0.08	0.13	0.18	0.96	1.44	1.86	2.30	0.98	0.77	0.12	0.61	-0.24	0.72		x		95.7	22	0.15	0.033
Camp.&Sidle '85, 10-1-80,u	0.01	0.09	0.37	1.09	1.41	1.50	1.63	0.89	0.60	-0.39	-0.74	-0.40	0.64		x		90.6	18	0.21	0.038
Reid & Frostick '86, 31.1.79	0.03	0.21	0.40	0.78	1.55	1.86	2.06	0.95	0.72	0.28	0.51	0.33	0.72		x		96.6	20	20	4
Hayward & Sutherland '74	0.09	0.31	0.47	0.88	1.39	1.57	1.88	0.92	0.59	0.10	0.50	0.10	0.79	x	xx		91.7	21	29	6
Hubbell et al. '87, lab	1.0E-03	0.12	0.31	0.92	1.49	1.76	2.17	0.93	0.74	0.09	0.72	-0.04	0.75		x		95.5	120	14	16.8
Kuhnle & Southard '88, H5	0.61	0.76	0.87	1.06	1.19	1.26	1.35	1.03	0.24	-0.21	-0.56	-0.20	0.95		x		80.3	60	100	60
Kuhnle & Southard '88, H3	0.34	0.53	0.61	0.95	1.29	1.44	1.97	0.97	0.47	0.17	0.64	0.00	0.98		x		86.7	120	100	120
Kuhnle & Southard '88, H1	0.38	0.54	0.62	0.95	1.30	1.52	1.85	1.00	0.47	0.19	0.46	0.04	0.89		x		87.2	300	100	300
Kuhnle & Southard '88, L2	0.30	0.48	0.61	0.97	1.33	1.51	1.87	0.99	0.50	0.11	0.62	0.00	0.89		x		87.9	300	100	300
Lisle '89, Prarie C	0.03	0.16	0.25	0.54	1.44	1.90	3.18	0.87	0.91	0.62	1.67	0.52	1.67	x			96.6	147	0.01	0.014
Lisle '89, Jacoby C	0.01	0.03	0.14	0.60	1.24	2.05	3.08	0.89	0.97	0.53	1.24	0.19	1.14	x			92.0	17	0.18	0.03
Carey '85, Obion R	0.03	0.11	0.20	0.52	1.66	2.10	2.70	0.91	0.90	0.61	1.08	0.56	0.75	x			95.9	122	0.083	0.102
Nanson '74, BC	0.02	0.06	0.08	0.15	0.83	1.54	4.09	0.58	0.98	0.91	3.35	0.81	2.23	x			81.8	18	0.47	0.085
Hamamori '61	0.03	0.15	0.27	0.75	1.53	1.97	2.81	0.95	0.87	0.41	1.00	0.25	0.90	x			100.0	100	1	100
Reid & Fro.'86, 24/25.12.78	1.0E-03	1.0E-03	0.11	0.49	1.24	1.98	3.56	0.82	1.03	0.62	1.56	0.40	1.30	x			90.9	23	20	4.6
Reid & Fro.'86, 28/29.12.78	0.03	0.07	0.13	0.61	1.56	1.90	2.39	0.86	0.82	0.45	0.63	0.33	0.68	xx	x		93.3	10	20	2
Bunte unpubl. Squaw C, net	0.05	0.15	0.22	0.60	1.60	2.01	2.19	0.92	0.79	0.51	0.51	0.46	0.64	xx	x		95.0	11	4.1	0.45
Kuhnle 1-18-87 small Q	0.19	0.41	0.47	0.68	1.00	1.25	2.27	0.78	0.53	0.44	4.17	0.51	1.61	x			88.8	37	0.16	0.059
Gomez '91 East FR 6-5-88	0.02	0.05	0.07	0.62	1.43	1.77	2.86	0.81	0.86	0.46	1.96	0.20	0.85	x			92.9	55	0.058	0.032
Dinehart '92, 4-5-91	0.07	0.29	0.39	0.60	1.58	1.84	2.60	0.91	0.77	0.59	0.91	0.64	0.87	x			95.0	17	0.021	0.004
Camp.&Sidle '85,10-1-80,lo	0.05	0.07	0.16	0.60	1.60	1.71	2.30	0.79	0.75	0.44	0.82	0.40	0.64	x			95.1	18	0.21	0.038
Emmett '80, East FR '75 vor	0.02	0.07	0.14	0.57	1.27	1.61	2.89	0.75	0.82	0.48	1.50	0.19	1.04	x			94.4	27	5.3	1.4
Emmett '80, East FR '75 HS	0.07	0.12	0.18	0.51	1.64	1.88	2.65	0.83	0.83	0.61	1.26	0.55	0.72	x			95.0	56	0.014	0.008
Milhou '73, spring '71	3.7E-05	6.5E-05	1.2E-04	1.3E-03	0.31	0.94	5.02	0.31	1.00	1.00	3.74	0.99	6.55	x			62.7	66	100	66
Carey & Hubbell '86, lab	1.0E-03	0.16	0.30	0.69	1.63	1.96	2.69	0.94	0.86	0.45	1.26	0.40	0.83	x			98.8	120	14	17
Bunte '91, Squaw C, 1hr.	0.09	0.18	0.30	0.66	1.28	1.72	3.10	0.85	0.84	0.50	2.46	0.28	1.26	x			95.4	408	20	81.8
Bunte '92, Squaw C, 5min.	0.05	0.34	0.34	0.68	1.37	1.54	2.74	0.86	0.71	0.48	2.27	0.33	1.07				94.4	864	173	20
Hoey & Sutherland '91, #1	0.22	0.38	0.41	0.73	1.50	1.88	2.31	1.00	0.69	0.52	0.88	0.41	0.79				93.6	176	100	176
Hoey & Sutherland '91, #2	0.08	0.17	0.27	0.59	0.76	0.84	0.98	0.54	0.30	-0.20	-0.04	-0.33	0.74				86.0	197	100	197
Kuhnle & Southard '88, L1	0.47	0.67	0.77	1.01	1.25	1.37	1.56	1.02	0.34	0.01	0.13	0.00	0.13				83.1	300	100	300
Reid & Fro.'86, 13/14.2.79	0.06	0.13	0.22	0.73	1.48	2.00	2.76	0.95	0.88	0.43	0.90	0.28	0.88				96.2	43	20	8.6
Camp.&Sidle '85, 10-17-81u	0.02	0.03	0.15	0.50	1.22	1.42	2.06	0.65	0.66	0.42	1.16	0.34	0.78				91.3	21	0.15	0.032
Lisle '89, Caspar C	0.01	0.04	0.05	0.29	1.34	1.80	3.93	0.71	1.03	0.79	1.57	0.62	1.24				89.4	39	0.33	0.13
Emmett '80, East FR '76 vor	0.01	0.05	0.32	0.72	1.57	1.85	2.69	0.87	0.85	0.37	1.11	0.36	0.88				97.6	52	12	6.3
Kuhnle 11-8-86 large Q	6.8E-05	0.02	0.13	0.53	1.61	2.14	3.22	0.90	1.02	0.59	5.97	0.46	0.89				93.3	125	0.47	0.59
Dinehart '92, 4-9-91	0.05	0.07	0.13	0.71	1.60	1.89	2.64	0.89	0.85	0.39	0.72	0.22	0.73				96.8	25	0.028	0.007
Dinehart '92, 12-5-89	0.01	0.10	0.28	0.53	1.65	2.04	2.50	0.89	0.86	0.57	0.90	0.64	0.74				99.0	30	0.021	0.006
Dinehart '92, 12-6-89	0.21	0.39	0.72	0.92	1.17	1.39	1.95	0.90	0.51	0.06	0.87	0.13	1.57				87.9	40	0.034	0.014
Dinehart '92, 1-11-90	0.03	0.09	0.30	0.79	1.38	1.83	2.59	0.91	0.82	0.31	0.85	0.10	0.97				97.6	37	0.034	0.013

The mean goodness-of-fit for a Gaussian distribution was slightly better (92.5%) than for the other two distributions (lognormal: 90.5% and Hamamori: 91.7%), but the standard deviations for the goodness-of-fit suggest that this difference is marginal at best.

**Table B-2; 3:** Mean, standard deviation and range of the calculated percent goodness-of-fit of all bedload data sets to a Gaussian, lognormal (Schleyer-test), and Hamamori distribution.

	Distribution		
	Lognormal	Gauss	Hamamori
Mean (%)	90.5	92.5	91.7
Std.Deviation	3.8	3.6	6.6
Range (%)	84.0 - 98.4	81.7 - 98.2	62.7 - 100

Since there is an excellent fit between the theoretical distributions and at least one of the data sets, there is a question of whether a high goodness of fit for one distribution will preclude a high goodness of fit for the other two distributions. **Figs. B-2: 1** indicate that for a given data set, there is no systematic relationship between the goodness-of-fit to a normal versus a lognormal distribution, or between the goodness-of-fit to lognormal and a Hamamori distribution. However, the data sets which had the highest goodness of fit for one distribution tended to have a lower goodness of fit for the other distributions (**Table B-2; 4**).

**Table B-2; 4:** Average percentage goodness-of-fit (%) of data sets that have the highest percent goodness-of-fit for a Gaussian, lognormal, or the Hamamori distribution, and the corresponding percent goodness-of-fit to the respective other distributions.

Distribution with highest % goodness- of-fit	Percentage Goodness-of-Fit to the respective other distributions		
	Lognormal	Gauss	Hamamori
Hamamori	89.5	91.7	95.5
Gaussian	90.9	94.5	87.8
Lognormal	94.6	91.0	86.6

***Comparison between the two test methods of normality and lognormality***

According to the *W*-test, 13 data sets were normally distributed and 17 data sets were lognormally distributed. 13 data sets were neither normal or lognormal at the 95% confidence level (**Table B-2; 2d**). Compared to the Schleyer-test, the *W*-test produced a much clearer distinction between the two distributions. Only two of the 13 data sets that tested positive for a normal distribution also tested positive for a lognormal distribution, and only one of the 17 lognormal distributions tested positively for a normal distribution. In cases where a sample data set fit more than one distribution, the data were assigned to the distribution for which they had the highest confidence level.

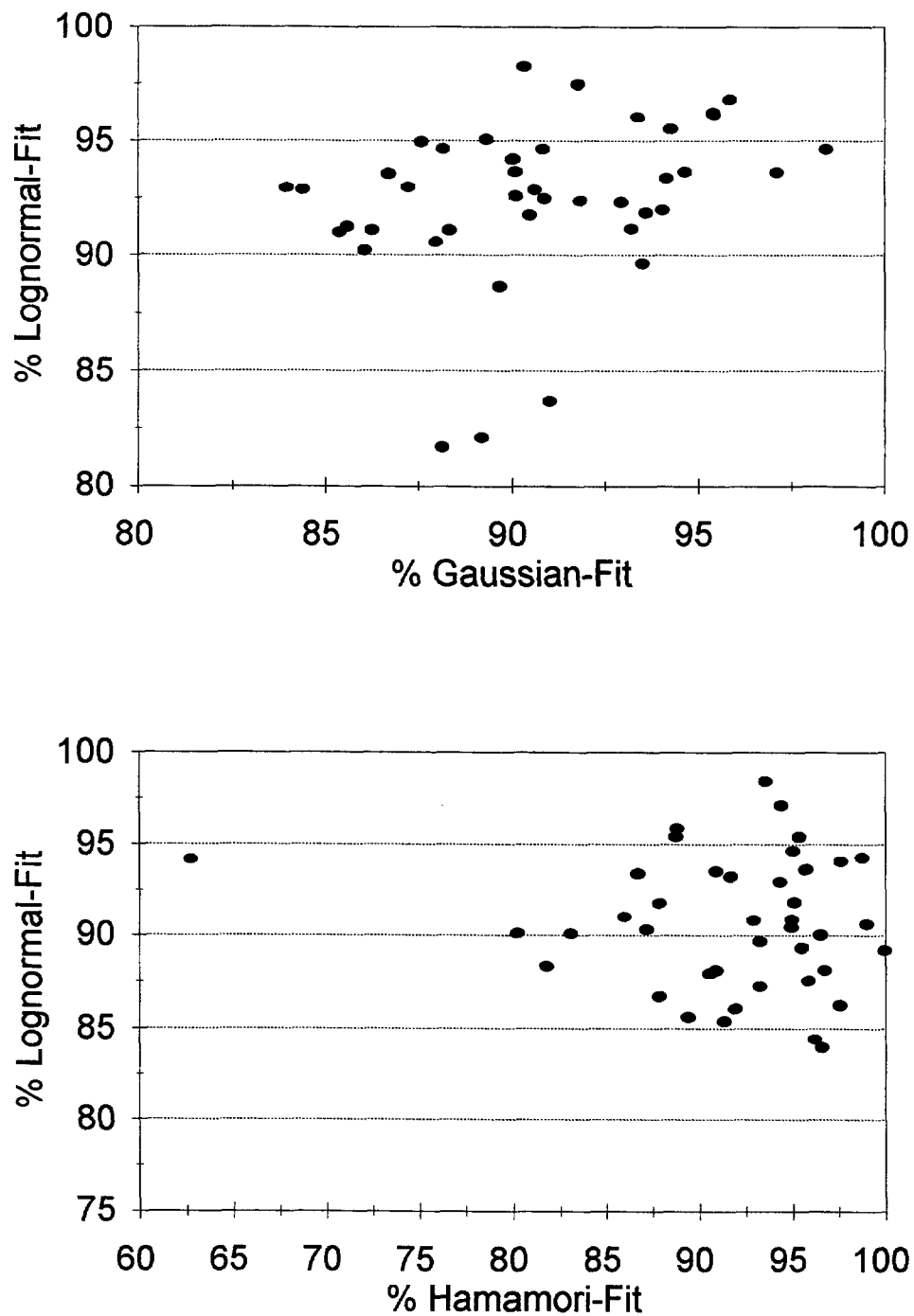


**Fig. B-2; 1:** Percent goodness-of-fit of relative transport rates for lognormal distributions versus percent goodness-of-fit for Gaussian distributions (top). Percent goodness-of-fit of relative transport rates to lognormal distribution versus goodness-of-fit to Hamamori distribution (bottom).

The results of the Schleyer and *W*-tests do not compare very well (Table B-2; 5). Some of the data sets that had a high goodness-of-fit for normality or lognormality according to the Schleyer-test did not test positive for normality or lognormality at the 95% confidence level. However, those data sets that were normally distributed according to the *W*-test had a higher mean goodness-of-fit for a normal distribution using the Schleyer-test (93.1%) than those data sets which did not test positively for normality (89.2%). A similar comparison showed only a small difference in mean goodness-of-fit between the data sets that were lognormally distributed (91.5%) and those that did not pass the *W*-test for lognormality (89.2%).

**Table B-2; 5:** Percent goodness-of-fit to a normal and lognormal distribution according to the Schleyer-test, and to the Hamamori distribution, of data sets for which normality and lognormality was approved or rejected by the *W*-test.

Result of <i>W</i> -test; confirmed distribution:	number of data sets	% Goodness-of-fit in		
		Schleyer-test to		to
		Lognormal	Gauss	Hamamori distr.
Gaussian	11	-	93.1	90.2
not Gaussian	28	-	89.2	-
lognormal	17	91.5	-	92.0
not lognormal	23	90.1	-	-
neither Gaussian, nor lognormal	13	89.6	92.1	92.6

For those data sets which could not be confirmed as normal or lognormal, the Schleyer-test indicated a low goodness-of-fit values (89.6%) for lognormality but a relatively high goodness-of-fit (92.1%) for normality and the Hamamori distribution (92.6%). These somewhat cloudy comparisons can be summarized as follows:

- The *W*-test shows moderate agreement with the Schleyer-test for Gaussian distributions.
- The agreement between the two testing procedures is poor for lognormal distributions. This can be attributed to the fact that data sets that tend to fit a lognormal distribution in either one of the tests are often short and have jagged frequency distributions. This has a negative effect on the percent goodness-of-fit. Contrarily, data sets that fit Gaussian distributions were often long and had smooth frequency distributions.
- Data sets for which the null hypothesis for normal or lognormal distributions was rejected in the *W*-test have a relatively high goodness-of-fit for the Gaussian (92.1%) and Hamamori (92.6%) distributions.
- The Hamamori distribution tested positive at the 95% confidence level for a lognormal distribution. Thus the Hamamori distribution is effectively a lognormal distribution with a particular parameters.

### 2.1.5 Distribution parameters: mean, sorting, skewness

In addition to the type of distribution, the data and the underlying distributions can be further characterized by parameters such as the mean, standard deviation, sorting, and skewness. For the purposes of characterization the normalized transport rates from the 40 data sets were sorted in ascending order. The percent frequency of occurrence of each value ( $n(qb_i)\%$ ) was calculated and summed ( $\sum n(qb_i)\%$ ) to establish the cumulative frequency distribution.

The percentiles  $p_5$ ,  $p_{16}$ ,  $p_{25}$ ,  $p_{50}$ ,  $p_{75}$ ,  $p_{84}$ , and  $p_{95}$  were computed using linear regression and linear interpolation as necessary. The mean, sorting, skewness, and kurtosis were calculated (eqs. 11 - 14) using the Folk and Ward (1957) procedure developed to characterize the grain-size distributions of river sediments. Since grain-size distributions are often truncated on their tails, the Folk and Ward (1957) procedure uses only the central 95 percent of the data. Sampling very large and very small bedload transport rates is often subject to sampling errors, and thus the Folk and Ward approach also seemed reasonable for characterizing bedload transport distributions. Thus the formulas used included:

$$\text{mean} = \frac{p_{16} + p_{50} + p_{84}}{3} \quad (10)$$

$$\text{sorting} = \frac{p_{84} - p_{16}}{4} + \frac{p_{95} - p_5}{6.6} \quad (11)$$

$$\text{skewness} = \frac{p_{16} + p_{84} - (2 \cdot p_{50})}{2 \cdot (p_{84} - p_{16})} + \frac{p_5 + p_{95} - (2 \cdot p_{50})}{2 \cdot (p_{95} - p_5)} \quad (12)$$

$$\text{kurtosis} = \frac{p_{95} - p_5}{2.44 \cdot (p_{75} - p_{25})} \quad (13)$$

Unfortunately, the value for skewness is very sensitive to the range of data used for its computation. Therefore, skewness was also calculated with two other procedures that use different data ranges. The calculation of skewness according to the "3rd moment method" (*skew.3rd.m.*) (Helsel and Hirsch 1992) takes into account all data:

$$\text{skew.3rd.m.} = \frac{n}{(n-1) \cdot (n-2)} \cdot \sum_{i=1}^n \frac{(qb_i - qb_m)^3}{s^3} \quad (14)$$

where  $qb_m$  is the mean of all  $qb_i$  and  $s$  is the standard variation.

This skewness coefficient (*skew.3rd.m.*) was compared with the skewness calculated as the *quartile skewness coefficient* (*skew.quart.*) which uses only the central 50 percent of the data.

$$skew.quart. = \frac{(p75 - p50) - (p50 - p25)}{p75 - p25} \tag{15}$$

The distribution parameters for all data sets are listed in **Tables B-2; 2a, 2b, 2c, and 2d**. Skewness coefficients are usually smallest when calculated from the interquartile range (eq. 18), and slightly larger when calculated according to Folk and Ward (1957) (eq. 12). The moment method (eq. 15) produces very high values for skewness in data sets that have a high 95th percentile (i.e., data sets that contain some large bedload transport rates) and a wide range of data (high sorting coefficient).

The calculated parameters (mean, sorting, and skewness) were not related in any systematic way to the goodness-of-fit to either a Gaussian or a lognormal distribution as determined by the Schleyer-test (**Fig. B-2; 2**). Even data sets with a higher than average goodness-of-fit for normality (or lognormality) are not distinctly different in their distribution parameters (**Table B-2; 6**). Contrarily, normally distributed transport rates (as confirmed by the *W*-test) have a relatively high mean of almost 1 *qb<sub>r</sub>*, and are intermediately-well sorted in terms of the Folk and Ward (1957) classification, while lognormal distributions have a lower mean, are poorly sorted, and--as expected--are highly skewed towards small values of *qb<sub>r</sub>*, (**Table B-2; 6**). Data sets which were neither normal nor lognormal had intermediate values for the mean, sorting and skewness. Data sets which fit the Hamamori distribution also had intermediate values, with poor sorting and highly skewed distributions.

**Table B-2; 6:** Distribution parameters for Gaussian, lognormal, and Hamamori distributions, as established by different techniques.

Test	Distribution	Distribution Parameters						
		eqs.	mean (11)	sorting (12)	skewness			kurtosis (14)
				skewF&W (13)	sk.3rd.m. (15)	sk.qrtl. (16)		
<b><i>W</i>-test</b>	<b>Gauss</b>		<b>0.96</b>	<b>0.56</b>	<b>0.05</b>	<b>0.31</b>	<b>-0.003</b>	<b>0.83</b>
Schleyer-test	better than avg. Gauss		0.88	0.71	0.39	1.61	0.31	1.24
<b><i>W</i>-test</b>	<b>lognormal</b>		<b>0.81</b>	<b>0.86</b>	<b>0.57</b>	<b>1.71</b>	<b>0.45</b>	<b>1.39</b>
Schleyer-test	better than avg. logn.		0.90	0.81	0.44	1.05	0.33	0.88
<b><i>W</i>-test</b>	<b>neither</b>		<b>0.85</b>	<b>0.73</b>	<b>0.37</b>	<b>1.33</b>	<b>0.27</b>	<b>0.88</b>
<b>Hamamori</b>	<b>ideal Hamamori</b>		<b>0.95</b>	<b>0.87</b>	<b>0.41</b>	<b>1.00</b>	<b>0.25</b>	<b>0.90</b>
Hamamori	better than avg. Hamamori		0.84	0.73	0.40	1.38	0.30	1.22

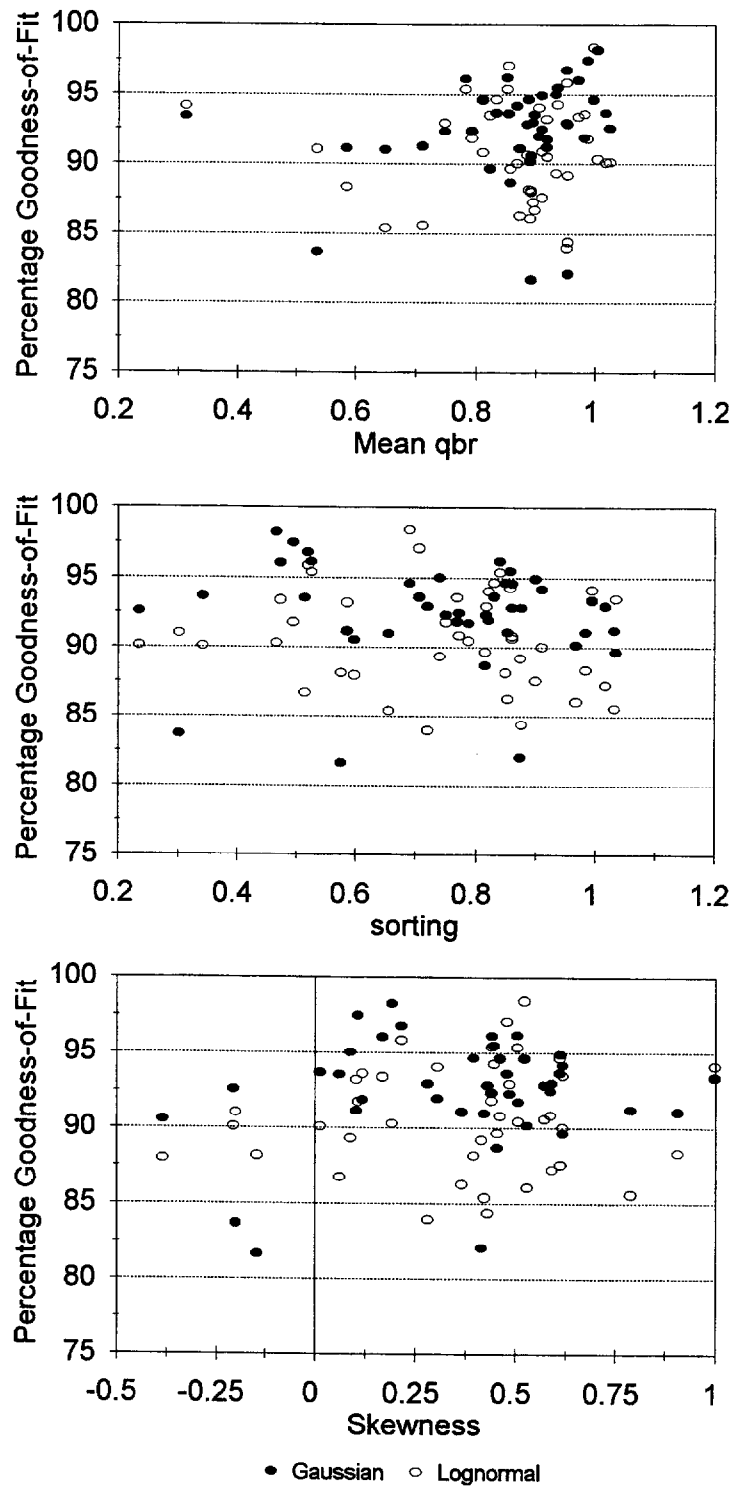
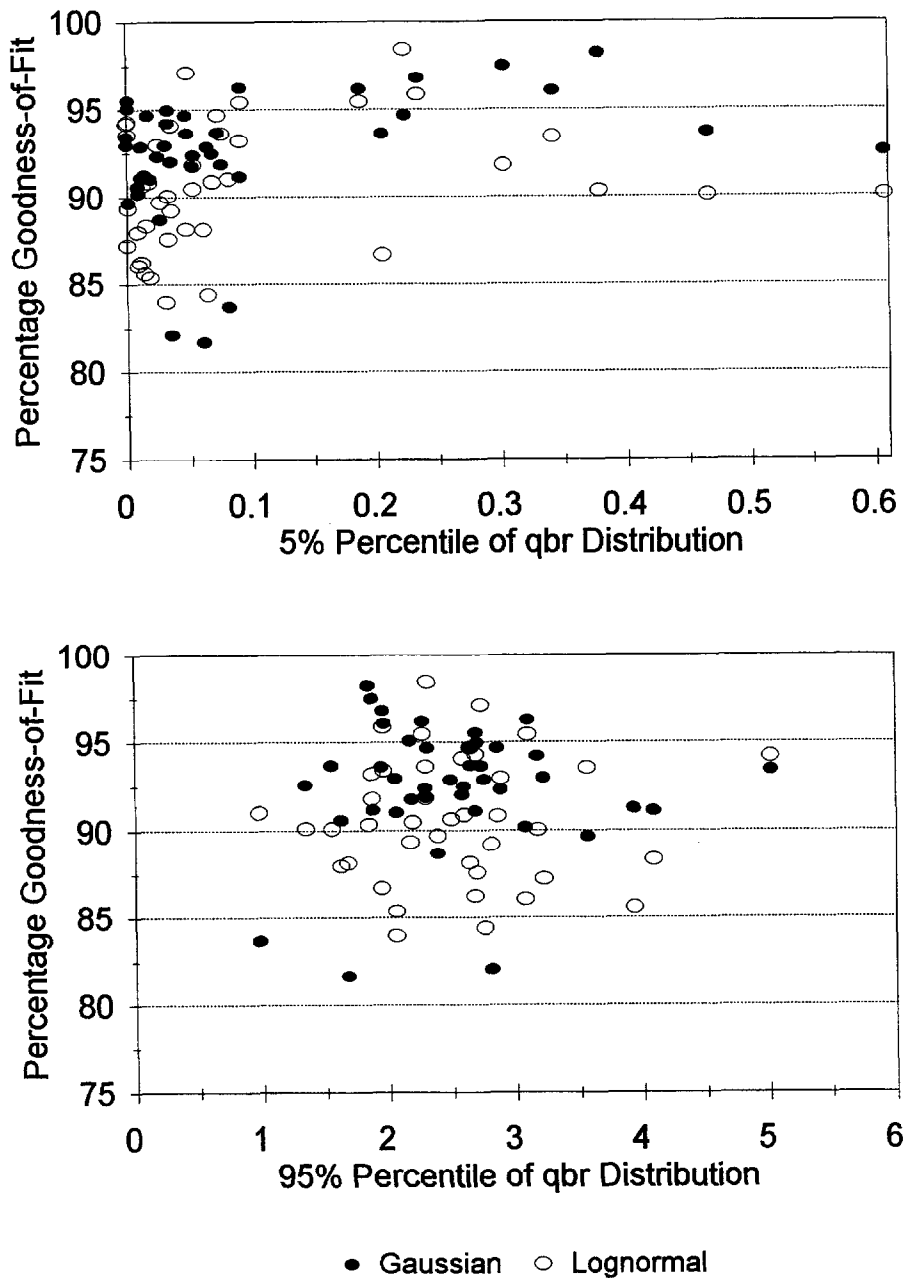


Fig. B-2; 2: Percent goodness-of-fit of relative transport rates  $qb_r$  for Gaussian and lognormal distributions versus mean (top), sorting (center), and skewness (bottom) of relative transport rates  $qb_r$ .

### 2.1.6 Shape of the cumulative distribution curves

The percentile values for the different distributions are given in **Table B-2; 7**. Since the distributions of relative bedload transport rates differ more in their tails than in their means, it was tested whether the 5th and 95th percentile varied with the percentage goodness-of-fit as determined by the Schleyer-test. Again, no systematic relation could be found (**Fig. B-2; 3**).



**Fig. B-2; 3:** Percent goodness-of-fit of relative transport rates  $qb_r$  for Gaussian and lognormal distributions versus the 5th (top), and 95th (bottom) percentile of the cumulative distribution functions of  $qb_r$ .

**Table B-2; 7:** Percentiles of relative transport rates by distribution type (Gaussian, lognormal, neither of the two, and Hamamori distributions, as determined by different procedures).

Test	Distribution	Percentiles						
		<i>p</i> 5	<i>p</i> 16	<i>p</i> 25	<i>p</i> 50	<i>p</i> 75	<i>p</i> 84	<i>p</i> 95
<b><i>W</i>-test</b>	<b>Gauss</b>	<b>0.19</b>	<b>0.35</b>	<b>0.51</b>	<b>0.95</b>	<b>1.38</b>	<b>1.57</b>	<b>1.88</b>
Schleyer-test	better than avg. Gauss	0.13	0.27	0.38	0.71	1.36	1.67	2.54
<b><i>W</i>-test</b>	<b>lognormal</b>	<b>0.04</b>	<b>0.12</b>	<b>0.20</b>	<b>0.54</b>	<b>1.34</b>	<b>1.77</b>	<b>2.96</b>
Schleyer-test	better than avg. logn.	0.05	0.15	0.27	0.68	1.51	1.86	2.59
<b><i>W</i>-test</b>	<b>neither</b>	<b>0.09</b>	<b>0.19</b>	<b>0.32</b>	<b>0.67</b>	<b>1.38</b>	<b>1.69</b>	<b>2.46</b>
<b>Hamamori</b>	<b>ideal Hamamori</b>	<b>0.04</b>	<b>0.15</b>	<b>0.27</b>	<b>0.75</b>	<b>1.53</b>	<b>1.97</b>	<b>2.81</b>
Hamamori	better than avg. Ham.	0.10	0.22	0.31	0.67	1.32	1.63	2.55

**Figure B-2; 4** compares the cumulative frequency distributions by distribution type as identified according to the *W*-test (**Fig. B-2; 4** (top)) and the Schleyer-test (**Fig. B-2; 4** (bottom)). These show that the cumulative frequency distributions are sorted by the Schleyer-test are relatively similar, while the cumulative frequency distributions as sorted by the *W* test are more distinct. **Figure B-2; 5** shows the respective frequency distributions, and this also suggests that the Hamamori distribution is intermediate with regard to the highly skewed lognormal distribution and the symmetrical normal distribution. **Table B-2; 8** helps quantify these differences by listing the percent frequency of small ( $< 0.5 qb_r$ ), medium ( $0.5-1.5 qb_r$ ), and large ( $> 1.5 qb_r$ ) relative transport rates for each of the three distribution types.

**Table B-2; 8:** Percentage of small, medium, and large relative transport rates ( $qb_r$ ) in each of the three distribution types as determined by the *W*-test.

Size	$qb_r$ Range	Distribution		
		Gaussian	Hamamori	lognormal
Small	$< 0.5$	25	38	48
Medium	$0.5 - 1.5$	57	37	30
Large	$> 2.0$	18	26	22

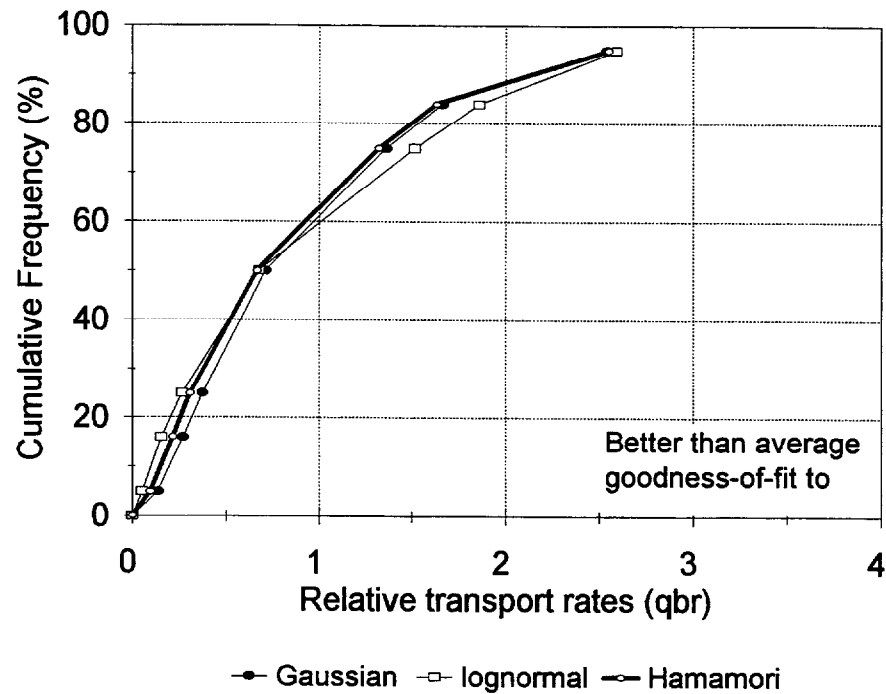
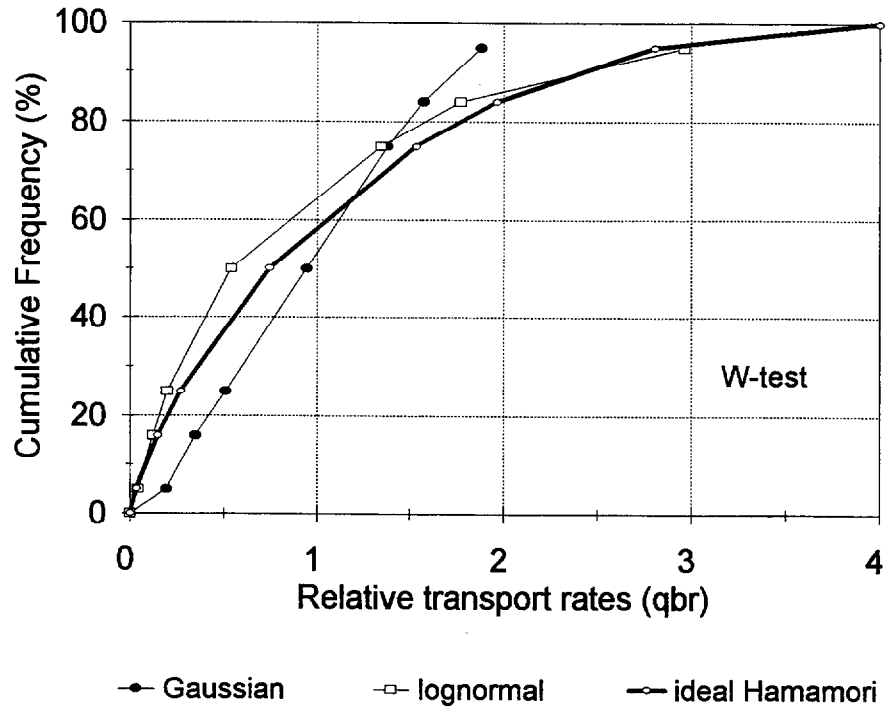


**Fig. B-2; 4:** Average cumulative distribution functions of relative transport rates  $qb_r$  for those data sets found to be normal or lognormal using the  $W$ -test, and the ideal Hamamori function (top). Average cumulative distribution functions for  $qb_r$ -data sets with better-than-average percentages of goodness-of-fit to Gaussian and lognormal distributions according to the Schleyer-test, and better-than-average percentage goodness-of-fit to the Hamamori distribution (bottom).

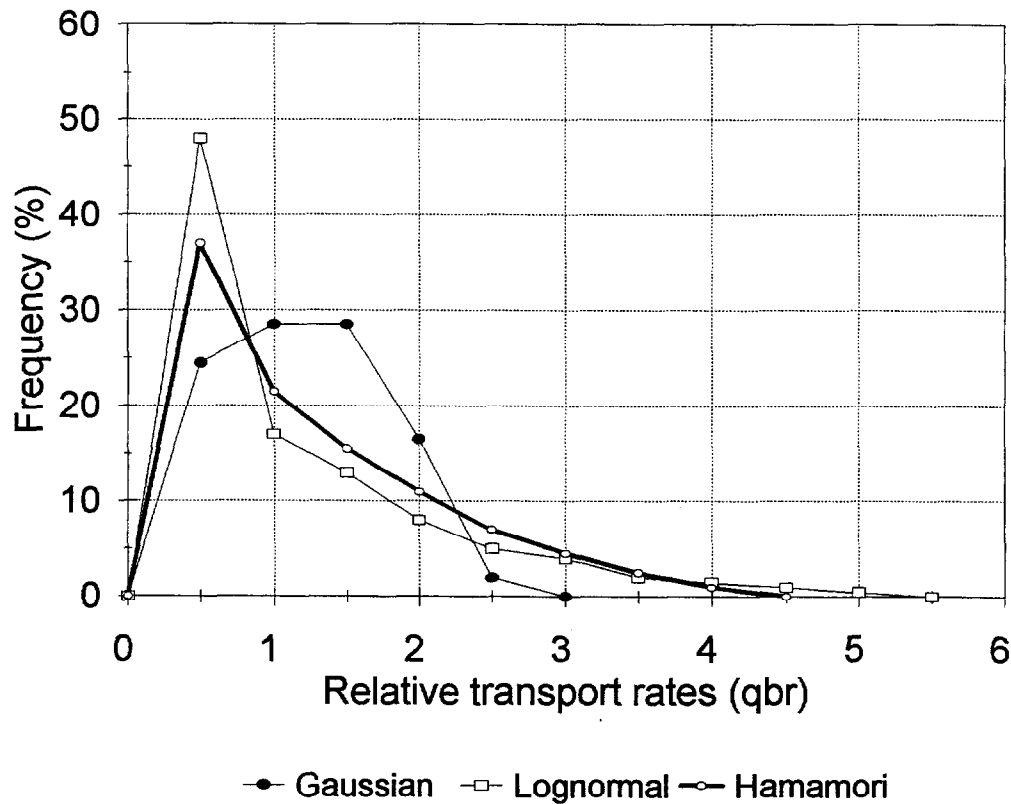


**Fig. B-2; 5:** Average frequency distributions of relative bedload transport rates for Gaussian and lognormal distributions (as determined by the  $W$ -test), and the ideal Hamamori distribution.

### 2.1.7 Summary of the test results

#### *Gaussian and lognormal distributions*

Table B-2; 8 and Fig. B-2; 5 show that data sets were Gaussian distributed when most of the measured bedload transport rates lay in the medium range, while in lognormally-distributed data sets almost half of the measurements were small ( $<0.5 qb_r$ ). In some lognormally distributed data sets, the maximum transport rate can reach up to 25 times the mean rates, as found for a cobble-bed stream by Shuyou et al. (1988). The lognormality of that distribution was confirmed by the Kolmogorov-Smirnov test with a 95% confidence interval.

#### *Hamamori distributions*

Data sets followed the Hamamori distribution when the frequency of small, medium, and large transport rates were more even. Although the Hamamori distribution has the highest percentage of large transport rates, maximum relative transport rates for the Hamamori distribution are fixed at  $4 qb_r$ . It was also found the ideal Hamamori distribution had a Folk and Ward (1957) sorting coefficient of 0.874, and distributions which had a sorting coefficient close to this value almost certainly would have a high goodness-of-fit for the Hamamori distribution (Fig. B-2; 6). No comparable relationship could be established between any of the other distributions and any of the distribution parameters (Fig. B-2; 7).

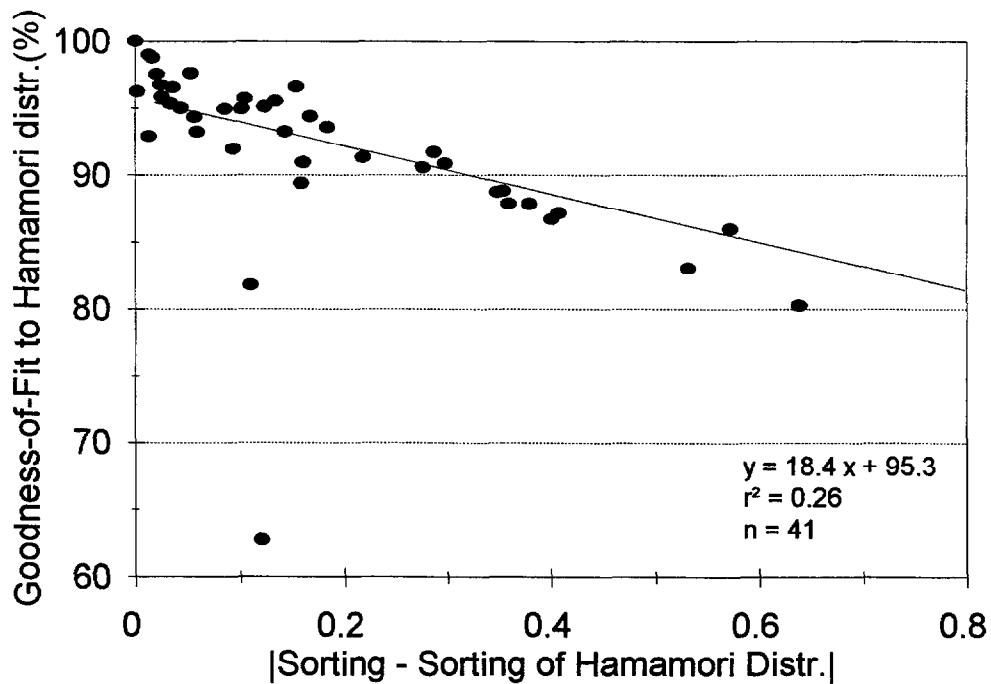


**Fig. B-2; 6:** Relationship between the goodness-of-fit of relative transport rates to a Hamamori distribution and the absolute difference between the sorting of relative transport rates and the value for sorting obtained from the ideal Hamamori distribution.

**Evaluation of the test methods**

The Schleyer-test for goodness-of-fit did not clearly differentiate data sets with a normal and a lognormal distribution. This lack of distinction may stem from the focus on the central 90% of the data, whereas most of the difference between the distributions seemed to lie in the tails of the distributions. Since the distributions were more clearly distinguished by the *W*-test, this separation is used in subsequent analyses.

**2.2 Effects on the statistical distribution type**

Since there is not a strong theoretical justification for a particular distribution of consecutive bedload measurements, and the data do not consistently follow a single distribution, it is important to determine those factors which control or may influence the observed distribution. In particular, it is necessary to ascertain the extent to which the observed distribution is controlled by the variability of bedload transport rates under different flow conditions. It further needs to be analyzed whether sampling schemes have any effects on the statistical distribution. McLean and Tassone (1987) indicated as much when they suggested that the goodness-of-fit to a Hamamori distribution depended on the constancy of the dune height (*m*-factor) and the timing of sampling relative to the speed of dune migration (*t*-factor).

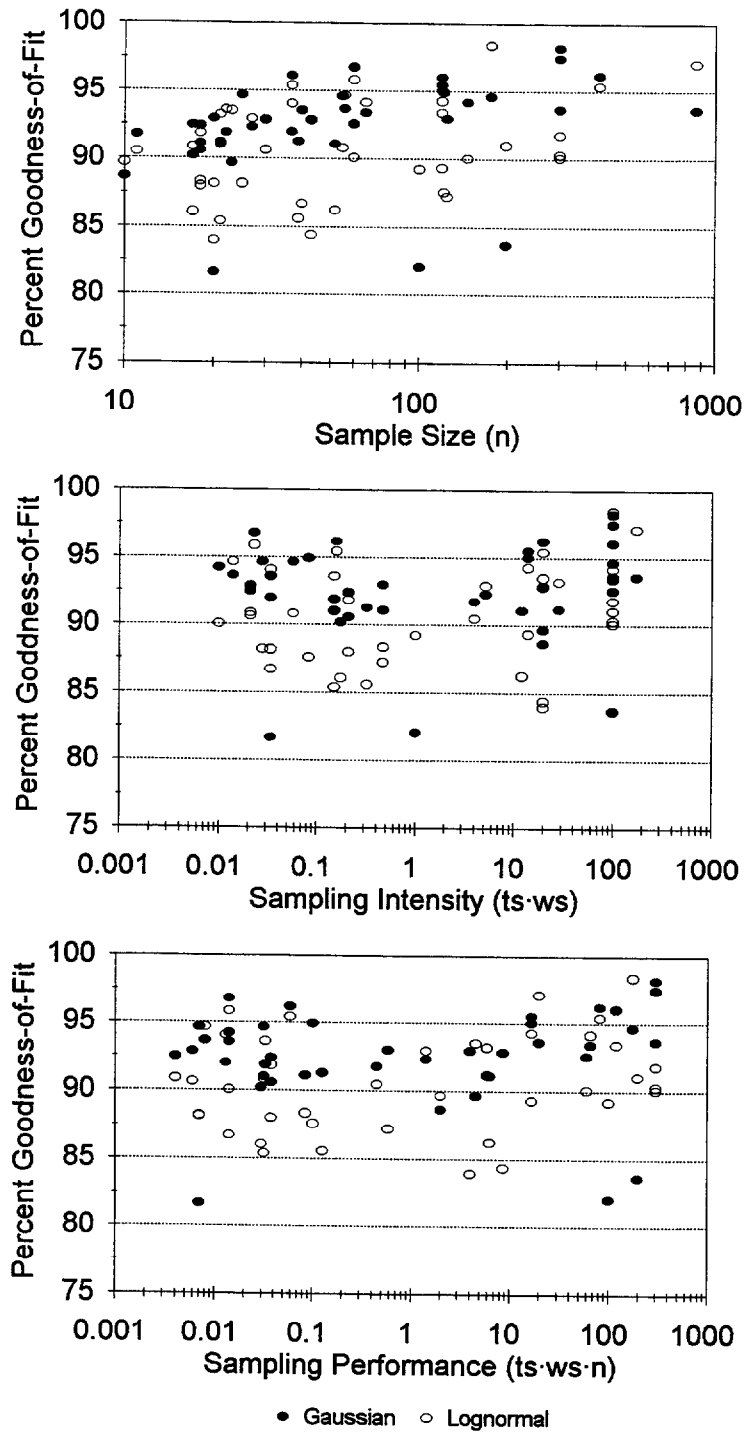


**Fig. B-2; 7:** Relationship between goodness-of-fit of relative transport rates to Gaussian and lognormal distributions and sample size (top), sampling intensity (center), and sampling performance (bottom).

The next section will examine the relationships between the statistical distribution of bedload transport rates, the natural variability, and the chosen sampling scheme. In particular, the effects of the following parameters will be examined:

- temporal scale of bedload transport variability (i.e., short-term or intra-event),
- sampling intensity and performance, and
- sampling types (continuous, sequential, and intermittent).

### 2.2.1 Short-term and intra-event variability

Short-term variability is associated with sampling during constant flow, while intra-event variability is associated with bedload sampling during unsteady flow. An absolute distinction between the variability of bedload transport at different temporal scales is not possible for most stream situations, because fluvial bedload transport rates are affected by several processes that operate concurrently at different temporal scales (see chapter B-1). Each of these processes has its own patterns of variability. Thus, measured short-term fluctuations of bedload transport are likely to be underlain by patterns of intra-event variability, while short-term fluctuations are superimposed on the intra-event variability. Despite this superimposition, the short-term variability of bedload transport under constant discharge will probably have a different statistical distribution than bedload transport rates at the intra-event scale during unsteady flow.

The results from the *W*-test for normality and lognormality, and the percentage goodness-of-fit to the Hamamori distribution showed that data sets taken during **constant** or almost constant discharge are more often Gaussian and Hamamori distributed than lognormal. Bedload transport rates from time periods of **unsteady** flow tend to follow a lognormal or Hamamori distribution (Table B-2; 9).

**Table B-2; 9:** Relationship between the temporal scale of bedload transport variability (constant vs. unsteady discharge) and distribution type. Normal and lognormal distributions were determined by positive *W*-tests. The top 50% in goodness-of-fit for a Hamamori distribution were then separated by constant and unsteady discharge.

Discharge Variability	No. of data sets	Number of data sets that obtained		
		positive <i>W</i> -test for lognormal	Gauss	better than average goodness-of-fit to Hamamori distribution
Constant	19	5	8	8
Unsteady	21	12	5	12

### 2.2.2 Sampling intensity and performance

In order to test whether sampling intensity affects the statistical distribution of bedload transport rates, several parameters related to sampling must first be defined. **Sampling type** refers to whether the sampling is continuous, sequential, or intermittent. **Continuous** sampling takes one bedload sample after the other with negligible unsampled time between samples. **Sequential** sampling leaves unsampled time between individual samples. During

constant flow, sequential samples are typically taken at intervals of a few minutes, and the total sampling period extends over roughly an hour or so. During unsteady flows, sequential samples are typically taken at intervals of 30-60 minutes, and sampling may extend over about a day or two. **Intermittent** sampling has a much lower sampling frequency, such as one sample per day or per week. Under relatively intensive intermittent sampling about 20 to 60 samples might be gathered during an entire highflow season, and these samples are usually taken on a fixed schedule with little or no regard to the variation in flow other than some effort to take more samples at higher flows.

**Sample size** ( $n$ ) is the total number of samples taken in a data set. **Sample duration**,  $t_{dur}$ , is the time period, or the length of time of one individual sample (e.g., "sampling for 30 seconds"). The **sampling interval**,  $t_{intv}$ , is the time period between the start of individual samples (e.g., "one sample each 30 minutes"). The **percentage time** sampled ( $t_s\%$ ) is the ratio between **sample duration** and **sampling interval**, expressed as a percent:

$$t_s\% = \frac{t_{dur} \cdot 100}{t_{intv}} \quad (16)$$

The **percentage of the stream width** sampled ( $w_s\%$ ) is the number of samples per cross-section multiplied by the ratio of sampler width  $w_{HS}$  to stream width  $w$  and expressed in percent.

$$w_s\% = \frac{n_s \cdot w_{HS} \cdot 100}{w} \quad (17)$$

**Sampling intensity** ( $I_s$ ) is the percentage of time sampled ( $t_s\%$ ) multiplied by the percent stream width sampled ( $w_s\%$ )

$$I_s = \frac{t_s\% \cdot w_s\%}{100} \quad (18)$$

The percent time sampled ( $t_s\%$ ) is 100% for continuous sampling, and will often drop below 1% for intermittent sampling. The percent width sampled ( $w_s\%$ ) is 100% when sampling covers the entire cross-section, as in the case of a vortex-type sampler, and typically drops to below 1% when samples are taken at one location during fast, sequential sampling. A sampling intensity of  $I_s = 100\%$  is only obtained when the entire sediment in transport within a cross-section is sampled at all the time. This can practically only be achieved in flume experiments, or at especially designed bedload transport measuring stations with vortex samplers or pebble counters. In research situations bedload sampling in streams using a 7.6 cm Helley-Smith sampler typically covers about 1-10% of the stream width, and 1-10% of the highflow duration, leading to sampling intensities between 0.01 and 1%. Baseline sampling for bedload usually comprises weekly sampling only, and if total sampling time for one cross-sectionally averaged sample takes one hour, only 0.6% of the time is actually sampled. Using a 7.6 cm (3-inch) Helley-Smith sampler in 1-meter increments over a 5 m wide stream yields 4 cross-sectional samples, and a  $w_s$  of 6.1%. Sampling intensity in this case is 0.036%, or 36/100,000 of the total possible samples.

**Sampling performance**

Sampling intensity does not necessarily quantify the quality of a data set in terms of sample size. For example, continuous sampling in 30-second increments across the entire stream width (e.g., using a vortex sampler) over a 5-minute period yields a sampling intensity of 100%, but only 10 samples. This sample size may be sufficient to calculate a mean, but is too small for detailed statistical analysis or to characterize the underlying distribution. For statistical purposes, and especially for the characterization of the discharge-bedload transport relationship, the value of a data set increases with the number of high-intensity samples taken throughout the flood event. This sampling quality can be expressed by a **sampling performance** ( $p_s$ ), defined as the product of sampling intensity ( $I_s$ ) and sample size ( $n$ ).

$$p_s = \frac{t_s \% \cdot w_s \% \cdot n}{100 \cdot 100} \quad (19)$$

Disregarding cross-sectionally variability and assuming only short-term variability of bedload transport, it does not matter statistically whether a high sampling performance is achieved by a few high-intensity samples or many low-intensity samples. But since bedload transport in streams is often affected by temporal variability resulting from processes operating at different time scales, a high number of low-intensity bedload samples should provide statistically better data sets than a few high-intensity samples that may not include the temporal variability occurring over longer time scales.

During periods of varying discharge, sampling performance should be evaluated over the entire flow event rather than over some arbitrary time period. For example, continuous sampling in 1-minute increments over a one hour period yields a sampling intensity of 100% and a sample size of 60. But if the entire high flow event lasts for two days, the overall sampling performance is not very high. Thus sampling performance needs to be defined in the context of the flow of interest, and in this case that would be the product of sampling intensity and the ratio of total sampled time to total duration of the high flow. But since this ratio is directly proportional to sample size, the definition of sampling performance as given in eq. (20) could probably be used to also quantify the sampling effort during unsteady flow.

The downside of sampling performance as defined in this study is that its actual value is difficult to evaluate. Typical values for sampling performance range between 0.01 and 0.1 for sequential sampling with a Helley-Smith sampler, and between 1 and 10 for continuous sampling with a few trap openings over the cross-section **Table B-2; 1**. Values of 100 and larger are possible for extended continuous sampling across the entire flow width. But since there is no limit regarding the number of samples taken per data set, there is also no limit as to how high the sampling performance can be.

Since our 40 data sets exhibit such a vast range in terms of sample size, sampling intensity, and sampling performance, an analysis of these values should be based on median rather than mean values. **Table B-2; 10** compares the median values of sample size, sampling intensity, and sampling performance among the different distribution types to determine the influence of sampling intensity and performance on the observed distribution of bedload transport rates. Data sets with large sample sizes, and data sets with high sampling intensity and high sampling performance tend to produce Gaussian distributions, while data sets generated by lower sampling intensities and performance tend to yield lognormal distributions. Intermediate values for sample size, sampling intensity, and performance yield Hamamori distributions.

**Table B-2; 10:** Relation between sampling schemes and the probability distribution of samples.

Distribution Type	Median Sample Size $n$	Median Sampling Intensity $w_s t_s / 100$	Median Sampling Performance $w_s t_s n / 100$
<i>Passed W-test at 95% significance level for:</i>			
Lognormal	37	0.2	0.1
Gauss	<b>60</b>	<b>20</b>	<b>6</b>
neither	40	0.5	0.6
<i>better than average goodness-of-fit for:</i>			
Hamamori	40	5	1
<i>better than average goodness-of-fit in Schleyer-test for:</i>			
Lognormal	55	17	6
Gauss	<b>120</b>	14	<b>10</b>

### 2.2.3 Continuous and sequential sampling

Both continuous and sequential sampling were used for sampling constant and unsteady flows. Sampling continuously at constant flow is characteristic of flume experiments, and most of these flume experiments yield Gaussian distributions (**Table B-2; 11a**). But our 40 data sets are not enough to reliably state which of the three distributions might apply to bedload transport measurements taken sequentially during constant flow, or either sequentially or continuously during unsteady flow. However, intermittent sampling with one or two samples per week during an entire highflow season yielded only lognormal and Hamamori distributions.

Differentiating according to the temporal scale of bedload transport, **Table B-2; 11a** shows a slight preference for Gaussian distributions to be obtained from sampling during constant flow (8 out of 13 Gaussian distributed data sets). The effect of temporal scale is indicated by the fact that lognormal distributions are preferentially obtained from sampling unsteady flows (12 out of 17 data sets). The Hamamori distribution again takes an intermediate position, with 8 out of the 20 data sets with a better-than-average goodness-of-fit coming from samples taken at constant flow, and the remaining 12 data sets from measurements taken during unsteady flow. A sorting by sampling type indicates a tendency for sequential and intermittent sampling to yield a lognormal distribution, and for continuous sampling to yield a normal distribution (**Table B-2; 11b**).

**Table B-2; 12** summarizes how temporal variability, sampling intensity, sampling type, and the sampled conditions affect the statistical distribution of the observed data. It should be kept in mind that these are general tendencies, and that the flow and sampling factors are not necessarily independent. Flume studies typically measure the short-term variability of bedload transport during constant flow, and this allows high sampling intensity and sampling performance. Under these conditions the data most often follow a Gaussian distribution. When bedload transport is measured in a stream during both constant and unsteady flow, sampling type does not seem to affect the resulting distribution of the data.

Intermittent sampling with only one or two samples per week are almost exclusively lognormal and Hamamori distributed, but not Gaussian.

**Table B-2; 11a:** Number of data sets falling into various sampling categories, and the distribution of those data sets by type of distribution.

Temp. scale of bedload transport	Discharge Variability	Sampling Type	Distribution Type					
			Lognormal		Gaussian		Hamamori	
			n	%	n	%	n	%
Short-term	$\pm$ Constant	19 {	- Continuous	9	1 (6)	5 (38)	3 (15)	
			- Sequential	10	4 (24)	3 (23)	5 (25)	
Intra-event	Unsteady	21 {	- Continuous	7	4 (24)	2 (15)	5 (25)	
			- Sequential	10	5 (29)	3 (23)	4 (20)	
			- Intermittent	4	3 (18)	0 (0)	3 (15)	
Total		40	40	17 (100)	13 (100)	20 (100)		

**Table B-2; 11b:** Percentage of lognormal-, Gaussian-, and Hamamori-distributed data sets falling into one of the three sampling types.

Sampling Type		Distribution Type					
		Lognormal		Gaussian		Hamamori	
		n	%	n	%	n	%
Continuous	9	5 (30)	7 (53)	8 (40)			
Sequential	10	9 (53)	6 (46)	9 (45)			
Intermittent	4	3 (18)	0 (0)	3 (15)			
Total	23	17 (100)	13 (100)	20 (100)			

### 2.3 Variability of bedload transport: coefficient of variation (CV)

Chapter B-1 provided several graphical examples of the temporal variability of bedload transport during constant and unsteady flow. This variability can be quantified by the coefficient of variation (CV). As will be shown in a later section of this chapter, the CV can be used to calculate how many bedload samples are needed to determine an accurate mean transport rate given that the underlying distribution is Gaussian.

Another reason for calculating the CV was to find out how much of the total variability of a data set is due to the effects of the unsteady flow. For this analysis we calculated the CV for bedload transport rates measured during unsteady flow ( $CV_{meas}$ ), and for data sets in which bedload transport was predicted from rating curves determined from measured transport rates ( $CV_{pred}$ ), and compared  $CV_{meas}$  to  $CV_{pred}$ .

**Table B-2; 12:** Preferential associations of stream and sampling parameters with a statistical distribution type.

Parameter	Statistical distribution type		
	Gaussian	lognormal	Hamamori
Scale of temporal variability (corresponding to) discharge patterns	short-term	intra-event	slight preference for intra-event variability during unsteady flow
Sampling intensity and performance	constant	unsteady	
Sampling type	mostly high	mostly low	intermediate
Bedload transport condition	slight preference for continuous sampling	preference for sequential sampling	no preference
	flume experiment	high flow event	high flow event

The coefficient of variation (CV) is the ratio of sample standard deviation divided by the sample mean (calculated from standard formulas as compared to the distributional characterization in Section 2.1.5):

$$CV (\%) = \frac{s}{m} \cdot 100 \quad (20)$$

The coefficients of variation (CV) for all data sets range from 30% to more than 200%, and these are presented with the sample means and standard deviations in **Table B-2; 1**. The coefficient of variation of bedload transport appears to be affected by several parameters, including the:

- grain-size distribution of the sediment being transported,
- temporal scale of bedload transport variability (short-term fluctuations during constant discharge and intra-event variation during unsteady flow), and
- sampling type and intensity.

The effects of these parameters on CV is analyzed in the following sections.

### 2.3.1 Effects of bedload particle-size

Several authors have reported that the coefficient of variation increases with increasing bedload particle sizes. Kuhnle and Southard (1988) showed that for gravel mixtures in lab experiments, the transport of small particles exhibited a relative small temporal variation, while transport rates of pebble-sized material fluctuated considerably. Jackson and Beschta (1982) and Beschta (1983) found a similar result for gravel-bed rivers in Oregon. Jackson

and Beschta (1982) sampled bedload at approximately 2-hour intervals for 5 to 60 seconds at 5 to 8 equally spaced intervals across the stream during a storm flow at Flynn Creek. The coefficient of variation in repetitive samples was about 50%. Although Jackson and Beschta (1982) could not attribute certain proportions of the variation to either sampling error or the temporal variability of bedload transport, they assumed that most of the variation was due to transport processes and not to unrepresentative sampling.

Similarly, the CV was about 45% for approximately 65 consecutive samples of total bedload transport taken at 3-minute intervals during the recession limb of a storm at Oak Creek, and this was strongly controlled by the particle sizes of the bedload particle sizes (Beschta 1983) (Table B-2; 11). Beschta (1983) assumed that some of the high variability of the pebble transport rates is due to the unrepresentative sampling efficiency of the Helley-Smith sampler for large particles, and he postulated that samplers with a larger orifice, bag size, and mesh width are needed to representatively sample the coarse part of bedload transport.

**Table B-2; 13:** Variation of CV with grain-size class at Oak Creek (from Beschta 1983).

	Grain size class (mm)				
	0.25-0.5	1-2	4-8	16-32	>32
CV (%)	17	29	58	70	150

A bedload sampler that met the above criteria was used during a snowmelt highflow at Squaw Creek, a mountain gravel-bed river in Montana. The sampler had an opening 0.3 m by 1.55 m, and the net was 3 m long with a 1-cm mesh (Bunte 1990, 1992a). The data obtained with this sampler clearly indicated that bedload particle size affects CV. But whether particle size increases or decreases CV is dependent on the number of samples included in the analysis, and on the variability of bedload transport rates within the data sets (Fig. B-2; 8 and Table B-2; 14). When relatively few bedload transport measurements are included, or when the range of measured bedload transport rates is relatively low, the variability tends to increase with particle size (see May 23/24 in Fig. B-2; 8). Within this overall trend, CV also tends to increase as additional samples taken during earlier highflow days with somewhat smaller discharges are included into the analysis (May 19-24). The same effect remains when bedload transport rates becomes larger and more variable during a later highflow day with slightly higher flows (e.g., June 5/6).

However, there is a large increase in CV when all bedload samples taken during snowmelt highflow are combined into one data set (May 19 - June 6). This larger data set also indicates that the transport rates of small pebbles becomes more variable than the transport rates of cobbles, and this is contrary to the trends described previously. This difference may be attributed to the fact that smaller pebbles are more subject to the effects of hiding and exposure. A higher temporal variability of fine bedload transport was also reported by Sidle (1988). Sidle postulated that the transport of fine bedload is mostly hydraulically controlled, while the coarse bedload was being temporarily stored behind large woody debris. Thus the effects of particle size on CV are not predictable *a priori*, but are controlled by the bedload transport processes as well as the number and variability of bedload samples used in the analysis.

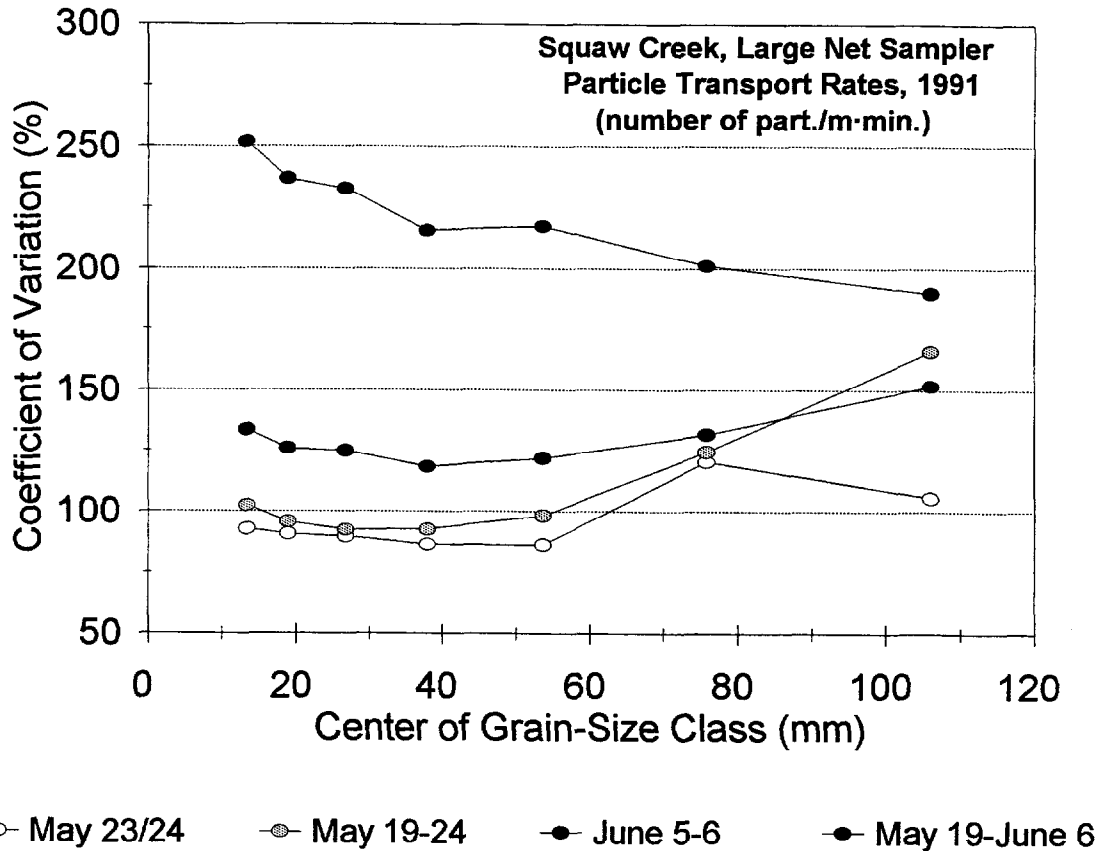


**Fig. B-2; 8:** Coefficient of variation in fractional bedload transport rates taken during different periods of snowmelt highflow at Squaw Creek, Montana. Bedload samples were taken with a large frame sampler. Size of the opening was 0.3 m by 1.5 m, and netting mesh width was 10 mm.

**Table B-2; 14:** Bedload sampling with a large net bedload sampler at Squaw Creek, 1991: transport rates and number of samples and sampling days.

Date of samples	Number of samples	Number of sampling days	Bedload transport rates	
			Range (kg/m·s)	$\frac{Qb_{max}}{Qb_{min}}$
May 23/24	11	1	0.5 - 11	22
May 19-24	17	3	0.5 - 11	22
June 5/6	8	1	9 - 340	38
May 19- June 6	25	4	9 - 340	38

### 2.3.2 Effects of the type of flow event and the respective bedload transport patterns

The effects of different types of flow on the variability of bedload transport rates will be examined below. We calculated the CV in percent for all 40 data sets (**Table B-2; 1**) and grouped the results according to flow types in **Table B-2; 15**. Although the number of data sets included in this study is somewhat small, and the accuracy of the calculated CV values cannot be assessed, certain trends are already discernible.

**Table B-2; 15:** Coefficients of variation (CV) for measured and predicted bedload transport rates for constant and unsteady flows in flumes and streams.

Flume/ Stream	Flow type	Sampling type	CV of bedload transport rates (%)	
			mean	range
Flume	constant	continuous	55	28 - 92
Stream	± constant	sequential	79	53 - 116
Stream	highflow event	continuous	97	74 - 125
Stream	highflow event	sequential	95	58 - 128
Stream	highflow season	intermit./cont.	145	88 - 269

While the average variability of bedload transport in flume studies is about 55%, the average CV increases to 79% when measured in a stream with nearly constant discharge. This difference reflects the wider range of possible bedload transport sources and sinks in streams as compared to flumes. The practical implication is that the variability of bedload transport rates in flume studies cannot be used to determine the minimum sample size for assessing the mean bedload transport rate in streams.

The high CV of bedload transport rates that are measured throughout an entire highflow season (145%) result from the wider range of flows and bedload transport rates encountered during a season as compared to within one flood event. There was a surprisingly small difference between the mean CV of bedload transport rates measured during almost constant flow (79%) and over individual flood events (97 and 95%). This difference of around 20% suggests that the variability at nearly constant flow can be nearly as large as the variability during a single high flow event.

For the sake of comparison, we also calculated the CV for the rating curve derived from the data sets collected over varying discharges. The calculated CV values for these rating curves were about 20% less than the CV values obtained from the original data. The higher CV values for the original data are, of course, due to the various processes that produce fluctuating bedload transport rates during flood events (Chapter B-1). The variability and uncertainty in estimating sediment loads with varying flows (e.g., using a rating curve approach) is covered in Chapter B-4.

## 2.4 Empirical sampling schemes and number of samples needed for preset levels of accuracy

Prior to initiating any attempt to detect a cumulative watershed effect, it is important to know the trade-off between the level of effort and the corresponding level of uncertainty for a particular stream. There are two approaches to estimating the sample size needed to estimate a mean transport rate for bedload. One can simply follow an empirical sampling scheme, based on existing studies and information for similar situations and stream types. This approach can provide a rough estimate of sampling accuracy, and will probably yield a workable compromise between sampling effort and sampling accuracy. The initial sampling will also provide some data which can be used to characterize the variability at the measuring site and then adjust the sampling scheme. The other, more precise approach is to use information from an explicit pilot study to determine the variability of bedload transport, estimate the underlying distribution, and then use equations or existing tables to define the appropriate sample size for a given variability and level of uncertainty. Both approaches will be explained below.

### 2.4.1 Empirical sampling schemes

Empirical sampling schemes for bedload transport are a compromise of sampling between the cross-sectional and the temporal variability of bedload transport. A summary and discussion of the strengths and weaknesses of several of these schemes are discussed below.

#### *Emmett's 20 x 2 equal width increment sampling*

The East Fork River in Wyoming is a 15-20 m wide gravel-bed river that transports mainly sand. Bedload transport is mostly confined to narrow pathways that wander more or less at random across the stream bed. Intensive studies have found a rather good agreement between bedload transport rates as measured with a 7.6-cm Helley-Smith sampler in 0.5 m increments across this stream, and cross-sectional bedload transport rates as measured with a vortex-conveyor belt sampler. On this basis Emmett (1980) concluded that bedload sampling had to focus on the cross-sectional variability of bedload transport. Emmett therefore suggested that one bedload sample at a site should consist of two traverses across the stream, sampling for about 30 seconds at each of 20 locations during each traverse. The 40 subsamples should then yield a good estimate of the total bedload transport at that cross-section.

This approach yields a total sampling time of about 20 minutes, while the field time for this sampling is about 1.0-1.5 hours. Emmett considers this period sufficiently long to account for the temporal variability in bedload transport. In the presence of bedload waves Emmett (1984) suggested that a more precise procedure would be to sample each location within the cross-section for a period sufficient to establish a mean local transport rate, but that the time required to do so would usually prohibit this approach.

Locations with different stream characteristics may require some modifications to this idealized sampling scheme. In narrower streams Emmett (1996) proposes to sample 13 locations with 3 traverses, or perhaps 10 locations with 4 traverses in yet narrower streams. Extremely high transport rates may also necessitate a reduction in sampling time at each location. Sampling periods as low as 10 seconds may be appropriate if this fills the sampler to half its capacity. On the other hand, extremely low transport rates may require much longer sampling times to collect a measurable amount of sediment. Other situations may demand a reduction in sample size and sampling time. For example, the number of

may demand a reduction in sample size and sampling time. For example, the number of subsamples can probably be reduced if the stream is less than 3 m wide, and the number of samples should probably be reduced if the flows are so flashy that discharge will change substantially in the time needed to take 40 subsamples of 30 seconds each (Emmett 1996).

**Hubbell and Stevens' 4 x 10 scheme**

Hubbell and Stevens (1986) and Hubbell (1987) compared the predicted error associated with sampling 4 and 20 cross-sectional locations, respectively, under various conditions. The relative temporal variability was kept equal at each location in the stream by assuming that bedload transport rates always followed the Hamamori distribution. On this basis Hubbell and Stevens (1986) and Hubbell (1987) created data sets of consecutive bedload transport rates, and each modeled scenario consisted of one large and one small mean transport rate. Within a cross-section, the ratio of large to small mean bedload transport rates was set to values of 1.5, 7, and 25 in order to account for different levels of lateral variability.

These data sets were then used to model three different characteristics of lateral transport distribution (Fig. B-2; 9): (1) a concentration of high transport rates in 25% of the stream width, and small mean transport rates in the remainder; (2) a central distribution scheme where large and small mean transport rates occupy equal portions of the stream width; and (3) a wide transverse distribution in which high bedload transport rate occupy 80% of the stream channel. Fig. B-2; 10 depicts the maximum probable errors associated with sampling 4 and 20 locations for three ranges of lateral variability (1.5-25:1) and the three distributions of high bedload transport as shown in Fig. B-2; 9. To better compare the performance of both sampling schemes, the small boxes in Fig. B-2; 10 mark the respective

**narrow concentration      central distribution      wide distribution**

Ratio of width covered by mean large and mean small transport rates:

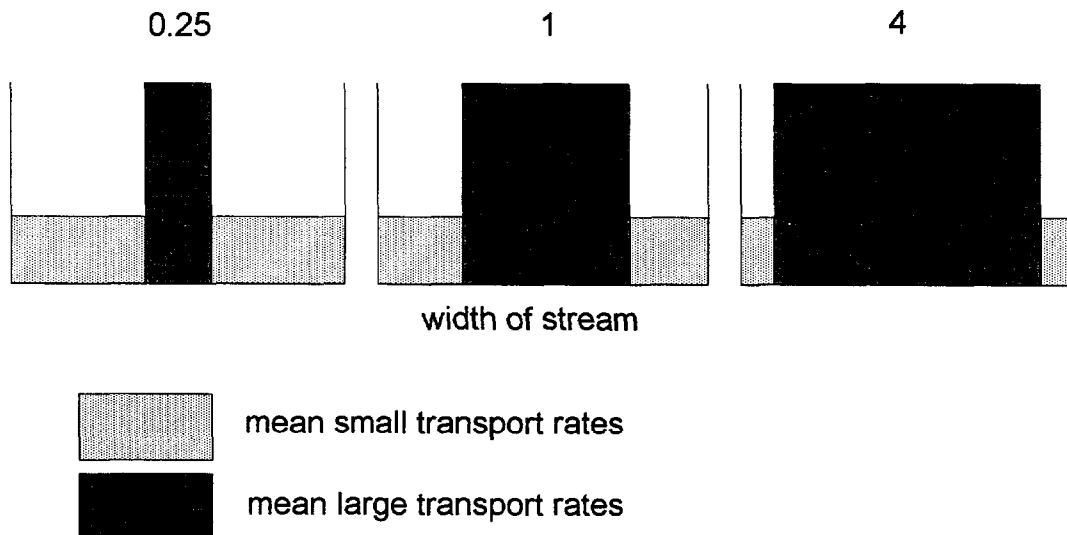


**Fig. B-2; 9:** Lateral distribution of bedload transport rates assumed in the transport models of Hubbell and Stevens (1986), and Hubbell (1987).

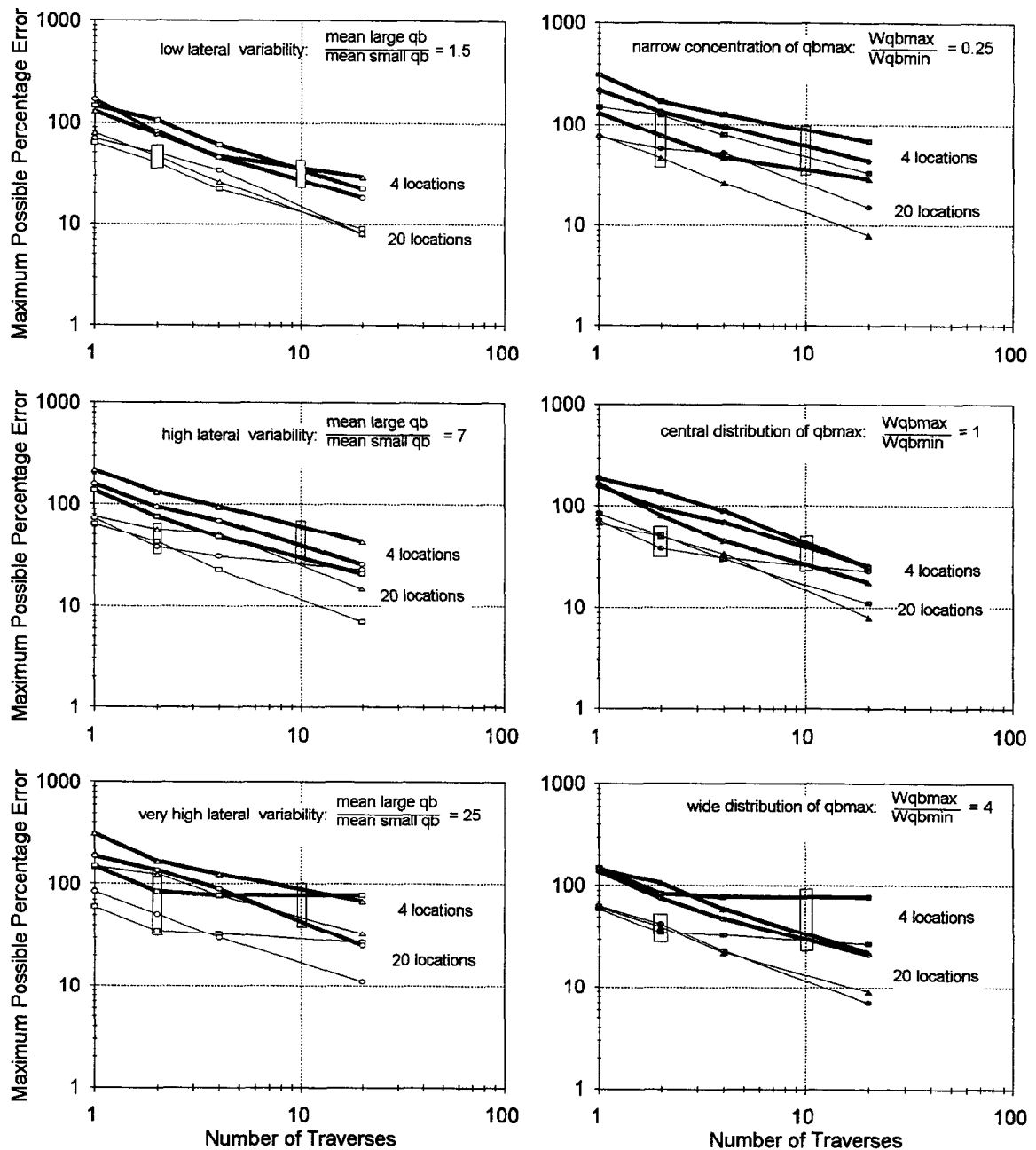


**Fig. B-2; 10:** Maximum percent error associated with two sampling schemes, different levels of variability in transport rates at individual locations (left-hand plots), and different spatial distribution of lateral variability within the cross-section (right-hand plots). Open symbols of  $\Delta$ ,  $\circ$ , and  $\square$  in the left-side plots represent narrow, equal, and wide distributions of large transport rates over the cross-section as shown in Figure B-2; 9. In the right-hand plots, closed symbols of  $\blacktriangle$ ,  $\bullet$ , and  $\blacksquare$  represent ratios of mean high to low transport rates of 1.5:1, 7:1, and 25:1, respectively. Heavy lines show the error associated with taking samples at only four cross-section locations, while thin lines represent the error associated with sampling at 20 cross-section locations. Boxes contain the maximum probable percent error for a sample size of 40. (Data plotted from Hubbell 1987).

maximum probable errors associated with taking 40 samples (actually subsamples) in each sampling scheme. The average percent error obtained for different degrees and characteristics of lateral variability are compared in **Table B-2; 16**. Taking 40 subsamples at 4 cross-sectional locations with 10 traverses yields either an equal or lower percentage error than taking 2 samples at 20 locations, except for the case when high bedload transport rates cover a wide section of the stream width (lower right plot in **Fig. B-2; 10**).

**Table B-2; 16:** Average maximum percent errors in bedload transport for 40 subsamples taken under two different sampling schemes with differing amounts and spatial distribution of high bedload transport rates.

Number of		Ratio of high to low mean transport rate			Ratio of stream width covered by large and small transport rates		
Verticals	Traverses	1.5	7	25	0.25	1	4
20	2	45	46	70	76	46	39
4	10	32	43	70	61	36	47

Hubbell (1987) then gives the maximum probable percent error for various sample sizes for two transport situations: (1) moderately nonuniform transport with a ratio of high to low mean transport rates of 1.5 and a central distribution of large transport rates; and (2) extremely non-uniform transport with a ratio of high to low mean transport rates of 25, and a wide lateral distribution of large transport rates (**Fig. B-2; 11**). For subsample sizes in the range of 10 to 100, and 10 to 400 samples respectively, sampling 4 locations and 10 traverses yields a lower percentage error than the 20 x 2 plan.

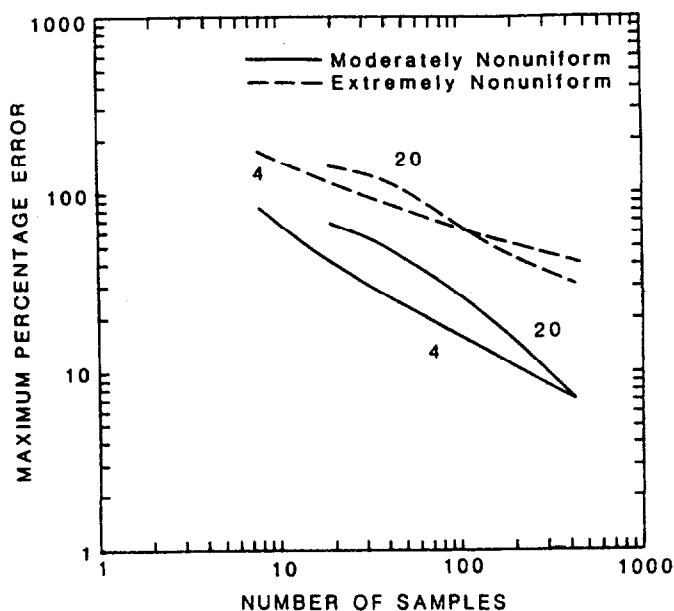


**Fig. B-2; 11:** Maximum probable percent error versus sample size for moderately nonuniform transport (ratio of high to low mean transport rates of 1.5:1, and equal widths of large and small transport rates), and extremely non-uniform transport (ratio of high to low mean transport rates of 25:1, and 80% of the stream width covered by transport rates) (from Hubbell 1987).

**Gomez's 5 x 21 at-a-point samples**

Based on analyses of the temporal variability of bedload transport by Carey and Hubbell (1986), Gomez et al. (1990, 1991), and Gomez (1991) also assume that the temporal variability of bedload transport rates usually follows the Hamamori distribution. The percentage error associated with sample size can be calculated from a formula given by Carey and Hubbell (1986):

$$\% \text{ error} = \pm t_{DF} \left( \frac{\sigma^2}{n} \right)^{1/2} \cdot 100 \quad (21a)$$

where  $t_{DF}$  is the value from the  $t$ -distribution for a given probability and  $\infty$  degrees of freedom,  $n$  is the sample size of random, serially uncorrelated samples, and

$$\sigma^2 = \frac{4m^2 + 2m + 1}{6m + 3} \quad (21b)$$

The variable  $m$  denotes the length of secondary dunes and was set to 1, and this resulted in a  $\sigma^2$  of 0.78. This equation for % error is plotted in Fig. B-2; 12 for 4 levels of confidence between 50 and 99%. At least 21 random measurements of about 30 seconds each, spaced at 10-minute intervals to avoid serial correlation, are needed at just one location within the cross-section to obtain an estimated mean transport rate that has a 99% probability of being within 50% of the true value. Twelve at-a-point samples would be needed if the confidence level was lowered to 95%. Gomez et al. (1990, 1991) further argue that the cross-sectional variability is often less than the temporal variability, and sampling effort should be allocated accordingly. This may also be true for many mountain streams, which are often supply-limited.

Nevertheless, there is a clear need to sample at multiple locations within the cross-section, particularly as discharge increases. Jackson and Beschta (1982) found that most of the increase in bedload transport and flow velocity at the onset of Phase II transport was in the center of the channel, with hardly any increase in velocity or transport in the other parts of the channel.

**Tang's equal transport rate spacing**

Tang (1990; 1991) noted that if there is negligible cross-sectional and temporal variability in bedload transport rates, the relative error (i.e., the difference in bedload transport rates between two repetitions of the same sampling scheme) is independent of whether the total sampling duration is assigned to many repetitions at a few cross-sectional locations, or fewer repetitions at many locations. In such situations the most efficient sampling design may be to measure bedload at only a few locations and have relatively few repetitions, but sampling for a longer time at each repetition. Of course, the assumption of negligible variability with respect to space, time, and grain-sizes will never be the case, and might only be approximated in some sand-bedded streams with minimal bedforms.

Since the relative sampling error is largest where mean transport rates and the magnitude of transport fluctuations are largest, and since sampling at more locations generally increases the sampling accuracy, Tang (1990; 1991) argues that sampling should be concentrated at

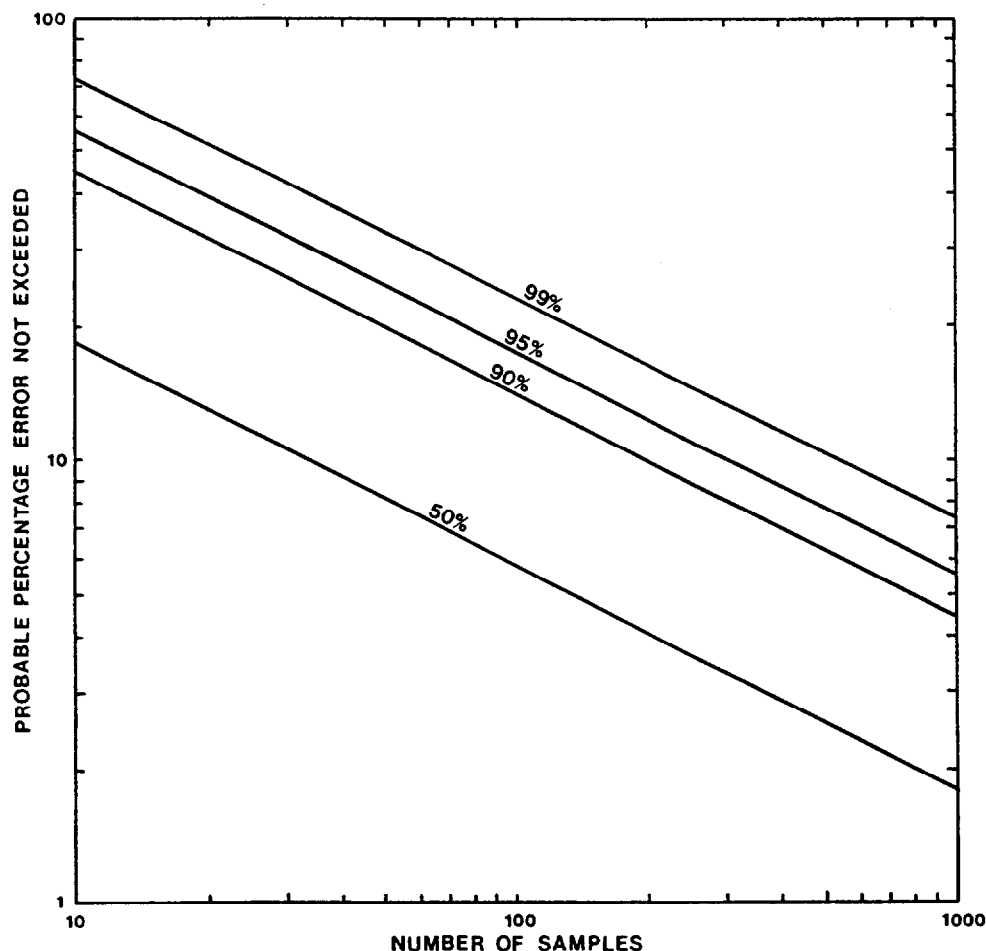


**Fig. B-2; 12:** Variation in the percent error (Eq. 21) of an estimate of the mean relative at-a-point bedload transport rate that can be expected not to be exceeded at the 99, 95, 90, and 50% confidence levels, with number of random samples. The relations are based on the Hamamori probability distribution function (Eq. 5) (from Gomez et al. 1990).

those locations where bedload transport rates are highest. Less sampling effort--in terms of locations, repetitions, and duration of sampling--should be devoted to those portions of the stream with lower transport rates. Tang suggested that such a sampling scheme could keep the relative mean square error below 10%, and he advocated sampling 8-12 locations in a gravel-bed stream with a unimodal distribution of bedload across the width, and 11 - 16 locations in a stream with a bimodal transverse distribution. In his scheme four repetitions would be collected at each sampling location, but one four minute sample would suffice if there is not much variation in transport rates or grain-size distributions over time.

Xiang and Zhou (1992) then showed that the standard deviation for two bedload transport measurements along equal-width increments was twice as high as the standard deviation resulting from two measurements at the same number of verticals but with the sampling locations based on equal transport rates. Alternatively, one could reduce the number of sampling locations from 9-16 sites under equal-width sampling to only six locations using equal transport rates with no reduction in accuracy. Such an increase in sampling efficiency

can only be achieved if one has relatively detailed *a priori* knowledge of the patterns and variability in sediment transport rates, and this again suggests need for a pilot study before embarking on any project to detect changes in sedimentary CWEs.

#### ***Comparison of sample sizes***

The sampling scheme of *equal transport rates* proposed by Tang (1990; 1991) required 32 to 64 subsamples for a mean square error to be below 10%, depending on the cross-sectional variability of transport rates. Gomez's (1991; Gomez et al. 1990; 1991) sampling scheme with at least 21 repetitions at 5 locations required 105 subsamples for an average sampling error of about 40%, whereas Emmett's (1980; 1984, 1996) equal width spacing suggested that 40 subsamples from 2 or 3 repetitions at 20 or 13 locations, respectively, would provide sufficient accuracy without explicitly stating the estimated error. Hubbell and Stevens (1986) and Hubbell (1987) showed that 40 subsamples yield a maximum probable error between 30 and 80%, depending on the lateral variability of bedload transport, with an overall average of about 54% error for the 20 x 2 scheme, and 48% for the 4 x 10 plan. Approximately 80 subsamples would have to be taken to lower the sampling error to about 40%.

These results all indicate that 40 to more than 100 bedload subsamples are needed to estimate the bedload transport rate at a given cross-section to an "acceptable" degree of accuracy (e.g., 10-80%). A direct comparison of the results is difficult, because much of the discrepancy in the recommended sampling schemes stems from the stream characteristics and the bedload transport processes at the site of concern, as well as the desired level of uncertainty. In order to clarify the trade-offs between sampling regimes, accuracy, and uncertainty, the following section analyzes the relationship between sample size and percent error for the different statistical distributions identified earlier and different degrees of variability within a given distribution.

### **2.4.2 Number of samples needed**

The accuracy of a mean sediment transport rate, and the number of samples needed to obtain a specified level of accuracy, will vary according to the statistical distribution of the parent population (i.e., all possible samples) and the variability within that distribution. The following sections will determine the minimum sample size required for Gaussian, lognormal, and Hamamori distributed bedload transport rates with different levels of variability. While these calculations have been carried out for bedload transport, they can also be applied to the parallel issue of sampling suspended sediment.

#### ***Gaussian distributions***

For Gaussian distributed samples the calculation of minimum sample size  $n_{min}$  is based on the coefficient of variation CV (Gilbert 1987; Kuhnle and Southard 1988), Kuhnle (1996). The minimum number of samples required ( $n_{min}$ ) is given by:

$$n_{min} = \left( \frac{k}{c} \cdot \frac{\sigma}{\mu} \right)^2 \quad (22)$$

where  $k = 1 - \alpha/2$ . If the confidence level,  $\alpha$ , is set to 0.05 for a two-sided test under a normal distribution,  $k$  is equal to 1.96.  $\sigma$  is the population standard deviation,  $\mu$  is the population mean, and  $c$  is the relative error (i.e., the variation of the sample mean from the population mean). The parameter  $c$  can also be considered as the allowable uncertainty. For example, if  $c$  is set to 0.1, this means that the sample mean should lie within 10% of the population mean. Of course the true mean and the standard deviation of the population are never known, but these can be estimated from the sample. If one assumes a Gaussian distribution, these values can be derived from the coefficients of variation calculated earlier. The number of samples required for the mean of a data set to be within 20% of the population mean is:

$$n_{min} = \left( \frac{1.96}{0.2} \cdot CV \right)^2 \tag{23}$$

Eqs. (22) and (23) were applied to the range of CVs encountered in the data sets with constant flow (see Table B-2; 15). These data sets are preferentially Gaussian distributed. Fig. B-2; 13 shows the exponential (i.e., power function) increase in the number of samples required to attain a more accurate estimate of the population mean given a coefficient of variation ranging from 50-125%.

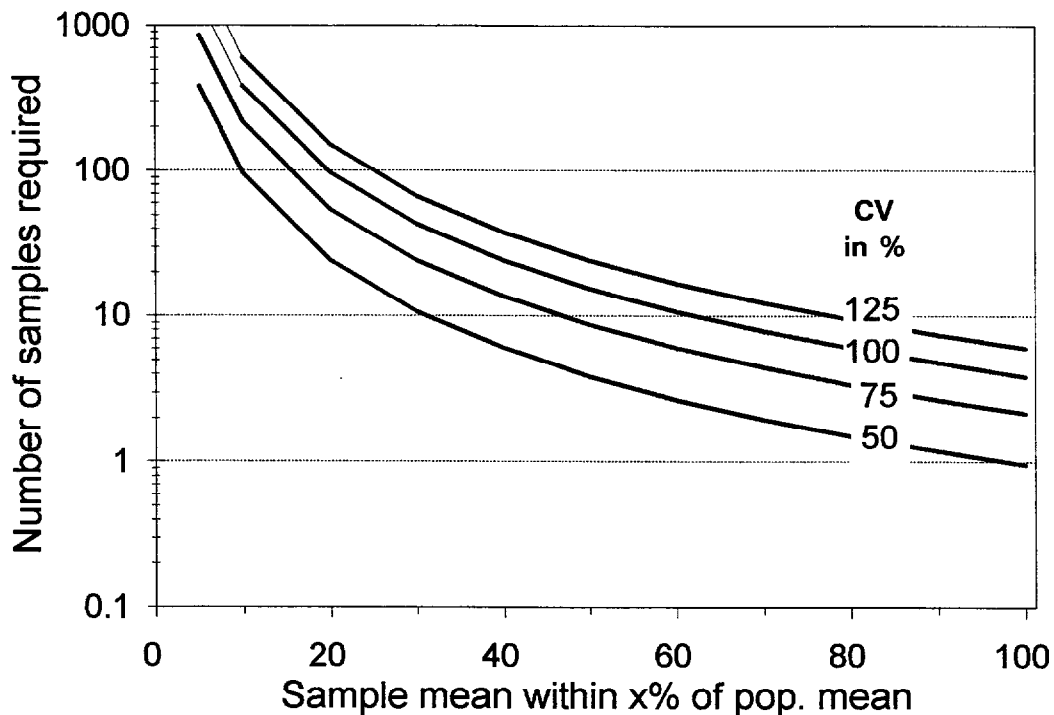


Fig. B-2; 13: Exponential increase in sample size with increasing accuracy of estimating the population mean with a 95% confidence interval; lines represent CV values between 50 and 125 percent.

If we assume a relatively low CV of 50-75% and we want to determine the mean transport rate to within 10% of the true value, approximately 100-200 samples are required. Increasing the allowable error to 20% reduces the estimated number of samples to around 20-50, while 10-25 samples are needed to determine the mean transport rate to within 30% of the population mean. Taking only 3 to 8 samples results in an uncertainty for the mean transport rate of 50%, while 1 or 2 samples yields an uncertainty of approximately  $\pm 100\%$ .

Chapter B-1 noted that the variability of bedload transport rates during a period of almost constant high flows can have a CV of more than 100%. If the CV is assumed to be in the range of 100-125%, **Fig. B-2; 13** indicates that more than a hundred samples are needed if the sample mean is to lie within 20% of the true mean at the 95% confidence level. Taking 15 to 24 samples will allow an estimate to within 50% of the true value, while 3 to 6 samples will yield an estimated mean transport rate that is accurate to a factor of two.

### ***Lognormal distributions***

Bedload transport rates measured during a period of almost constant high flows are often lognormally distributed. In this case the minimum number of samples for determining the *median* transport rate for a specified relative error (or uncertainty) can be estimated based on the sample variance ( $s^2$ ) and the total possible number of samples ( $N$ ) within the time and space of the sampling period for one sample (a sample being the estimated bedload transport for the cross-section at the time that sample is taken). Gilbert (1987) gives the following equation for temporally and spatially uncorrelated data sets<sup>3</sup>:

$$n_{min} = \frac{k^2 \cdot s^2}{(\ln(c+1))^2} + \left( \frac{k^2 \cdot s^2}{N} \right) \quad (24)$$

$k$  is again set to 1.96 for  $\alpha = 0.05$ , and  $c$  is the specified percent error expressed as a decimal.  $s^2$  is the variance of the log-transformed individual bedload transport rates for a data set ( $\ln qb_i$ ) and given as

$$s_{\ln qb_i}^2 = \frac{1}{n-1} \sum_{i=1}^n (\ln qb_i - \overline{\ln qb_i})^2 \quad (25)$$

where  $\overline{\ln qb_i}$  is the arithmetic mean of the individual log-transformed bedload transport rates for a given data set. The additive term in eq. (24) substantially decreases the sample size ( $n$ ), especially if the allowable error is small and  $N$  also becomes small. For an indefinitely large pool of possible samples  $N$ , the additive term is neglected. In most cases  $N$  can be assumed to be quite large and thus negligible. For example, a stream 8 m wide has a total of 12,000 possible samples when sampling for 30 seconds with a 7.6-cm Helley-Smith sampler over a period of one hour. Even if the stream width is reduced to 0.8 m and the

<sup>3</sup> It may not be possible to sample temporally uncorrelated bedload samples, especially in the presence of recurring bedload dunes or bedload waves from sudden upstream sources. In these cases sampling must be carried out before, during, and after bedload waves in order to ensure representative sampling that includes a variety of large and small transport rates. Spatial correlation of bedload samples may occur when migrating bedload sheets cover a wide section of the stream bed. Again, it is important to recognize the presence of such phenomena and to sample as representatively as possible.

flow is assumed to remain relatively steady for a half-hour sampling period, there are still 600 possible samples.

**Fig. B-2; 14** (top) indicates that the difference in sample size is most pronounced when attempting to minimize the uncertainty, and the sample size can span an order of magnitude if the allowable error is around 20%. Around 50-100 samples are needed to estimate the median to within 50%, depending on the variance and the number of possible samples. As the allowable uncertainty increases the range of sample size becomes somewhat narrower, but still varies by a factor around four for a 100% relative error.

**Fig. B-2; 14** (top) also shows the effects of variance on the number of samples needed. Those data sets taken under nearly constant flow conditions and small values of  $s^2$  ( $< 1.2$ ) generally have low values for the Folk and Ward (1957) parameters for sorting ( $\approx 0.6$ ) and skewness ( $\approx 0.2$ ). Those data sets tend to Gaussian distributed, with rather poor percentage goodness-of-fit to Hamamori distributions. Data sets with higher variance ( $s^2$  between 1.7 and 2.2) are less well sorted ( $\approx 0.9$ ), more skewed ( $\approx 0.5$ ), and more likely to be lognormal or Hamamori distributed. **Fig. B-2; 14** (top) shows that the number of samples needed approximately doubles as  $s^2$  increases from 1.7 to 2.2.

For bedload transport rates that follow the Hamamori distribution, Gomez et al. (1990) provide equations with which to estimate the at-a-point sample size needed to estimate the mean transport rates within preset levels of accuracy (eqs. 22 a and b). These at-a-point sample sizes then have to be multiplied by the number of sampled cross-sections in a stream. If one follows Gomez et al. (1990) and assumes that five sampling locations within a cross-section is sufficient, the sample sizes estimated from equations 22 a and b must be multiplied by a factor of five.

**Fig. B-2; 14** (bottom) compares the minimum sample size for a given level of accuracy for Gaussian (eq. 23 and 24), lognormally (eq. 24), and Hamamori (eqs. 22 a and b) distributed data sets. The number of samples needed for Gaussian distributions, assuming a CV of 50-100%, is shown in the gray-shaded band. The center line within this band is for a CV of 75%. The difference in sample size between a Gaussian distributed data set with a typical CV of 75%, and a lognormally distributed data set with a typical  $s^2$  of about 2 is almost one order of magnitude if the allowable uncertainty is greater than 50%, and decreases to a factor of about 6 for smaller allowable errors. Thus a sample size of 60 and 12 samples would yield respective sampling accuracies of 20 and 40% for Gaussian distributed bedload transport rates, but more than 100 samples would have to be taken to achieve a 40% accuracy if the underlying distribution is lognormal.

A change in sediment transport rates can be a useful indicator of CWEs if this is more sensitive than a change in channel morphology or other indicators of stream channel condition (e.g., intergravel dissolved oxygen or number of fish). In other words, the change in sediment transport should be detected prior to other adverse changes, but the "threshold" for channel morphologic change in response to a change in sediment load will vary with stream type and is not easily predicted. The analyses presented to this point suggest that it is very difficult to detect less than a 25-50% change in bedload transport at a discharge large enough to transport substantial amounts of bedload.

Under the best circumstances, which means that sediment transport rates are no more variable than in a laboratory flume, there is no variation in sediment supply, and cross-sectional variability is minimal, Emmett-style sampling with 40 subsamples could be accurate to within 25-30%. The problem is that such conditions are not found in gravel-bed rivers.

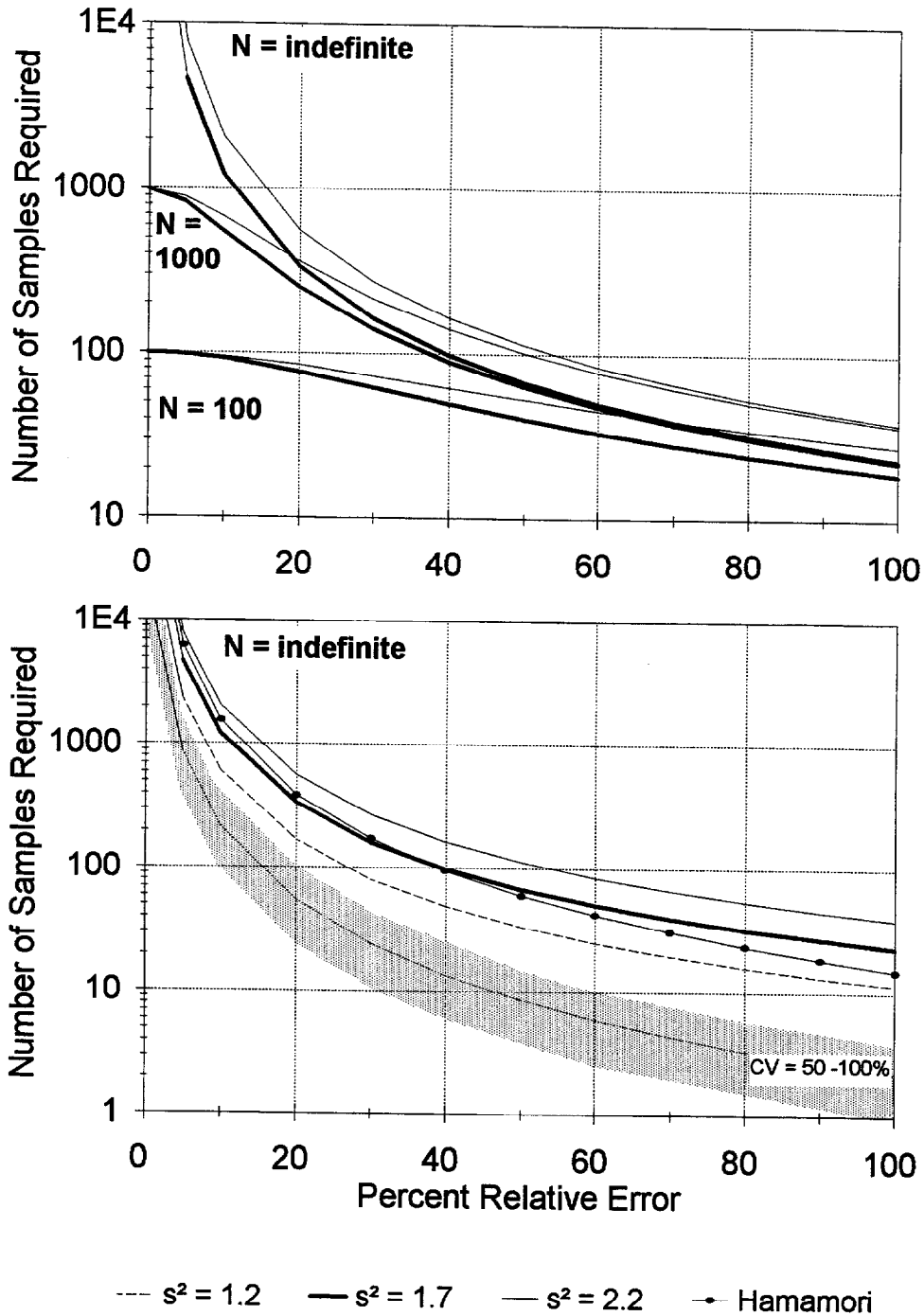


**Fig. B-2; 14:** Number of samples needed to estimate the median transport rate with 95% confidence as a function of percent relative error in lognormally distributed data. The top figure shows sample size to be a function of variance ( $s^2$ ) and the potential number of samples ( $N$ ), with the heavy lines representing a lower variance than the thinner lines. The bottom figure shows the variation in sample size required to estimate the mean and median transport rates for Gaussian and lognormally distributed data sets, respectively. The gray band represents Gaussian-distributed data sets with a CV between 50 and 100%; the broken line in the center indicates a CV of 75%. The three upper lines without symbols represent the number of samples required for lognormally distributed data with the indicated variance.

Given the variability in existing short-term records, one generally should not expect that a given set of measurements will represent the true bedload transport rate to better than a factor of 50%. This uncertainty in measuring bedload transport at a given flow and point in time must then be combined with the variability at the intra-event and inter-event scale in order to determine the relative sensitivity to detecting a change in sediment transport rates at a given flow, and these issues are discussed in subsequent chapters of this report.

### 2.4.3 Total sampling time and sampling performance needed

The previous section determined sampling accuracy in terms of the minimum number of samples needed. Although the number of samples required for a given accuracy depends on the variability of the bedload transport rates (i.e., small values of CV require small numbers of samples for a given accuracy), there is no standard with regard to how much sampling constitutes an individual bedload transport sample.

The sampling scheme advocated by Emmett (1980) consists of about 40 subsamples, and a total sampling time of 20 minutes. The total time necessary for such a sample probably adds up to 1-1.5 hours, and the sampling uncertainty may be in the range of 25-30% if a CV of 75-100% and a Gaussian distribution can be assumed, or 70-100% if the underlying distribution is lognormal and the variance is 1.7-2.2 log units.

Gomez et al. (1990, 1991) and Gomez (1991) argued that sampling should focus on the short-term variability in bedload transport, and that around 20 subsamples of 30 seconds each should be taken at about 5 cross-section locations. This yields more than 100 subsamples, a total sampling time of 53 minutes, and a field time of at least 2-3 hours. Sampling uncertainty for each location is about 30% if the underlying distribution is Gaussian, and 60 to more than 100% if the underlying distribution is lognormal.

Kuhnle and Southard (1988) and Kuhnle (1996) found that total sampling times of 20-50 minutes were needed to get to the point where additional sampling did not substantially improve their estimated sediment transport rates, and this was for laboratory flumes with no changes in sediment supply and no need to account for cross-sectional variability. Dietrich and Whiting (1989) defined the appropriate sample time  $t_{min}$  as the sampling period needed to catch enough particles for an accurate characterization of the particle-size distribution.

$$t_{min} = \frac{\rho_s \cdot (\pi/6) \cdot D_i^3}{p_i\% \cdot qb_i \cdot w_s} \quad (26)$$

where  $p_i\%$  is the weight percentage of the  $i$ th particle-size fraction,  $qb_i$  is the transport rate of the  $i$ th size fraction, and  $w_s$  is the width of the sampler. Sampling times determined with this equation commonly ranged from several minutes to more than one hour.

Although this variety of suggested sampling procedures may be confusing, a standard, fixed sampling procedure for all streams is not feasible or realistic given the diversity of stream and sampling conditions. However, if it was possible to express sampling accuracy in terms of actual sampling performance required, this value could then be allotted over space and time in such ways that it optimally covers the spatial and temporal variability for the specified stream and sampling location.

Therefore, the next step in the analysis was to calculate the minimum total sampling time,  $t_{min}$ , needed for a mean transport rate to be within 10, 20, 30 or more than 30% of the true

mean transport rate for all 19 data sets with constant or near-constant flow. The minimum number of samples ( $n_{min}$ ) needed for the mean transport rate to be within 10, 20 or 30% of the true transport rate (eq. 22) was multiplied by the sampling duration  $t_{dur}$  (e.g., 30 seconds) and the number of traverses ( $n_{trav}$ ) completed.

$$t_{min} = n_{min} \cdot t_{dur} \cdot n_{trav} \quad (26)$$

This time was expressed in a unit of hours (Table B-2; 1) and compared to the total sampling time of the respective data set.

Most of the data sets from flume experiments, which have CVs < 60% and a sampling performance (eq. 19) of about 100 or more, have total sampling times sufficiently long for the mean bedload transport rate to be within 10% of the true mean transport rate. In most of the stream studies with near-constant flow total sampling time sufficed for a 30% accuracy. However, these studies represent research situations where sampling performance, and thus sampling accuracy, is much higher than in many of the sampling projects carried out for annual sediment yield estimates.

The total sampling time needed can also be expressed in terms of sampling intensity and sampling performance. Median values of sampling intensity and sampling performance were estimated from data sets in which the total sampling time had yielded a better than 10, 20, and 30% sampling accuracy (Table B-2; 17). Values in Table B-2; 17 had to be expressed as median values because within one class of sampling accuracy there are only about 5 data points for each parameter and the respective individual values can span two orders of magnitude.

It is not surprising to note that all sampling parameters increased with increasing percent accuracy. Since sampling performance incorporates three parameters which represent different aspects of sampling intensity, sample accuracy is most strongly affected by sampling performance. Additional values could not be incorporated into Table B-2; 17 because the values are empirically-derived rather than theoretical.

**Table B-2; 17:** Median values of sampling parameters associated with different sampling accuracies.

Sampling Accuracy higher than %	Total sampl.time needed (hrs.)	Sample Size $n$	% width sampled $w_s$ %	% time sampled $t_s$ %	Sampling Intensity $w_s \cdot t_s / 100$	Sampling Performance $w_s \cdot t_s \cdot n / 10,000$	CV %
10	2.5	300	100	100	100	300	47
20	1.0	120	0.5	17	0.1	1	69
30	0.3	31	0.5	9	0.05	0.02	87

The values in Table B-2; 17 are useful in terms of indicating a relative magnitude and a general trend. A larger data set would be required to increase the accuracy of these analyses. It would also be desirable to have separate tables for different stream types since the variability of bedload transport rates vary by stream type.

Nevertheless, if we assume that the values are representative, then **Table B-2; 17** can be used to estimate the percent accuracy associated with various values of sampling performance. For example, 10 repetitions of 30 seconds at each of five cross-sectional locations in a 5-m wide stream with a 7.6-cm Helley-Smith sampler within a 30-minute time period would sample 7.7% of the width and 25% of the time. Total sampling intensity is 1.9, and sampling performance is 0.19. Interpolating between the values for sampling performance suggests that an accuracy of around 25% could be expected. If only two traverses had been made, sampling performance would drop to 0.04 and the sampling accuracy would be closer to 30%.

Without knowing the conditions at a new sampling site it is probably best to conduct an initial sampling program with high spatial and temporal resolution. This should indicate the magnitude of variation and primary patterns of the variation in bedload transport at that site. For example, if transport rates at the sides of the river are found to be relatively low during all flow conditions, it would then be best to focus one's sampling efforts in the center of the stream where transport rates are high and therefore have the greatest effect on the total bedload transport. On the other hand, multi-thread channels or rivers "a mile wide and an inch deep" require an Emmett-style sampling procedure. Once the patterns of bedload transport are known, it might then be possible to set up a locally adapted and less intensive sampling program that would still give relatively accurate transport rates. However, it must also be remembered that patterns of bedload transport can change over time. Thus the appropriateness of a chosen sampling strategy must be regularly checked by carefully reviewing the data at each location and checking the temporal variability at key locations within the cross-section.

## 2.5 Summary

The number of bedload samples required for representative sampling can be estimated if the statistical distribution of consecutive bedload transport rates is known. Sample size can either be determined by a formula (e.g., eq. 22 or 23), or the sampling can be continued until measured transport rates show a reasonable agreement with a statistical distribution that might be expected in a given situation. Although the literature suggests that bedload transport rates follow a Gaussian, (Kuhnlé and Southard 1988), lognormal (Shuyou et al. 1988), or Hamamori distribution (Hamamori 1962; Carey and Hubbell 1986; Hubbell 1987, and Gomez et al. 1989), there is no comprehensive study that determines how the underlying distribution is affected by bedload transport conditions or sampling regime. Such information is essential to estimating the uncertainty and thus the detectability of a CWE.

For these reasons a first step in this study was to analyze the short-term variability of consecutive bedload transport measurements in 40 data sets extracted from the literature. Data sets included stream and flume studies, and varied with respect to flow conditions, particle sizes, and sampling characteristics (e.g., continuous sampling in traps, or sequential sampling with samplers). The following aspects were analyzed for all data sets:

- fit to one of the statistical distribution types (Gaussian, lognormal, or Hamamori);
- effects of flow variability, sampling schemes, and sampling types on the statistical distribution; and
- coefficient of variation, number of samples, and total sampling time needed to estimate a mean value with a given range of uncertainty and confidence in that estimate.

Data sets were tested for Gaussian and lognormal distributions using the Schleyer-test (Schleyer 1987) and the *W*-test (Gilbert 1987), and for goodness-of-fit to the theoretically-derived Hamamori distribution (Hamamori 1962).

Results showed that the *W*-test is better suited to distinguish between distribution types than the Schleyer-test. Although both procedures showed some agreement for Gaussian distributions, the different procedures showed little agreement for lognormal distributions. The reason for this discrepancy may be the often jagged frequency distributions of small data sets, and the fact that the Schleyer-test excludes the tails of the distribution (<5% and >95%). Of the 40 data sets tested, the *W*-test indicated that 11 data sets were Gaussian distributed and 17 were lognormally distributed. The goodness-of-fit with respect to the Hamamori distribution ranged from 63 to 99%. Average characteristics of data sets with Gaussian, lognormal, or better-than-average goodness-of-fit to the Hamamori distribution are summarized in **Table B-2; 18**.

**Table B-2; 18:** Average values of selected distribution parameters of relative bedload transport rates  $qb_r$ , by type of distribution.

Distribution Parameter	Distribution type		
	Gaussian	ideal Hamamori	lognormal
Mean $qb_r$	0.96	0.95	0.81
Sorting	0.57	0.87	0.86
Skewness	0.05	0.41	0.57
95th percentile	1.88	2.96	2.81
Maximum $qb_r$	2.4	4	~5

The three types of distributions are most variable for small and medium relative transport rates. The proportion of transport rates smaller than 0.5  $qb_r$  are one quarter for a Gaussian distribution, three-eighths for the Hamamori distribution, and one-half for lognormally-distributed data. These proportions are essentially reversed for transport rates between 0.5 and 1.5  $qb_r$ . Maximum relative transport rates rarely exceed three times the mean rate in Gaussian distributions and are fixed at four times the mean rate in the Hamamori distribution, but the maximum value in lognormally-distributed data can be up to 25 times the mean rate (Shuyou et al. 1988).

In order to analyze the effects of flow variability, sampling types, and sampling schemes on the statistical distribution, sampling type was classified as continuous, sequential, and intermittent. Sampling intensity was defined as the product of the proportion of the period sampled time the proportion of the stream width which was sampled. Sampling performance was defined as the product of sampling intensity and sample size.

The following flow and sampling conditions were generally associated with the three types of distributions analyzed in this study:

#### Gaussian distributions

- constant flows (short-term variability of transport rates),
- slight preference for continuous sampling, but no intermittent sampling; and
- mostly large sample sizes, high sampling intensities, and high sampling performance.

All of the above attributes are typically present in flume experiments.

### Lognormal distributions

- unsteady flows (intra-event variations of transport rates),
- sequential sampling, and
- mostly small sample sizes, poor sampling intensities, and poor sampling performance.

### Hamamori Distribution

- unsteady flows (intra-event variations of transport rates),
- intermediate sample sizes, sampling intensities, and sampling performance; and
- sequential sampling.

The coefficient of variation (CV) can be used to quantify the variability of bedload transport rates. The variability of bedload transport rates increases with the temporal variability of flow, and the CV also seems to increase with increasing grain-size. The latter trend is not as strong if large particles become the dominant component of the grain-size distribution during a transport event.

Empirical sampling schemes tend to focus on either the cross-sectional variability or the temporal variability. No single sampling scheme will be preferred in all cases, and the appropriateness of a particular sampling scheme will depend on how well this captures the primary causes of variability in measured transport rates at a particular site. Thus an optimal sampling scheme should concentrate on locations where bedload transport rates are highest and most variable.

Bedload transport rates in flume experiments with constant flow commonly have CVs in the range of 50-75%. More than a hundred samples would be needed to determine the mean transport rate in those data sets with an accuracy of 10% and a confidence level of 95% (i.e., the mean of the sampled distribution is within 10% of the "true" population mean). About 20-50, 10-25, and 4-8 samples are needed if the sample mean is to be within 20, 30, and 50% of the population mean.

The CV of bedload transport rates in natural streams during near-constant flow can reach 100 or even 125%. This level of variability would require several hundred samples to determine the mean with a 10% accuracy, and roughly 100 samples if our estimated mean is to be within 20% of the true mean at the 95% confidence level. If a 50% accuracy is tolerable, this will still require 15-25 samples, while 3-6 samples will result in a 100% relative error.

Sample sizes of almost an order of magnitude more are needed to obtain the same levels of sampling accuracies in estimating the *median* transport rate in lognormally distributed data sets. For a typical variance of  $s^2 = 1.7$ , 40 and 20 samples give a 70 and 100% uncertainty. 300 to 100 samples are needed to increase sampling accuracies to a relative error of 20 and 40%, respectively. Somewhat smaller sample sizes are required if the data follow the Hamamori distribution.

An attempt was made to express the necessary amount of sampling in terms of total sampling time and sampling performance as well as sample size. Since there is no sampling standard for all bedload transport and sampling conditions, the estimation of sampling time or sampling performance may provide a better index than sample size and allow a more flexible allotment of bedload sampling over space and time.

The analyses described in this chapter can only provide a small insight into the statistical variability of bedload transport, and the processes which affect it. A substantially larger number of data sets would have to be analyzed to improve the accuracy of the results.

### 3. Measurement Techniques and Uncertainty

#### 3.1 Introduction

The analyses in the previous chapters have implicitly assumed that an individual sample or subsample accurately represents the sediment transport rate at that point in time and space. However, due to the constraints inherent to most sampling devices, the accuracy of individual bedload and suspended sediment samples cannot be taken for granted. This chapter discusses the uncertainty inherent in a wide variety of sediment sampling techniques, as the varying accuracy of different techniques has implications for detecting cumulative watershed effects. The focus is more on bedload sampling because of the greater problems in accurate and representative sampling relative to suspended sediment, and because bedload commonly comprises the bulk of the sediment load in forested, montane streams where most CWE analyses are being conducted. In Squaw Creek, for example, there was an initial flush of suspended load during the first part of the snowmelt high flow, but the total suspended load over the course of the 14-day high flow period accounted for less than 30% of the total sediment load (Table B-3; 1). An understanding of the limitations and uncertainty associated with different measuring techniques will improve our interpretation of sediment data, and provide some guidance to minimize the errors associated with different sampling techniques.

**Table B-3; 1:** Mean daily values of bedload transport rates and suspended sediment load during a typical snowmelt highflow season at Squaw Creek, a gravel-bed mountain stream in Montana (drainage area: 105 km<sup>2</sup>) (Data from Bunte et al. 1987; Bunte 1996).

Day of event	Discharge (m <sup>3</sup> /s)	Susp.Sed. concentration (g/l)	Bedload transport rates		Susp. Sed. load (kg/d)	Bedload (kg/d)
			Helley-Sm. (kg/m·s)	Net-sampl. (kg/m·s)		
1	5.50	0.25	0.005	0.02	4950	3960
2	6.00	0.30	0.008	0.05	6480	10022
3	5.75	0.20	0.0065	0.07	4140	12668
4	5.80	0.10	0.007	0.08	2088	14532
5	5.85	0.30	0.007	0.09	6318	16343
6	5.70	0.30	0.0062	0.05	6156	9226
7	5.70	0.20	0.0062	0.05	4104	9226
8	5.40	0.05	0.0045	0.01	972	2255
9	5.10	0.02	0.003	0.002	367	734
10	5.20	0.03	0.003	0.003	562	899
11	5.70	0.12	0.0062	0.05	2462	9226
12	5.2	0.03	0.003	0.003	562	899
13	5.2	0.02	0.003	0.003	374	899
14	5.8	0.1	0.007	0.08	2088	14532
Seasonal totals					<u>42000</u>	<u>105000</u>

### 3.2 Measurement techniques and uncertainties of bedload sampling

A disproportional sampling of certain grain-size fractions, or a misrepresentative sampling of transport rates in general, can be due to the characteristics of the sampling device, its inappropriateness in a given sampling situation, and poor operating skills. The first step towards avoiding measurement problems is to be aware of bedload transport processes, their contribution to the temporal and spatial variability of bedload transport and the grain-size distribution of the sediment, and the extent of this variability. The second step is to employ bedload sampling devices that are matched to the particular material, sediment transport processes, and flow conditions; a better match will lead to smaller measurement errors.

Bedload can be measured directly or indirectly. Direct methods sample the bedload material being transported in a particular location with portable bedload samplers, continuously registering bedload traps, or debris basins. Indirect measurements include the acoustic recordings of inter-particle collisions or particles banging against a hydrophone, or detect the passage of magnetically or otherwise traced particles over a sensor. Besides their variable accuracy in given stream situations, measurement techniques vary greatly with respect to construction and operating costs, portability and maneuverability, degree of sophistication, and the potential temporal and spatial resolution of the measurements. Overviews of various bedload sampling techniques are available from Hubbell (1964), Ergenzinger (1985), and DVWK (1992).

Among the direct measurement techniques, portable bedload samplers are the most common. Some samplers operate on the principle of pressure-difference, such as Helley-Smith type samplers, and these are generally designed for sampling bedload particles in the range of fine gravels. Coarser bedload is sampled with basket and net samplers in which a comparatively coarse wire mesh lets the water flow through with less resistance than a fine mesh bag. By definition these types of samplers are not dependent on pressure differences. The respective problems and advantages of both sampler types are discussed below.

#### 3.2.1 Helley-Smith-type samplers: effects on sampling efficiency

Although Helley-Smith-type samplers are in widespread use, there is contradictory information regarding the conformity or difference of transport rates measured with a Helley-Smith-type sampler and "true" transport rates. There may also be considerable differences in transport rates measured with different types of Helley-Smith samplers. Helley and Smith (1971) based their sampler on the Arnhem-sampler developed by the Delft Hydraulics Institute. The fine mesh bag at the downstream end is designed to catch particles larger than very fine sand (0.2-0.3 mm), but the resistance due to this bag reduces the flow velocity inside the sampler body. To compensate for this reduction, flow is accelerated at the sampler entrance by means of a flared sampler entrance region. The area ratio is defined as the area at the sampler exit ( $A_{exit}$ ) divided by the area at the sampler entrance ( $A_{entr}$ ), and this is 3.22 for the standard Helley-Smith sampler (Fig. B-3; 1).

$$area\ ratio = \frac{A_{exit}}{A_{entr}} \quad (1)$$

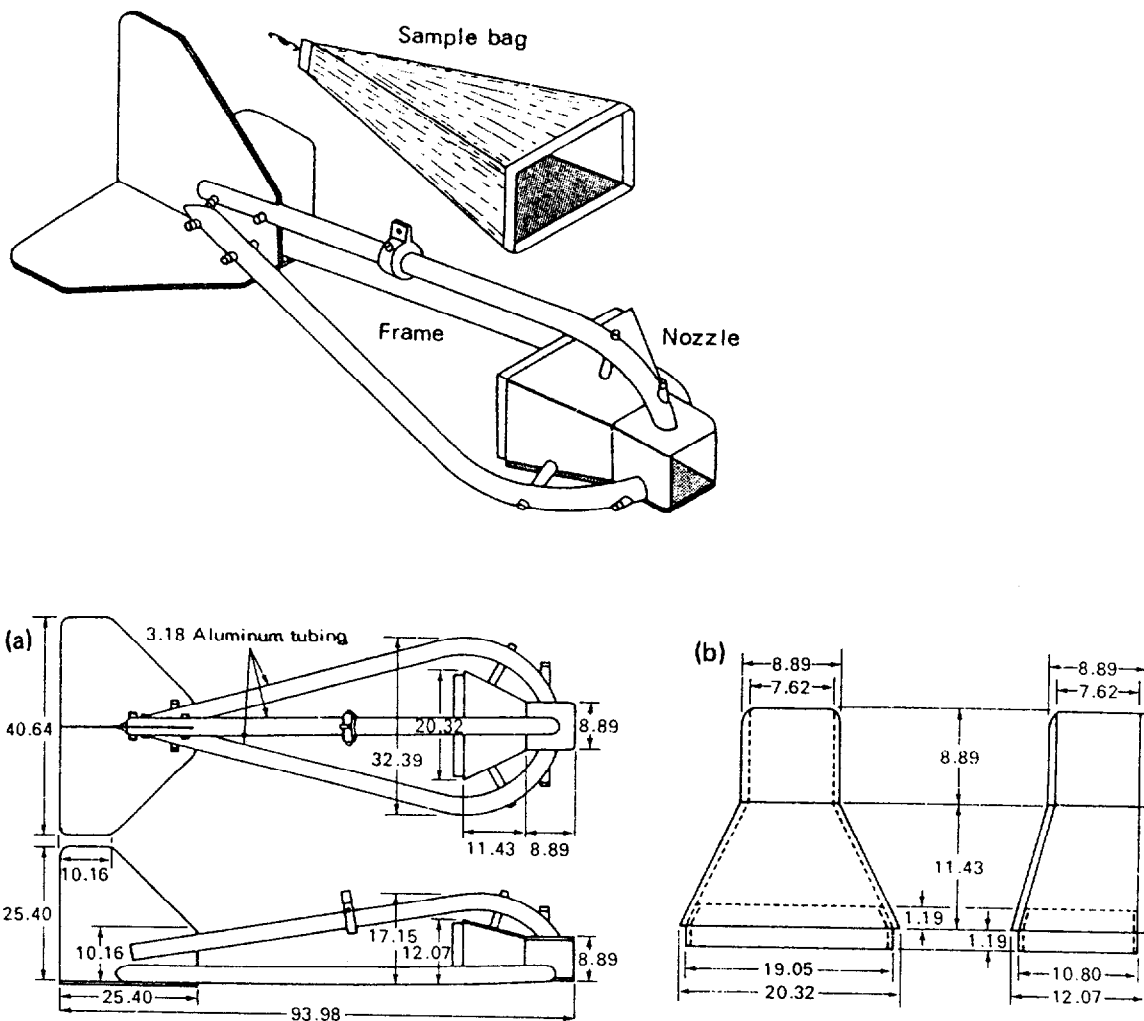


**Fig. B-3; 1:** 3 x 3 inch standard Helley-Smith bedload sampler (7.6 cm x 7.6 cm). Oblique (top), plan and side elevation views of (a) the entire sampler, and (b) the sampler nozzle. All dimensions in cm (from Emmett 1981).

The flared design causes the flow lines to converge in front of the orifice, and this creates a suction of water into the sampler (Fig. B-3; 2). The mean flow velocity within the sampler orifice ( $v_{ml}$ ) is thus larger than the undisturbed mean flow velocity in front of the sampler ( $v_{mv}$ ). The hydraulic efficiency is:

$$\text{hydraulic efficiency} = \frac{v_{ml}}{v_{mv}} \quad (2)$$

and for pressure-differential samplers like the Helley-Smith this ratio is always greater than 1.

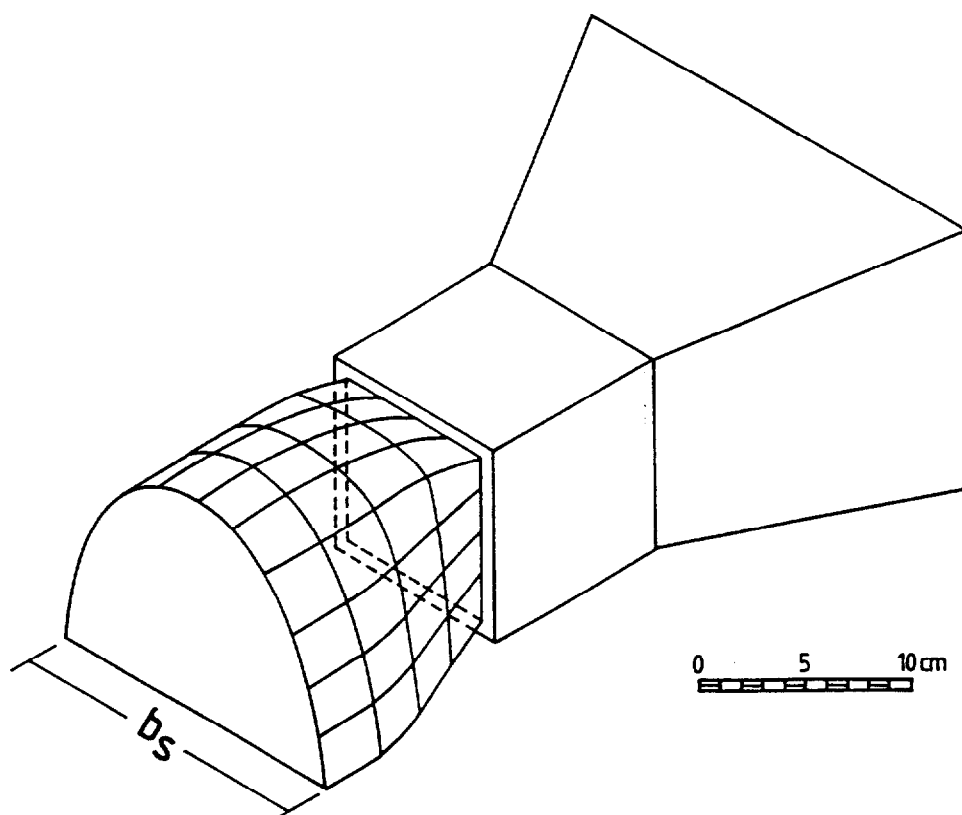
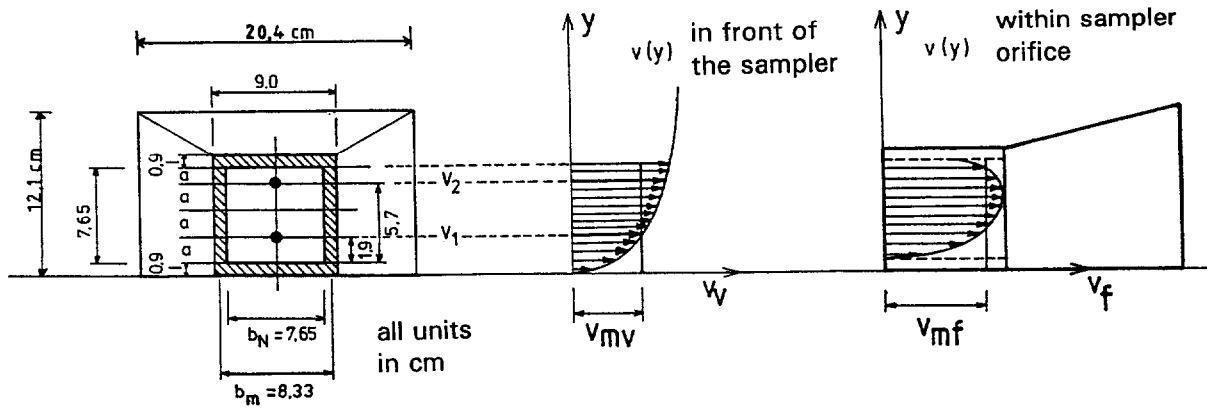


**Fig. B-3; 2:** Zone of converging streamlines in front of the standard Helley-Smith sampler (after Druffel et al. (1976), from DVWK 1992).

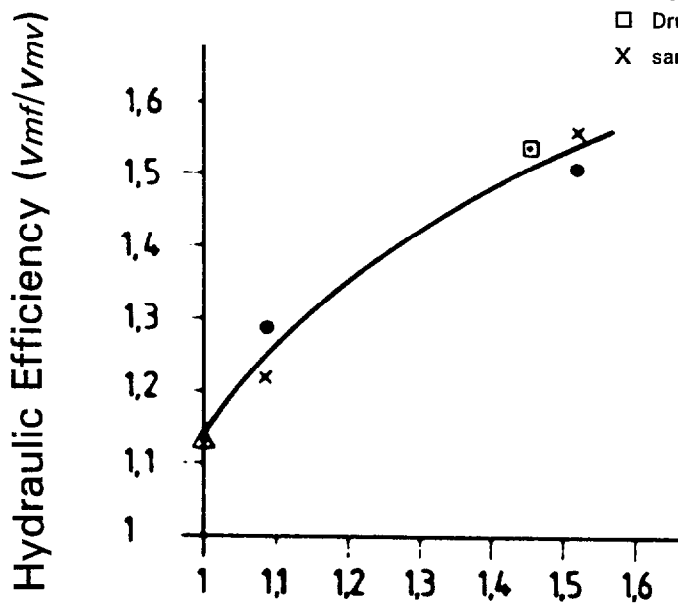
Many modifications have been made to the original Helley-Smith sampler to adjust for local sampling conditions, stream-bed characteristics, sediment transport phenomena, and flow. Thus there is a wide variety of Helley-Smith type samplers currently in use (**Table B-3; 2**), and these vary with respect to:

- orifice size
- area ratio
- bag size, and
- mesh width.

Changes in these characteristics alter the hydraulic efficiency, and most versions of the Helley-Smith have values between 1.1 and 1.6 (**Fig. B-3, 3**). A precise specification of the hydraulic efficiency is difficult, because this depends not only on the sampler specifications (see above), but also on the flow field in front of the sampler, which is controlled by the curvature of the velocity profile. Thus the hydraulic efficiency should increase with bed material roughness and discharge, and decrease with increasing depth of flow. However, Emmett (1984) states that the standard Helley-Smith sampler retains a constant hydraulic efficiency of 1.54 for a range of flows applicable to natural streams.



- Federal Institute of Hydraulic Engineering (BAW, Germany)
- △ Helley and Smith (1971), ( $v_m = 0.5$  m/s)
- Druffel et al. (1976), ( $v_m = 0.7$  m/s)
- X sampler constructed by the BAW



Curvature of the velocity profile  
Ratio of upper to lower velocity ( $v_2/v_1$ )

Fig. B-3; 3: Velocity profile in front of and within the sampler orifice (top); Increase of hydraulic efficiency ( $v_{mf}/v_{mv}$ ) with curvature of the velocity profile ( $v_2/v_1$ ) within the sampler orifice (bottom) (from DVWK 1992).

The accuracy of a sampler is defined by the sampling efficiency, which is the ratio of sampled material ( $Qb_s$ ) to the material that would have been transported if the sampler had not been there ( $Qb$ ).

$$\text{sampling efficiency} = \frac{Qb_s}{Qb} \quad (3)$$

Sampling efficiency depends not only on hydraulic efficiency, but also on site characteristics such as:

- bedload transport rates
- bedload particle sizes
- contact of the sampler with the river bed, and
- sampler handling and alignment.

Thus sampling efficiencies will not only vary between different versions of the Helley-Smith-type samplers, but also between different sites and even different individuals.

The appropriateness of specific bedload samplers in particular situations is still a matter of controversy. Although there are a few studies that compare the effects of sampler size and shape on sampling efficiency for total and fractional bedload transport rates, such studies can't cover all types of samplers or the full range of stream conditions. Field comparisons are also hindered by the variability of bedload transport in space and time (see Chapter B-1). One solution is to collect a large number of samples using different samplers, as done by Gray et al. (1991).

Another possibility is "probability matching", and this was employed by Hubbell et al. (1985), Hubbell and Stevens (1986) and Hubbell (1987) to compare sampling efficiencies of various samplers at different transport rates. In these studies the longer-term bedload transport rates were held constant during the runs, but transport rates fluctuated within the run due to the formation of dunes and ripples. Transport rates were varied between runs. As it was thought inappropriate to compare individual data or mean values, cumulative frequency distributions of bedload samples taken by different samplers in repetitive flume experiments were used for comparison. The validity of this procedure is still controversial.

Another problem in comparing Helley-Smith type samplers of different dimensions is that the samplers are typically collecting all the material above a certain grain-size which is flowing through the sampled area. The samplers are thus capturing some "suspended" load as well as bedload, and the sampling efficiency will vary according to the grain-size being collected.

There is a wide variety of different pressure difference samplers currently in use, including the Delft Nile sampler (Gaweesh and Van Rijn 1994) and the Chinese Yangtze-78 (Y-78) sampler (Xiang and Zhou 1992), and the sampling efficiencies for these samplers can range from 5 to 300%. The following section will review how sampling efficiency is affected by sampler dimensions and sediment transport conditions for Helley-Smith type samplers, and the dimensions of the various samplers included in this analysis are listed in **Table B-3; 2**.

**Table B-3; 2:** Pressure difference samplers and their dimensions (after Hubbell et al. 1985).

Common Name of sampler	Orifice size (width x height)		Area Ratio	Hydraulic Efficiency
	(inch)	(cm)		
Standard Helley-Smith	3 x 3	7.6 x 7.6	3.22	1.54
BL-84; BL-86-3	3 x 3	7.6 x 7.6	1.4*	1.35
...	3 x 3	7.6 x 7.6	1.1*	1.15
6-inch Helley	6 x 6	15.2 x 15.2	3.22	1.54
...	12 x 6	30.5 x 15.2	1.4*	1.4
...	12 x 6	30.5 x 15.2	1.1*	1.15

\* estimated

### 3.2.1.1 Orifice size and large particles

The relatively small sampler entrances in Helley-Smith type samplers of 7.6 x 7.6 and 15.2 x 15.2 cm hamper the collection of pebbles and cobbles. The resulting bedload samples can be artificially truncated and unrepresentative, and this will also contribute to more variable transport rates for larger particles sizes (Beschta 1983; Bunte 1991). While particles larger than the sampler orifices obviously cannot be sampled, there is much confusion and disagreement regarding the threshold particle size for which the sampling efficiency becomes intolerably low. The standard Helley-Smith sampler was designed for sampling bedload in the size range from 2 to 10 mm. Bagnold (1977) suggested using a Helley-Smith sampler only when the  $D_{50}$  of bedload transport is one order of magnitude smaller than the sampler opening. Even if the  $D_{50}$  of bedload is not to exceed 8 mm for the 3-inch Helley-Smith and 16 mm for the 6-inch Helley-Smith, the respective  $D_{95}$  values would be about 32 and 64 mm, respectively, if one assumes a rather well-sorted gravel with a standard deviation of  $\sigma = 1.0$  (equal to Inman's (1952) sorting coefficient of  $(\phi_{84} - \phi_{16})/2$ ). Emmett (1981, 1984) assumed that the 3-inch Helley-Smith could accurately sample particles up to 16 mm, which would be a half  $\phi$ -size lower than the threshold suggested by Bagnold (1977), but a half  $\phi$ -size higher than suggested by Helley and Smith (1971). (Since  $\phi = -\log_2$  of the diameter, a one-unit increase in  $\phi$  decreases the particle size by a factor of two; conversely, a one-unit decrease in  $\phi$  increases the particle size by a factor of two.) Wolcox et al. (1996) compared debris pond samples to bedload samples taken with a Helley-Smith sampler, and found that the latter did not representatively sample the 5-35 mm particles that represented the  $D_{75}$  to  $D_{90}$  of the grain-size distributions. The  $D_{75}$  to  $D_{90}$  determined from the Helley-Smith samples were 0.5-1.5  $\phi$ -sizes larger than the comparable percentiles accumulated in the debris basin (see also **Table B-3; 4** in the next section).

This bias in the Helley-Smith sampler against pebble-sized bedload poses a problem for sampling in gravel-bed rivers, as it is usually not known *a priori* which part of the bed material grain-size distribution will actually be transported as bedload. While Phase I transport may only yield sand-sized particles as bedload, the gravels and cobbles in the armor layer start to become mobile after the onset of Phase II transport (Jackson and Beschta 1982; Beschta 1987). Depending on stream type and sediment supply, this shift in bed materials could happen annually, during flows with a 2-5 year recurrence interval, or hardly ever. Switching to a 6 x 6-inch or a 12 x 6-inch Helley-Smith sampler in the middle of the flood is not necessarily the solution. Not only may it become impossible to hold this larger sampler in the stream when flow velocity is high, but samples collected with different

samplers are not directly comparable. As discussed later, sampling efficiency and the sample grain-size distribution are both dependent on sampler size and shape.

A pilot study using several samplers and a painted pebble experiment can be used to indicate whether a 76- or 152-mm sampler is appropriate for a given site, or whether a basket-type sampler might also be required.

### 3.2.1.2 Area ratio and hydraulic efficiency

Hubbell et al. (1985), Hubbell and Stevens (1986), and Hubbell (1987) used flume experiments to test the sampling efficiency of six Helley-Smith-type samplers of different size and shapes. These values were compared to bedload transport rates sampled with a continuously weighable bedload trap that was assumed to yield true transport rates (Table B-3; 2). Bed material consisted of very well-sorted pea-sized gravels with a  $D_{50}$  of 6.5 mm, and  $D_{16}$  and  $D_{84}$  of about 5 and 7.5 mm, respectively. Mean flow velocities ranged from 1 to 1.6 m/s, and mean bedload transport rates ranged from 0.02 to 0.5 kg/m·s. The study found that most samplers oversampled true transport rates, and that oversampling increased with orifice size, hydraulic efficiency, and bedload transport rates, and decreased with particle size.

The effect of orifice size and hydraulic efficiency on oversampling is quite understandable, as a larger orifice means that more saltating and even suspended particles will get into the sampler. Accordingly, a higher hydraulic efficiency means that more particles that are not inertia-controlled are sucked into the sampler. For the 3 x 3 inch Helley-Smith-type samplers only the non-flared sampler with an area ratio of 1.1 sampled "true" rates. The BL-84 (area ratio of 1.4), and the standard Helley-Smith sampler (area ratio of 3.22) oversampled by factors of 1.3 and 1.5, respectively. These differences were more than doubled for the 6 x 6 inch Helley-Smith sampler (area ratio of 3.22), while the 12 x 6 inch sampler (area ratio of 1.4) still oversampled by a factor of 2 for transport rates smaller than 1.5 kg/m·s. The non-flared 12 x 6 sampler (area ratio of 1.1) yields a good correspondence with true transport rates as long as transport rates stay below 1.5 kg/m·s (Fig. B-3; 4).

A similar discrepancy between the 3 x 3 and 6 x 6 inch samplers was reported by Bagnold (1977). When the mean diameter of bedload abruptly changed from 0.5 mm to 50 mm, bedload transport rates measured with the 3-inch Helley-Smith sampler were about one order of magnitude lower than the transport rates measured with the 6-inch Helley-Smith sampler.

Childers (1991) compared the sampling efficiency of the BL-84 sampler (area ratio of 1.4) and the "standard" Helley-Smith (area ratio of 3.22) under a wide range of flow and bedload transport conditions at the Toutle River (WA), the Cowlitz River (WA), and the East Fork River (WY). 30 to 80 samples were collected at each stream. Mean flow velocities ranged from 0.6 to 2.6 m/s, mean bedload transport rates ranged from 0.02 to about 3 kg/m<sup>2</sup>·s, and mean bedload particle sizes ranged from sand to 10 mm. Mean transport rates sampled with the standard Helley-Smith were 10-200% (average of 75%) higher than the transport rates obtained with the BL-84 sampler. The median sampled bedload particle size was also 5-50% larger in the standard Helley-Smith sampler as compared to the BL-48. Similar results were also reported by Gray et al. (1991) for bedload transport during low flows in the sand-bedded Colorado River near Supai, AZ, using the BL-86-3 (also a 3 x 3 inch opening and an area ratio of 1.4) and the standard Helley-Smith sampler. The ratio between

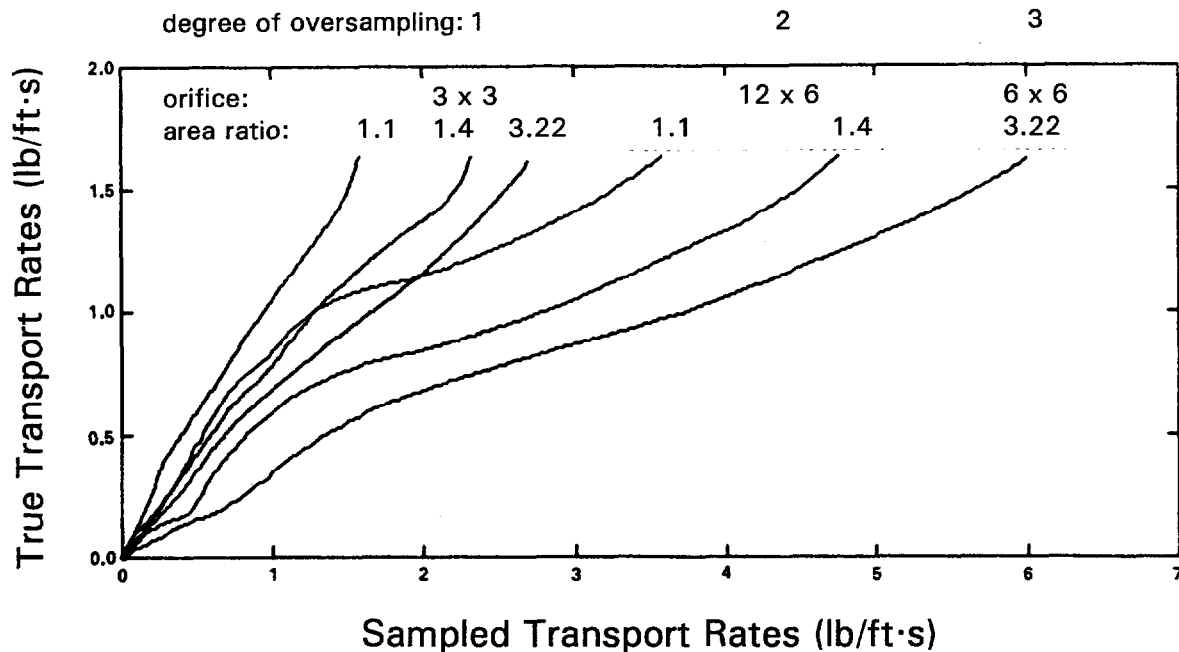


**Fig. B-3; 4:** Calibration curves for sampling efficiency of various Helley-Smith-type samplers for well-sorted bed material with a  $D_{30}$  of 6.5 mm (after Hubbell and Stevens 1986; Hubbell 1987).

BL-86-3 and Helley-Smith samples for increasing bedload transport rates was described by a linear regression (**Fig. B-3; 5 (top)**):

$$Qb_{BL-86-3} = 0.24 Qb_{HS} + 0.33 \quad (4)$$

From this regression function one can plot the percent difference in transport rates between the Helley-Smith and the BL-86-3 sampler. **Fig. B-3; 5 (bottom)** shows that the BL-86-3 oversampled the Helley-Smith for small transport rates, but when bedload transport rates exceeded 0.5 tons/day-foot (0.017 kg/m·s), the standard Helley-Smith oversampled relative to the BL-86-3. At the moderately high transport rate of 2 lb/day-foot (0.069 kg/m·s) the standard Helley-Smith was capturing 150% more bedload.

The difference in bedload transport rates as measured with these two rather similar samplers can reach a factor of 3 (**Fig. B-3; 4**). The implication of these types of differences is that the use of different samplers in different locations could create a disparity in bedload transport rates that might otherwise be attributed to a CWE. It is therefore quite important that CWE analyses either be conducted at comparable sites with identical procedures, or that intercomparisons of bedload transport rates be made at different times and locations with the different types of samplers being used in the study.

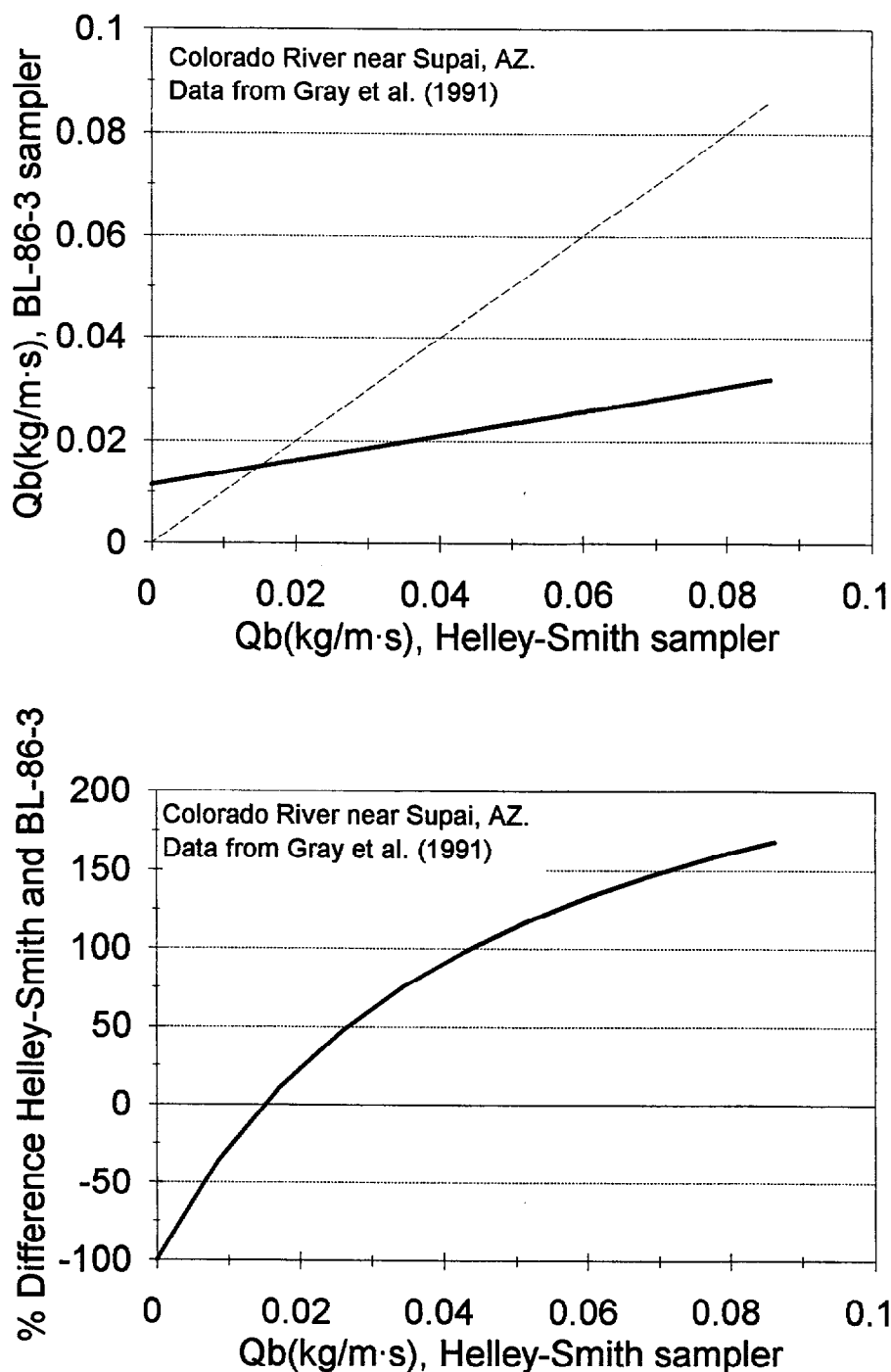


**Fig. B-3; 5:** Comparison between bedload transport rates sampled with the standard Helley-Smith sampler and the BL-86-3 at the Colorado River near Supai, AZ, during low flows. Top: dotted line represents perfect agreement and the solid line is the observed regression given by Gray et al. (1991). Bottom: percent difference between bedload transport rates sampled with the standard Helley-Smith sampler and the BL-86-3.

### 3.2.1.3 Bedload transport rates

The graphs in Fig. B-3; 4 all show that Helley-Smith type samplers tend to oversample as bedload transport rates exceed 1.5 lb/foot·s, and this is more true for the larger samplers with a larger area ratio. Fig. B-3; 6 shows very clearly that the degree of oversampling becomes more severe as bedload transport rates exceed 1.0 lb/foot·s, but the degree of oversampling is a function of particle size and the area ratio. However, the issue of

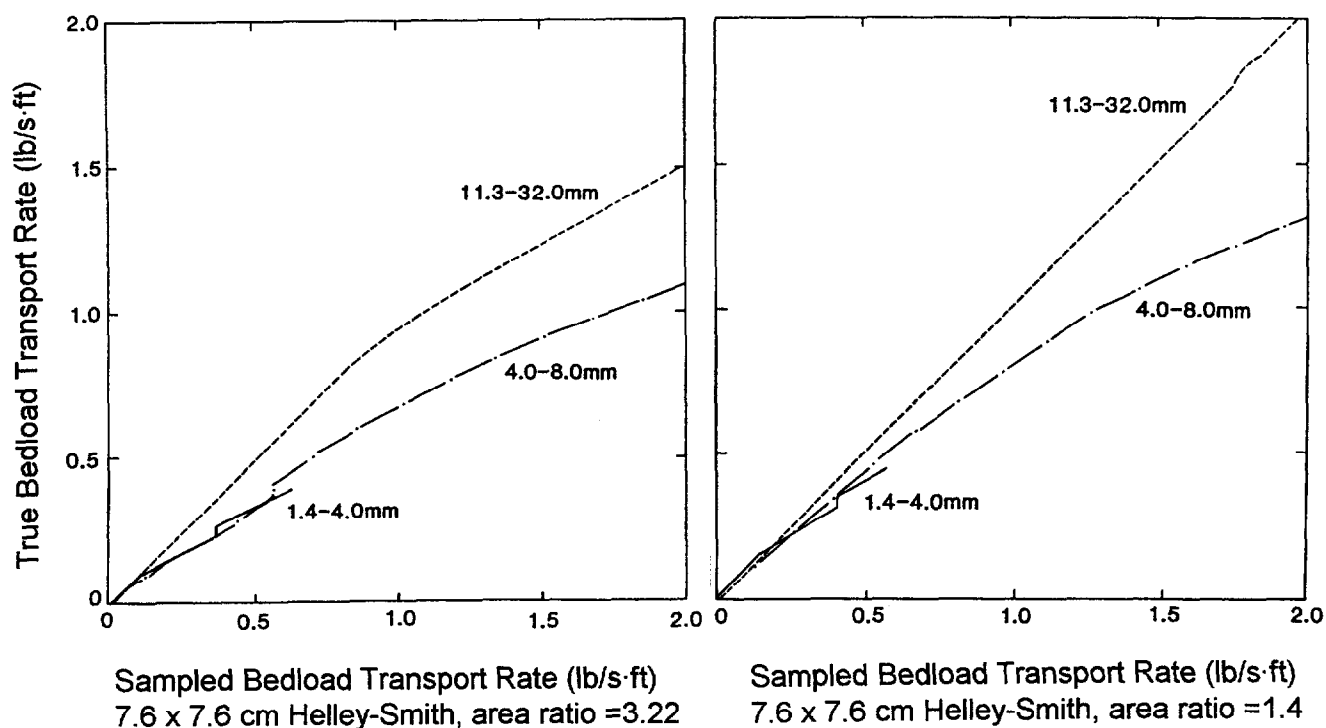


**Fig. B-3; 6:** Calibration curves for adjusting sampled rates of various size fractions of material collected with the standard Helley-Smith sampler (left) and the BL-84 (right). The diagonal is the line of perfect agreement (from Hubbell and Stevens, 1986; Hubbell, 1987).

oversampling for large transport rates needs to be put into perspective by comparison with commonly sampled bedload transport rates. Table B-2; 1 in the previous chapter provided mean transport rates from various streams, while Table B-3; 3 provides data on mean bedload transport rates during high flow events for various streams.

Most of the values in Table B-3; 3 are less than 1 lb/foot·s, which converts to the very high bedload transport rate of 1.49 kg/m·s (not 0.138 kg/m·s as indicated by Hubbell (1987)). Thus the higher oversampling values shown in Fig. B-3; 4 (bedload transport rates in excess of 4 lb/foot·s or 6 kg/m·s) will almost never be observed in practice. Nevertheless, the problem of oversampling is still substantial for most of the Helley-Smith-type samplers currently in use.

**Table B-3; 3:** Mean bedload transport rates during high flow events in various streams.

Stream	Reference	Stream bed characteristics	Bedload material	Mean bedload transport rates (kg/m·s)
Fraser Exp.St. (CO)	Troendle et al. '96	GB*, -- gravel supply	sand + gravel	0.005
Turkey Br. (UK)	Reid & Frostick '86	GB, -- gravel supply	sand + gravel	0.003-0.02
Squaw Cr. (MT)	Bunte '96	GB	gravel + sand	0.005-0.02
St. Louis Cr. (CO)	Ryan & Troendle '96	GB	sand + gravel	0.01
Caspar Cr.	Lisle '89	GB	sand + gravel	0.03
Jacoby Cr.	Lisle '89	GB	sand + gravel	0.05
Prairie Cr.	Lisle '89	GB	sand + gravel	0.06
E. Fork R. (WY)	Emmett '80	GB, + sand supply	mostly sand	0.05-0.10
Bambi Cr. (AK)	Campbell & Sidle '85	GB	sand + gravel	0.06-0.13
Oak Cr. (OR)	Milhaus '73	GB	sand + gravels	0.1
Duck Cr. (WY)	Whiting et al. '88	SB#&GB	mostly sand	0.4
Cowlitz R. (WA)	Childers '91	SB	sand	0.3-0.5
SF Obion R.(TN)	Carey '85	SB	sand	0.5
Toutle R. (WA)	Childers '91	SB, ++ sand supply	sand	0.5-2
Toutle R. (WA)	Childers '91	SB&GB, ++supply	sand + gravels	2-3
NF Toutle R.(WA)	Dinehart '92	GB, ++ pebble supply	mostly pebbles	1-5

\*GB = gravel-bed river; #SB = sand-bed river; -- very little sediment supply; - little sediment supply; ± moderate sediment supply; + high sediment supply; ++ very high sediment supply.

### 3.2.1.4 Bedload particle size

Although the standard Helley-Smith sampler was designed for sampling bedload in the range of 2 - 10 mm, the sampler is frequently used for sampling bedload transport beyond this range of grain sizes. Depending on the grain sizes in motion, this can result in severe measurement uncertainties.

Comparisons of the standard Helley-Smith sampler to the conveyor belt sampler at the East Fork River indicated that the Helley-Smith slightly undersampled particles 0.5-16 mm in diameter regardless of flow, and there was no size-dependent variation in sampling efficiency (Emmett 1981; 1984). However, particles in the size fraction of 0.25-0.5 mm were oversampled, and particles larger than 16 mm were undersampled (Emmett 1980).

**Fig. B-3; 7** combines data on sampling efficiency for different-sized particles from several sources. These data indicate a trend of decreasing sampling efficiency with increasing particle size. Comparisons with **Fig. B-3; 6** shows that oversampling becomes more pronounced with decreasing particle size and higher bedload transport rates. For a transport rate of 0.5 lb/foot·s (i.e., 0.75 kg/m·s), the standard Helley-Smith accurately sampled particles larger than 11 mm, but tended to oversample 1.4-8 mm particles by roughly 60%. However, mean transport rates in many mountain gravel-bed streams are typically much lower (e.g., 0.005 to 0.1 kg/m·s). Such transport rates are in the very low range of **Fig. B-3; 6** (0.003 to 0.067 lb/foot·s), and oversampling is much less pronounced.

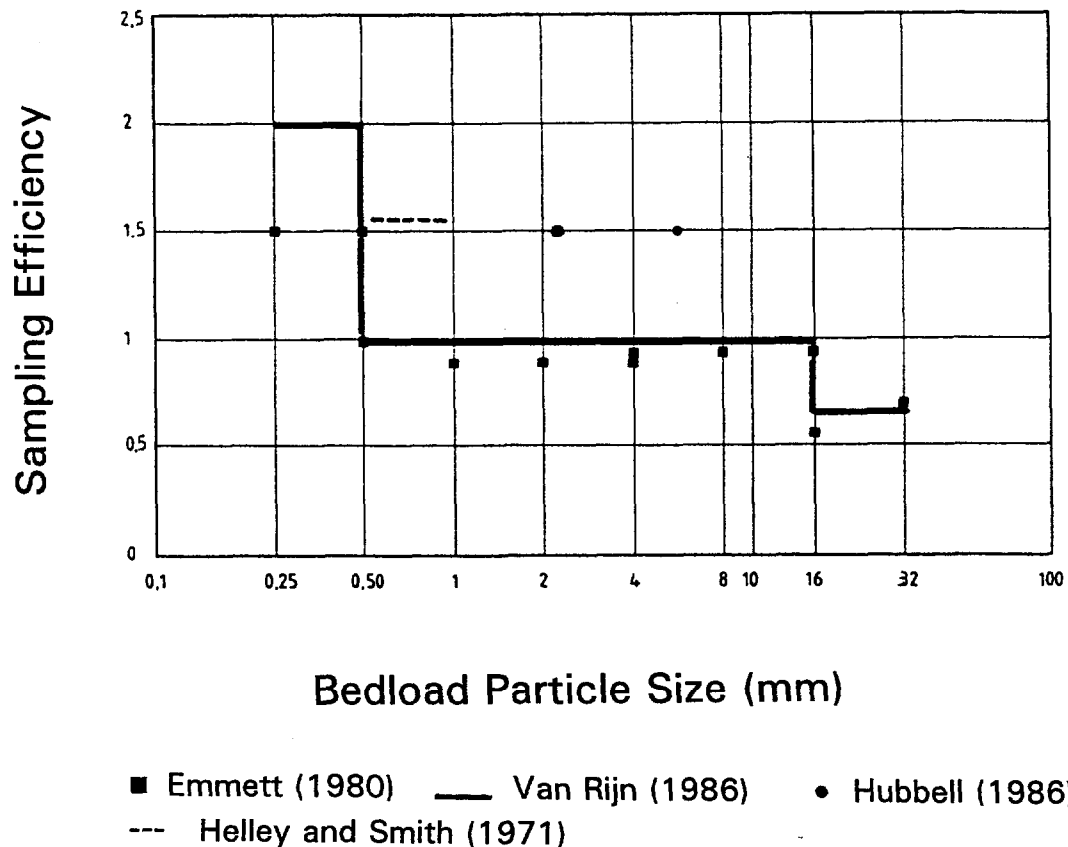


**Fig. B-3; 7:** Measured values of sampling efficiency for the standard Helley-Smith sampler and resulting interpolated curve (after DVWK 1992).

Oversampling of small particle sizes at higher transport rates is attributable to the fact that during high bedload transport rates much of the sand moves in suspension. The high hydraulic efficiency then leads to the sampler capturing more sediment than would normally pass through that cross-sectional area. Another reason for the oversampling of small particles is that flow velocities are usually high during times of high bedload transport, and this increases the hydraulic efficiency. Larger particles are less affected by the converging stream lines.

**Fig. B-3; 8** integrates this information into a conceptual model that shows the interplay between the particle size, transport rates, and sampler size and shape on sampling efficiency. Sampling efficiency generally increases steeply as the sampled sediment size approaches the mesh size, and continues to increase until it reaches a maximum value in the sand range. Sampling efficiency slowly decreases with increasing particle size, and then decreases more rapidly as particle size reaches the pebble range and approaches the upper size limit for sampling. The range in which sampling efficiency is relatively independent of particle size increases as the area ratio, hydraulic efficiency, and bedload transport rates all decrease.

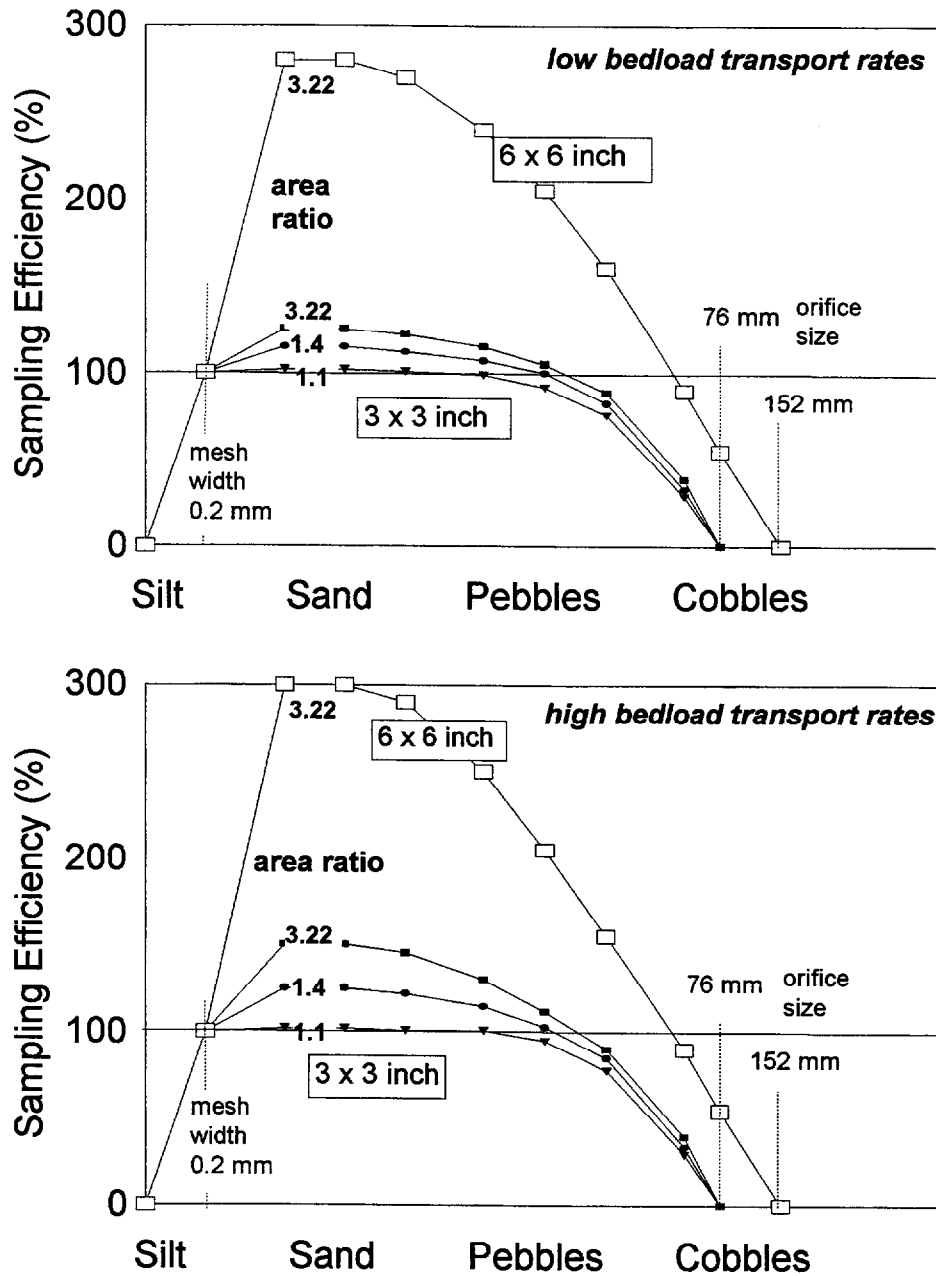


**Fig. B-3; 8:** Conceptual model demonstrating the combined effects of particle sizes and bedload transport rates on sampling efficiency for three differently-shaped 3 x 3-inch Helley-Smith samplers (area ratios of 1.1, 1.4, and 3.22) and the standard 6 x 6-inch Helley-Smith sampler with an area ratio of 3.22 for low bedload transport rates (top) and high bedload transport rates (bottom)..

**3.2.1.5 Bag size, mesh width, and sampling duration**

The Helley-Smith sampler was not designed to sample large amounts of sandy sediment. Using a small bag size (about 2000 cm<sup>2</sup>), a fine mesh width (0.2 mm), and long sampling

duration (30 s or more) can severely decrease the sampling efficiency. Johnson et al. (1977) compared bedload sampled with different bag and mesh sizes during three days of peak flows in a gravel-cobble river in Idaho. Results of that study are plotted in Fig. B-3; 9.

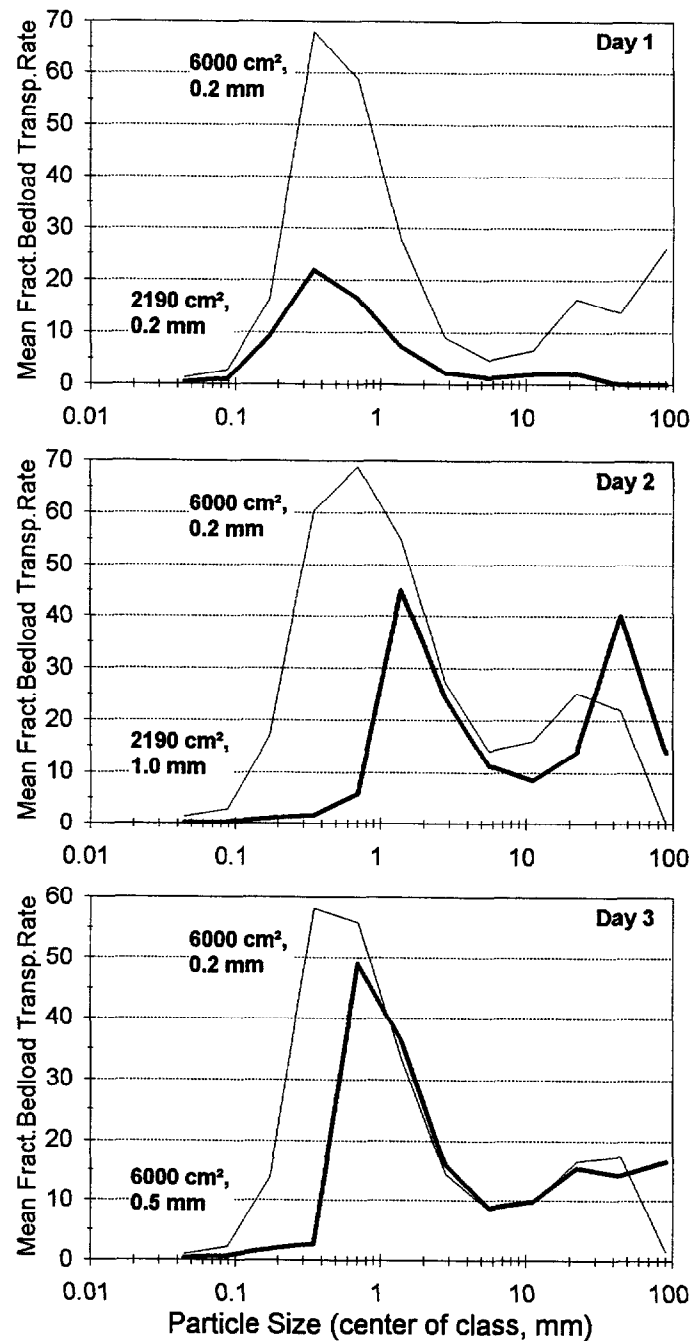


**Fig. B-3; 9:** Effects of bag size and mesh width on sampled mean bedload transport rates by grain-size. The thin line in each graph represents the bedload captured with a 6000 cm<sup>2</sup> bag with a 0.2-mm mesh (data from Johnson et al. 1977).

***Bag size and mesh width***

Bag size was shown to greatly affect the amount of bedload collected. The 2190 cm<sup>2</sup> bag caught only about one quarter of the material that was caught with the 6000 cm<sup>2</sup> bag, and particles larger than a few millimeters were not caught when using the small bag (Fig. B-3; 9). This difference is due to the combination of a small mesh size (0.2 mm) and the small bag size. Fine sand and organic debris clogged the pores in the fine mesh, and this had a large effect on the hydraulic efficiency when the bag was relatively small and rapidly became clogged.

A comparison of a small bag with a wide (1.0 mm) mesh to a large bag with a small (0.2 mm) mesh indicates that the coarser mesh doesn't capture much sediment smaller than 1 mm, but the small bag still captured more sediment than the small bag with a 0.2-mm mesh (compare the top and middle figures in Fig. B-3; 9). A comparison of the large bag with a small mesh and the small bag with a coarse mesh indicated that sampling efficiency was similar for particles larger than 1 mm. This shows that an increase in mesh size can partially compensate for a small bag size.

For large bags, mesh size controlled the minimum particle size, but had little effect on the larger particles. Taken together, these results show that clogging can be a severe problem when smaller bags are used that rapidly become full. A larger bag can be coupled with a smaller mesh size to capture a better distribution of the grain-sizes being transported, but the duration of sampling must be carefully controlled in response to the observed bedload transport rates as discussed in the next section.

***Sampling duration***

Similar observations of clogged meshes in small bag sizes led Beschta (1981) to analyze how progressive clogging affected the sampled bedload weight, and the degree to which clogging caused sampling efficiency to decrease with increasing sampling duration. As in the study by Johnson et al. (1977), Beschta found that the 6000 cm<sup>2</sup> bag posed no problem, irrespective of the mesh size, because the sampled fines collected in the downstream part of the bag where they do not obstruct the flow. But using a small 1950 cm<sup>2</sup> bag in the same flume experiments severely decreased the sample weight, and this decrease became more pronounced as the sampling duration was extended (Fig. B-3; 10). Flume experiments indicated that when the sand feed rate was 0.2-0.3 kg/m·s, the weight of the sampled sand increased at a progressively slower rate as sampling duration increased. After 30 s of sampling, sampling efficiency was already reduced to 40%. Sampling for 60 s diminished sampling efficiency to 20%, while at the end of two minutes sampling efficiency had dropped to only 10%.

Since measured bedload transport rates may easily be influenced by sampling duration, Beschta (1981) concluded that transport rates from different sampling durations cannot be compared when a small bag is used. In order to ensure that sampling efficiency in sandy sediment is not affected by sampling duration or mesh size, bedload sampling in streams with substantial amounts of sand transport should only use a large (6000 cm<sup>2</sup>) bag.

Sampling efficiency can also decrease when the bag fills to the point that hydraulic efficiency is reduced. Emmett (1981) therefore suggests not to fill the sample bag to more than 40% of its capacity. This means that one must select an appropriate sampling duration for the bedload transport rates being measured.

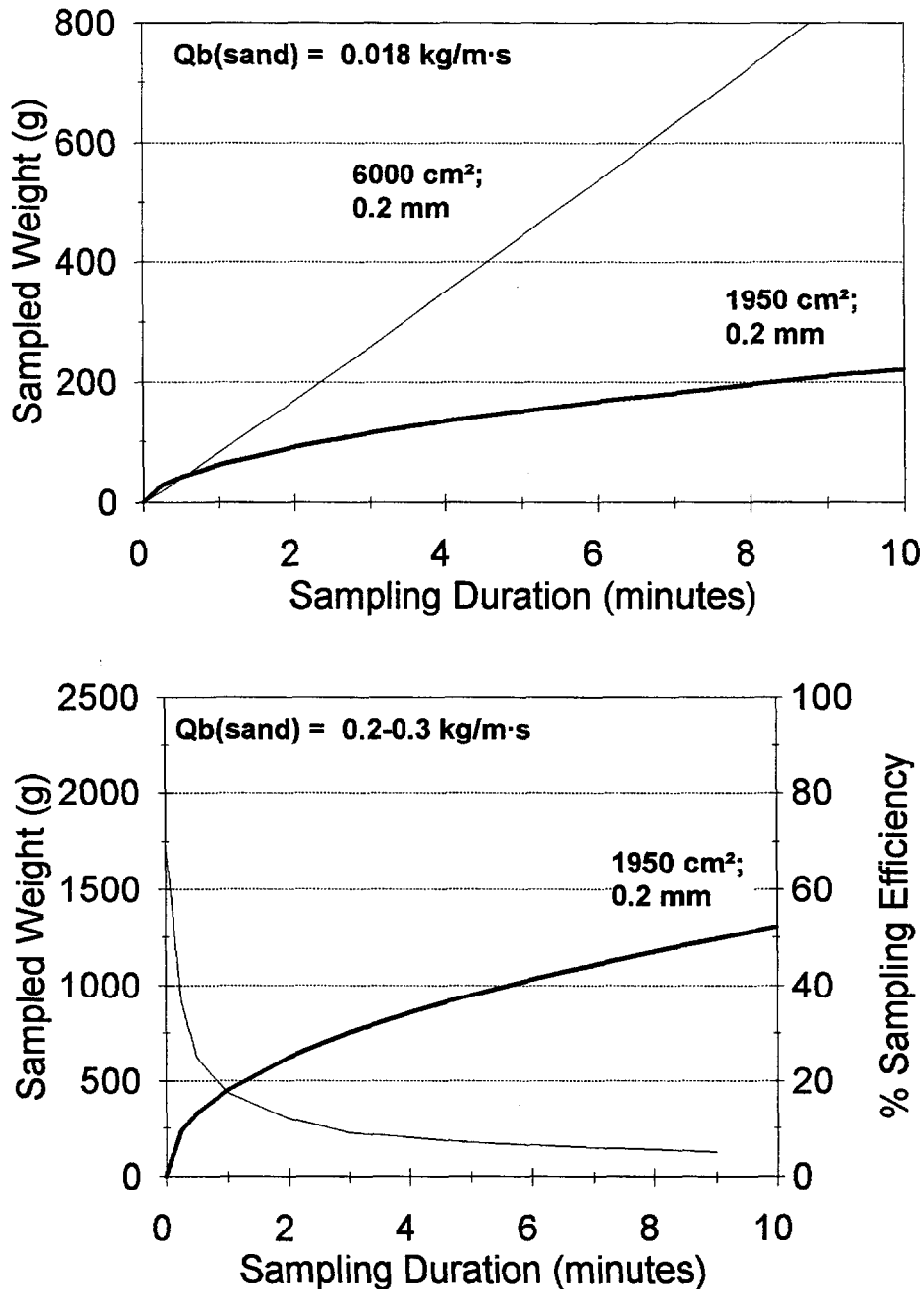


**Fig. B-3; 10:** Effects of bag size and sampling duration on weight of sandy bedload sampled with a standard 3 x 3 inch Helley-Smith sampler. Sampled weight does not increase linearly with time for small bags (top). This effect is more pronounced for higher transport rates (bottom), and sampling efficiency (thin line) decreases strongly within the first minute of sampling (data replotted from Beschta 1981).

### 3.2.1.6 Contact with the river bed

The previous discussion was based on the condition that no fine sediment passes under the sampler when placed onto the stream bed. Likewise, it was assumed that no scour hole developed around the sampler entrance, as this would supply additional material to the

sampled sediment. Both phenomena are frequently encountered in bedload sampling, with the former more common in coarse-bedded streams and scour a larger problem in sand-bedded streams.

**Coarse gravel beds**

In coarse gravel-bed rivers much of the fine sediment can easily pass under the sampler if the sampler is not in perfect contact with the river bottom. Wilcox et al. (1996) compared bedload samples taken with a 3 x 3 inch Helley-Smith sampler at a wooden sill on the upstream side of a debris pond, and at a cross-section 45-60 m further upstream in three gravel-bed rivers. While sampling on a wooden sill did not make much difference to sampling on the stream bottom at Coon Creek (WY), the grain-size distribution of bedload sampled on the stream bottom was 1.5 - 2.5 times coarser than the bedload sampled on sills at East Fork Encampment Creek (CO), and East St. Louis Creek (CO) (Table B-3; 4). The larger size and amount of pebbles in the stream-bottom samples could be due to pebble "scooping", or to fewer pebbles reaching the samplers placed on the sills. If it is assumed that the sills were flush with the river bed and did not protrude into the flow, the almost two-fold increase of fine sand for the samples taken on the sill (Fig. B-3; 11) could indicate that about 50% of the sand finer 1 mm escaped under the sampler when sampling directly on the stream bottom. At Coon Creek a similar comparison indicated that only about 20% of the sand less than 1 mm in diameter was lost under the sampler.

**Table B-3; 4:** Bedload grain-size distributions (mm) sampled with a 3 x 3 inch Helley-Smith sampler on a wooden sill, in a stream cross-section, and excavated from a debris basin (data from Wilcox et al. 1996).

	Coon Cr. (WY)					EF Encampment Cr. (CO)					E. St. Louis Cr. (CO)				
	D <sub>10</sub>	D <sub>25</sub>	D <sub>50</sub>	D <sub>75</sub>	D <sub>90</sub>	D <sub>10</sub>	D <sub>25</sub>	D <sub>50</sub>	D <sub>75</sub>	D <sub>90</sub>	D <sub>10</sub>	D <sub>25</sub>	D <sub>50</sub>	D <sub>75</sub>	D <sub>90</sub>
sill	0.39	0.61	1.8	7.2	25	0.40	0.62	1.3	4.6	13	0.31	0.52	1.3	4.1	8.5
x-sect.	0.40	0.72	2.1	6.8	19	0.60	1.10	3.0	5.5	29	0.50	1.15	3.2	6.7	12
basin	0.48	0.86	2.1	12	30	0.39	0.76	2.2	15	35	0.62	1.22	3.6	11	24

As the potential loss of fines under the sampler may be quite high, sampling on sills is advisable (Johnson et al. 1977). Sampling on sills becomes especially important for CWE analysis where the detection of an increase in the amount of sand transport is of interest. Some hydrologists may argue that the loss of fine sediment under the sampler compensates for the tendency for Helley-Smith samplers to oversample fine sediment, but this means that one is trading a better known error for an almost completely unknown error. A better and more accurate approach is to avoid fine sediment loss under the sampler, and correct for oversampling by using calibration curves.

**Scour hole development in sand-bedded streams**

Bedload sampling in sand-bedded streams is frequently faced with the problem of scour hole development around the entrance of the sampler. This supplies additional sediment to the sampler and severely disturbs the sample. Some bedload samplers have been specially designed to minimize this problem (Zhou et al. 1981; Gao 1991; Xiang and Zhou 1992; Gaweesh and Van Rijn 1994), and these generally feature an entry plate in front of the sampler that covers the transition between the sampler and the stream bed. These samplers also have a low hydraulic efficiency to prevent excessive suction of sand into the sampler.

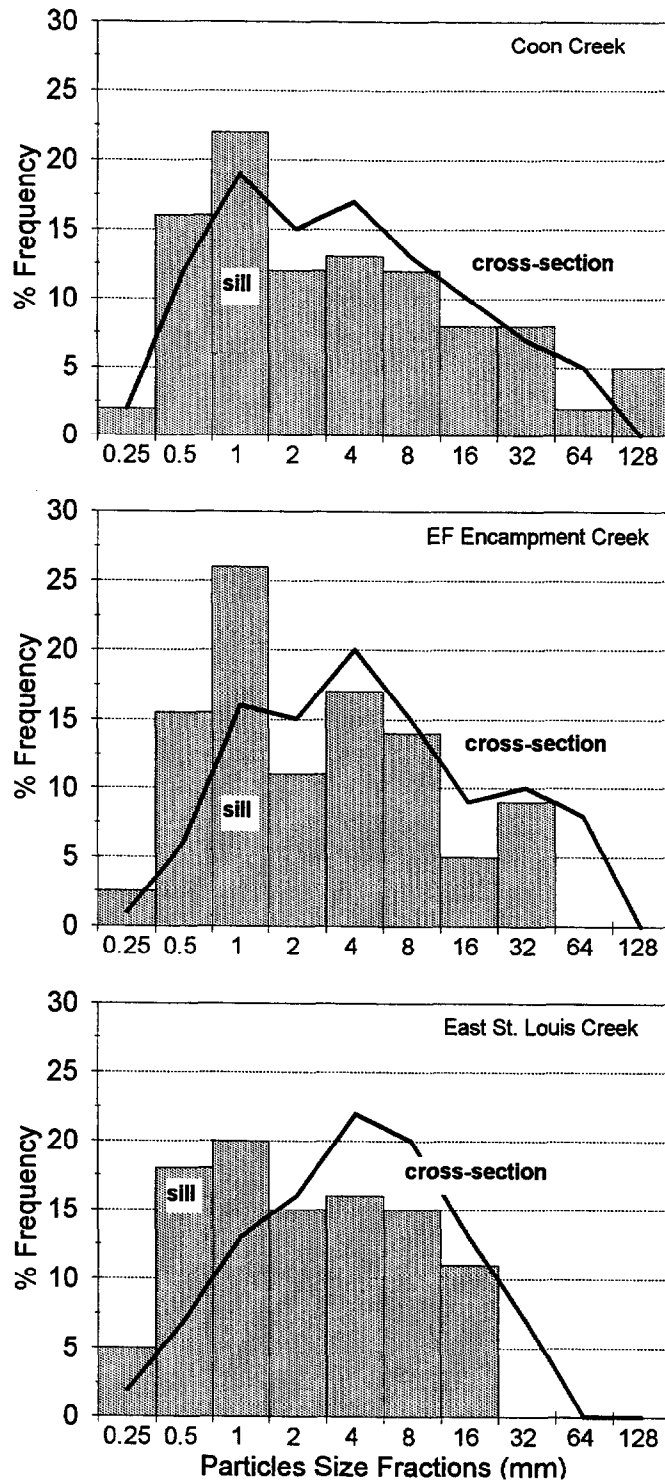


**Fig. B-3; 11:** Comparison of grain-size distributions sampled at three gravel-bed streams with a 3 x 3-inch Helley-Smith sampler directly on the stream bottom (solid line) and at a sill (bars) (data from Wilcox et al. 1996).

This is achieved by using a box-shaped sampler in which sampled sediment can settle, while the flow, deprived of its sediment, escapes through a slot at the top rear. However, not all sand settles in the sampler body, and sampling efficiency typically takes values between 40 and 60% for the Chinese Yangtze-73 and Yangtze-78 samplers (Zhou et al. 1981; Gao 1991; Xiang and Zhou 1992).

The Delft Nile sampler can have sampling efficiencies in a range as low as 80 to 130%, depending on particle size, when used in a flume with long sampling durations of 10 minutes (Gaweesh and Van Rijn 1994). But in field tests the amount of sampled sediment is strongly affected by the degree of contact with the river bed, the initial bottom touch which stirs up sediment, and by subsequent scour development. This makes bedload sampling in sand-bedded streams extremely difficult and prone to large errors, especially if the depth of the flow prohibits wading and visual observation. Childers (1996) even proposes not to venture into any bedload sampling projects in sand-bedded streams. Unless there are special provisions for accurate bedload sampling, sediment transport in sand-bedded streams is probably better sampled at locations that bring the entire sediment load into suspension, and then use suspended sediment sampling techniques. Another method for sampling bedload in a sand-bedded stream is to use a standard suspended sediment sampler (DH-48) at the downstream side of a wooden board set on edge into the stream bottom. The sampler can then be lowered until the nozzle touches the sill.

### 3.2.1.7 Poor operating

#### ***Sampler misalignment***

Last but not least, sampling accuracy can be grossly decreased by poor operating skills. Good handling ensures that the sampler is properly aligned with the flow. This may become a problem when sampling near stream confluences, in meander bends, or anywhere where the lateral flow component is large. Using a standard 3 x 3 inch Helley-Smith sampler in a sand-bedded flume ( $D_{50} = 0.24$  mm, sorting =  $(D_{84} - D_{16})/2 = 0.56$ ), Gaudet et al. (1991) analyzed how sampler misalignment with respect to the main direction of flow affects the relative sampling efficiency. Compared to perfect alignment, a misalignment of  $10^\circ$  reduced the relative sampling efficiency to 56% in three experiments with Froude numbers ranging from 0.27 to 0.67. A misalignment of  $45^\circ$  produced a 45% reduction in relative sampling efficiency. This undersampling is only partially due to the reduced width of the sampler opening that is exposed to flow. The main reason is that hydrodynamics in the sampler entrance are altered. The effects of misalignment on sampling efficiency are most pronounced at low velocities.

#### ***Scooping and stirring up sediment***

Good handling also tries to prevent the scooping and stirring up of sediment when putting the sampler onto the stream bottom. The effect of scooping sediment becomes especially large when transport rates are small. In gravel-bed rivers pebbles are most likely to get scooped, and a single pebbles in a bedload sample that otherwise consists of a few spoonfuls of sand should always be suspicious. Sediment that got into the sampler due to stirring up the bottom sediment is harder to identify because this sediment is likely to be fine and fit in with the grain-size distribution in the rest of the sample. To avoid scooping and stirring up sediment, one needs to make sure that the tail of the sampler first touches the stream bottom, and the sampler is then tipped towards a more horizontal position. The effect of scooping or stirring up sediment can also be minimized by longer sampling durations.

Operating problems are most likely to increase when flow velocities are high, and when wading the stream becomes a task in itself. Sampling bridges, guide ropes, and teamwork can all help reduce operator errors. Sampling bedload in sand-bedded streams during high flows is most likely to encounter stirring and scour problems.

### 3.2.1.8 Summary

A wide range of bedload grain-sizes in a stream, and varying grain-size distributions during a high flow event, may require the use of different samplers to match the momentary bedload transport conditions. Sampling efficiencies will vary according to the sampler size and shape, as well as the bedload transport conditions. This variability makes it necessary to calibrate individual samplers in order to calculate accurate bedload transport rates. Unfortunately, the few calibration curves now available vary with bedload transport conditions do not cover the full range of flow and sediment conditions. Lacking any better alternative, one should attempt to assess sampling accuracy of bedload sampling by extrapolating from studies of sampling efficiency under comparable conditions. A knowledge of the effects of sampler configuration and transport processes on sampling efficiency are essential. Such assessments of sampling efficiency are important for accurately assessing the accuracy of measured bedload transport rates and detecting CWEs. A failure to consider the changes in sampling efficiency in different streams and sediment transport conditions could contribute to an incorrect assessment regarding the presence or absence of change in sediment transport rates or annual loads.

### **3.2.2 Basket and net samplers**

Basket samplers are designed for sampling pebble and cobble bedload. The bottom of basket samplers can be either a solid plate, or loosely woven iron rings that conform to the shape of the bed. Sides and top of the sampler are usually of mesh wire. Hubbell (1964) gives a comprehensive descriptions of older basket samplers. A net sampler consists of large, strong nylon netting attached to a sampler opening (Bunte 1992, 1996). Due to the rather large mesh widths, flow can pass through these samplers relatively unobstructed. The force exerted on the sampler by the flow is therefore relatively small compared to the large sizes of the samplers. All grain sizes smaller than the mesh width pass through the sampler, while larger particles are retained. This creates bedload samples that are artificially truncated on the fine end, but which may rather accurately represent the coarse end of bedload grain-size distributions.

Basket samplers are not flared (i.e., their area ratio is 1), but hydraulic efficiencies and sampling efficiencies may nevertheless vary. Engle and Lau (1981) expressed sampling efficiency of basket samplers as functions of several dimensionless parameters, each relating to the characteristics of the sampler, flow, and bed material. Conducting experiments in a sand-bedded flume with three sizes of basket samplers, each with a 0.6-mm wire mesh, Engle and Lau (1981) found that sampling efficiency  $E$  was mostly affected by the following two dimensionless parameters

$$E = f \left( \frac{L_s}{D_{50}}, \frac{t^* \cdot u^*}{L_s} \right) \quad (5)$$

where  $L_s$  is the sampler width,  $t^*$  is sampling duration, and  $u^* =$  shear velocity defined as  $\sqrt{g \cdot d \cdot S}$ , with  $g =$  acceleration due to gravity,  $d =$  flow depth, and  $S =$  slope (Fig. B-3; 12).

While there is no significant effect of the ratio  $L_s/D_{50}$  on sampling efficiency for  $L_s/D_{50}$  in the range of 80-160, sampling efficiency was reduced for a  $L_s/D_{50}$  ratio of 27 obtained in other experiments with larger mesh sizes and coarse sediment.

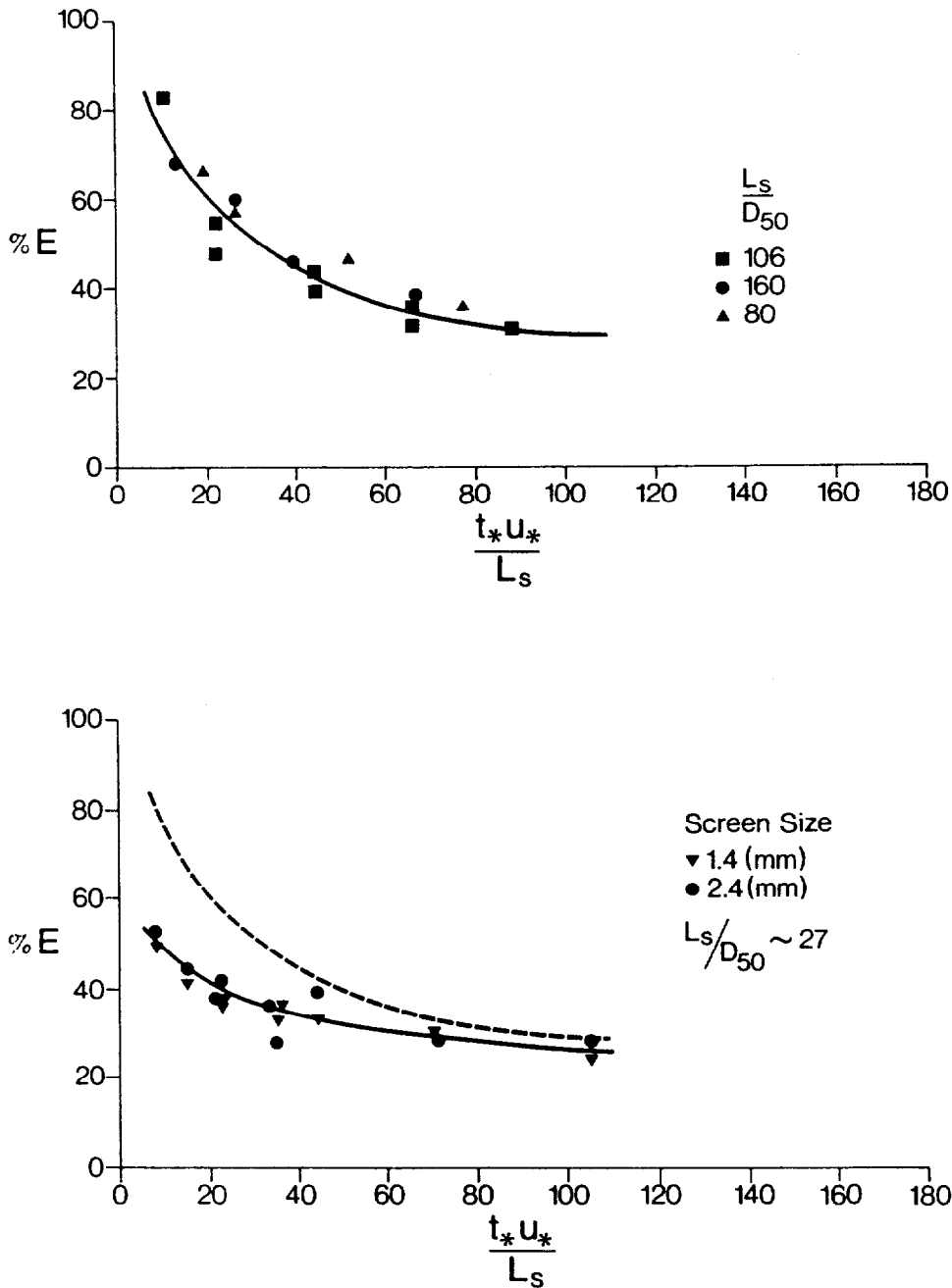


**Fig. B-3; 12:** Percent sampling efficiency (%E) as a function of the ratio of sampling duration  $t^*$  times shear velocity  $u^*$  and sampler size  $L_s$ . The three values of  $L_s/D_{50} = 80, 106,$  and  $160$  plot on one curve (top). A different curve is obtained for a smaller ratio of  $L_s/D_{50} = 27$ . Stippled curve is curve from the plot above (bottom) (from Engel and Lau 1981).

Besides the  $L_s/D_{50}$  ratio, sampling efficiency varies with sampling duration and shear velocity. Sampling efficiency decreased from 80% to 30%, and from 50 to 30%, respectively, as the sampler filled up during long sampling duration. The decrease of sampling efficiency with increasing shear velocities may be due to more particles being transported in suspension, or bouncing higher when saltating. Constant sampling efficiency for all sampling, flow, and sampler characteristics cannot be assumed. Thus calibration curves are necessary to obtain accurate bedload transport rates.

The basket samplers tested by Engle and Lau (1981) had a rather fine mesh of 0.6 mm, and were calibrated in a sand-bedded flume. The different behavior of sampling efficiency for coarser bed material (**Fig. B-3; 12b**) suggested that the calibration proposed by of Engel and Lau (1981) cannot be directly applied to cobble-bed streams with pebble-sized bedload. Gao (1991) and Xiang and Zhou (1992) compared the sampling efficiencies of two basket samplers developed in China (Yangtze-64 and Yangtze-80) with two pressure-difference samplers (6 x 6-inch Helley-Smith and the Toutle River sampler).

**Table B-3; 5:** Characteristics of bedload samplers compared by Gao (1991) and Xiang and Zhou (1992).

Sampler Name		Entrance dimensions		Flume determined		Sampler Mass (kg)	Sampling Capacity (kg)	Bedload Size Range (mm)
		Width (cm)	Height (cm)	Heff.* (%)	Seff# (%)			
Helley-Smith	PD <sup>§</sup>	15.2	15.2	154	varies	100	20	1- 32
Toutle River	PD	30.5	30.5	140	varies	300	50	1- 64
Yangtze-80	B <sup>§</sup>	30.0	30.0	92	53	200	20	5-128
Yangtze-64	B	50.0	50.0	89	42	240		10-128?

\* Heff = hydraulic efficiency; # Seff = sampling efficiency; § PD = pressure difference sampler; § B = basket sampler

When tested in flume experiments with bedload grain-sizes ranging between 5 and 200 mm, the Chinese basket samplers Yangtze-64 and Yangtze-80 had an almost constant sampling efficiency for all bedload particle sizes, while the sampling efficiencies of the Toutle River sampler, and especially the 6 x 6-inch Helley-Smith, strongly decreased with particle size (Gao 1991) (**Fig. B-3; 13a**). The 6 x 6 Helley-Smith sampler<sup>4</sup> had the highest sampling efficiency, as bedload transport values were greater than the Yangtze-80 sampler by a factor of 2-4, and a factor of two larger than the Toutle River sampler (**Fig. B-3; 13b**). Seen the other way round, the Yangtze-80 sampler catches only 20 to 40% of the bedload sampled by the 6 x 6-inch Helley-Smith (**Fig. B-3; 13c**).

The relative sampling efficiency was also tested in field experiments in the upper Yangtze River with bedload in the range of 1-150 mm (Gao 1991; Xiang and Zhou 1992). Although the general trend of the curves is maintained, relative sampling efficiencies differ between field and flume tests (**Fig. B-3; 13d and e**). This difference makes it difficult to transfer flume calibration curves to field situations. Unfortunately, field experiments did not provide "true" bedload transport rates, so **Fig. B-3; 13d and e** cannot tell which of the samplers deviated most from the sampling efficiency established in the flume runs.

<sup>4</sup>The sampling efficiency of the 6 x 6 Helley-Smith sampler was "deduced" in the Chinese study, but the methods for doing so were not given. The present study assumes that the results are correct.

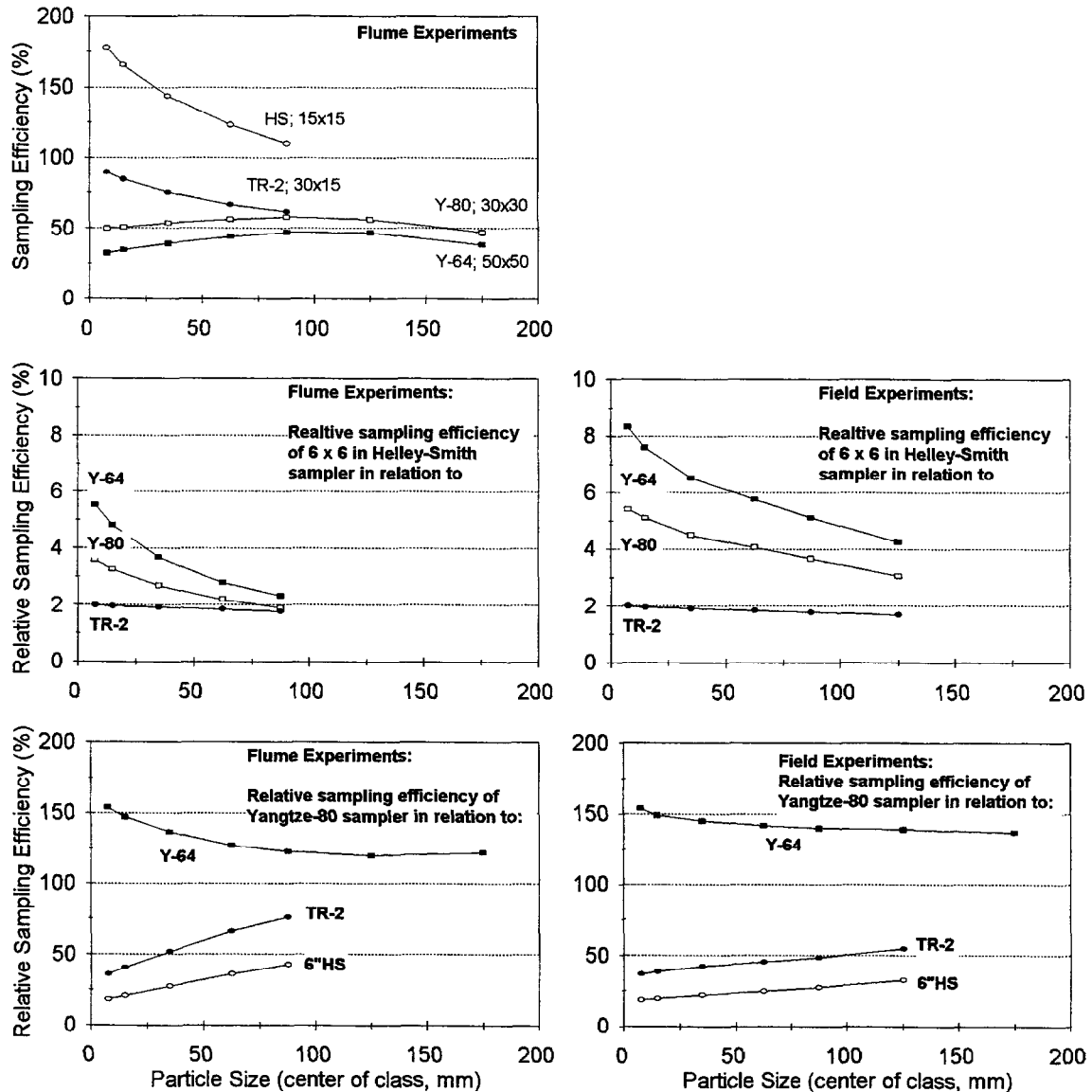


**Fig. B-3; 13:** (a) Percent sampling efficiency as a function of particle size for two basket-type samplers (Y-64 and Y-80, and two pressure-difference-type samplers (TR-2 and 6 x 6-inch HS) in flume experiments (upper left); (b) Factor by which 6 x 6 inch Helley-Smith sampler oversampled Y-64, Y-80, and TR-2 sampler in flume experiments (center left); (c) Relative sampling efficiency of Y-80 sampler in flume experiments (lower left); (d) Factor by which 6 x 6-inch Helley-Smith sampler oversampled Y-64, Y-80, and TR-2 sampler in field measurements (center right); (e) Relative sampling efficiency of Y-80 sampler in field experiments (lower right) (Data from Gao 1991; Xiang and Zhou 1992).

### 3.2.3 Annual surveying or excavation of bedload traps or debris basins

Sediment accumulated in a bedload trap or a debris basin can yield accurate measurements of bedload transport over more extended time periods provided that the trap efficiency for bedload is 100%, that the trapped bedload can be accurately surveyed, and the bulk density

can be accurately determined. The alternative is to excavate and weigh the accumulated bedload.

#### ***Trap efficiency***

Trap efficiency for finer bedload particles may often be less than 100%, as fine sand can be flushed through the trap without settling. The determination of trap efficiency can be difficult, as this can be affected by the time of sampling as well as the problems of accurately measuring the bedload reaching or passing through the sediment ponds. Data from Wilcox et al. (1996) for three gravel-bed rivers shows that the debris basins yielded only one-half to three-quarters of the amount of sand <1mm obtained by bedload samples taken on a sill at the upstream end of the debris basins (Fig. B-3; 14). This could indicate an insufficient trap efficiency for sand, but the smaller amount of sand in the debris basins could also result from a higher than average percentage of sand transported during the bedload sampling period as compared to the annual average. Correct estimates of trap efficiency would require a comparison of bedload samples upstream and downstream from the debris basins.

For smaller sediment traps the efficiency will vary with flow. Suspended sediments may be captured during low flows, while not all of the fine bedload may be captured during high flows.

### **3.2.4 Continuously recording bedload traps**

Ordinary debris basins will give an annual or perhaps an event-based bedload yield, but some studies may require a record of the temporal variation of bedload during a high flow event. This can be achieved with continuously recording bedload traps. Continuous sampling of bedload that is transported over the entire cross-section provides the most accurate method of determining instantaneous bedload transport rates, provided the trap efficiency is 100% for a wide range of flow and bedload transport conditions (see section 3.2.4). The downside of the potentially very accurate sampling enterprise is that one needs to build a rather substantial sampling station equipped with either a vortex sampler, weighable traps, or continuously surveyable debris basins.

#### ***Vortex samplers***

A vortex sampler is a tube typically about 0.5 to 2 feet in diameter that has about a quarter of its circumference cut out. The opening of the tube is flush with the river bed. The vortex tube usually extends - sometimes diagonally - over the entire channel width (Fig. B-3; 15). Some systems are designed so that different sections of the trap can be independently opened and closed during a high flow event. All bedload particles over the tube are trapped in the vortex and moved to the stream bank either by a helical swirl in the vortex sampler, or with the help of a conveyor belt. A continuous stream of water and sediments gushes from the end of the vortex tube into a pit, where manual samples can be taken as desired. Samples can be retained for further analysis, or directly returned to the stream in a bypass canal. This system makes it possible to obtain a detailed record of the temporal and spatial variability of bedload transport and its grain-size distribution, but in order to operate it needs to be manned. The more people are engaged in the sampling, the more detailed the record can be.

Atkinson (1994) presents a methodology for calculating the trapping efficiency of vortex samplers. The trapping efficiency is the proportion of the total sediment transport below the

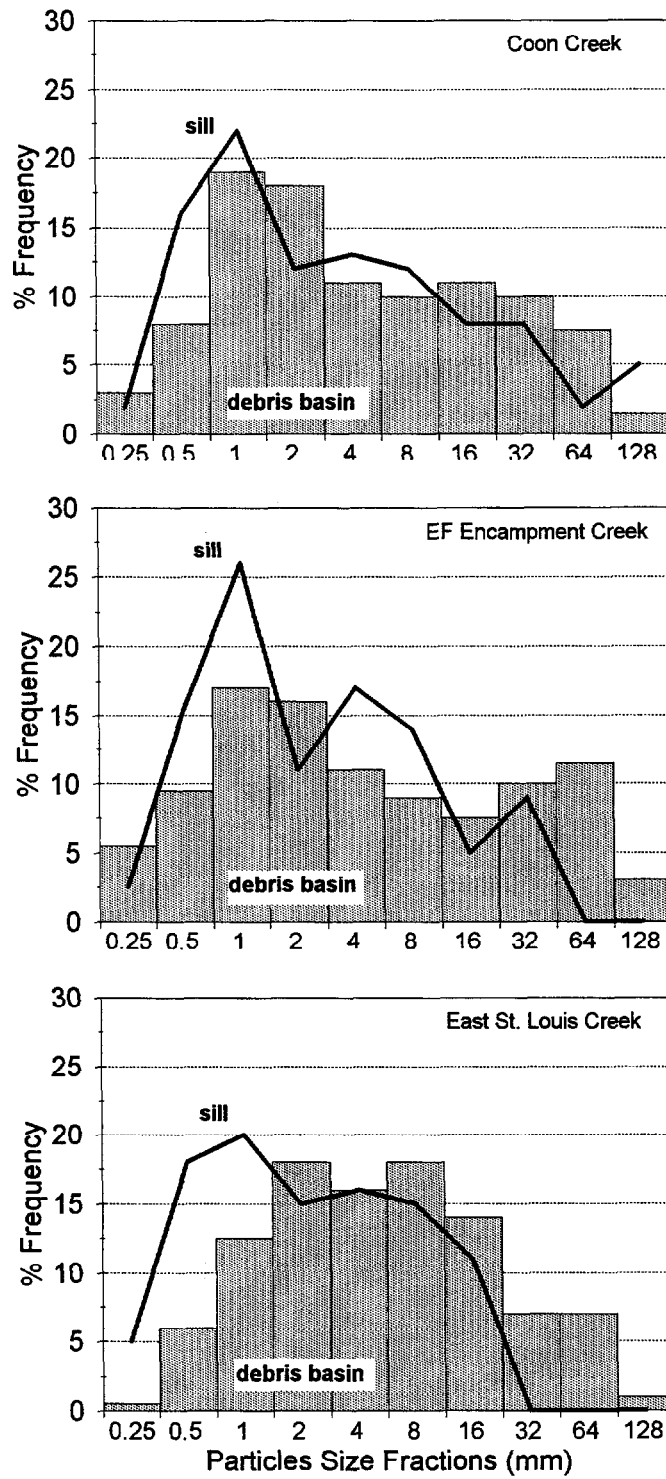


**Fig. B-3; 14:** Comparison of grain-size distributions sampled at three gravel-bed streams with a 3 x 3 inch Helley-Smith sampler at a sill (solid line), and the grain-size distributions of bedload accumulated in debris basins (bars) (data from Wilcox et al. 1996).

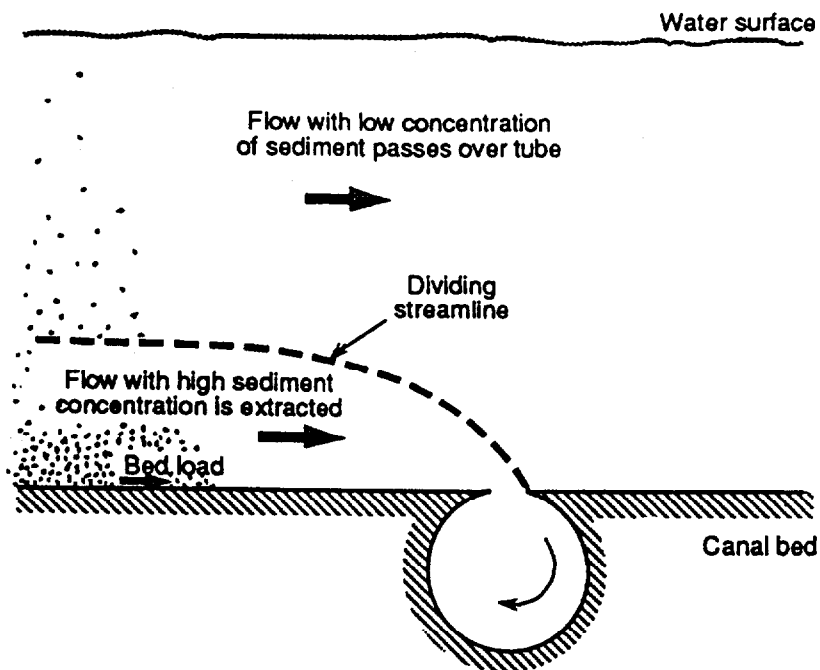
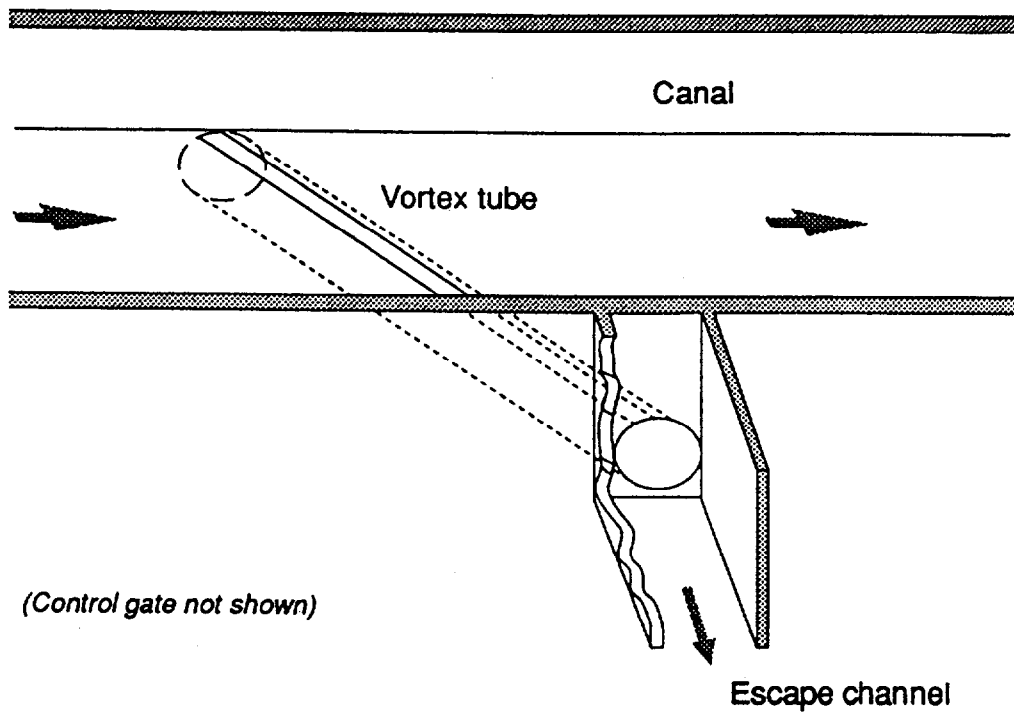


**Fig. B-3; 15:** Schematic diagram of a vortex sampler (top); Elevation of streamline dividing between sediment that goes into the sampler and sediment that passes over it (bottom) (from Atkinson 1994).

height of the dividing stream line in the channel upstream from the vortex tube to the sediment transport rate extracted into the vortex tube. Thus, vortex samplers not only sample sediment that actually moves on the bottom of the stream, but all sediment that moves below the dividing stream line<sup>5</sup>. Trapping efficiency depends on the flow hydraulics, grain-size distribution, the resulting sediment concentration profiles, and the height of the dividing stream line which in turn is determined by the dimensions of the vortex tube. Trapping efficiency is further dependent on the exact location of the vortex tube within the encasing canal. Atkinson (1994) calculated trap efficiencies and analyzed the discrepancy between observed and predicted trapping efficiencies for 120 measurements at six samplers in five sand-bedded canals. Although the mean discrepancy ratio of all 120 measurements was 1, individual values varied by a factor of 2 and included examples of both over- and undersampling relative to the predicted trapping efficiency. In most cases, however, the discrepancy ratios ranged between +25% and -20%.

The sampling efficiency of vortex tubes can be optimized by selecting the proper dimensions of the tube given the expected flow range and bedload transport conditions. However, a vortex sampler can only entrap particles that move below the dividing stream line, and if flows are high enough to move a substantial part of the sediment as "high" suspended load above the dividing stream line, it will pass over the sampler.

Due to high construction and operating costs, vortex samplers are restricted to a few, well-equipped measuring sites. Vortex samplers have been used at Oak Creek in Oregon (Milhous 1973), the Torless Stream in New Zealand (Hayward and Sutherland 1974; Hayward 1980), the East Fork River in Wyoming (Leopold and Emmett 1976, 1977; Emmett 1980; Emmett et al. 1980; Klingemann and Emmett 1982), and at Virginio Creek in Italy (Billi and Tacconi 1987).

#### ***Continuously weighable bedload traps (Birkbeck Sampler)***

Continuous measurements of bedload transport can also be made with bedload traps in the bottom of the stream that continuously weigh the accumulated bedload (i.e., Birkbeck sampler) (Reid et al. 1984, 1985; Reid and Frostick 1984, 1986; Lewis 1991; Laronne et al. 1992; Powell et al. 1995). These traps have a volume of about 0.25-1 m<sup>3</sup>, and they are designed to measure rather small transport rates or for short events. Ergenzinger et al. (1994) report that the error of the weighable trap used in desert flash floods increased with decreasing transport rates, being 2.2 and 13% for weighing intervals of 60 and 10 seconds at a transport rate of 5 kg/m·s (submerged weight), and increasing to 11 and 67% for transport rates of 3 and 1 kg/m·s, respectively.

The downside of these samplers is that the capacity of these traps is limited, and they are often filled before the end of the high flow. It is also not possible to obtain a temporal record of grain-size distributions. The advantage of these systems is that they can be automated, thereby allowing their use in remote areas and precluding the need for observers to be present during the flow event.

A slightly different version of weighable sediment traps is introduced by Miyamoto et al. (1992). They used a bypass structure in which a water-bedload mixture is directed through a screen that separates out the water and collects the sediment in a tipping bucket. The bucket is continuously weighed, and as soon as a preset weight is reached the accumulated bedload is discharged.

---

<sup>5</sup>This may be an explanation for the rather good agreement in Emmett's (1980) comparison between bedload transport rates sampled with the 3 x 3 inch Helley-Smith and the bedload trap at East Fork River.

***Continuously surveyable debris basins***

A continuously surveyable debris basin has been designed for mountain torrents with flashy floods and huge amounts of coarse sediment transported as bedload, hyperconcentrated flow, or in suspension. A concrete channel funnels the flow over (or through) a steeply inclined coarse mesh from which pebbles and cobbles roll into a debris basin, while the water, sand, and smaller particles pass through the grid and are conducted back to the stream. The accumulated pile of coarse sediment is continuously scanned by a sonar device, and this allows a fully automated continuous record of coarse bedload transport over long periods of time (Lenzi et al. 1990; D'Agostino et al. 1994). The accuracy of this method was not reported and may be very difficult to evaluate. Again, such devices are only available at a few research sites.

**3.2.5 Indirect methods of bedload transport measurements**

Indirect measurements of bedload transport include the acoustical record of noise from either inter-particle collisions or particles banging against a hydrophone, or the detection of magnetically or otherwise marked particles over a sensor.

***Self-generated noise***

Measuring bedload transport rates by the self-generated noise utilizes the acoustic detection of inter-particle collisions using a submerged hydrophone (Schlatte, 1984; Heathershaw and Thorne, 1985; Thorne et al. 1989; Williams et al., 1989b; Rouse 1994). Rating curves relating transport rates of particles in a rotating drum to voltage output in a hydrophone at the drum wall indicated a scatter 20-40% scatter of data around the mean value (Rouse 1994).

***Acoustic and piezoelectric sensors***

Bänzinger and Burch (1990) and Rickenmann (1994) registered the acoustic signals created by the impact of bedload particles as they pass over a cross-section that had nine hydrophones built into the bottom. The accuracy of this measuring system cannot be well established. A plot of the increment in accumulated sediment and the sum of hydrophone signals within that time period showed that the 11 data points extended over two orders of magnitude on each axis, with a scatter of about half an order of magnitude about the regression line.

Tanaguchi et al. (1992) recorded the noise of bedload particles hitting a submerged pipe that had a microphone inside, and they reported only a 30% difference between the hydrophone data and direct measurements of bedload transport. This error increased for high bedload transport rates.

**3.3.6 Measuring bedload transport using tracer techniques****3.3.6.1 Techniques and recovery rates*****Tracer techniques for bedload particles***

By definition, the tracer population must be representative of the material whose dispersion is to be investigated. A literature review about the various tracer techniques and the

possibilities for their recovery was compiled by Hassan et al. (1984) and Bunte and Ergenzinger (1989). Possibilities to trace sediment particles include:

- **Natural tracers:**
  - obvious petrology
  - natural magnetism
  - large volume of external sediment (artificial input: Hansen and Alexander 1976; natural input: Sullivan et al. 1987)
- **Surface manipulation:**
  - visual tracing:
    - painting with color (Thompson 1994; Emmett and Myrick 1985)
    - numbering (Gintz 1990, 1994; Gintz and Schmidt 1991, 1995; Gintz et al. 1996)
  - property tracing:
    - coating with magnetic material
    - coating with radioactive material (Hubbell and Sayre 1964; Sayre and Hubbell 1965)
- **Interior manipulation:**
  - passive detection:
    - inserting iron tracer (Gintz 1990, Gintz and Schmidt 1991, Schmidt and Ergenzinger 1992, Schmidt et al. 1992)
    - inserting magnetic tracer (Ergenzinger and Conrady 1982; Gintz 1990, 1994; Gintz and Schmidt 1991, 1995; Gintz et al. 1996; Schmidt and Ergenzinger 1992; Schmidt et al. 1992; Schick et al. 1987a and b; Hassan 1990; Hassan et al. 1984, 1991, Hassan and Church 1994)
    - enhancing magnetic properties (Arkell et al. 1983)
  - active detection
    - inserting radio tracer (Buskamp and Ergenzinger 1991, Schmidt and Ergenzinger 1992, Schmidt et al. 1992)
- any combination of the above (artificially magnetized particles are usually painted and numbered)
- artificial substitute particle with several tracing properties (Gintz 1990, 1994; Gintz and Schmidt 1991, 1995; Schmidt and Ergenzinger 1992; Schmidt et al. 1992; Gintz et al. 1996)

Each tracing method has its advantages and disadvantages that arise from the interplay between the costs and efforts to manufacture a tracer, the lifetime of the tracing property, the ease and range of detection, the research question, and the feasibility for a given situation.

#### ***Tracer recovery rates***

The quality of tracer studies is directly linked to the recovery rate of the traced particles. The recovery rate usually decreases with the duration of the tracer experiment and the dispersion of the tracers. Searching for tracers becomes a tedious enterprise once tracers have dispersed over a long distance downstream. The lateral dispersion may deposit some tracers close to the last flood bank line where tracers may lie hidden in the riparian vegetation. The vertical dispersion into the bed material might make it especially difficult to

relocate and retrieve the traced particles. A long lifetime of the tracing property, and the ease and range of detection help to ensure a high recovery rate.

The recovery rate for visually traced particles decreases proportionally to the amount of tracers that become buried by other sediment. The amount of particles that become buried and the burial depth increases with the flashiness of the flood, the vigor and the time period of the bedload transport event. A recovery rate as low as 50% is typical for visual tracers after a single (flashy) flood event (Hassan et al. 1984). The cumulative effect of this low recovery rate is that after a few flood events only insignificantly few tracer particles can be found (Table B-3; 6). Artificial magnetic tracers, however, can be located with a magnetometer even when tracers are buried 50 or 60 cm deep. The recovery rate is therefore much higher and often exceeds 90% (Hassan et al. 1984). This high recovery rate allows one to follow the downstream movement of tracers over many flood events, thus providing a better view on the long-term transport behavior of bedload sediment.

**Table B-3; 6:** Percentage of original tracers particles recovered after consecutive floods for low (50%) and high (90%) tracer recovery rates.

Number of consecutive floods	Recovery Rates	
	50%	90%
1	50	90
2	25	81
3	13	73
4	6	66
5	3	59
6	2	53

A new generation of tracers are radio tracers that actively emit signals which are received by antennas. Radio tracers generally have a 100% recovery rate, as they continuously disclose their current position. This allows one to analyze the stepwise motion of bedload transport and investigate the statistical distribution of motion and rest phases (Buskamp and Ergenzinger 1991; Ergenzinger et al. 1989; Schmidt et al. 1989; Schmidt and Ergenzinger 1992).

### 3.3.6.2 Transport rates and continuous transport records

#### ***Detection of travel distance and travel speed of traced particles***

Tracer particles can be used to detect the travel speed and travel distance of bedload particles. A comprehensive study on tracer dispersion and mean annual travel distances is provided in chapter C-4 of this report.

#### ***Estimating bedload transport rates based on tracer particle dispersion***

Information on the travel speed, or distance of a single or a group of tracers from an input point, as well as depth to which tracer particles are worked into the river bed can be used to calculate mean bedload transport rates ( $qb_m$  in kg/m·s) using different formulae. Carling (1987) gives the following formula:

$$qb_m = d_{sc} \cdot v_{Dm} \cdot \rho_s \cdot (1 - \lambda), \quad (6)$$

where  $d_{sc}$  is the depth of a scour layer,  $v_{Dm}$  is mean sediment travel velocity,  $\rho_s$  is sediment density, and  $\lambda$  is the porosity of the gravel layer. Scour depths are indicated by the vertical depths of tracers in the bottom sediment. However, Carling (1987) cautions that the transport rates calculated by the above formula would only equal measured transport rates for discharges larger than bankfull.

Kirkby (1991) defines the event bedload transport per unit flow width ( $Qb$  in  $m^3/m$ ) for a line transect of painted pebbles as a sum of individual tracer movements:

$$Qb = \sum_{i=1}^n A_d \cdot \frac{l_i}{w} \quad (7)$$

where  $A_d$  is the cross-sectional area of a tracer particle in the plane of the transect,  $l_i$  is the travel distance of an individual tracer, and  $w$  is the lengths of the transect (or the width of the stream).

For the movement from a stream area ( $A_{st}$ ) or the volume beneath this stream area, Kirkby (1991) sums the event bedload transport as:

$$Qb = \sum_{i=1}^n V_i \cdot \frac{l_i}{A_{st}} \quad (8)$$

where  $V_i$  is the volume of a tracer from this area.

#### ***Detection of the passage of bedload tracers***

A variety of tracer techniques can be used for continuous measurement of bedload transport at a measuring station. To ensure a good quality of this record, tracer particles must constitute a high percentage of bedload. The duration of the record is determined by the supply of traced particles. Natural tracers have the advantage that their supply is usually unlimited, and that the ratio of tracer particles and untraced particles is basically constant.

Ergenzinger and Conrady (1982), and Reid et al. (1984) registered the signals generated by large, artificially-magnetized particles as they passed over a detector device. However, the relatively small number of tracer particles that can be fabricated limits the amount of information that can be obtained on the temporal variability of bedload transport. The natural magnetism common in volcanic rocks makes a usable tracer that can be put to work in many areas with volcanic rocks (Custer 1992). The magnetic tracer technique was developed (Ergenzinger and Custer 1982; 1983; Custer et al. 1986, 1987) to the point that Spieker and Ergenzinger (1990) and Ergenzinger et al. (1994) were able to record the individual passages of naturally magnetic pebbles and cobbles larger than about 30 mm over a detector log installed at the bottom of Squaw Creek, a mountain river in Montana. The quality of the records allowed detailed analyses of the temporal variability of bedload

transport (Custer et al. 1987; Bunte et al. 1987; Bunte 1991, 1992a, 1996; De Jong 1995).

Conversions of the resulting particle counts to bedload transport rates is difficult, since one would have to sample both the coarse particles which cause the signals and the small particles which are not detected with a bedload sampler. This sampling would have to take place very close to the detector without producing electronic noise, and this calibration problem that has not yet been satisfactorily solved.

Each of these indirect bedload sampling techniques depend on a good calibration to convert signal rates to bedload transport, but such calibrations are difficult. Thus these techniques may provide an excellent temporal record and are very useful to examine the processes and variability of bedload transport. The use of such techniques to detect a sedimentary CWE may be limited because they are an uncertain index rather than an absolute measurement of bedload transport.

### **3.2.7 Summary: measurement uncertainties of bedload sampling**

Bedload samplers are advantageous in that they are portable, relatively cheap, can be used in natural channels, and do not require much training. On the other hand, bedload samplers have highly variable and somewhat unpredictable sampling efficiencies. With all other conditions held constant, sampling efficiency of bedload samplers generally increases with:

- orifice size,
- area ratio,
- bedload transport rate,
- bag size,
- mesh width, and
- scooping, stirring, and scour hole development.

Sampling efficiency decreases with:

- bedload particle sizes,
- sampling duration,
- degree of misalignment, and
- lack of contact with the river bed.

Most of the factors which decrease sampling efficiency are likely to increase during high flows.

It is impossible to predict the combined effect of all parameters on sampling efficiency, because the relation between each parameter and sampling efficiency can take a variety of different curves depending on the other parameters. Thus, neither sampling efficiency, nor the accuracy of sampled bedload transport rates, will be known for a given sampling situation, and calibration is very difficult.

A few studies have attempted to analyze the interplay between 2 or 3 parameters, which is doable because samplers only come in a few orifice sizes, area ratios, bag sizes, and mesh widths. But more comprehensive studies are scarce, and information has to be pieced together from small individual studies.

Well-constructed and well-operated debris basins can provide a near-perfect degree of sampling accuracy and are suitable for CWE analysis, if a seasonal or annual time frame is sufficient. Continuously recording bedload sampling stations can provide detailed data on bedload transport and its grain-size distribution, but the costs to install and run such stations makes them impractical for general monitoring purposes.

Indirect measurements of bedload transport supply a continuous, mostly automated record of bedload, with lesser construction requirements than direct sampling. But the high error associated with the calibration of signal rates may make indirect methods inappropriate for analyzing CWEs.

Proper sampling and measurement techniques can improve the detectability of CWEs by reducing the uncertainty and bias inherent in bedload measurements. An awareness of the problems with sampler efficiency is also necessary to minimize the confounding inherent in comparisons between sites. In other words, an observed difference in measured bedload transport rates between two sites may be due to differences in sampling efficiencies as well as management actions. In most cases any estimates of sampling bias will have to be drawn from the existing literature as summarized here, since a calibration of samplers for a given range of conditions is a difficult, if not impossible, task, given the problems of obtaining "true" data and the numerous interacting factors which affect sampling efficiency and measurement accuracy.

This study cannot provide specific nomograms or formulas to compute sampling efficiency for all sampler specifications and site characteristics. However, some general recommendations can be provided to improve the accuracy of bedload sampling:

- understand bedload transport processes and estimate expected transport rates, grain-size distributions, and variability in order to select the most appropriate sampling gear and sampling regime,
- understand how sampling efficiency is affected by sampler specifications and bedload transport characteristics;
- use the proper sampler specifications (orifice size, area ratio, bag size, mesh size, etc.) for a given situation, and use multiple sampler sizes and shapes if necessary;
- use the 3 x 3 inch Helley-Smith sampler only if the expectable bedload size does not exceed the designated size range of 2 - 10 mm;
- use a sampler with a larger orifice if bedload includes coarser particles (i.e., > 10-15 mm);
- use a specifically designed sand bedload sampler for sand-bedded streams, and watch for scour holes;
- use a basket-type sampler if bedload consists of mostly pebbles and cobbles;
- use a less flared sampler if most of the bedload is sand,;
- whenever possible install a sill into or onto the stream bed, as this ensures proper placement of the sampler and will greatly reduce problems such as scooping and underflow;

- use measuring bridges and guide ropes as necessary to ensure proper placement of the sampler, and this is particularly necessary for larger samplers during high flows;
- try to calibrate samples against transport rates, especially when using different types and sizes of samplers;
- take sampler accuracy and bias into account when comparing sites or changes in bedload transport over time, as these factors may account for some of the observed differences or diminish the differences; and
- educate the sampling team, as the persons conducting the sampling can greatly affect the measured values, and their input is necessary to adjust the sampling to observed conditions.

### **3.3 Measurement techniques and uncertainty of suspended sediment sampling**

Measurement and sampling issues tend to be less acute for suspended sediment because the fine sediments tend to be better mixed within the cross-section and exhibit less short-term variability than the coarser sediments which move as bedload and stay closer to the channel bottom. Thomas (1985) exhaustively discusses different sampling methods and sampling schemes for small mountain rivers and gives suggestions for representative sampling.

#### **3.3.1 One-point bottle sampling**

The error associated with one-point suspended sediment sampling depends on several factors:

- turbulence of flow and how well grain sizes are mixed in the flow;
- presence of short-term fluctuations;
- sampling quantity and sampling duration; and
- suspended sediment concentration.

As noted earlier, the grain-size distribution and the concentration of suspended sediment can show widely varying responses to increasing flow (Walling and Moorehead 1989). Both a fining and a coarsening of suspended sediment with time is possible. It is therefore especially important for one-point-sampling to choose a measuring site in which turbulent flow conditions provide an adequate mixing of the suspended sediments within the cross-section. Similarly, the concentration of suspended sediment can also fluctuate considerably with time. The resulting measurement uncertainty can be reduced by either taking repeated samples or by taking a large volume of water for a sample (i.e., extending the sampling period over some time (perhaps a minute). The problem with taking a larger sample is that this will generally result in a greater disturbance of the stream flow lines, and this will adversely affect the sampling efficiency.

The sediment concentration can also affect the measurement uncertainty. Branski (1967, cited in Branski 1981) quantified the mean quadratic errors of one-point-suspended sediment sampling with a Polish 2-liter silt bottle sampler (PIHM-1) and found sampling errors to be largest when sediment concentrations were lowest (Table B-3; 7).

**Table B-3; 7:** Mean quadratic error in percent for single-point suspended sediment sampling using the Polish 2 liter bottle sampler (from Branski 1981).

<u>Suspended sediment concentration (mg/l)</u>				
5	10	20	50	100
48	27	20	19	18

### 3.3.2 DH-48 width and depth integrated sampling

Width- and depth-integrated sampling with a DH-48 sampler is recommended in order to account for the cross-sectional and short-term variations in suspended sediment concentration. However, the standard DH-48 cannot sample the last five centimeters above the channel bottom. This sampling artifact can lead to an underestimation of the coarse fraction of the suspended sediment concentration (Walling and Webb 1981), since the larger inorganic suspended particles are usually more concentrated close to the channel bottom.

### 3.3.3 One-point pump samplers

A time series of suspended sediment concentration data is needed in order to establish a rating curve and to estimate hysteresis effects. This can be done with an automatic sampler that pumps water samples into a carousel of lab bottles. With the proper electronics sampling can be driven by:

- stage;
- flow volume;
- time (either fixed or random intervals); or
- a combination of the above.

Measurement uncertainties of pump samplers are associated with:

- location of the intake nozzle within the channel cross-section;
- orientation of the nozzle with respect to the direction of flow;
- poor mixing of suspended sediment at the intake location;
- disturbance of the water and particle flow lines by the pumping action, and
- sample quantity and duration;
- insufficient number of bottles to sample through the entire event.

Some of these problems can be overcome by careful installation and maintenance of the sampler, and a knowledgeable choice of the preset sampling program. The issues of taking representative water samples within a cross-section are generally resolved by coupling a manual sampling program that samples the entire cross-section with the point samples taken by an automated pump sampler. It is also possible to locate multiple water intakes at different heights, and to place these within a venturi canal where shooting flow should provide relatively uniform mixing, but such modifications may be difficult and expensive. Continuous pumping can be used to impede clogging, but this greatly increases the power requirements as well as the wear on the pump. Supervising the pump sampler during highest flow can certainly help to prevent failures.

### **3.3.4 One-point continuous turbidity monitoring and calibration with episodic, instantaneous measurements of $C_s$**

The temporal sampling issues and the problem of sample storage can be overcome by continuously monitoring the turbidity of the flow. The trade-off is that the continuous turbidity measurements have to be calibrated to suspended sediment concentrations by regularly taking width- and depth integrated suspended sediment samples.

The timing and the frequency of the suspended sediment samples depends on the persistence and accuracy of the relationship between the cross-sectional suspended sediment concentration and turbidity. A change in water or sediment color, grain-size distribution, or the ratio of organic to inorganic matter content commonly occur within a storm event and between storm events, and this means the turbidity signal needs to be frequently calibrated against the suspended sediment concentration. For example, Bley and Schmidt (1991) showed how the relation between turbidity units (NTU) and suspended sediment concentration varied according to the type of precipitation event for a catchment in the northern Alps. A very steep increase of  $C_s$  with NTU resulted from a hailstorm that provided an unusually high proportion of relatively large suspended particles.

The cross-sectional location of the sample intake in the stream greatly affects both the turbidity and the amount of suspended sediment sucked into the hose. A high sand content is detrimental to pump-based turbidity monitoring for two reasons: the pumping action is usually not strong enough to hold the sand particles in suspension where the turbidity is measured, and the sand can clog the hose system. Stronger pumps may not be feasible because of a limited power supply, or desirable because they may resuspend sediment from the river bottom.

### **3.3.5 Reservoirs or stilling ponds, annual survey or excavation**

Measurements of suspended sediment that has accumulated over a period of time (usually a year) in a reservoir or a stilling pond require that the trap efficiency of the sediment trap is known. In most cases the trap efficiency is less than 100%. For this reason the suspended sediment concentrations and its grain-size distribution at the outflow of the sediment detention structure has to be measured and used to calculate the trap efficiency. A concrete structure that can be completely emptied down helps to obtain accurate results when excavating and weighing the accumulated sediment. The surveying of accumulated fine sediments may be problematic if the sediment contains organic material that compacts or decays over time. This is an especially large source of error if annual sediment yield is calculated as the difference between consecutive surveys. Any errors in the first survey will also carry over to the determination of the volume in the second survey, and the inaccuracy in successive surveys have been known to generate negative annual sediment yields (Rice et al. 1979).

### **3.3.6 Summary: measurement uncertainties of suspended sediment sampling**

It is difficult to give a general value for the uncertainty associated with suspended sediment measurements. The measurement uncertainty depends on a number of factors which have been discussed above. Mead et al. (1990) state that the measurement error of instantaneous suspended sediment concentration or sediment yield can be as small as 10% if the sampling was sufficiently intensive and careful, and there is not a rapid shift in the

amount of sand transported in suspension versus bedload. There is probably no limit for the error associated with measuring suspended sediment or annual deposition if measuring conditions, instrumentation, sampling design, and personal initiative are poor. The success of suspended sediment sampling has to be evaluated for each sampling site given the variation in site conditions and the dynamics of suspended sediment transport.

## **4. Sampling Schemes for Rating Curves and Annual Load Estimates: Do we know or are we guessing?**

### **4.1 Introduction**

The previous chapters addressed the issues of sample size, and the accuracy of a compound sample to represent the cross-sectional transport rate over the period of time required to take that sample. We also discussed the accuracy of an individual sample with regard to the true transport rate at that point in time and space. We now address the accuracy and precision of annual sediment load estimates, and for convenience we will assume that the individual samples are accurate.

The accuracy of annual load estimates is often critical to the detection of CWEs, as a change in calculated annual sediment loads is commonly an objective of monitoring programs and a guide to management. However, the assessment of any purported change in annual sediment yields depends on the uncertainty of the estimates and the interannual variability of the annual sediment load estimates. The uncertainty, or alternatively, the accuracy of a load estimate refers to how well a calculated sediment load agrees with the "true" sediment load, and this is the primary topic for this chapter. The next chapter will deal with the annual variability of sediment loads, which is another consideration in whether a cumulative effect can be detected.

Annual sediment load estimates are commonly determined by one of three methods:

- measuring the weight or volume of sediment that accumulates in a sediment traps (see previous chapter);
- using a sediment rating curve to estimate the sediment load from measured discharge, or
- summation of incrementally determined sediment loads.

In the latter two cases, calculations are based on concurrent measurements of discharge and sediment transport. These paired observations are then used to estimate sediment transport rates for time increments substantially longer than the sampling duration.

Research regarding the uncertainties associated with either method seem to be better developed for suspended sediment load than for bedload. This chapter will therefore focus on the accuracy and precision of annual suspended load estimates associated with rating curve and load summation methods, with the understanding that the same principles will generally apply to bedload measurements.

### **4.2 Accuracy and precision of suspended sediment load estimates**

The accuracy of suspended sediment load estimates can range from relatively good (e.g., within 30%) to very poor. An extensive literature review led Meade et al. (1990) to assume an average error of 50% for annual sediment load estimates derived from sediment rating curves. In some cases the error may be as little as 20% if suspended sediment concentrations and discharge are consistently and closely related. Walling (1977) reported that estimates of monthly sediment loads were between 10 and 900% of the true sediment load for the River Creedy in Great Britain.

As many researchers have observed large errors in the rating curve approach, the reliability and applicability of this technique has been questioned (e.g., Walling, 1977; Rákóczy, 1977; Walling and Webb, 1981, 1982, 1987, and 1988; and Olive and Rieger, 1985). Some of the factors that contribute to a large error in the rating curve approach include:

- Estimates of the annual sediment load will vary with the temporal schemes of the sampling (e.g., hourly, daily, weekly, or event-based sampling), and with the number of high flow samples included in the data set.
- Large scatter in the relationship between  $C_s$  and discharge, and this is due to the various hysteresis effects as well as sediment exhaustion, various sources of sediment supply, and other factors as discussed below and in Chapter B-2.
- The rating curve technique suffers from an inherent statistical flaw that requires correction factors; and
- Little is known about the precision of annual load estimates unless replicate computations are done. Most data sets are not detailed enough to allow replicate computations.

Each of these points is discussed in the following sections of this chapter.

## **4.2.1 Rating curve problems for sediment load estimates**

### **4.2.1.1 Effects of sampling schemes**

On an annual basis sediment transport is usually concentrated into a few short periods of transport activity separated by long periods with little or no sediment transport. Thus the majority of sediment is typically transported within a small fraction of the total time. This is especially true for small streams that respond to local weather situations. Depending on the respective discharge regime, sediment transport can be concentrated within one season (e.g., snowmelt or rainy season), or occur in numerous events throughout the year (frontal rains and local storms). The concentration of sediment transport into a few periods creates difficulties with regard to the timing of sampling. Fixed-interval sampling (e.g., on a weekly basis) is not likely to catch the high flow events, but will retrieve many low flow samples with little sediment transport. However, fixed interval sampling fits well with office hours.

As noted earlier, event-based sampling will provide a much better estimate of sediment transport because more samples are being taken during periods with high sediment transport rates. Unless an automated sediment sampling system is employed, event-based sampling is much more inconvenient and difficult to carry out. This is particularly true for smaller basins that respond rapidly to a storm event, and for streams that are more remote or difficult to access during high flow events. Nevertheless, some human presence during high flows is highly conducive to reliable sampling, especially in the early stages of a sampling program. Over time it may be possible to develop a reliable automated sampling station, but these need to be calibrated against more intensive samples in order to accurately predict transport rates for the entire cross-section and range of particle sizes. There is also some truth to the principle that unforeseen problems will arise at the most inconvenient and critical times.

There are also problems with the procedure used to calculate annual sediment loads. Walling and Webb (1981) provide several examples where annual sediment yields were

calculated by two different parties and the results differed by almost two orders of magnitude, even when the computations were based on the same data set. These enormous differences were ascribed to the different temporal resolutions chosen for the computations.

The effects of different sampling schemes on total load estimates was also demonstrated by Rákóczi (1977). Three Hungarian streams with different sediment response behaviors were shown to require different sampling schemes to account for the same percentage of total load. Sampling every other day was able to account for 87% of the annual suspended sediment transport at the Danube, where almost 50% of the annual transport takes place in 15% of the time. In the same percentage of time about 80% of the sediment passed at the Zala River. The consistency in sediment transport rates meant that weekly sampling could account for more than 80% of the total sediment. In contrast, the flashy Szamos River required event-based sampling because 95% of the annual load occurred during only 20% of the total time.

#### ***Effects of number of high flow samples***

The effect of the number of high flow samples on the accuracy of the estimated sediment load using the rating-curve approach was comprehensively studied by Walling and Webb (1981). They based much of their results on the analysis of a 7-year continuous record of turbidity, hourly values of  $C_s$ , and a well-defined relation between turbidity and  $C_s$  for the River Creedy in Great Britain. This data set was used to compare six different sampling strategies with regard to their accuracy in estimating annual sediment loads. Fifty repetitions of each sampling scheme provided information on the precision of the different strategies. The five sampling schemes differed with respect to the number of high flow data that were added to weekly samples in the development of a rating curve (Table B-4; 1)

**Table B-4; 1:** Various sampling strategies used by Walling and Webb (1981) to compute the annual sediment load using the rating curve approach.

Sampling Type Number	Weekly samples = 7 x 52 samples = 364 samples	Number of samples taken at discharges		Total number of samples	4 rating curves for: winter, summer, rising, and falling limb
		>15 m <sup>3</sup> /s	>30 m <sup>3</sup> /s		
1	364	-	-	364	-
2	364	200	-	564	-
3	364	150	50	564	-
3a	364	150	50	564	yes
4	364	750	250	1364	-
4a	364	750	250	1364	yes

Regardless of the sampling scheme, the scatter in the relation between  $C_s$  and discharge was found to extend over two orders of magnitude. Adding more high flow data greatly increases the amount of data at the upper end of the rating curve, and this caused the correlation coefficients to improve from 0.70 for Type 1 sampling to 0.87, 0.86, and 0.88 for sampling types 2, 3, and 4. The wide scatter in the data used to construct the rating curve and the limited number of high flow data resulted in a wide range of rating curves with different slopes when these were derived from time-invariant weekly sampling regimes. Conversely, the addition of extra data at high flows always increased the data range and led

to similar rating curves for all replicates. The more data for high discharges were added, the steeper the slopes of the rating curves, and the higher the correlation coefficients.

***Effect of temporal resolution of the flow series***

Applying these rating curves to the 7-year flow record, Walling and Webb (1981) then calculated annual sediment loads based on hourly and daily flows, respectively. Weekly samples from hourly flow series resulted in estimated sediment loads that were, on average, only 17-19% of the true total sediment load (Fig. B-4; 1). The addition of more high flow data as one progresses from Type 1 to Type 4 sampling, improved both the accuracy (estimates approached 77% of the true load) and the precision of the estimated annual sediment load. The coefficient of variation (CV) decreased from 22% for strictly weekly sampling to 3% when weekly sampling was supplemented by 1000 high flow samples.

Total load estimates based on daily mean flow data were consistently lower (17-61% of the true total sediment load) than total load estimates based on hourly mean flow data (19-77% of the true value). Using separate rating curves for winter and summer and separating rating curves according to rising and falling limb (Type 3a and 4a sampling) improved the prediction from 58 to 74%, and from 73% to 77% of the true total load, respectively.

In short, accuracy and precision of total load estimates increased with:

- increasing number of high flow data incorporated into the rating curve,
- employing several rating curves to represent seasonal and hysteresis effects, and
- increasing temporal resolution of the hydrograph from daily to hourly mean flows.

These results indicate that by adding sufficient high flow data, the rating curve should produce an accurate and precise estimate of the annual sediment load. However, it may be unrealistic to expect to collect 1000 sediment measurements at high flow in addition to the 364 weekly data (7 years x 52 weeks) for Type 4 sampling. In this case almost 75% of the data set consisted of high flow data, and this distribution of data can only be obtained by event-based sampling. The availability of such intensive data sets at high flows may also permit the estimation of the annual load by a potentially more accurate methodology, such as a summation procedure with small time increments, and this alternative is discussed later on in this chapter.

As might be expected, there is also the issue of declining gains in precision and accuracy with increasing sample size. Walling (1977) found that the total sediment load was overestimated when he used a very intensive sampling scheme.

Little is usually known about the precision of a sediment load estimate. In order to assess precision one needs replicates of sediment load estimates calculated for one sampling strategy. If it is assumed that replicate results are normally distributed, the minimum number of replicates ( $n_{min}$ ) necessary to estimate the total sediment load within a certain percentage of the true value can be calculated by:

$$n_{min} = \left( \frac{1.96}{0.2} \cdot CV \right)^2 \quad (1)$$

where 1.96 (=  $z_{1-\alpha/2}$ ) is a factor that corresponds to the 95% confidence level (Gilbert 1987), and the 0.2 in the denominator indicates that the estimated mean of the total load

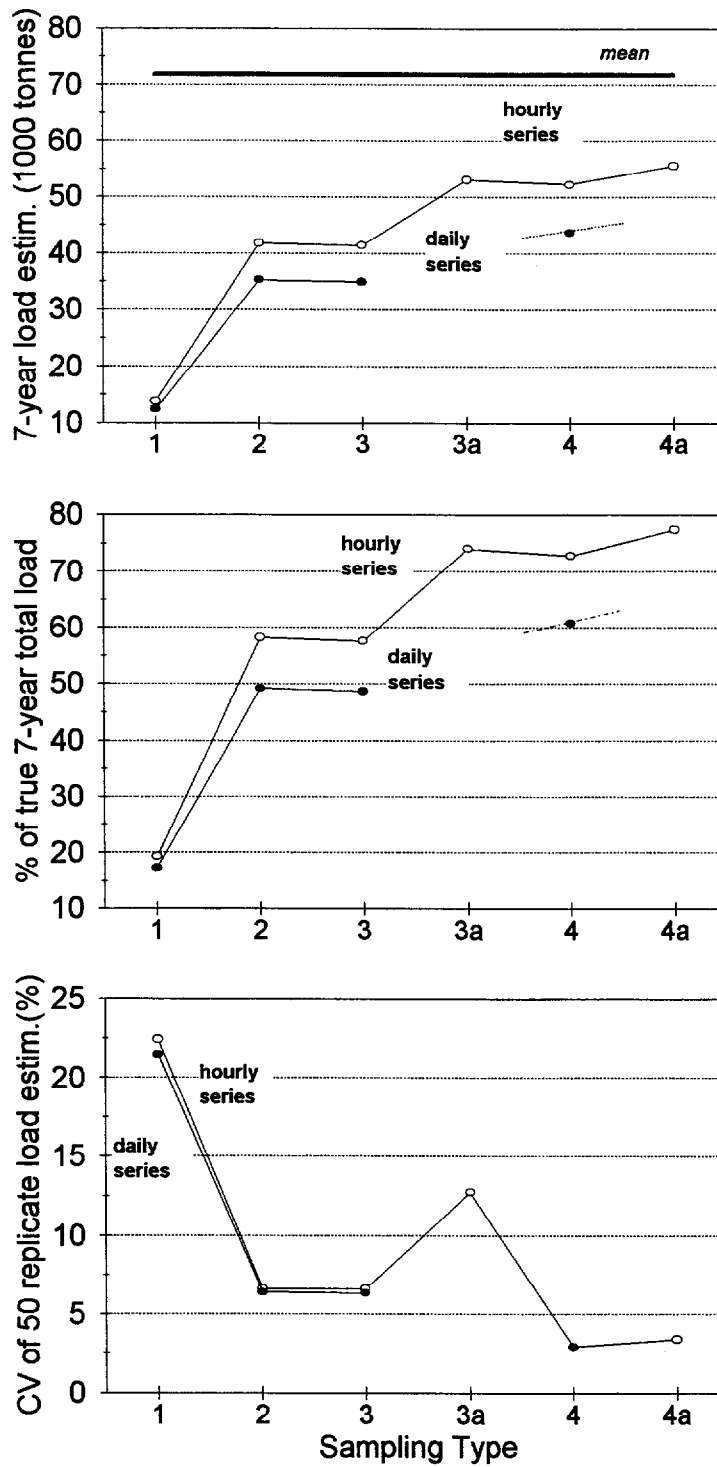


**Fig. B-4; 1:** Effect of sampling type (as defined in Table B-4; 1) and the temporal resolution of the flow series (i.e., hourly and daily values) on the accuracy of the total load estimates in terms of absolute values (top), percentage values (center), and variability (i.e., the CV of 50 replicate load estimations) (bottom).

should be within 20% of the true load. The coefficient of variation (*CV*) for simple weekly rating curves (Type 1) is about 20% (Table B-4; 1). Solving eq. (1) for a level of precision of 20% indicates that about 4 replications are required. If the level of precision is raised to 10%, 15 repetitions are needed. This leads to a similar paradox as above: if the sampling program is weekly, it is not possible to do replicate calculations of annual sediment yield based on different weekly sampling days. If sampling had been performed daily, a summation procedure will probably provide a more accurate estimate of the annual sediment load.

#### 4.2.1.2 Accounting for hysteresis and rating curve variability

The hysteresis of an event-based rating curve can take numerous shapes depending on the interplay of the various processes of stream flow generation, sediment delivery, and sediment transport. A few examples of conditions that lead to hysteresis, and the resulting hysteresis shapes, are summarized from the more detailed review presented in chapter B-1.

A flood wave without much sediment supply from tributaries will probably have a peak in *C<sub>s</sub>* that precedes the discharge peak, due to the resuspension of readily available sediments from the stream bed as the flow increases. A high input of suspended sediment from overland flow into the stream might also lead an early response of *C<sub>s</sub>*, and thus to a clockwise hysteresis. The hysteresis effects can be enhanced by an increasing contribution of groundwater to the runoff hydrograph. The sequential arrival of sediment from several sources might lead to multiple peaks in the concentration of *C<sub>s</sub>* over time, and this can cause successive hysteresis loops. A series of storms can lead to a depletion of sediment supply, where each successive storm transports less sediment than the prior storm. If consecutive storms increase in intensity, new sediment sources might be available to each storm and prevent supply exhaustion. Variations in the hysteresis loop can also be due to the differences in flow generation (e.g., intense thunderstorms versus snowmelt or less intense frontal storms), land use, and the intra-basin variability in rating curves due to different physiographic conditions. Different rating curve hysteresis loops for suspended sediment concentration are depicted in Olive and Rieger (1985), Rieger and Olive (1986) and Williams (1989) (see chapter B-1). We are not aware of any studies that have analyzed the error of annual load estimates for different shapes and degrees of hysteresis.

The following section discusses how the scatter in the relationship between *C<sub>s</sub>* and discharge, and the resulting uncertainty in annual load estimates, might be improved by taking into consideration those factors that contribute to a wide or irregular hysteresis. Walling and Webb (1982, 1987, 1988) suggest:

- relate *C<sub>s</sub>* only to storm flow, as the baseflow is clear and dilutes *C<sub>s</sub>*,
- consider different detachment and transport capacities on the rising and falling limbs of the hydrograph,
- use different rating curves for different intervals between storms, and
- include the concept of a variable source area into the rating curves.

Walling and Webb (1981) found that they could improve the accuracy of total load predictions by using separate rating curves for summer and winter, rising and falling limbs, or some combinations thereof (e.g., falling limbs of winter flows; Walling and Webb 1988). The success of these methods depends on how well seasonal patterns are established in the hydrograph and sediment production, and whether hysteresis effects follow regular patterns. This approach did not work out for Ketcheson (1986) when he attempted to establish four seasonal rating curves for the Idaho Batholith region.

Several of these factors have also been proposed by other researchers (e.g., Bathurst et al. 1986; Bathurst 1987). Beschta (1983) and VanSickel and Beschta (1983) developed a prediction model for suspended sediment yield that addressed the temporal variation in sediment availability in and near to the stream, including a supply-depletion function. The model was believed to show promise as a predictive and conceptual tool for understanding the supply dynamics of suspended sediment sources and their influence on sediment concentrations in mountain streams.

The number of factors that ought to be considered or included in the development of rating curves depends on the characteristics of the relation between  $C_s$  and discharge, and thus varies tremendously between streams. A special set of rating curves have to be established for each stream. This is not only a more complex exercise than simply plotting sediment versus discharge, but it also requires a data base with at least several years of detailed flow and sediment records.

Parker and Troutman (1989) abandoned the single-storm rating curve technique, and concentrated their sampling on the large annual events that produce almost all of the annual suspended sediment yield. They obtained better predictions of the annual sediment load by relating annual peak flow to the corresponding sediment yield for that flood. This relation is combined with a log-Pearson type III distribution for annual floods to produce a frequency distribution of sediment yields.

#### 4.2.1.3 First-time rating curve: general sedimentary state of the river, its tributaries and the basin:

If a sampling strategy needs to be set up for a watershed with no previous records of the sediment-discharge relationship, it should generally be assumed that a single rating curve will not accurately estimate annual sediment yields. The likely shape of the sediment-discharge relationships, and the need to consider the variability between seasons, storms, and the rising and falling limbs of the hydrograph, could be assessed by a watershed analysis. This should include a rough sediment budget of the drainage basin, the tributaries, and the river itself. Both the location and the expected grain-size distribution of the different sediment sources are needed to estimate the discharges at which this sediment will become available.

"Fingerprinting" techniques as suggested by Peart and Walling (1986, 1988) can be used to identify the sources and sinks of naturally or artificially traced sediments. Once it is known which storages are tapped during certain flow events (e.g., prolonged winter season rain, summer storm flow, spring snowmelt, etc.), and what kind of sediment is likely to be transported under different conditions, an initial sampling program could be developed. Regular data analysis is then necessary to optimize the sampling scheme (i.e., focus sample collection on the high transport periods with the most variability). Annual sediment yields can then be calculated as the sum of the sediment loads calculated from each rating curve or high-flow event.

#### 4.2.1.4 Effects of bias correction

Ferguson (1986, 1987) noted that rating curves based on a power function between sediment concentration ( $C_s$ ) and discharge ( $Q$ ) ( $C_s = a \cdot Q^b$ ) results in a systematic underestimation of total sediment load. This bias can be explained as follows: when the least square regression is calculated for a power function relationship between  $C_s$  and  $Q$ ,

both the data for  $Cs$  and  $Q$  are log-transformed and a linear regression is typically derived in the form of:

$$\log Cs_i = a + b \log Q_i \tag{2}$$

in which  $Cs_i$  and  $Q_i$  are paired values. The expression is then antilogged ( $10^x$ ) to obtain the prediction of  $Cs_i'$

$$Cs_i' = 10^a \cdot Q_i^b \tag{3}$$

This transformation poses no problem if the regression is perfect ( $r^2 = 1$ ). However, the inevitable scatter in the data causes a bias in the predicted sediment concentration or transport. This is because the predicted value of  $Cs_i'$  is based on the geometric mean rather than the arithmetic mean. For example, the arithmetic mean ( $m_a$ ) of the series 1, 2, 3 is 2.0, while the geometric mean ( $m_g$ ) is the  $n$ th root of the product of  $n$  numbers or 1.82 for the same series:

$$m_g = \sqrt[3]{1 \cdot 2 \cdot 3} = 1.82 \tag{4}$$

The geometric mean is always smaller than the arithmetic mean. Therefore,  $Cs_i'$  predicted by the power function relation is always smaller than the "true"  $Cs_i$ . Ferguson (1986) gives the following example: a regression might interpolate between values of 1.7 and 2.3 of  $\log Cs_i$  at some given  $Q$ , and predict  $\log Cs_i$  to be 2.0, the antilog of which is  $10^2 = 100 = Cs_i'$ . Likewise, the antilogs of 1.7 and 2.3 ( $10^{1.7}$  and  $10^{2.3}$ ) are 50 and 200. The arithmetic mean of 50 and 200, however, is 125 and not 100 which is the geometric mean. In this case, the estimated  $Cs_i'$  (100) is only 80% of the "true"  $Cs_i$  (125).  $Cs_i'$  has been underpredicted by 20%. This underprediction becomes the more pronounced, the wider the scatter of the data is. (For example, the antilogs of 1.5 and 2.5 are 32 and 316, and their arithmetic mean is 174. Thus, the predicted  $Cs_i'$  (100) underpredicts the true  $Cs_i$  (174) by more than 40%.)

In order to compensate for this systematic underprediction inherent to the log-transformed regressions of rating curves, Ferguson (1986, 1987) suggested to use a correction factor ( $CF_1$ ) with which to multiply the rating curve-based sediment load.

$$CF_1 = e^{(2.651 s^2)}, \tag{5}$$

where  $s$  is the log of the standard error of estimate of the rating curve (Ferguson 1987); if natural logarithms are used, the correction factor ( $CF_2$ ) becomes

$$CF_2 = e^{(s^2/2)}. \tag{6}$$

A third correction factor ( $CF_3$ ) was introduced by Koch and Smillie (1986).

$$CF_3 = \frac{1}{n} \sum_{i=1}^n 10^{e_i} \quad (7)$$

with  $e_i = \log(C_i) - \log(Ce_i)$ .  $\log(C_i)$  is the log of sediment concentration observation  $i$ ,  $\log(Ce_i)$  is the estimated log value of concentration for the same observation derived from the regression using the appropriate value of discharge, and  $n$  is the number of observations.

Ferguson (1986, 1987) reported major improvements of total load estimates after correcting for the bias, and he claimed that the corrected values of estimated mean sediment loads deviated less than 10% from the true loads. An inherent assumption of his approach (known as a quasi-maximum likelihood estimator, or QMUE) is that the errors in the sediment rating curve are normally distributed in the log domain, or lognormally distributed in the real domain. Cohn et al. (1989) noted that Ferguson's approach was still biased, and he proposed a minimum variance unbiased estimator (MVUE). Several authors have indicated that the latter approach, while more complicated, is unbiased and does minimize the root mean square error of estimated sediment loads. Both the QMUE and the MVUE assume that the residuals from the sediment rating curve are lognormally distributed.

Walling and Webb (1988) cautioned that the bias corrections alone do not necessarily provide a major improvement in the reliability of rating curves, because of the other factors that contribute to rating curve errors. Walling and Webb (1988) applied the bias correction factors  $CF_1$  and  $CF_3$  to total load estimates for three rivers in Great Britain. The rating curves are based on regular weekly sampling (Type 1), and regular weekly sampling with hundreds of extra data added for high discharge values (Type 4). Rating curve estimates of sediment concentration were applied to hourly flow series, and resulting hourly loads were summed over the entire time period of available data. Data span 10 years for the River Dart, 8 years for the River Creedy, and 2 years for the Exe. Results of this study are given in **Table B-4; 2**. Annual load estimates from Tables 3 and 4 in Walling and Webb (1988) are expressed as a percentage of the true load, averaged over the entire available time period for each river.

Weekly sampling predicted only about 10% of the total load, and bias correction, especially the  $CF_3$  correction factor, increased total load predictions by roughly a factor of 3-4. Although the correction factors greatly improved the estimates, the uncorrected estimates were so far off that bias correction alone could not make the results tolerable. Besides, the precision became worse. Bias corrections were more successful when applied to load estimates based on weekly sampling supplemented by 1000 high flow samples which predicted on average about 18% of the total load. Bias correction increased the percentage of estimated sediment load to about 70% of the true load, and the precision of the estimates was only slightly reduced.

Thus, it seems advisable to routinely apply the correction factors, especially if the rating curve is well defined. However, correction factors are not the cure for poor rating curve performances in general. Walling and Webb (1988) suggest that the main reason for the poor performance of rating curve estimates of sediment load for their rivers are not a lack of correction factors, but factors like data scatter, seasonal variations in the sediment-

**Table B-4; 2:** Percentage of true sediment load and coefficient of variation (CV) obtained for uncorrected rating curve load estimates, and for corrected rating curve estimates of sediment load for three rivers and 50 replicates of two different sampling schemes: regular weekly sampling (weekly) and regular weekly sampling plus flood period sampling ( $w+Q$ ). (Data from Walling and Webb 1988).

	<u>Simple rating</u>		<u>CF<sub>1</sub> correction</u>		<u>CF<sub>3</sub> correction</u>	
	weekly	$w+Q$	weekly	$w+Q$	weekly	$w+Q$
<i>Percentage of true sediment load</i>						
River Dart	4	7	10	23	22	36
River Creedy	19	27	48	71	58	78
River Exe	7	19	25	116	43	86
<i>Coefficient of variation</i>						
River Dart	16	12	27	19	24	15
River Creedy	14	13	14	12	29	23
River Exe	25	19	36	18	31	21

discharge relationship, lack of coincidence of sediment concentration and discharge responses during storm runoff, and hysteresis as well as exhaustion effects. These effects are so large that a simple straight-line rating curve approach is not appropriate. Furthermore, the extreme concentration of sediment transport during a few annual events makes it unlikely that regular sampling programs will obtain a sufficient and representative sample of high flows.

#### 4.2.2 Summation of daily sediment loads

Besides rating curve-based estimates, annual sediment load can be calculated by a summation procedure. Although there are several methods, the basic idea is to multiply discharge times  $C_s$  for each time interval, and sum the products for the time of interest. The chosen time increments can vary from minutes to months, but are most often based on hourly, daily, or weekly mean values. Accuracy and precision of summation procedures not only depends on the particular summation procedure chosen, but also on the time interval represented by each data pair.

The error associated with this method can be as small as 5% for large rivers with high concentrations of fine suspended sediment and a sampling program explicitly designed to define average daily suspended sediment concentrations (Colby 1956, cit. after Walling 1977). The error can be of "almost unlimited magnitude" (Walling 1977: 531) for small catchments with flashy hydrographs, varied sediment sources with different grain sizes, poor discharge records, and less frequent  $C_s$  measurements (e.g., only once per day). Similar results were reported by Walling et al. (1992) and Bley and Schmidt (1991).

##### ***Effect of selected summation procedure***

Walling and Webb (1981) analyzed the effects of six different summation procedures on sediment load estimates. The main differences between the summation methods are the time spans over which individual measurements of  $C_s$  and discharge are integrated, and the order of mathematical operations (i.e., whether data are first averaged, or first multiplied) (Table B-4; 3). For example, one method combines the instantaneous measurements of  $C_s$

into weekly or monthly means and multiplies these by the mean discharge for the same period of time, while another method first multiplies the instantaneous values of  $C_s$  and discharge, extends these to a specific time interval (e.g., a week), and sums these to obtain an annual total.

**Table B-4; 3: Sediment load summation procedures (from Walling and Webb 1981).**

Method	Numerical Procedure
1	Total load = $K \left( \sum_{i=1}^n \frac{Cs_i}{n} \right) \left( \sum_{i=1}^n \frac{Q_i}{n} \right)$
2	Total load = $K \sum_{i=1}^n \left( \frac{Cs_i Q_i}{n} \right)$
3	Total load = $K Q_r \left( \sum_{i=1}^n \frac{Cs_i}{n} \right)$
4	Total load = $\frac{K \sum_{i=1}^n (Cs_i Q_i)}{\sum_{i=1}^n Q_i} Q_r$
5	Total load = $K \sum_{i=1}^n (Cs_i Q_{pi})$
6	Total load = $K \sum_{m=1}^{12} (Cs_m Q_m)$

- $K$  = conversion factor to take account of period of record  
 $Cs_i$  = instantaneous concentration associated with individual samples (mg/l)  
 $Q_i$  = instantaneous discharge at time of sampling ( $m^3/s$ )  
 $Q_r$  = mean discharge for period of record ( $m^3/s$ )  
 $Q_{pi}$  = mean discharge for interval between samples ( $m^3/s$ )  
 $Cs_m$  = mean monthly concentration  
 $Q_m$  = mean monthly discharge  
 $n$  = number of samples

Using an extensive data set from the River Creedy in Great Britain, Walling and Webb (1981) compared the accuracy and precision of total load estimates obtained by replicates of the same summation method (i.e., by varying the day of the week and the time of day in the sampling strategies) with the "true" load obtained by hourly integration of discharge and sediment concentration.

At first sight the two summation methods (nos. 2 and 4) that multiply instantaneous rather than average values of discharge and  $C_s$  seem to accurately predict the true load regardless of sampling interval (Fig. B-4; 2). However, it needs to be kept in mind that these results present the mean obtained from 50 replicates of the same procedure, and not the result of a single computation. The lower graph in Fig. B-4; 2 indicates that the precision from these two procedures is very poor, as the coefficient of variation increases from about 10% to more than 40% with longer sampling intervals. Predictions from the fifth method are 40-80% of the true load, while methods 1, 3, and 6 consistently underestimate the total sediment load by about 70% or more with little regard to the sampling interval.

The adverse effects of using time-averaged discharge and  $C_s$  (methods 1, 3, 5 and 6) for estimating total load was also demonstrated by Keller and Weibel (1991) for rating curves. They found that the scatter in the rating curve could be reduced from two to one order of magnitude by using instantaneous sediment concentration and discharge data instead of weekly data.

#### ***Effect of time scale***

Increasing the sampling interval from one to 14 days increases the coefficient of variation for the load estimates from less than 10% to 25-45% (Fig. B-4; 2). Since one will generally only have the one sample (the measured values at the selected time interval), the 95% confidence interval--assuming that the estimated sediment loads are normally distributed--will be approximately twice these values on either side of the mean. Thus daily values could yield estimated sediment loads to within 15-20% of the true value, while weekly values would yield estimates that are only within 40-60% of the mean.

The fifth method of calculation underestimates the true load by 40-80%, depending on the sampling interval (Fig. B-4; 2). This level of accuracy is better than the uncorrected rating curve estimates applied to daily flows, as the latter estimates were only 20-60% of the true annual sediment load (see Fig. B-4; 1). A time integration method similar to Walling and Webb's (1981) fifth summation procedure was used by Ketcheson (1986) to estimate total annual sediment load from hand-sampled sediment data in snowmelt-dominated streams in the Idaho Batholith.  $C_s$  and bedload transport were sampled every other day, alternating morning and afternoon samples. Ketcheson (1986) found that the summation method, in which instantaneous values of  $C_s$  and bedload were assumed to represent a period of about two days, generally yielded comparable results to the rating curve approach. Both methods predicted sediment load within a 50% error band only in about 75% of all years. In about 50% of the time the annual load predictions were within 25%, and about 25% of the time the predictions were within 10%. Both the rating curve and the summation procedure tended to underpredict annual sediment load in years with generally low sediment yields, and consistently underpredicted sediment load in years with high sediment loads. In years with medium sediment loads, both procedures generally overpredicted annual sediment loads.

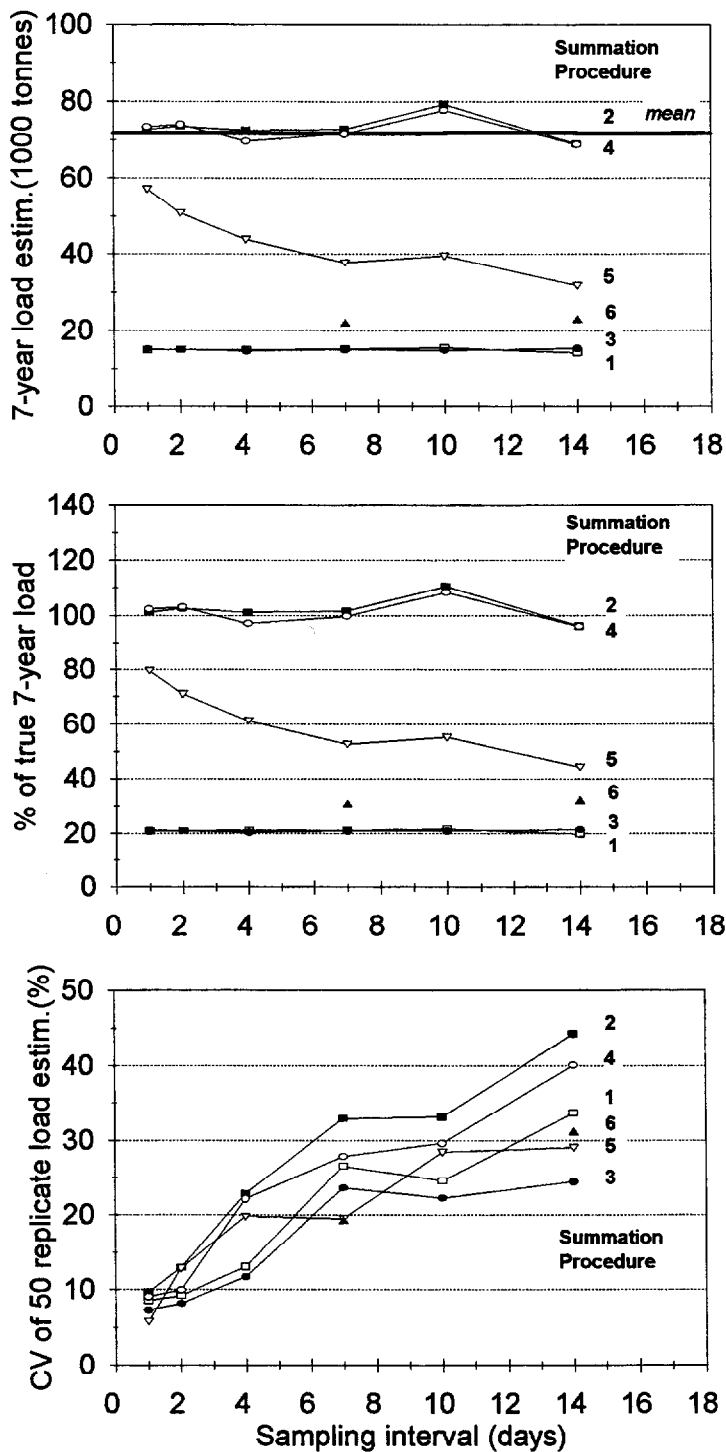


**Fig. B-4; 2:** Effect of sampling interval and summation procedures (as defined in Table B-4; 3) on sampling accuracy in terms of total values (top), percentage values (center), and variability (i.e., the CV of 50 replicate load estimations) (bottom).

### 4.2.3 Rating curves or summation procedures?

Previous results by Walling and Webb (1981) indicated that a rating curve approach would estimate annual sediment load to within almost 80% of the true load when sampling was supplemented by hundreds of high flow samples (sampling type 4), separate rating curves were used for summer and winter, rising and falling limbs, (sampling type 4b), and when the rating curve was applied to hourly flows. The precision of 50 replicate load estimates from those rating curves was high, yielding a CV less than 3%. Two of the summation procedures (procedures 2 and 4) precisely predicted sediment load when the results of 50 replicate analyses were averaged. The use of daily sampling intervals reduced the precision to about 10%. The question arises as to whether a rating curve estimate or a summation procedure provides a more accurate and precise estimate of the true sediment load.

Given the known coefficient of variation of 50 replicate analyses of sediment load estimates, equation 1 (Chapter 4.2.1.1) can be used to determine the minimum number of replicate analyses needed for the load estimate to be within a preset percentage of the average of all 50 replicate analyses. This analysis was done for the best sediment load estimates obtained from rating curves Type 3, 4 and 4a and summation procedures 2 and 4 (Fig. B-4; 3). The results indicate that the summation methods provide a more accurate estimate of the total sediment load, but that the uncertainty of the estimates increases substantially as once samples less than once every 1-2 days. A rating curve approach with intensive high flow sampling can lead to precise but less accurate estimates. In practice, few people will have the number of samples necessary to develop separate rating curves by season, rising vs. falling limb, or whatever other factor accounts for some of the variability within a specific rating curve. It should also be kept in mind that these results were developed from intensive sampling of larger streams in a humid environment, and the streams would therefore not be as subject to the rapid changes in flow and sediment concentration as low-order streams in forested areas. Further investigations are therefore needed to assess the relative accuracy of the summation and rating curve approaches in other environments.

### 4.2.4 Summary: Suspended sediment load estimates

Errors in the estimated sediment load can reach about one order of magnitude for monthly loads (Walling 1977), and average 50% for annual loads (Meade et al. 1990).

Annual suspended sediment load is commonly estimated by three methods:

- estimating weight or volume of sediment in debris basins or reservoirs,
- using a rating curve approach, and
- summing incrementally determined short-term sediment loads.

The accuracy of the first method depends mainly on the trap efficiency, and this varies with sediment size and retention time. The accuracy of the other two methods is dependent on the representativeness of the  $C_s$  samples for a given discharge or sampling interval, respectively. The representativeness of  $C_s$  samples can be improved by:

- incorporating more high flow samples into a fixed-interval sampling scheme,
- applying  $C_s$  estimates to discharge data with a high temporal resolution,
- establishing separate rating curves (rising and falling limb, summer and winter),
- using bias correction factors, and
- doing replicate sediment load computations.

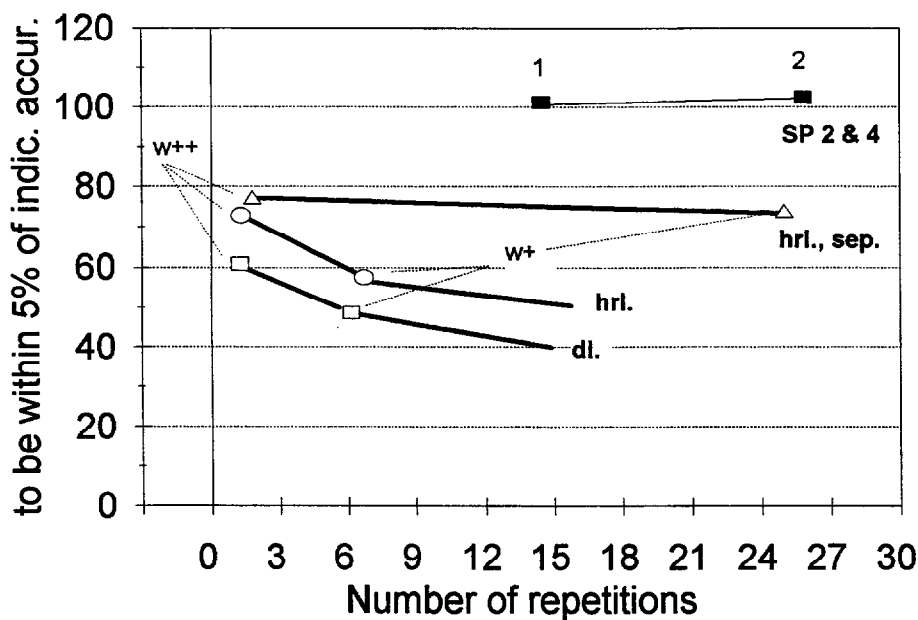
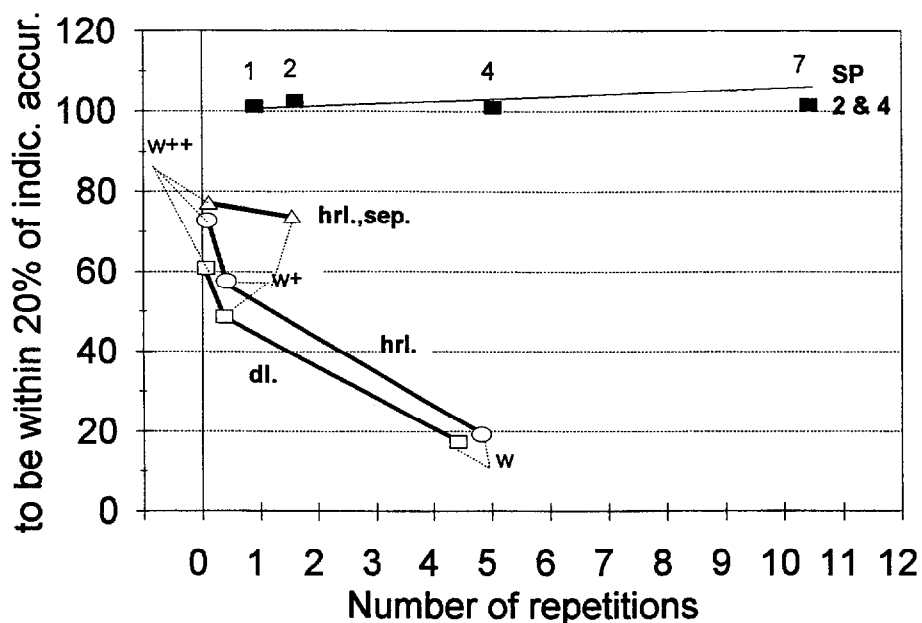


**Fig. B-4; 3:** Number of repetitions of 50 replicate sediment load analyses needed for the estimated sediment load to be within 20% (top), and 5% (bottom) of the indicated accuracy (i.e., the percentage of total load averaged from 50 replicate analyses). Full symbols refer to summation procedures SP, and the corresponding numbers indicate the sampling interval in days. Open symbols indicate rating curve load estimates based on 7 years of weekly (w) sampling (Sampling Type 1); w+ = weekly sampling plus 200 high flow samples (Sampling Type 3), w++ = weekly sampling plus 1000 high flow samples (Sampling Type 4). These sampling types were applied to hourly (hrl.), and daily (dl.) flow series; and hourly samples with separate rating curves for summer and winter, rising and falling limb (hrl., sep.) (Sampling Types 3a and 4a, respectively).

The analysis by Walling and Webb (1981) showed that annual load estimates derived from weekly sampling yielded less than 20% of the true load, and this estimate improved to 50-60% of the true load when hundreds of high flow data were added to the rating curve. Applying the rating curve estimate of  $C_s$  to hourly instead of daily data further increased the load estimate to 60-70%. Using separate rating curves to adjust for seasonal and hysteresis effects improved the sediment load estimate by about another 10%, but the best result--using separate rating curves and hundreds of additional high flow data points--still yielded estimates that were less than 80% of the true load. The variability as quantified by the coefficient of variation also decreased from 22% for weekly sampling to 3% when sampling was supplemented by numerous high flow samples. Walling and Webb (1988) used another data set to show that bias correction greatly improves the load estimate, but this cannot correct for the errors due to limited or unrepresentative sampling.

The accuracy and precision of summation procedures varied greatly according to the method used. The methods which extrapolated from the instantaneous product of discharge and  $C_s$  generally performed much better than methods which first averaged values before calculating a mean load for the period of averaging. More frequent sampling was most beneficial in terms of reducing the uncertainty rather than improving the accuracy. Sampling every 1-2 days yielded relatively accurate samples with a coefficient of variation of around 20% (i.e., a 95% probability that the estimate would be within approximately 40% of the true value).

According to Walling et al. (1992) load estimates based on summation procedures can range from a 90% underprediction to an overprediction of more than 400% if an "insufficient" number of samples is taken, or the time interval over which the measurements were integrated was too large. In their literature review, Meade et al. (1990) state that a 20-25% error can be expected for the mean annual sediment yield based on the summation of load from daily measurements over a 15-year record. The mean error increased to about 50% for rating curve estimates, and was about 20% when there was little scatter in the  $C_s$ -discharge relation.

While the rating curve approach seems to yield less accurate estimates of the annual sediment load than summation procedures, repetitive sampling suggests that the rating curve estimates are more consistent (precise) than the summation approach. The most accurate estimates of annual sediment loads are derived from summation procedures that utilize the product of instantaneous sediment concentrations and discharge measurements. With smaller time intervals the accuracy of the estimates are improved.

The accuracy and precision indicated in this report represent the results of the various studies by Walling and Webb, and reflect the conditions of their particular streams in Great Britain. Absolute values of accuracy and precision of sediment load estimates depend on the degree of scatter and the shape of the hysteresis of the discharge- $C_s$  relationship. Therefore it is necessary to repeat these types of analyses in streams with different flow regimes, sediment loads, and sediment delivery processes.

Annual load estimates based on weekly sampling were generally of low accuracy or precision depending on whether a rating curve or a summation procedure was used. For this reason Walling and Webb (1981, 1982, 1987, and 1988), Thomas (1985), and Thomas and Lewis (1993) all recommend event-based sampling and a high resolution record for flow and  $C_s$ . More recently, Thomas (1988, 1991) has suggested that a random sampling scheme should provide the best estimate of annual suspended sediment load.

### 4.3 Uncertainties in annual load estimates of bedload transport

The previous section discussed the uncertainty of suspended sediment load estimates and found that the uncertainty was due to rating curve scatter and sampling schemes. In order to analyze the uncertainty of total bedload estimates, one needs to compare the degree of scatter in suspended sediment and bedload transport rating curves, and the sampling schemes employed for the two transport modes.

#### 4.3.1 Differences in rating curves of suspended sediment and bedload transport

The scatter in the relation between discharge and sediment transport can be mainly attributed to two factors:

- physical processes of instream sediment transport (sediment transportability and storage), and
- the temporal and spatial variability of sediment delivery to the stream system.

Both aspects are present in streams with fine and coarse sediment, but their effect varies from stream to stream, and is loosely tied to sediment sizes and watershed area.

##### ***Physical processes of bedload transport***

As suggested above, there is almost always a very wide scatter in the relationship between discharge and bedload transport, and this is due to the many physical processes which control bedload transport besides discharge (Chapter B-1). These processes include the stochastic single step motion of bedload, the effects of turbulent bursts, migration of bedforms, distance from a pool-riffle section with its particular patterns of bedload transport, wash-out of fines in the beginning of a high flow, delayed entrainment of pebbles from "hidden" locations, possible break-up of the armor during the latter stages of a high flow event, and the sudden occurrence of bank collapse and sediment release from log jam bursts. All of these processes add to the temporal and spatial variability of bedload transport, and are only loosely linked to discharge.

##### ***Sediment storage dynamics***

The variability of suspended sediment transport is usually less than the variability in coarse sediment transport. Fine sediment, once mobilized, usually travels further than coarse sediment, and is less likely to be stored in instream locations. In contrast, bedload is frequently stored within the stream system. In larger rivers much of the sediment will be stored on bars or in the stream bed, while bedload transport in small forested streams is often controlled by the formation and decay of LWD. The effects of storage dynamics on rating curve variability was shown in Ketcheson's (1986) analysis of bedload transport rating curves from the Idaho Batholith region. The variability between rating curves of the same catchment over several years, and the difference in rating curves between neighboring catchments, was attributed to sediment storage dynamics, especially to LWD that trapped and released bedload at unpredictable time intervals. These storage effects caused so much variability in the bedload rating curves between 1975 and 1982 that it was not possible to detect a statistically-significant difference in sediment loads pre- and post-logging. In another 118-ha basin, bedload transport rating curves changed significantly over several years, although no management activities had been underway during that time.

***Hydraulic control***

Another factor that affects the bedload rating curve is the degree of hydraulic control on sediment transport. If there is ample instream supply of sediment within the size ranges that the flow is competent to transport, sediment transport becomes transport-limited and the amount of sediment in transport is a more direct function of flow strength. In this case sediment transport is mainly hydraulically controlled. Sediment particles that are not bonded by cohesion (e.g., clays), covered by a pavement, or interlocked within the pavement, are most likely to be hydraulically controlled in their transport rates.

An example of the different processes to which fine and coarse sediment respond was provided by King (1979) and Ketcheson (1986) in their comparison of the coefficients of determination ( $r^2$ ) for bedload and suspended sediment rating curves. Approximately 45% of the  $C_s$  rating curves were statistically significant at the 95% level, and only 11% had  $r^2$  values greater than 0.6. Conversely, 71% of the bedload transport rating curves were significant, and approximately 50% of all bedload rating curves had a  $r^2$  value greater than 0.6.

King (1979) reported that the coefficients of determination ( $r^2$ ) for suspended sediment rating curves ranged between 0.28 and 0.67 for water years 1975 and 1976. Incorporating the data from the very dry water year of 1977 increased the scatter and caused the  $r^2$  to drop to values between 0.20 and 0.49. In contrast, the bedload rating curves for all three years yielded  $r^2$  values between 0.68 and 0.97.

One reason for the lesser scatter of bedload is that the bedload was comprised primarily of sand ( $D_{90}$  of 3-7 mm). This size range responds rather well to hydraulic conditions. Similar results were reported by Shen (1972), Holeman (1975), and Rannie (1977) (all cited by Ketcheson 1986) who found bedload transport to be more closely related to stream flow, while suspended sediment concentration of large rivers was more dependent on watershed properties and disturbance.

***Sediment delivery***

A major cause of the differences in sediment response is the difference in the delivery of fine and coarse sediment to the stream channel. It can be argued that there is a greater temporal and spatial variation in the delivery of fine sediment to the stream system, and this is due in part to the multitude of storage locations for fine sediment within the watershed. Sediment delivery for pebble and cobble bedload tends to be more closely tied to the distance between sediment source and the stream system, unless coarse sediment is rapidly conveyed by debris flows and gullies.

Although the above examples all indicated that bedload rating curves had higher regression coefficients than the corresponding  $C_s$  rating curves, one cannot generalize to the statement that bedload rating curves usually have a better fit than  $C_s$  rating curves. Temporal and spatial variability of sediment delivery poses a major problem for rating curves of suspended sediment (Walling 1983), while instream storage and a limitation of sediment supply cause a large scatter in the rating curves for coarse bedload transport. The least scatter in rating curves can be expected for bedload transport in large streams with ample supply of transportable sediment, where transport is largely hydraulically controlled, and most of the sediment is delivered from instream sources.

### 4.3.2 Effects of sampling on rating curve correlations

The strength of the relationship between sediment and discharge is usually quantified by the coefficient of determination ( $r^2$ ). A change in the rating curve may not necessarily be an accurate indicator of management effects because the correlation between discharge and sediment is affected by factors such as sample size and range of flows sampled, as well as by the sediment transport patterns and sediment supply Ketcheson (1986).

In the first step of analysis we computed the  $r^2$  of power function regressions ( $Qb = a \cdot x^b$ ) between individual bedload transport rates and discharge values in the data sets used to analyze the temporal variability of transport rates (Chapter B-2).  $r^2$  values for the data sets with varying discharge ranged from 0.13 to 0.95 (Table B-2; 1, sixth to the last column). These 21 data sets covered a partial or an entire high flow event, a high flow season, or all events of an entire year. The  $r^2$  values generally increased with a larger range of sampled flows, the ability of the sampling technique to represent a large proportion of the transported bedload, and decreased with increasing bedload particle sizes.

A relatively high  $r^2$  of 0.82 was obtained for a group of data in which bedload sampling extended over an entire season with a large range of flows. In this group of data, bedload was sampled with a vortex trap and the streams contained a high percentage of easily transportable sand and fine gravels. The  $r^2$  for data sets that covered the entire season dropped to 0.64 and 0.56 when less representative sampling techniques (Helley-Smith or a basket sampler, respectively) were used, or when bedload particle sizes became larger. Another data set in which bedload was sampled over an entire high flow season with a high temporal resolution yielded an  $r^2$  of only 0.56. We attributed this low  $r^2$  value to the fact that discharge only spanned a factor of 2, the recurrent daily hysteresis effects, short-term bedload fluctuations, sediment exhaustion over successive high flows, and that only large pebbles and cobbles were being monitored.

#### 4.3.2.1 Range and variability of sediment transport, range of flows and sample size

In order to take a closer look at the effects of statistical and sampling issues on the  $r^2$  of rating curves, we created a few simple data sets in which the range and the variability of bedload transport, the number of high flow samples, and sample size was varied. We selected a sample size of 12 as our initial value. Although this may be a little on the low side, it reflects the fact that bedload transport measurements typically have a very low temporal resolution and sampling intensity as defined earlier.

Bedload transport values were evenly distributed over a 15-fold range in discharge that was subsequently reduced to a factor of 10. Sediment transport rates were chosen to obtain rating curve exponents of 1 to 3, a range commonly found in bedload rating curves for gravel-bed mountain streams. Results of these analyses are listed in Table B-4; 4, and graphically presented in Fig. B-4; 4.

Decreasing the magnitude of the sediment transport rates from a rating curve exponent of 3.1 to 1.1, while maintaining a one order of magnitude data range in both cases, reduced the  $r^2$  from 0.94 to 0.66 (Fig. B-4; 4 upper left). The higher  $r^2$  for the steeper rating curve suggests that a steeper rating curve is "better", but in reality the spread of the data around the mean is the same in both cases. This effect of increasing the range of sediment transport data should be kept in mind when comparing rating curves and streams.

**Table B-4; 4:** Sediment transport range (arbitrary unit), factor of scatter, discharge range (arbitrary unit), and sample size used for regression analysis, and the resulting rating curve  $r^2$ , exponents, and coefficients.

Total data range $Qb_{min} - Qb_{max}$	Factor of scatter for highest discharge $Qb_{min} - Qb_{max}$	Sample size	Discharge range	Rating curve		
				$r^2$	exponent	coefficient
1 - 2,621,440	10	12	1.4 - 64	0.94	3.1	2.6
1 - 640	10	12	1.4 - 64	0.66	1.1	2.6
1 - 40,960	10	12	1.4 - 64	0.88	2.1	2.6
1 - 2,621,440	>10,000	12	1.4 - 64	0.46	2.3	1.8
1 - 40,960	10	12	1.4 - 16	0.88	3.1	2.6
1 - 160	10	12	1.4 - 16	0.49	1.1	2.6
1 - 2,560	10	12	1.4 - 16	0.77	2.1	2.6
1 - 40,960	>1,000	12	1.4 - 16	0.39	2.4	2.0
1 - 40,960	10	8	1.4 - 64	0.87	2.9	3.3
1 - 160	10	8	1.4 - 64	0.38	0.9	3.3
1 - 2,560	10	8	1.4 - 64	0.74	1.9	3.3
1 - 40,960	>1,000	8	1.4 - 64	0.21	1.4	5.6

In the upper right plot of Fig. B-4; 4, the variability of the data was varied from one order of magnitude for the smallest discharge values to 4.5 orders of magnitude for the highest flows. This spread of the data not only decreased the  $r^2$  value from 0.88 to 0.46, but also slightly altered the steepness of the rating curve. This difference in the spread of the data corresponds to the variations in bedload transport as controlled by storage dynamics.

The two central plots of Fig. B-4; 4 show the effects of excluding high flow samples from the analysis while maintaining the same sample size. This example reflects the situation where flows barely exceed the threshold of bedload motion. The drop in  $r^2$  (from 0.66 to 0.49) is most pronounced for data sets with a small range of transport rates. The rating curve steepness is not much affected if sample size is maintained. But if high flow barely exceeds the threshold of bedload motion and no additional bedload samples can be taken at lower flows to maintain the sample size, the  $r^2$  drops even more strongly (from 0.66 to 0.38), and reduces the value of the rating curve exponents (see lower plots of Fig. B-4; 4). For highly variable transport rates, the exclusion of high flow samples lowered the  $r^2$  from 0.46 to 0.21 (bottom right plot).

This analysis shows that sediment rating curves and their regression coefficients respond to changes in the range of measured flows and to sample size, even without any changes in the transport dynamics. These effects become larger with smaller sediment transport rates, and should therefore be most pronounced in supply-limited, armored gravel-bed mountain streams. Such streams are also quite likely to exhibit a large variability in measured transport rates because sediment transport is partly controlled by the dynamics of large woody debris. This suggests that considerable care should be taken in attempting to link a change in the sediment rating curve to the effects of management activities.

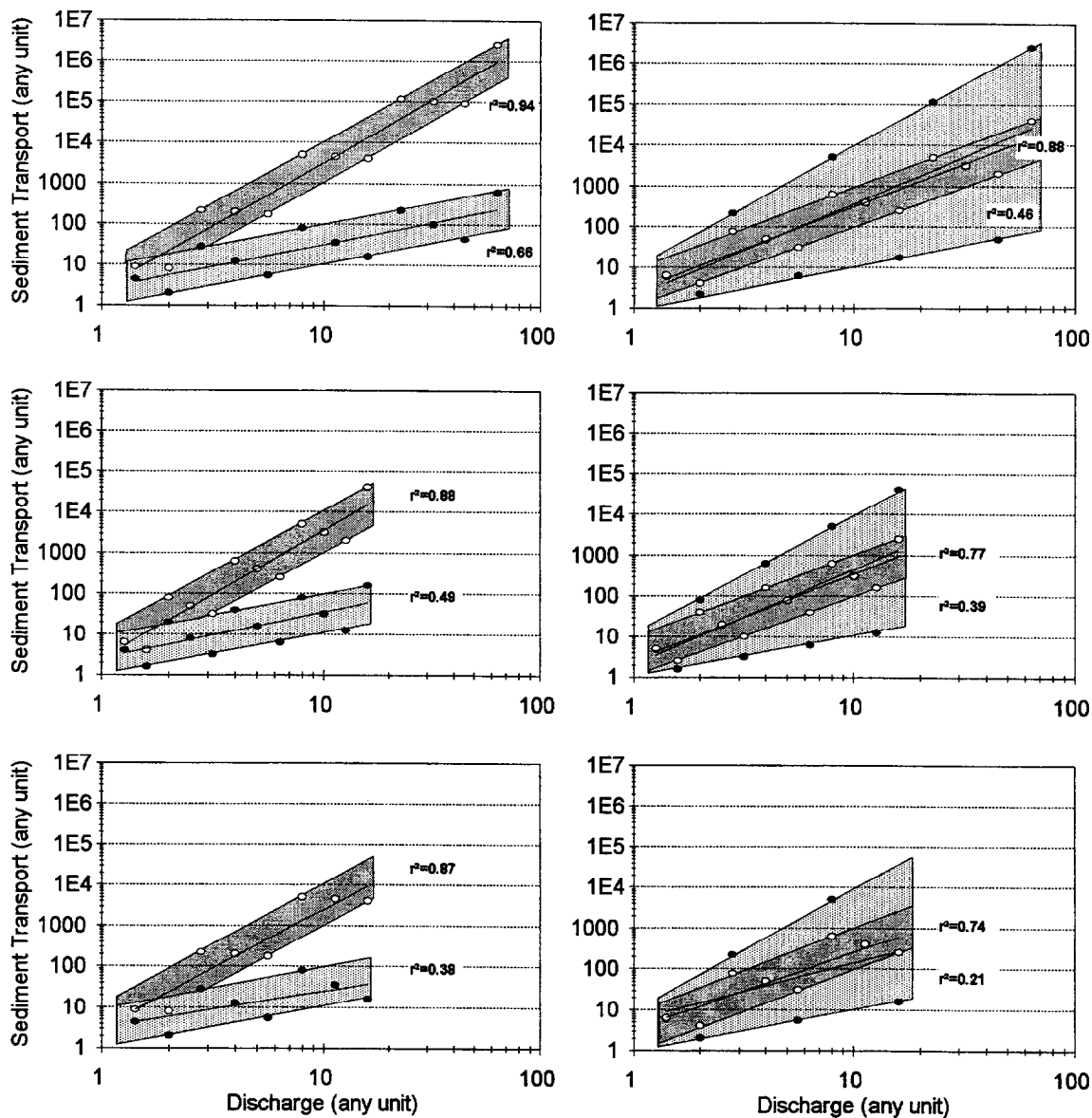


**Fig. B-4; 4:** Effects of range of flows, range of sediment transport rates, variability in sediment transport, and sample size of sediment transport on rating curve  $r^2$  and regression functions. Shaded areas depict the data ranges.

#### **Sampling interval**

The correlation between bedload transport rates and discharge is also affected by the temporal resolution of the sampling. For this analysis we used the data sets of continuous bedload signal rates created by the passage of naturally magnetic pebbles and cobbles over a detector log at Squaw Creek (Bunte 1992, 1996). One data set consisted of 864 consecutive 5-minute samples over three days of a snowmelt high-flow. A second data set consisted of 408 consecutive hourly signal rates covering 17 days, or almost the entire period of snowmelt high flows. In a third data set, these hourly signal rates were averaged to form mean hourly signal rates per day, and a day was defined from one day's low flow to the next day's low flow.

A sampling duration of 5 minutes yielded a very poor relationship between discharge and particle transport rates ( $r^2 = 0.13$ ) (Fig. B-4; 5 (top)). A scatterplot showed the data to

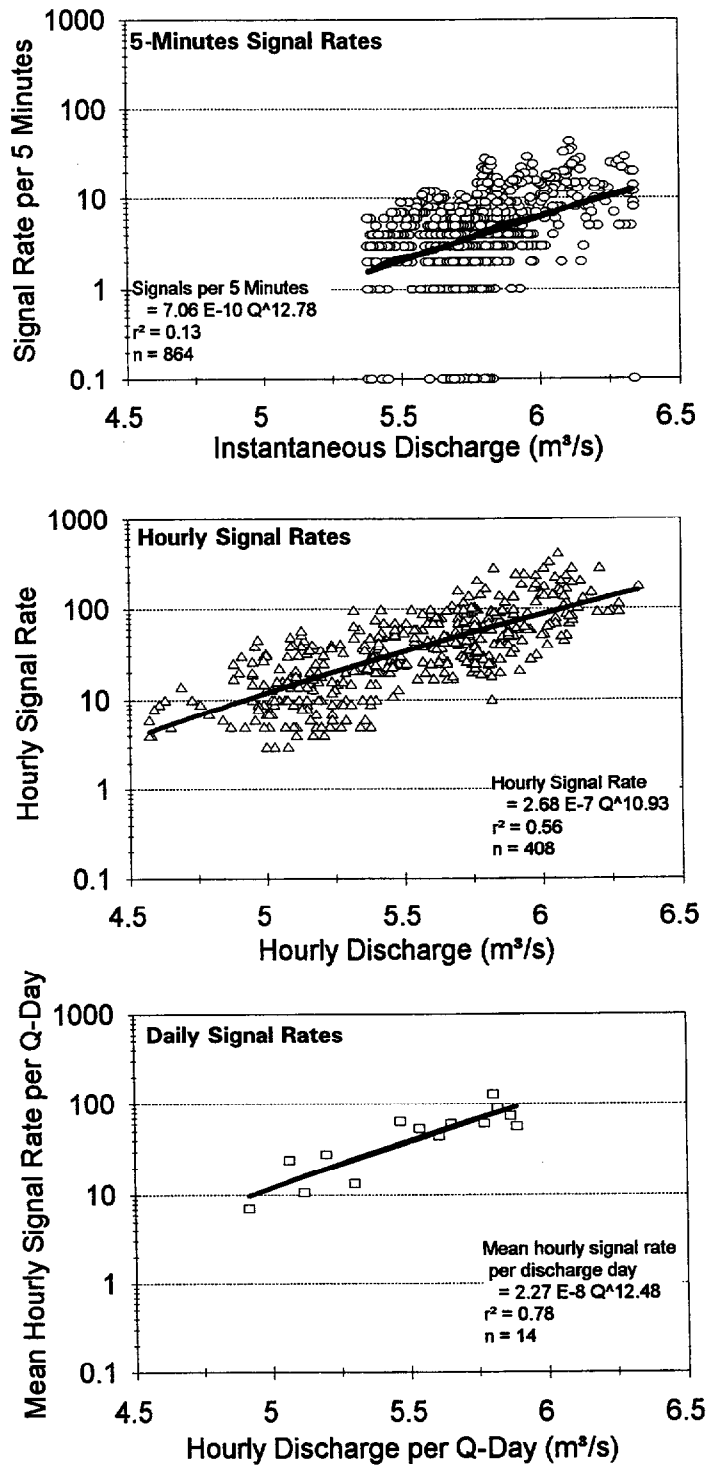


Fig. B-4; 5: Relation between bedload signal rates and discharge at Squaw Creek, a gravel-bed mountain stream, for various levels of temporal resolution: 5 minutes (top), 1 hour (center), and 1 day (bottom).

vary by approximately 1.5 orders of magnitude. Increasing the sampling period generally increased the correlation between signal rates and discharge. For hourly samples the  $r^2$  improved to 0.56 (Fig. B-4; 5 center), and the data generally lay within an order of magnitude of the line of best fit. For daily samples the  $r^2$  increased to 0.78, and the scatter was reduced to approximately half an order of magnitude (Fig. B-4; 5 (bottom)). The lower  $r^2$  with shorter sampling times is presumably due to the higher short-term variability associated with the stochastic movement of particle groups and the storage and release of sediment within the riffle-pool morphology of the channel bed.

The above results confirm the importance of sampling in controlling the correlation between discharge and sediment transport. In general, correlation coefficients can be expected to improve with:

- a greater range of sampled flows,
- an increase in the number of samples,
- a greater range of sediment transport rates,
- the representativeness of the sampling techniques employed (trap samplers vs. Helley-Smith-type samplers), and
- the degree of averaging of transport rates.

#### 4.3.2.2 Effect of sample size and bias correction on the prediction of total load

The effects of sample size is a recurring topic in any discussion on the detectability of CWEs. Since the rating curve approach is the most common procedure to estimate bedload transport, we undertook a more intensive study on the effects of sample size on the accuracy and uncertainty of estimating bedload transport. Four bedload transport data sets were used for this study:

- 52 values from the East Fork River during the 1976 snowmelt highflow, (Emmett 1980);
- 408 hourly bedload data from Squaw Creek 1986 (Bunte 1992, 1996) during snowmelt highflow;
- 147 15-minute bedload data from Prairie Creek (Lisle 1989, and pers. communication) during a single storm event; and
- 125 data from Goodwin Creek during a storm (Kuhnle, written communication).

For each data set a sediment rating curve was developed, and the estimated sediment transport from all the data points was defined as the "true" value. The statistical characteristics of each data set were also determined, and these were used to generate a new, synthetic data set which had the same statistical parameters and appearance as the original data set.

The expected value and standard deviation of the predicted sediment load was then estimated for sample sizes ranging from 5 to 100 (the maximum sample size for the first data set was limited to 40 because the original data set only had 52 values). These estimates were obtained by repeated sampling from both the synthetic and the actual data sets. Each estimate was also corrected for the bias discussed in Section 4.2.1.4 using Ferguson's (1986) quasi-maximum likelihood estimator (QMLE), Colby et al.'s (1989) minimum variance unbiased estimator (MVUE), and a first-order approximation (FOA) developed by Dr. Pepe Salas under the auspices of this project.

The results indicate that for the first three data sets, the MVUE provides the best estimate of the total bedload transport with the lowest standard deviation of the estimates (Figs. B-4; 6-9). Ferguson's QMLE provides the poorest performance, and Dr. Salas's FOA performs

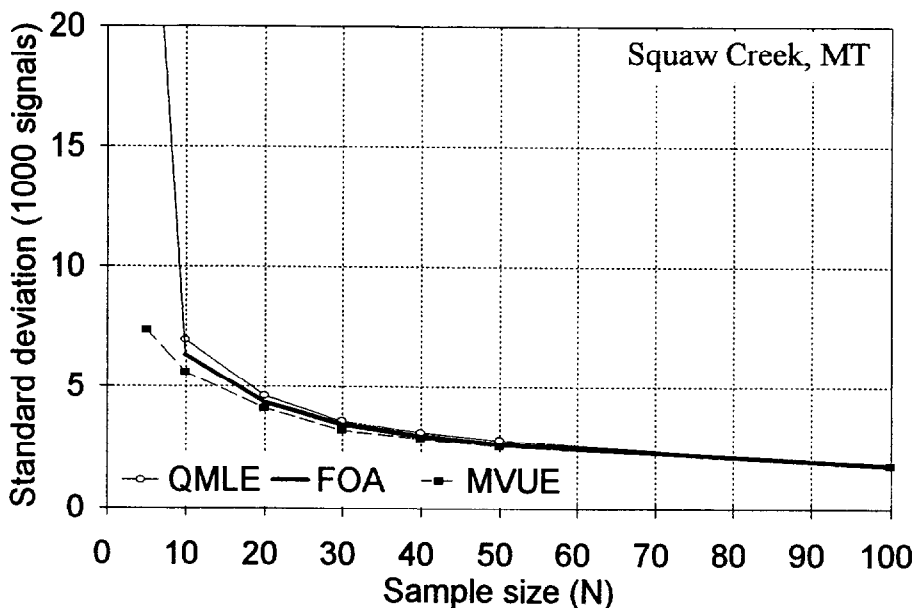
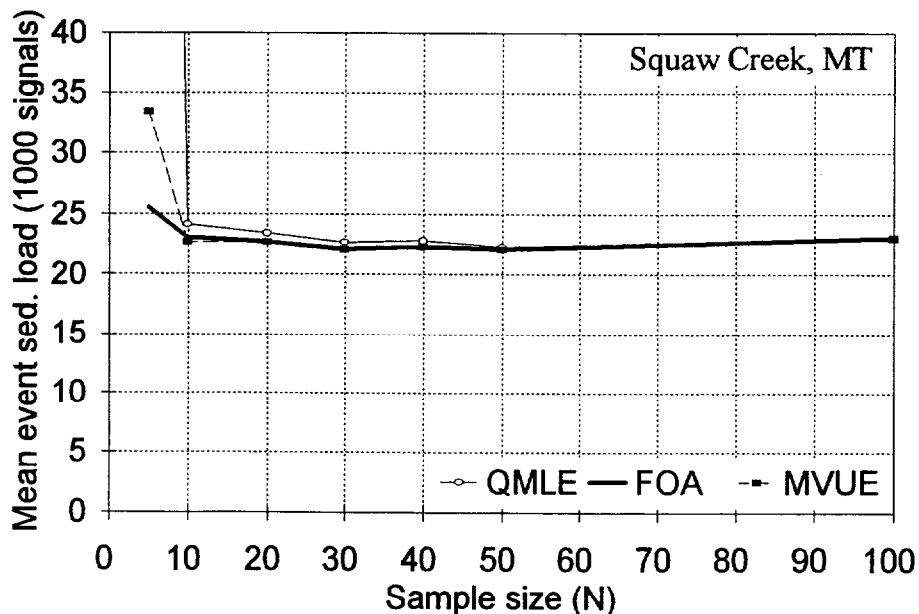


Fig. B-4; 6: Mean (top), and standard deviation (bottom) of total signal load as a function of sample size  $N$  obtained from actual data based on the rating curve estimators QMLE, FOA, MVUE for Squaw Creek, Montana (data from Bunte 1991).

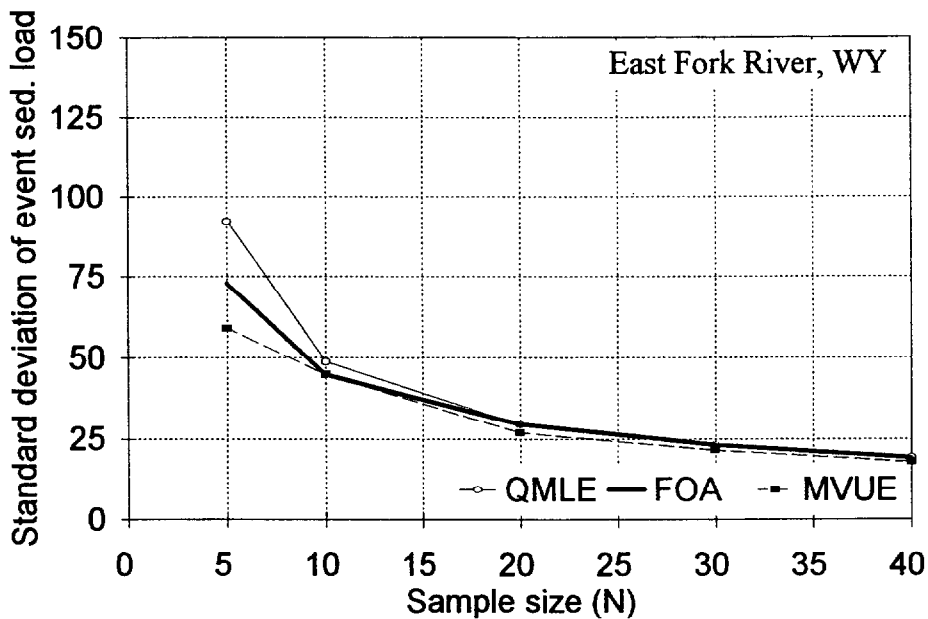
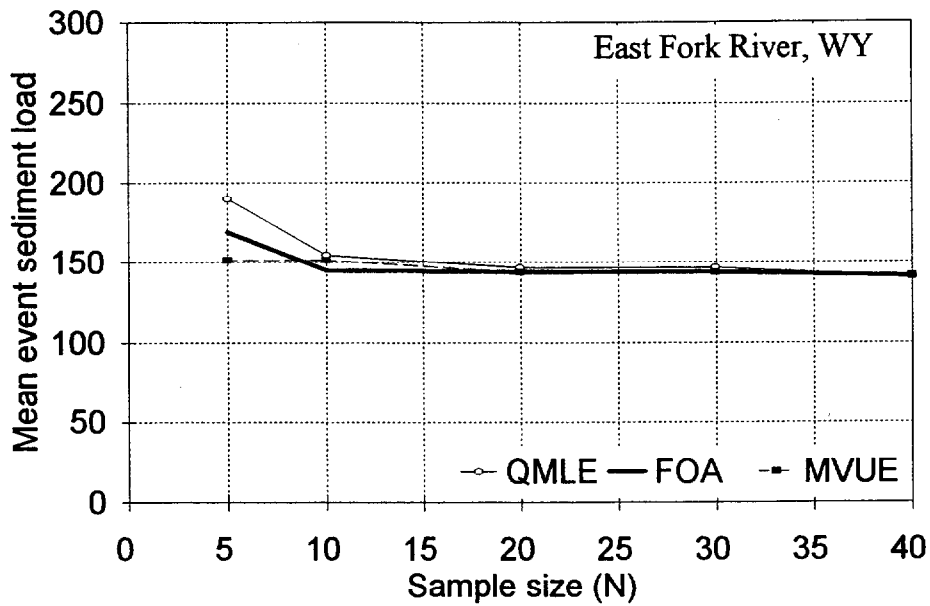


Fig. B-4; 7: Mean (top), and standard deviation (bottom) of total sediment load as a function of sample size  $N$  obtained from actual data based on the rating curve estimators QMLE, FOA, MVUE for the East Fork River, Wyoming (data from Emmett 1980).

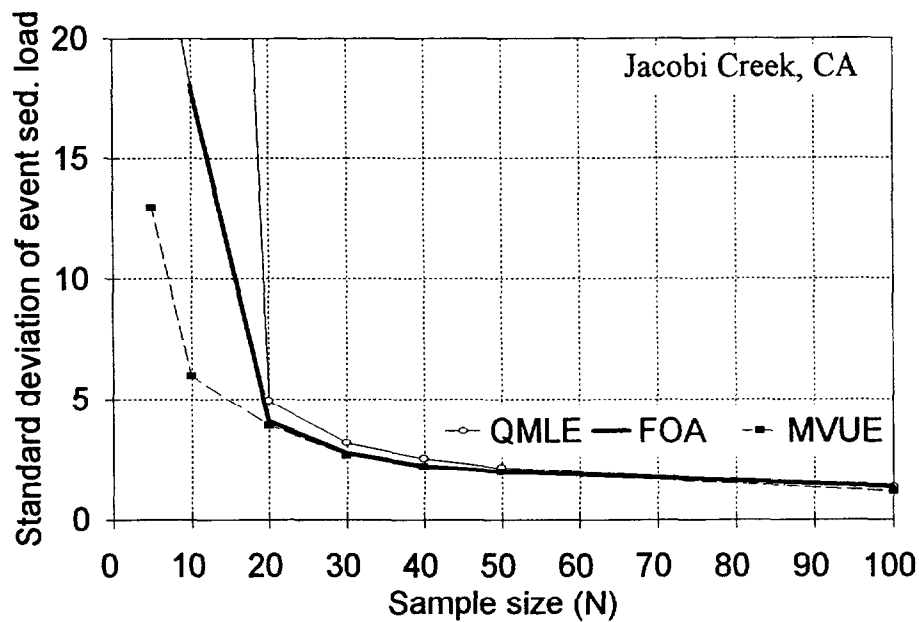
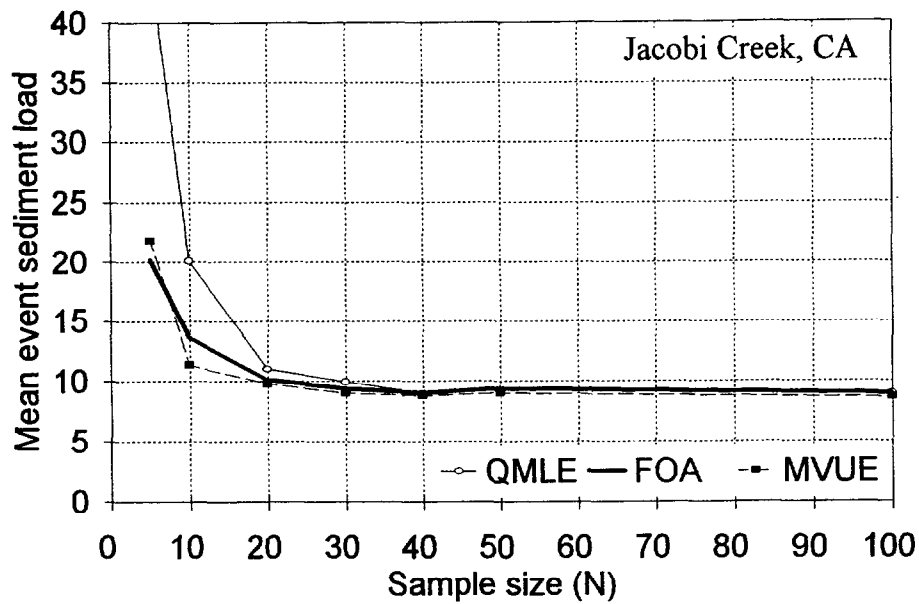
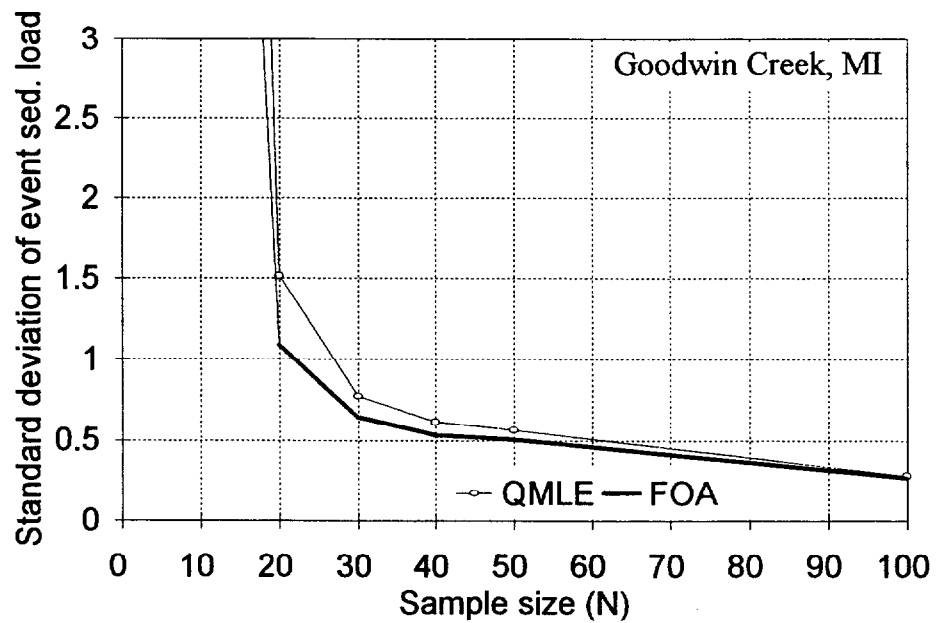
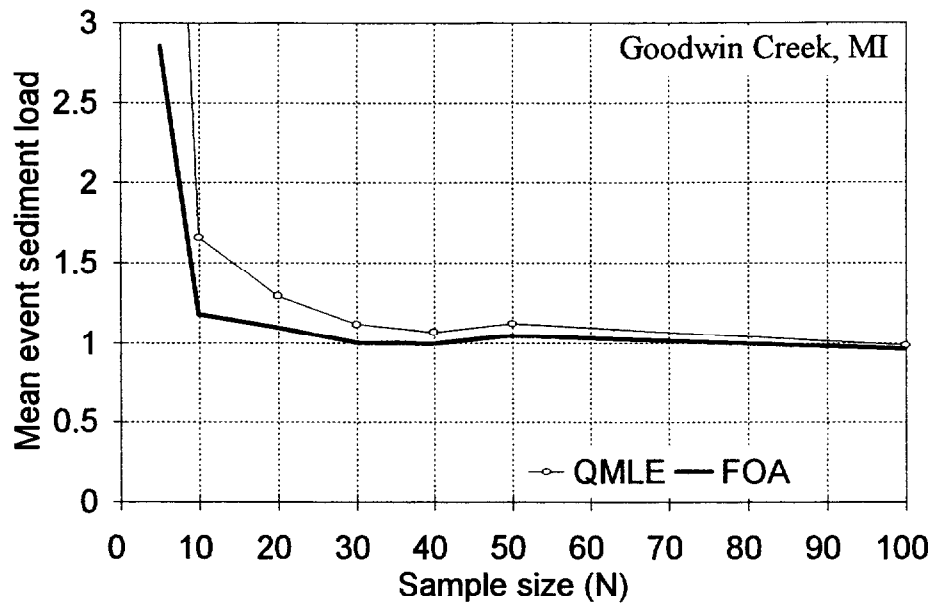


Fig. B-4; 8: Mean (top) and standard deviation (bottom) of total sediment load as a function of sample size  $N$  obtained from actual data based on the rating curve estimators QMLE, FOA, MVUE for Prairie Creek (data from Lisle 1989, and Lisle pers. com.).



**Fig. B-4; 9:** Mean (top), and standard deviation (bottom) of total sediment load as a function of sample size  $N$  obtained from actual data based on the rating curve estimators QMLE, and FOA for Goodwin Creek, Mississippi (data from Kuhnle, pers. com.).

almost as well as the MVUE. However, the MVUE approach does not converge in the case of the data from Kuhnle, and in this case the FOA provides the best estimate of the total sediment load.

**Figures B-4; 6-9** also indicate a relatively rapid decline in the uncertainty of the estimated sediment load as the sample size increases from 5 to 20. For data sets that are less well-behaved (i.e., a poorer relationship between discharge and bedload transport), there is also a substantial improvement in the accuracy of the estimate as the sample size is increased to 30 or 40 samples, with the magnitude of this increase varying according to the estimation method used. In practical terms, the coefficient of variation for the four synthetic data sets ranged from about 20 to 150% when the sample size was 20. When the sample size was increased to the maximum value of 40 or 100 samples, all three methods converged and the coefficient of variation still ranged from about 15 to 50%. Sampling the actual data generally led to a slightly lower coefficient of variation as compared to the results for the synthetic data.

These evaluations of the uncertainty of bedload transport estimates provide another indication of the likely uncertainty of sediment load predictions, and thus our ability to detect change. It would obviously be useful to conduct a similar analysis on other high-resolution data sets, and to evaluate why the preferred estimation method (MVUE) did not work for Kuhnle's data set.

#### 4.3.2.3 The effect of time of day on the representativeness of bedload sampling: favorable measuring times in a snowmelt regime

Since sampling typically occurs over a very small fraction of the total period of bedload transport, and the high flow values are most critical for determining annual sediment yield, one should ideally sample at those high flow periods which are most representative of the mean bedload transport rate. It should be noted, however, that the mean transport rate of interest is for a given discharge when using the rating curve approach, or a specific period of time when using the summation approach. The question then becomes whether one can identify specific periods which would better approximate the mean transport rate, as this would then reduce the uncertainty of the estimated sediment load and thus increase the sensitivity to detect a change in the sediment load.

The 17-day continuous record of particle transport rates from a snowmelt high flow at Squaw Creek was used to analyze the patterns of temporal variation with regard to the mean daily bedload transport. Over this 17-day period there was a gradual change in the daily hysteresis loop from a steep clockwise pattern (i.e., a higher transport rate on the rising limb) to an almost horizontal counter-clockwise hysteresis (suggesting sediment exhaustion or equal mobility). Within this 17-day period we identified those hourly periods that were most favorable for sampling according to two criteria representing two different sampling objectives (Bunte and MacDonald 1993). The first objective was to sample those three-hour periods which were close to the average transport rate observed over the entire snowmelt high flow. The second objective was to identify those periods that best represented the mean transport rate on a calendar day as well as a discharge day.

For the first objective we first identified those times when the mean transport rate for a single hour was 90-120 percent of the mean transport rate for the entire snowmelt high flow. These times periods are shaded in the second but last column in **Tables B-4; 5-7**. We also identified all periods at least three hours in length when the mean transport rate for each hour was within 75-150% of the overall mean transport rate. The more frequent

Table B-4; 5: Relative signal rates, normalized by mean signal rate of the entire high flow period

Time	May				June													fav.mes. periods	avg.hrlly. sig.rate	Time
	28	29	30	31	1	2	3	4	5	6	7	8	9	10	11	12	13			
0 - 1	319	338	113	85	301	66	70	19	38	357	47	19	19	53	126	43	8	3	126	0 - 1
1 - 2	639	169	113	96	272	122	49	30	30	470	56	28	15	171	100	64	8	3	151	1 - 2
2 - 3	545	132	94	96	117	132	45	19	70	545	38	38	47	122	304	54	15	2	150	2 - 3
3 - 4	451	113	94	141	173	56	113	75	77	274	56	19	58	39	188	28	8	2	122	3 - 4
4 - 5	357	188	75	77	180	94	188	60	56	396	66	13	23	167	135	17	9	2	131	4 - 5
5 - 6	263	225	56	45	122	85	90	85	66	143	19	13	45	188	98	9	9	1	97	5 - 6
6 - 7	225	207	188	47	62	169	113	98	38	201	39	6	113	60	68	19	6	1	103	6 - 7
7 - 8	38	150	75	53	70	188	184	109	30	145	17	17	113	103	47	11	13	2	84	7 - 8
8 - 9	19	132	56	177	75	103	122	73	58	62	24	28	175	53	49	9	9	2	76	8 - 9
9 - 10	56	113	56	77	32	98	90	56	51	75	47	17	179	38	47	17	11	2	66	9 - 10
10 - 11	56	75	132	49	32	92	38	60	28	186	34	6	216	38	38	11	9	3	68	10 - 11
11 - 12	94	132	150	79	47	62	28	56	38	197	19	9	293	45	32	9	9	2	81	11 - 12
12 - 13	169	113	75	70	47	39	75	73	32	263	17	19	252	34	32	17	11	2	83	12 - 13
13 - 14	113	94	75	132	77	54	62	49	32	182	9	30	197	47	47	9	13	2	76	13 - 14
14 - 15	38	94	132	70	56	38	70	36	47	154	19	23	143	47	24	24	17	2	63	14 - 15
15 - 16	150	132	132	105	98	34	39	38	56	85	41	30	158	36	38	26	19	3	75	15 - 16
16 - 17	75	113	188	113	75	88	75	24	86	73	19	28	96	85	132	19	26	4	81	16 - 17
17 - 18	319	169	319	75	184	68	41	19	73	113	17	28	85	54	103	39	9	3	107	17 - 18
18 - 19	432	150	470	100	267	269	28	34	66	85	17	17	94	41	68	34	19	4	136	18 - 19
19 - 20	225	113	75	160	160	261	38	75	143	83	19	9	132	71	94	26	17	3	105	19 - 20
20 - 21	395	113	319	182	132	173	49	26	188	92	15	9	128	49	73	19	15	4	123	20 - 21
21 - 22	545	169	545	338	122	60	38	28	225	113	24	13	122	47	79	23	8	3	156	21 - 22
22 - 23	451	132	395	173	120	81	19	92	207	56	30	32	98	64	43	13	8	3	125	22 - 23
23 - 24	789	150	282	376	47	81	39	58	263	47	28	11	58	117	21	11	11	2	149	23 - 24

occurrence of these favorable measurement periods are shaded in the first and last columns of **Tables B-4; 5-7**.

The drainage area of 106 km<sup>2</sup> meant that daily flows peaked near midnight, while daily low flows occurred in mid-afternoon. In general, the most favorable sampling periods occurred during the first part of the rising limb between 1500 and 200 hours (**Table B-4; 5**). The more stringent first criterion meant that the most favorable sampling times were limited to the early-to-mid part of the rising limb (1700-2000) and the early-to-mid part of the falling limb (0500-0700). For both cases the most favorable sampling times were very early in the morning or in the late afternoon or evening. These times are not particularly conducive to sampling, as fall at the end or outside of normal working hours.

For the second objective, we identified those periods which approached the mean daily transport rate for a calendar day and a discharge day (defined as the period from low flow to next day's low flow). We found that the periods of favorable measuring times are more frequent when one is only attempting to estimate the mean daily transport rate, and this is probably due to the correlation between the daily and the hourly values. At Squaw Creek, three or more blocks of favorable measuring times occurred at almost any time of day except for the pre-dawn period (**Table B-4; 6**). Transport rates which were close to the mean daily value were slightly more frequent from 0800-1000 on the falling limb and intermittently between 1400 and 2200 on the rising limb of flow. However, if a sample is taken at exactly the same hour each day, the most favorable hours on average are in the middle of the falling limb in the very early morning (500-800) and the entire rising limb between 1700 and 0100. The discrepancy between the recommended periods stems from the distinction between the number of days with transport rates very close to the mean daily values (which show a lot of variability from day to day) versus taking the average transport rate for each hour across all 17 days.

If the definition of a day is changed from a calendar to a discharge day, there are somewhat fewer favorable measuring periods, and these occur during the second half of the daily falling limb (800-1100) and the latter parts of the daily rising limb (2000-2200) (**Table B-4; 7**). If the bedload measurements are to be repeated at the same time each day, the optimum timing for transport rates to be close to the daily mean are during the middle and end of the falling limb of flow (500-800 and 1000-1400), and then intermittently on the rising limb.

Although these results are specific to Squaw Creek, they emphasize the daily variability in sediment transport and the point that the pattern of sediment transport is not consistent despite the strong diurnal pattern in flow. The long lag between peak snowmelt (typically early afternoon) and peak flow (from early evening until after midnight, depending on the size of the basin) means that bedload transport measurements made in conjunction with office hours will sample close to the daily minimum flow when bedload transport would also be expected to be relatively low. Again an understanding of the temporal patterns in discharge and sediment transport for the basin of interest must be understood if one desires to accurately estimate sediment loads by either a rating curve or a summation approach.

#### **4.3.3 Sediment transport equations**

Bedload transport equations represent another possible approach to estimating sediment transport and annual sediment loads. There are about twenty bedload transport equations that are more or less widely used, and a number of studies have compared the use of certain equations in various fluvial environments. The general outcome of those studies is

Table B-4; 6: Relative signal rates, normalized by mean signal rate of a calendar day

Time	May				June													fav.mes. periods	avg.hrly. sig.rate	Time
	28	29	30	31	1	2	3	4	5	6	7	8	9	10	11	12	13			
0 - 1	113	231	64	70	252	63	98	35	45	195	157	98	16	71	152	187	63	2	115	0 - 1
1 - 2	227	116	64	79	228	117	69	56	36	256	188	146	13	232	120	277	63	3	139	1 - 2
2 - 3	193	90	54	79	98	126	64	35	84	297	126	195	39	166	368	236	125	2	141	2 - 3
3 - 4	160	77	54	116	145	54	159	140	93	150	188	98	49	54	227	122	63	2	118	3 - 4
4 - 5	127	128	43	63	151	90	265	112	68	216	220	68	19	227	164	73	78	2	127	4 - 5
5 - 6	93	154	32	37	102	81	127	157	79	78	63	68	38	255	118	41	78	2	95	5 - 6
6 - 7	80	141	107	39	52	162	159	181	45	110	132	29	95	82	82	81	47	4	99	6 - 7
7 - 8	13	103	43	43	58	180	260	202	36	79	57	88	95	140	57	49	110	5	94	7 - 8
8 - 9	7	90	32	146	63	99	172	136	70	34	82	146	147	71	59	41	78	6	87	8 - 9
9 - 10	20	77	32	63	27	93	127	105	61	41	157	88	150	51	57	73	94	6	76	9 - 10
10 - 11	20	51	75	40	27	88	53	112	34	102	113	29	182	51	45	49	78	4	67	10 - 11
11 - 12	33	90	86	65	39	59	40	105	45	108	63	49	246	61	39	41	78	3	73	11 - 12
12 - 13	60	77	43	57	39	38	106	136	38	144	57	98	212	46	39	73	94	4	79	12 - 13
13 - 14	40	64	43	108	64	52	87	91	38	99	31	156	166	64	57	41	110	4	75	13 - 14
14 - 15	13	64	75	57	47	36	98	66	56	84	63	117	120	64	30	106	141	6	69	14 - 15
15 - 16	53	90	75	87	82	32	56	70	68	46	138	156	133	48	45	114	157	4	81	15 - 16
16 - 17	27	77	107	93	63	84	106	45	104	40	63	146	81	115	159	81	220	6	87	16 - 17
17 - 18	113	116	182	62	154	65	58	35	88	62	57	146	71	74	125	171	78	4	99	17 - 18
18 - 19	153	103	268	82	223	257	40	63	79	46	57	88	79	56	82	146	157	7	114	18 - 19
19 - 20	80	77	43	132	134	250	53	140	172	45	63	49	111	97	114	114	141	6	104	19 - 20
20 - 21	140	77	182	150	110	165	69	49	226	50	50	49	107	66	89	81	125	6	104	20 - 21
21 - 22	193	116	311	279	102	57	53	52	271	62	82	68	103	64	95	98	63	6	125	21 - 22
22 - 23	160	90	225	142	101	77	26	171	248	31	101	166	82	87	52	57	63	5	114	22 - 23
23 - 24	280	103	161	310	39	77	56	108	316	26	94	59	49	158	25	49	94	3	119	23 - 24

Table B-4; 7: Relative signal rates, normalized by mean signal rate of a discharge day

Time	May				June													fav.mes. periods	avg.hrlly. sig.rate	Time
	28	29	30	31	1	2	3	4	5	6	7	8	9	10	11	12	13			
0 - 1		144	109	47	220	62	66	38	83	431	57	23	23	114	273	94	16	2	112	0 - 1
1 - 2		72	109	53	199	116	47	60	66	566	68	34	18	371	216	139	16	2	134	1 - 2
2 - 3		56	91	53	85	125	43	38	153	657	45	45	102	265	661	118	33	3	161	2 - 3
3 - 4		48	91	78	126	53	107	151	169	331	68	23	127	86	408	61	16	2	121	3 - 4
4 - 5		80	72	43	132	89	179	121	124	478	79	16	49	363	294	37	20	3	136	4 - 5
5 - 6		96	54	25	89	80	86	170	144	172	23	16	98	408	212	20	20	3	107	5 - 6
6 - 7		88	181	26	45	160	107	196	83	242	48	7	245	131	147	41	12	3	110	6 - 7
7 - 8		64	72	29	51	178	175	219	66	174	20	20	245	224	102	24	29	1	106	7 - 8
8 - 9		56	54	98	55	98	116	147	128	75	29	34	380	114	106	20	20	4	96	8 - 9
9 - 10		48	54	43	23	93	86	113	111	91	57	20	388	82	102	37	24	4	86	9 - 10
10 - 1		32	127	27	23	87	36	121	62	224	41	7	469	82	82	24	20	4	92	10 - 1
11 - 12		56	145	44	34	59	27	113	83	238	23	11	637	98	69	20	20	2	105	11 - 12
12 - 13		48	72	39	34	37	72	147	70	317	20	23	547	73	69	37	24	1	102	12 - 13
13 - 14		40	72	73	56	52	59	98	70	220	11	36	429	102	102	20	29	2	92	13 - 14
14 - 15		40	73	39	41	36	66	72	57	186	23	27	310	102	53	53	37	1	76	14 - 15
15 - 16	64	127	73	77	93	32	79	75	68	102	50	36	343	78	82	57	41	2	87	15 - 16
16 - 17	32	109	104	82	71	84	151	49	104	88	23	34	208	184	286	41	57	2	100	16 - 17
17 - 18	136	163	177	55	175	64	83	38	88	136	20	34	184	118	224	86	20	2	106	17 - 18
18 - 19	183	145	261	73	253	256	57	74	79	102	20	20	204	90	147	73	41	3	122	18 - 19
19 - 20	96	109	42	117	151	249	75	165	172	100	23	11	286	155	204	57	37	3	120	19 - 20
20 - 21	167	109	177	133	125	165	98	58	227	111	18	11	278	106	159	41	33	5	119	20 - 21
21 - 22	231	163	302	247	116	57	75	62	272	136	29	16	265	102	171	49	16	4	136	21 - 22
22 - 23	191	127	219	126	114	77	38	202	249	68	36	39	212	139	94	29	16	3	116	22 - 23
23 - 24	335	145	156	275	45	77	79	128	317	57	34	14	127	253	45	24	24	1	126	23 - 24

that one or two formulas will yield reasonable results for a given stream, while the majority of predicted transport rates will be off by a factor of 2 to 10 (e.g., Raudkivi 1976, citing results from Vanoni et al. 1961; Hayward 1980; Allen 1981; Bathurst et al. 1987; Gomez and Church 1989; Kuhnle et al. 1989; Williams et al. 1989b; Georgiev 1990; Bechteler et al. 1994; Blizzard 1994). Although there is a wide variability of predicted transport rates in for all stream types, the predictions seem to be worst for small gravel-bed streams where there is less of a direct bedload transport response to changes in the flow hydraulics. The various comparisons also do not identify any formula that generally predicts bedload transport rates more accurately than the other formulas. Thus the success of bedload transport predictions depends on how well a particular bedload equation is adjusted to the specific conditions and transport processes in a given stream.

Beschta (1983a) was referring particularly to the problem of temporal variability when he summarized the state-of-the-art as:

*"The inherent variability in particle size distribution, degree of armoring, highly variable channel geometry, transient nature of storm runoff and the role of structural features such as bedrock controls and large organic debris indicate the extrapolation of equations developed under conditions of steady flow, uniform particle size and uniform channel geometry may result in large estimation errors. The development of deterministic equations that can accurately predict bedload transport in mountain streams may not be possible; perhaps a stochastic approach could be emphasized."*

In their handbook "Sediment Transport Technology", Simons and Sentürk (1992) analyzed some of the bedload equations developed for sand- and gravel-bed streams. It is not only important to use a formula from the proper group of equations (i.e., a sand formula for sand-bedded streams, and a gravel formula for gravel-bed streams), but it was also implied that trial and error plays a role, and that it is prudent to use a formula that "fits". Simons and Sentürk (1992 p., 696) further conclude: "Sediment transport problems encountered involve much more than applying selected transport relationships to estimate the rate of bed material transport in a reach of river" and "There is a continuing need to develop transport relationships specifically related to field conditions." They urge that the spatial variation of channel and flow conditions, as well as the temporal variability, must be included in sediment transport calculations. They also emphasize that the persons who aspire to use bedload transport equations must be well acquainted with sediment transport processes in order to select an appropriate formula and produce meaningful results.

Many bedload equations predict bedload transport rates according to the critical shear stress required to move the  $D_{50}$  of the bed material size. Other equations, such as the original Einstein (1942) equation, predict transport rates for each particle size present in the bed material based on the respective critical shear stress for that particular particle size. Estimating the  $D_{50}$  of the bed material size can be a difficult task in mountain streams. Several studies have indicated that the amount of bed material needed for an accurate determination of the particle size distribution can amount to hundreds of kilograms if the particle size spectrum includes large cobbles (e.g., Church et al. 1987; Bunte 1995).

When using a formula that is based on only one particle size percentile, such as the  $D_{50}$ , it is critical to accurately determine the  $D_{50}$  because predicted bedload transport rates are so strongly dependent on particle size. A detailed analysis of the sensitivity of the Ackers and White (1973) sediment transport formula for sand-bedded streams showed that an underestimation of  $D_{50}$  by 50% can lead to an overestimation of predicted transport rates by a factor of 2 to 10, while an underprediction of the  $D_{50}$  by as little as 20% may lead to overpredictions of transport rates by as much as 25 to 70% (Bunte 1994).

Accurate measurements of flow hydraulics are also crucial for accurate bedload transport predictions. For the Ackers and White equation, a 20 and 50% overestimate of flow velocity resulted in an overprediction of sediment transport by about 90 and 280%, respectively. The sensitivity of bedload transport equations to poor bed material and flow parameters may be somewhat less pronounced for gravel-bed rivers, but this lesser sensitivity is counteracted by the higher probability of inaccurately measuring bed material and flow parameters in gravel-bed rivers.

In view of these problems, the original Einstein (1942) equation seems to be most appropriate for bedload transport predictions in gravel-bed streams. As this equation is based on the critical shear stress of individual size fractions, one does have to accurately determine the percentage of each size fraction on the channel bed. The Einstein (1942) equation also includes a hiding factor that accounts for the decreased mobility of small particles when surrounded by large particles, and the increased mobility of exposed large particles. However, the original Einstein (1942) equation does require a rather large computing effort.

#### **4.3.4 Summary: Uncertainty of estimates of annual bedload transport**

The prediction of annual bedload transport from rating curves is subject to the same issues and limitations as the prediction of suspended sediment loads. One difference, however, is that much of the scatter in the rating curve for suspended sediment is often due to the spatial and temporal variability in sediment delivery, while the scatter in the bedload rating curve is probably due more to irregular transport patterns and storage dynamics. The coefficient of determination for bedload rating curves are affected by a number of factors related to both sediment transport and sampling, including:

- range of sediment transport rates;
- variability in sediment transport due to a wide variety of processes;
- range of sampled flows;
- sample size,
- representativeness and relative efficiency of the sampling techniques at different flows, sediment transport rates, and grain-size distributions; and
- sampling intensity and duration; and
- temporal scale over which the data are averaged.

Surprisingly, the coefficient of determination for bedload rating curves is often higher than for suspended sediment rating curves. Nevertheless, the interannual variability in bedload rating curves is sufficiently large to preclude using a change in rating curves to detect CWEs.

A relatively small number of samples (e.g., <20) may be sufficient to provide a first-order estimate of the total sediment load, but the uncertainty of this estimate can vary from more than a factor of two to less than 50%. Increasing the sample size will decrease the uncertainty, especially if the additional measurements are taken at high flows. A reduction in the standard error of the rating curve or an improvement in the accuracy of a summation procedure may also be achieved by sampling at times that are more likely to be representative of the bedload transport rate for that discharge or time period. Selecting this time requires an understanding of the flow and sediment transport dynamics in the stream being sampled. Sampling bedload transport in snowmelt-dominated areas is particularly difficult because peak flows occur in the evening or at night, depending on the size of the basin. In most cases the use of a summation procedure to predict annual bedload transport

will be hindered by the temporal resolution of the data; automated sampling techniques are only possible for a few well-equipped measurement stations. Sediment ponds represent an alternative to direct measurement, and in cases where regular sampling is difficult these can offer a relatively low-tech and low effort procedure to accurately estimate the annual sediment load.

Bedload transport formulas are another means for predicting sediment loads, but the use of different formulas will generate predicted transport rates that vary over 1-2 orders of magnitude. Bedload transport equations have to be matched to the stream type and bed material, and checked against actual data if they are to have any validity. Small errors in estimating key variables, such as the median particle size or flow velocity, can greatly affect the predicted transport rate. The uncertainty associated with bedload transport formulas severely limits their ability to distinguish or accurately predict CWEs.

## 5. Annual Variability of Sediment Yield (Total Load)

The determination of a management-induced change in sediment yields is dependent on the magnitude of that change relative to the interannual variability in the absence of management. If a paired-basin approach is followed, the strength of the relationship between the basins must also be assessed in order to determine the detectability of a management-induced change in sediment yields.

Previous chapters have evaluated the accuracy and variability of sediment measurements, as well as the procedures to extrapolate from a few measurements to estimating the annual sediment load. Each of these issues directly affect the reliability of the estimated annual sediment load, and thus must be addressed prior to any analysis of the interannual variability of suspended load, bedload, or total load. The following investigation of the variability of annual sediment yields is directed at the following questions:

- What is the interannual variability in sediment yields within a basin, and how does this vary with basin size and basin characteristics?
- What level of consistency can we expect in annual sediment yields between paired basins?
- Based on the data from the first two questions, how large does a management impact have to be before it can be detected?

### 5.1 Extent and evaluation of natural variability

The accuracy of the estimated annual sediment yield is dependent on the short-term and intra-event variability, measurement and sampling errors, and the calculation procedures employed to determine annual load. The discussion of these topics in previous chapters indicated that the potential error from each of these factors can be quite large. Specific values are difficult to quantify because they are so case-dependent, but it can be assumed that they range from as little as 10-20% under optimal conditions and intensive sampling, to an order of magnitude or more. The potential effect of all these sources of error and uncertainty are not incorporated in the following analyses because the data are generally not available to estimate these, and the simultaneous consideration of all of these issues is simply not practical or even feasible given the present state of knowledge and the time available for this project.

The determination of mean annual sediment yield is affected by the time span over which it is determined, and the extent of the interannual variability observed during this time period. When estimating mean annual sediment yield ( $Q_{sa}$ <sup>1</sup>), several factors need to be taken into consideration:

- Number of years of data,
- Climatological and environmental conditions of the watershed during the period of record;
- Occurrence of extreme events; and
- Persistence of extreme events (sediment storage or depletion for the following years).

Unfortunately there are very few long-term data sets from basins that have not been subjected to anthropogenic change, and those data sets that are available are generally for

---

<sup>1</sup>Unless it is clear from the context that  $Q_{sa}$  specifically refers to suspended sediment yield,  $Q_{sa}$  refers to annual sediment yield in general with no distinction between suspended sediment and bedload.

very small research basins. The analysis of longer-term data sets from larger basins is hampered by a lack of detailed information on changing conditions within the basin, and our ability to link land use changes with specific changes in annual sediment yields. Another limitation is that the existing records of annual sediment yields may not necessarily be representative of the longer-term means and variability. This is particularly true for basins that are subject to relatively infrequent events that can produce very large amounts of sediment (e.g., landslides, debris flows, glacial lake outbursts, etc.). Thus the observed distribution of data are only valid with respect to the period of observation, and the possibility of much more extreme events cannot be excluded.

## 5.2 The Data set

For the analyses presented here, 37 data sets of annual sediment yield ( $Q_{sa}$  or  $Q_{ba}$ ) in mountainous areas have been collected from various sources, including the USGS Water Resources Data Base, data sets published in the literature, and personal communications. We generally selected data sets with at least twelve years of nearly continuous data for our analysis. Unfortunately, many data sets in the USGS Water Resources Data Base were not continuous. Some gaps could be closed because there were only a few days missing and the sediment yields for these days could be interpolated from the surrounding data. Other times the gaps were too large to be filled by interpolated values. Time limitations meant that most of the data on the long-term annual sediment yield of large rivers has been drawn from USGS records in Montana and the Rocky Mountain region.

For Hubbard Brook annual sediment data were obtained from published literature. However, Bilby (1981) and Martin and Hornbeck (1993) give completely different values of annual sediment yield for the time period after 1973. We gave preference to the newer source. Another source of data were personal communications. J. Stednick (Department of Earth Resources, CSU) provided us with data from the Alsea watershed and C. Troendle and J. Nankervis (USFS, Fort Collins) provided data sets from the Fraser Experimental Forest.

An overview of all 37 data sets is given in **Table B-5; 1**. All data on annual sediment yield have been converted to metric tons per km<sup>2</sup> per year, unless an analysis was limited to a single data set. The 37 data sets vary with respect to their time length (11 - 35 years), the method of determining annual sediment yield (daily suspended sediment sampling or determining the volume of sediments caught in debris basins), the drainage area (0.1 - almost 200,000 km<sup>2</sup>), stream gradient, precipitation and flow regime, and watershed treatments (unimpaired to heavily managed). Some data sets included relatively extreme event like a debris flow or a large flood. For each data set we determined the mean, annual sediment yield, the standard deviation, the coefficient of variation, and the type of distribution (Gaussian or lognormal). In cases where multiple basins had been monitored, or the monitoring had extended over a period of change within the basin, we also analyzed the regression relationships between basins or over time.

Mean  $Q_{sa}$ ,  $CV$ , and regression coefficients were used for intra- and inter-basin comparison. Knowledge of the distribution type (Gaussian or lognormal) is necessary to assess the number of years of record needed for the calculated mean annual sediment yield to be within a certain level of accuracy.



Further analyses included graphical plots of:

- time series,
- ranking from largest to smallest event,
- summations of sediment yields over time (double-mass curves), and
- cumulative frequency distribution.

Time series of annual sediment yields were plotted to visually compare records from adjacent basins. Regression analyses of time series from adjacent basins provides useful insight into the interbasin variability. The ranking of data was used to determine the importance of the most extreme events; we specifically calculated the percentage of the total sediment yield over the period of record that was contributed in the year with the largest observed annual sediment yield ( $Qsa_{max}$ ) and the two largest annual sediment yields ( $Qsa_{max} + Qsa_{2max}$ ). The frequency distribution helps identify outliers and is the prerequisite for computing the median ( $Qsa_{50}$ ) and a cumulative frequency distribution. Only a few of the 185 plots prepared are included in this report, but they are available upon request. The statistical results are summarized in Table B-5; 1.

### 5.3 Annual variability of sediment yield: mean values and extreme values

The mean annual sediment yield ( $Qsa$ , t/km<sup>2</sup>-a) of basins <10km<sup>2</sup> was found to vary from 1 to almost 700 t/km<sup>2</sup>. This variation is, however, not well related to basin size.  $Qsa$  seems to be mostly a function of the interplay between topographical, geological, hydrological, and management conditions of the catchment. Catchments in the Pacific Northwest produce a higher natural  $Qsa$  than catchments in the Colorado Rocky Mountains (Fraser Experimental Forest) or New Hampshire (Hubbard Brook Experimental Forest).

Data sets are usually skewed due to the occurrence of a few years with high sediment yields, and this causes the mean sediment yield to be up to 2 times larger than the median sediment yield. Mean annual sediment yield is typically only exceeded in 20-40% of the years. In extreme cases in the Pacific Northwest, the mean is 3 to 10 times larger than the median.

The maximum annual sediment yield ( $Qsa_{max}$ ) typically accounts for 15-30% of the total sediment yield in data sets that extend over a 15 to 30-year period. The cumulative sediment yield of the two years with the highest sediment yield ( $Qsa_{2max}$ ) accounted for about 50% of total observed sediment yield in small basins with large mean  $Qsa$ , around 30% of total observed sediment yield for small basins with low  $Qsa$ , and about 35% for large basins in Montana.

The range of the annual sediment yield within each data set is quite wide. Data sets from the Pacific Northwest are often characterized by a series of relatively small annual sediment yields interrupted by one or more years with much larger values. The interannual variability over one or a few decades commonly extends over a range of at least one order of magnitude, and can be more than two orders of magnitude. The most extreme example of this case is watershed #3 in the H.J. Andrews Experimental Forest, where sediment yield generated by a debris flow during one storm event accounted for 82% of the total sediment yield over a 31-year period (Grant and Wolff 1991).

The coefficient of variation is generally greater than 100% for basins in the Pacific Northwest. The CVs for annual sediment loads from the Fraser and Hubbard Brook Experimental Forests range from 70 to over 100%, while large streams in Montana have a slightly lower average CV but a similar range. Streams in the Piceance Creek basin in

northwestern Colorado have a somewhat higher average CV (103%), although these values were derived from basins with relatively short records.

At first glance the relatively high CVs for basins in the Pacific Northwest might be attributed to the steep, landslide-prone terrain. Another factor may be the large variability in storm events as compared to snowmelt-dominated areas. One could also note the fact that most of the annual sediment load from the Pacific Northwest basins is suspended sediment, while most of the annual sediment yield in the Fraser and Hubbard Brook Experimental forests is bedload. (For this analysis we did not consider the dissolved load, even though this may be the largest loss in terms of mass.)

#### **5.4 Inter- and intra-basin variability in undisturbed basins within one experimental forest**

The mean annual variability of undisturbed catchments, and the interbasin differences or similarities in annual sediment yield, were analyzed using data sets from the Hubbard Brook Experimental Forest in New Hampshire and from the Fraser Experimental Forest in central Colorado. Data and background information on Hubbard Brook were extracted from Bilby (1981), Martin and Hornbeck (1993), and Federer et al. (1990). Data and background information for the Fraser Experimental Forest were provided by C. Troendle and J. Nankervis (pers. comm.), Troendle (1993), and Troendle and King (1985). These data sets were chosen because the common period of record was at least 13 years and there was an absence of catastrophic events which could affect annual sediment yield for several years.

##### **5.4.1 Hubbard Brook Experimental Forest**

Mean annual bedload yield from three undisturbed control watersheds at the Hubbard Brook Experimental Forest are 5.4, 3.1, and 2.3 t/km<sup>2</sup> for WS 1, 3, and 6, respectively, for the 16-year period from 1975 to 1990. A comparison of the time series of annual sediment yields shows relatively little consistency among these three undisturbed catchments, despite their presumed similarity and proximity in space (Fig. B-5; 1). An analysis of annual runoff showed much more consistency, and this suggests that there were not substantial differences in the large-scale climatic regime between the three basins (Fig. B-5; 2 and 3). An analysis of the relationship between annual streamflow ( $Qa$ ) and the annual yield of bedload ( $Qba$ ) indicated that there was almost no correlation for any of the three undisturbed watersheds (1, 3, and 6) over the 14-year time period for which common data exist. The coefficients of determination ( $r^2$ ) for these regressions were 0.044, 0.004, and 0.043, respectively.

Martin and Hornbeck (1993) suggested that the annual sediment yield at Hubbard Brook might be better related to individual storms than to total annual water yield. Fig. B-5; 4 shows the highest annual instantaneous discharge ( $Qi_{max}$ ) for WS 3 between 1975 and 1988, and these values explained 37% of the interannual variability in bedload yields. These instantaneous maximum annual discharges ( $Qi_{max}$ ) at WS 3 were also related to the annual bedload yields ( $Qba$ ) at WS 1 and WS 6 ( $r^2=0.20$  and 0.65, respectively). These results suggest that individual storms do affect annual bedload yield, but other factors must also come into play.

A comparison of annual sediment yields over the entire 16-year period shows that each control basin had a unique pattern (Fig. B-5; 1). In WS 1, for example, annual sediment

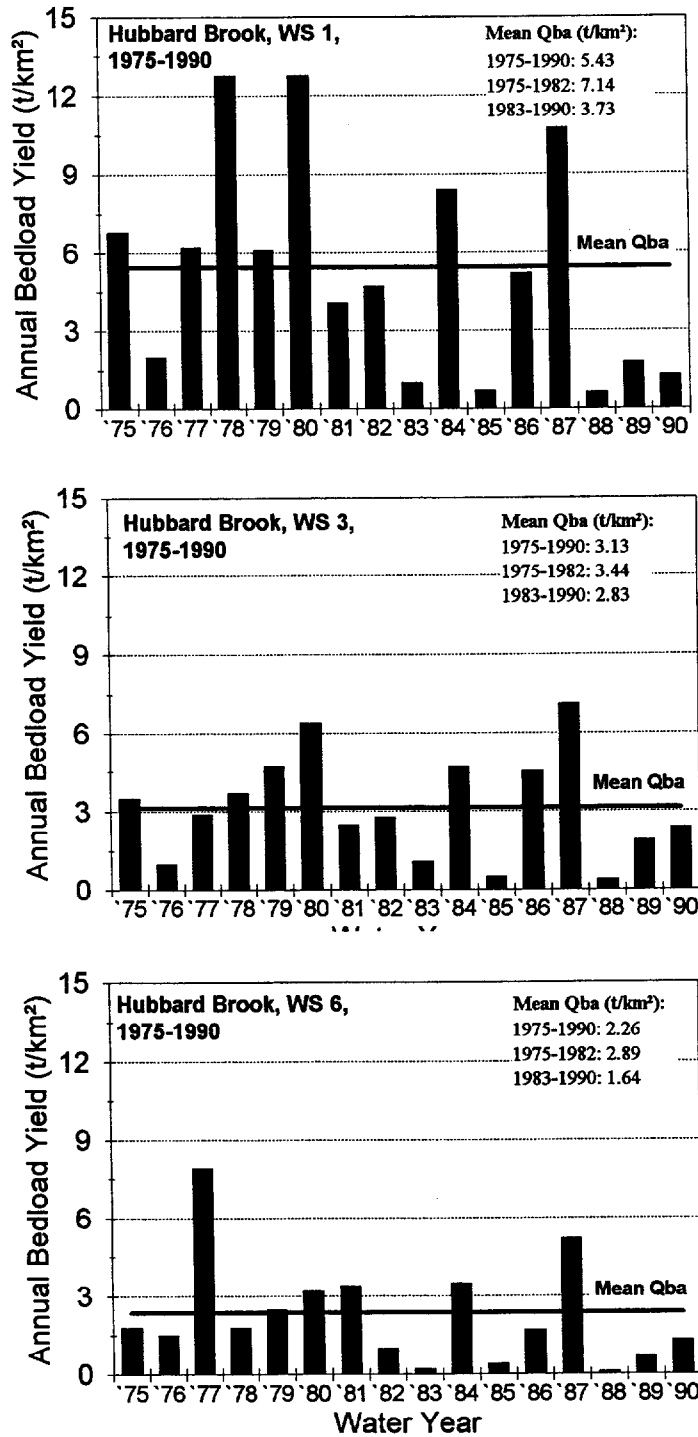


**Fig. B-5; 1:** Annual bedload yields from three undisturbed control watersheds (WS 1, 3, and 6) at the Hubbard Brook Experimental Forest for 1975 to 1990.

yields for 1978 and 1980 were about 2.5 times the average. In WS 3, 1978 is only slightly above average, while 1980 is twice the average. In WS 6, annual sediment yield in 1978 is slightly below average, while 1980 was only slightly above average. In 1977 the sediment yield in WS 6 was nearly three times the average, while sediment yields in the other two catchments were about average.

Regressions were developed between each of the three basins, as this is the usual procedure in any kind of paired basin experiment. The  $r^2$  values for the three comparisons (3 vs. 1, 6 vs. 3, and 1 vs. 6) were 0.72, 0.30, and 0.26, respectively (Table B-5; 2). In an attempt to identify the source of the variability between the three basins, the 16-year record was subdivided into two 8-year periods. The first period spanned the slightly wetter years of 1975-1982, while the second period of 1983-1990 was somewhat drier. During this second period the annual sediment yield was much more consistent among the three basins (Fig. B-5; 1), with  $r^2$  values of 0.92, 0.91, and 0.95. For the first eight-year period the relationships were not nearly as consistent ( $r^2$  values of 0.64, 0.004, and 0.001) (Table B-5; 2). The reliability of even the best set of regressions is questionable given the variation in slopes and the relatively high standard errors of the regressions.

**Table B-5; 2:** Linear regressions between annual sediment yields of undisturbed (WS 1, 3, 6) and disturbed watersheds (WS 2 and 5) at Hubbard Brook Experimental Forest for the entire period of 1975 (or 1976) - 1990, the period of higher flows and higher sediment yields 1975 (or 1976)-1982, and the period of lower flows and sediment yields, 1983 - 1990. For each regression, *a* is the slope, *b* is the y-intercept,  $r^2$  is the coefficient of determination, and StE is the standard error of the regression.

		Entire period 1975 (or 1976)- 1990			High sediment yield, wetter period 1975 (or 1976)- 1982			Low sediment yield, dryer period 1983 - 1990		
WS 1, 3, and 6 undisturbed	<b>WS</b>	<b>3 &amp; 1</b>	<b>6 &amp; 3</b>	<b>1 &amp; 6</b>	<b>3 &amp; 1</b>	<b>6 &amp; 3</b>	<b>1 &amp; 6</b>	<b>3 &amp; 1</b>	<b>6 &amp; 3</b>	<b>1 &amp; 6</b>
	<i>a</i>	1.86	0.56	1.08	0.30	0.08	0.06	0.58	0.73	2.12
	<i>b</i>	-0.39	0.50	2.98	1.30	2.60	6.97	0.67	-0.41	0.25
	$r^2$	<b>0.72</b>	<b>0.30</b>	<b>0.26</b>	<b>0.64</b>	<b>0.004</b>	<b>0.001</b>	<b>0.92</b>	<b>0.91</b>	<b>0.95</b>
	StE of y	2.38	1.77	3.88	1.04	2.36	4.61	0.72	0.60	0.98
WS 2 cut and sprayed with herbicides in 1965	<b>WS</b>	<b>2 &amp; 1</b>	<b>2 &amp; 3</b>	<b>2 &amp; 6</b>	<b>2 &amp; 1</b>	<b>2 &amp; 3</b>	<b>2 &amp; 6</b>	<b>2 &amp; 1</b>	<b>2 &amp; 3</b>	<b>2 &amp; 6</b>
	<i>a</i>	0.36	0.92	0.95	0.07	-0.17	0.48	0.84	1.44	1.86
	<i>b</i>	1.22	0.28	0.99	2.74	3.81	1.74	-0.02	-0.97	0.05
	$r^2$	<b>0.32</b>	<b>0.44</b>	<b>0.48</b>	<b>0.024</b>	<b>0.023</b>	<b>0.33</b>	<b>0.83</b>	<b>0.89</b>	<b>0.86</b>
	StE of y	2.47	2.24	2.15	2.12	2.12	1.76	1.61	1.28	1.46
WS 5 clear-cut with heavy equip- ment in the winter of 1983/1984	<b>WS</b>	<b>5 &amp; 1</b>	<b>5 &amp; 3</b>	<b>5 &amp; 6</b>	<b>5 &amp; 1</b>	<b>5 &amp; 3</b>	<b>5 &amp; 6</b>	<b>5 &amp; 1</b>	<b>5 &amp; 3</b>	<b>5 &amp; 6</b>
	<i>a</i>	0.63	1.87	1.77	0.41	1.36	1.49	1.30	2.24	2.90
	<i>b</i>	3.40	0.98	2.82	3.35	1.56	1.94	2.56	1.07	2.64
	$r^2$	<b>0.24</b>	<b>0.43</b>	<b>0.41</b>	<b>0.17</b>	<b>0.27</b>	<b>0.61</b>	<b>0.53</b>	<b>0.57</b>	<b>0.55</b>
	StE of y	5.11	4.41	4.49	4.12	3.87	2.83	5.25	5.02	5.10

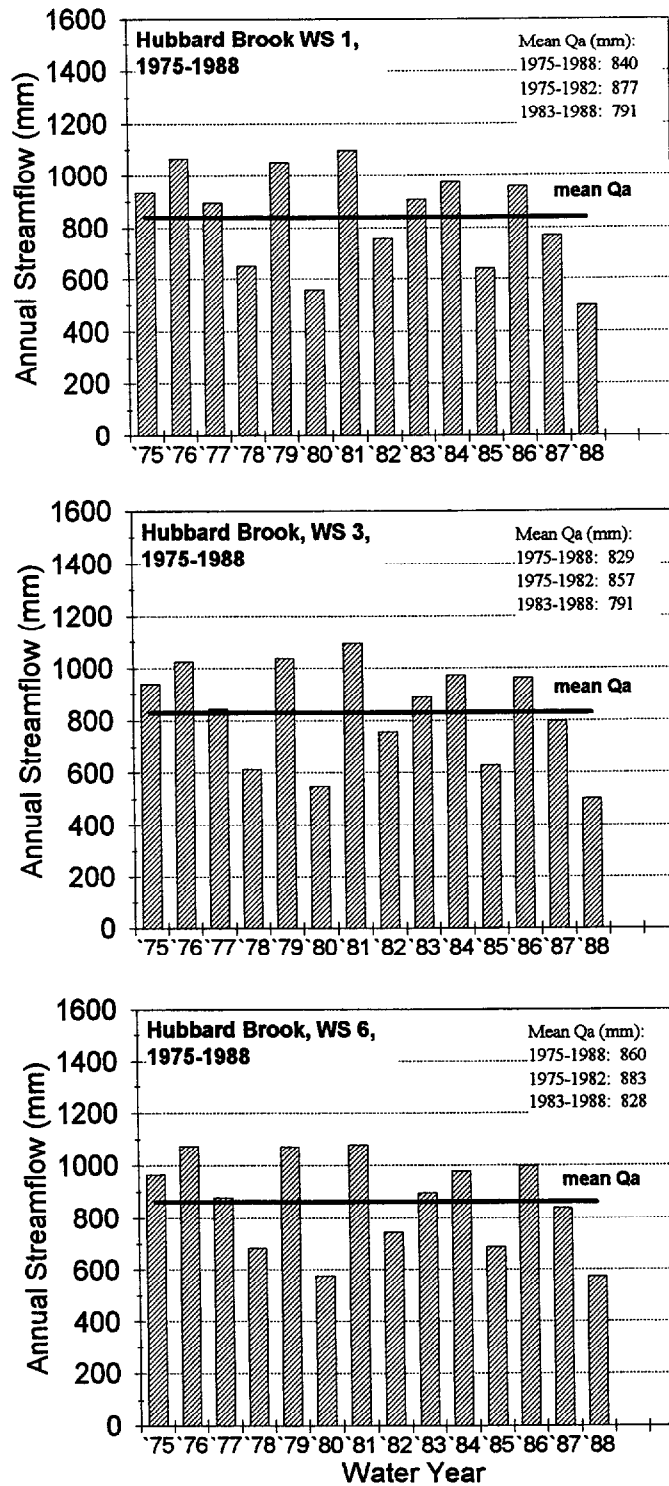
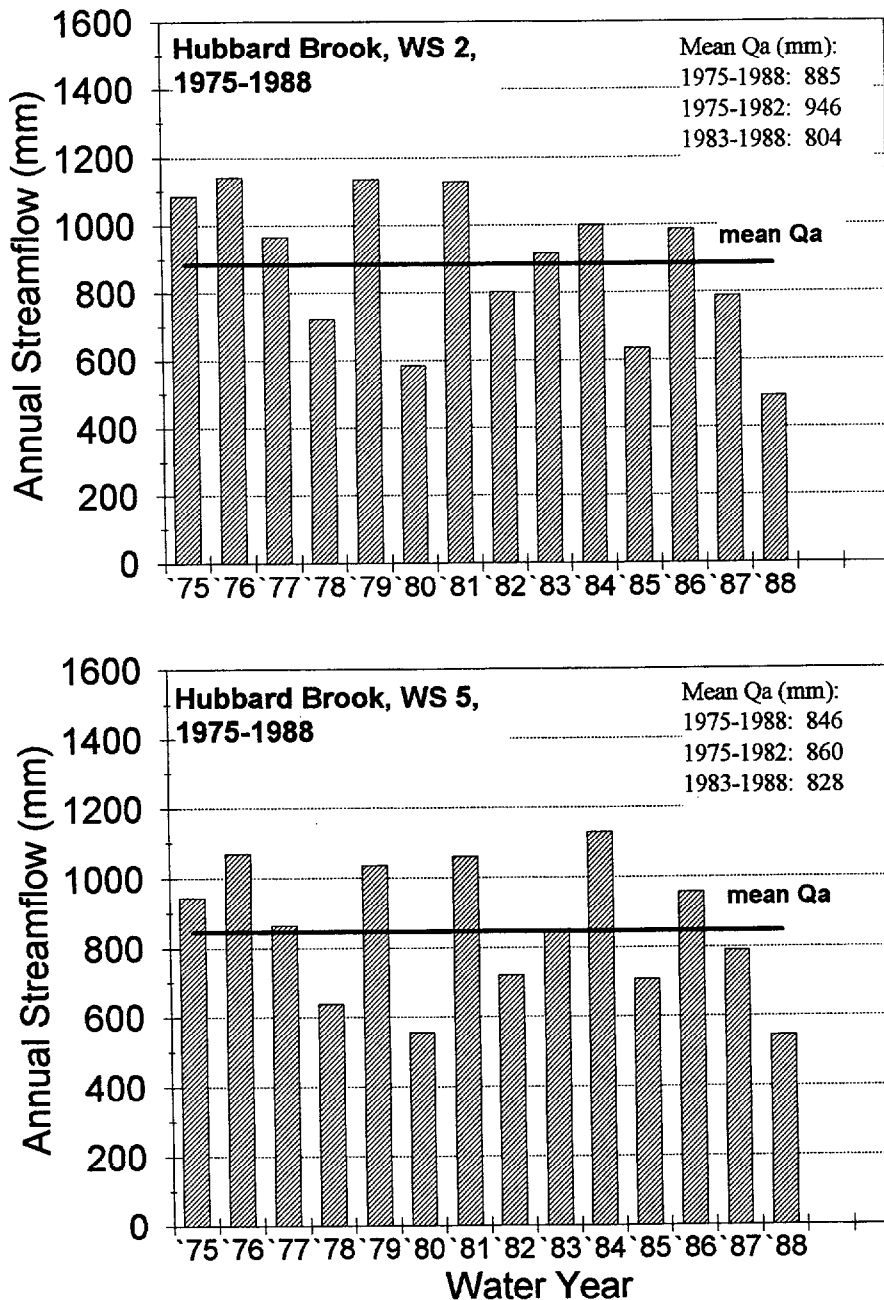


Fig. B-5; 2: Annual streamflows in the three undisturbed control watersheds (WS 1, 3, and 6) at the Hubbard Brook Experimental Forest from 1975 to 1990.



**Fig. B-5; 3:** Annual streamflows in the two disturbed watersheds (WS 2 and 5) at the Hubbard Brook Experimental Forest from 1975 to 1990.

A comparison of mean annual sediment yields and mean annual streamflows was conducted for the two time periods in order to further elucidate why sediment yields between basins should be poorly correlated from 1975-1982 and highly correlated from 1983-1990 (Table B-5; 3). One possibility is that the slightly higher stream flows in 1975-1982 could result in a higher production of sediment, but this sediment might not reach the stream or be stored within the stream network. If sediment transport is more affected by storage dynamics than

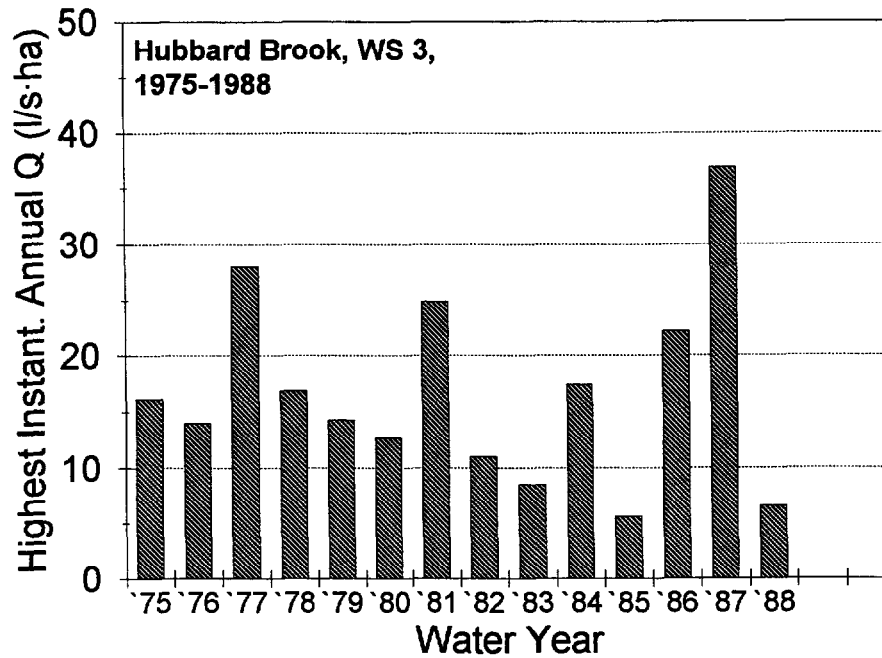


Fig. B-5; 4: Highest instantaneous annual streamflow at WS 3, 1975-1988.

actual flows, this would cause the poor observed relationship between  $Q_a$  and  $Q_{ba}$ . The second period was characterized by slightly lower annual stream flows (6-10%) and annual sediment yields (18-48%). Fig. B-5; 4 indicates that there was more variability in peak flows during the second period, and this may have improved the correlation between sediment and water yields. Another factor may be the occurrence of low flows, as all the watersheds had very low bedload yields in years with no major storms. The absence of storms may have then primed the stream for higher bedload transport during the next year with a large flow event, but the different watersheds would naturally exhibit more variability during the years with higher sediment yields.

Table B-5; 3: Mean annual bedload yields ( $Q_{ba}$ , t/km<sup>2</sup>) and mean annual streamflow ( $Q_a$ , mm) over various time periods for three undisturbed watersheds at the Hubbard Brook Experimental Forest.

Time period	$Q_{ba}$ (t/km <sup>2</sup> )			$Q_a$ (mm)			Time period
	WS 1	WS 3	WS 6	WS 1	WS 3	WS 6	
1966-1990	-	-	2.37	-	-	831	1966-1988*
1966-1973	-	-	2.58	-	-	767	1966-1973
1975-1990	5.43	3.13	2.26	840	829	860	1975-1988*
1975-1982	7.14	3.44	2.89	877	857	883	1975-1982
1983-1990	3.73	2.83	1.64	791	791	828	1983-1988*
Difference (%)	-48	-18	-43	-10	-8	-6	

\* note the slightly different time intervals between compared periods of  $Q_{ba}$  and  $Q_a$ .

### 5.4.2 Fraser Experimental Forest

The question arises whether the variation in the relationship between flow and annual sediment yields observed at Hubbard Brook can also be found in other catchments. Of particular interest is whether these relationships show a similar variability over time and between control basins. The watersheds in the Fraser Experimental Forest in central Colorado provided another data set that could be used for this analysis.

The Fraser Experimental Forest has two control watersheds, and these are East St. Louis Creek (8.03 km<sup>2</sup>) and Lexen Creek (1.24 km<sup>2</sup>). Both of these catchments have steep, boulder-strewn streams with step-pool profiles cutting through glacial moraines. The patterns of annual runoff are very similar in both catchments (Fig. B-5; 5). Again, however,

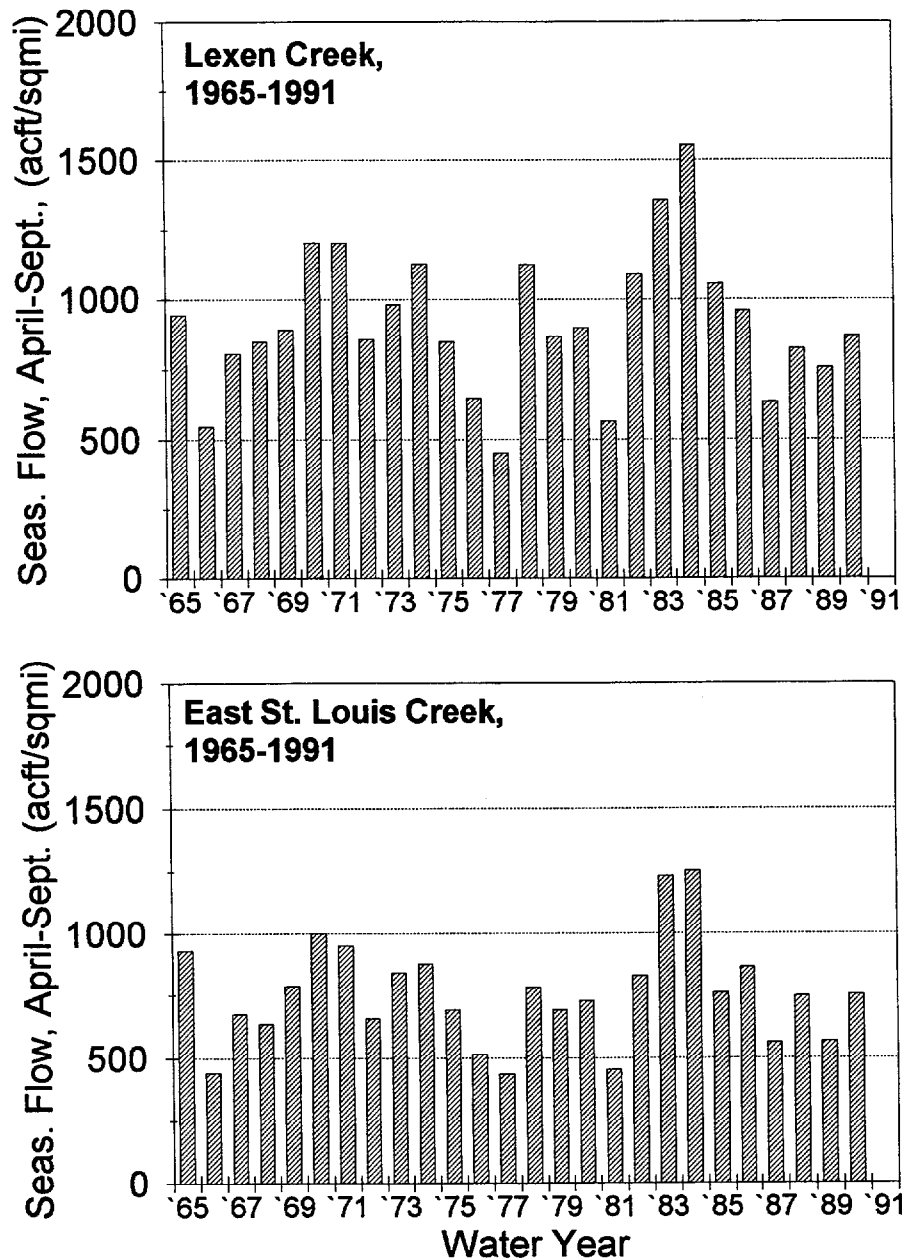


Fig. B-5; 5: Seasonal streamflows (April -September) from two control watersheds (Lexen Creek and East St. Louis Creek) at Fraser Experimental Forest, 1965-1991.

the time series of annual sediment yields from these two catchments, despite their proximity and presumed comparability, show surprisingly little similarity (Fig. B-5; 6) except for a few high sediment yields in some years (1983, 1984) and a few very low sediment yields in other years (1977, 1979). A basic similarity in bedload generation and transport is suggested by the similar mean annual bedload (as measured in debris basins) for the 15-year period common to both catchments (Table B-5; 5).

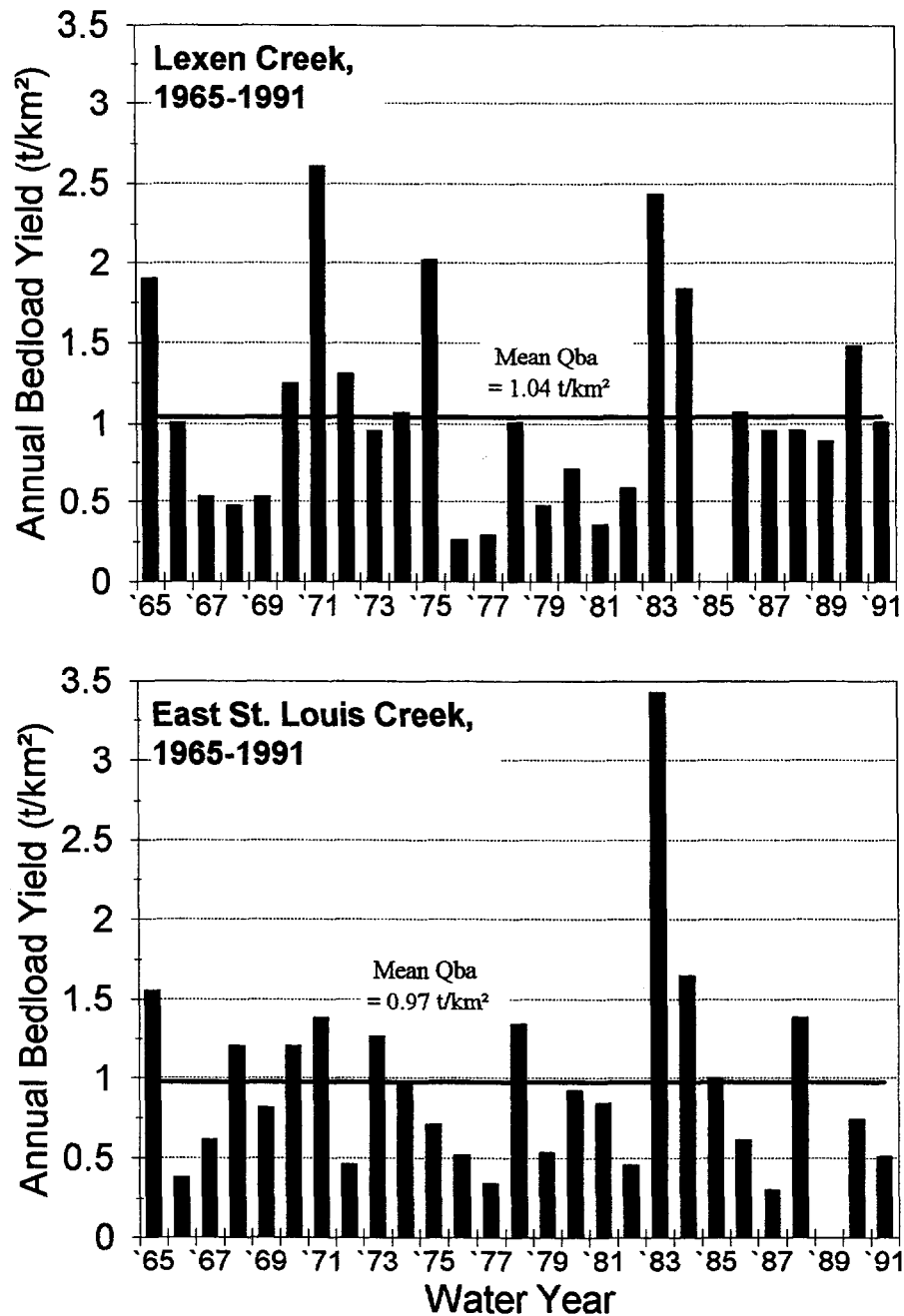


Fig. B-5; 6: Annual sediment yields from two control watersheds (Lexen Creek and East St. Louis Creek) at Fraser Experimental Forest, 1965-1991.

Regression analysis indicated that seasonal streamflow could account for 56% of the annual variability in sediment loads on East St. Louis Creek, but only 30% of the annual sediment load for Lexen Creek. If the 26 years of record are broken into three successive periods that were somewhat wetter, drier, and wetter than average, it can be seen that the correlations between runoff and sediment yields were generally stronger during the wet periods and very poor for the intervening dry period (Table B-5; 4). The relationship between flow and sediment yield was generally stronger for East St. Louis Creek than Lexen Creek.

**Table B-5; 4:** Correlation coefficients ( $r^2$ ) of linear regressions of annual sediment yields versus seasonal flow (April-Sept.) for various time periods for the undisturbed basins East St. Louis Creek and Lexen Creek at Fraser Experimental Forest, Colorado.

Time Period	East St. Louis Creek	Lexen Creek
1965-1990	0.56	0.30
1965-1974 wet	0.60	0.25
1975-1982 dry	0.13	0.17
1983-1990 wet	0.61	0.33

A comparison of the annual sediment yields from these two basins indicates a relatively weak relationship for the total period of record and all periods except the wetter years from 1983-1991. The rather high  $r^2$  for this last period appears to be due primarily to the high bedload yields in both 1983 and 1984 data in both catchments. These high sediment yields extend the range of data, and this generally increases the correlation coefficient.

**Table B-5; 5:** Mean annual sediment yields and seasonal stream flow for various time periods at East St. Louis Creek and Lexen Creek, Fraser Experimental Forest, Colorado, and the coefficients of determination for linear regressions between the annual sediment yields of the two watersheds.

Time Period	Mean Annual Sediment Yield (t/km <sup>2</sup> )			Mean Seasonal Flow (April-Sept.) (mm)	
	E. St. L. Cr.	Lexen Creek	$r^2$	E. St. L. Cr.	Lexen Creek
1965-1991	0.97	1.09	0.37	357	437
1965-1974 wet	0.99	1.17	0.12	371	447
1975-1982 dry	0.71	0.72	0.12	305	386
1983-1991 wet	1.20	1.39	0.78	387	476

The previous chapter showed that at Hubbard Brook the prediction of annual sediment yield could be improved when the annual maximum instantaneous flows were used for prediction rather than mean annual flows. But the concentration on the highest flows is not necessarily the remedy for improved bedload yield estimates for all streams. At the Fraser Experimental Forest, Troendle (1993) found that the best predictor for annual sediment yield was the number of days which equalled or exceeded bankfull flow (Table B-5; 6). Bankfull flow is approximated by 93 l/s·km<sup>2</sup> at East St. Louis Creek, and 104 l/s·km<sup>3</sup> at Lexen Creek.

**Table B-5; 6:** Coefficients of determination ( $r^2$ ) between the duration of various flow levels and annual sediment yields for two control basins at Fraser Experimental Forest (from Troendle, 1993).

	Coefficients of Determination ( $r^2$ )	
	East St. Louis Cr.	Lexen Cr.
N (years)	22	27
Peak flow	0.61	0.21
Total flow	0.59	0.16
Duration* > 66 l/s·km <sup>2</sup>	0.35	0.03
Duration > 87 l/s·km <sup>2</sup>	0.53	0.26
Duration >109 l/s·km <sup>2</sup>	0.74	0.50
Duration >130 l/s·km <sup>2</sup>	0.64	0.28
Duration >153 l/s·km <sup>2</sup>	0.30	0.23

\* number of consecutive days in which indicated flow is equalled or exceeded

This comparison of inter- and intra-basin variability for undisturbed basins at the Hubbard Brook and Fraser Experiment Forests shows that the value of mean annual sediment yield is affected by the runoff conditions of the time period chosen. Generally, wetter years produce higher sediment yields (Tables B-5; 3 and 5). At Hubbard Brook, wetter years had a slightly lower variability in annual sediment yields (Table B-5; 7). This lower variability may have contributed to a poorer relationship between the sediment yields of adjacent, undisturbed basins. On the other hand, the pronounced response of sediment yields at Hubbard Brook to higher flows during drier years caused a greater variability of annual sediment yields and, in turn, a better relationship between annual sediment yields in neighboring basins. In contrast, the behavior of the two control basins at Fraser Experimental Forest was generally less predictable. Variability of annual sediment yields, the correspondence between neighboring basins, and the predictability by annual flow varies less systematically between wetter and drier periods.

Snowmelt-dominated areas are often presumed to be less variable than rain-dominated areas, but even in the former the minimum CV for annual sediment yields is 50% (Table B-5; 7). Values of 100% can easily be obtained, and there appears to be no support for the hypothesis that a longer record will decrease the coefficient of variation.

**Table B-5; 7:** Coefficient of variation (in percent) for various time periods for undisturbed watersheds at Hubbard Brook and Fraser Experimental Forest. Time periods in the left-hand column are for Hubbard Brook; time periods in the extreme right-hand column are for Fraser.

Time period	Hubbard Brook			Fraser		Time period
	WS 1	WS 3	WS 6	E. St. L. Cr.	Lexen	
1966-1990	-	-	99	66	60	1965-1991
1966-1973	-	-	121			
1975-1990	80	64	91	41	55	1965-1974 wet
1975-1982 wet	60	47	76	45	50	1975-1982 dry
1983-1990 dry	106	85	111	83	41	1983-1991 wet

These results indicate that for a typical calibration period of 3-5 years, one could obtain either a very good or a very poor relationship between annual sediment and water yields, depending upon the streamflow patterns of the years used for calibration. The ability to detect a change in sediment yield would vary accordingly. If a well-correlated period was used for calibration and this was followed by years of poor correlation, the estimated effect of treatment could be seriously in error. Interbasin comparisons of water yields are usually much stronger than the interbasin comparisons of sediment yields. Comparisons over time on a single basin (e.g., prior to and after treatment) are only valid if they are conducted over periods with similar patterns of bedload transport.

## **5.5 Comparison of variability of sediment yields in disturbed and undisturbed basins**

The analyses of annual sediment yields from undisturbed basins indicated a relatively large variability in annual sediment yields, varying responses to flows, and a surprising degree of inconsistency between neighboring basins. This information is critical for evaluating the next question, which is the relative effect of management activities on the mean and variance of annual sediment yields.

### **5.5.1 Difference in mean and coefficient of variation in disturbed and undisturbed basins**

The difference in mean annual sediment yields between managed and unmanaged catchments can be very large or only slightly noticeable (Table B-5; 1). In the Pacific Northwest the mean annual sediment yield in managed basins was approximately three times larger in the Alsea watershed, and about seven times larger for the H.J. Andrews Experimental Station, than in undisturbed basins. If an extreme event occurs shortly after management or if management triggers an extreme event like a debris flow, annual sediment yield can increase up to about 30 times the background  $Q_{sa}$  (e.g., WS 3, H.J. Andrews Experimental Forest).

At Fraser Experimental Forest in central Colorado, mean annual sediment yields from managed basins are about twice the values from control watersheds. At Caspar Creek in northern California annual sediment yields are generally very high, but the difference between a logged and unlogged catchment was only 7%. At Hubbard Brook in New Hampshire, managed basins have a sediment yield 1-3 times larger than the control basins, but the differences between control (unmanaged) basins can be almost as large.

The extensive literature on the effects of forest harvest indicate that forest management activities will generally increase the amount and variability of annual sediment yield, and the corollary is that control watersheds should have the lowest mean and the lowest variability within an Experimental Forest. The data presented in Table B-5; 1 indicate that this is generally the case. Only at the Alsea watersheds did the control catchment have a slightly mean annual sediment yield as well as a higher standard deviation in terms of tons per square kilometer per year. However, it is also of interest to note that the relative variability, expressed in terms of a coefficient of variation, was not consistently lower in the control catchments as compared to the managed catchments.

The general conclusion from this overview is that mean annual sediment yield is likely to increase as a result of management, but it does not necessarily follow that there will be an increase in the interannual variability when expressed in relative terms as a coefficient of variation. The implication is that the natural variability of sediment yield in undisturbed basins is so high that it is difficult to identify any added variability due to management. This view is supported by findings from Ferguson et al. (1991) and Olive and Rieger (1991).

### 5.5.2 Amount and duration of sedimentary effects in disturbed basins

The comparison of the three control watersheds at the Hubbard Brook Experimental Forest showed that drier years tended to have more intrabasin variability and less interbasin consistency with regard to annual bedload yields. At Fraser Experimental Forest the intrabasin variability and interbasin consistency showed little evidence of being systematically related to annual runoff patterns. The next step in evaluating the detectability of CWEs is to determine how the pattern of annual sediment yields varies between undisturbed and disturbed basins. A poor correlation will further compromise the ability to detect management changes, while a more consistent relationship will facilitate the detection of change. An additional confounding factor in the comparison of sediment yields between disturbed and undisturbed basins is the rate of recovery. **Table B-5; 1** clearly shows that disturbed basins will generally have a higher annual sediment yield, but a rapid reduction in this additional sediment yield will reduce the strength of the relationship between the disturbed and undisturbed basins, and thereby hinder the detection of significant change, particularly in view of the high interannual and interbasin variability.

#### *Hubbard Brook*

A comparison of mean annual sediment yields for various periods after disturbance shows a clear but relatively short-term increase in annual sediment yields at Hubbard Brook, and a smaller long-term effect. One of best-known disturbed watersheds is WS 2, and this was felled in 1965 but no wood was removed. The watershed was then sprayed with herbicides to prevent revegetation for several years. The expected increase in sediment yield began after a two-year delay in 1967 and continued for about six years. Exceptionally high sediment yields were observed in 1969 and especially 1970 (**Fig. B-5; 7**). Mean annual bedload increased to 12.5 t/km<sup>2</sup> over the 8-year period (1966-1973) following the initial clearing, and this is four times the mean bedload yield of 3.15 t/km<sup>2</sup> obtained for the post-logging period of 1975-1990 (**Table B-5; 8**). The observed increase in sediment yields was attributed to the release of sediment stored behind decomposing logs in the stream (Bilby 1981).

The post-logging period can be divided into a wetter phase (1975-1982) and a drier phase (1983-1990). During this first period sediment yields were relatively low (**Table B-5; 8**), and this suggests that the initial supply of sediments had been flushed away. Thus the consistency of annual bedload yield between WS 2 and the control (WS 6) was rather low ( $r^2 = 0.33$ , **Table B-5; 2**). The patterns of annual sediment yield between WS 2 and WS 6 come back into phase in about 1982 or 1983, or more than 15 years after the initial clearing, and this leads to a relatively high  $r^2$  of 0.86 for the period 1983-1990 (**Table B-5; 2** and **Fig. B-5; 7**).

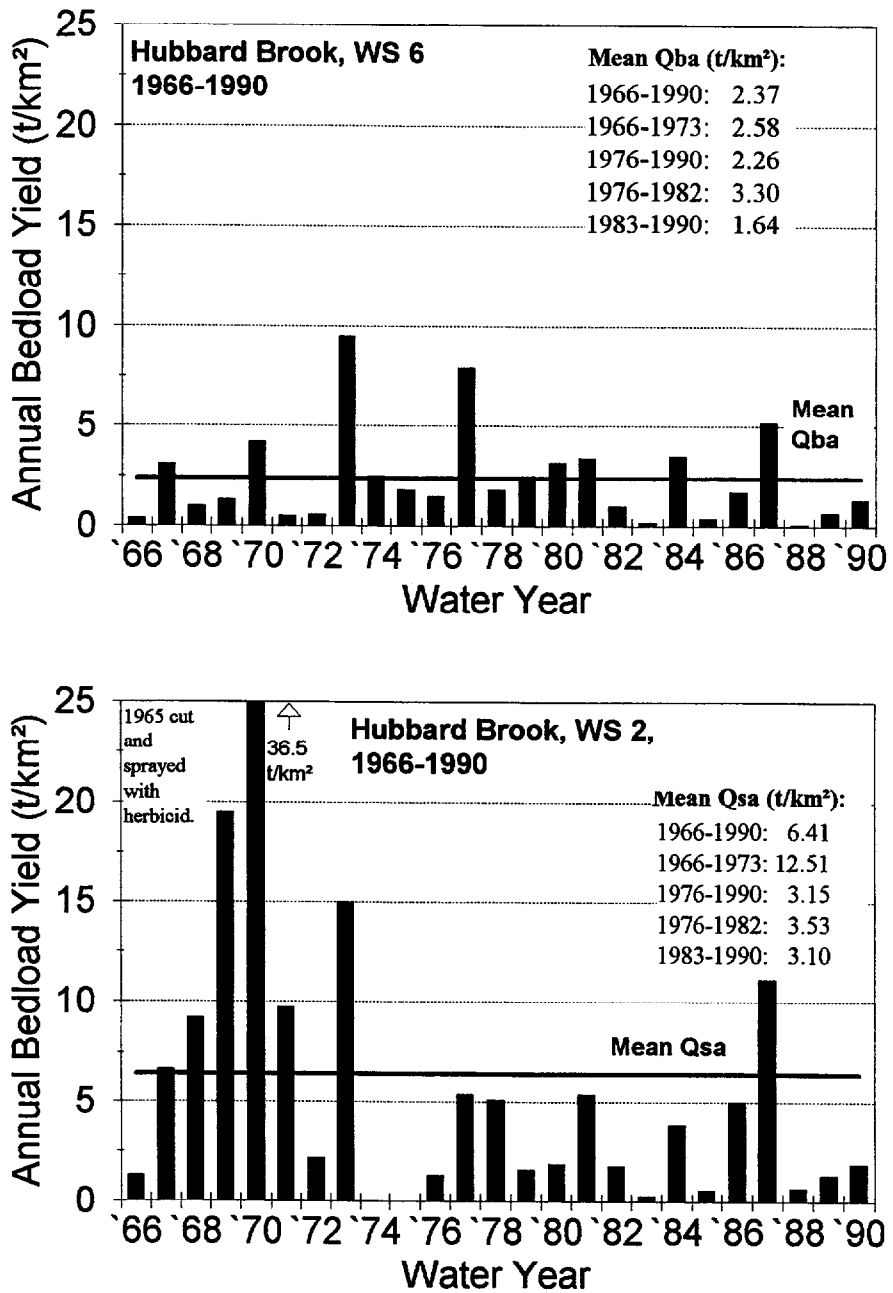


Fig. B-5; 7: Annual sediment yields from the undisturbed WS 6 and the disturbed WS 2 at the Hubbard Brook Experimental Forest from 1966 to 1990.

WS 5 is the other treated watershed at the Hubbard Brook Experimental Forest, and the pre-disturbance sediment yield for WS 5 was more than twice that of WS 6 (Table B-5; 3 and 8). During the calibration period of 1975-1983 WS 5 showed a similar pattern in annual

**Table B-5; 8:** Mean annual bedload yields (t/km<sup>2</sup>) for disturbed basins at Hubbard Brook and Fraser Experimental Forest for various time periods.

Time period	Hubbard Brook		Fraser, Deadhorse Cr.			Time period
	WS 2	WS 5	North	South	Main	
1966-1990	6.41	-	-	-	1.93	1965-1991
1966-1973	12.51	-	-	-	1.62	1965-1974 wet
1975-1990	3.15	6.82	2.35	1.95*	2.11	1975-1991
1975-1982 wet	3.21	6.25	2.09	1.21	0.92	1975-1982 dry
1983-1990 dry	3.10	7.40	2.59	2.60	3.09	1983-1991 wet
Year of disturbance	1965	1983/84	1981	1977/78	1983	

\*1976-1990

sediment yields to WS 6 (Fig. B-5; 8) as indicated by a  $r^2$  of 0.61 (Table B-5; 2). In water year 1984 WS 5 was clearcut with use of heavy machinery. Annual sediment yields in the next three years were 6, 3 and 2 times the expected sediment yield as determined from the regression with WS 6. These three years of high sediment yields increased the mean sediment yield for the drier period of 1983-1990 by 118%, while annual sediment yields in all the undisturbed basins declined relative to the previous eight years (Table B-5; 10). From about 1986 or 1987, or approximately three years after treatment, the pattern of annual sediment yields seems to again follow WS 6 (Fig. B-5; 8). The relative shortness of the obvious sedimentary impact may be due in part to the low runoff in the following years (1988-1990) which results in relatively low sediment transport capacities.

The coefficient of variation of mean sediment yield (Table B-5; 9) tends to show a slight increase during the period of maximum change in the annual sediment yield in the disturbed watersheds. Nevertheless, the coefficient of variation was always lower in WS 5 than in the

**Table B-5; 9:** Coefficient of variation (in percent) of mean annual bedload yields (t/km<sup>2</sup>) for disturbed basins at Hubbard Brook and Fraser Experimental Forest for various time periods.

Time period	Hubbard Brook		Fraser, Deadhorse Cr.			Time period
	WS 2	WS 5	North	South	Main	
1966-1990	128	-	-	-	110	1965-1991
1966-1973	91	-	-	-	99	1965-1974 wet
1975-1990	91	83	91	71**	113	1975-1991
1975-1982 wet	61	67	86	88	118	1975-1982 dry
1983-1990 dry	117	96	96	52	92	1983-1991 wet
Year of disturbance	1965	1983/84	1981	1977/78	1983	

\*\*1976-1990

undisturbed WS 6 (Table B-5; 9). This might be explained by the fact that the mean sediment yields in undisturbed basins are relatively low and can easily vary by a factor of 2 or 3.

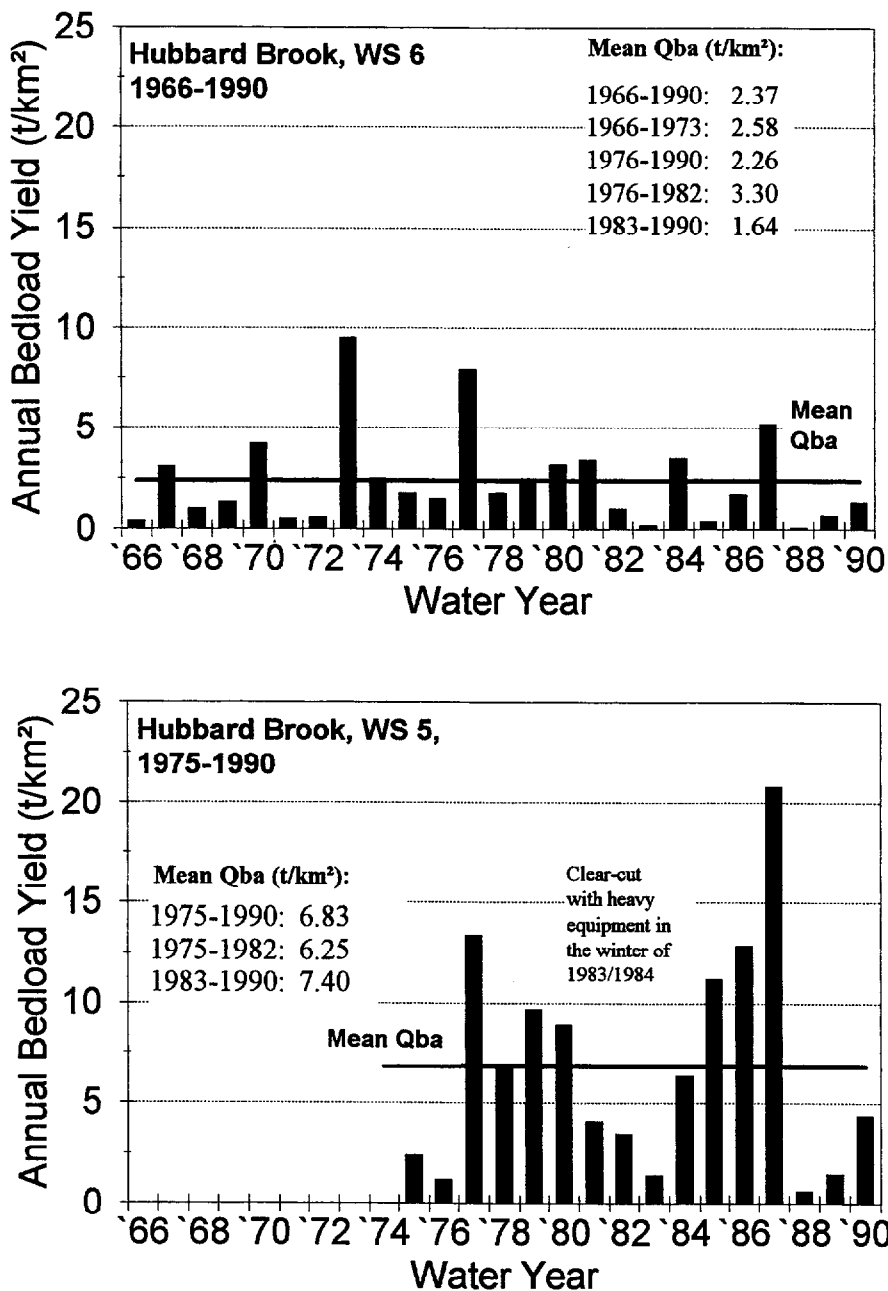


Fig. B-5; 8: Annual bedload yields from the undisturbed WS 6 and the disturbed WS 5 at the Hubbard Brook Experimental Forest from 1966 to 1990.

**Table B-5; 10:** Percent difference in mean and CV of annual sediment yields between a wet (1975-1982) and dry (1983-1990) period at Hubbard Brook, and a dry (1975-1982) and wet (1983-1991) period at Fraser Experimental Forest.

	Hubbard Brook					Fraser Experimental Forest				
	undisturbed			disturbed		undisturbed		dist., Deadhorse Cr.		
	WS 1	WS 3	WS 6	WS 2	WS 5	E.S.L.*	Lexen	North	South	Main
Mean	-48	-18	-43	-3	118	169	193	117	215	336
CV	177	181	146	192	143	169	-18	124	-41	-22

\* E.S.L. = East St. Louis Creek

### **Fraser Experimental Forest**

The pattern of runoff within the last two decades at Fraser Experimental Forest is contrary to that in Hubbard Brook—a wet phase followed by a dry phase. This led to almost a doubling (169 and 193%, respectively) of the mean sediment yields during the wetter phase in the two undisturbed basins, East St. Louis and Lexen Creek (Table B-5; 10). The timber harvest in Deadhorse North and Deadhorse South occurred in 1981 and 1977/78, respectively, which is within the first, drier period of 1975-1982. The upper parts of the Deadhorse Creek, Main, basin were logged in 1983, which marked the beginning of the wetter period. In the disturbed basins the mean annual sediment yield during the wetter phase was either slightly increased (Deadhorse North) or doubled (Deadhorse South) when the disturbance still occurred in the dry phase (Table B-5; 8 and 10). Sediment yields tripled in Deadhorse Main, as the disturbance during the wetter phase combined with the effects of climate (Fig. B-5; 9).

The relative variability of mean annual sediment yields in the Fraser Experimental Forest appears to be more a function of the basin characteristics than the presence or absence of disturbance. Deadhorse Main, for example, consistently has a higher CV than Deadhorse South or North. Similarly, the increase in mean sediment yields seems to be due more to the shift towards wetter conditions than an increase due solely to management (Table B-5; 10). In contrast, the effects of disturbance are equal to or larger than the effect of a wetter period versus a drier period (Table B-5; 10). Both disturbed watersheds at Hubbard Brook also showed a small increase in their CV during the drier period. While these results would be affected by the relative magnitude of the change in climatic conditions, they indicate that the variation in discharge is a confounding factor, and the importance of this factor can vary considerably. The implication is that short-term changes in annual sediment yield must be carefully analyzed for climatic influences.

The occurrence of wet and dry periods at Fraser Experimental Forest had a less systematic effect on the correlations between the different control watersheds than the climatic variations at Hubbard Brook. We also found that a slight shift in the timing of an interbasin comparison could have a dramatic effect on the quality of the relationship as indicated by the coefficient of determination. For example, the  $r^2$  for the regression between Lexen and East St. Louis Creeks drops from 0.65 for 1976-1982 to 0.12 if the period is extended by one year to include 1975. This difference is due to the relatively high sediment yield of Lexen Creek in 1975, as this is not reflected in the annual runoff nor in the 1975 sediment yields for any other basin. A even greater sensitivity to the range of data can be seen in the change in  $r^2$  between Deadhorse North and Deadhorse South with the control watershed of Lexen Creek; in these examples a one-year increase in the time range decreases the  $r^2$  from 0.83 and 0.94 to 0.04 and 0.07, respectively (Table B-5; 11). Similar regressions between

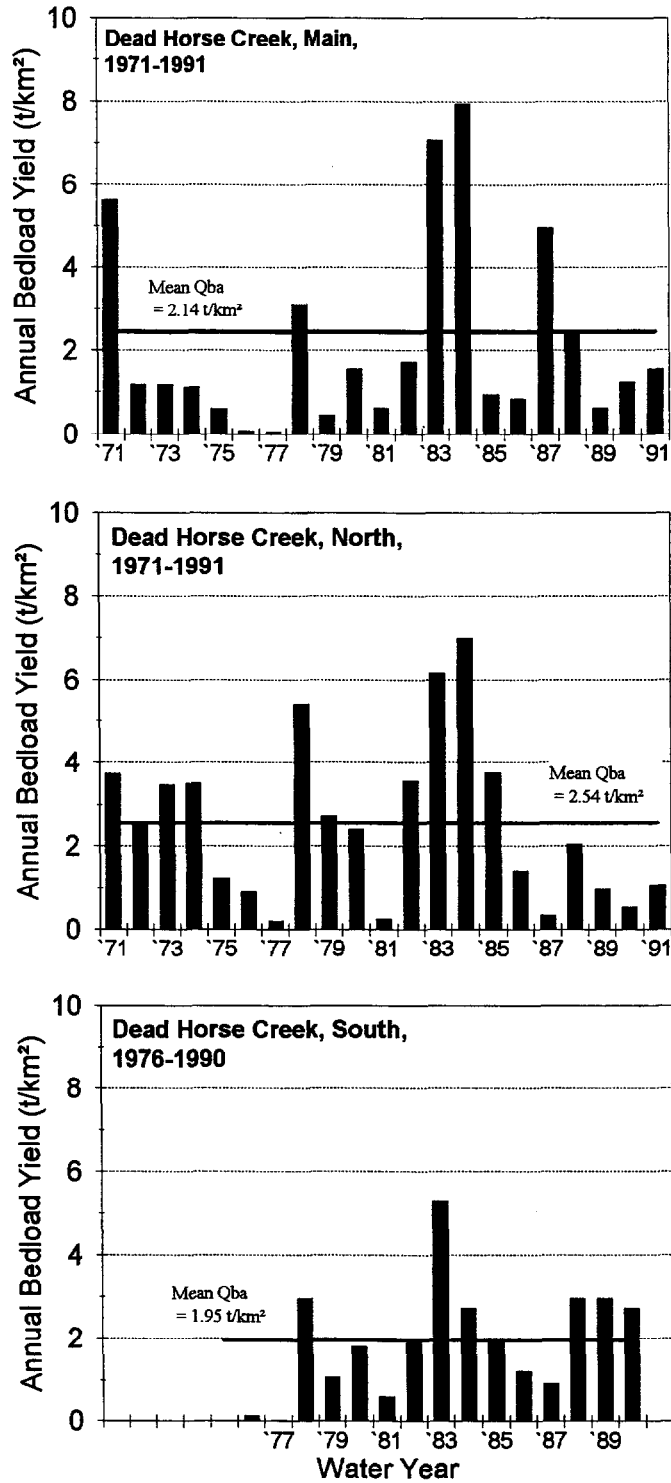


Fig. B-5; 9: Annual bedload yields from three disturbed watersheds (Deadhorse Creek - Main, Deadhorse Creek - North, and Deadhorse Creek - South) at Fraser Experimental Forest, 1965-1991.

the two Deadhorse basins (North and South) with the control watershed of East St. Louis are relatively immune to this shift because none of these basins had a high sediment yield in 1975. In general, the  $r^2$  values obtained for the drier period at Fraser Experimental Forest are lower than the  $r^2$  values obtained from the wetter period of 1983-1991 with its correspondingly higher sediment yields (Table B-5; 11).

**Table B-5; 11:** Regression equations for annual sediment yields between undisturbed (Lexen and East St. Louis Creek) and disturbed watersheds (Deadhorse Creek North, South, and Main) at Fraser Experimental Forest for the entire period of 1975-1990, the period of high sediment yield (1975-1982), and the period of low sediment yield (1983-1990)<sup>#</sup>. (*a* is the slope, *b* is the y-intercept, and *StE* represents the standard error of the regression.)

	Entire period 1975 - 1991		Low sediment yield Drier period 1975 - 1982		High sediment yield, Wetter period 1983 - 1991		
Lexen Creek and East St. Louis Creek, undisturbed	<u>Lexen &amp; East.St. Louis</u>		<u>Lexen &amp; East.St. Louis</u>		<u>Lexen &amp; East.St. Louis</u>		
	<i>a</i>	0.84		0.19		1.67	
	<i>b</i>	0.09		0.57		-1.10	
	$r^2$	<b>0.48</b>		<b>0.12</b>		<b>0.78</b>	
	<i>StE of y</i>	0.59		0.33		0.53	
North Deadhorse Cr., logged in 1981	<u>NDH &amp; Lex</u>	<u>NDH &amp; ESL</u>	<u>NDH &amp; Lex</u>	<u>NDH &amp; ESL</u>	<u>NDH &amp; Lex</u>	<u>NDH &amp; ESL</u>	
	<i>a</i>	1.77	2.05	0.64	3.21	3.97	2.07
	<i>b</i>	0.52	0.40	1.63	-0.20	2.87	0.10
	$r^2$	<b>0.27</b>	<b>0.53</b>	<b>0.04</b>	<b>0.33</b>	<b>0.67</b>	<b>0.66</b>
	<i>StE of y</i>	1.97	1.58	1.90	1.87	1.72	1.75
South Deadhorse Cr.**, logged in 1977/78	<u>SDH &amp; Lex</u>	<u>SDH &amp; ESL</u>	<u>SDH &amp; Lex</u>	<u>SDH &amp; ESL</u>	<u>SDH &amp; Lex</u>	<u>SDH &amp; ESL</u>	
	<i>a</i>	1.98	1.53	3.91	2.26	2.21	1.31
	<i>b</i>	-0.03	0.32	-0.86	-0.39	-0.58	0.87
	$r^2$	<b>0.76**</b>	<b>0.78**</b>	<b>0.95**</b>	<b>0.54**</b>	<b>0.71</b>	<b>0.89</b>
	<i>StE of y</i>	0.75	0.72	0.25	0.79	0.95	0.57
Main Deadhorse Cr., logged in 1983	<u>MDH &amp; Lex</u>	<u>MDH &amp; ESL</u>	<u>MDH &amp; Lex</u>	<u>MDH &amp; ESL</u>	<u>MDH &amp; Lex</u>	<u>MDH &amp; ESL</u>	
	<i>a</i>	2.47	2.22	0.46	2.53	3.57	1.76
	<i>b</i>	-0.26	0.16	0.69	-0.78	-1.26	1.54
	$r^2$	<b>0.42</b>	<b>0.50</b>	<b>0.07</b>	<b>0.61</b>	<b>0.48</b>	<b>0.42</b>
	<i>StE of y</i>	1.95	1.82	1.09	0.71	2.31	2.44

<sup>#</sup>Data from 1985 and 1989 were not available from Lexen and East St. Louis Creeks, and for this reason these two years are not included in any regression.

\*\*Years 1975 and 1991 not included in any regression with Deadhorse South Creek, because no data are available.

Summing up the effects of disturbance on sediment yield shows that management impacts generally increased the annual sediment yield. The extent of the increase is at least partly dependent on the length of the time interval for comparison between disturbed and control watersheds, and the climatic conditions during the period of comparison. There does not seem to be a consistent change in the relative variability of annual sediment yield with

disturbance. At Hubbard Brook the interbasin consistency of annual sediment yields between disturbed and undisturbed basins was slightly lower during wetter periods with higher sediment yields. At the Fraser Experimental Forest the reverse was true, in that there was somewhat greater consistency in annual sediment yields between disturbed and undisturbed basins during wetter periods with higher sediment yields. The inclusion or exclusion of a single year with anomalously high or low sediment yields can greatly affect the strength of the relationship between two basins.

### 5.5.3 Predictability of annual sediment yield from interbasin comparisons

#### *Hubbard Brook*

The predictability of annual sediment yields in a paired watershed analysis can be assessed from the coefficient of determination and standard error of a regression between the two watersheds. **Table B-5; 2** provided a matrix of the regressions: (1) between the undisturbed basins in the Hubbard Brook Experimental Station (WS 1, 3, and 6); (2) between each of the disturbed basins (WS 2 and 5) and each of the undisturbed basins. The regression statistics are shown for both the entire period of record, and for the wetter and drier subperiods, and the latter data clearly shows the dependence of the regressions on the selected interval. At Hubbard Brook both the coefficient of determination and the standard error of the regressions between the undisturbed basins were markedly better for the drier time periods with generally low annual sediment yields (**Table B-5; 2**). On the other hand, the strength of the regressions for the entire period of record are generally not that strong, even among the undisturbed basins. Thus the inclusion of a disturbed period may not necessarily have that large of a detrimental effect on the relationship between basins. Of course a larger degradation in the regression would be expected with a greater change in sediment yields, particularly if that change was only present for part of the post-disturbance period.

#### *Fraser Experimental Forest*

The corresponding matrix of regression equations for watersheds at the Fraser Experimental Forest is shown in **Table B-5; 11**. In contrast to Hubbard Brook, the interbasin comparisons were generally stronger for the wetter period than for the drier period. There was not any distinct difference in the strength of the regressions between the undisturbed basins as compared to the relationships between the disturbed and the undisturbed basins. This suggests that, at least for the levels of disturbance at Fraser, the climatic effects and the interbasin variability are at least as important as the management effects.

So far, the results of this study agree with Olive and Rieger (1991) who found that suspended sediment concentrations following disturbance were frequently within the observed range prior to disturbance. Since the natural variability was greater than the magnitude of the increase associated with basin disturbance, Olive and Rieger (1991) suggested that research should focus on the analyses of the processes acting in disturbed and undisturbed basins. Ferguson et al. (1991) also found that the effects of logging on suspended sediment concentration could not be determined by a paired watershed analysis because the natural variability of suspended sediment concentration was too large. Ferguson et al. (1991) concluded that sufficient pre-disturbance monitoring is essential to quantify the natural variability.

## 5.6 Variability: years of record needed and downstream change

As discussed in Section B-2.4.2, it is possible to estimate the number of years of data needed to determine the mean annual sediment yield ( $Q_{ba}$ ) within a certain percentage of the long-term mean. This requires both the coefficient of variation (CV) and the underlying distribution of the annual series of sediment yield data. This information can then be used to determine what magnitude of change can be detected over what time period.

### 5.6.1 Coefficient of variation

The previous chapters showed that the mean and CV of annual sediment yields are very sensitive to the time period over which they are determined. While wetter or dryer periods consistently led to an increase or decrease, respectively, in the mean annual sediment yield for that period, the variability could be either increased or decreased. Since it is not possible to determine a consistent adjustment factor for these changes due to climatic variation, the only possible approach is to use the CV determined over the entire period of record. If the record is relatively short, then it may be helpful to evaluate the CV for other basins for various overlapping periods to assess the representativeness of the short record.

The coefficients of variation for small catchments of 0.1 -10 km<sup>2</sup> (Table B-5; 2) are summarized below:

38%	at Carnation Creek in the Vancouver Coast Range,
52 - 141%	for Piceance River and its tributaries in western Colorado,
31 - 114%	for large rivers in Montana with drainage areas of 730-179,000 km <sup>2</sup> ,
66 - 105%	for small basins in the Fraser Experimental Forest in Colorado,
64 - 128%	for small basins in the Hubbard Brook Experimental Forest in New Hampshire,
74 - 128%	in the Alsea Watershed of the Oregon Coast Range,
90 - 130%	at Caspar Creek in northern California,
105 - 156%	for tributaries and upper reach of the Deschutes River, Washington Cascades,
122 - 466%	for small basins in the H.J. Andrews Experimental Forest in the Oregon Coast Range.

A key question is whether higher sediment yields are generally associated with a higher CV. A plot of the data from Table B-5; 2 (Fig. B-5; 10) provides some indication of a positive relationship between these two characteristics. A power function regression between CV and  $Q_{sa}$  yielded the equation

$$CV = 66.81 \cdot Q_{sa}^{0.118}, \quad (1)$$

and a correlation coefficient  $r^2$  of 0.24. Thus there does appear to be some increase in CV with increasing mean annual sediment yields ( $Q_{sa}$ ). Since CV is a relative measure, the flatness of the regression means that the dominant trend is that the absolute variability tends to increase more or less proportionally to the increase in mean annual sediment yields.

### 5.6.2 Distribution type and number of samples needed

The *W*-test developed by Shapiro-Wilk (Gilbert 1987) was run for all data sets to determine the underlying distribution (see Section B-2.1.3). Most series of annual sediment yield were

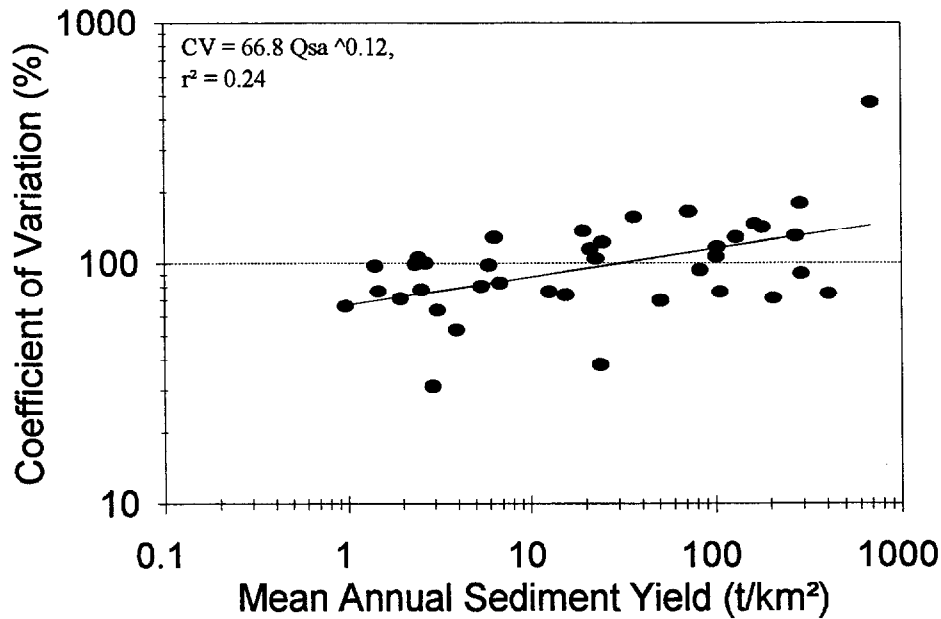


Fig. B-5; 10: Coefficient of variation versus mean annual sediment yield for 38 basins.

lognormally distributed as suggested by Van Sickle (1981). For almost one-third of the data sets the null-hypothesis of a Gaussian distribution could not be rejected at a 95% significance level. These Gaussian distributed data sets were characterized by relatively low coefficients of variation (38-83%). If the CV exceeded 83%, the distribution was lognormal.

The number of years of record needed for the mean annual sediment yield to be within a certain percentage of the true mean annual sediment yield can be calculated for Gaussian distributed data sets employing the equation:

$$n_{min} = \left( \frac{1.96}{c} \cdot CV \right)^2 \tag{2}$$

where  $n_{min}$  is the minimum number of samples (or years in this case), 1.96 is the tabulated value for 95% confidence intervals, and  $c$  is the level of accuracy with  $c = 0.2$  if the estimated mean  $Qba$  is to be within 20% of the true mean  $Qba$  (see Section B-2.4.2). The number of years needed for the sample mean to be within 10, 20, 30, 50 and 100% of the population mean was calculated for all data sets and these are listed in **Table B-5; 1**. For those data sets that are not normally distributed it is assumed that equation 2 gives at least a rough approximation of the minimum number of years needed. **Table B-5; 12** indicates the minimum length of record needed for a very low value (38%) and a low range (70-83%) of CV.

For Gaussian-distributed data sets with exceptionally low annual variability (38%), more than 50 years of record are needed if the mean annual sediment yield is to be within 10% of the true mean. If the level of accuracy is reduced to 30%, only six years of record are

**Table B-5; 12:** Number of years of record for annual sediment yields needed for the sample mean to be within 10, 20, 30, 50 and 100% of the population mean for Gaussian distributed time series of annual sediment yields.

Coefficient of Variation (%)	<u>Percent difference between sample mean and true mean</u>				
	10%	20%	30%	50%	100%
38	56	14	6	2	1
70-83	200-263	47-66	20-25	7-11	2-3

needed. For basins with more typical, but still low CVs of 70-83%, more than two centuries of data records are needed for a 10% accuracy. For 30% and 50% accuracy, 20-25 years and 7-11 years, respectively, are still required. If we assume a typical calibration period of 3-7 years, this means that the mean annual sediment yield can only be estimated to an accuracy--at the 95% confidence level--of slightly less than 100%.

### 5.6.3 Downstream decrease of annual variability in sediment load

To evaluate the importance of scale considerations in sediment yield it is necessary to know if the variability of sediment yield changes downstream. One might expect that headwater streams exhibit more variability in annual sediment yields than larger rivers because they are more subject to specific storm- or sediment-producing events. The question of scale can be further refined according to the constituent of concern--i.e., is the annual variability of suspended sediment concentrations more scale-dependent than annual yields of bedload? If the temporal scale is changed from annual to intra-event or seasonal variability, does that affect whether there is a scale-dependence of suspended or bedload sediment yields? Ideally, this analyses could be conducted on high-resolution data sets from undisturbed nested basins that extend across a relatively wide range of spatial scales. Unfortunately there are no locations where such data sets are readily available, as the larger basins within the experimental forests are composed of a matrix of disturbed and undisturbed basins, and sediment transport data are often not available at this larger scale.

A search through the USGS Water Resources Data Base yielded only two data sets from mountainous areas in the western U.S. that had sediment yield data from a series of nested basins over a sufficiently long and overlapping time period. The more complete data set covered seven common years of nested basin data for Piceance Creek and its left-hand tributaries in the White River Basin in northwestern Colorado (Section C: 4.1.1). In order to determine if the variability of annual sediment yields systematically changes in a downstream direction or with increasing catchment size, the coefficient of variation was calculated for the seven common years of data. These values were then plotted versus drainage basin size for four stations on Piceance Creek and three tributary stations (Fig. B-5; 11). The data show no systematic variation in relative variability in a downstream direction. The uppermost station on the mainstem at Piceance Creek did have a relatively high CV, while the CV was virtually constant for the next three stations downstream. The three tributaries, all of which had smaller drainage areas than the first station on the mainstem of Piceance Creek, had CVs that were similar to the stations further downstream (i.e., less than the first mainstem value on Piceance Creek). The importance of a common data period is demonstrated by determining the CVs for the full data sets for the three upper stations at Piceance Creek. The additional two to four years of data at these stations would nearly

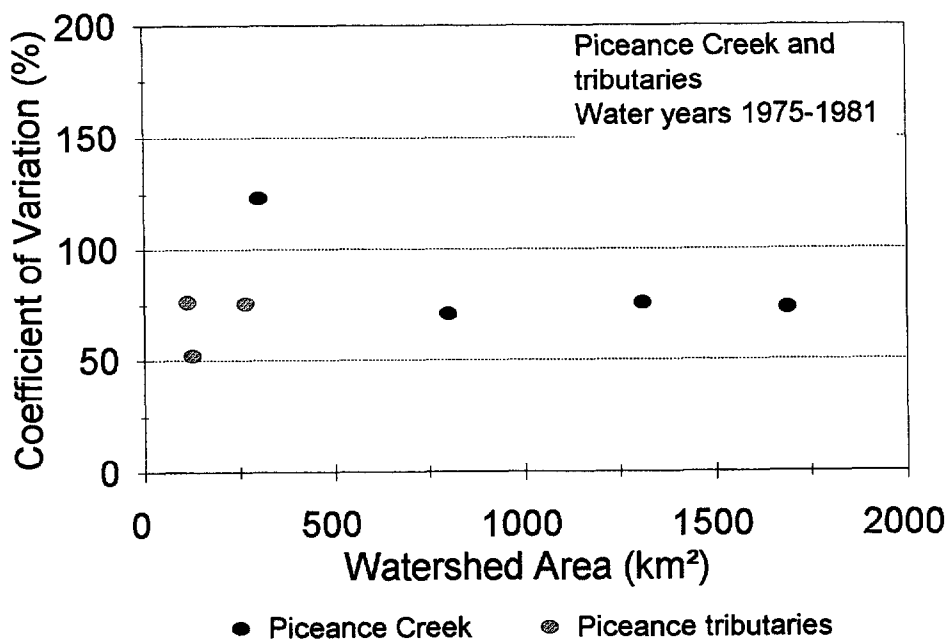


**Fig. B-5; 11:** The coefficient of variation of annual suspended sediment yield for Piceance Creek in northwestern Colorado and its tributaries as a function of basin area. Data were calculated from values measured from 1975 to 1981, inclusive.

double the respective CV values, and this was due to some exceptionally large annual suspended sediment yields within these additional years.

In an additional, cruder attempt to detect a downstream change in CV, we simply plotted the CVs for all the data in **Table B-5; 1** against watershed area (*A*) (**Fig. B-5; 12**). Although these data extended over more than six orders of magnitude, a power function regression yielded the equation:

$$CV = 101.05 \cdot A^{-0.020}, \tag{3}$$

which had a *r*<sup>2</sup> of only 0.031. The negative exponent indicates a slightly decreasing trend, but area could only explain 3% of the variability in the coefficient of variation. Given the wide range of CVs present in the data and the numerous other factors which have been shown to affect the variability of annual sediment loads, we cannot presume any relationship between spatial scale and a change in relative variability in the downstream direction.

The results shown in **Fig. B-5; 12** suggest that it is a great oversimplification to expect a decrease in the variability in annual sediment loads in the downstream direction. We know that disturbance increases the mean annual sediment load, but this may not affect the CV unless the disturbance is of sufficient magnitude to cause a large (e.g., 5-10 fold increase) over a relatively short time period. For such a disturbance to affect the variability of downstream sediment yields, the increased sediment yield must be transported downstream.

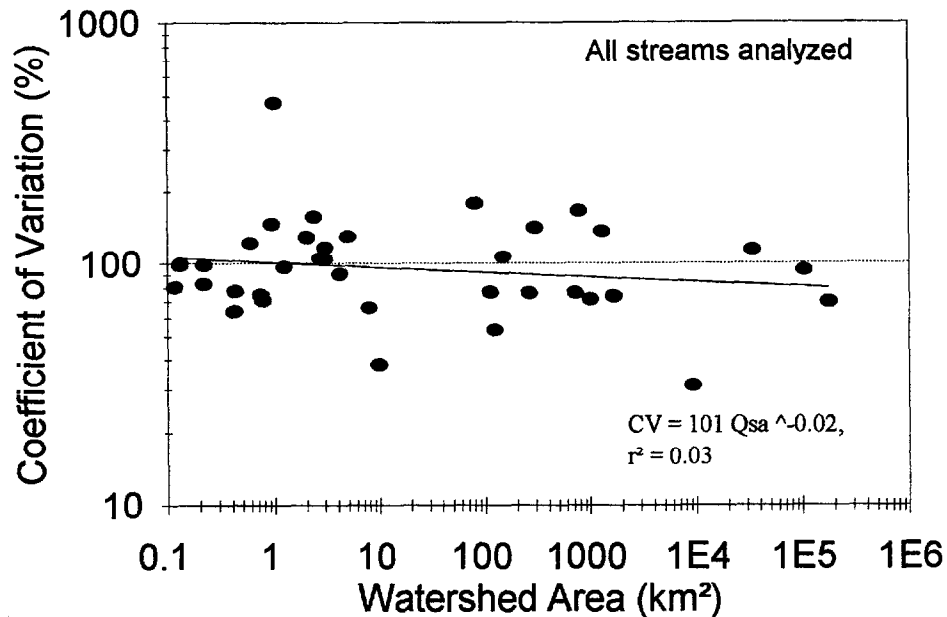


**Fig. B-5; 12:** Coefficient of variation of annual sediment yield versus watershed area for 38 basins.

In reality, increased sediment yields will usually originate from various causes, occur in different parts of a basin, and be distributed over various time periods.

For example, mining activities in many areas of the Rocky Mountains introduced large amounts of sediment into the headwater creeks as well as into some of the larger streams. The concurrent need for fuelwood and construction timber led to extensive clearing, and this may also have increased the supply of sediment logging. Hydraulic mining and dredging greatly altered the amount of sediment available to the streams in both small and large valleys.

Similarly, the forested watersheds in the Pacific Northwest have been subjected to logging and road-building activities. In the absence of buffer strips or best management practices, these activities caused substantial increases in sediment yields. The key question is how are these increased sediment yields translated downstream, and this is not a simple question of spatial scale. The downstream movement of coarse sediment will depend on factors such as the change in water yield as well as the change in sediment yield, the amount of available storage due to large woody debris, and the downstream succession of stream types. Aggradation is the expected response in low-gradient gravel-bed rivers where the channel gradient decreases, but this will not necessarily be the case in all stream systems.

A primary reason why we might assume a downstream decrease in the variability of annual sediment yields is that much of the sediment supplied to the stream is commonly stored within the fluvial system. This stored sediment can be used to build a floodplain or alluvial fan, or slowly released as the upstream supply wanes. Mountainous areas in the eastern parts of the U.S. have already gone through one or more cycles of logging. These sediments were deposited in the stream system, but have since been reentrained and still being reworked within the fluvial system. Many of the flatter streams in the eastern and

central parts of the U.S. were also subject to extensive siltation as a result of clearing and agriculture. With the introduction of soil conservation methods and the return of some areas to forest cover, the sediment input into the streams was decreased and the rivers started to cut through their former deposits. Thus the original sources of sediment may be largely eliminated, but the rivers are maintaining their sediment load by reworking existing deposits.

Both natural and anthropogenic disturbances can occur in any part of the watershed and cause a temporary disequilibrium in any part of the stream system. It is not possible to generalize that the variability of sediment transport is either larger in the upstream reaches or in the downstream reaches. A local investigation of where the stream is disturbed is necessary to those reaches where a change in sediment transport is to be expected. Measurements can be concentrated at the site of the impact or at the projected sites which will be most affected. In the latter case the downstream effects can appear over time scales ranging from days to decades or more.

## **5.7. Sedimentary response in the years following the large event**

The previous section suggests that after a certain amount of sediment has been mobilized following a disturbance, the increase in mean annual sediment yield over a 2-year period, for example, could be negligible if the mobilized sediment has not yet arrived, or relatively severe if the sediment was rapidly transmitted through the intervening stream reaches. Quantification of a disturbance effect by a statement like "sediment yield increased by x% over the predicted value in the first two years" may be misleading or of limited value, since it does not indicate how much sediment is still to be expected. The true extent of the sedimentary watershed disturbance can only be evaluated after all the mobilized material has passed the reach. From a regulatory point of view, the change in sediment yield then has to be related to some resource or designated beneficial use, and this linkage may be difficult or fraught with uncertainty.

The effect of anthropogenic activities on sediment and other resources can be expressed in terms of severity, duration, and lag time. Given the variability discussed in the different sections of this report, it is usually difficult to predict the full range of a sedimentary response to watershed disturbance. The following sections, as well as the next chapter, present some concepts and tools that might be used to predict and define a sedimentary response.

### **5.7.1 Cumulative sediment yield**

One technique to identify the response in annual sediment yield to a storm or major watershed disturbance is to plot the cumulative annual sediment yield. Three kinds of response can be identified and associated with watershed and sediment transport conditions as follows (Fig. B-5; 13):

- 1) Post-impact sediment yields remain high, indicating either a continuing disturbance or a slow rate of travel, a wide longitudinal dispersion, or a release of stored sediment;
- 2) Post-impact sediment yields remain low, indicating a depletion of sediment from the drainage system;
- 3) Post-impact sediment yields return back to normal, indicating that the excess material has been flushed out of the system above the measuring point.

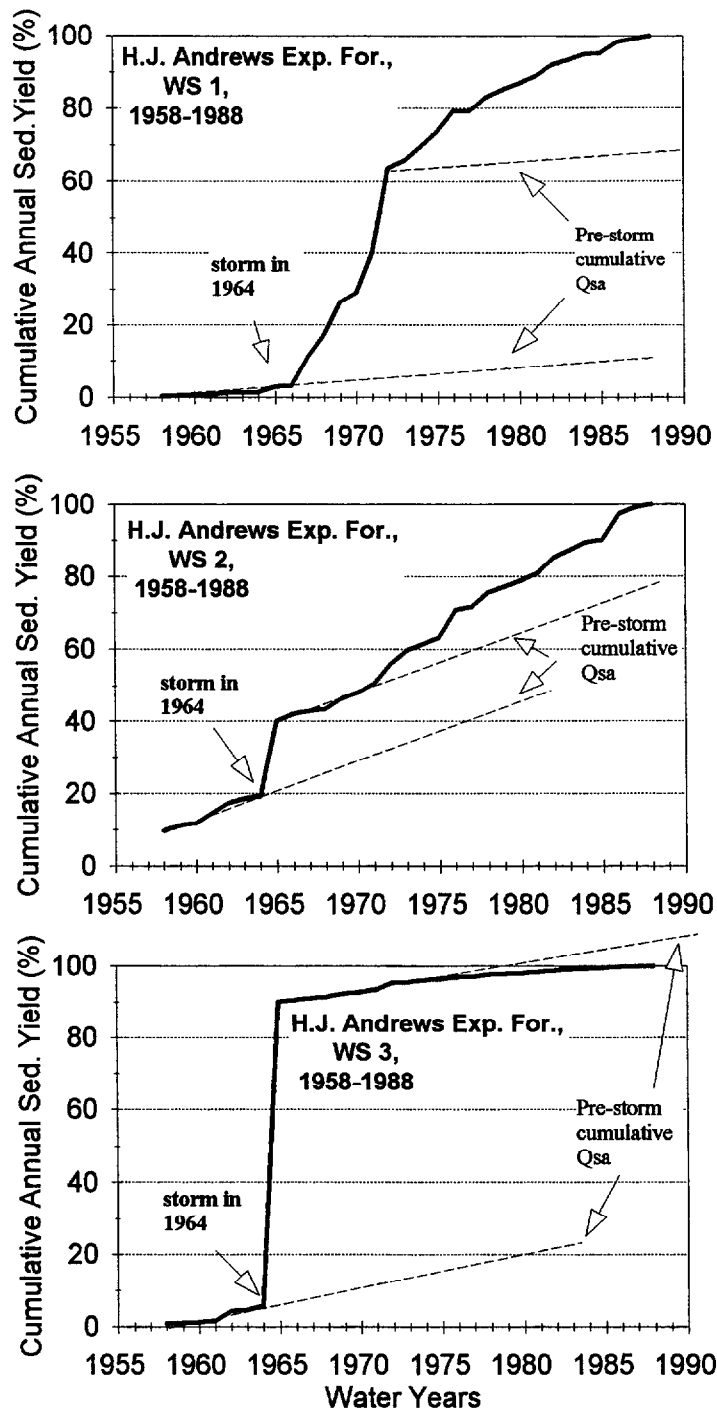


**Fig. B-5; 13:** Three different responses of watersheds to management impacts at the H.J. Andrews Experimental Forest, 1958-1988 (after Grant and Wolff 1991).

Post-impact sediment yields remain high when the effects of a large sediment pulse due to a storm or other disturbance persist for a number of years. This can be due to the continuing release of sediment from upstream storage areas or destabilized hillslopes and channels, both of which can provide a continuous source for high sediment yields for consecutive smaller events. Increased sediment yields following a major event have been observed at the Deschutes River in Washington (Sullivan et al., 1987:51-55) and in Watershed 1 at the H.J. Andrews Experimental Forest (Fig. 2 in Grant & Wolff, 1991).

The opposite response, which is below-average annual sediment yields after the disturbance, can occur when the upstream sediment sources have been emptied by increased flows or by a major sediment transport event, leaving little sediment available for transport in by subsequent flows. Examples include WS 3 in the H. J. Andrews Experimental Forest (Fig. 2 in Grant and Wolff, 1991) and WS 2 at Hubbard Brook, where sediment depletion was observed after deteriorating logs no longer provided any sediment storage (Bilby 1981).

The third possible response is a relatively rapid return to pre-disturbance conditions, indicating that the excess material has been flushed through the system. This has been observed in headwater streams in the Deschutes following road construction in erosion-resistant volcanic rocks (Sullivan et al. 1987) and in the H.J. Andrews undisturbed control watershed 2 after a storm.

### **5.7.2 Time until first response occurs**

The response time for sediment depends on the distance between the input and the measuring location, and on the rate of travel of introduced sediments. The rate of travel is highly dependent on the grain size and on the question whether the sediments are already in the stream or still on the slopes. Naturally, slope, channel and flow conditions further affect the travel velocity and travel distance of sediment. (see chapter C-4). Ketcheson (1986) reported a 6 year delay in response to logging operations for a 163 ha Silver Creek tributary until a higher than average spring high flow triggered the emptying of the sediment storage and caused a shift in the rating curve. However, road building in an adjacent 102 ha tributary in proximity to the stream prompted an immediate response in terms of increased sediment concentrations. Sullivan et al. (1987) found the same immediate response of suspended sediment to road building in a small headwater tributary to the Deschutes River. However, the coarse fraction of suspended sediment concentration took a 4 year delay in its response to debris flows that entered the stream 15 to 20 km upstream in the Deschutes River headwater areas. Megahan et al. (1986) also examined the volumes and travel velocity of slope deposits originating from road construction in granitic basins in Idaho. Over a 4 months period (June to October) they measured mean and maximum travel velocities from fill slopes, which produced relatively little sediment, to be 6 and 64 m, respectively. Culvert deposits, producing much more sediment, travelled at a much faster rate of 32 m (mean) and 118 m (maximum).

A cumulative plot of annual sediment yields can be an appropriate tool to identify how far along the watershed is with its response. However, a geomorphological analysis of the watershed drainage system might be the best method to predict how much more sediment is to be expected from a particular disturbance. The prediction of the arrival time of this sediment requires some knowledge about the dispersion and travel time of different sediments in different stream types.

## 5.8 Summary

This chapter has shown that the interannual variability of annual sediment yields is quite large. Very few records of annual sediment yields have a coefficient of variation of less than 50%, and most values are closer to 100%. Values of 100-150% appear to be quite common, and in basins subject to extreme sporadic events, such as landslides or debris flows, the CV can be several hundred percent. The variability in annual sediment yields for undisturbed watersheds tends to be slightly larger for watersheds in the Pacific Northwest than for basins in Colorado or New Hampshire. There is a weak tendency for the relative variability, as indicated by the coefficient of variation, to increase with increasing sediment loads, but there appears to be no significant relationship between basin size and the relative variability of annual sediment yields. This means that despite the tendency for sediment yields to diminish in the downstream direction, we cannot expect a downstream reduction in interannual variability.

Basins with a low CV tended to have a normal distribution of annual sediment yields, while basins with higher CVs tended to have a lognormal distribution of annual sediment yields. Although there is a wide range of variability, approximately a decade of monitoring is needed to estimate the annual sediment yields to within 50% of their true value at the 95% confidence level.

The data collected and analyzed in this study also showed a relatively high interbasin variability, even within a single experimental forest. In some cases the measured sediment loads on one basin explained less than 10% of the variability on an adjacent undisturbed basin. We also found a wide variability in the strengths of the relationship between various flow parameters (e.g., maximum annual flows, annual water yield, or duration of a given flow) and annual sediment yields. Depending on the hydrological and sedimentological conditions of the basin, the interbasin predictability may be better or worse for wetter periods as compared to drier periods. In many cases the strength of the relationship, as indicated by the  $r^2$  value, can change quite dramatically with a change in the time period being compared, or even with the addition or exclusion of a single year.

The data clearly indicate that forest management activities increase the annual mean sediment yield, but this does not necessarily mean that there is a concomitant increase in the variability of the annual sediment loads. The extent and duration of the sedimentary response varies from basin to basin, and this means that the observed change in the mean and variability of annual sediment yields will be highly dependent on the length of the post-disturbance period chosen for analysis.

The true extent of the sedimentary watershed disturbance can only be evaluated after all the mobilized material has passed the reach, and this could take a few days, several storms, or more than several decades. Geomorphological field assessments and plots of cumulative sediment yields can help identify how far along the watershed is with its response, how much more sediment is to be expected, and the potential for various sources of sediment to overlap and create a sedimentary CWE.

## Part C: Downstream Transport of Sediment

### 1. Introduction

The previous chapters showed that individual sediment transport measurements, load estimates, and determinations of mean annual sediment yield are of rather low accuracy. This was attributed to the high temporal and spatial variability of sediment transport, the poor or inconsistent sampling efficiencies, and low sampling intensities. Since annual sediment yields may be only poorly correlated to annual runoff or the annual sediment yields of neighboring basins, there is considerable uncertainty in determining whether a significant change in sediment yield has actually occurred in response to management. Some of this uncertainty can be reduced if care is taken in choosing the location of sampling, the devices for sampling, and the allocation of sampling effort. It is also necessary to decide what level of certainty is desired, and then assess whether the proposed monitoring regime is likely to achieve those objectives given the natural variability, the period of record, the degree of change that one wishes to detect, and when an answer is desired (or possible).

Although the sampling issue has been discussed in some detail, the location of sampling has only been briefly mentioned in conjunction with these other topics. Altering the locations of sampling is another means to improve the detectability of a change in sediment transport or sediment loads. In theory, the most sensitive location to detect a change in sediment supply is as close as possible to where the additional sediment enters the stream. This presumes that the sediment source can be clearly defined, and most land management activities create diffuse, nonpoint sources of sediment. Sediment can also be delivered to the stream by means of various pathways such as road ditches, surface erosion from compacted areas, gullies, debris flows, and unstable hillslopes. An increase in water yield can also lead to the generation of additional sediment from within the stream channel due to streambed erosion, bank erosion, or the collapse of log jams. Sampling headwater streams can also pose difficulties with regard to access, and the duration of high flow events will also be shorter in headwater locations. Finally, the increase in sediment yield at an upstream location may be of limited significance because it does not directly affect a designated beneficial use.

If sediment sampling close to the various sediment sources is a difficult or unrewarding task, sampling needs to be concentrated further downstream where sediment from various sources has combined. However, the further one goes downstream, the more difficult it becomes to attribute a sedimentary effect to a particular watershed disturbance. It has also been repeatedly documented that as sediment travels downstream, an increasing proportion of the sediment is deposited and can remain in storage over time periods ranging from minutes to centuries. As the introduced slug of sediment becomes dispersed over increasingly longer increments of space and time during its downstream travel, the increase in sediment concentration or transport rates are diminished in the downstream direction until the effects may be lost in the extensive background "noise". On the other hand, the effects of several watershed disturbances may combine and overlap to produce a sedimentary CWE when each individual effect may not be individually recognizable. In order to predict, and hopefully avoid, sedimentary CWEs, the downstream travel behavior of sediment needs to be investigated.

This more explicit analysis of spatial scale considerations focusses on the questions of: (1) where might we expect sedimentary CWEs within the stream system; and (2) where might

we best detect sedimentary CWEs. Even though these are the fundamental issues which initiated the study, their explicit consideration is dependent on the fuller understanding of the physical processes, measurement uncertainty, and natural variability in sediment transport at different scales. The determination of where to look requires a knowledge of how far sediments are likely to travel per unit time, as only then can we predict when the sediment from a particular source or disturbance is likely to pass through a specific monitoring location, or be deposited in a particular stream reach. All monitoring is of little use if one "misses" the sediment passage because it has not yet arrived, or because it has already passed through. Predicting the arrival of various slugs of sediment introduced from upstream areas is a difficult task because the rate of sediment travel depends on numerous factors. Prominent among these are the size of the introduced sediment, its predominant transport mode (suspended or bedload), the energy available for sediment transport (which in turn depends on stream gradient, flow depth, and flow velocity), the stream type and sediment regime (transport-limited or supply-limited), the sequence of stream types between the source area and the location of concern, and the frequency and magnitude of runoff events. The following sections will discuss each of these topics in more detail.

#### ***Prediction of downstream sediment yield***

Several potential methods exist to estimate downstream sediment yield. The predictive options fall into two main categories: the Eulerian and the Lagrangian approach. The Eulerian (synoptic) approach quantifies sediment loads at a series of downstream locations. Once the downstream variation of cross-sectional sediment loads is known, their differences can be compared and the reaches with maximum sediment transport rates indicate the current location of the sediment wave in the stream system. If there are several reaches with high transport rates and these reaches progress downstream at different speeds, the potential for synergistic sedimentary effects can be foreseen. However, this approach requires a high sampling effort to accurately measure sediment transport at multiple locations in the stream system.

Eulerian methods can vary with respect to sampling effort and the sediment sizes to be addressed. An upstream-downstream comparison of sediment loads will require a high sampling effort, and this may incorporate all sediment sizes. The application of sediment transport formulas to the annual hydrograph will result in a greatly reduced accuracy but requires little sampling effort. The prediction of downstream sediment loads is easiest for clays and other fine sediments for which deposition can be neglected. Thus downstream sediment loads become a function of the dilution or enrichment which can easily be calculated from estimated discharges over time and their respective concentrations of fine sediment. All sediment is subject to deposition and storage within the stream system, and this storage of sediment with increasing basin size is the basis for the widely-used sediment delivery ratios. As will be discussed later, these curves appear to be basin or region-specific, and they implicitly assume a universal ratio regardless of grain size or stream types.

Lagrangian methods follow sediments through the fluvial system rather than relying on the sequential synoptic views of the Eulerian approach. In principle the Lagrangian approach attempts to quantify both the transport distance and the rest periods of the various particles of interest. One common technique is tracer studies, which monitor or track the downstream movement of sediment. This method can be used for all particles sizes, provided that the sediment has either natural properties that can be traced (e.g., petrology, natural magnetism), or that the particles can be "fingerprinted" by attaching an artificial tracer (e.g., dye, magnetization, radioactive substances). The monitoring effort depends on the tracer detectability and dispersion of the tracer particles. Another possibility to assess downstream sediment transport is through the use of high-resolution sediment routing models (Stow and Chang 1987; Chang and Stow 1988, and 1989).

### ***Geomorphological analysis of channel change***

A third category of methods is the analysis of the local sedimentary state of the stream. Annual comparisons of the volume of sediment stored within a reach can determine if the reach is aggrading or degrading, and this may indicate whether a sediment wave is arriving at a reach or is leaving it. Another geomorphological approach is to repeatedly analyze the downstream variability in stream bed parameters such as channel geometry and bed material sizes, as these parameters can also be used to indicate the sedimentary state of a channel reach. This topic will not be discussed here, but a recent study under the direction of the second author of this report provides an excellent literature review and identifies those variables which best indicate the effects of forest management (Madsen 1994).

The next two sections of this study (Chapters C-2 and C-3) will discuss several Eulerian approaches to determine the downstream sediment yield. This includes the applicability of delivery ratio curves, and a discussion of how sediment delivery ratio curves could be modified to account for the variation in stream types and sediment transport conditions. This is followed by a discussion of how one might predict the downstream concentration of the fine sediment that is not subject to much storage in the downstream direction, and how the detectability of a change in these concentrations will vary according to different dilution scenarios.

The last part of this section (Chapter C-4) tackles the Lagrangian approach. The few systematic studies show that the downstream travel of coarser sediment is quite intermittent across various temporal scales, and that micro- and macro-scale stream morphology plays a major role in determining transport distances. We also review the more numerous case studies that report the travel distances for a particular flood event or series of events, and the limitations of these studies with respect to their temporal duration (i.e., there are very few tracer studies that have extended for a year or more).

## **2. Sediment Delivery Ratios**

### **2.1 Definition and development**

One potential method of addressing the downstream delivery of sediment is through the use of sediment delivery ratios. The sediment delivery ratio (*DR*) is defined as the ratio of the sediment exported from a basin (sediment yield) to the amount of sediment produced in the basin by erosion processes. Hence the delivery ratio is determined by erosional processes as well as by transport processes. Since a decrease in *DR* with increasing basin size is the usual rule, sediment delivery ratios implicitly refer to the relationship between the sediment delivery ratio and basin size.

This concept of *DR* curves was invented in order to predict the siltation of reservoirs by fine material exported from agricultural or rangeland basins through the fluvial system without measuring sediment yields (Maner and Barnes, 1953). Basin area sediment production is assessed by either mapping local erosion volumes or by calculating areal sheet erosion losses with formulas like the USLE (Wischmeyer and Smith, 1978). A sediment delivery ratio curve can then be used to estimate mean annual sediment yield for a given basin area. The negative relations between *DR* and the size of the catchment area are commonly described by negative power functions in the form of:

$$DR = a \cdot A_d^{-b} \quad (1)$$

where  $A_d$  is the drainage area, and  $a$  and  $b$  are coefficients.

A number of sediment delivery ratio curves has been developed in different agricultural and rangeland areas (e.g. Maner and Barnes 1953; Glymph 1954; Maner 1958). Roehl (1962) and Renfro (1975) collected data from several authors and combined them in a single  $DR$  curve. Both curves are identical, but Roehl's (1962) curve includes the wide variation of  $DR$ s for a given basin size. The variability of  $DR$  curves is also indicated by Piest et al. (1975). The American Society of Civil Engineers, however, gives only a single  $DR$  curve in their handbook on Sedimentation Engineering (ASCE 1975). The National Engineering Handbook published by the Soil Conservation Service (USDA 1983) again shows a wide band around their  $DR$  curve indicating the wide variability of  $DR$ s for a given basin area. Another fairly recent collection of published  $DR$  curves is provided by Walling (1983) (Fig. C-2; 1), and he makes no attempt to combine all the published  $DR$  curves into one "universal" curve.

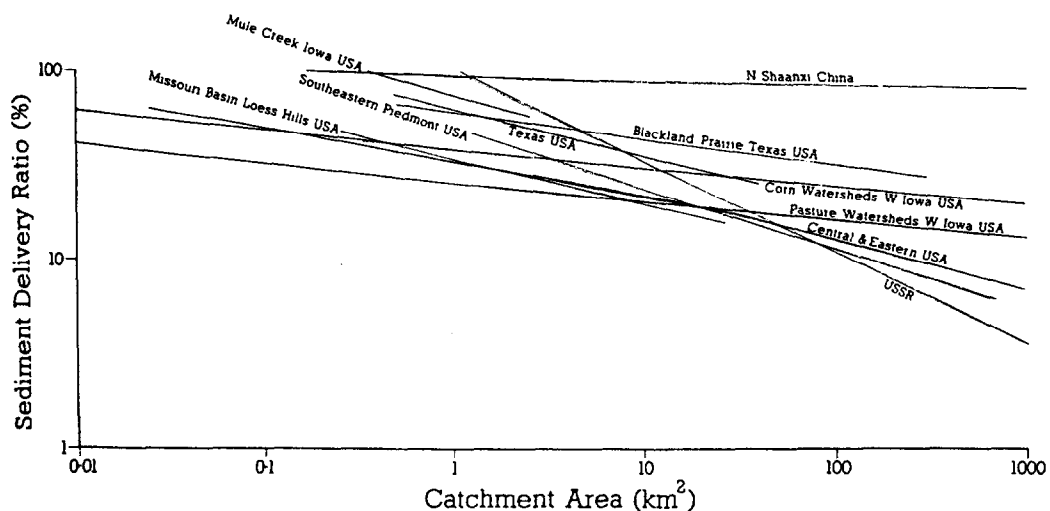


**Fig. C-2; 1:** Relationship between sediment delivery ratio and drainage basin area for different regions based on data from Roehl (1962), Sokolovskii (1968), Piest et al. (1975), Renfro (1975), A.S.C.E. (1975), Williams (1977), and Mou and Meng (1980) (from Walling 1983).

The downstream delivery of sediment would be greatly facilitated if one could determine whether there is a common or "typical" exponent for  $DR$  curves. For agricultural or rangeland catchments in hilly areas of the USA the exponents tend to scatter around -0.2 (Roehl 1962; USDA 1983). It is of interest to note that the slope of the USDA curve is slightly different than the  $DR$  curves from Roehl (1962) and Renfro (1975), even though the range of the data is the same as Roehl (1962). This difference might be due to the fact that the National Engineering Handbook took an arithmetic mean of the data range to produce their  $DR$  curve instead of a power function regression. The general negative exponent of  $DR$  curves as proposed by the American Society of Civil Engineers is only -0.125, leading to a less steep curve and therefore less storage. Walling (1983) shows that  $DR$  curves from other geographic areas can deviate substantially from the curves developed in the U.S. The variation in the delivery ratios for a given basin size and the exponents ( $b$ ) of generalized  $DR$  curves from published collections are given in **Table C-2; 1**.

**Table C-2; 1:** Reported values for the exponent (*b*) and variability in the range of *DRs* (in percent) for various drainage basin areas in published collections of *DRs* and *DR* curves.

Reference	Drainage basin area (km <sup>2</sup> )				Exponent of power function regression
	1	10	100	1000	
Roehl (1962)	15-70	10-45	5-25	2-10	-0.23
A.S.C.E. (1975)	-	-	-	-	-0.125
Walling (1983)	30-90	20-60	10-40	4-20	-
U.S.D.A. (1983)	15-65	10-45	5-25	2-10	-0.24

## 2.2 General applicability of *DR* curves

If reliable measurements of sediment yield are not available, a delivery ratio curve is a tempting tool to estimate sediment yield for a given downstream location. The only required input variables are basin size and an estimate of sediment production. These can be obtained from geographic information systems or other sources. Before advocating the use of *DR* curves, however, it is necessary to evaluate two key questions with regard to the applicability of this methodology, and these are: (1) the interbasin and temporal variability of *DR* curves, and (2) the downstream variability of *DR* curves.

### 2.2.1 Interbasin and temporal variability of sediment delivery ratios

Sediment production and transport processes are controlled by many different factors which fall under the terms basin physiography and management impacts. Both can be highly variable among catchments. This means that both disturbed and unimpaired basins will feed a variety of sediments into the streams at different rates. Once the sediment is in the stream system, its transport rate depends on flow and stream conditions. All the variability in physiography, sediment production, and transport rates from different stream type will in turn be reflected in temporally- and spatially-varying sediment delivery ratios.

Walling (1983) provides an excellent review which discusses the problems that occur when temporal and spatial processes of sediment production and transport are lumped into a *DR*. Following Walling's review, an abundance of literature appeared that highlighted several aspects of the variability of delivery ratios in adjacent basins and the temporal and interbasin variability of *DRs*. Matherne and Prestegard (1988), for example, show how different parts of the basin vary in their hydrologic response to rainfall. Different subcatchments then varied in their sediment production and sediment delivery.

Roberts and Church (1986) calculated *DRs* for four small (4-13 km<sup>2</sup>) undisturbed, fourth- to fifth-order watersheds in coastal British Columbia. The geographical conditions were similar for all four streams, but the catchments differed in their geology. *DRs* at the drainage basin outlets varied from 0.3 to 0.9 and **increased** with drainage basin size. Post-logging *DRs* varied in an unsystematic manner from 0.1 to 0.8. A comparison of the pre- and post-logging *DRs* showed changes ranging from an increase, indicating high sediment input and transport, to a decrease, suggesting that the presumed increase in sediment production due to logging had not yet reached the measuring station. In other cases there was no apparent trend in the *DRs* following forest harvest. The results show that there was tremendous

variability in the *DR* curves among basins, and these curves changed in an unpredictable manner following management activities.

Stott et al. (1986) found the *DR* for suspended sediment yields to be close to 1 in a paired watershed (forested and moorland) analysis in Scotland, indicating that virtually all of the suspended sediment left the basins. In contrast, the *DR* for bedload was 0.7 in the forested catchment and only 0.03 for the moorland catchment. In the case of the moorland catchment, the low *DR* suggested that most of the bedload is stored during the high-frequency, low magnitude events, and the low-frequency, high-magnitude events may then empty out some of the accumulated bedload storage.

Megahan et al. (1986) found that 15, 6, and 2 percent of sediment was delivered in three neighboring streams in Idaho following road construction. Although these catchments varied with respect to the number of stream crossings and distances between the roads and the stream, the different delivery ratios were attributed primarily to the road condition and the construction phase when the storms hit.

Coleman and Scatena (1986) found variable *DRs* in suburban Washington D.C. After identifying sediment sources and assessing their delivery potential, they emphasized that the *DR* in multi-source areas includes processes governing both sediment supply (erosion) and transport to the stream channel. They found the density and magnitude of sediment sources to be mainly controlled by land use, while transport and storage processes were mainly controlled by local hillslope topography. Similarly, Novotny et al. (1986) found that *DR* is controlled by runoff energy in agricultural and urbanizing sub-basins, while in urban and suburban sub-basins the drainage paths are more important. Urban drainages with a storm sewer system can have *DRs* as high as 1, while grass swales, common in suburban natural drainages, reduced the average *DR* to 0.1.

Walling and Quine (1991) found *DRs* of agricultural fields in Great Britain to vary between 0.27 and 0.86, depending on the amount of runoff as well as the soil texture and erodibility. Grant and Wolff (1991) also found different responses of suspended and bedload sediment to storm flows after logging in a paired watershed analyses (Fig. B-5; 13) in the previous chapter). Watershed 1 was completely logged, but there was a two-year delay between logging and the onset of what turned out to be a six-year increase in bedload and suspended sediment yields; values then slowly returned to the original conditions. Sediment yields in the nearby control watershed (#2) had a one-year peak in response to a major storm event, then returned to normal for seven years. There was then a continuous increase in sediment yield as the previously-stored sediment finally began to reach the measuring station. In watershed 3 debris slides and debris flows occurred and these reached the stream channel. The resulting high transport rates flushed most of the sediment out of the reach, so subsequent years were left with lower than average sediment yields due to a depleted supply. These different responses of sediment yield to a storm event were attributed to the complex interplay between treatment activities, the timing of the storm events, and differences in geological and geomorphic properties (see Section B-5.8)

Another contribution to the variability of *DRs* is the seasonal and long-term temporal variation of sediment storage. For a small catchment in Luxembourg, Duijsings (1986), reported a winter *DR* of 0.25 to 0.50 when sediment is supplied to near-stream locations or retained in in-stream storage. These stored sediments are flushed out during summer thunderstorms, and this caused the summer *DRs* to range between 1 and 3.5. These seasonal variations mean that the time of sampling can greatly affect the estimated *DR*. The average annual *DR* of nearly 100% indicates a very efficient transport system, and this is due to a rapid breakdown of the soil into particle sizes that are easily transported.

Laird and Harvey (1986) reported an episodic change in basin sediment delivery following a wildfire and large amounts of precipitation. The resulting hillslope erosion led to an accumulation of eroded material in the upper tributaries but a degradation of the main river due to increased runoff. After eight years the hillslopes were stabilized. Then the tributaries degraded, and the outflow of sediment from the tributaries caused aggradation in the main channel. This indicates that drainage basins can undergo cycles of geomorphic states, and the delivery ratios will vary over these cycles and with the scale of the basin being evaluated.

This literature review clearly indicates a high interbasin and temporal variability of *DRs* due to the different processes of both sediment production and sediment transport. This variability is due to both natural and anthropogenic causes. The high interbasin and temporal variability of *DRs* means that one cannot easily transfer *DRs* and *DR* curves from one basin to another, and this is especially true if the interbasin heterogeneity--both natural and anthropogenic--is large. In summary, trying to predict downstream sediment yield with generalized *DR* curves does not seem to be a good option for predicting sedimentary CWEs.

### 2.2.2 Downstream variability of sediment delivery ratios

The second question is whether single, logarithmic *DR* curve can be used to predict the downstream variation of sediment yield. Since a *DR* curve describes continuously decreasing *DRs* in a downstream direction, this implies that an increasing proportion of sediment is being stored on the way downstream. The widely observed spatial variability of delivery and sediment transport processes make it seem very doubtful that a single *DR* curve could be used to predict sediment yields for consecutive downstream locations with increasing drainage areas. The use of a single smooth delivery ratio curve might be justified in very homogeneous areas where sediment production, delivery to the stream, and transport through the stream systems does not exhibit much variability in processes. These conditions might be found in relatively flat or even gently sloped areas with consistent land use, which are the types of catchments for which *DR* curves were originally developed. But forested mountainous catchments, especially after logging operations, do not have a homogeneous sediment budget. Spatially varied processes of sediment production and transport should lead to a downstream alternation of various *DRs*, particularly since there will be considerable variability in particle sizes and stream types. Those parts of a catchment with high sediment production and high sediment inputs into the streams can experience long periods of aggradation, or the streams can be rapidly flushed, depending on stream and sediment characteristics. Other reaches with low sediment production (including the delivery from upstream sources) might be scoured or maintain an equilibrium state.

### 2.3 Modified *DR* curves to detect changes in sediment yield

The previous sections suggested that in steep, forested catchments that are affected by management activities, neither ready-made *DR* curves, nor *DR* curves transferred from adjacent catchments can be used to predict sediment yields at different downstream locations. In topographically complex basins it also seems to be nearly impossible for one *DR* curve to predict sediment yield at various downstream locations. Walling (1983) suggested two alternatives. The first is to fully address the complexity of sediment delivery processes through the development of physically-based erosion and sediment transport models that simulate the interaction between various parameters for small increments of space and time. Since 1983, physically-based soil erosion models such as WEPP (Nearing

et al. 1989; Lane et al. 1993), RETIC (Baird et al. 1993), EROSION 2D (Schmidt 1993), and EUROSEM (Morgan et al. 1992) have been developed to predict soil detachment, transport, and deposition in agricultural environments, but these models each have their limitations (e.g., WEPP is not intended to simulate sediment transport in perennial channels or areas larger than a square mile). Any model predictions must be evaluated and verified for different land uses and environments. The middle road or second alternative as suggested by Walling (1983) is to develop models that combine the simplicity of *DR* curves with the (presumed) accuracy and general applicability of more physically-based models.

If one follows this second alternative, which is probably more realistic for most management purposes, modified *DR* curves could be developed and differentiated according to:

- processes of sediment production and delivery to the stream,
- grain sizes and sediment transport processes, and
- sediment storage dynamics and sequence of stream types in the basin of interest.

### **2.3.1 Differentiation according to sediment production and delivery processes**

As the delivery ratio is defined as the ratio of sediment yield to sediment production, Coleman and Scatena (1986) have suggested that the assessment of sediment delivery should distinguish between the production and delivery of sediment from the source to the stream, and sediment transport within the stream system. In mountain environments disturbed by forest management activities, sediment production and delivery to the stream stems from a wide variety of distinct and diffuse sources, both natural and anthropogenic, and there can be a wide range in the amount of sediment produced. For example, Neill and Mollard (1982) estimated that the Old Man River, which drains part of the Rocky Mountains in Canada, contributed only minor amounts of sediment. In contrast, Kronfellner-Kraus (1982) considered mountain torrents in the eastern Alps of Austria to be a large source of sediment.

One important anthropogenic sediment source is forest roads. Numerous studies have documented the effects of road construction and road use on erosion rates and sediment yields (e.g., Trimble and Weitzman 1953; Megahan and Kidd 1972; Megahan et al., 1986, 1991; Weaver and Madej 1981; Weaver et al. 1987; Hagans and Weaver 1987; Reid et al. 1981; Reid and Dunne 1984; Swift 1988). Road cuts and washed-out culverts can produce a large slug of sediment followed by continuing erosion, especially, if road-induced landslides and debris flows are involved. A continuing supply of fine, or in some cases coarse sediments, can come from unpaved road surfaces, road cuts, and gullies that develop from excessive, concentrated road drainage.

Another source of sediment in steep forested catchments are various types of mass movements (Orme 1991; Benda and Dunne 1987; Sullivan et al. 1987; Grant and Wolff 1991). Several studies have documented an increased occurrence of mass movements or debris flows following logging activities (Swanston and Swanson 1976; Klock and Helvey 1976; Swanston 1979, 1981; Swanson et al. 1981; Swanston and Marion 1991).

The proportion of sediment delivered to the stream system and the length of the reach which is subjected to increased sediment are both highly variable. Mass movements often deliver sediments directly to the stream channels. Roadside ditches extend the drainage network and facilitate the delivery of road-derived sediments to the stream system. Such sources are relatively distinct and almost act like point sources. Certain stream reaches (a

section with unstable banks) can also be a fairly distinct source (e.g., Madsen, 1994). Deposits from mass movements, debris fans, or sediment in the channel may be more intermittent deposits that continue to deliver sediment to the streams over a longer time period. In contrast, sediment from soil creep or biogenic transport is delivered to the streams as a much more diffuse source, and is therefore more difficult to quantify.

Several approaches have been used to predict sediment production in steep, forested, mountainous basins. Equations are available to predict sediment yield from forest access roads in different conditions (Reid et al. 1981; Reid and Dunne 1984, Megahan et al. 1991). Dissmeyer (1984) developed formulas to predict slope sediment yields following different logging and post-logging treatments. Sediment yield from heavily disturbed sites (road cuts, mass movement deposits) might be predicted from a USLE-type formula with a "delivery ratio" term to account for the distance of overland travel between the construction site and the receiving stream (Holberger and Truett, 1976). A similar approach was suggested by Kronfellner-Kraus (1982).

A different approach is to explicitly account for the different processes that produce sediment yield. Mutchler and Ritchie (1979) defined the denominator of the *DR* as the sum of sheet erosion, gully erosion, and fluvial erosion. A more recent attempt to predict sediment loads from debris flows was built into the proposed classification for headwater streams by Whiting and Bradley (1993). Using general relations pertaining to slope stability, valley and fluvial geomorphology, and sediment entrainment, headwater streams are classified according to the likelihood of debris flow occurrence, debris flows reaching the streams, and debris flow material being entrained in the stream. An alphanumeric code then predicts the likelihood of a headwater stream to receive and convey debris flow sediments.

Sediment with different properties is produced from these various sources and delivered to the stream system. Thus the sediment delivery varies in accordance with the:

- grain-size distribution,
- rate and total amount of sediment production,
- response to different hydrologic events, and
- spatial location with respect to the channel.

In some cases it may be possible to identify specific conditions and management actions which could lead to "typical sedimentary events". This might be the flush of fines from road surfaces during storms, or the predictable response of gullies during storms, or the sustained contribution of mixed sediments from a debris flow following a major storm. Each of these sources might be characterized with regard to their typical or probabilistic grain-size distribution and delivery to the stream channel. It might then be possible to establish *DRs* and *DR* curves for "typical sedimentary events" by source process and location. While in some basins the interplay between the source, the sediment type (sizes and amounts), and response to specific storms can be used to identify a distribution of "typical sedimentary events", this classification might be impossible in other basins. In the latter basins a different approach, such as the definition of *DRs* and *DR* curves by grain sizes and sediment transport processes, will have to be undertaken.

### **2.3.2 Differentiation of *DR* according to grain sizes and sediment transport processes**

Delivery ratio curves were derived for agricultural catchments where most of the sediment was eroded by surface erosion processes and consisted of particles ranging in size from clay

to silt or sand. Most of these sediments are transported in suspension. Despite the relatively small range of grain-sizes associated with agricultural erosion, the interbasin variability of delivery ratio curves is tremendous. Forest management activities can produce both fine (e.g., from roads) and coarse sediments (e.g., from mass movements or instream sources resulting from direct disturbance or a change in flows). Mountain rivers typically transport a wide range of grain-sizes because they have the necessary transport capacity and because there is a wide range of sediment sizes available for transport. It should not be surprising that a lumping of all these sediment sizes contributes to the variability of sediment delivery curves. Bathurst et al. (1986) therefore proposed that the transport of individual grain-size classes should be assessed separately. Establishing *DR* curves for different grain-size classes should reduce the variability of *DRs* by accounting for the different transport capacity and competence of a given flow for different grain sizes.

Although the transport capacity and competence of a given flow are not just a function of grain size, one could expect that the coarser the sediment, the higher up in the basin they will be deposited or stored. Thus the problem of excess coarse bedload should be kept, at least for a while, in the lower-order streams, while the suspended sediment problem is likely to be rapidly exported downstream to the very low gradient reaches. This transport behavior would suggest relatively flat *DR* curves (exponent of power functions close to 0) for fine sediments and increasingly steep *DR* curves (exponents below -0.2) for increasingly coarser sediment.

It is uncertain how much the development of a set of *DR* curves for selected grain-size classes will improve the predictability of downstream sediment delivery and the likelihood of CWEs. Size-selective sediment transport occurs even within a relatively small range of grain sizes and can lead to different *DRs*. For fine sediment, this variation can be attributed to factors like aggregation, dispersion, and cohesion, which in turn affect entrainment and transport. Peart and Walling (1982) found different *DRs* for the different particle sizes within the suspended load because of the differences in transport efficiency.

For coarse sediments the position of a certain grain size within the overall grain-size spectrum can strongly affect its entrainment and transport behavior (Fenton and Abbott 1977; Komar 1987). A given grain size is much easier to erode and to transport when surrounded by smaller particles than when the same particle is surrounded by larger particles ("hiding factor"). These findings were further developed into the concept of "equal mobility", which means that once coarse bedload starts to be transported, all coarse grain-size classes are transported without any preference for the smaller gravels (Parker and Klingemann 1982; Parker et al. 1982; Andrews 1983; Andrews and Parker 1987). This concept is in opposition to findings from other researchers who observed a grain-size dependence for entrainment and transport rates in response to varying flows (e.g. Ashworth and Ferguson 1989, Shih and Komar 1990a, b; Komar and Shih 1992; Bunte 1992a, b). This conflict might be resolved if bedload transport shifts from selective transport during the initial, low stages of sediment transport to equal mobility during the latter, higher stages of sediment transport. In alluvial gravel-bed rivers with an excess of transportable material there may be little difference between the discharges for selective transport and equal mobility. The difference in flows needed to initiate selective transport and equal mobility, respectively, may become larger as streams become more supply-limited than transport limited. In steep mountain rivers equal mobility will not be reached during ordinary high flows, as it would take an event of catastrophic magnitude to get the entire bed, including the largest clasts, into motion (Bunte 1990; 1992).

Other factors that affects the *DR* of a grain-size class are the temporary depletion or oversupply of a certain grain size. A temporal variation in transport rates of fine and coarse bedload is a common feature in mountain gravel-bed rivers. During the first days of high

flow fine sediment is often winnowed out from the interstices of the coarse bed material and this constitutes most of the bedload. Later, after the sand has been flushed out, the same discharge transports mainly gravels (Beschta 1987; Bunte 1990).

Sidle (1988) documented a variety of transport responses for fine (< 1mm) and coarse bedload (> 8mm) in pool-riffle sequences. The interannual variations in bedload transport reflected the dynamics of sediment storage and release by LWD. The intra-annual variations in bedload transport were attributed to antecedent storm history and cumulative flows, as these both determined the availability of fine bedload. During high flows the pools were repeatedly scoured and filled. The coarse bedload was less reactive than the finer materials, and this led to a general aggradation which was interrupted by scour during large floods and subsequent highflows when the armor had not yet consolidated.

Emmett (1976) and Gomez (1983) noted a deficiency of fine material when armoring occurred during receding flows. Although the flow capacity would allow the transport of fines, the developing armor layer limited the supply. Church et al. (1991) analyzed the mobility of the fine fraction (< 2mm) during bedload transport. The instantaneous grain-size distribution of this fine fraction depended on the flow history, sediment supply from upstream, and discharge. However, over the course of an entire season, the grain-size distribution of the fine bedload was equal to their proportion in the subsurface bed material. This means that in the long term equal mobility can be assumed, at least for the finer fraction of the bed material.

### 2.3.3 Differentiation of *DR* according to sediment storage dynamics

An evaluation of downstream sediment transport must also recognize that episodic storage and remobilization is part of the long-term sediment budget of rivers. Much of the sediment within a stream system is stored at various locations in, along, or adjacent to the river (channel bed, gravel bars, LWD, beaver dams, banks, etc.). These storage locations have different volumes and store different grain sizes for various periods of time. These factors, plus the timing of sediment retrieval, greatly affects the temporal variation of sediment delivery. Hence the capacity of potential storage sites for particles of different sizes and their respective residence times need to be assessed.

While the location and volume of sediment storage can be assessed from a combination of topographic maps, aerial photography and ground verification, the time period over which the sediment is likely to stay in storage is much more difficult to estimate. However, this information is needed when addressing sediment *DRs*. Therefore, dating and modeling of storage residence times (Kelsey et al. 1986; Madej 1987), the calculation of mean annual rates of sediment release, and the estimation of the sediment storage budget is a major issue in assessing the downstream delivery of sediment.

Cumulative storage can occur over a long sequence of high frequency, low magnitude events. This stored sediment can be abruptly emptied during a low frequency, high magnitude event (Stott et al. 1986; Knox 1988). Sometimes the storage residence time can be predicted with the help of a flood-frequency curve. Knowing the flood stage for a given location, it can be estimated which storage locations or how much of a particular storage location will be accessible and possibly eroded during a given flood.

Other factors besides high flows can release stored sediment, and this is especially true for sediment stored by LWD. Storage around LWD is only temporary and is subject to remobilization after the LWD has been artificially removed or after log-jam bursts (Bilby

1981, 1984; MacDonald and Keller 1987; Klein et al. 1987; Bugosh and Custer 1989; Federer et al. 1990). Sudden releases of sediment can cause aggradation and channel widening. The resulting change in the budgetary state of the river (Section A: 2) may substantially alter the previously-defined *DRs*.

Sediment deposited along the river banks and in upstream tributaries is subject to remobilization when the fluvial system changes its budgetary state, e.g., from transport-limited (leading to deposition) to supply-limited (leading to scour) (Phillips 1987). This change in budgetary state can be due to altered management practices in the upstream drainage basin (Dissmeyer 1976, Trimble 1976, Trimble 1983, Thorne 1991, Froehlich and Starkel 1993), or a downstream disturbance due to practices such as dredging, gravel mining, hydraulic mining, stream diversion (Simon and Hupp 1990; Kondolf and Mathews 1993; Lehre et al. 1993; James 1991; Rieffenberger and Baird 1991), or sediment retention structures (Ruby 1976). These issues were also discussed in Section A-3.

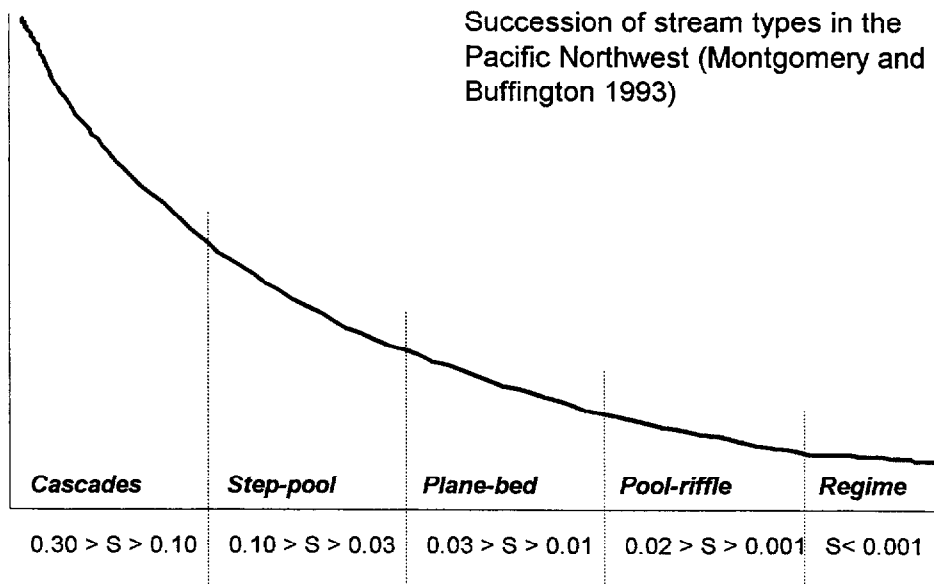
Some of the material that is excluded from transport by being temporarily stored may be compensated for by scour downstream of storage locations such as check dams or LWD. The almost stochastic behavior of storage associated with the movement of LWD will contribute to the poor predictability of *DR* curves. Procedures need to be developed to predict the storage dynamics of LWD. Once the amount and grain-size distribution of sediment stored and released by LWD are known, the net downstream sediment transport over time can be calculated.

#### **2.3.4 Stream Type and Grain-size Selective Stream Delivery Ratios**

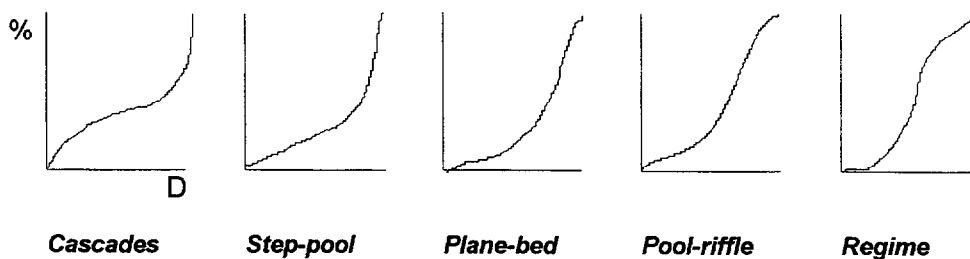
In some steep forested watersheds, soil creep, treethrow, and other biogenic processes may deliver sediment from the hillslopes to the streams in a relatively predictable manner. If these hillslopes are the main sources of sediment and the stream network is relatively consistent at the scale of interest, a grain-size adjusted *DR* curve might give acceptable results. In other watersheds these hillslope sources may be negligible in comparison to the amount of sediment from upstream sources such as road ditches, gullies, and debris flows. In such catchments the sediment delivery ratio approach might better predict downstream sediment yield if the *DR* is redefined as a "stream delivery ratio". A stream *DR* would be the ratio of sediment output from a reach divided by the sediment input into a reach. This could be done separately for various grain sizes and one would obtain a grain-size selective *DR*. If this ratio was related to the distance downstream it could form a grain-size selective stream *DR* curve.

The selection of a suitable reach length is important. It would be impractical to compare *DR* from cross-section to cross-section in tightly spaced intervals. It would also not be appropriate or advantageous to relate stream *DR* curves to the entire length of a stream, since the budgetary state of the stream will vary from headwaters to fifth-order streams. An intermediate and practical spatial scale for grain-size selective stream *DR* curves could be the distance over which a stream maintains a specific morphology, since the morphology of a reach is indicative of the budgetary state. The stream *DR* curve could therefore be related to the length over which a stream follows the stream classification developed by Montgomery and Buffington (1993, 1997). A schematic view of the downstream succession of stream types in mountainous terrain is shown in Fig. C-2; 2. Consistent stream types would define each reach, and one might expect the lengths of the stream types for consecutively lower gradients (plane bed, riffle-pool, and regime) to be progressively longer. As the stream profile often varies, particularly in glacially formed or tectonically active regions, the downstream sequence of stream types will also vary. A cascading stream might be followed by a riffle-pool type stream in a meadow and then

change into a step-pool stream as the gradient steepens. In some cases it might be possible to combine certain stream types, such as the presence of a steeper gradient section (e.g., a step-pool reach) within a much longer, lower-gradient reach.



**Expected bedload grain-size distributions in different stream types**



**Expected unit bedload transport rates in different stream types**

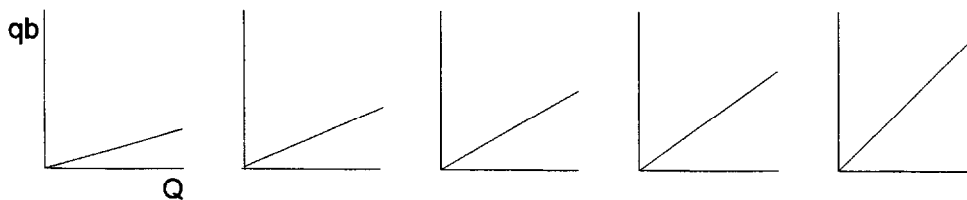


**Fig. C-2; 2:** Conceptual downstream sequence of channel types (Montgomery and Buffington, 1993, 1997), bedload grain-size distributions, and expected unit bedload transport rates.

As stream *DRs* can be defined as the ratio of sediment output from a reach to sediment input into a reach, then certain values for stream *DRs* might be associated with the budgetary state of the stream:

- stream *DR* smaller than one indicates sediment storage and aggradation;
- stream *DR* equal to one indicates a reach-scale equilibrium with a throughflow of sediment;
- stream *DR* larger than one indicates scour and long-term sediment depletion.

A stream *DR* greater than one in mountain streams is inherently a transient situation. Once the stream channel has been depleted of all erodible material, scour eventually leads to either a bedrock channel or a cascade channel in which the bed material cannot be entrained. Scour basically ceases and the stream *DR* approaches 1.0.

A *DR* of 1.0 should apply for "bankfull" floods in almost all streams that are not aggrading. In fluvial environments that are aggrading, the *DR* can differ according to the sediment supply of the flood event. During relatively large floods when the sediment supply exceeds the transport capacity, sediment is deposited either in the stream bed or next to the stream bed on alluvial fans or floodplains. This deposition leads to a *DR* of less than 1.0. During floods with less sediment supply and without large amounts of overbank deposits the stream *DR* would probably be close to 1 or even scouring ( $DR > 1$ ).

A conceptual model for grain-size dependent stream delivery curves is shown in Fig. C-2; 3.

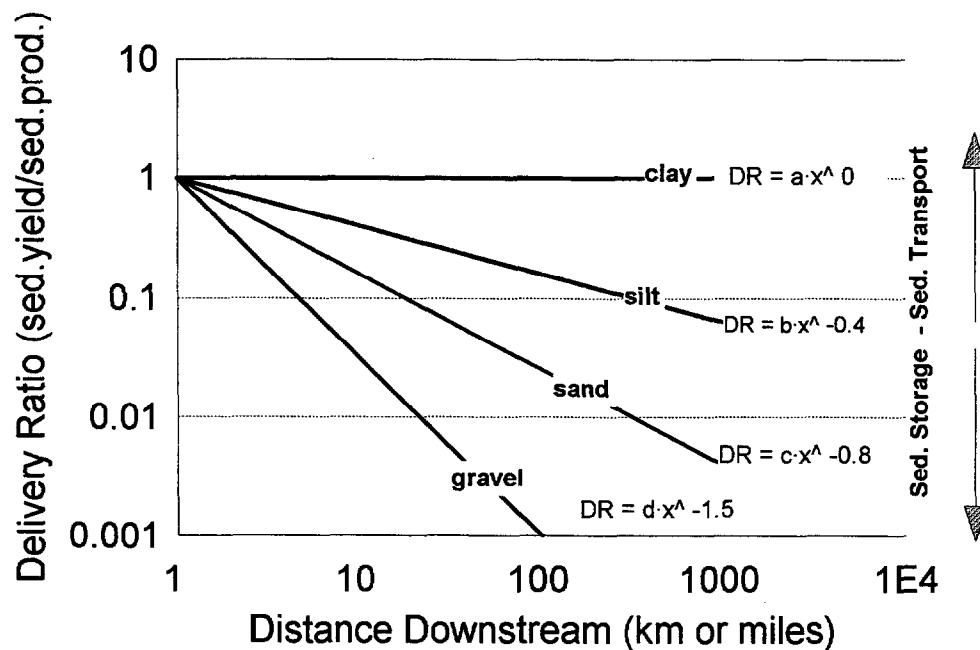


Fig. C-2; 3: Conceptual grain-size sediment delivery curves, assuming a constant stream type.

The  $b$  exponent decreases with particle size, and this indicates the progressively larger proportion of deposited sediment with increasing grain size. The general formula for these delivery ratios is:

$$DR_D = a \cdot L^{-b}, \quad (2)$$

where  $DR_D$  is the delivery ratio of a given grain-size class,  $L$  is the distance downstream, and  $a$  and  $b$  are coefficients.

The exponent of the delivery ratio for clayey material can be set to zero if one assumes that only negligible amount of clay settle out during downstream transport in steep mountainous catchments. However, clay-sized particles could settle out in backwater area, and during large storms, overbank deposits could occur. Both of these processes lead to a  $DR$  of less than 1.0. The  $DR$  could even exceed 1.0 if there is a concentration of sediment concentration in the downstream direction. Such enrichment has been observed where clay-sized material is readily available (Novotny et al., 1986).

The exponents of the delivery ratio curves for the transport of silt, sand, gravel, and cobbles should be progressively smaller, since the average downstream transport distance decreases with grain size. The change in exponent has a physical basis as the transport mode switches from suspended to intermittent bedload transport with increasing grain size. However, the roughness of the river bed can lead to special conditions of grain-size selective entrainment due to the effects of hiding or the temporary storage or entrapment of certain grain-sizes. These mechanisms often reduce the availability of the smaller grain-sizes (see chapter B-2.3.2).

The use of grain-size selective  $DR$  curves by stream types can be considered as simple sediment routing models. The two methods discussed in the following sections represent increasing sophistication (and perhaps increasing success) in estimating the downstream transport of sediment. Both methods are Lagrangian, in that they predict the downstream transport over time, and these are: (1) sediment routing models for shear-erodible beds, and (2) field methods for tracking the downstream movement of particles identified by natural or artificial tracers.

### 2.3.5 Summary

$DR$ s were invented to predict mean annual suspended sediment yield and the lifetime of reservoirs in relatively homogeneous agricultural or rangeland areas. In this setting  $DR$  curves may produce a reasonable estimate when averaged over a number of years. The interannual variation of  $DR$ s due to the timing of storms and sediment production, or the delayed response of sediment yield due to short-term storage, are not important in this situation.

The  $DR$  curve concept is a black-box procedure that lumps together all transport and storage processes over different temporal and spatial scales. A literature review indicates that  $DR$ s differ substantially among basins as well as between storms or years. This suggests that a given  $DR$  should only be used in the specific area and stream types where it was developed, and a  $DR$  should be based on multiple years of data.

If sediment yield data aren't available and  $DR$  curves are the only feasible alternative, the predictive capability of  $DR$  curves can be improved by using  $DR$ s modified to reflect the

specific sediment production and delivery processes operating in the basin of interest. Surface erosion and mass movements, for example, will generally have different grain-size distributions and delivery rates to the stream network. In some cases the physical conditions and management activities may make it possible that the interplay between the source type, the sediment type (sizes and amounts), and response type (e.g., to storms or major events), can lead to characteristic "typical sedimentary events". In other basins this classification might be impossible.

A differentiation of *DR* according to grain-sizes and transport processes might be another approach to account for the large variability in grain-sizes encountered in mountain rivers. Such an approach will be limited by the complexities of predicting the entrainment and transport of certain grain sizes (e.g., hiding and exposure, entrapment etc.).

In most basins more sediment is stored than transported, and a poor understanding of sediment storage will lead to poor results when trying to apply *DR* curves. Procedures are needed to analyze and incorporate sediment storage dynamics, especially by LWD, into *DRs*. Once the amount and grain-size distribution of sediment stored and released by LWD are estimated, the problem of how to calculate the net downstream sediment transport can be tackled.

Differentiation by stream type as well as grain-size would be another step towards a more sophisticated and hopefully more accurate use of *DRs*. Such an approach would be based on the ratio of the output of a certain size fraction from a reach to the input of that size fraction into a reach. A reasonable spatial scale for a reach could be the length of stream section that has a common budgetary state, or possibly the length of a stream type in Montgomery and Buffington's (1993, 1997) classification. This approach implicitly requires the delineation in space of specific sediment sources, and in disturbed basins many of the natural and management-induced sources (e.g., poorly-sorted material from debris flows, fines from roads) are--at least on the basin-scale--effectively point sources. More diffuse sources, such as soil creep, might have to be addressed at the reach scale.

It follows that *DR* curves that do not differentiate between the various processes of sediment production, transport and storage dynamics, and the budgetary states of streams, are poorly positioned to predict the likelihood and magnitude of cumulative watershed effects. Modified *DR* curves should greatly improve the predictability of downstream sediment yields and cumulative watershed effects, but a knowledge of the sedimentary processes in the basin is required to appropriately modify or choose *DR* curves. The use of specific sediment delivery ratios for various grain-sizes and stream types is in effect a crude sediment routing model, but one that is approachable in a management context.

### 3. Modeling the effect of dilution on the downstream decrease of sediment concentration

#### 3.1 Applicability of a dilution model

As suspended sediment travels downstream and clearwater tributaries join in, the sediment concentration of the muddy stream is diluted by mixing with the clear tributaries. It might therefore follow that the detectability of an increase in suspended sediment load will decrease accordingly in the downstream direction. This simplistic view of dilution, which might be applicable over a short turbulent reach, cannot necessarily be applied to estimate downstream sediment concentrations. First, the concept of dilution may only account for part of the downstream reduction in sediment loads because suspended sediment is not in solution like the dissolved load. Suspended sediment particles are constantly subjected to settling forces, and they stay in suspension only to the extent that the settling forces are counteracted by lift forces. If we assume a constant particle density and a spherical shape, then the magnitude of settling forces is proportional to the size of the particle. The finest clay particles can travel in suspension for quite a while, but the occurrence of low flow velocity and the presence of back water zones increases the probability that a clay particle will settle out.

Any attempt to predict the decline in downstream sediment yield due to dilution carries several explicit or implicit assumptions. The first assumption is usually that the sediment delivery ratio is 1. A *DR* of 1 is only valid when the river reach in question is relatively short and steep (see chapter C: 2.3.4), as the high turbulence will ensure continued suspension of the sediment particles. Even if we allow some settling, the implicit assumption is a constant sediment delivery ratio, and this is unlikely except in the case of a consistent stream types and changes in discharge in the downstream direction. The second implicit assumption is that the downstream reaches are not contributing fine sediments from storage. Such a scenario is most easily found in unimpaired, high-energy mountain rivers, although an efficient conveyance of suspended sediment with no storage losses was also reported by Lambert and Walling (1986) for the gravel-bed river Exe in Devon, UK.

Studies documenting an efficient conveyance of fine sediment are outnumbered by studies reporting less than 100% sediment delivery (e.g., Olive and Rieger, 1986; Campbell et al., 1986; Walling et al., 1986) and studies indicating a substantial storage of fine sediments in or close to the river channel (e.g., Melville and Erskine, 1986; Miller and Shoemaker, 1986). Rosgen (1976) documented different scenarios for the downstream behavior of suspended sediment during a snowmelt high flow in the West Fork of the Madison river in southwestern Montana. Increases or decreases in downstream sediment concentration depended on the river order and on the erodibility of the stream bed material. Color infrared (CIR) photography from a helicopter showed high sediment concentrations in some headwater streams due to overland flow, rilling, and gulying. The receiving streams had much lower transport capacity than the headwater streams. This resulted in relatively rapid declines in suspended sediment concentrations. However, when the rivers were incised into easily erodible material, both large and small streams showed a downstream increase in suspended sediment concentration due to channel bed erosion. This downstream increase in suspended sediment concentration was not observed in those rivers that were incised into coarse angular material.

### 3.2 The dilution model

The downstream conveyance of fine, clayey sediments from a basin with a branched tributary system can be calculated if the delivery ratio is set to 1. A 500-ha watershed model with a water yield of 0.1 l/s·ha and a bifurcation ratio of 4 was chosen (similar to MacDonald, 1989) for these simulations. Sediment concentration was determined for a fourth-order stream. Since a bifurcation ratio of four was chosen, the watershed model contained four third-order tributaries, 16 second-order subbasins, and 64 first-order tributary basins. The area of the first-order headwater basins was set to 5 ha because Schumm (1956) had found a 1:10 ratio for the relation between the areas of a first- and a fourth-order stream, and this 5-ha value is also above the channel head initiation threshold defined by Montgomery and Dietrich (1994) for steep valleys with a general slope gradient of 10-40%. This area ratio allows for 64% of the entire fourth-order basin to be covered by first-order basins. The other 36% of the basin are areas that contribute directly to higher order streams without a defined stream channel.

Six scenarios were modeled, and these varied with regard to the background water yield and sediment concentrations as well as the assumed change in water yield and sediment concentration due to management. For the undisturbed portions of the watershed the assumed runoff was 0.1 l/s·ha and the assumed suspended sediment concentration is 0.

#### 3.1.1 Modelled scenarios

The following six scenarios were modeled:

- (1) A single sediment source producing high sediment concentrations in one of the first-order catchments in the otherwise undisturbed watershed. The model assumes an even water yield from all locations in the watershed.
- (2) Water yield from the disturbed basin is doubled along with the increase in suspended sediment yield.
- (3) Increased sediment yields occur in 10 headwater basins totalling 50 ha,
- (4) Doubled water yield from all the disturbed basins together with the increase in suspended sediment yield,
- (5) Disturbance increased to 80% of the catchment, and
- (6) Water yield from the disturbed basins is again doubled to 0.2 l/s·ha.

In each of these six scenarios the sediment concentration of the impaired watershed area ( $C_{s_i}$ ) was varied in steps of one order of magnitude from 0.001 to 10 g/l. The downstream decrease of suspended sediment concentration was simulated for four conditions of background sediment concentration in the entire basin, ranging from "clean" conditions with clear water to "dirty" conditions with background sediment concentrations of up to 0.1 g/l. The downstream sediment concentration at the fourth order basin ( $C_{s_{tot}}$ ) was calculated as follows. A water yield of 0.1 l/s·ha was multiplied by the unimpaired watershed area (495 ha, 450 ha, and 100 ha, respectively) to yield the discharge  $Q_4$  at the fourth-order measuring site:

$$q_{A4} \cdot A_4 = Q_4 \quad (1)$$

Multiplying the discharge of the impaired basin  $Q_i$  by a chosen sediment concentration  $C_{s_i}$  of 0.0, 0.001, 0.01 and 0.1 gives the four background sediment yields at the measuring site:

$$Q_4 \cdot Cs_4 = Qs_4 \tag{2}$$

The discharge of the impaired basin area  $Q_i$  (5 ha, 50 ha, and 400 ha respectively) is also calculated by multiplying the respective water yields  $q_{Ai}$  (0.1 l/s·ha and 0.2 l/s·ha) by the area of the impaired basins  $A_i$ :

$$q_{Ai} \cdot A_i = Q_i \tag{3}$$

Multiplying the various sediment concentrations  $Cs_i$  produced by different degrees of basin impairment gives the sediment yield from the impaired basins:

$$Q_i \cdot Cs_i = Qs_i \tag{4}$$

Sediment yields from the unimpaired watershed area are added to the sediment yields from the impaired parts of the basin area:

$$Q_{tot} = (q_{A4} \cdot A_4) + (q_{Ai} \cdot A_i) \tag{5}$$

Dividing the total sediment yield by the total discharge  $Q_{tot}$  in the watershed yields the sediment concentrations found at the measuring site:

$$\frac{Qs_4 + Qs_i}{Q_{tot}} = Cs_{tot} \tag{6}$$

Summing equations (1) to (6) yields the following function for the sediment concentration at the measuring site:

$$Cs_{tot} = \frac{(q_{A4} \cdot A_4 \cdot Cs_4) + (q_{Ai} \cdot A_i \cdot Cs_i)}{(q_{A4} \cdot A_4) + (q_{Ai} \cdot A_i)} = \frac{Qs_4 + Qs_i}{Q_{tot}} \tag{7}$$

If the water yield of the unimpaired watershed areas  $q_{A4}$  (l/s·ha) equals the water yield  $q_{Ai}$  of the impaired parts of the basin (scenarios 1 and 3), water yield cancels out.

## 3.2 Results

### 3.2.1 Sediment concentration from impaired basin and background

The effects of the different levels of impairment (in terms of sediment concentration, impaired area, increased water yield, and background sediment concentrations) on downstream sediment concentration  $Cs_{tot}$  is shown in Fig. C-3; 1a-f. The problem with

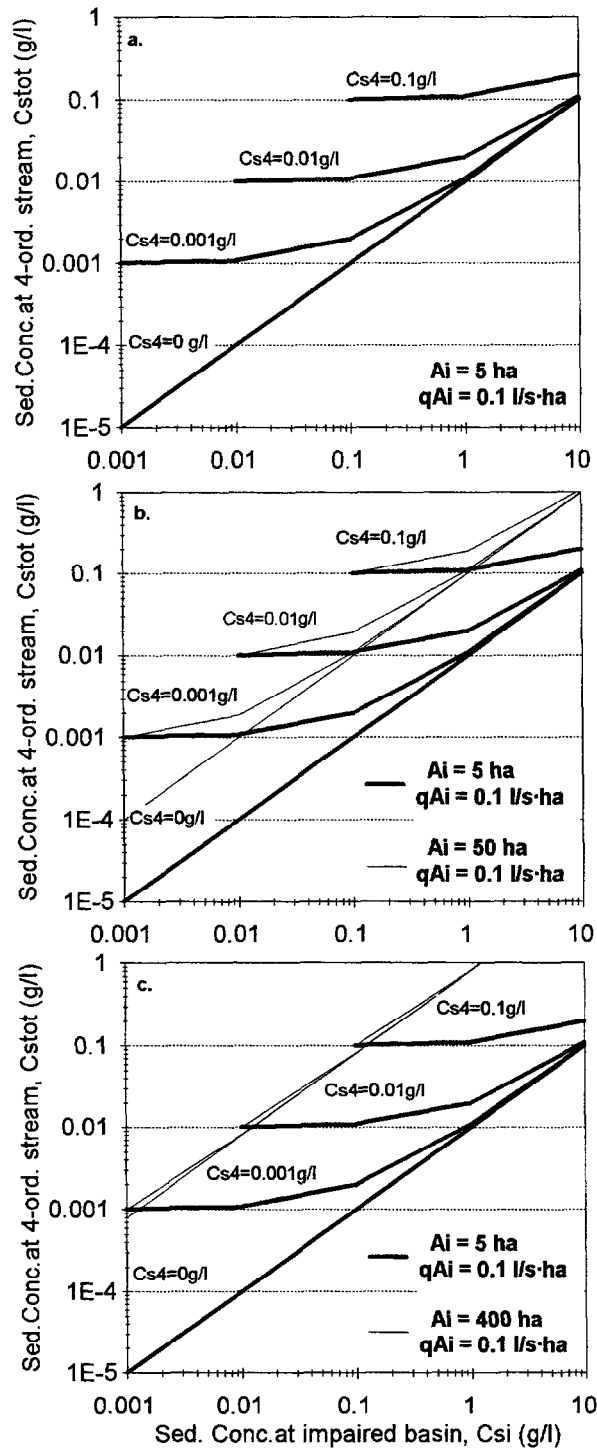


**Fig. C-3; 1a to 1c:** (a) The effects of dilution (background suspended sediment concentration, ( $C_{s4}$ ) on downstream total sediment concentration ( $C_{stot}$ ) for different increases in suspended sediment concentration from an impaired watershed ( $C_{si}$ ). (b) Size of the impaired basin ( $A_i$ ) is increased from 5 to 50 ha. (c) Size of the impaired basin ( $A_i$ ) is increased from 5 to 400 ha.

graphically presenting the relationships between  $Cs_i$  and  $Cs_{tot}$  is that sediment concentrations in the fourth-order stream commonly extends over 3 orders of magnitude (0.001 to 1 g/l), while the process of dilution produces linear relationships between  $Cs_i$  and  $Cs_{tot}$ . Using a double logarithmic scale makes it difficult to identify the nature of the relationships between any two variables, since a linear relationship can plot as a straight line or as a curve depending on whether the constant equals zero.

- Since the model is based on a delivery ratio of 1 (the effect of this assumption is discussed later in this section), sediment concentration in the impaired basin  $Cs_i$  yields a positive linear relationship with sediment concentration at the measuring site  $Cs_{tot}$ . The general form of the relationship between  $Cs_i$  and  $Cs_{tot}$  is:

$$Cs_{tot} = a + b \cdot Cs_i \tag{8}$$

where  $a$  is the constant and  $b$  is the slope.

- A change in the impaired area ( $A_i$ ) causes a proportional change in the sediment concentration at the measuring site ( $Cs_{tot}$ ) (Fig. C-3; 1a and 1b).
- A change in the water yield from the impaired area also affects the slope of the function. Doubling the water yield  $q_{Ai}$  of the impaired area without reducing the sediment concentration almost doubles the rate at which  $Cs_{tot}$  increases with  $Cs_i$  (Fig. C-3; 1d). The slope ( $b$ ) of the above function can be approximated by the relationship between the impaired basin discharge and total basin discharge:

$$b \approx \frac{A_i \cdot q_i}{A_4 \cdot q_4} \tag{9}$$

The effect of doubling the water yield from the impaired basin becomes less pronounced as the area of the impaired basin increases (i.e., less dilution). If water yield from a 50-ha impaired basin is doubled to 0.2 l/s·ha, the observed change in  $Cs_{tot}$  is reduced to 1.8. A doubled water yield from a 400-ha area increases the rate of change only by a factor of 1.1.

- An increase in background sediment concentration,  $Cs_4$ , does not affect the rate at which the sediment at the measuring site increases with increasing  $Cs_i$  of the basin (lines are parallel to each other), but does affect the constant  $a$ . The value of  $a$  can be approximated by:

$$a \approx Cs_4 - \frac{A_i \cdot q_i}{A_4 \cdot q_4} \tag{10}$$

This indicates that  $a$  is directly proportional to the background sediment concentration of the unimpaired basin. Pronounced dilution effects occur when sediment concentration from the impaired basin is low and the impaired area is small. The masking effect due to higher background sediment concentrations is less pronounced with higher sediment concentrations from the impaired basin.

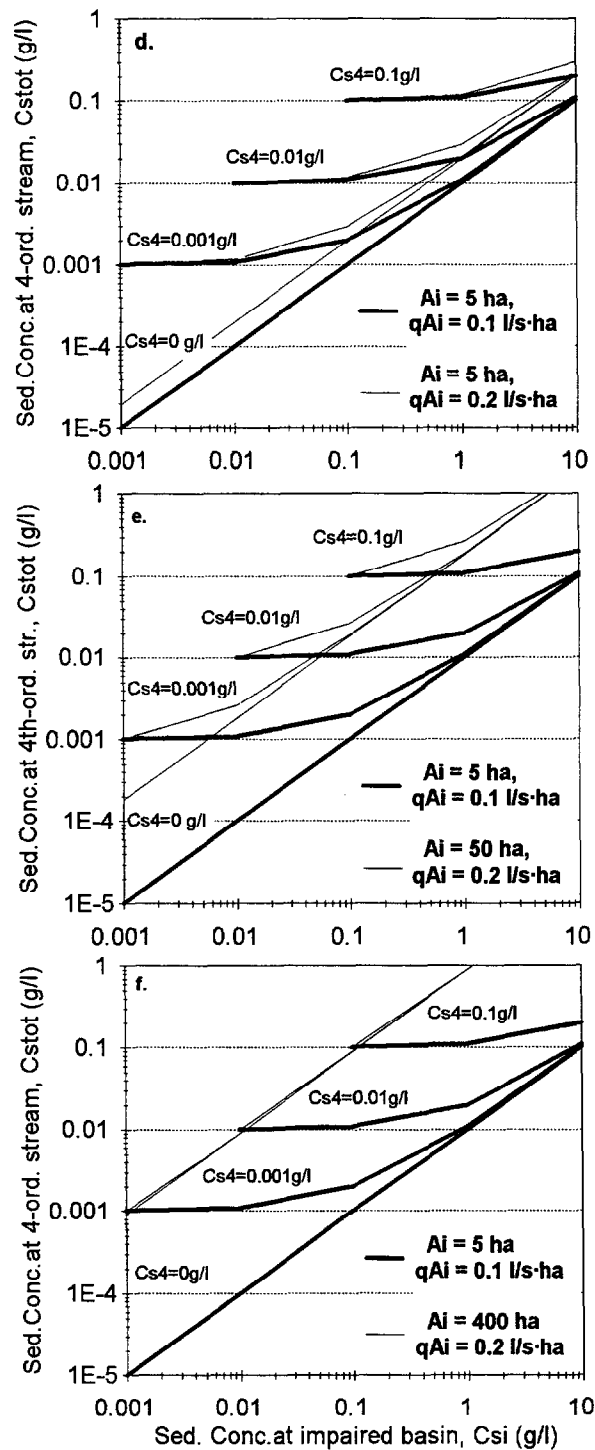


**Fig. C-3; 1d to 1f:** (d) The effects of dilution (background suspended sediment concentration, ( $C_{s4}$ ) on downstream total sediment concentration ( $C_{stot}$ ) for different increases in suspended sediment concentration from an impaired watershed ( $C_{si}$ ). Water yield ( $qA_i$ ) is increased from 0.1 l/s·ha to 0.2 l/s·ha. (e) Size of the impaired basin ( $A_i$ ) is increased from 5 to 50 ha, and water yield ( $qA_i$ ) is increased from 0.1 l/s·ha to 0.2 l/s·ha. (f) Size of the impaired basin ( $A_i$ ) is increased from 5 to 400 ha, and water yield ( $qA_i$ ) is increased from 0.1 l/s·ha to 0.2 l/s·ha.

From a mathematical point of view, the background sediment concentration and the different types of disturbance (increasing sediment concentrations from the disturbed basin or an increase in the affected area) are equally effective in increasing the total sediment concentration, regardless of the order of magnitude of fine sediment pollution. However, from an ecological and a practical point of view, a doubled sediment concentration at the measuring site is of less concern at very low concentrations (1 or 2 mg/l) than at very high concentrations (1 or 2 g/l) (Fig. C-3; 1g).

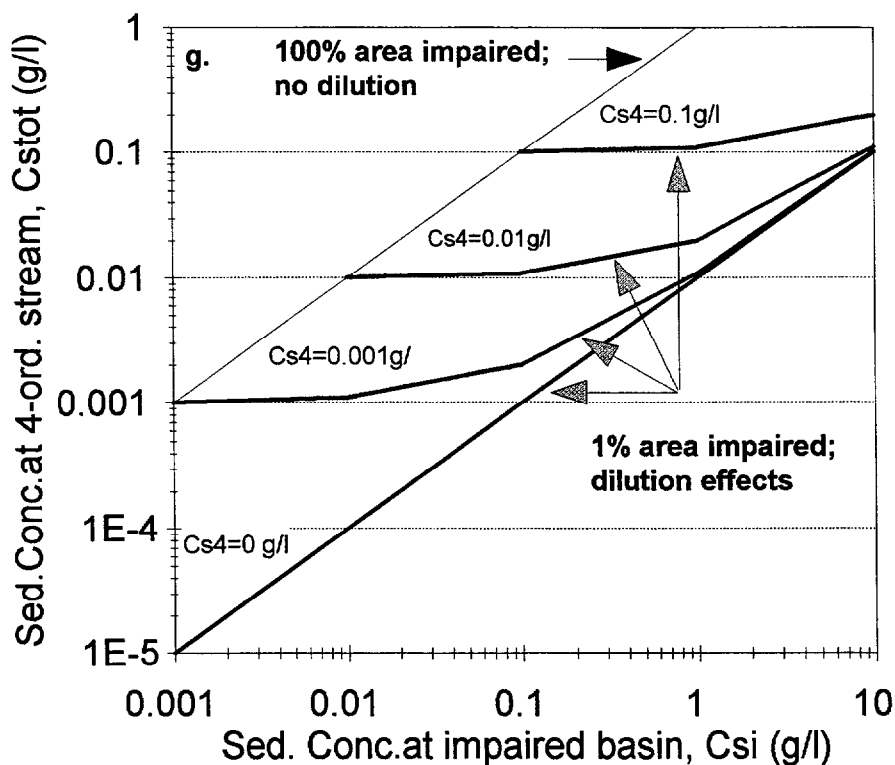


**Fig. C-3; 1g:** Generalized model of dilution effects on suspended sediment concentrations in a fourth-order basin as a function of the sediment concentrations from an impaired (disturbed) basin, the proportion of the basin that is disturbed, and the background concentration of suspended sediment from the unimpaired portions of the fourth-order basin.

### 3.2.1 Different scenarios of stream flow

This interplay between the impaired area, change in water yield, and change in sediment concentration should be related to flow conditions that might cause certain sediment concentrations.

For easier reference, the sediment concentrations of the impaired basin are termed "low", "medium" and "extreme", while the background concentrations are called "slight", "moderate" and "high". The detection limit is assumed to be 0.001 g/l. These terms are

relative, since a "low" concentration in a fairly erodible environment may already be considered a "medium" sediment concentration in a more erosion-resistant environment. A sediment concentration of 1 mg/l is the order of magnitude that can still be determined by standard filtration practices.

The combination of low sediment concentrations from the impaired basin with clear or slight background sediment concentrations characterizes low flow conditions (lightly shaded zone in Fig.C-3; 1h). Medium sediment concentrations from the impaired basin, combined with clear or moderately increased background concentrations, characterize the intermediate flows that might be due to wet or moderate snowmelt conditions (medium shaded zone). Medium-to-extreme sediment concentrations in the impaired basin and moderate-to-high background sediment concentrations are characteristic of storm flows or peak snowmelt runoff (heavily shaded zone in Fig.C-3; 1h).

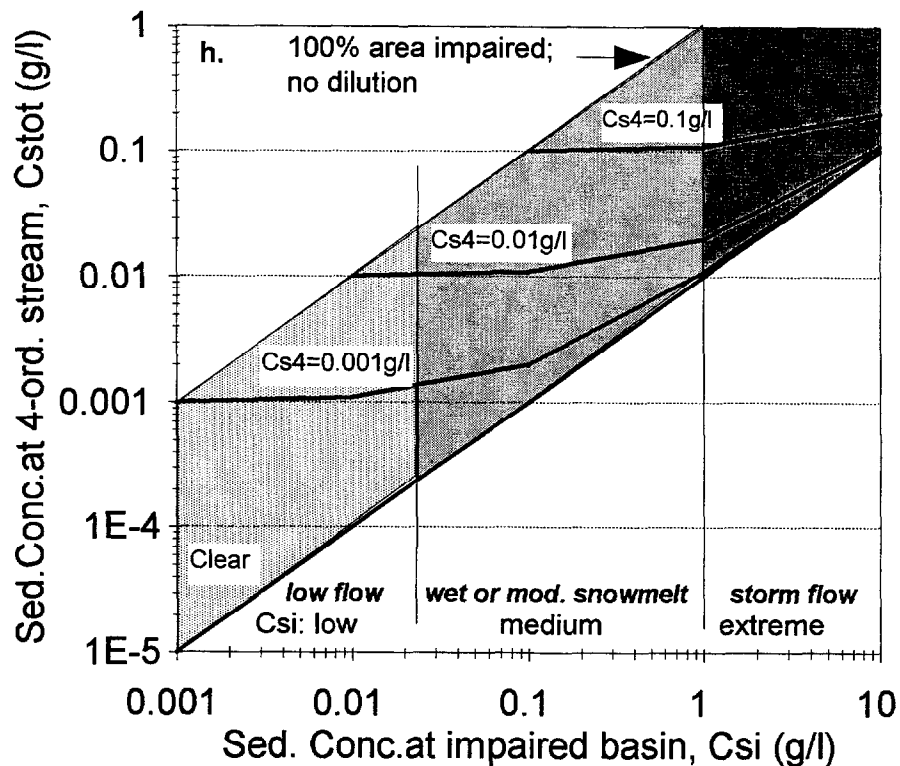


Fig. C-3; 1h: Effects of dilution on suspended sediment concentrations in a fourth-order basin under different runoff conditions as a function of the sediment concentrations from an impaired (disturbed) basin, the proportion of the basin that is disturbed, and the background concentration of suspended sediment from the unimpaired portions of the fourth-order basin.

During low flows the clear water input from the tributaries dilutes the sediment input from the impacted area to below the assumed detection limits of 1 mg/l (Fig.C-3; 1h). A large increase in impaired basin area, its sediment yield, or in the background sediment concentration is necessary to cause a measurable increase in total sediment concentration.

During intermediate flow conditions with a relatively low sediment concentration from the impaired basin (e.g., 0.1 g/l), the sediment concentration in the fourth-order stream will be increased almost as much by a ten-fold increase in background sediment concentration (from 0.001 to 0.01 g/l) as by a ten-fold increase in affected basin area (Fig. C-3; 1b). During high flow conditions that feature both high sediment concentrations from the impaired basin and a relatively high background  $Cs_4$ , a ten-fold increase in background sediment concentration leads to a much less than 10-fold increase in sediment concentration at the measuring site, while the increase in impaired basin area still proportionally increases total sediment concentration at the measuring site. Thus the effect of increased basin area becomes more pronounced with higher sediment concentrations from the impaired basin.

These simple simulations showed that, given the detection limits obtained with ordinary equipment and procedures (sampling bottle, filtration, weighing), one may be better able to detect a sediment input from an upstream source when the water from other sources has some background turbidity. If all the tributaries deliver clear water the fine sediment input from a single first order headwater stream can be diluted beyond standard detection limits by the time it reaches a fourth-order stream. In contrast, the input of suspended sediment from the tributaries in the moderate and high flow scenarios prevented excessive dilution. Although this slightly reduced the relative effect of the increase in suspended sediment from the impaired basin, it did allow the detection of the disturbance effect in a fourth-order stream.

It should be noted that the assumption of a perfect conveyance efficiency ( $DR = 1$ ) affects the expected magnitude of change but not the basic principles. During stormflow conditions there would be more turbulence, but any overbank flow would result in a reduced velocity and a deposition of fine sediments in these areas (see chapter C-2.3.4). An increase in water yield could induce channel scour, and this would partially compensate for storage of sediment in the downstream direction that is implied by the negative slope of most delivery ratio curves.

## 4. Travel distance and travel velocity of downstream sediment transport

### 4.1 Introduction

The downstream movement of bedload sediment in disturbed watersheds can adversely affect downstream reaches, particularly when sediment from different sources simultaneously arrives at the same location. Sand- and silt-sized sediment in gravel-bed rivers damages the habitat of salmon and trout populations, and can encourage vegetation encroachment during subsequent low flows. Once vegetation has established itself, it can further propagate the deposition of fine sediment, leading to a positive feedback loop. An increase in sediment yield of sand or coarser material can cause aggradation of the streambed, pool-infilling, and stream widening which then may lead to bank collapse. This input of additional local sediment further promotes aggradation and stream widening and degrades or severely disrupts the riparian zone (MacDonald et al., 1991; Meehan, 1992).

The analysis and prediction of sedimentary CWEs would be greatly facilitated if the velocity of the downstream movement of sediment could be specified for a given stream reach. Knowledge of the mean annual travel distance of different sediment sizes in different stream types is also necessary to set up a cost-effective monitoring system, as noted by Wolman (1977) and the participants in the EPA-USFS Technical Workshop on Sediments (Proceedings of the Technical Workshop on Sediments 1992). (Although we are interested in the distance travelled per unit of time, in this chapter we are generally using the term "travel distance" to refer to mean annual transport distance, and this is done in order to distinguish the annual velocity from the much faster but much shorter-term velocity of a particle in motion.)

Unfortunately, sediment transport from source areas through the channel system is a sequence of unsteady or discontinuous processes in which episodes of relatively fast transport alternate with relatively long periods of storage (Chapter B-2). This unsteady transport of sediment has been investigated across a range of temporal and spatial scales. For bedload transport these studies range from the analysis of travel times, step lengths, and rest periods of single particles (Buskamp and Ergenzinger, 1991) during a flood event to the residence time of sediments in river terraces on a millennia time scale (e.g., Kelsey et al., 1986; Madej et al., 1987) and the downstream transport of sediment waves derived from the Pleistocene glaciation (Slaymaker 1990). Other studies pointed out that introduced sediment disperses not only in a downstream direction, but also laterally and vertically, and downstream sediment transport depends on a number of factors such as channel characteristics, sediment characteristics (size, shape), the flow regime (Gintz 1991, 1994; Schmidt and Ergenzinger 1992), and channel micromorphology (Brayshaw et al. 1983; Brayshaw 1985).

There are no systematic studies that have determined mean annual transport distances of different sediment sizes through different stream types over a time scale of several years or longer. With regard to suspended sediment, there apparently are only a few detailed studies that have quantified travel paths, travel distances, and storage. Faced with this lack of information, this report study addressed the issue of travel distance of suspended sediment and bedload transport in several ways. For suspended sediment the following sections will:

- point out the newly-developing tracing techniques for suspended sediment ("fingerprinting"),
- compare downstream sediment loads measured at consecutive U.S. gaging stations, and
- synthesize existing data on the travel distance of suspended sediment.

In order to gain more insight into mean annual travel distance of bedload transport, this study:

- reviewed published information on the three-dimensional dispersion of sediment;
- reviewed the effects of stream morphology and micromorphology on the travel distances of different bedload particle sizes;
- analysed the problems with extrapolating to mean annual travel distances from short-term studies; and
- synthesized the data on mean annual bedload travel distances as inferred from about 30 individual studies in different stream types.

We focussed our review and analysis on studies that employed tracer techniques or monitored the downstream migration of bedforms and bars. In theory, downstream sediment transport could be calculated from sediment routing procedures using some of the many sediment transport models (e.g., Federal Interagency Sedimentation Conferences, 1976; 1986; 1991; Abt and Gessler, 1988; Wang, 1989). The basic concept of many of these models has been analyzed and compared by Fan (1989). We did not employ any sediment transport models because these models provide only an approximate solution to the specific problem or situation for which the model was developed. Their application to a different situation has to be evaluated for each case, and the appropriate adjustments have to be made and assumptions verified. The differences in predictions from different models implies that the results of a given simulation are highly sensitive to model selection, and thus not easily generalized.

## 4.2 Suspended sediment transport

CWEs due to suspended sediment could be detected and predicted more easily if one could mark individual sources of suspended sediment and track their respective paths through the fluvial network. Studies on hillslopes and small agricultural watersheds have been able to track the path of fine sediment from source areas to sinks using "fingerprinting" techniques (see Section C-4.2.1). This option is less feasible in larger catchments because of the required high sampling intensity and the dilution in space and time of the marked particles. A second possibility to estimate downstream travel distance is a comparison of suspended sediment loads from sequential or nested measuring stations within a catchment. Although this approach is limited by the scarcity of such data sets, a greater problem is that one cannot uniquely label the different sources of sediment passing by a given monitoring station. How does one know if all of the sediment passing through the upstream cross-section is also passing through the downstream cross-section, or whether an exchange of sediment has taken place? Despite these problems, we did attempt to quantify the travel distance of suspended sediment on an annual basis for a basin in Colorado which had a series of rather closely spaced monitoring stations with temporally overlapping records. A third source of information on the travel distance of suspended sediment is the scientific literature, and in this report we summarize the limited data that we were able to uncover. The following sections review each of these approaches in turn.

#### 4.2.1 Fingerprinting sources of fine sediment, its travel paths and sinks

New developments in active and passive tracer techniques have greatly improved our ability to trace the sources, paths, and sinks of fine sediment, and to distinguish the relative contributions of sediment from different sources to the total sediment yield (Peart and Walling, 1986; 1988). Sediments are traced by their petrology, color, natural magnetite content,  $^{137}\text{Cs}$  adsorption, or the ratios of  $^{226}\text{Ra}$  or  $^{232}\text{Th}$  (Sobocinsky et al. 1990; Cerling et al. 1990). If the sedimentary properties are unsuitable to serve as tracers, artificial tracers such as crushed magnetite can be used (Parson et al. 1993). Appropriate techniques are then used to detect the marked sediment in different locations. Relevant studies include: Walling et al. (1986); Walling and Bradley (1988); Campbell et al. (1986); Walling and Quine (1991); and Olley et al. (1993).

These tracer techniques were developed to detect and analyze sediment sources and sediment travel paths in relatively small areas on hillslopes and agricultural fields. Tracer concentrations are typically compared before and after an event for source, sink, and transport locations. The sampling effort is not unreasonably large since travel paths are usually visible and sample locations can be easily identified. The spatial scale of the sampling in these type of hillslope erosion studies is relatively small, and the temporal scale is also tractable because there is little or no change between events.

Unfortunately these techniques and assumptions are not easily applied in drainage basins, as the greater mobility of fine sediments in streams requires a much more intensive sampling effort. A sufficiently large stretch of stream and its adjacent riparian areas would have to be sampled at a sufficiently high spatial and temporal resolution to detect the erosion, deposition, and transport of sediment stemming from different sources (e.g., channel bottom, upper and lower banks, upstream sources, and inputs from the adjacent hillslopes).

An exception in terms of sampling effort and fluvial applicability was Rosgen's (1976) use of aerial infrared photography to evaluate suspended sediment concentrations during a high flow event. The results showed that internally-derived (allochthonous) and externally-derived (autochthonous) sediments may have different transport dynamics. Fine sediment added to the stream from outside sources (bank collapse, overland flow) might quickly settle out, while the high transport capacity that was capable of eroding fine sediment from the channel bottom was more capable of keeping the latter sediments in suspension, thereby increasing their transport distance.

Another method to distinguish between suspended sediments from different sources was proposed by Symader et al. (1989). Sediment from different locations in the catchment often can be identified by their mineralogical or geochemical properties. Combined geochemical and mineralogical analyses of water and sediment can identify resuspended sediment, since remobilization of channel bottom sediment frequently releases dissolved zinc, iron, and manganese from the interstitial water to the river, but doesn't release much phosphate. An increase in suspended sediment concentration together with an increase of zinc, iron, or manganese would suggest an autochthonous sediment source, while the lack of the heavy metals in the stream water would suggest external sediment sources. Sediment stemming from bank collapse can be identified because it dilutes the concentration of most suspended solids.

Symader et al. (1989) also suggested that it might be possible to identify seasonal response patterns in sediment sources. For example, summer storms on dry soil tended to produce externally-derived sediment that can be transported over hundreds of meters in tire tracks on dirt roads before it reaches the stream. High sediment concentrations from external

sources, combined with relatively low runoff, prevents resuspension within the channel. During the wetter autumn season there is little overland flow but more interflow, and the resulting streamflows are more likely to resuspend the recently-deposited river bottom sediments. In winter storms bank collapse is the primary source of fine sediments.

#### 4.2.2 Estimating transport distances by comparing downstream loads

An attempt was made to estimate the annual downstream travel distances of suspended sediment by comparing sediment loads from consecutive downstream measuring stations. This approach will only yield meaningful results if certain assumptions or conditions are met, including:

- sediment load estimates must be reliable (see chapter B-4);
- the sediment load from all incoming tributaries between monitoring locations is negligible or known; and
- there is no exchange of suspended sediment with sediment from instream sources.

None of these three conditions could be verified in the data set used in our analysis, and it could be argued that the first and third conditions can almost never be satisfied. Nevertheless, we believe that these limitations do not invalidate the basic results.

##### 4.2.1.1 Data sets and methodology

A search through the USGS Water Resources Data for several western states identified two nested basins suitable for such an analysis: Piceance Creek in northwestern Colorado (Fig. C-4; 1) and the Wind River Basin in central Wyoming. We focussed on the Piceance Creek catchment because there were more monitoring stations with a larger number of overlapping years. Piceance Creek is within the White River basin, and it drains the Tertiary sand and shale layers of the Green River formation in the Roan Plateau. The basin is dominated by forest and rangelands with some irrigated agriculture along the streams. The data sets used for the analysis are summarized in Table C-4; 1.

**Table C-4; 1:** Area, mean daily suspended sediment load, years of record, and location of mainstem and tributary stations with suspended sediment data along a 40-km reach of Piceance Creek.

Station	Basin area (km <sup>2</sup> )	<i>Qsd</i> * (t/d)	Years of record	Location
Piceance 1	303	37	1975-1985	about 500 m above the confluence with Stewart Gulch
Stewart Gulch	114	0.5	1975-1982	
Willow Creek	125	1.5	1974-1982	
Piceance 2	800	46	1975-1985	about 1.5 km below Willow Creek
Black Sulph. Cr.	267	10	1975-1981	
Piceance 3	1311	51	1972-1983	about 500 m below the confluence with Ryan Gulch and 7 km below Black Sulphur Creek
Piceance 4	1689	80	1975-1981	at the confluence with the White River

\*Mean daily suspended sediment load in English tons per day from 1975-1981.

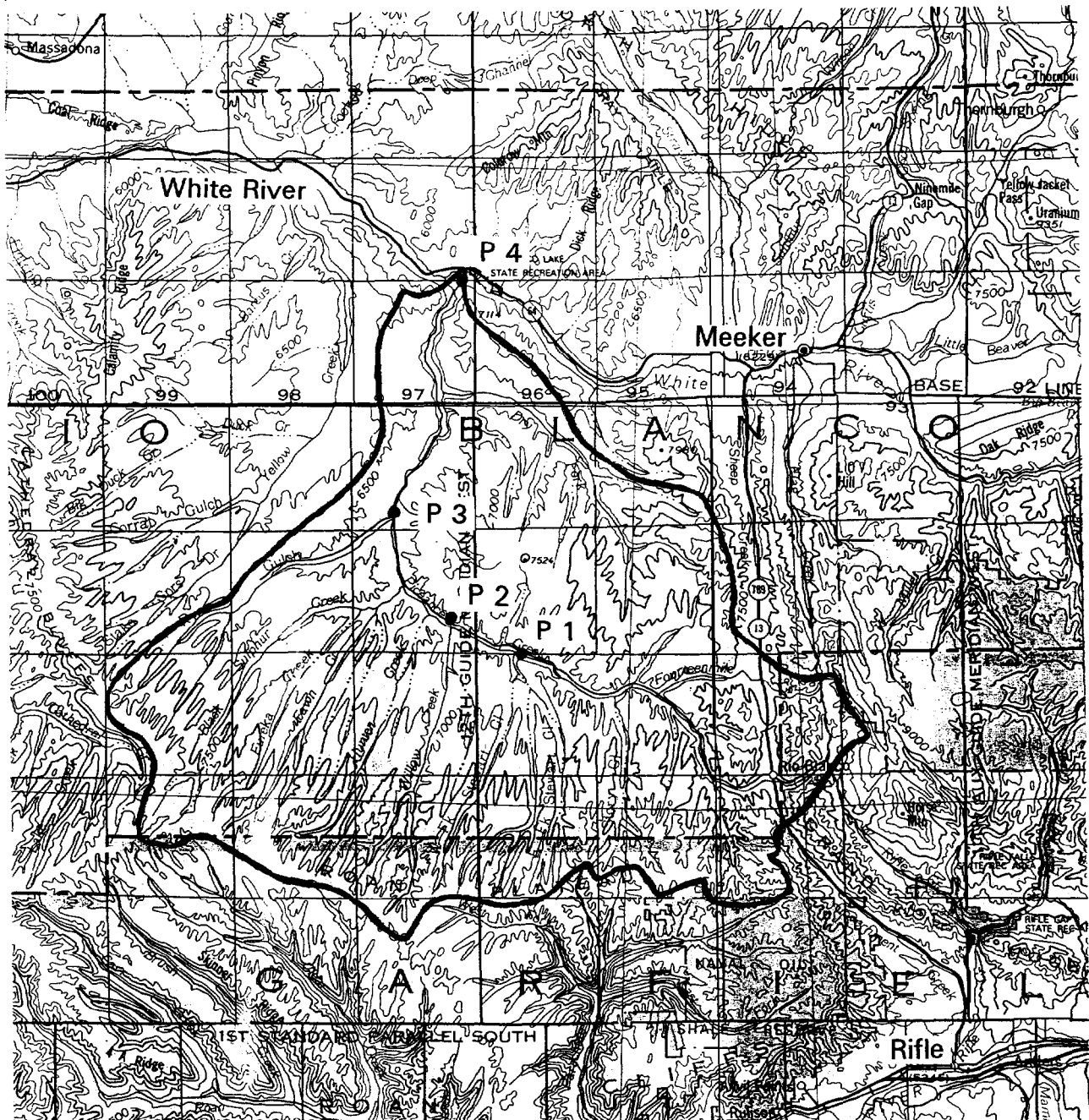


**Fig. C-4; 1:** Map of the Piceance Creek basin in northwestern Colorado. Scale is 1:500,000.

The ephemeral streams which comprise the three forks of Stewart Gulch are each about 20 km long. Willow Creek is perennial and about 25 km long. Black Sulphur Creek is perennial and about 35 km long with several ephemeral tributaries. The stations at Piceance Creek are numbered in downstream sequence (P1 - P4). The distances between stations P1 and P2, P2 and P3, and P3 and P4 are about 7, 12, and 20 km, respectively.

Annual sediment load is expressed in terms of mean daily sediment load ( $Q_{sd}$ ) from 1975-1981. Since data are only used for comparative purposes, the units have not been converted and are in American tons (907 kg) per day. Mean daily sediment load is plotted for the seven years with data (1975-1981) from all four stations along Piceance Creek (Fig. C-4; 2) and its tributaries (Fig. C-4; 3). A comparison of these figures shows that the effect of the upper two tributaries (Stewart Creek and Willow Creek) on the total suspended sediment load at Piceance Creek 2 is negligible.

#### 4.2.1.2 Scour and storage in the reaches between the stations

The station at Piceance 2 has a mean daily sediment load of 46 t/d. This exceeds the sum of the loads from the upstream station at Piceance 1 (37 t/d) and Willow Creek (1.5 t/d). If we assume that there are no other significant sources of sediment, then there must have been net scour within the reach between Piceance 1 and Piceance 2 over the period of common data.

Black Sulphur Creek and Ryan Gulch feed into the reach between Piceance 2 and 3. The data record for Ryan Gulch was not complete, but Hadley and Shown (1976) report that the average sediment delivery for Ryan Gulch is about 0.3 t/d, and that most of the sediment that reaches the stream is stored in fan-like areas and does not contribute to sediment yield. The sum of mean daily loads from Piceance 2 (46 t/d) and Black Sulphur Creek (10 t/d) is approximately 5 t/d larger than the mean daily load at Piceance 3 of 51 t/d. Some additional sediment from Ryan Gulch also is delivered to this reach, and this further increases the discrepancy between upstream and downstream sediment loads. Hence the data indicate that this reach is slightly aggrading.

The average sediment load at Piceance 2 is 23% larger than the average sediment load at Piceance 1. By multiplying the sediment load at Piceance 1 by 1.23 we can obtain a predicted value for the sediment load at Piceance 2. A comparison of the predicted load at Piceance 2 with the actual mean daily sediment load shows that for any given year the downstream increase in total sediment load can be quite different from this average value of 23%. In some years the downstream sediment load is disproportionately large and in other years it is disproportionately small (Fig. C-4; 4).

The same procedure can be applied for Piceance 3, which has a mean sediment load 12% larger than Piceance 2. The 20-km reach between Piceance 3 and 4 has only one major tributary, Dry Creek, but no sediment data are available for this tributary. Between Piceance 3 and 4 the mean daily sediment load increases from 51 to 80 t/d, or 55%. The estimated drainage area of Dry Creek is 600 km<sup>2</sup>, or more than twice the area of Black Sulphur Creek which has a mean daily suspended sediment load of 10 t/d. Thus the increase of more than 28 t/d between Piceance 3 and 4 can either be attributed to sediment inputs from Dry Creek or other areas along this reach, or to net scour between these two stations.

In 1975, only half the load arrived at Piceance 2 which would have been expected given the load at Piceance 1 (Fig. C-4; 4). A mean sediment load of almost 30 t/d must have been stored between the two reaches. In 1976 sediment loads were surprisingly low at the upstream station compared to the relatively high load in the tributaries. Sediment loads were also proportionally too large at the downstream site, indicating that about 10 t/d must have been scoured between Piceance 1 and Piceance 2. During the drought year of 1977 there was a low sediment contribution from upstream and a large amount of scour between Piceance 1 and Piceance 2, as the downstream sediment load at Piceance 2 was more than 60 t/d larger than the known sediment inputs. Over the next three years there was an

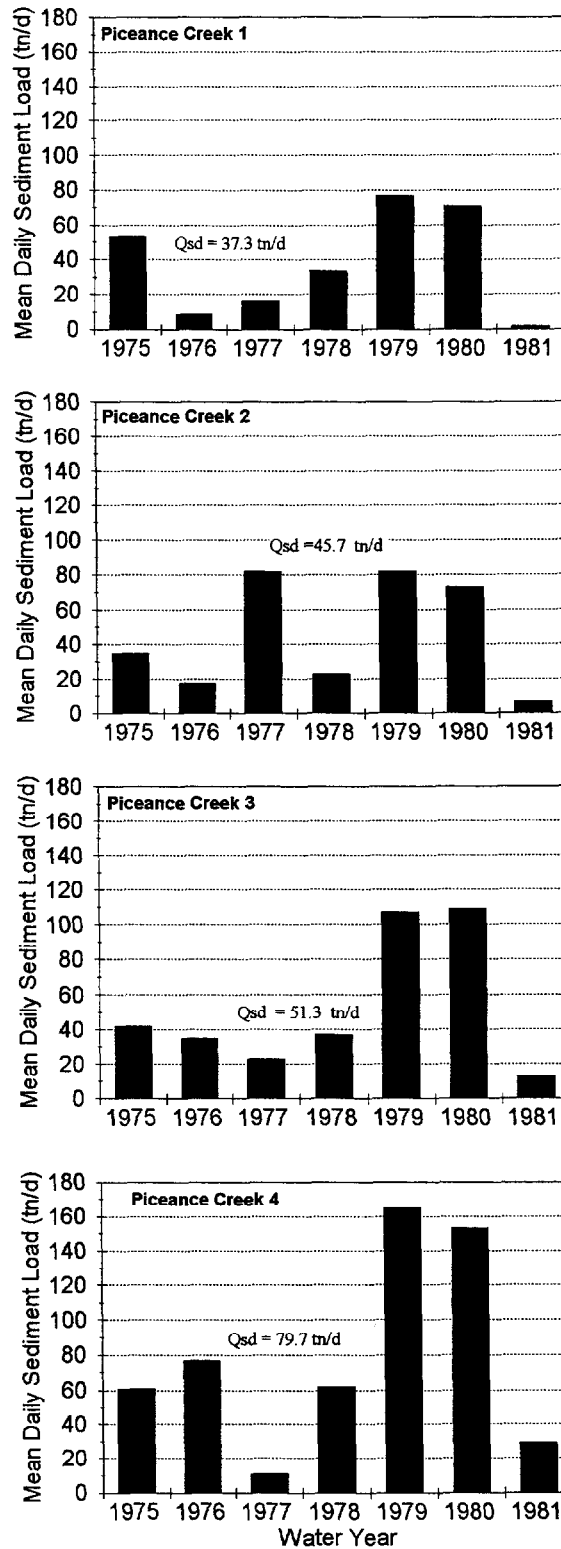


**Fig. C-4; 2:** Mean daily suspended sediment load for four stations (P1 to P4) along Piceance Creek in northwestern Colorado, 1975 - 1981.

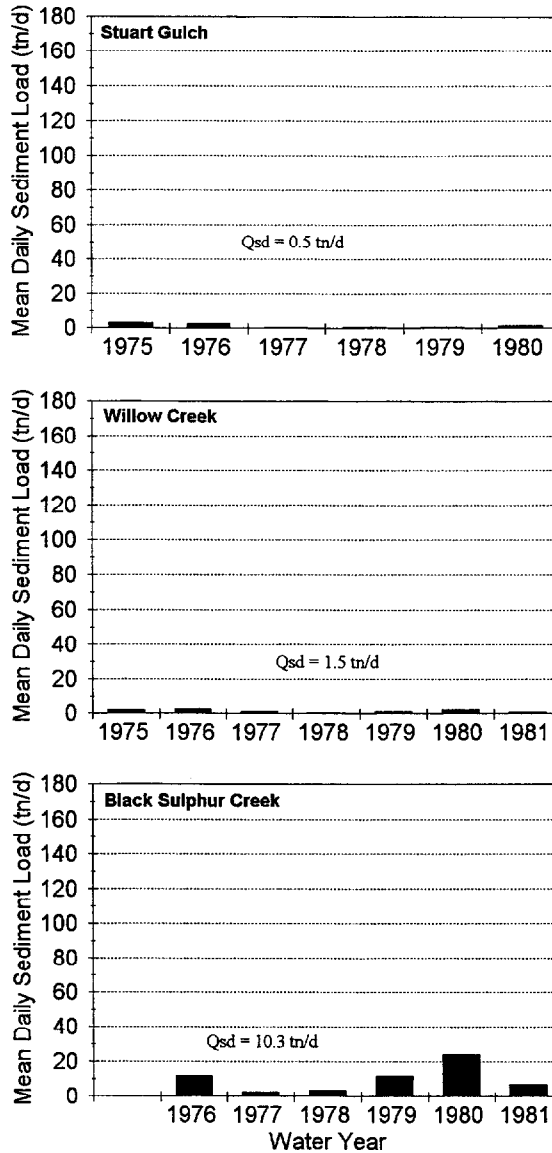
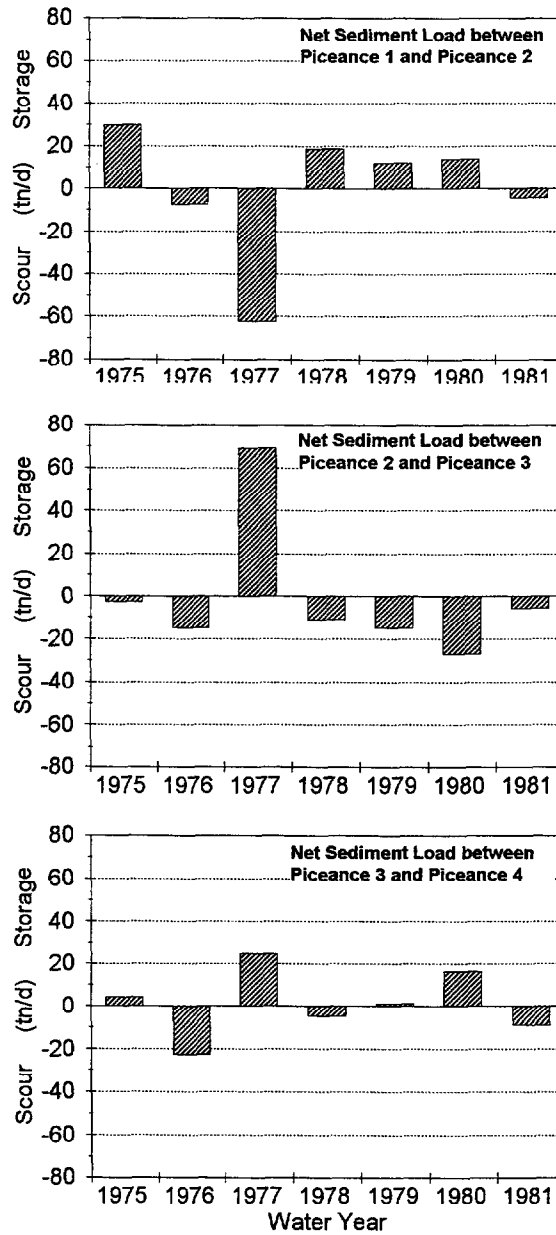


Fig. C-4; 3: Mean daily suspended sediment load for three tributaries to Piceance Creek, 1975 - 1981.

estimated net daily storage of 10-20 t/d in this 9 km reach. By 1981 the sediment budget was again slightly negative (i.e., there was net scour) (Fig. C-4; 4).

The pattern of scour and fill for the next reach downstream (between Piceance 2 and 3) is exactly opposite to the pattern described for the reach between Piceance 1 and 2 (Fig. C-4; 4). Years with storage in the upstream reach are years with scour in the downstream reach and vice versa. The large amount of sediment scoured in the upstream reach in 1977 appears to then be stored in the downstream reach. In the following years the upstream scour seems to have slowly filled in, while the downstream storage is degraded. The only exceptions to this pattern are in 1976 and 1981, when extremely low loads in the upstream reach were associated with scour in all the downstream reaches. These opposing patterns



**Fig. C-4; 4:** Annual deviation (in percent) of the mean daily suspended sediment loads at a downstream station relative to the mean increase between the two stations over the period of record.

in the upstream and downstream reaches can be interpreted as the passage of a slug of sediment through the channel system, and this movement can also be traced down through the last reach.

The large net movement of sediment in 1977 from reach P1-P2 to P2-P3 appears to also have deposited some sediment in reach P3-P4. This indicates that the bulk of the sediment moved more than 10 km, whereas some material deposited in reach P3-P4 must have moved about 20 km in that year. The following two years appear to level out the 1977

event in the upper two reaches, and had little effect on the net balance of the lower reach. After a little scour in 1978, equilibrium was reached in 1979. The large scour in reach P2-P3 in 1980 seems to have caused some deposition in the downstream reach.

The question arises as to what kind of event(s) could cause the movement of a slug of sediment through the channel system during a year of extreme drought. We can only speculate on possible explanations, and these might include:

- localized thunderstorm activity that caused short periods of flooding with direct sediment contribution to the main stream without excessive sediment contribution into the upper reaches of the stream;
- cattle trampling in the upstream reaches of Piceance Creek in search for water, thereby mobilizing sediment that is subsequently flushed during minor increases of flow;
- major channel disturbance (bank collapses, bridge building, etc.), or
- a slug of sediment was already in the channel upstream of reach P1-P2, and this simply migrated downstream.

#### **4.2.3 Review of data on the downstream travel distance of turbidity**

Some information on the travel velocity of suspended sediment (turbidity) is also available from the Deschutes River, a managed basin in the western Washington Cascades with a series of turbidity monitoring stations. Sullivan et al. (1987: 23-31) reported that it took 3-5 months for the peak of turbidity to travel approximately 600 m downstream following a sediment input due to road construction. This lag was in a very steep (13% average gradient) third-order stream with a narrow boulder-cobble channel and numerous cascades and falls. In Lincoln Creek, a debris avalanche deposited 4000 m<sup>3</sup> of sediment into the stream about one kilometer upstream from the confluence with the Deschutes River. Increased turbidity was observed over the next four months at a measuring station about one kilometer downstream, and this again was in a very steep channel. None of this sediment could be detected at a station 17 km downstream (Sullivan et al., 1987; p. 45). If we assume a constant transport velocity, an annual transport distance of 1.5 and 2.5 km/yr, respectively, could be crudely estimated for these two situations.

A third indication of travel distance is from the Deschutes River itself. A 50-year storm in December 1982 triggered numerous landslides in several of the headwater basins. The total weight of the landslide material was estimated to be 35,000 tonnes. During the winter of 1982-83, the sediment from those landslides apparently did not measurably increase the sediment export 15-20 km downstream. Only during 1984 did the summer dry season turbidity start to increase (Sullivan et al. 1987, p. 52). If this increase in turbidity can be associated with the landslides, as assumed by the authors, about 1.5 years were required for the suspended sediment to travel 15 to 20 km. This would indicate an average travel velocity of 10-13 km/yr. In contrast, water flowing at a rate of only 1 ft/sec (0.3 m/s) would travel 26 kilometers per day.

Another sudden increase in suspended sediment export occurred in the Deschutes River in 1986. This could not be related to rainfall and discharge, even though annual sediment yield in the Deschutes River is believed to be closely related to rainfall and discharge. In 1986 there also was a change in the sediment rating curve and a coarsening of the suspended sediment was reported. Sullivan et al. (1987: p. 52) attributed this change to the passage of landslide material generated 4 years earlier and 15-20 km upstream. If this is the case, then the sand fraction of this suspended sediment wave travelled approximately 5 km/yr.

These examples indicate that externally-supplied suspended sediment travels surprisingly slowly in steep mountain streams. Transport velocities increase after the sediment reaches the main river and becomes autochthonous material, and this is consistent with Rosgen's (1976) findings. As expected, fine suspended sediment travels faster than coarse suspended sediment.

An unusually large annual travel distance can be extrapolated from the experiments at Hunt Creek, a groundwater-fed pool-riffle stream in Michigan (Hansen and Alexander 1976). The turbidity cloud associated with an artificial input of sand travelled through a one-mile reach in 30 to 60 minutes, suggesting a travel velocity of 19-38 km/day.

The above suggests that the suspended sediment may travel faster with increasing stream size (or, in most cases, with distance downstream). Hence transport distance in small, steep, hydraulically-rough headwater streams may be less than in larger rivers with a lower gradient. This is contrary to what one might initially predict, and this is discussed in more detail in the review of tracer experiments later in this chapter.

### **4.3 Processes affecting the downstream travel distance of bedload sediment**

The primary means to obtain information on the travel paths, travel velocity, and mean rate of travel is to track the path of sediment from various sources to the different storage areas. Determining the rate of movement and storage requires the use of natural or artificial tracers and regular monitoring of their location. Tracers suitable for such tasks need to be durable and detectable even when buried deeply in the river sediments. A description of various sediment tracer techniques is given by Bunte and Ergenzinger (1989).

#### **4.3.1 Information needed for long-term mean annual travel distances**

Sediment transport through the fluvial system is a three-dimensional process with a long-term storage component. On their downstream journey, particles move not only longitudinally, but are also dispersed vertically and laterally. Longitudinal dispersion is affected by the temporary storage of bedload particles on the stream bed, and by the exchange between particles in motion and particles from the stream bed. Vertical dispersion is associated with the burial of tracers into the river sediment, and their subsequent excavation during high flows. Lateral dispersion refers to the deposition of sediment on bars, where sediment is stored until a later flood reentrains the sediment or the bar is scoured away by lateral erosion. Storage within the stream bed and on gravel bars can occur over widely-varying time scales.

Long-term observations of the downstream movement of individual bedload particles would, by definition, provide data on this three-dimensional dispersion and sediment storage. However, to the best of our knowledge, tracer studies on the downstream travel velocity of bedload are limited to shorter-term studies over single events, or medium-term observations extending over a few flood events or several years. These studies have generally focussed on only certain aspects of downstream transport, such as dispersion, or the effects of particle characteristics, stream morphology, or flow characteristics on travel distance. Long-term observations of the downstream conveyance of traced bedload particles in perennial mountain streams, which could provide information on the mean annual transport distances

over a time span of years or decades, are virtually non-existent. Thus the published results of the various short- and medium-term observations need to be combined to help infer the longer-term mean annual travel distance of bedload particles.

Unfortunately, the inferred travel distances from short- and medium-term observations pose a number of problems. One set of problems is associated with dispersion phenomena, while another set of problems is associated with the dynamics of bedload transport and how travel speeds are affected by particle size, stream morphology, and flow duration. Dispersion phenomena include the fact that the short-term travel speed of introduced tracers decreases as the tracers become part of the active bed material layer. Another problem is that the effects of medium-term storage in the bed or on gravel bars are only seldom included in analyses of travel speed. More importantly, the long-term storage of particles in the bed and on bars can almost never be integrated into an analysis of mean annual travel distances.

To infer or predict longer-term travel distance, four questions need to be investigated, and these are:

1. How can the downstream dispersion of bedload particles be statistically described?
2. How is the dispersion process affected by sediment properties, stream channel characteristics, and flow regime?
3. How does short-, medium- and long-term sediment storage affect dispersion?
4. How can the medium- or long-term velocity of various bedload particles in different stream types be inferred from a short-term study?

The next section will focus on the problems of tracer dispersion, while the next section will focus on the issues of particle size, particle shape, and stream morphology. Since these issues are inherently linked, any effort to systematically review these topics is faced with the problem of overlapping information, and some redundancy could not be avoided.

### **4.3.2 Studies addressing the dispersion of bedload sediment**

As noted previously, tracer particles disperse downstream (longitudinally), vertically (burial into the river sediment and reexcavation), and laterally (storage on bars and reentrainment). These topics and the relevant studies are briefly introduced in the following sections. In some cases the data stemming from certain studies are summarized in latter sections because the specific results are so closely intertwined.

#### **4.3.2.1 Longitudinal dispersion: travel distances**

To determine bedload travel rates, one needs to introduce large amounts of either natural or artificial sediment or tracers into a stream system. A large volume or number of tracers is needed to account for the high variability associated with individual particles, and to detect the change in transport rates over time at various measuring stations. Such monitoring studies, when conducted over several years, can provide a good indication of annual tracer distances, especially when the concerned stream does not have much medium- and long-term sediment storage.

Relatively precise measurements of travel paths and travel distances can be obtained when particles can be reliably identified and measured. Hubbell and Sayre (1964) and Sayre and Hubbell (1965) monitored the longitudinal dispersion of radioactive sand tracers in daily

intervals over a 12-day period at a sand-bedded stream in Nebraska. While the temporal extent of this experiment is somewhat short, it was included in our analysis of mean annual transport distances because terminal transport velocities seem to have been reached, and flows during the experiment were near the mean annual flow. Emmett and Myrick (1985) carried out several medium-term tracer experiments at the East Fork River (Wyoming), a gravel-bed river with a bedload comprised primarily of sand. They injected a fluorescently-marked sand and monitored its downstream migration over a snowmelt highflow season.

Ferguson et al. (1995) monitored the downstream dispersion and travel distance of one bedload tracer population over two years in a Scottish gravel-bed river. Intensive one-season studies with individually marked pebbles and cobbles were carried out at the Lainbach, a mountain gravel-bed river in the German Alps (Gintz, 1990; 1995; Gintz and Schmidt 1991; Schmidt and Ergenzinger 1992; Schmidt and Gintz 1995; Gintz et al., 1996). Thompson (1994) measured pebble and cobble travel distances during snowmelt highflow in a Rocky Mountain stream. The travel distances from these studies will be discussed in Section C-4.3.5.

#### 4.3.2.2 Statistical distribution of longitudinal dispersion

Several short-term tracer studies have studied various statistical aspects of the downstream dispersion of bedload, particularly:

- the transport step length of individual sand particles;
- the transport step lengths and rest phases of individual pebbles and cobbles;
- the transport distances of sand, and
- the transport distances of individual pebble and cobble tracers.

Grigg (1970) found that the frequency distribution of step lengths and rest periods of single radioactively-marked sand particles can be described by gamma or Poisson functions. Einstein (1937 and 1942) had presumed that a particle step length was about 100 times the particle diameter, but Busskamp and Ergenzinger (1991) and Schmidt and Ergenzinger (1992) found that particles moved at least 200 times their diameter. Step lengths increased for higher discharges and rest phases approached zero when the entire bed was in motion. The frequency distribution of step-lengths could be described by both a negative exponential and a gamma distributions. Over time, the frequency distribution of particles at various downstream locations flattens out and becomes more elongated, and this temporal development of the longitudinal particle dispersion can be characterized by a Poisson process. It must be emphasized that all of these studies monitored tracer movements over a period of hours or days, and these measurements of transport distances were not meant to be extrapolated to mean annual transport distances.

The longitudinal dispersion of radioactive sand particles was found to follow a gamma distribution (Hubbell and Sayre, 1964; Sayre and Hubbell, 1965). Daily monitoring over a 12-day period of steady flow showed that the temporal variation of the longitudinal dispersion of the bulk of sediment movement also can be characterized by a Poisson process.

Schick et al. (1987b) measured transport distances of individually traced pebbles and cobbles after flash floods in desert streams. The longitudinal frequency distributions, especially in the beginning of the dispersion process, were extremely skewed. A few particles moved very far, most particles moved only a short distance, and some particles did not move at all. Hence a mean transport distance is almost a meaningless number. If the longitudinal transport distribution has advanced to the point where it is described by a

negative exponential function, then transport distances should at least be given as a median rather than a mean, as the latter could be substantially larger as a result of a few particles travelling a long distance. However, most studies only report mean transport distances, and this limits the use of the published data to predict CWEs.

Schmidt et al. (1992) described that the longitudinal dispersion of cobble tracers in an Alpine step-pool stream. They found that after only one flood the dispersion followed a negative exponential function. For another population of tracers, Schmidt and Ergenzinger (1992) found that the longitudinal dispersion changed from a negative exponential distribution to an almost uniform dispersion over a two-year period in a 400-m reach.

Schick et al. (1987a) noted that the dispersion of particles for a single event is different from the longitudinal dispersion resulting from several events. The maximum dispersion distance ( $l_{max}$ ) from two short events is larger than the range of dispersion measured after one long event. Because the mean is so strongly affected by  $l_{max}$ , it also would be larger for two short events. Statistically, those particles that travelled a long distance in the first event had a low probability of experiencing another long travel step if the flood continued over a longer time period or was immediately followed by a second event. Particles that travelled a greater distance were more often deposited in shielded places (gravel bars, interstices, clusters, around boulders). In contrast, the median displacement length of one long event or two closely-spaced events is larger than the combined medians of two single events. A simulation of longitudinal dispersion indicated that a group of tracers will eventually be evenly distributed over the reach (i.e., the longitudinal dispersion approaches unity) (Hassan et al. 1991).

A summary of information on longitudinal dispersion and descriptive modeling is provided in Kirkby (1991). Empirical data sets and mathematical reasoning are used to explain why the cumulative longitudinal dispersion of tracers follows negative exponential and gamma distributions. Negative exponential distributions result from the observation that only a small proportion of all the tracers move, and from the fact that only those tracers that move more than a predefined distance ( $>l$ ) are part of the calculations. This situation would be mostly encountered in streams with pebble and cobble tracers during a relatively small high flow event. The negative exponential function gives the number of particles ( $n$ ) that move farther than the distance ( $l$ ) as:

$$n_{(>l)} = n_o \cdot \exp\left(-\frac{l}{l_m}\right) \tag{1}$$

where  $n_o$  is the number of tracer particles that actually moved, and  $l_m$  is the mean travel distance.

Kirkby (1991) used a stochastic approach to derive a gamma distribution of travel distances according to the number of steps that a tracer takes per flood event. Compared to the exponential distribution, which was based on a relatively low tracer mobility, the gamma distribution better describes the longitudinal dispersion for the case that all grains move during a relatively large flow. By combining Figures 2a and 8 from Kirkby (1991), we can obtain the cumulative distribution of travel distances for both a negative exponential distribution and a gamma distribution (Fig. C-4; 5). This indicates that a gamma function describes the situation in which all particles move, but most of them move only a short distance. In contrast, the negative exponential function applies to the situation when some particles do not move and relatively fewer particles move a short distance, but more particles travel a relatively large distance. Before addressing the extent to which these

distributions apply in natural streams, some aspects of vertical and lateral dispersion must first be discussed.

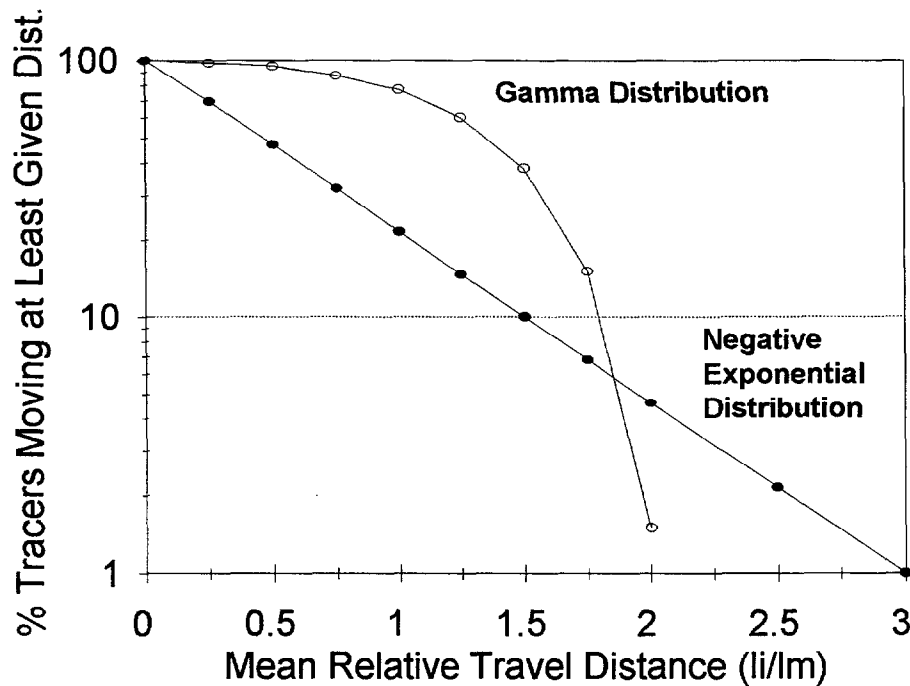


**Fig. C-4; 5:** Cumulative distributions of relative travel distances ( $l_i/l_m$ ) for a negative exponential distribution (straight line) and a gamma distribution (curved graph) (after Kirkby 1991). Note that the y-axis is a logarithmic scale so that the negative exponential distribution plots as a straight line.

#### 4.3.2.3 Vertical dispersion: processes and effects on travel distances

The vertical dispersion of coarse pebbles and cobbles, and the temporal variation of this vertical dispersion, has been studied in both short- and medium-term tracer experiments. Hassan et al. (1984) and Schick et al. (1987a, b) used magnetically-tagged tracer particles that can be relocated and retrieved even when deeply buried. Individual particles were buried up to 50 cm as a result of flash floods in the ephemeral streams of Nahal Og and Nahal Hebron in the Negev and in the Judean Desert in Israel. Hassan (1990) found that the time and depth of burial and the time of exposure varies with the morphologic location in the stream. Particles were buried deeper in the thalweg and in pools than in bars. Schick et al. (1987a) observed that after a few floods, only about one-third of the tracers placed on the surface were exposed. This proportion was relatively constant as particles previously buried were exposed and exposed particles were buried. The exchange rate was assumed to increase with the magnitude of the flood event.

Hassan and Church (1994) examined the temporal aspect of the burial process more closely using data from desert flash floods, a stream with a storm regime on Vancouver Island (Carnation Creek), and a stream with a snowmelt regime in the interior of British Columbia

(Harris Creek). At the beginning of an event particles become exposed. As the event progresses, particles are incorporated into the channel bottom. By combining the data from these different streams, Hassan and Church (1994) formulated a general description of vertical dispersion. This states that after a single flood event, the vertical distribution of tracer particles follows an exponential decay function. The majority of particles are near the surface and only a few particles are deeply buried. This vertical distribution is subsequently affected by the number of consecutive flood events, the magnitude and duration of the floods, and by the structure and texture of the bed material. The vertical distributions become skewed or the exponential decrease is weakened if the armor was poorly developed, or if a long flood event (e.g., snowmelt) occurred. With an increasing number of events, more tracer particles were incorporated into the sediments on the bottom of the channel. Hassan and Church (1994) then extrapolated beyond the period of their observations by modeling the vertical distribution of the tracer particles over time. The results indicated that in the final stage of tracer dispersion, the vertical distribution of tracers in the channel bottom becomes uniform, since the deeply buried particles have only a small chance of being exposed and re-entrained.

The question arises whether vertical dispersion affects downstream travel velocity. Clearly a pebble or cobble tracer cannot move downstream when it is buried in the stream bed, and so its travel distance will be very low compared to those tracer particles that are on the bed surface and therefore available for entrainment. However, it appears that these subsurface particles make up for some of their immobile storage time by having an exceptionally large transport step following reexposure. Schick et al. (1987a, b) explain that in desert flash floods reexposure is associated with local scour, and the strong flows causing the local scour provide a stronger entrainment "push". Transport distances of particles that were reexposed during a flood event were three times greater than particles which were on the surface before and after the flood (Section C-4.3.3.2).

A low recovery rate of marked particles should indicate that a large number of tracers has been worked into the bed through particle exchange. More particle exchange and a lower recovery rate should be associated with larger, more turbulent, and longer-duration flood events. In such cases the average travel velocity of surface and subsurface tracer particles could well be the same. In his experiments in desert flash floods, Hassan (1990) noted no difference in the transport distance of surface particles as compared to the particles which had been buried.

If the majority of flood events is not able to generate much vertical dispersion, the long-term mean travel distance of the surface particles will probably be farther than the mean travel distance for those particles which were buried but not reexposed. No systematic study has examined the channel, sediment, and flow conditions under which the mean travel distance and velocity of surface particles represent the mean of all tracer particles.

#### 4.3.2.4 Lateral dispersion

We could only find a few references regarding the lateral dispersion of tracer particles in mountain streams (Gintz and Schmidt 1991; Schmidt and Ergenzinger 1992). One would expect that lateral dispersion is closely related to channel characteristics such as presence and size of gravel bars, entrenchment, sideslope morphology, and the magnitude of high flow events. Gintz and Schmidt (1991) and Schmidt and Ergenzinger (1992) report that in tracer experiments carried out during several, moderately-sized short summer floods at the Lainbach, a mountain step-pool stream in Bavaria, flows were not high enough to entrain any significant amount of tracer particles seeded on lateral gravel bars. Of all the tracers

entrained from various other starting positions within the deeper parts of the stream, only 6% were deposited on bars (see also Section 4.3.3.4).

### 4.3.3 Effects of particle size and shape, bedforms, and stream morphology on the downstream travel distance

A literature review of tracer studies indicated that the downstream travel distance and longitudinal dispersion is affected by the following sediment, flow, and channel properties:

- particle size and shape,
- magnitude and duration of flow,
- bed micromorphology,
- channel and valley morphology, and
- the type and amount of large woody debris.

Since all of these affect the long-term travel distance, each of these items is discussed in the following sections.

#### 4.3.3.1 Particle size and shape

Church and Hassan (1992) conducted a literature review on the relationship between grain-size and travel distance. Surprisingly, many authors found no relationship between the transport distance of tracers and their grain size. However, their analyses of data sets from several authors showed that transport distances of free surface particles generally **declined** with particle size. This decline in travel distance with grain size is less pronounced for relatively small particles (smaller than twice the  $D_{50}$  of the subsurface material) because these smaller particles can hide behind larger particles or be trapped in the interstices within a rough gravel bed (Hassan and Church 1992). For larger particles (larger than twice the  $D_{50}$  of the subsurface) the decline in transport distance with particle size is very pronounced and reflects the counteracting forces of inertia and particle weight.

The magnitude of the flood event also affects the relationship between particle size and travel distance (Hassan and Church 1992). Size-dependent transport behavior is most pronounced for relatively large flows that mobilize the surface layer. In smaller high flows that just exceed the threshold of particle motion, transport lengths of small particles may be handicapped by hiding during entrainment and trapping during deposition. Decreased entrainment probabilities and increased deposition probabilities counteract the positive effects of a lighter weight on transport distances, and this diminishes the effects of grain-size on transport distances in relatively small floods.

These concepts do not always hold, however. Kirkby (1991) showed a decreasing size dependency with increasing flow for Crimple Beck, a sand-bedded river in north Yorkshire (Great Britain). The transport distances for the leading edge of the tracer wave decreased with grain size (5-10 mm, 10-15 mm, and 15-20 mm) for a given peak flow. At flows sufficient to make bedload movement more important than suspended load, the grain-size dependency became negligible. Kirkby (1991) attributed this phenomenon to the presumed onset of equal mobility during high flows, while sediment transport during low flows was grain-size dependent.

A strong grain-size dependency for the leading edge of pebble-sized particles was also recorded in a single flash flood event (Tazioli, 1981). In this study radioactive pebbles were

inserted into a small stream in southern Italy. Maximum transport distances exceeded 240, 125, and 70 m for particles of 19-25, 20-30, and 24-39 mm, respectively. No information on the channel characteristics were provided. Ketcheson and Megahan (1991) noted a systematically higher mobility of finer grain sizes in their tracer experiments with sand and fine gravel in Idaho streams.

A systematic size dependency in sediment transport was also found at Allt Dubhaig, a gravel-bed stream in Scotland (Ashworth and Ferguson, 1989). Pebbles with an intermediate diameter of 40 mm were moved more often and transported further than cobbles with an intermediate diameter of 180 mm. However, the smallest grain-size class (27-38 mm) had a lower mobility rate than the next larger grain-size class (38-54 mm). A similar phenomenon had been shown by Laronne and Carson (1976) for tracers ranging from 4 to 256 mm in a steep (gradient of 2.1-8.6 percent) boulder-bedded stream. Mean transport lengths varied from 53 to 112 m during a spring highflow and generally decreased with particle size, but there was a large amount of scatter in the data. Again the greatest transport distances were not in the smallest weight group (0.1-1 grams, representing particles in the 10-20 mm size range), but in the next larger group of 1-10 grams. Transport distance then declined with each larger size class.

A recent tracer study in a pool-riffle stream in the Colorado Front Range also showed that the smallest size class had a lower mean transport distance than most of the larger size classes, but there was a consistent decline in transport distance with grain-size for all the larger classes (Table C-4; 2) (Thompson, 1994). Again the scatter in the data was large, with coefficients of variation in excess of 100%.

**Table C-4; 2:** Transport distances by size class over a larger than normal snowmelt highflow in North St. Vrain Creek (from Thompson 1994).

	Grain size classes (mm)					
	16-32	32-45	45-64	64-90	90-128	128-256
Mean distance (m)	27.5	51.9	41.5	25.5	7.6	1.3
standard deviation	34.9	68.3	50.5	32.5	10.4	2.5
CV (%)	127	132	122	127	137	200
No. of recov. tracers	15	17	30	38	45	4

Thompson (1994) also observed that sand apparently did not get washed out of the pools during the entire high flow season. Horizontal vortices in pools caused the sand to be deposited in backwater areas during high flows, and this sand then slumped back towards the pool center as flows receded. If such vortices persist during high flows, sand-sized material may not be as readily transported in pool-riffle rivers as might otherwise be assumed.

The wide scatter within the general trend of decreasing transport distance with particle weight and particle size have also been noted in a series of tracer experiments in the Lainbach, an alpine step-pool stream in southern Germany (Gintz and Schmidt, 1991; Schmidt and Ergenzinger, 1992; Schmidt et al., 1992; and Gintz, 1994). The gradient is about 0.026, and high flows are generated either by spring snowmelt, long-duration frontal systems, or summer storms. The size of the tracer particles ranged from 50 to 170 mm, and this corresponds to  $D_{45}$  and  $D_{75}$ , respectively, of a volume sample from the channel.

However, another experiment showed the opposite behavior, with tracers weighing 100 g travelling less than particles weighing 500 g. Apparently the small tracers were trapped in the interstices of larger particles on the stream bed, especially in the coarse structure of the natural steps. The decreased mobility of small particles due to trapping in interstices and gravel pockets has also been observed by Barta et al. (1993).

The effect of particle shape on transport distance and the variation in transport distance has also been studied during the Lainbach experiments (Gintz, 1990; 1994; Gintz and Schmidt, 1991; Schmidt and Gintz, 1995; and Gintz et al., 1996). Hundreds of artificial concrete tracers were placed in the stream. These all weighed 1.0 kg, but there were four different shapes representing the three corners and the center of the Sneed and Folk (1958) diagram of particle shape. These shapes can be classified as ellipsoids, rods, discs, and spheres. They found that transport distance in the hydraulically rough Lainbach was strongly dependent on particle shape. Mean transport distances after two consecutive floods increased from discs (19 m) to spheres (61m) to ellipsoids (66 m) and then to rods (76m). The low transport distances of discs can be attributed to their stable position in imbrication structures and their relatively small cross-sectional area (*b*-axis times *c*-axis) exposed to flow. Other studies have also shown that higher shear stresses are required to entrain disc-shaped particles than rounded particles, and this causes disk-shaped particles to have a shorter mean transport distance (Ashworth and Ferguson, 1989; More and Diplas, 1994). The effects of particle shape and orientation on entrainment and transport velocities was further analyzed in flume experiments by Carling et al. (1992), and these results showed that the effect of particle shape varied with the roughness of the channel bed.

#### 4.3.3.3 Magnitude and duration of flow

Although many studies have shown that travel distance generally increases with magnitude and duration of the flood event, Hassan and Church (1992) combined data from several authors to plot transport distance per flood ( $l_m$ ) event against excess stream power ( $\omega - \omega_o$ ) in kg/m·s (Bagnold 1966; 1980). The resulting power function is :

$$l_m = 1.0 \cdot (\omega - \omega_o)^{1.2}. \quad (2)$$

Using data by Leopold et al. (1966) from desert streams in New Mexico, Hassan and Church (1992) found that the travel distances of pebbles and cobbles was about 30-50 times larger in hydraulically smoother sand-bedded streams. Differentiating data sets by grain-size had relatively little effect on the nearly one order of magnitude of scatter (Hassan et al., 1992). By combining all of their data sets Hassan et al. (1992) empirically defined the relationship between mean transport distance and excess stream power ( $\omega - \omega_o$ , in  $W \cdot m^2$ ) as:

$$l_m = 0.0283 \cdot (\omega - \omega_o)^{1.44}. \quad (3)$$

This regression had an  $r^2$  of 0.77.

Hassan et al. (1992) then examined the "virtual rate of travel", which was defined as the travel velocity during the period when discharge exceeded the threshold of motion ( $v_{dm}$ , in m/h). Using peak discharge to calculate excess stream power, they found:

$$v_{bm} = 2.56 \cdot 10^{-4} \cdot (\omega - \omega_0)^{2.02} \tag{4}$$

The rather poor  $r^2$  of 0.40 was improved by using only the duration and excess stream power of the first discharge peak to calculate the virtual rate of travel. The revised relationship was:

$$v_{bm} = 2.93 \cdot 10^{-4} \cdot (\omega - \omega_0)^{2.07} \tag{5}$$

and this has an  $r^2$  of 0.74. The implication of these results is that mobility is greatly affected by the initial location of the tracers.

Gintz (1994) also investigated the relationship between transport distance and excess stream power from her tracer data from the Lainbach (Fig. C-4; 6). Her data are a factor of 5-10 below the data presented by Hassan and Church (1992). This difference can be attributed to the steeper step-pool profile of the Lainbach, where much of the flow energy is lost in the nearly vertical plunge of water off the steps. The data sets used by Hassan and Church (1992) and Hassan et al. (1992) were derived primarily from streams with lower gradients which do not have a step-pool morphology.

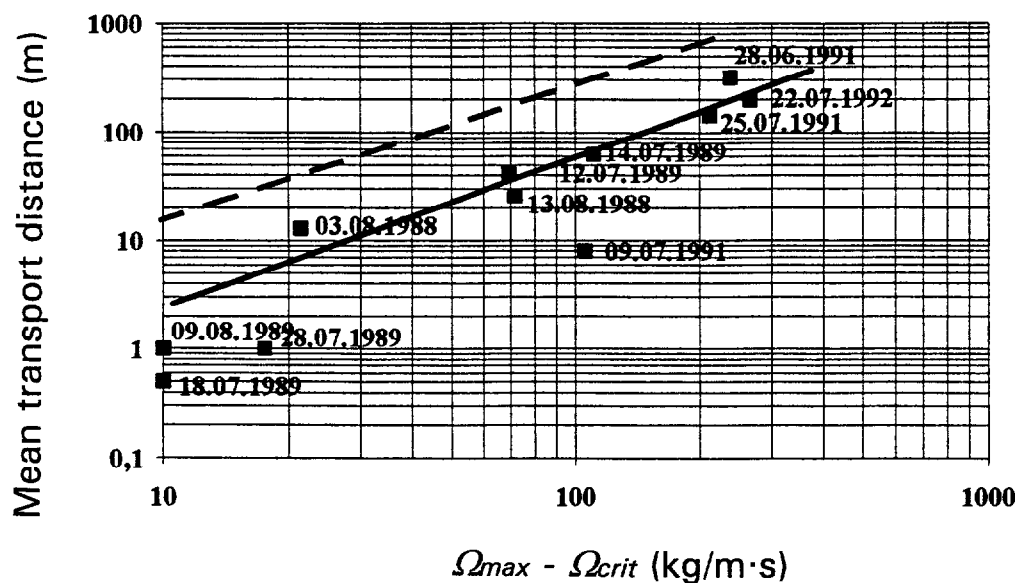


**Fig. C-4; 6:** Mean transport distance (m) of pebble and cobble tracers versus excess stream power ( $\Omega_{max} - \Omega_{crit}$  in kg/m·s) of peak flows for various flood events at the Lainbach, a step-pool stream in Bavaria (Gintz 1994). The dashed line represents the data from Hassan et al. (1992) for less steep streams that do not have a step-pool morphology.

The difference in energy expenditure also has an effect on travel velocities (Fig. C-4; 7). Gintz's data yields substantially lower transport velocities and a much slower increase in transport velocity with excess stream power as compared to the results from Hassan et al. (1992). This lower rate of increase in transport velocity may be attributed to a generally decreased particle mobility in the cobble-bedded, step-pool Lainbach compared to the hydraulically smoother streams in Hassan's studies. The indication of decreased mobility in steeper streams is consistent with many of the observations for suspended sediment transport (Section C-4.2.3), namely that transport distance seems to decrease with increasing steepness and roughness of the stream. However, Ketcheson and Megahan (1991) found that the number of sand and fine gravel tracers which left the test reaches in four small creeks in Idaho increased with increasing gradient. Since the highest peak discharges were associated with the streams that had steepest gradients, the higher mobility of sand and fine gravels in the steeper streams may be due to their higher peak discharges.

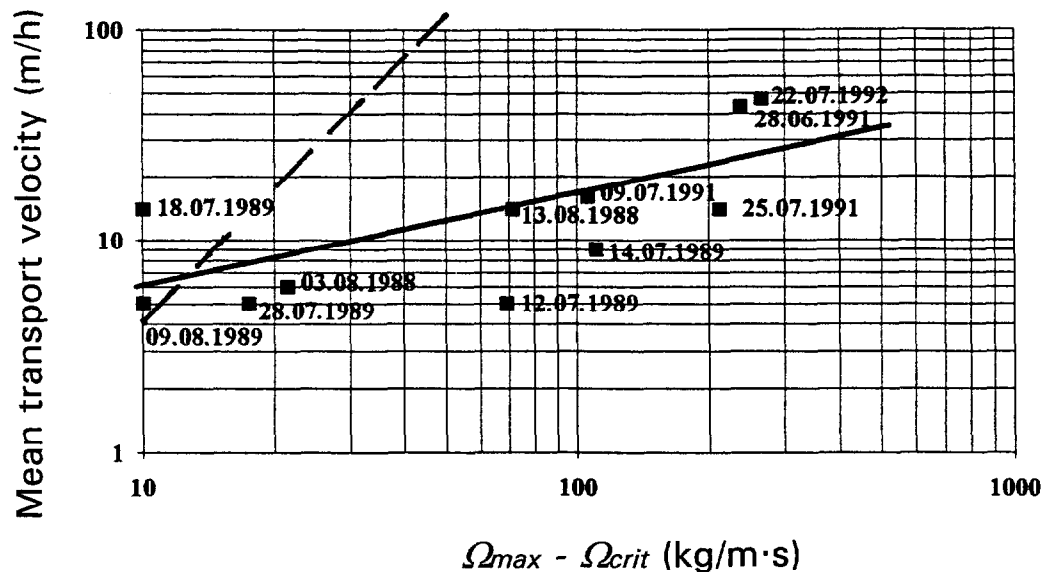


Fig. C-4; 7: Mean travel velocity (m/h) of pebble and cobble tracers versus excess stream power ( $\Omega_{max} - \Omega_{crit}$  in kg/m·s) of peak flows for various flood events at the Lainbach, a step-pool stream in Bavaria (from Gintz 1994). The dashed line represents data from Hassan et al. (1992) for less steep streams that do not have a step-pool morphology.

#### 4.3.3.4 Bedforms and micromorphology

Travel distances and the dispersion of tracers are affected by bedforms and the channel micromorphology. For example, bedload can be incorporated into ripples and dunes. In such bedforms a particle might travel quite fast (e.g., up the stoss side and down the lee side), but the net downstream advance of bedload is equal to the migration velocity of the bedform, since the entire bedform passes over the particle deposited on the lee side. This mechanism is quite obvious for small ripples, but it also has to be taken into account for larger-scale sand and gravel dunes that may be tens of meters in length.

Bedload transport distances can also be increased by vortex scour and the helical flow field that develops around local flow obstructions like bridge piers (e.g., Laursen 1963) or large rocks in a finer matrix (Karcz 1968; Leopold et al. 1966). Small particles are easily scoured and entrained in the vortex at the stoss of a flow obstruction. During relatively low high flows, most of the particles are deposited in the wake eddy, while relatively strong flows can carry entrained particles through the lateral scour channels and deposit them further downstream where the helical motion of the scour vortex fades (Bunte and Poesen 1993b, 1994).

Another example of the effect of local scour on transport distances comes from the studies carried out in the Negev desert in Israel. After flashy desert floods Schick et al. (1987a, b) and Hassan (1990) found tracer particles to be deeply buried, but during the next flood local scour can reexpose even deeply buried particles. Hassan (1990) found the deepest scours in the thalweg and in the pool areas. Although the transport distance of the particles reentrained by local scour exceeded the transport distance of surface particles by three times (Schick et al. 1987a), this larger transport distance was more than counteracted by their much lower entrainment probability (Hassan 1990).

Several studies have found that the bed micromorphology, and especially the formation of particle clusters, decreases transport distances. In Turkey Brook, a gravel-bed river in Great Britain, Frostick et al. (1984) noted that particles within clusters were generally less mobile than particles in open plane-bed positions. This finding is consistent with the observation that higher flows are required to move particles with a closer spacing on the bed than to move particles that are further apart from each other (Leopold et al., 1996).

The entrainment probability of a particle is also dependent on its location within a particle cluster. Frostick et al. (1984) found that 100% of the particles in an open position on the plane-bed positions were moved, as compared to 50-60% of the particles in wake positions and 40% of the particles in stoss positions. Likewise, mean transport distances per event decreased from about 10 m for entrainment from plane-bed positions, to 2-7 m and 2-3 m for entrainment from wake and stoss positions, respectively (Brayshaw et al. 1983; Brayshaw 1985).

Stoss and wake positions around boulders also proved to be unfavorable locations for the entrainment and transport of cobble tracers in the Lainbach (Gintz and Schmidt 1991; Gintz 1994). While 100% and 80% of the tracer particles were entrained from pool and step areas, respectively, the entrainment probability dropped to only 29% for stoss positions. Mean transport distances after two consecutive summer storms from stoss positions were quite low (27m) compared to mean transport distances for particles from pools (86 m) and steps (55 m) (Table C-4; 3). Particle clusters therefore seem to act as another sediment storage location from which sediment is less frequently exchanged relative to those parts of the channel bottom without clusters.

#### 4.3.3.5 Channel and Valley Morphology

Several authors have noted that the downstream transport distance of both fine and coarse bedload sediment is affected by the channel morphology. Laronne and Carson (1976) observed the greatest transport distances for particles entrained from the steepest reaches, while particles seeded in reaches with a lower stream gradient were not transported as far.

**Table C-4; 3:** Effects of channel morphology and micromorphology on entrainment probability, transport distances, and deposition probability of 480 artificial 1.0 kg tracers. Data were obtained after either one or two consecutive summer flood events in a mountain stream (from Gintz and Schmidt 1991; Schmidt and Ergenzinger 1992).

	Morphological Feature or Position				
	Pools	Steps	Stoss	Lee	Lateral Bars
Entrainment probability (%)	100	80; 63*	29; 47*	-#	-#
Transport distance (m)	86	55	27	-#	-#
Deposition probability (%)	32	13	19	7	6

\* after two consecutive floods; #value not measured or too small to be significant

Downstream dispersion and travel distance are often associated with the recurring elements of stream morphology. Tracer experiments at the East Fork River in Wyoming indicated that sediment is scoured from the pools during rising flows and deposited in pools during waning flows (Emmett and Myrick, 1985). On average the  $D_{50}$  of the bed material was coarse sand, but the bed material composition varied longitudinally between sand-filled pools, gravelly riffles, gravel bars, and bedrock.

During tracer experiments at the East Fork River, particles ranging in size from 0.25-8 mm were injected onto the stream bed. About 300 m downstream of the injection point a longitudinal dispersion of the tracers into 2 or 3 modes started to become visible. The bulk of the sediment was deposited near a cross-section 2356 meters downstream from the injection point, while large amounts of sand were deposited in pools at 1901, 2356, and 2608 m (Meade et al. 1981; Meade 1985). This polymodal longitudinal transport distribution was most marked for the two finest grain-size classes (0.25-0.5 mm, and 0.5-1.0 mm), indicating that the pools were especially effective in trapping the fine material as the snowmelt high flow receded. For the next two larger grain-size classes (1-2 and 2-4 mm), the distance between peak concentration peaks was smaller, and the first peak represented the bulk of the sediment. For the largest grain-size class (4-8 mm) the longitudinal distribution was unimodal.

For the pink tracers used at the East Fork River by Emmett and Myrick (1985), the longitudinal dispersion of tracers over the snowmelt high flow was strongly grain-size dependent (Table C-4; 4). The distance to the leading edge consistently declined from 2.5

**Table C-4; 4:** Seasonal transport distances and dispersion (m) of "pink" tracers of various grain-size classes during snowmelt highflow at the East Fork River in 1979 (data from Emmett and Myrick, 1985).

	Grain-size classes in mm				
	0.25-0.5	0.5-1.0	1-2	2-4	4-8
First sediment peak	550*	450*	450	350	-
Second sediment peak	1150	700	700*	700*	550
Leading edge	2500	1550	1050	750	600
Dispersion range	2000	1100	600	400	50

\* bulk of sediment

km for the finest grain-size class to 600 m for pea gravel (4-8 mm). There was less variation in the travel distances for the main body of sediment with grain size.

The data in **Table C-4; 4** effectively represent the annual travel velocity. At a finer scale of resolution travel velocity was relatively constant for about 2-3 weeks over the peak rates of snowmelt high flows. As the discharge slowly receded transport velocities gradually decreased until almost all particles came to rest. The point at which the travel velocity starts to decrease is somewhat arbitrary, but **Table C-4; 5** indicates the difference in mean daily travel velocities (m/d) during the snowmelt season for the primary and secondary peak discharges.

**Table C-4; 5:** Travel velocities (m/d) of "pink" tracers of various grain-size classes during snowmelt highflows at the East Fork River in 1979 (data from Emmett and Myrick, 1985).

	Grain-size classes in mm				
	0.25-0.5	0.5-1.0	1-2	2-4	4-8
Secondary peak	18*	20*	9	10	-
Primary peak	34	24	20*	20*	23
Leading edge	71	61	38	28	36

\* bulk of sediment

The velocity of the bulk of the sediment ranges between about 10 and 30 m/d. For the smaller particles (0.25-1.0 mm) the leading edge and the secondary peak had a greater travel distance than for the larger particles (1-8 mm), but this trend was not apparent during the primary peak and was not discernible within these larger size classes.

Meade et al. (1981) and Meade (1985) provide evidence that sediment is scoured from the pools during the beginning of the high flow and deposited in the pools towards the latter recession part of the seasonal high flow. During the initial rising flows sediment is scoured out of one pool and starts its downstream journey as a sediment wave. The bulk of the sediment has only reached the next pool as the snowmelt highflows recede, and the distance covered is, on average, about one pool spacing per year; on the East Fork River this is about 20-30 stream widths or 400-600 m. This interpretation is consistent with the results from the analyses presented in **Table C-4; 5**.

The recognition that mean annual sediment transport distances (*l<sub>m</sub>*) are a multiple of pool spacings could be helpful for estimating annual transport distances in low-gradient streams where pool spacing is very large and particles may only be transported one or two pools per year. Unfortunately, this knowledge is of little practical value for estimating annual travel distances in streams with a closer spacing of pools and particles may be transported through many pools within a given year.

The fact that pools have a major effect on transport distances and transport probabilities of individual pebble and cobble tracers was also noted by Gintz and Schmidt (1991), Schmidt and Ergenzinger (1992) and Gintz (1994) at the Lainbach. Pools proved not only to be the optimum entrainment position for coarse gravels, but particles from pools also travelled the greatest mean distance (86m) as compared to particles eroded from steps (55 m). Pools were also the most favorable location for deposition (Section 4.3.3.2).

Travel distance in meandering streams also seems to be a multiple of the meander bends, since the pools in the outside bends are scoured during rising flows and filled during waning flows (Dietrich and Smith 1984; Anthony and Harvey 1991). Travel distances in meandering streams can also be evaluated from the perspective of theoretical particle trajectories. Particles that travel along the thalweg are less subject to the start-and-stop pattern of transport and deposition, and are therefore more likely to travel a greater distance than the particles scoured in an outside bend. In meandering streams the latter particles are more likely to be deposited on the upstream end of the next point bar. Particles scoured a little further upstream in the bend will be deposited further downstream on the point bar (Holtorff 1989). Particles deposited on a point bar will stay until a higher flow reentrains them or until the downstream migration of meander bends erodes the former point bar. Tracer experiments by Gintz (1994) confirmed that sediment residence times for frequently flooded gravel bars are longer than those in pools.

The effect of sediment storage in gravel bars on the short- and medium-term downstream dispersion was also addressed by Hassan et al. (1991) in desert streams. For the first transport event(s) after tracer injections the longitudinal dispersion of coarse particles could generally be described by negative exponential, gamma, or Poisson distributions. But as the longitudinal tracer displacements approached the spacing of gravel bars, tracers started to become worked into the gravel bed. This process disturbed the dispersion process to such a degree that it could no longer be satisfactorily described by any of the above statistical distributions. Hassan et al. (1991) claimed that, once the transport distance extends beyond the spacing of channel storage sites like bars and pools, thousands of traced particles would be needed to test which distribution would best fit the long-term transport distances associated with a slug of introduced particles.

Reference has already been made to the study of sediment transport in four small streams in Idaho (Ketcheson and Megahan, 1991). Of the tracer particles still present in the test reaches after a snowmelt highflow, 47% of the sand and fine gravel tracers was in deposits behind LWD, 12% was around rocks, and the remaining 40% was contained in other channel locations (e.g., pools, channel bed, or point bars). It is obvious that the dispersion of introduced sediment will be interrupted when bedload is trapped behind LWD. In such cases one might expect that the mean bedload velocity will be determined by the spacing and half-life of the LWD. However, the stored sediment might not be remobilized, as the larger sediment deposits behind LWD can form terrace-like features that may persist long after the loss of the initial LWD (Abbe et al., 1993).

#### 4.3.3.6 Long-term sediment storage

Most tracer studies have focussed on the short-term (event scale) and medium-term (seasonal or perhaps annual scale) effect of sediment storage on tracer dispersion and transport distances, and this is the usual scale for evaluating CWEs. Nevertheless, the longer-term storage of sediment is of equal importance, and sediment storage on this scale has been addressed for gravel-bed rivers by Kelsey et al. (1986), Madej et al. (1987), Madej (1984 and 1989 (with the latter cited after Meade et al. 1991)), and Abbe et al. (1993). Sediment residence times can extend up to millennia, depending on the location relative to the stream channel and the magnitude of the subsequent events. Nakamura et al. (1987) estimated sediment residence times of 10-30 years for near-stream storage locations.

Numerous studies have also evaluated the storage of suspended sediment in higher-order streams (e.g., Dissmeyer 1976; Trimble 1976, 1977, 1981, 1983, and 1993; Phillips 1987, 1989, 1991, 1992, and 1993; and Marron 1992). These studies have generally shown that high erosion rates in headwater basins during the 19th and early 20th centuries led to

extensive deposition in lower-gradient downstream reaches. Sediment does not begin to be removed from these storage locations until 50 or 100 years later, when erosion control measures in the headwaters deplete sediment supply and initiate erosion of the former alluvial deposits. The high sediment yields stemming from this more recent erosion of the older deposits may then lead to another generation of floodplain deposits still further downstream.

#### **4.3.3.7 Summary**

##### ***Effects of particle size***

Although transport distances generally decrease with particle size, individual studies report a large scatter or even an inconsistent relationship between transport distance and grain size. This variability can be attributed to hiding and trapping as well as particle shape. Both mechanisms are especially effective during the smaller high flows when the threshold of motion is just exceeded, but the coarse armor layer is not yet broken up. The relationship between grain size and transport distance is often stronger for the larger flows that entrain all grain sizes, as transport distances are more strongly controlled by the counteracting forces of inertia and particle weight.

##### ***Magnitude and duration of the flow event***

Transport distances and virtual rates of travel generally increase with the magnitude and duration of the flood event. However, the large energy expenditure associated with the extremely turbulent flow in steep mountain streams can lead to a decrease of transport distances as the stream bed becomes steeper and rougher.

##### ***Bed micromorphology, bed forms, and stream morphology***

A rough channel bed, imbrication, and particle clustering all seem to decrease entrainment probabilities and encourage deposition. By acting as small, instream sediment storage locations, mean transport distances are correspondingly reduced. Similarly, individual particles may be rapidly transported when on the surface of ripple and dune bedforms, but mean transport rates are reduced by the time that particles are buried by the advancing ripple or dune. Thus the mean particle transport velocity is simply the velocity of the bedforms. Entrainment probabilities and transport distances are increased by the occurrence and vigor of vortex erosion and local scour.

Transport distances appear to be greatest for particles entrained from steep locations, pools, and the outside of meander bends. There is some evidence that transport distances are multiples of pool spacings. Since the dispersion process is also affected by the occurrence of other sediment storage locations (e.g., gravel bars and behind LWD), transport distances might also be a multiple of bar spacings (Kondolf and Matthews 1986) or large jams of LWD.

##### ***Stream type - stream gradient***

It follows that the roughness of the stream bed and the proportion of energy dissipated in turbulence are important controls on the distance of sediment transport. In large, hydraulically-smooth streams with ample sediment supply, transport distances should increase with unit stream power, and thus with stream gradient. In small, hydraulically-rough mountain streams, transport distances may not increase with unit stream power because much of the flow energy is dissipated in the tumbling flow around or over

obstructions. One might even predict that mountain streams could have a negative relationship between stream gradient and transport distance. Unfortunately, there are no systematic studies of transport distances as a function of gradient, bed material, sediment supply, and stream morphology.

In summary, the downstream dispersion of a given sediment input is disturbed by a variety of mechanisms operating at different spatial and temporal scales. Large particle sizes, smaller flood events, certain channel features (e.g., armor layer, roughness, particle clusters, imbrication), and irregular sediment storage sites (e.g., LWD or beaver dams) delay or impede the three-dimensional dispersion process. Conversely, smaller particle sizes, relatively large floods, and certain channel features (hydraulic smoothness, lack of an armor layer) facilitate a smoother and possibly more predictable dispersion of sediment. Although not explicitly expressed in the literature, a process that increases the dispersion of sediment will also tend to increase transport distances. Over longer time periods the dispersion of sediment becomes more predictable, but the same is not necessarily true for the downstream travel of sediment. The uncertainty of transport distances can severely hinder the downstream prediction of CWEs and the effect of spatial scale, and the ability to extrapolate from the shorter-term, smaller-scale studies is the focus of the next section of this report.

#### **4.3.4 Extrapolation of short-term and medium term tracer experiments?**

The duration of the tracer experiments cited in the previous section is generally too short to reliably determine mean annual travel distances. Nevertheless, the results of these shorter-term studies are critical to understanding the processes that affect mean annual travel distance. This knowledge is essential to preventing an inappropriate extrapolation of the published data to different streams or over longer time periods.

In the absence of long-term studies, the question arises as to how one might evaluate or predict the long-term travel distance for different grain sizes in various stream types. Since so many different variables affect the downstream dispersion of sediment, it is questionable whether the long-term dispersion and mean annual travel distance can be extrapolated from existing data. Specifically, several questions arise regarding the estimation of longer-term travel distances:

- 1) Many tracer studies were done in flashy ephemeral streams. Are the respective results of tracer movements transferable to the different flow regimes of perennial streams?
- 2) Much of the introduced tracer material becomes worked into the channel bottom and stays buried for various periods of time. Do measured tracer surface transport distances accurately represent the bulk sediment transport rate?
- 3) Should the average transport distances be derived from the arithmetic mean, the median, or the mode of the dispersion distribution?
- 4) Can the long-term sediment transport behavior be estimated by summing several short-term studies of sediment transport?
- 5) Are the models used to describe short-term dispersion applicable to longer-term estimates of sediment displacement?
- 6) Can the long-term downstream travel distance of bedload be predicted by the extrapolation of short-term (e.g., a few days or a seasonal high flow) tracer results?
- 7) Does the dispersion process and the travel velocity of introduced tracers change over time, irrespective of flow hydraulics?
- 8) If long-term tracer experiments are necessary, how might these be designed and what are the required tracer characteristics?

From the information gathered to this point, we put forth the following "answers":

***(1) Can we use data from ephemeral streams for perennial streams?***

Flash floods in desert channels have many of the features that lead to a smoother dispersion and greater travel distances. We might therefore expect that travel distances per flood event observed in these studies might be larger than the travel distances for flood events of comparable duration and frequency in perennial streams.

***(2) Does surface tracer velocity equal bulk tracer velocity?***

Hassan (1990) found the travel distance of pebbles and cobbles in desert flash floods, where vertical exchange commonly reaches deep into the subsurface, to be equal for particles on the surface and buried in the subsurface. We would expect that in perennial streams where the armor layer is not torn up with each flood event, at least the smaller surface particles will move more frequently and thus further than particles which were buried and cannot be moved until they are reexposed during the next large event. The mean transport distance of surface particles in perennial mountain streams will therefore be substantially larger than the bulk transport rate, and the ratio will depend on the weighted average duration of storage for each storage location.

***(3) Should we rely on the mean, median, or mode of transport distances?***

The longitudinal dispersion process seems to pass through several stages. For bedload particles, the dispersion pattern in the initial stages of a flood event is characterized by a few particles travelling a large distance while most particles travel only a short distance or not at all. An effort to quantify transport distances only seems to make sense after appreciable sediment transport has occurred and the tracers have dispersed to the extent that one could determine an appropriate probability distribution such as a negative exponential. At this stage the median is the best description of average transport lengths. As the longitudinal spread of the tracers further increases over time, the dispersion might be better described by a gamma function, and the mode might be a more suitable measure of average transport distances. In most cases the mean will be greatly affected by the small number of particles that travel a great distance.

The choice of the median or mode will depend in part upon the question one is trying to address. The median is of more interest if one is trying to track a specific sedimentary event, while the mode may be more important if one is trying to predict the maximum convergence of sediment from several sources in a downstream reach. The arrival of the leading edge may also be of interest if this is associated with a certain contaminant or the initial arrival might interfere with a sensitive and biologically important process such as the suitability of spawning habitat.

***(4) Can one sum short-term behaviors to estimate long-term displacement?***

Particle dispersion is increased over time as successive floods transport the tracers downstream. This means that a large number of tracers would be needed to reliably establish the long-term dispersion pattern. To accurately represent the long-term pattern of dispersion and transport the tracer particles would have to successively represent the evolving distribution that would be found over time. Most tracer experiments do not place the particles in locations where they are unlikely to move, even though most experiments have shown that a large proportion of the tracers end up in locations where they are not readily accessible to transport by the next high flow. Since the storage component is so important on any time scale beyond an individual flood event or seasonal high flow, a sediment budget appears to be the only approach that can be used to estimate the longer-

term bulk transport of sediment. The deposition and retrieval of particles from different storage sites is a key aspect that still needs to be better understood and quantified.

***(5) Can the short-term dispersion models be applied to longer-term estimates of sediment displacement?***

The longitudinal dispersion over relatively small displacements can be characterized by dispersion models. Different descriptive models are required at different evolutionary stages, but numerous factors (e.g., magnitude of flow events, micromorphology, channel morphology, storage) lead to dispersion patterns that deviate from the theoretical distribution functions. Kirkby (1991, p. 119) states that "In the absence of process constraint the negative exponential distribution is the most likely, but process behavior may constrain movement, particularly inter-particle movement, and so modify the distribution." For pebble and cobble tracers Hassan et al. (1991) and Hassan and Church (1992) found that dispersion models ceased to work when dispersion reached the scale of bar spacing, as the burial of particles on the bars greatly delayed any further downstream travel. Regular bedforms, such as steps and pools or pools and riffles, disrupt the dispersion by depositing a disproportionate number of particles in certain locations (e.g., pools) relative to other locations, such as steps. These regular bedforms may also cause transport distances to be partly determined by the distance between bedforms. Thus the applicability of the models for the short-term dispersion and transport of sediment will also depend on the size of the stream and the spatial scale of interest.

***(6) Can the long-term travel distance be predicted by extrapolating from short-term transport distances?***

In the absence of other tools, it is tempting to use the relationships presented by Hassan et al. (1992) and Gintz (1994) to predict mean travel distances by employing a rating curve for excess stream power and a flow duration curve. However, these results were generally derived from short-term tracer experiments where the dispersion pattern was still in the initial stages and the placement of tracers on the bed of the channel promoted large transport distances. Given that freshly seeded tracers often have relatively favorable entrainment conditions, and that tracers have not yet been deposited in locations unfavorable for reentrainment, the mean annual travel distance derived from short-term tracer experiments should be larger than the sum of the travel distances obtained by flow duration curves and the relationships between travel distance (or virtual rates of travel) and excess stream power. On the other hand, one could argue that the travel distance from two short events could be larger than the travel distance from an event of the same magnitude but twice as long. The initiation of motion for pebbles and cobbles in gravel-bed streams is often delayed until sand and small debris is winnowed out of the stream bed. Bedload transport during one long-lasting flood event would experience this entrainment delay only once, and not twice as in two shorter floods.

Another caveat in determining travel distances from flow duration curves is that the relationship between travel distance and stream power seems to be dependent on stream type. Gintz et al. (1996) show that travel distances for a given excess stream power were larger after a huge flood event that changed the former step-pool morphology of a mountain stream into a braided stream.

Results from Schick et al. (1987b) and an understanding of dispersion processes both indicate that mean travel distances summed from several individual events will overestimate the mean travel distance for a longer time period. On the other hand, the sum of *median* travel distances from individual events might be smaller than the *median* travel distance

determined from one long event. An additional complication is that the travel velocities were all derived from floods which might be described as "moderate" or less. We did not find any data on tracer travel distances or tracer velocities during extremely large flood events in perennial streams. Although travel distances and dispersion generally increase with flood magnitude, transport behaviors and dispersion patterns are likely to differ for floods of different magnitudes. Furthermore, the dispersion patterns are likely to be influenced by flood history (i.e., the order in which floods of different magnitude follow each other). Multiplying the average transport distance of an average magnitude event times the number of floods to be expected over a long time period will not truly represent the long-term travel distance, but will probably be in the right order of magnitude if the proportion of sediment in the different storage locations is accurately characterized and taken into consideration.

***(7) Does the travel velocity slow over time?***

The answers to the previous questions suggest that transport distances will generally decline over time as more particles are stored within or adjacent to the channel. Since no study has distributed particles in proportion to the various storage locations, it is not possible to determine whether this trend would be true if the placement of tracer particles did not create an inherent bias in the data. The extent of this bias can be determined for the short-term from the data collected by Sayre and Hubbell (1965) on the daily transport of sand tracers. Using their data, we calculated the mean and the mode of the displacement of the sand tracer and plotted this on a daily basis (Fig. C-4; 8). The results show a nearly 50% decrease in the mean transport velocity over a 12-day period, and about a 30% decrease in the mode. After seven days there appeared to be little change in the transport velocity of the mode (23 m/d), but there was a continuing decline in the mean over the 12-day period of the experiment. The mean flow velocity varied between 0.66 and 0.72 m/s, but the small variation in velocity did not seem to affect the calculated sediment transport velocities.

***(8) Which tracer properties are necessary for long-term observations?***

The validity of a tracer experiment depends on the methodology used, and it is important to take the methodology into account before applying the results of a particular experiment to the situation of interest. To accurately represent bulk sediment transport, a tracer must be able to be detected on the channel surface and when deposited in storage. This implies a tracer that is easily seen and that can be located when buried, usually with a magnetometer. The tracer also must be durable in order to withstand abrasion over an extended period, and it may be desirable to coat the tracer to preclude the growth of algae. A sufficient number of tracers must be used to provide a representative sample for each important transport process and storage location. Of particular importance is the need to carry out longer-term experiments in different stream types.

These answers indicate that it is problematic to infer long-term travel distances from the available short-term data, and that an extrapolation will generally result in an overprediction of travel distances. Nevertheless, the analysis and prediction of sedimentary CWEs requires some estimate of the mean annual travel distance through the stream system. The next section of this report will compile and combine the information from individual short- and medium-term studies in different streams.

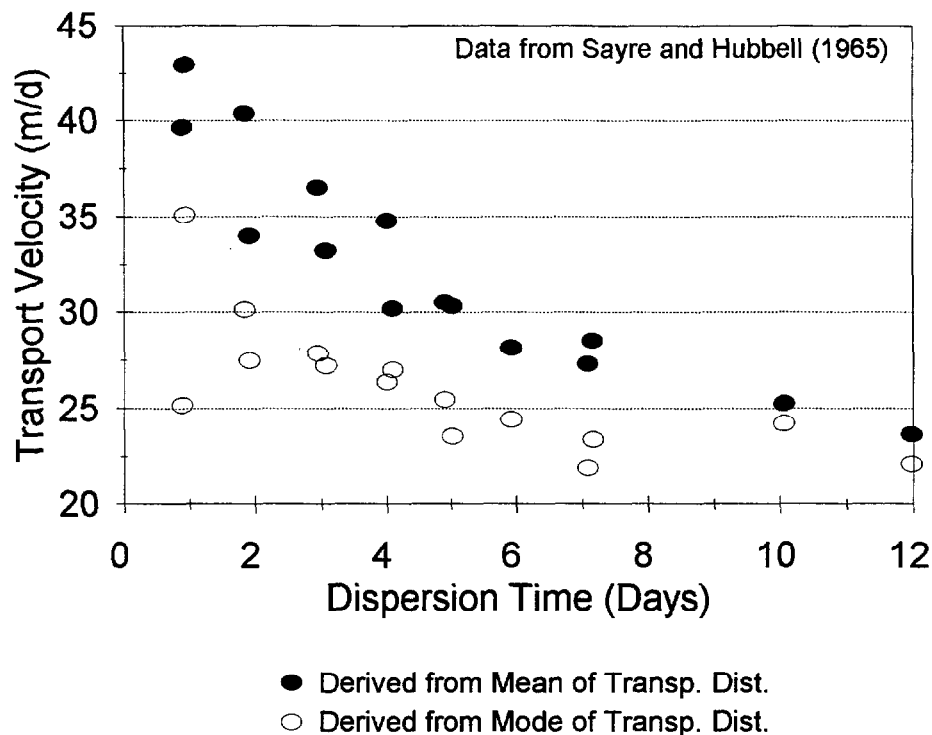


Fig. C-4; 8: Daily transport velocities as the ratio of displacement distance and dispersion time for modes and means of displacement distances at North Loup River (data from Sayre and Hubbell 1965).

#### 4.4 Extrapolation of mean annual travel distances from medium- and short-term studies

Extrapolation from short-term studies should ideally be based on a detailed evaluation of the flow conditions over the period of study relative to the longer-term flow-duration curve.

One should also evaluate the individual studies with respect to the stream type, and consider the median as well as the mode of the observed sediment transport.

Unfortunately, none of the published studies had this detailed information, and for practical reasons we were forced to simply utilize the published data on mean transport distances, despite its potential bias due to a few large transport distances. Similarly, we usually did not know the frequency of the flow event during which travel distances were measured, much less the transport distances in an event larger or smaller than the measured events. Based on whatever scarce information was provided in the individual studies, and supplemented by our general hydrological and geographical knowledge, we estimated the relative frequency of the sampled period and multiplied the observed mean travel distance by the estimated frequency to obtain a crude estimate of mean annual travel distances. To increase the size of the data base, we also assumed that the transport distances inferred from tracer experiments were comparable to transport distances inferred from the migration of bedforms (Section C-4.3.3.4). We are very aware of the limitations of the resulting compilation, but we believe that the results should be within the right order of magnitude and useful for demonstrating trends.

A total of 55 references were found that contained some information on sediment travel distances in various stream types. About 40 of these references contained information that allowed us to estimate mean annual travel distances. The following paragraphs summarize some of the key studies on annual, event-scale, or daily transport velocities of sands, small gravels, pebble and cobble tracers, and the migration rate of bedforms used to infer mean annual transport distances.

#### 4.4.1 Downstream movement of sands and fine gravels

##### ***Hunt Creek: artificial sand wave***

Under certain conditions no tracers are needed to detect the downstream movement of bedload. The amount of artificially or naturally added sediment to the stream can be so large that it forms a sediment wave that is morphologically and sedimentologically distinguishable from the original channel sediments. Hansen and Alexander (1976) added sand into Hunt Creek, a riffle-pool, groundwater-fed Michigan stream. This sediment formed a sand wave that migrated downstream with a velocity of 2.5 m/d. Since flow does not vary much over the course of a year, this value might be extrapolated to yield an annual travel distance of about 800 m/yr. As this sand wave migrated downstream, the associated stream aggradation led to increases in channel width and gradient, and decreases in depth, especially in the pools.

##### ***North Loup River: decreasing travel velocity of sand***

Hubbell and Sayre (1964) and Sayre and Hubbell (1965) measured the dispersion of a radioactively-marked sand in the North Loup River in Nebraska. The bed material had a  $D_{50}$  of 0.29 mm and was formed into large dunes 0.4 m high and 3.70 long. The measured discharge was 7.4 m<sup>3</sup>/s (260 cfs), which is close to the mean annual flow. Depth was 0.76 m and the gradient was 0.083%. For the tracer experiment, radioactive sand was deposited in two-pound lots on the bottom of the stream bed at intervals of two feet across the channel width. Each day, the downstream dispersion of this traced material was tracked, and the mode and mean of the dispersion were recorded for 12 consecutive days. The gradual and even dispersion process could be statistically characterized by a gamma or Poisson function. As shown in Fig. C-4; 8, the mean terminal longitudinal dispersion velocity decreased to about 23 m/d. If it is assumed that flows close to the mean annual flow prevailed for much of the year and the transport velocity of 23 m/d could be sustained for 200 days per year, the mean annual transport distance is 4600 m/yr.

##### ***East Fork River study: from pool to pool each year***

The bulk transport distance of fluorescently-marked sand-to-gravel-sized particles was observed over several weeks of the snowmelt highflow in 1979 at the East Fork River in Wyoming. The transport distance for medium sand (0.25-0.50 mm) was 550 -1150 m, and this decreased to 400-700 m for coarse sand and fine gravel (0.5-4mm). Pea gravel of 4-8 mm had a bulk transport distance of 550 m (Section C-4.3.3.4). On a mass basis the average annual travel distance for all particle sizes was about 650 m. The mean bulk travel distance of coarse sand corresponded to about one pool spacing. Daily travel velocities ranged from 10 to 30 m/d, and this was affected by grain-size. The mean gradient of the East Fork River in the study reach was 0.07%.

#### 4.4.2 Single particle tracers of pebbles and cobbles

##### *Lainbach: longitudinal dispersion and effects of entrainment position and particle shape.*

Annual transport distances were observed over a three-year period with a relatively typical range of flows (Schmidt and Ergenzinger 1992). During an initial summer flood in 1986, the tracers spread over a 200 m reach and the mean travel distance for all tracers was 33 m. At the end of three years less than 20% of the original tracers were found within a 800 m reach. In another experiment 150 cobble tracers ranging in weight from 300 to 5020 g (median weight of 1330 g) were placed in a pool. After one summer with eight flood events the mean total travel distance was 274 m; the minimum and maximum transport distances were 44 and 763 m, respectively (Schmidt and Ergenzinger 1992). Mean transport distances for a third population of 1-kg magnetic tracers over two consecutive summer flood events were 27-86 m, depending on entrainment position, and 19-76 m, depending on particle shape.

Gintz (1994) presents transport distances for each of twelve flood events between 1989 and 1992 (Table C-4; 6). If it is assumed that the recorded summer floods represent one-third to one-half of the annual flood activity, then cumulative mean annual transport distances would range between 200 and 300 m/yr for 1989. The 1990 flood had an estimated recurrence interval of 100 years, and this converted the channel from a step-pool to a braided stream. Later floods reworked these deposits and started to restore the former step-pool morphology. The large estimated annual transport distance of 1.0-1.4 km in 1991 still reflects the abundance of transportable sediments and the relatively smooth channel morphology.

**Table C-4; 6:** Flood events, mobility, and transport distances between 1989 and 1992 at the Lainbach (from Gintz, 1994).

Date	Event		Tracer				
	$Q_{max}$ ( $m^3/s$ )	Duration (h)	Mobility (%)	Mean transp. distance (m)	Transport velocity (m/h)	Recovery rate (%)	Mean transport dist. of moved tracers (m)
7.12.89	8.3	12	42	41	5	95	60
7.14.89	12.2	9	52	63	9	93	86
7.18.89	3.4	0.5	7	0.5	14	100	7
7.28.89	3.9	1	18	1	5	100	4
8.09.89	3.4	2	11	1	5	95	9
6.30.90	165	52	94	115	2	25	120
6.28.91	8.7	11	56	317	43	80	451
7.09.91	3.6	1	11	8	16	100	16
7.14.91	19.2	67					
7.17.91	8.3	17					
7.25.91	7.4	16	65	143	14	71	222
7.22.92	10.2	6	73	199	47	88	271

##### *North St. Vrain: size-dependent transport distances*

Thompson (1994) measured the mean transport distance during the long-lasting and vigorous snowmelt highflow in 1993 at the North St. Vrain River in central Colorado. In this relatively low gradient (0.7%) step-pool stream the mean transport distance was 28 m for small pebbles (16-32 mm) and 52 m for medium pebbles (32-45 mm). Mean travel

distances then decreased to 42, 26 and 8 m for the grain size classes of 45-64, 64-90, and 90-128 mm, respectively. The measured mean transport distance of 52m/yr for the medium pebbles (32-45 mm) was assumed to be representative of the bed material transport.

***Seale's River in Quebec: local gradient and particle size dependency***

Laronne and Carson (1976) determined the mean travel distance of tracers in a steep bouldery stream (2.1-8.6% gradient) over the snowmelt highflow. For particles ranging in size from 4 to 256 mm the observed transport distances ranged from 53 to 112 m, depending on particle size and the gradient below the emplacement location. Median travel distance decreased with size, except for the fact that the smallest size class (0.1-1g) was not transported as far as the next larger size class. Averaging over all emplacement locations and reading data to the nearest 5 m from Fig. 12 in Laronne and Carson (1976), we calculated the median travel distances to be 125, 140, 85, 65 and 25 m for the weight classes 0.1-1, 1-10, 10-100, 100-1,000, and 1,000-10,000 g, respectively. This reduced to a general transport distance for all gravels of approximately 100 m/yr in a channel with an average gradient of 0.05.

***Ephemeral streams in Israel: Nahal Og and Nahal Hebron***

Hassan (1990) measured the transport distances associated with flash floods in two ephemeral desert streams, Nahal Hebron (gradient of 0.016) and Nahal Og (gradient of 0.014). The pebble and cobble tracers represented the upper 50% of the bed material particle-size distribution and the upper 85% of the surface particle-size distributions at both sites. About four floods occur each year at Nahal Hebron and five floods at Nahal Og, but only one or two of these are able to transport the coarse bedload. The mean annual floods are 10-15 m<sup>3</sup>/s. Mean transport distances for Nahal Hebron ranged from 0 to 65 m per flood for four of the 21 floods recorded over a three-year period, yielding a cumulative mean transport distance of 154 m. Assuming that a flood with bedload transport capacity occurs on average once per year yielded a mean annual transport distance of about 50 m per year. At Nahal Og, mean transport distances ranged from 0 to 146 m for six floods over a two-year period. This gives 80 m/yr as an estimate of mean annual transport distances at Nahal Og.

***Steep torrents in Japan***

By defining transport distance as the length of one unit of a sequence from scour to deposition, Nakamura et al. (1987) determined the mean annual bedload transport distances for five mountain streams in Japan (Table C-4; 7). Transport distances varied from 10 to 165 m per year--values that are consistent with the transport distances for pebble and cobble tracers from other studies.

**Table C-4; 7:** Basin area, stream characteristics, sediment residence times, and mean annual transport distances for five mountain rivers in Japan (from Nakamura et al., 1987).

Stream	Basin area (km <sup>2</sup> )	Stream gradient (m/m)	Storage capacity (10 <sup>3</sup> ·m <sup>3</sup> /km)	Sediment exchange (10 <sup>3</sup> ·m <sup>3</sup> /km·a)	Residence time (years)	Stream width (m)	Mean annual transport dist. (m)
Furano River	23	0.10	26	2.6	10.2	34	<b>30 - 50</b>
upper reaches	23			2.5	9.2	29	35 - 55
lower reaches	29			2.7	10.5	39	30 - 50
Haruki River	21	0.091	222	12.4	17.9	128	<b>45 - 75</b>
Ogawa River	11	0.083	27	1.0	26.8	25	<b>10 - 20</b>
Usubetsu River	65	0.04	61	2.2	27.7	36	<b>10 - 20</b>
Saru River	1345	0.0036	126	12.1	10.4	151	<b>105 - 155</b>
upper reaches	85			9.0	9.4	135	<b>105 - 155</b>
lower reaches	175			16.0	10.9	171	115 - 165

#### 4.4.3 Predictability of mean annual travel distances by stream type and gradient?

The complete set of estimated mean annual travel distances is summarized in **Table C-4; 8**. It is important to recognize that, in view of the inherent bias in most of these studies, these values are more likely to represent a maximum distance than a "typical" value.

The importance of this data set is that it might facilitate the prediction of the downstream movement of sediment and hence the prediction of sedimentary CWEs. Although our earlier analysis showed that many factors affect the downstream movement, we wanted to try and identify the relationship between the mean annual travel distance and key factors that might be readily assessed by field personnel. A plot of all the data from **Table C-4; 8** against stream gradient showed a weak trend of decreasing travel distance with increasing gradient (**Fig. C-4; 9** (top)).

Since travel distances should increase with gradient for hydraulically smooth streams but decrease with gradient in hydraulically rough streams (section C-4.3.3.4), we separated the data into two groups: (1) braided and severely aggrading streams, and (2) step-pool, riffle-pool, unspecified "mountain" streams, ephemeral streams, large streams more than 50 m wide, streams with alternate bars, and sand-bedded streams. For the first group of data mean annual travel distance does generally increase with gradient (**Fig. C-4; 9** (center)). In contrast, mean annual travel distance appears to decrease with stream gradient in streams that are hydraulically rough (i.e., where much of the flow energy is dissipated by turbulence) (**Fig. C-4; 9** (bottom)). The trends were sufficiently strong that regression functions were calculated. For the hydraulically smooth streams the mean (which might really be a maximum) travel distance ( $l$ ) increases with stream gradient ( $S$ ) by:

$$l = 80,600 \cdot S^{1.29} \quad (6)$$

**Table C-4; 8:** Estimated mean annual bedload travel distances (m) based on individual studies and predicted mean annual travel distances based on regression functions (Eqs. 6 and 7).

Reference	Stream Type	Stream grad. (m/m)	$D_{50}$ (mm)	Mean ann. travel dist.(m)	Tracer size range (mm)	Pred. travel dist.(m)
<i>Braided and steep, aggrading streams:</i>						
Ferguson et al. 1995	pool-riffle, aggr.	0.0018	22	22	16 - 90	23
Wathen et al. 1995	pool-riffle, aggr.	0.0020	22	24	19 - 76	27
Butler 1977	braided	0.0037	40	155	34 -116	59
Ferguson et al. 1995	pool-riffle, aggr.	0.0038	40	35	16 - 90	61
Ferguson et al. 1995	pool-riffle, aggr.	0.0053	46	83	16 -128	93
Ferguson et al. 1995	pool-riffle, aggr.	0.0087	57	59	16 -128	177
Goff and Ashmore 1994	braided	0.010	30	1250	bedform propag.	212
Ferguson et al. 1995	braided	0.012	129	85	16 -180	268
Ferguson et al. 1995	braided	0.016	115	96	32 -256	389
Chaco et al. 1989	braided	0.018	24	2000	39 - 72	452
Emmett et al. (in press)	braided	0.018	24	2900	40 - 70	452
Griffith 1993	braided	0.025	25	600	bedform propag.	691
Carson and Griffith 1989	braided	0.025	25	600	bedform propag.	691
Schmidt and Gintz 1995	braided	0.035	50	863	42 -113	1067
Gintz et al. 1996	braided	0.035	50	1000	42 -113	1067
Pickup et al. 1983	braided	0.045	2	1300	0.025 - 16	1475
Chaco et al. 1994	braided	0.050	60	1100	66 - 86	1690
<i>Step-pool, pool-riffle, "mountain", alternate bars, ephemeral, large, and sand-bed streams:</i>						
Crickmore 1967	sand-bed	0.0003	0.3	4000	0.2 - 0.3	1843
Rakoczi 1992	meandering?	0.0004	17	3000	4 - 25	1502
Emmett et al. 1983;	pool-riffle	0.0007	1.28	650	0.25 - 8	1010
Emmett and Myrick 1985	pool-riffle	0.0007	1.28	650	0.25 - 8	1010
Meade 1985	pool-riffle	0.0007	1.28	750	0.25 - 8	1010
Hubbell and Sayre 1964	sand-bed	0.0008	0.29	4600	0.29	918
Rakoczi 1992	meandering?	0.0008	17	2500	4 - 25	918
Thomsen 1980	sand-bed	0.0008	0.5	500	0.5 - 0.6	918
Hansen & Alexander 1976	pool-riffle	0.0008	0.5	800	0.5 -918	918
Kondolf & Mathews 1986	pool-riffle	0.0030	50	65	130-359	358
Nakamura et al. 1987	mountain	0.0036	130	-	calc. sed. migr.	316
Jaeggi 1987	alternate bars	0.004	150	-	bar propagation	293
Zeller 1967	alternate bars	0.004	300	-	bar propagation	293
Thompson 1994	pool-riffle	0.007	50	52	16 - 128	197
Sobocinski et al. 1990	pool-riffle	0.008	sd/gr.	265	1 - 2	179
Cencetti et al 1994	altern. bars	0.008	16	500	16 - 128	179
Sobocinski et al. 1990	pool-riffle	0.008	sd/gr.	160	8 - 16	179
Ferguson et al. 1995	pool-riffle	0.010	75	93	23 - 256	153
Hassan et al. 1992	ephemeral	0.014	35	80	30 - 180	120
Hassan 1990	ephemeral	0.016	64	38	30 - 180	109
Gintz et al. 1996	step-pool	0.020	50	200	42 - 113	93
Schmidt & Ergenzinger 1992	step-pool	0.020	50	350	68 - 333	93
Gintz 1994	step-pool	0.020	50	300	100	93
Schmidt and Gintz 1995	step-pool	0.020	50	190	42 - 113	93
Nakamura et al. 1987	mountain	0.040	15	-	calc. sed. migration	57
Laronne and Carson 1976	step-pool	0.050	50	124	5 - 200	49
Nakamura et al. 1987	mountain	0.083	15	-	calc. sed. migration	34
Nakamura et al. 1987	mountain	0.091	60	-	calc. sed. migration	32
Nakamura et al. 1987	mountain	0.100	40	-	calc. sed. migration	30

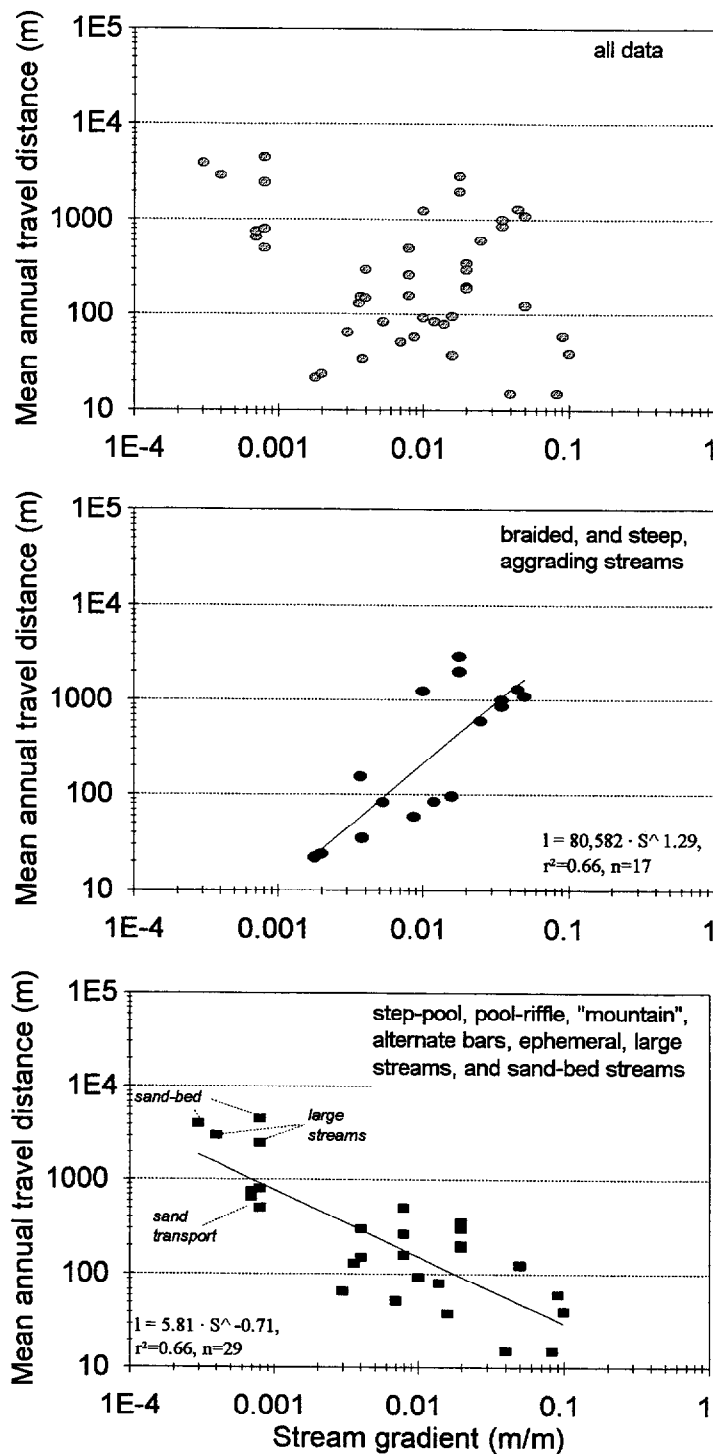


**Fig. C-4; 9:** Mean annual travel distance of bedload transport as a function of stream type and gradient. All data sets (top); data from braided, and steep, aggrading streams (center), and data from streams classified as step-pool, pool-riffle, mountain, alternate bars, ephemeral, large streams, and sand-bedded streams.

For hydraulically rough streams the mean (maximum) annual transport distance is related to stream gradient by:

$$l = 5.81 \cdot S^{-0.71} \tag{7}$$

Although both regressions had a  $r^2$  of 0.66, the data range over approximately one order of magnitude. This variability hinders the use of these regressions for CWE analyses, but they can help indicate when and where one might initiate a monitoring effort, or expect an impact from various sediment sources. Obviously these general trends would have to be evaluated within the context of a particular basin, size of the introduced sediment, flow regime, etc. More long-term studies on travel distance and the associated flow regime would help confirm these trends and possibly either reduce the existing scatter or allow a further stratification.

#### 4.4.4 Annual travel distances as a function of grain-size

As stated earlier (Section C-4.3.3.7), transport distances generally decrease with particle size. This statement especially refers to the three large size classes of (a) silt and finer, (b) sand, and (c) gravels. However, within each of these large particle size classes, individual studies report controversial results regarding particle-size dependent travel distances. Some studies found a strong, others a weak size dependency, while again others found no consistent relation between particle size and travel distance at all. It appeared that a size dependency of travel distances was less well developed for relative small flow events and in hydraulically rough streams. Due to the variability encountered in size dependent transport distance within the large particle size classes, we only looked at size dependency of transport distances between the three large size classes.

If the short- and medium-term transport distances of suspended sediment (Section C-4.2.3), and for sand and gravel bedload transport listed in **Table C-4; 8** are sorted by grain-size and its prevalent mode of transport, there is a remarkable consistency in the order of magnitude of annual travel velocities for suspended sediment, sand bedload, and pebble-cobble bedload in (mountain) streams (**Table C-4; 9**). This consistency in travel distance might be partly coincidental and may also stem from an unrepresentative set of studies. This argument, however, is belied by the wide range of estimated travel distances for gravels in braided and aggrading streams.

**Table C-4; 9:** Range of mean annual transport distances ( km/year) for suspended sediment, predominantly sand-sized bedload, and single pebbles or cobbles.

Sediment size	Mean annual transport distances	
	Range (km/yr)	Mean (km/yr)
Suspended sediment in mountain streams	2 - 20	10
Sand as the predominant bedload	0.5 - 5	2
Pebbles and cobbles in mountain streams	0.02 - 0.5	0.1
Gravels in braided streams	0.02 - 5	-

If we wish to evaluate a potential site for sedimentary CWEs that is 10 km downstream from an assumed disturbance in the headwater areas, **Table C-4; 9** suggests that CWEs due to suspended sediment might be expected within a year, or at most several years. If sand was the predominant constituent of concern, it might be several years to more than a decade until CWEs are observed. Sedimentary impacts due to the arrival of pebbles and cobbles from upstream disturbed areas could take decades in hydraulically rough streams. However, if a steep mountain stream receives large amounts of sediment supply and becomes hydraulically smooth, mean annual travel distances could increase by an order of magnitude and affect a potential site 10 km downstream within a few years.

## **Part D: Conclusions and Recommendations**

### **1. The issue of spatial scale in sedimentary cumulative watershed effects**

Cumulative watershed effects (CWEs) arise from the overlapping effects of management activities in time or in space. Although CWEs can be expressed in terms of runoff, nutrients, temperature, or other parameters important for aquatic ecosystems, we focussed on sediment because this is critical to several designated uses and often the limiting constraint on forest management activities. The basic precept behind this project was that the detectability of a sedimentary CWE is controlled by the variability across a range of temporal scales, measurement uncertainty, the storage and dilution of the constituents of concern, and the magnitude and duration of the changes induced by management activities.

Both temporal and spatial scales affect the occurrence and detectability of CWEs (Bunte and MacDonald 1995). For example, the short-term temporal variability controls the uncertainty associated with a given measurement, while the interannual variability in annual sediment loads governs the magnitude of change that can be detected within a given time period. Similarly, spatial scale issues range from the variability in sediment transport across a stream cross-section to the basin-scale decline in sediment delivery with increasing area and the variability in annual sediment loads between adjacent basins. The principal focus of this report has been on the extent to which potential increases in sediment load from forest management activities can be transported downstream, our ability to detect these changes, and the extent to which these cumulative effects are scale dependent.

This issue of spatial scaling is intuitively obvious for the extreme cases, but has only recently been explicitly addressed in state and federal documents to guide cumulative effects analyses. Both the USFS and the State of Washington procedures (Ecosystem Analysis at the Watershed Scale, 1995; Washington Forest Practices Board, 1992) suggest that the appropriate spatial scale for watershed analysis is 20-200 square miles (50-500 square kilometers), and this range was derived at least in part from the hydrologic considerations set out in Harr (1989). However, it is not necessarily true that this scale is most appropriate for sedimentary cumulative effects.

Of particular concern is the fact that sediment is not transported downstream with the water unless we assume perfect suspension. In contrast to discharge, management-induced inputs of sediment are much more subject to storage in or adjacent to the channel. Scale considerations for sedimentary cumulative effects are also complicated because changes in flow can increase the amount of sediment, sediment is much more difficult to measure than discharge, and the downstream transport of sediment is dependent on numerous factors such as the particle size of the introduced sediment, stream gradient, degree of confinement, bed characteristics, available storage, and the magnitude, duration, and frequency of high flows. The likelihood of cumulative sedimentary effects will also be highly dependent on the current condition and budgetary state of the stream, and thus the effect of management activities cannot be considered in isolation from the natural processes and long-term geomorphic context in the basin of interest.

The mechanistic approach that can be applied to hydrologic cumulative effects is also of limited applicability for sedimentary cumulative effects because the timing of sediment

inputs are often much more persistent and complex with regard to time. Again the particle size of the introduced sediment will combine with the pattern of discharge, the stream channel characteristics, and the overall sedimentary state of the basin to create a relatively unique and somewhat unpredictable downstream response. Thus certain aspects of the scale problem can be generalized, but the relevant spatial scale for analyzing cumulative watershed effects is a unique function of the basin under consideration, the issues of primary concern, and the extent to which a particular effect needs to be documented rather than presumed. It should be obvious, for example, that the construction of roads and forest harvest on several small watershed in the upper reaches of the Mississippi Valley will not be detectable in Minneapolis much less in New Orleans or St. Louis, but that some--presumably quite small--proportion of the introduced sand will eventually be transmitted downstream and contribute to the building of the Mississippi delta in the same way as every other natural and anthropogenic sediment source.

## **2. Detectability of CWEs**

From a forest management perspective, the question is whether a specific set of activities can lead to a detectable change in sediment transport rates, stream channel condition, or the designated beneficial uses. From a regulatory perspective, the absence of explicit standards for many variables, such as the bed material particle size or stream channel condition, leads to the difficult problem of translating some physical measurement of the channel into an adverse effect on one or more designated beneficial uses. While these issues are beyond the scope of this report, they ultimately affect the extent to which one should attempt to detect a sedimentary cumulative effect, where one might look for such effects, and what changes are of principal concern. Again there will be different levels of concern associated with the input of sediment into particular water bodies, such as Lake Tahoe or Crater Lake, as compared to a small steep stream that may empty directly into the Pacific Ocean.

## **3. Measurement uncertainty**

If one accepts that we wish to detect either a measurable increase in the sediment load or the effects thereof, then one first has to address the issue of measurement uncertainty. The first chapter of this report documented the large temporal fluctuations in sediment transport rates at several scales. Short-term fluctuations in bedload transport rates (e.g., on the order of seconds to a few hours) at a relatively constant discharge typically extend over one order of magnitude. These short-term fluctuations are associated with a variety of physical processes, including the passage of bedforms, local turbulence, selective transport, the interaction of particles on the bed of the stream, and sudden events such as bank collapse or the movement of a piece of large woody debris. The net result is that these fluctuations are largely unpredictable, and one either has to capture this variability through intensive sampling or accept the fact that a single sample has a very high degree of uncertainty with regard to its representativeness of the mean transport rate. These short-term fluctuations in sediment transport rates are generally several times greater for bedload transport than for suspended sediment.

Measurement of bedload transport in both flumes and streams suggest that high-intensity, sequential sampling tends to produce a lognormal distribution. Typical coefficients of variation during periods of constant discharge are 55-100%. This means that 12-40 samples are required to be 95% certain that the estimated mean is within a factor of two of the true mean.

Fluctuations in sediment transport rates will also occur over the time scale at which changes in discharge are apparent. Unfortunately discharge is not necessarily a good predictor of sediment transport rates, as our review of intensively sampled high flows indicated that discharge accounted for 13-85% of the observed variability in bedload transport rates. This variability in discharge-sediment transport relationships is due to a variety of physical processes such as sediment exhaustion, changing inputs of sediment from tributaries, and sudden events such as the break-up of the armor layer, bank erosion, or the movement of large woody debris. A clockwise hysteresis loop between a storm hydrograph and sediment transport rates cannot be assumed, and thus the separation of a sediment rating curve into rising and falling limbs may not significantly improve the predictability of either bedload or suspended sediment transport rates. Other studies have shown that there may also be a seasonal dependence in sediment supply and sediment transport rates as a result of different types of storm events, the resulting variations in runoff processes, and seasonal variations in erodibility and erosion processes.

For any given flow sediment transport rates can be expected to vary by 1-2 orders of magnitude. Typical coefficients of variation for sediment transport rates during high flows for a single event are around 90-110%, and these increase to around 150% for high flows over a single snowmelt high flow. The relatively small increases in the coefficient of variation over changing discharges again suggest that smaller changes in discharge (e.g., a factor of two) are not well correlated with changes in sediment transport rates. Thus the sampling of sediment transport rates is constantly subject to the trade-off between costly and intensive sampling to better characterize the mean, or less intensive measurements with a correspondingly higher degree of uncertainty. The limited data also suggest that an increasing grain size is associated with a higher variability in bedload transport rates.

The measurement of sediment transport rates is also complicated by the corresponding and interacting spatial variability. Over the short-term one has to account for the variation in sediment transport rates across the cross-section and, in the case of suspended sediment, in the vertical dimension. Generalizations about the magnitude and distribution of cross-sectional variability are difficult, and different authors suggest quite different allocations of bedload sampling effort to account for the short-term temporal variability vis-a-vis the spatial variability across the cross-section. Is it better to have 10 replicate samples at just four cross-section locations or just two replicate samples at 20 locations? One can optimize sampling effort to minimize the uncertainty in the total estimated bedload transport rate, but this requires a knowledge of both the short-term temporal variability and the variability across the cross-section. Our literature review and analyses suggest the short-term variability is so severe in single-thread channels that it is probably better to repetitively sample fewer locations than to sample more locations with a lower intensity. It should be noted that this generalization is more likely to be true for coarse-bedded mountain streams than low-gradient, fine-bedded streams with a high width-depth ratio. Again the cross-sectional variability is greatly reduced for suspended sediment, but the variation with depth must be accounted for by depth-integrated sampling if one wishes to estimate actual sediment loads.

At a slightly larger spatial scale, there may be some variation in measured sediment transport rates according to the location of the sampling cross-section relative to the local bedforms. Sediment transport rates will differ between pools and riffles, and this difference can be expected to change with changing discharge. On the reach scale, sediment transport rates will vary if the upstream reaches are either aggrading or degrading. This means the selection of a sampling location requires a basic understanding of the existing sedimentary state of the stream with regard to the material to be sampled (bedload or suspended load), the particle size of the incoming sediment, and the transport capacity of the intervening stream reaches.

Another critical component of measurement uncertainty is simply the intensity and the accuracy of the sampling techniques. We defined sampling intensity as the proportion of the channel sampled times the proportion of time that sampling actually took place over the period of interest. One hour per week of actual sampling time with a 7.5-cm Helley-Smith in a 5-m wide stream equates to a sampling intensity of 0.036%, or a little more than one-three thousandth of the samples that would be taken by continuous sampling across the entire cross-section over a one-week period. The point is that most typical field sampling regimes require very high levels of extrapolation to estimate total sediment loads. This extrapolation is further hindered by the fact that high flows rarely occur at times that are conducive to sampling. Peak daily runoff in snowmelt-dominated basins typically occurs in the evening or at night, depending on the size of the basin. The timing of mean daily transport rates is both unpredictable and inconsistent, and this again indicates that a relatively intensive sampling regime is necessary to accurately estimate sediment transport rates for a specific period of time (e.g., daily) or a specific discharge.

The accuracy of an individual sample is typically defined by the sampling efficiency. A sampling efficiency of one means that the sampler captured exactly the same mass of sediment that would have passed through the sampling location had the sampler not been there. In reality, the definition of sampling efficiency should be strengthened by specifying that the sample should also have a similar grain-size distribution, as different-sized particles have different likelihoods for being sampled. This is important because different particle sizes have varying implications for channel morphology and aquatic life.

Since all samplers disturb the flow lines, an efficiency of 100% is not possible. Sampling efficiency will vary with the velocity profile in front of the sampler, the particle sizes being sampled, and the characteristics of the sample reservoir or net. The choice of samplers, sampling duration, and sampling location is a compromise between competing objectives. Pressure-difference samplers, such as a Helley-Smith bedload sampler, tend to oversample smaller (<8 mm) particles and undersample larger (>11 mm) particles. Use of a larger (e.g., 15 x 15 cm) bedload sampler will generally increase the oversampling of smaller particles to better capture the larger particles, but the mechanics of using a larger sampler at high flows means that the measured sediment loads may not be very accurate. The use of any bedload sampler under high flow conditions is very difficult, as it is almost impossible to control the exact placement of the sampler. The problems of scooping, stirring, and misalignment are particularly difficult for bedload samplers in coarse-bottomed streams. Several studies have developed calibration factors for specific particle sizes under specific conditions, but there is not a comprehensive set of calibrations that might be used to correct data from a variety of stream types and flow conditions by sampler and particle size. The placement and use of log or concrete sills is recommended for more accurate bedload sampling in streams.

The limitations of measuring suspended sediment are not quite as severe as measuring bedload, but standard techniques result in an unsampled zone immediate above the bottom of the stream where concentrations are expected to be at a maximum. Pump samplers only sample one point in space, and the hydraulics of pumping distort the flow lines and therefore produce an unrepresentative sample with regard to particle size and possibly also concentration.

The net result is that all sediment samples are really an index of sediment transport, and we can only crudely estimate the likely errors. In practical terms, this means that a change in measurement techniques can have a substantial effect on the estimate sediment load, and a "cumulative watershed effect" could be created by simply shifting from a 7.5- to a 15-cm Helley-Smith, or from depth-integrating to point sampler. Sediment ponds may be the most

practical means to obtain an accurate estimate of sediment transport rates, but these raise questions of cost, stream channel disturbance, and what to do with the captured sediment.

#### 4. Determination of annual sediment loads

A final component of measurement uncertainty is the integration and extrapolation from individual measurements to estimates of total loads over time. Sediment rating curves (using discharge to predict sediment transport rates) are a common approach, but measured sediment transport rates typically range over two orders of magnitude for a given discharge. The use of a log-log scale for sediment rating curves often leads to a substantial underestimate of sediment transport rates because interpolation between log values produces a geometric mean, while interpolation between antilogged values yields the more accurate and higher arithmetic mean. Incorporating a bias correction factor for a sediment rating curve based on weekly samples will usually increase the estimated annual sediment load by several times.

The reliability of a sediment rating curve is highly dependent on the extent to which sediment transport is directly related to hydraulic factors. Thus sediment rating curves tend to be most effective for bedload transport in sand-bedded streams, and are less appropriate in situations where the entrainment of particles is not readily predictable and sediment transport rates are highly dependent on sediment inputs from outside the immediate channel. Sediment rating curves are generally improved by incorporating a wider range of data, averaging over longer time periods, and increasing the sample size.

Sediment rating curves and estimated sediment yields are particularly sensitive to the number and value of high flow samples. Increasing the number of high flow samples will typically result in more consistent sediment rating curves, higher coefficients of determination, higher estimates of sediment loads, and estimated sediment loads that are closer to the true value.

Meade et al. (1990) estimated an average error of about 50% for annual sediment loads derived from suspended sediment rating curves. Sediment rating curves for bedload transport will typically explain around 50% of the variation in bedload transport rates, but one should also expect that in smaller basins the coefficient of determination ( $r^2$ ) may well be less than 25%. A number of studies have also indicated that sediment rating curves can exhibit considerable seasonal and interannual variation. A change in the sediment rating curve is often, but not necessarily, associated with a change in sediment supply. Changes in sediment rating curves must be explicitly considered in any effort to detect sedimentary CWEs, and this implies a continuing and moderately-intensive sampling regime.

Summation procedures are an alternative to sediment rating curves, and these estimate total sediment loads by multiplying each sediment transport measurement by the time represented by that measurement, and summing these values for the desired time period. Summation procedures are most effective if sediment transport data are available every 1-2 days, and in such cases the summation procedure may provide a more accurate estimate of total sediment loads than a rating curve. Ketcheson (1986) found that using the summation procedure for samples taken every other day had similar errors to the more common rating curve technique; in both cases the estimates were within 50% of the true value in 75% of the years.

On the other hand, the use of a summation procedure for weekly samples can underestimate annual sediment loads by a factor of two or more. The process by which data are averaged and then summed can also greatly affect the estimated annual sediment load (Walling and

Webb 1981; 1988; Walling et al. 1992). With regard to scale, one would expect the summation procedure to be more accurate in larger basins where the changes in discharge are more gradual, but we could not find any explicit consideration of this factor in the literature. A separate analysis of this issue, using data sets from basins of varying size in different geomorphic regions, would be of interest.

## 5. Interannual and interbasin variability in sediment loads

The final scale of temporal and spatial variability considered in this report is the interannual and interbasin variation in annual sediment loads. A high degree of interannual variability would suggest that long measurement periods would be needed to detect all but the largest changes in annual sediment loads, while a high interbasin variability would call into question the validity of comparisons between disturbed and undisturbed basins (e.g., a paired catchment approach). An analysis of 37 data sets with 11-35 years of data indicated that the typical coefficient of variation for annual sediment loads was 70-130%, while the range was from 38 to 467%. The variability in annual sediment loads for undisturbed watersheds tended to be slightly larger for basins in the Pacific Northwest than for basins in Colorado or the northeastern U.S. There was a weak trend towards increasing variability with increasing sediment loads ( $r^2=0.24$ ), but there appears to be no significant relationship between basin size and the relative variability of annual sediment yields. This means that despite the tendency for sediment yields to diminish in the downstream direction, we cannot expect a downstream reduction in interannual variability as originally hypothesized.

Annual sediment yields tended to be normally distributed in basins with a low coefficient of variation (CV), while basins with higher CVs tended to have a lognormal distribution of annual sediment yields. Although there is a wide range of variability, approximately a decade of monitoring is needed to estimate average annual sediment yields to within 50% of their true value at the 95% confidence level, while 3-7 years may suffice to estimate the annual sediment load to within a factor of two. Given a typical CV of approximately 100%, approximately 15 years of pre- and post-disturbance monitoring would be required to detect a twofold change in annual sediment yields at a 95% confidence level. We also found a wide variability in the strengths of the relationship between various flow parameters (e.g., maximum annual flows, annual water yield, or duration of a given flow) and annual sediment yields.

The various data sets also showed a relatively high interbasin variability, even within a single experimental forest. In some cases the measured sediment loads on one undisturbed basin explained less than 10% of the variability in annual sediment loads on an adjacent, theoretically paired, undisturbed basin. Depending on the hydrological and sedimentological conditions of the basin, the interbasin predictability may be better or worse for wetter periods as compared to drier periods. In many cases the strength of the relationship, as indicated by the  $r^2$  value, can change quite dramatically with a shift in the time period being compared, or even with the addition or exclusion of a single year. At the Fraser Experimental Forest, for example, the  $r^2$  between two undisturbed catchments (East St. Louis and Lexen Creeks) dropped from 0.65 to 0.12 if the seven-year period of comparison was extended by one year. The implication is that the relationship between paired basins can change quite dramatically depending on the time period selected for calibration. Thus a relative decrease in sediment from a paired basin should not automatically be attributed to the initiation of additional management activities, nor should a decrease be automatically attributed to restoration activities or natural recovery.

A comparison of sediment yields from managed and unmanaged basins indicates that forest management activities have increased mean annual sediment yields by 7-200%, but this

does not necessarily mean that there is a concomitant increase in the variability of the annual sediment loads in managed basins. In many cases the range in annual sediment yields in undisturbed basins was comparable to the range of annual sediment yields following forest management activities. Several other studies have also noted a lack of significant change in the mean or variability of annual sediment loads following the initiation of forest management activities.

The detectability of a change in annual sediment loads may be further hampered by the timing and duration of the increase in sediment loads due to management. Some data sets from smaller basins show a several-year lag between management activities and an apparent increase in sediment yields, while in other cases there was a sudden increase and then a relatively rapid decline in annual sediment yields as the catchment "recovered". The timing and duration of an increase in sediment yields is highly dependent on the source of the sediment, the delivery of this sediment to the stream channel, and the delivery of this sediment to the monitoring location. For example, a change in sediment yields due to a decrease in root strength and an increase in mass movements might not be expressed for more than a decade, whereas much of the fine sediment from roads or bank erosion would be generated in the year of construction and might be rapidly routed into and through the stream channel. Similarly, a slug of sediment that is introduced in one reach may take years or decades to reach the monitoring location. Thus the observed change in the mean and variability of annual sediment yields will be highly dependent on the timing of the sediment being generated and the routing of the sediment through the stream system. Both temporal and spatial scales come into play because the change in the mean and variability will be an interacting function of the monitoring location and the length of the post-disturbance period chosen for analysis.

## **6. Downstream travel velocity**

The amount and rate of downstream sediment transport is critical to the prediction and efficient detection of sedimentary CWEs. In a given basin sedimentary CWEs could appear in different locations and at different times depending on the particle sizes being evaluated. Sediment delivery ratios (SDRs) are usually assigned solely as a function of basin area. Thus the implicit assumption in applying SDRs is that there is a general homogeneity in terms of geomorphic processes and climatic conditions within the basin. SDRs have been derived primarily from agricultural areas and for smaller particle sizes, and the application of such SDRs to topographically diverse and geomorphically complex basins is highly questionable. The reality is that SDRs have been shown to vary widely within a basin, between seasons, among years, and especially among basins. At present there is a large gap between the oversimplified approach of delivery ratios and more complex physically-based models, and there may be some potential to develop more specific SDRs for certain combinations of sediment sources, sediment sizes, and stream types.

Conceptually we know that the downstream transport of sediment is largely a function of the size of the introduced sediment, the mode of transport (i.e., bedload or suspended load), the energy available (which itself is primarily a function of discharge, slope, depth, and velocity), the amount of available sediment, and stream type. The problem is that our physically-based models can't accurately predict sediment transport rates unless they have been explicitly calibrated to the situation of interest, and they require more data and effort than most land management agencies are prepared to invest. Modifying sediment delivery ratios according to some of the key factors controlling sediment transport may provide an intermediate level of analysis that would be both practical and more realistic in terms of predicting sedimentary CWEs. We might expect, for example, that specific grain-size distributions can be associated with particular erosional processes. A simple mapping of

stream types or even stream gradients can be used to indicate the likely rate of travel and accumulation. By also considering the existing sedimentary state of the stream network (i.e., aggrading, degrading, or in quasi-equilibrium), a relatively simple model could be developed to predict downstream sedimentary CWEs.

For suspended sediment we can't assume that the delivery ratio will simply be 1.0. Deposition will occur, particularly in lower-velocity areas such as overbank flows, side channels and backwater eddies. Fine sediment may also infiltrate into the streambed if there are sufficiently large interparticle pore spaces and the bed material is not in motion. Although the deposition of fine sediment will not be solely a function of basin area, SDRs may be a useful first step towards predicting the downstream transport of suspended sediment. Results from a simple watershed-scale model suggest that, depending on the detection limit an increase in suspended sediment loads may be more detectable when this is superimposed on "dirty water" than clean water.

The section reviewed and analyzed the travel rates of different-sized particles in various stream types. Approximately forty individual studies were identified that had traced the downstream movement of particles over time. These studies indicate that the downstream dispersal of tracer particles generally follows a Poisson process, and the resulting spatial distribution is described by either a gamma or a negative exponential distribution. These patterns are consistent with the precept set forth in the first chapter on sediment transport processes, namely that individual particles are mostly at rest with only occasional periods of movement. Mean transport rates are not necessarily a valid indicator of sediment transport or an appropriate means to predict sedimentary CWEs, as a few particles may travel a great distance while the vast majority of particles travel only a short distance. Transport distance was found to be partly a function of particle shape, with disk-shaped particles traveling only about one-third as far as ellipsoids, spheres, or rod-shaped particles of the same mass and density.

One would also expect transport distance to increase with decreasing particle size, but this was not always the case. The equal mobility concept suggests that when the entire bed is in motion, bedload particles should move at approximately the same rate regardless of size, and this was observed in some of the tracer studies. On the other hand, if sediment transport is selective, the smaller particles should be more easily entrained and exhibit a correspondingly greater travel distance per unit time. Overall, the smaller grain sizes did tend to have a greater travel distance per unit time than the larger particles, although the relative difference varied according to stream type, the type of flow event(s), and the grain sizes being compared.

Our analysis also indicated that the hydraulic roughness of the stream bed is an important control on the rate of downstream particle movement. In streams with a wide distribution of particle sizes, the smaller particles may be trapped or hidden by the larger particles. Bedload particles generally seem to be transported further in hydraulically-smooth streams as compared to steep step-pool or cascade channels, despite the greater amounts of energy being dissipated in the latter. There is also an interaction between gradient and hydraulic roughness, as the data indicate that travel distances generally increase with increasing gradient in braided and aggrading streams, but decreased with gradient in streams that were characterized as hydraulically rough. This latter result is somewhat surprising, as it suggests that the average annual travel distance for bedload may be smaller in steep headwater streams than in some of the lower-gradient, higher-order "response" reaches. If these results are confirmed by future tracer studies, the implication is that sedimentary CWEs might occur higher in the basin and be more persistent than commonly believed. On the other hand, this decrease in travel distance with gradient in hydraulically rough streams

probably does not apply to the finer particle sizes. The problem is that there are very few data on travel rates for small particles in steep mountain streams.

Efforts to determine "average" annual transport distance by particle size were hampered by several limitations of the compiled data sets. First, most tracer experiments were conducted over relatively short time periods. Extrapolation to average annual travel distances would require detailed information on the average number, magnitude, and duration of high flow events, but this information was generally not readily available. Such extrapolations would also implicitly assume that travel distances are highly correlated with discharge and that the observed travel velocities were representative. In reality, many studies had relatively low tracer recovery rates, and it is likely that most of the unrecovered particles were buried within the bed or other sediment storage locations. Particles still in an active transport phase were more likely to be recovered, and this bias in recovery would tend to increase the average estimated travel distance. Similarly, the placement of particles on the bed surface increases their likelihood of entrainment, and the few studies with more frequent measurements did suggest a decline in transport distance over time. Thus there is an inherent bias in the reported average transport distances, and a more accurate estimate of average annual transport distances would need to account for the proportions of particles in storage versus the proportion of particles on the surface of the stream bed and thus readily available for entrainment and downstream transport.

Although these limitations in the data could not be fully resolved, we nevertheless estimated the range and mean of annual travel distances (in kilometers per year) as follows:

<u>Particle Size and Stream Type</u>	<u>Range</u>	<u>Mean</u>
Suspended sediment in mountain streams	2 - 20	10
Sand as the predominant bedload	0.5 - 5	2
Pebbles and cobbles in mountain streams	0.02 - 0.5	0.1
Gravels in braided streams	0.02 - 5	--

## 7. Detecting a sedimentary cumulative watershed effect

These rates of particle movement can be used as a first, crude estimate of the likely arrival of sediment waves originating from upstream source areas. This type of estimate can then help indicate where one might initiate a monitoring effort, and the time period that might be necessary to detect the initiation and passage of one or more sediment inputs. Clearly a much longer monitoring period will be needed for coarser particles and to document a return to pre-disturbance conditions or background levels with respect to sediment transport rates.

The extended lags in producing and delivering sediment to the monitoring location means that the true extent of the change in sediment loads can only be evaluated after all the directly and indirectly mobilized material has passed the monitoring location. Because this will usually require an extended period of monitoring, the results of such studies will be of more use in guiding future activities than for adjusting management on the basin being monitored.

Given the difficulties in making accurate measurements and the tremendous natural variability across a range of spatial and temporal scales, a more immediate feedback to adaptive management may be better provided by geomorphological field assessments. Such assessments may be criticized as subjective and highly dependent on the paradigm of the observer, but these objections can be largely overcome in controversial situations by relying

on the consensus of several observers, each of whom is familiar with the landscape and geomorphic processes in the area. A variety of supporting data can also be utilized, and this might include quantitative assessments of key channel characteristics or, if available, plots of data collected to date (e.g., cumulative sediment yields or stream channel characteristics). These data, when combined with data from comparable basins, can then help determine how the stream has evolved to its present condition, and hence how it might be expected to respond in the future to a given set of sediment inputs.

If our short- and long-term objectives are to protect and enhance aquatic resources, then we clearly will have to rely on current assessments and relatively crude predictive tools. We acknowledge and have tried to point out the key issues with regard to measuring sedimentary CWEs, and that the complexity of stream-sediment issues poses severe challenges to the development of any rigorous, quantitative, and reliable predictive technique. Land management decisions can rarely wait until we have collected the necessary long-term data to define a trend or a change at the 90 or 95% confidence level. A universal sedimentary CWE model is simply not realistic given the diversity and complexity of sediment production and transport processes.

In effect we see two paths into the future. The first is continuing research to improve our understanding, and this must encompass shorter-term process studies and longer-term studies to better understand rates and variability. The other path is to conduct better quality, shorter-term assessments to provide immediate guidance to resource managers. In terms of aquatic resource management, both paths will lead to failure unless there is close interaction between each set of activities. We must also recognize the limitations of our efforts, as we will never have perfect, universal tools for prediction and analysis, and our imperfect short-term decisions will have longer-term implications for the health of our aquatic resources.

## Part E: References

- A.S.C.E. (American Society of Civil Engineers), 1975. *Sedimentation Engineering. Manual and Reports on Engineering Practice*, No. 54, A.S.C.E., New York, N.Y., 745 pp.
- Abbe, T.B., D.R. Montgomery, K. Fetherston and E.M. McClure, 1993. A process-based classification of woody debris in a fluvial network: preliminary analysis of the Queets River, WA. *EOS, Transactions, American Geophysical Union*, Supplement to Vol. 74(43), p. 296.
- Al-Ansari, N.A. and G.T. Al-Sinawi, 1988. Periodicity of suspended sediment concentration in the River Tigris at Bagdad identified using short interval sampling. In: *Sediment Budgets*. IAHS Publ. no. 174: 353-358.
- Allen, P.B., 1981. Measurement and prediction of erosion and sediment yield. U.S. Dept. of Agriculture, Science and Education Administration, Agricultural Reviews and Manual, ARM-S-15, 23pp.
- Anastasi, G., 1984. Geschiebeanalysen im Felde unter Berücksichtigung von Grobkomponenten. [Field analyses of gravels with special emphasis to coarse particles]. *Mitteilungen der Versuchsanstalt für Wasserbau, Hydrologie und Glaziologie der ETH Zürich*, No. 70.
- Andrews, E.D., 1983. Entrainment of gravel from naturally sorted riverbed material. *Geological Society of America Bulletin* 94: 1225-1231.
- Andrews, E.D. and G. Parker, 1987. Formation of a coarse surface layer as the response to gravel mobility. In: *Sediment Transport in Gravel-Bed Rivers*. C.R. Thorne, J.C. Bathurst and R.D. Hey (eds.). John Wiley and Sons, New York.
- Anthony, D.J., and M.D. Harvey, 1991. Stage-dependent cross-section adjustments in a meandering reach of Fall River, Colorado. *Geomorphology* 4:187-203.
- Apperley, L.W., and A.J. Raudkivi, 1989. The entrainment of sediments by the turbulent flow of water. *Hydrobiologia* 176/177: 39-49.
- Arkell, B., G. Leeks, M. Newson and F. Oldfield, 1983. Trapping and tracing: some recent observations of supply and transport of coarse sediment from upland Wales. *Special Publications of the International Association of Sedimentation* 6: 107-119.
- Ashworth, P.J. and R.I. Ferguson, 1989. Size-selective entrainment of bed load in gravel bed streams. *Water Resources Research* 25(4): 627-634.
- Atkinson, E., 1994. Vortex-tube sediment extractors. I: Trapping efficiency. *Journal of Hydraulic Engineering* 120 (10): 1110-1125.
- Atkinson, E., 1994. Vortex-tube sediment extractors. II: Design. *Journal of Hydraulic Engineering* 120 (10): 1126-1138.
- Bagnold, R.B., 1966. An approach to the sediment transport problem from general physics. *U.S. Geological Survey Professional Paper* 422-I, 37pp.
- Bagnold, R.B., 1977. Bed load transport by natural rivers. *Water Resources Research* 13(2): 303-312.
- Bagnold, R.B., 1980. An empirical correlation of bedload transport rates in flumes and natural rivers. *Proceedings of the Royal Society of London, Series A*, 372: 453-473.
- Baird, A.J., J.B. Thornes, and G.P. Watts, 1993. Extending overland flow models to problems of slope evolution and the representation of complex slope surface topographies. In: *Overland Flow. Hydraulics and Erosion Mechanics*. A.J. Parsons and A.D. Abrahams (eds.), UCL Press, London.
- Bänzinger, R., and H. Burch, 1990. Acoustic senses (hydrophones) as indicator for bed load in a mountain torrent. In: *Hydrology in Mountainous Regions*. IAHS Publ. no. 193: 207-214.
- Barta, A.F., P.R. Wilcock and C.C. Shea, 1993. Entrainment of gravel in steep streams. *EOS, Transactions, American Geophysical Union*, Supplement to Vol. 74(43), p. 311.

- Bathurst, J.C., 1987. Measuring and modelling bedload transport in channels with coarse bed material. In: *River Channels. Environment and Process*. K.S. Richards (ed.), The Institute of British Geographer Special Publication Series, Basil Blackwell, Oxford, p. 272-294.
- Bathurst, J.C., G.J.L. Leeks, and M.D. Newson, 1986. Relationship between sediment supply and sediment transport for the Roaring River, Colorado, USA. In: *Drainage Basin Sediment Delivery*. IAHS Publ. no. 159: 105-117.
- Bathurst, J.C., W.H. Graf and H.H. Cao, 1987. Bed load discharge equations for steep mountain rivers. In: *Sediment Transport in Gravel-Bed Rivers*. C.R. Thorne, J.C. Bathurst and R.D. Hey (eds.), John Wiley and Sons, New York.
- Bechteler, W., 1986. (ed.) *Transport of Suspended Solids in Open Channels*. A.A. Balkema, Rotterdam.
- Bechteler, W., H.-J. Vollmers and S. Wieprecht, 1994. Model investigations into the influence of renaturalization on sediment transport. In: *Dynamics and Geomorphology of Mountain Rivers*. P. Ergenzinger and K.-H. Schmidt (eds.), Lecture Notes in Earth Sciences 52: 37-52, Springer Verlag, Berlin.
- Benda, L. and T. Dunne, 1987. Sediment routing by debris flows. In: *Erosion and Sedimentation in the Pacific Rim*. IAHS Publ. no. 165: 213-223.
- Beschta, R.L., 1978. Long-term Pattern of sediment production following road construction and logging in the Oregon Coastal Range. *Water Resources Research* 14(6): 1011-1016.
- Beschta, R.L., 1979. Debris removal and its effects on sedimentation in an Oregon Coast Range stream. *Northwest Science* 53:71-77.
- Beschta, R.L., 1981a. Increased bag size improves Helley-Smith bed load sampler for use in streams with high sand and organic matter transport. In: *Erosion and Sediment Transport Measurement*. IAHS Publ. no. 133: 17-25.
- Beschta, R.L., 1981b. Patterns of sediment and organic-matter transport in Oregon Coast Range Streams. *Erosion and Sediment Transport in Pacific Rim Steeplands*, IAHS Publ. No. 132: 179-188.
- Beschta, R.L., 1983a. Sediment and organic matter transport in mountain streams of the Pacific Northwest. In: *Proceedings of the D.B. Simons Symposium on Erosion and Sedimentation*, R.-M. Li (ed.), Simons, Li & Associates, Ft. Collins, Colorado, p. 1.69-1.89.
- Beschta, R.L., 1987. Conceptual models of sediment transport in streams. In: *Sediment Transport in Gravel-Bed Rivers*. C.R. Thorne, J.C. Bathurst, and R.D. Hey (eds.), John Wiley, Chichester, p. 387-419.
- Bevenger, G.S. and R.M. King, 1995. A pebble count procedure for accessing watershed cumulative effects. USDA, Forest Service, Rocky Mountain Forest and Range Experiment Station, Research Paper RM-RP-319, 17 pp.
- Bilby, R.E., 1981. Role of organic debris dams in regulating the export of dissolved and particulate matter from a forested watershed. *Ecology* 62(5): 1234-1243.
- Bilby, R.E., 1984. Removal of woody debris may affect stream channel stability. *Journal of Forestry* 82: 609-613.
- Bley, D., and K.-H. Schmidt, 1991. Die Bestimmung von repräsentativen Schwebstoff-Konzentrationsgängen - Erfahrungen aus dem Lainbachgebiet/Oberbayern. (Determination of representative temporal variations of suspended sediment concentration - experiences from the Lainbach/upper Bavaria). In: *Forschungen zur Fluß- und Hangdynamik. Freiburger Geographische Hefte* 33: 121-129.
- Blizard, C.R., 1994. Hydraulic Variables and Bedload Transport in East St. Louis Creek, Rocky Mountains, Colorado. Thesis submitted in partial fulfillment of the requirements of the degree of Master of Science, Colorado State University, Colorado.
- Bluck, B.J., 1982. Texture of gravel bars in braided streams. In: *Gravel-bed Rivers. Fluvial Processes, Engineering and Management*. R.D. Hey; J.C. Bathurst and C.R. Thorne (eds.), John Wiley and Sons, Chichester, p. 339-355.

- Branski, J., 1981. Accuracy of estimating basin denudation processes of suspended sediment measurements. In: *Erosion and Sediment Transport Measurement*, IAHS-Publ. No. 133: 213-218.
- Brayshaw, A.C.; L.E. Frostick and I. Reid, 1983. The hydrodynamics of particle clusters and sediment entrainment in coarse alluvial channels. *Sedimentology* 30: 137-143.
- Brayshaw, A.C., 1985. Bed microtopography and entrainment thresholds in gravel-bed rivers. *Geological Society of America Bulletin* 96: 218-223.
- Bridge, J.S. and J. Jarvis, 1976. Flow and sedimentary processes in the meandering river South Esk, Glen Clova, Scotland. *Earth Surface Processes and Landforms* 1: 303-336.
- Bridge, J.S. and J. Jarvis, 1982. The dynamics of a river bend: a study in flow and sedimentary processes. *Sedimentology* 29: 499-543.
- Brown, G.W. and J.T. Krygier, 1971. Clear-cut logging and sediment production in the Oregon Coast Range. *Water Resources Research* 7(5): 1189-1198.
- Bugosh, N., and S.G. Custer, 1989. The effect of a log-jam burst on bedload transport and channel characteristics in a head-waters stream. In: *Proceedings of the Symposium on Headwaters Hydrology*. W.W. Woessner, and D.F. Potts (eds.), Missoula, MT, USA, p. 203-211.
- Bunte, K., 1989. Locations of gravel bars and sediment storages in the lower 6 km reach of Squaw Creek, a mountain stream in Montana. Unpublished manuscript.
- Bunte, K., 1990. Experiences and results from using a big-frame bed load sampler for coarse material bed load. In: *Hydrology in Mountainous Regions*. IAHS Publ. no. 193: 223-230.
- Bunte, K., 1991a. Untersuchung der zeitlichen Variation des Grobgeschiebetransportes und seiner Korngrößenzusammensetzung (Squaw Creek, Montana, USA). [Temporal variation of coarse material bedload transport and its grain-size distribution (Squaw Creek, Montana, USA.)]. Ph.D. thesis submitted to the Dept. of Earth Sciences at the Freie Universität Berlin, Germany, 223 pp.
- Bunte, K., 1991b. Bedload samples collected with the net-sampler at Squaw Creek in 1991: transport rates and grain-size distributions. Unpublished manuscript.
- Bunte, K., 1992a. Particle number grain-size composition of bedload in a mountain stream. In: *Dynamics of Gravel Bed Rivers*. P. Billi, R.D. Hey, C.R. Thorne and P. Tacconi (eds.), John Wiley, Chichester, p. 55-72.
- Bunte, K., 1992b. Discussion of Komar and Shih (1992): Equal grain mobility versus changing grain sizes in gravel-bed streams. In: *Dynamics of Gravel Bed Rivers*. P. Billi, R.D. Hey, C.R. Thorne and P. Tacconi (eds.), John Wiley, Chichester, p. 93-96.
- Bunte, K., 1994. Modeling bedload transport in sand-bed streams using the Ackers and White (1973) sediment transport formula. Report prepared for the Stream Technology Center, Rocky Mountain Forest and Range Experiment Station, US Forest Service, Fort Collins, Colorado, 56pp.
- Bunte, K., 1996. Field manual for sampling surface and subsurface particle size distribution in natural gravel-bed streams for use in bedload transport computations. Report prepared for the Stream Technology Center, Rocky Mountain Forest and Range Experiment Station, US Forest Service, Fort Collins, CO, 109pp.
- Bunte, K., 1996. *Analyses of the temporal variation of coarse bedload transport and its grain size distribution (Squaw Creek, Montana, USA)*. English translation of Bunte (1991). U.S.D.A., Forest Service, Rocky Mountain Forest and Range Experiment Station, Fort Collins, CO., General Technical Report RM-GTR-288, 124 pp.
- Bunte, K. and P. Ergenzinger, 1989. New tracer techniques for particles in gravel bed rivers. *Bulletin de la Societé Geographique de Liège* 25: 85-90.
- Bunte, K. and L.H. MacDonald, 1993. Temporal Variation of coarse bedload transport during snowmelt high flow and implications for sampling. *EOS, Transactions, American Geophysical Union*, Supplement to Vol. 74(43), p. 295.
- Bunte, K. and J. Poesen, 1993a. Effect of horseshoe vortex erosion on sediment yield from soils covered by rock fragments. *Zeitschrift für Geomorphologie* 37(3): 327-335.

- Bunte, K. and J. Poesen, 1993b. Effects of rock fragment covers on erosion and transport of non-cohesive sediment by shallow overland flow. *Water Resources Research*, 29 (5), 1415-1424.
- Bunte, K. and J. Poesen, 1994. Effects of rock fragment size and cover on overland flow hydraulics, local turbulence and sediment yield on an erodible soil surface. *Earth Surface Processes and Landforms* 19: 115-135.
- Bunte, K., S.G. Custer, P. Ergenzinger, and R. Spieker, 1987. Messung des Grobgeschiebe-transportes mit der Magnettracertechnik. [Measuring coarse material bedload transport with the magnetic tracer technique.] *Deutsche Gewässerkundliche Mitteilungen* 31(2/3): 60-67.
- Buskamp, R., 1994. The influence of channel steps on coarse bed load transport in mountain torrents: Case study using the radio tracer technique 'PETSU'. In: *Dynamics and Geomorphology of Mountain Rivers*. P. Ergenzinger and K.-H. Schmidt (eds.). Lecture Notes in Earth Sciences, Springer Verlag, Berlin, 129-139.
- Buskamp, R., 1994. Erosion, Einzelaufwege und Ruhephasen: Analyse und Modellierung der stochastischen Parameter des Grobgeschiebetransportes. [Erosion, individual travel distances, and rest phases: analysis and modeling of the stochastic parameters of coarse bedload transport.] Ph.D. Dissertation submitted to the Department of Earth Sciences at the Freie Universität Berlin, Germany.
- Buskamp, R., and P. Ergenzinger, 1991. Neue Analysen zum Transport von Grobgeschiebe: Messung Lagrangescher Parameter mit der Radiotracer-technik (PETSU). [New analyses of coarse bedload transport: Measurements of Lagrangian parameters with the radio tracer technique (PETSU)]. In: *Deutsche Gewässerkundliche Mitteilungen*. 35(2): 57-63.
- Buskamp, R. and D. Gintz, 1994. Geschiebefrachterfassung mit Hilfe von Tracern in einem Wildbach (Lainbach/Oberbayern). [Bedload transport determination using tracers in a mountain torrent (Lainbach/Upper Bavaria)]. In: *Messungen in fluvialen Systemen. Feld- und Laboruntersuchungen zur Erfassung des Wasser- und Stoffhaushaltes*, D. Barsch, R. Mäusbacher, K.-H. Pörtge and K.-H. Schmidt (eds.), Springer Verlag, Heidelberg, p. 179-193.
- Butler, P.R., 1977. Movement of cobbles in a gravel-bed stream during a flood season. *Geological Society of America Bulletin* 88: 1072-1074.
- Campbell, A.J. and R.C. Sidle, 1985. Bedload transport in a pool-riffle sequence of a coastal Alaska stream. *Water Resources Bulletin*, American Water Resources Association 21(4): 579-590.
- Campbell, B.L., R.J. Loughran, G.L. Elliot, and D.J. Shelly., 1986. Mapping drainage basin sediment sources using caesium -137. In: *Drainage Basin Sediment Delivery*. IAHS Publ. no. 159: 437-446.
- Carey, W.P., 1983. Variability in measured bedload transport during constant and slowly changing water-discharge conditions. In: *Proceedings of the Advanced Seminar on Sedimentation, August 15-19, 1983, Denver, Colorado*. US Geological Survey Circular 953: 37-38.
- Carey, W.P., 1985. Variability in measured bedload-transport rates. *Water Resources Bulletin*, American Water Resources Association 21(1): 39-48.
- Carey, W.P., 1993. Sediment-Transport characteristics of Cane Creek, Lauderdale County, Tennessee. *Water-Resources Investigations Report 93-4067*, U.S. Geological Survey, Nashville, Tennessee, 19pp.
- Carey, W.P., and D.W. Hubbell, 1986. Probability distributions for bedload transport. In: *Proceedings of the Fourth Federal Interagency Sedimentation Conference*, Las Vegas, Nevada. Vol. I. Subcommittee on Sedimentation of the Interagency Advisory Committee on Water Data, p. 4.131-4.140.

- Carling, P.A., 1987. Discussion of Schick et al. (1987b): Bedload transport in Desert Floods: Observations in the Negev. In: *Sediment Transport in Gravel-Bed Rivers*, C.R. Thorne, J.C. Bathurst and R.D. Hey (eds.), John Wiley and Sons, New York, p. 636-637.
- Carling, P.A., 1988. The concept of dominant discharge applied to two gravel-bed streams in relation to channel stability thresholds. *Earth Surface Processes and Landforms* 13:355-367.
- Carling, P.A., 1991. An appraisal of the velocity-reversal hypothesis for stable pool-riffle sequences in the River Severn, England. *Earth Surface Processes and Landforms* 16: 19-31.
- Carling, P.A., A. Kelsey and M.S. Glaister, 1992. Effect of bed roughness, particle shape and orientation on initial motion criteria. In: *Dynamics of Gravel Bed Rivers*. P. Billi, R.D. Hey, C.R. Thorne and P. Tacconi (eds.), John Wiley, Chichester, p. 23-36.
- Carling, P.A. and N. Wood, 1994. Simulation of flow over pool-riffle topography: A consideration of the velocity reversal hypothesis. *Earth Surface Processes and Landforms* 19: 319-332.
- Carson, M.A. and G.A. Griffiths, 1987. Bedload transport in gravel channels. *Journal of Hydrology (N.Z.)*, 26(1): 1-151.
- Cencetti, C., P. Tacconi, M. del Prete and M. Rinaldi, 1994. Variability of gravel movement on the Virginio gravel-bed stream (central Italy) during some floods. In: *Variability in Stream Erosion and Sediment Transport*. IAHS Publ. 224: 3-11.
- CSQ 1978. Regulation 1508.4, Council on Environmental Quality.
- Cerling, T.E., S.J. Morrison, R.W. Sobocinski and I.L. Larson, 1990. Sediment-water interaction in a small stream: adsorption of  $^{137}\text{Cs}$  by bed load sediments. *Water Resources Research* 26(6): 1165-1176.
- Chacho, E.F., R.L. Burrows and W.W. Emmett, 1989. Detection of coarse sediment movement using radio transmitters. *International Association for Hydraulic Research (IAHR)*, Proceedings of the 23. Congress, Technical Session B : B367-B373.
- Chacho, E.F., W.W. Emmett and R.L. Burrows, 1994. Monitoring gravel movement using radio transmitters. In: *Hydraulic Engineering '94*. Proceedings of the 1994 Conference, G.V. Cotroneo and R.R. Rumer (eds.), ASCE, New York, Vol. 2: p.785-789.
- Chang, H.H. and D.A. Stow, 1988. Sediment delivery in a semi-arid coastal stream. *Journal of Hydrology* 99: 201-214.
- Chang, H.H. and D.A. Stow, 1989. Mathematical modeling of fluvial sand delivery. *Journal of Waterway, Port, Coastal, and Ocean Engineering* 115(3): 311-326.
- Childers, D., 1991. Sampling differences between the Helley-Smith and BL-84 bedload samplers. In: *Proceedings of the Fifth Federal Interagency Sedimentation Conference, March 18-21, 1991, Las Vegas, NV.*, Subcommittee of the Interagency Advisory Committee on Water Data, p. 6.31-6.38.
- Childers, D., 1996. Bedload samplers and sampling techniques. Handout provided for the Bedload Sampling Workshop, coordinated by D. Childers during the *Sixth Federal Interagency Sedimentation Conference, March 10-14, Las Vegas, Nevada*. Interagency Advisory Committee on Water Data, Subcommittee on Sedimentation, 17p.
- Church, M., 1985. Bed load in Gravel-Bed Rivers: Observed phenomena and implications for computation. In: *Proceedings of the Canadian Society for Civil Engineering Annual Conference, Saskatoon, Sk.*, p. 17-37.
- Church, M. and M.A. Hassan, 1992. Size and distance of travel of unconstrained clasts on a streambed. *Water Resources Research* 28(1): 299-303.
- Church, M. and D. Jones, 1982. Channel bars in gravel-bed rivers. In: *Gravel-bed Rivers. Fluvial Processes, Engineering and Management*. R.D. Hey; J.C. Bathurst and C.R. Thorne (eds.), John Wiley and Sons, Chichester, p. 291-338.
- Church, M., D.G. McLean and J.F. Walcott, 1987. Bed load sampling and analysis. In: *Sediment Transport in Gravel-Bed Rivers*, C.R. Thorne, J.C. Bathurst and R.D. Hey (eds.), John Wiley and Sons, New York.

- Church, M., J.F. Wolcott and W.K. Fletcher, 1991. A test of equal mobility in fluvial sediment transport: behavior of the sand fraction. *Water Resources Research* 27(11): 2941-2951.
- Clarke, R.T., 1990. Statistical characteristics of some estimators of sediment and nutrient loadings. *Water Resources Research* 26(9): 2229-2233.
- Clifford, N.J., J.R. French and J. Hardisty, (eds.), 1993. *Turbulence. Perspectives on Flow and Sediment Transport*. John Wiley & Sons, Chichester, 360pp.
- Colby, B.R., 1961. Effect of depth of flow on discharge of bed material. *Studies of Flow in Alluvial Channels. U.S. Geological Survey Water-Supply Paper 1498-D*, 12pp.
- Colby, B.R., 1963. Fluvial sediments - a summary of source, transportation, deposition, and measurement of sediment discharge. *U.S. Geological Survey Bulletin 1181-A*, 47 pp.
- Colby, B.R., 1964. Discharge of sand and mean-velocity relationships in sand-bed streams. *Sediment Transport in Alluvial Channels. Geological Survey Professional Paper 462-A*, 47 pp.
- Colby, B.R. and C.H. Scott, 1965. Effects of water temperature on the discharge of bed material. *Sediment Transport in Alluvial Channels. Geological Survey Professional Paper 462-G*, 25 pp.
- Coleman, D.J. and F.N. Scatena, 1986. Identification and evaluation of sediment sources. In: *Drainage basin sediment delivery*. IAHS Publ. no. 159: 3-18.
- Crickmore, M.J., 1967. Measurement of sand transport in rivers with special reference to tracer methods. *Sedimentology* 8 (3): 175-228.
- Culbertson, J., 1977. Influence of flow characteristics on sediment transport with emphasis on grain size and mineralogy. In: *Proceedings of a Workshop on the Fluvial Transport of Sediment-Associated Nutrients and Contaminants*, held at Kitchener, Ontario Oct. 20-22, 1976, H. Shear and A.E.P. Watson (eds.), p. 117-113.
- Custer, S.G., 1992. A review of natural-gravel-transport-detection experiments at Squaw Creek, Montana, 1981-1991. Paper presented at the U.S. Army Corps of Engineers Workshop, Oct. 27, 1992.
- Custer, S.G., K. Bunte, R. Spieker and P. Ergenzinger, 1986. Timing and location of coarse bedload transport: Squaw Creek, Montana. *EOS, Transactions, American Geophysical Union*, Vol. 67(44), p. 943.
- Custer, S.G., P.E. Ergenzinger, N. Bugosh and B.C. Anderson, 1987. Electromagnetic detection of pebble transport in streams: a method for measurement of sediment transport waves. In: *Recent Developments in Fluvial Sedimentology*. F. Ethridge and R. Flores (eds.), Society of Paleontologists and Mineralogists Special Publication 39: 21-26.
- D'Agostino, V., M.A. Lenzi and L. Marchi, 1994. Sediment transport and water discharge during high flows in an instrumented watershed. In: *Dynamics and Geomorphology of Mountain Rivers*. P. Ergenzinger and K.-H. Schmidt (eds.), Lecture Notes in Earth Sciences 52: 67-81, Springer Verlag, Berlin.
- Darbyshire, E.J. and J.R. West, 1993. Turbulence and cohesive sediment transport in the Parrett Estuary. In: *Turbulence. Perspectives on Flow and Sediment Transport*. N.J. Clifford, J.R. French and J. Hardisty (eds.), John Wiley and Sons, Chichester, 215-247.
- De Jong, C., 1995. Temporal and spatial interactions between river bed roughness, geometry, bedload transport and flow hydraulics in mountain streams - examples from Squaw Creek, Montana (USA) and Lainbach/Schmiedlaine, Upper Bavaria (Germany). *Berliner Geographische Abhandlungen* 59, Institut für Geographische Wissenschaften der Freien Universität Berlin, 229pp.
- Dickinson, W.T., R.P. Rundra, and D.J. Clark, 1986. A delivery ratio approach for seasonal transport of sediment. In: *Drainage Basin Sediment Delivery*. IAHS Publ. no. 159: 237-253.
- Dietrich, W.E. and J.D. Smith, 1984. Bed load transport in a river meander. *Water Resources Research* 20(10): 1355-1380.

- Dietrich, W.E., J.W. Kirchner, H. Ikeda, and F. Iseya, 1989. Sediment supply and the development of the coarse surface layer in gravel-bedload rivers. *Nature* 340: 215-217.
- Dietrich, W.E and P. Whiting, 1989. Boundary shear stress and sediment transport in river meanders of sand and gravels. In: *River Meandering*. S. Ikeda and G. Parker (eds.), Water Resources Monograph 12, American Geophysical Union, Washington, DC, p. 1-50.
- Dinehart, R.L., 1992. Evolution of coarse gravel bedforms: field measurements at flood stage. *Water Resources Research* 28(10): 2667-2689.
- Dinehart, R.L. (in prep.). Sediment transport at gaging stations near Mount St. Helens, Washington, 1980 -90. Data collection and analysis. *Water-Supply Paper*.
- Dissmeyer, G.E., 1976. Erosion and sediment from forest land uses, management practices and disturbances in the southeastern United States. In: *Proceedings of the Third Federal Inter-Agency Sedimentation Conference, Denver, CO.*, Sedimentation Committee of the Water Resources Council. p. 1-140 - 1-148.
- Dissmeyer, G.E. and G.R. Foster, 1984. A guide for predicting sheet and rill erosion on forest land. U.S.D.A. Forest Service, Southern Region, Technical Publication R8-TP6, 28pp.
- Drake, T.G., R.L. Shreve, W.E. Dietrich, P.J. Whiting, and L.B. Leopold, 1988. Bedload transport of fine gravel observed by motion-picture photography. *Journal of Fluid Mechanics* 192: 193-217.
- Duijsings, J.J. H.M., 1986. Seasonal variation in the sediment delivery ratio of a forested drainage basin in Luxembourg. In: *Drainage Basin Sediment Delivery*. IAHS Publ. no. 159: 153-164.
- DVWK (Deutscher Verband für Wasserwirtschaft und Kulturbau e.V.), Fachausschuß "Sedimenttransport in Fließgewässern", 1992. Geschiebemessungen. [Bedload transport measurements.] *DVWK-Regeln zur Wasserwirtschaft* 127. Verlag Paul Parey, Hamburg, 53pp.
- Ecosystem Analysis at the Watershed Scale: Federal Guide for Watershed Analysis, 1995. Regional Ecosystem Office, U.S. Forest Service, Portland, OR.
- Ehrenberger, R., 1931. Direkte Geschiebemessung an der Donau bei Wien und deren bisherige Ergebnisse. *Wasserwirtschaft* 34.
- Einstein, H.A., 1937. Der Geschiebetrieb als Wahrscheinlichkeitsproblem. [Bedload transport as a probability problem]. *Mitteilungen der Versuchsanstalt für Wasserbau an der Eidgenössischen Technischen Hochschule in Zürich*.
- Einstein, H.A., 1950. The bed-load function for sediment transportation in open channel flows. In: *U.S. Dept. of Agriculture, Soil Conservation Service, Technical Bulletin* 1026.
- Emmett, W.W., 1975. The channels and waters of the Upper Salmon River area, Idaho. *Geological Survey Professional Paper* 870-A, 116pp.
- Emmett, W.W., 1976. Bedload transport in two large, gravel-bed rivers, Idaho and Washington. In: *Proceedings of the Third Federal Inter-Agency Sedimentation Conference, Denver, Colorado*, Sedimentation Committee of the Water Resources Council, p. 4.191-4.114.
- Emmett, W.W., 1980. A field calibration of the sediment trapping characteristics of the Helley-Smith bedload sampler. *Geological Survey Professional Paper* 1139, Washington, DC.
- Emmett, W.W., 1984. Measurement of bedload in rivers. In: *Erosion and Sediment Yield: Some Methods of Measurement and Modelling*. R.F. Hadley and D.E. Walling (eds.), Geo Books, Norwich, Great Britain, p. 91-109.
- Emmett, W.W. and R.M. Myrick, 1985. Field data describing the movement and storage of sediment in the East Fork River, Wyoming. Part V. Bed material tracers, 1979 and 1980. *United States Dept. of the Interior, Geological Survey, Open File Report* 85-169, 339 pp.

- Emmett, W.W., R.L. Burrows and E.F. Chacho. Coarse-particle transport in a gravel-bed river. Submitted to UNESCO's *Nature and Research*, 1995.
- Emmett, W.W., L.B. Leopold, and R. M. Myrick, 1983a. Some Characteristics of fluvial Processes in Rivers. In: Proceedings of the Advanced Seminar on Sedimentation, Aug. 15-19, 1983, Denver, CO. *U.S. Geological Survey Circular* 953.
- Emmett, W.W., L.B. Leopold and R.M. Myrick, 1983b. Some characteristics of fluvial processes in rivers. In: *Proceedings of the Second International Symposium on River Sedimentation*, Nanjing, China, Oct. 11-16, 1983, p. 730-754.
- Emmett, W.W., R.H. Myrick and R.H. Meade, 1980. Field data describing the movement and storage of sediment in the East Fork River, Wyoming. Part I. River hydraulics and sediment transport, 1979. *U.S. Geological Survey, Open-File Report* 80-1189, 43pp.
- Emmett, W.W., R.H. Myrick and R.H. Meade, 1982. Field data describing the movement and storage of sediment in the East Fork River, Wyoming. Part III. River hydraulics and sediment transport, 1980. *U.S. Geological Survey, Open-File Report* 82-359, 289pp.
- Emmett, W.W., B. Gomez and M.L. Smalley, 1996. Data that describe cross-channel spatial and temporal variation in bedload -- East Fork River, Wyoming, and Fall River, Colorado. *U.S. Geological Survey, Water Resources Investigations Report* (in press), 115 pp.
- Engel, P. and Y.L. Lau, 1981. The efficiency of basket type bed load samplers. In: *Erosion and Sediment Transport Measurement*. IAHS Publ. no. 133: 27-34.
- Ergenzinger, P., 1985. Messung der Geschiebebewegung und des Geschiebetransportes unter Naturbedingungen. [Measurement of bedload movement and bedload transport under natural conditions]. *Landschaftsökologisches Messen und Auswerten* 1(2/3): 141-157.
- Ergenzinger, P., 1988. The nature of coarse material bed load transport. In: *Sediment Budgets*. M.P. Bordas and D.E. Walling (eds.), IAHS publ. no 174: 207-216.
- Ergenzinger, P. and J. Conrady, 1982. A new tracer technique for measuring bedload in natural channels. *Catena* 9: 77-80.
- Ergenzinger, P.J. and S.G. Custer, 1983. Determination of bedload transport using naturally magnetic tracers: first experience at Squaw Creek, Gallatin County, Montana. *Water Resources Research* 19(1): 187-193.
- Ergenzinger, P. and C. De Jong, 1995. Dynamic roughness, sediment transport and flow structures in a mountain stream. Paper presented at the Gravel-Bed Rivers IV Workshop -- *Gravel-Bed Rivers in the Environment* --, held at Gold Bar, WA, Aug. 20-26, 1995.
- Ergenzinger, P., C. de Jong, and G. Christaller, 1994. Interrelationships between bedload transfer and river bed adjustment in mountain rivers: an example from Squaw Creek, Montana. In: *Process Models and Theoretical Geomorphology*. M.J. Kirkby (ed.), John Wiley and Sons, New York, p. 141-158.
- Ergenzinger, P., K.-H. Schmidt, and R. Busskamp, 1989. The pebble transmitter system (pets): first results of a technique for studying coarse material erosion, transport and deposition. *Zeitschrift für Geomorphologie N.F.* 33(4): 503-508.
- Ergenzinger, P., C. De Jong, J. Laronne and I. Reid, 1994. Short term temporal variations in bedload transport rates: Squaw Creek, Montana, USA, and Nahal Yatir and Nahal Estemoa, Israel. In: *Dynamics and Geomorphology of Mountain Rivers*. P. Ergenzinger and K.-H. Schmidt (eds.). Lecture Notes in Earth Sciences, Springer Verlag, Berlin, 251-264.
- Everitt, B., 1993. Channel response to declining flows on the Rio Grande between Ft. Quitman and Presidio, Texas. *Geomorphology* 6: 225-242.
- Fan, S.-S., 1989. An overview of computer stream sedimentation models. In: *Sediment Transport Modeling*. S.S.Y. Wang (ed.), American Society of Civil Engineers, New York, p. 362-367.
- Federer, C.A., L.D. Flynn, C.W. Martin, J.W. Hornbeck and R.S. Pierce, 1990. Thirty years of hydrometeorologic data at the Hubbard Brook Experimental Forest, New Hampshire. USDA Forest Service, Northeastern Forest Experimental Station, *General Technical Report* NE-141, 44pp.

- Fenton, J.D and J.E. Abbott, 1977. Initial movement of grains on a stream bed: the effects of relative protrusion. In: *Proceedings of the Royal Society of London A* 352: 523-537.
- Ferguson, R.I., 1986. River loads underestimated by rating curves. *Water Resources Research* 22(1): 74-76.
- Ferguson, R.I., 1987. Accuracy and precision of methods for estimating river loads. *Earth Surface Processes and Landforms* 12: 95-104.
- Ferguson, R.I., I.C. Grieve and D.J. Harrison, 1991. Disentangling land use effects on sediment yield from year to year climatic variability. *Sediment and Stream Water Quality in a Changing Environment: Trends and Explanation*. IAHS publ. No. 203: 13-20.
- Ferguson, R.I., K.L. Prestegard and P.J. Ashworth, 1989. Influence of sand on hydraulics and gravel transport in a braided gravel-bed river. *Water Resources Research* 25(4): 635-643.
- Ferguson, R.I., T.B. Hoey, S.J. Wathen, A. Werritty, R.I. Hardwick and G.H. Sambrook Smith, 1995. Downstream fining of river gravels: an integrated field, lab and modelling study. Paper presented at the Gravel-Bed Rivers IV Workshop -- *Gravel-Bed Rivers in the Environment* --, held at Gold Bar, WA, Aug. 20-26, 1995.
- FISP, 1991. *Proceedings of the Fifth Federal Interagency Sedimentation Conference, March 18-21, 1991, Las Vegas, NV.*, Subcommittee of the Interagency Advisory Committee on Water Data.
- FISP, 1996. *Sixth Federal Interagency Sedimentation Conference, March 10-14, Las Vegas, Nevada.* Interagency Advisory Committee on Water Data, Subcommittee on Sedimentation.
- Foley, M.G., 1976. Scour and fill in an ephemeral stream. In: *Proceedings of the Third Federal Inter-Agency Sedimentation Conference, Denver, CO*, Sedimentation Committee of the Water Resources Council, p. 5.1-5.12.
- Folk, R.L. and W.C. Ward, 1957. Brazos River Bar: a study in the significance of grain size parameters. *Journal of Sedimentary Petrology* 27(1): 3-26.
- Francis, J.R.D., 1973. Experiments on the motion of solitary grains along the bed of a water-stream. *Proceedings of the Royal Society of London, Series A*, 332: 443-471.
- Gao, H., 1991. The comparison tests of gravel bed load samplers. *Proceedings of the Fifth Federal Interagency Sedimentation Conference, March 18-21, 1991, Las Vegas, Nev.*, Subcommittee on Sedimentation of the Interagency Advisory Committee on Water Data, p. 6.55-6.62.
- Gaudet, J.M., A.G. Roy and J.L. Best, 1994. Effects of orientation and size of Helley-Smith sampler on its efficiency. *Journal of Hydraulic Engineering* 120 (6): 758-766.
- Gaweesh, M.T.K. and L.C. van Rijn, 1994. Bed-load sampling in sand-bed rivers. *Journal of Hydraulic Engineering* 120 (12): 1364-1384.
- Georgiev, B.V., 1990. Reliability of bed load measurements in mountain rivers. In: *Hydrology of Mountainous Regions I*, IAHS Publ. no. 193: 263-270.
- Gessler, J., 1976. The dilemma of setting standards. In: *Proceedings of the Third Federal Inter-Agency Sedimentation Conference, Denver, Colorado*, Sedimentation Committee of the Water Resources Council, p. 2.158-2.167.
- Gilbert, R.O., 1987. *Statistical methods for environmental pollution monitoring*. Van Nostrand Reinhold, New York.
- Gilvear, D.J. and G.E. Petts, 1985. Turbidity and suspended solids variations downstream of a regulating reservoir. *Earth Surface Processes and Landforms* 10: 363-373.
- Gintz, D., 1990. Die Messung der Grobgeschiebebewegung mit Hilfe von Eisen- und Magnettracern am Lainbach, Oberbayern. [Measurements of coarse bedload movements using iron- and magnetic tracers at the Lainbach, upper Bavaria]. M.S. thesis submitted to the Dept. of Physical Geography at the Freie Universität Berlin, Germany.

- Gintz, D., 1995. Transportdistanzen und räumliche Verteilung von Grobgeschieben in Abhängigkeit von Geschiebeeigenschaften und Gerinnemorphologie - Tracerversuche im Lainbach/Obb. [Transport distances and spatial distribution of coarse bedload particles as a function of particle properties and channel morphology - tracer experiments at the Lainbach, upper Bavaria]. Ph.D. These submitted to the Department of Physical Geography at the Freie Universität Berlin, Germany. Also published 1995 in *Berliner Geographische Abhandlungen - Beihefte*, Heft 3, 107 pp, Institut für Geographische Wissenschaften der Freien Universität Berlin.
- Gintz, D. and K.-H. Schmidt, 1991. Grobgeschiebetransport in einem Gebirgsbach als Funktion von Gerinneform und Geschiebemorphometrie. [Coarse material bedload transport in a mountain stream as a function of channel shape and particle morphometry]. *Zeitschrift für Geomorphologie*, Supplement Band 89: 63-72, Berlin.
- Gintz, D., M.A. Hassan and K.-H. Schmidt, 1996. Frequency and magnitude of bedload transport in a mountain river. *Earth Surface Processes and Landforms* 21: 433-445.
- Glymph, L.M. (Jr.) 1954. Studies of sediment yield from watersheds. In: *Proc. of the General Assembly in Rome 1954*. IASH Publ. no. 36: 178-191.
- Goff, J.R. and P. Ashmore, 1994. Gravel transport and morphological change in braided Sunwapta River, Alberta, Canada. *Earth Surface Processes and Landforms* 19: 195-212.
- Gölz, E., and B. Dröge, 1989. Zur morphologischen und sedimentologischen Charakteristik des Rheins. [Morphological and sedimentological characteristics of the Rhein]. *Deutsche Gewässerkundliche Mitteilungen* 33(3/4): 85-91.
- Gomez, B., 1983. Temporal Variations in Bedload Transport Rates: The Effect of Progressive Bed-Armouring. *Earth Surface Processes and Landforms* 8: 41-54.
- Gomez, B., 1991. Bedload transport. *Earth-Science Reviews* 31: 89-132.
- Gomez, B. and W.W. Emmett, 1990. Data that describe at-a-point temporal variations in the transport rate and particle-size distribution of bedload -- East Fork River, Wyoming and Fall River, Colorado. *U.S. Geological Survey, Open File Report* 90-193, 48 pp.
- Gomez, B., W.W. Emmett, and D.W. Hubbell, 1991. Comments on sampling bedload in small rivers. In: *Proceedings of the Fifth Federal Interagency Sedimentation Conference, March 18-21, 1991, Las Vegas, NV.*, Subcommittee of the Interagency Advisory Committee on Water Data, p. 2.65-2.72.
- Gomez, B., D.W. Hubbell and H.H. Stevens Jr., 1990. At-a-point-bed load sampling in the presence of dunes. *Water Resources Research*, 26(11): 2717-2731.
- Gomez, B., R.L. Naff, and D.W. Hubbell, 1989. Temporal variation in bedload transport rates associated with the migration of bedforms. *Earth Surface Processes and Landforms* 14: 135-156.
- Goodwin, P. and R.A. Denton, 1991. Seasonal influences on the sediment transport characteristics of the Sacramento River, California. In: *Proceedings of the Institute of Civil Engineers, Part 2 - Research and Theory* 91: 163-172.
- Graf, J.B., 1983. Measurement of bedload discharge in nine Illinois streams with the Helley-Smith sampler. In: *Proceedings of the Advanced Seminar on Sedimentation*, Aug. 15-19, Denver, CO. U.S. Geological Survey Circular 953: 39-40.
- Grant, G.E., 1987. Assessing effects of peak flow increases on stream channels: a rational approach. In: *Proceedings of the California Watershed Management Conference*, Wildland Resource Center, Div. of Agric. and Nat. Resources, University of California, Report no. 11: 142-149.
- Grant, G.E., and A.L. Wolff, 1991. Long-term patterns of sediment transport after timber harvest, western Cascade Mountains, Oregon, USA. In: *Sediment and Stream Water Quality in a Changing Environment: Trends and Explanation*. IAHS Publ. no. 203: 31-40.
- Gray, J.R., R.H. Webb and D.W. Hyndman, 1991. Low-flow sediment transport in the Colorado River. *Proceedings of the Fifth Federal Interagency Sedimentation Conference, March 18-21, 1991, Las Vegas, Nev.*, Subcommittee on Sedimentation of the Interagency Advisory Committee on Water Data, p. 4.63-4.71.

- Griffiths, G.A., 1993. Sediment translation waves in braided gravel-bed streams. *Journal of Hydraulic Engineering* 119(8): 924-936.
- Grigg, N.S., 1970. Motion of single particles in alluvial channels. *Journal of the Hydraulics Division*. Proceedings of the American Society of Civil Engineers, 96(HY12): 2501-2518.
- Guy, H.P., 1970. Fluvial sediment concepts. *U.S. Geological Survey Techniques Water-Resources Investigations*, Book 3, chapter C1, 55 pp.
- Hadley, R.F. and Shown 1976.
- Hagans, D.K. and W.E. Weaver, 1987. Magnitude, cause and basin response to fluvial erosion, Redwood Creek basin, northern California. In: *Erosion and Sedimentation in the Pacific Rim*. IAHS Publ. no. 165: 419-428.
- Hamamori, A., 1962. A theoretical investigation on the fluctuation of bed-load transport. *Hydraulics Laboratories Delft*, Report R4, Serie 2.
- Hansen, E.A., 1974. Total sediment discharge sampling over sills. *Water Resources Research* 10(5): 989-994.
- Hansen, E.A. and G.R. Alexander, 1976. Effect of an artificially increased sand bedload on stream morphology and its implications on fish habitat. In: *Proceedings of the Third Federal Inter-Agency Sedimentation Conference, Denver, CO*, Sedimentation Committee of the Water Resources Council, p. 3.65-3.76.
- Harr, D.R., 1981. Scheduling timber harvest to protect watershed values. In: *Proceedings of the Interior West Watershed Management Symposium*, D.M. Baumgartner (ed.), Washington State University, Cooperative Extension, Pullman, p. 269-280.
- Harr, D.R., 1989. Cumulative effects of timber harvest on streamflows. Paper presented at the Soc. Am. Foresters 1989 Annual Convention, Spokane, WA, 24 p.
- Hartman, G.F. and J.C. Scivener, 1990. Impacts of forestry practices on a coastal stream ecosystem, Carnation Creek, British Columbia. *Canadian Bulletin of Fisheries and Aquatic Sciences* 223, 148 pp.
- Hassan, M.A., 1990. Scour, fill, and burial depth of coarse material in gravel bed streams. *Earth Surface Processes and Landforms* 15: 341-356.
- Hassan, M.A. and M. Church, 1992. The movement of individual grains on the streambed. In: *Dynamics of Gravel Bed Rivers*. P. Billi, R.D. Hey, C.R. Thorne and P. Tacconi (eds.), John Wiley, Chichester, p. 159-175.
- Hassan, M.A. and M. Church, 1994. Vertical mixing of coarse particles in gravel bed rivers: a kinematic model. *Water Resources Research* 30(4): 1173-1185.
- Hassan, M.A., M. Church and P.J. Ashworth, 1992. Virtual rate and mean distance of travel of individual clasts in gravel-bed channels. *Earth Surface Processes and Landforms* 17: 617-627.
- Hassan, M.A., M. Church and A.P. Schick, 1991. Distance of movement of coarse particles in gravel bed streams. *Water Resources Research* 27(4): 503-511.
- Hassan, M.A., A.P. Schick and J.B. Laronne, 1984. The recovery of flood-dispersed coarse sediment particles. *Catena Supplement* 5: 153-162.
- Hayward, J.A. and A.J. Sutherland, 1974. The Torlesse stream vertex-tube sediment trap. *Journal of Hydrology (N.Z.)* 13(1): 41-53.
- Hayward, J.A., 1980. Hydrology and stream sediments in a mountain catchment. In: *Tussock Grasslands and Mountain Lands Institute Special Publ.* 17, 236 pp.
- Heathershaw, A.D., and P.D. Thorne, 1985. Sea-bed noises reveal role of turbulent bursting phenomenon in sediment transport by tidal currents. *Nature* 316: 339-342.
- Heede, B.H., 1991. Stop sediment on the watershed, not in the stream. In: *Sediment and Stream Water Quality in a Changing Environment: Trends and Explanation*. IAHS Publ. no. 203: 41-55.
- Helley, E.J. and W. Smith, 1971. Development and calibration of a pressure -difference bedload sampler. *USDI, Geological Survey, Water Resources Division, Open File Report*, Menlo Park, California, 18pp.

- Helsel, D.R. and R.M. Hirsch, 1992. *Statistical methods in water resources*. Elsevier, Amsterdam, 522 pp.
- Hjulström, F., 1935. Studies of the morphological activities of rivers as illustrated by the River Fyris. *Bulletin of the Geological Institute*, University of Uppsala 25: 221-527.
- Höfner, T., 1994. Erfassung des fluvialen Sedimenttransfers in der zentralalpiner Periglazialstufe. [Determination of fluvial sediment transfer in the central Alpine periglacial region]. In: *Messungen in fluvialen Systemen. Feld- und Laboruntersuchungen zur Erfassung des Wasser- und Stoffhaushaltes*, D. Barsch, R. Mäusbacher, K.-H. Pörtge and K.-H. Schmidt (eds.), Springer Verlag, Heidelberg, p. 195-205.
- Hoey, T.B. and A.J. Sutherland, 1991. Channel morphology and bedload pulses in braided rivers: a laboratory study. *Earth Surface Processes and Landforms* 16: 447-462.
- Holberger, R.L. and J.B. Truett, 1976. Sediment yield from construction sites. In: *Proceedings of the Third Federal Inter-Agency Sedimentation Conference, Denver, CO., Sedimentation Committee of the Water Resources Council*. p. 47-58.
- Holtorff, G., 1989. The formation of meandering and braided channels. In: *Sediment Transport Modeling*, S.S.Y. Wang (ed.), American Society of Civil Engineers, New York, p. 70-75.
- Hong, R.-J., M.F. Karim and J.F. Kennedy, 1984. Low temperature effects on flow in sand-bed streams. *Journal of Hydraulic Engineering* 110 (2): 109-125.
- Horowitz, A.J., F.A. Rinella, P. Lamothe, T.L. Miller, T.K. Edwards, R.L. Roche and D.A. Rickert, 1989. Cross-sectional variability in suspended sediment and associated trace element concentrations in selected rivers in the US. In: *Sediment and the Environment*, R.F. Hadley and E.D. Ongley (eds.), IAHS Publ. no. 184: 57-66.
- Hubbell, D.W., 1964. Apparatus and techniques for measuring bedload. *Geological Survey Water Supply Paper* 1748, 74p.
- Hubbell, D.W., 1987. Bed load sampling and Analysis. In: *Sediment Transport in Gravel-Bed Rivers*. C.R. Thorne, J.C. Bathurst and R.D. Hey (eds.), John Wiley, Chichester, p. 89-118.
- Hubbell, D.W. and D.Q. Matejka, 1959. Investigation of sediment transportation, Middle Loup River at Dunning, Nebraska, with application of data from turbulence flume. *U.S. Geological Survey, Water Supply Paper* 1476, 123pp.
- Hubbell, D.W. and W.W. Sayre, 1964. Sand transport studies with radioactive tracers. *Journal of the Hydraulics Division*. Proceedings of the American Society of Civil Engineers, 90(HY3): 39-18.
- Hubbell, D.W. and H.H. Stevens Jr., 1986. Factors affecting accuracy of bedload sampling. *Proceedings of the Fourth Federal Interagency Sedimentation Conference, Las Vegas, Nevada*. Vol. I. Subcommittee on Sedimentation of the Interagency Advisor Committee on Water Data, p. 4.20-4.29.
- Hubbell, D.W., H.H. Stevens, J.V. Skinner and J.P. Beverage, 1985. New approach to calibrating bed load samplers. *Journal of Hydraulic Engineering*, 111(4): 677-694.
- Hubbell, D.W., H.H. Stevens Jr., J.V. Skinner, and J.P. Beverage, 1987. Laboratory Data on Coarse-Sediment Transport for Bedload-Sampler Calibrations. *U.S. Geological Survey Water-Supply Paper* 2299: 1-31.
- Hupp, C.R. and A. Simon, 1991. Bank accretion and the development of vegetated depositional surfaces along modified alluvial channels. *Geomorphology* 4: 111-124.
- Ibbeken, H., 1974. A simple sieving and splitting device for field analysis of coarse grained sediments. *Journal of Sedimentary Petrology* 44(3): 939-946.
- Ice, G.G., 1984. Cumulative effects - concepts and modeling of observed water quality responses. *NCASI Technical Bulletin* 435: 1-13.
- Ichim, I. and M. Radoane, 1990. Channel sediment variability along a river: a case study of the Siret River (Romania). *Earth Surface Processes and Landforms* 15: 211-225.

- Ikeda, H. and F. Iseya, 1987. Thresholds in the mobility of sediment mixtures. In: *International Geomorphology*, Part I. V. Gardiner (ed.), John Wiley and Sons, Chichester, p. 561-570.
- Iseya, F., and H. Ikeda, 1987. Pulsations in bedload transport rates induced by longitudinal sediment sorting: a flume study using sand and gravel mixtures. *Geografiska Annaler* 69A(1): 15-27.
- Jackson, W.L. and R.L. Beschta, 1982. A model of two-phase bedload transport in an Oregon Coast Range stream. *Earth Surface Processes and Landforms* 7: 517-527.
- Jaeggi, M., 1983. Alternierende Kiesbänke. [Alternating gravel bars.] *Mitteilungen der Versuchsanstalt für Wasserbau, Hydrologie und Glaziologie* 62, ETH Zürich, 286 pp.
- Jaeggi, M.N.R., 1987. Interaction of bed load transport with bars. In: *Sediment Transport in Gravel-Bed Rivers*. C.R. Thorne, J.C. Bathurst, and R.D. Hey (eds.), John Wiley, Chichester, p. 829-841.
- James, A.L., 1991. Incision and morphologic evolution of an alluvial channel recovering from hydraulic mining sediment. *Geological Society of America Bulletin*, 103: 723-736.
- Johnson, C.W., R.L. Engleman, J.P. Smith and C.I. Hanson, 1977. Helley-Smith bed load samplers. *Journal of the Hydraulics Division* 103(HY10): 1217-1221.
- Kappesser, G., 1995. Riffle stability index. Unpublished draft manuscript for review and comment. George Washington and Jefferson National Forests, Roanoke, VA, 21p.
- Karcz, I., 1968. Fluvial obstacle marks from wadis of the Negev (Southern Israel). *Journal of Sedimentary Petrology* 38 (4): 1000-1012.
- Keller, E.A., 1970. Bed-load movement experiments: Dry Creek, California. *Journal of Sedimentary Petrology* 40(4): 1339-1344.
- Keller, E.A., 1971. Areal sorting of bed-load material: the hypothesis of velocity reversal. *Geological Society of America Bulletin* 82: 753-756.
- Keller, E.A., 1972. Areal sorting of bed-load material: the hypothesis of velocity reversal: reply. *Geological Society of America Bulletin* 83: 915-918.
- Keller, E.A. and J.L. Florsheim, 1993. Velocity-reversal hypothesis: a model approach. *Earth Surface Processes and Landforms* 18: 733-740.
- Keller, E.A. and W.N. Melhorn, 1978. Rhythmic scaping and origin of pools and riffles. *Geological Society of America Bulletin* 89: 723-730.
- Keller, H.M. and F.J. Swanson, 1979. Effects of large organic material on channel form and fluvial processes. *Earth Surface Processes* 4: 361-380.
- Keller, H.M. and P. Weibel, 1991. Suspended sediments in stream water - indicators of erosion and bedload transport in a mountainous basin. In: *Sediment and Stream Water Quality in a Changing Environment: Trends and Explanation*. IAHS Publ. no. 203: 53-61.
- Kelsey, H., M.A. Madej, J. Pitlick, P. Stroud, and M. Coghlan, 1981. Major sediment sources and limits to the effectiveness of erosion control techniques in the highly erosive watersheds of north coastal California. In: *Erosion and Sediment Transport in Pacific Rim Steeplands*. IAHS Publ. no. 132:493-509.
- Kelsey, H.M., R. Lamberson and M.A. Madej, 1986. Modeling the transport of stored sediment in a gravel bed river, northwestern California. In: *Drainage Basin Sediment Delivery*. IAHS Publ. no. 159: 367-391.
- Ketcheson, G.L., 1986. Sediment rating equations: an evaluation for streams in the Idaho Batholith. *U.S.D.A., Forest Service, Intermountain Research Station, General Technical Report INT-213*, 12pp.
- Ketcheson, G.L. and W.F. Megahan, 1991. Sediment tracing in step-pool granitic streams in Idaho. In: *Proceedings of the Fifth Federal Interagency Sedimentation Conference, March 18-21, 1991, Las Vegas, NV.*, Subcommittee of the Interagency Advisory Committee on Water Data, p. 4.147-4.153.
- King, J.G., 1979. Water quality characteristics of the Horse Creek watersheds in north central Idaho. Idaho Water Resources Institute, University of Idaho, Moscow, Idaho. Research Technical Completion Report, Project A-051-IDA, 118pp.

- King, J.G., 1989. Streamflow responses to road building and harvesting: a comparison with the equivalent clearcut area procedure. *USDA, Forest Service, Intermountain Research Station, Research Paper INT-401*, 13p.
- King, R.M. and J.P. Potyondy, 1993. Statistically testing Wolman pebble counts: changes in percent fines. In: *Stream Notes*, October 1993. USDA Forest Service, Stream Technology Center, Fort Collins, CO.
- Kirkby, M.J., 1991. Sediment travel distance as an experimental and model variable in particulate movement. In: *Catena Supplement* 19: 111-128.
- Klein, R., R. Sonnevil and D. Short, 1987. Effects of woody debris removal on sediment storage in a northwest California stream. In: *Erosion and Sedimentation in the Pacific Rim*. IAHS Publ. no. 165: 403-404.
- Klingeman, P.C. and W.W. Emmett, 1982. Gravel bedload transport processes. In: *Gravel Bed Rivers. Fluvial Processes, Engineering and Management*. R.D. Hey, J.C. Bathurst, and C.R. Thorne (eds.), John Wiley, Chichester, p. 141-179.
- Klock, G.O. and J.D. Helvey, 1976. Debris flows following wildfire in north central Washington. In: *Proceedings of the Third Federal Inter-Agency Sedimentation Conference, Denver, CO, Sedimentation Committee of the Water Resources Council*. p. 91-97.
- Knox, J.C., 1989. Long- and short-term episodic storage and removal of sediment in the watersheds of southwestern Wisconsin and northwestern Illinois. In: *Sediment and the Environment*. IAHS Publ. no. 184: 157-164.
- Komar, P.D., 1987. Selective entrainment by a current from a bed of mixed sizes: a reanalysis. *Journal of Sedimentary Petrology* 57(2): 203-211.
- Komar, P.D. and S.-M. Shih, 1992. Equal mobility versus changing bedload grain size in gravel-bed streams. In: *Dynamics of Gravel Bed Rivers*. P. Billi, R.D. Hey, C.R. Thorne and P. Tacconi (eds.), John Wiley, Chichester, p.73-106.
- Kondolf, G.M. and W.V.G. Matthews, 1986. Transport of tracer gravels on a coastal California River. *Journal of Hydrology* 85: 265-280.
- Kondolf, G.M., and W.V.G. Matthews, 1993. Coarse sediment management in regulated rivers of California. *EOS, Transactions, American Geophysical Union*, Supplement to Vol. 74(43), p. 321.
- Kronfellner - Kraus, G., 1982. Estimation of extreme sediment transport from torrential drainage basins in the East Alps. In: *Recent Developments in the Explanation and Prediction of Erosion and Sediment Yield*. IAHS Publ. no. 137: 269-273.
- Kuhnle, R.A., 1996. Unsteady transport of sand and gravel mixtures. In: *Advances in Fluvial Dynamics and Stratigraphy*, P.A. Carling and M. Dawson (eds.), John Wiley, Chichester, p. 183-201..
- Kuhnle, R.A., and J.B. Southard, 1988. Bed load transport fluctuations in a gravel bed laboratory channel. *Water Resources Research* 25(2): 247-260.
- Kuhnle, R.A., J.C. Willis, and A.J. Bowie, 1989a. Variations in the transport of bed load sediment in a gravel-bed stream, Goodwin Creek, northern Mississippi, U.S.A. In: *Fourth International Symposium on River Sedimentation, Beijing, China*. p. 539-546.
- Kuhnle, R.A., J.C. Willis, and A.J. Bowie, 1989b. Total sediment load calculations for Goodwin Creek. In: *Sediment Transport Modeling*, S.S.Y. Wang (ed.), American Society for Civil Engineers, New York, p. 700-705.
- Laird, J.R. and M.D. Harvey, 1986. Complex-response of a chaparral drainage basin to fire. In: *Drainage Basin Sediment Delivery*. IAHS Publ. no. 159: 165-183.
- Lambert, C.P. and Walling, D.E., 1986. Suspended sediment storage in river channels: a case study of the river Exe, Devon, UK. In: *Drainage Basin Sediment Delivery*. IAHS Publ. no. 159: 263-276.
- Lane, L.J., M.A. Nearing, J.M. Lafren, G.R. Foster and M.H. Nicols, 1993. Description of the US Department of Agriculture water erosion prediction project (WEPP) model. In: *Overland Flow. Hydraulics and Erosion Mechanics*. A.J. Parsons and A.D. Abrahams (eds.), Chapman & Hall, New York.

- Lane, S.N., K.S. Richards and J.H. Chandler, 1995. Morphological estimation of the time-integrated bed load transport rate. *Water Resources Research* 31(3): 761-772.
- Lane, S.N. and K.S. Richards, 1995. Discharge and sediment supply controls on erosion and deposition in a dynamic alluvial channel. Paper presented at the Gravel-Bed Rivers IV Workshop -- *Gravel-Bed Rivers in the Environment* --, held at Gold Bar, WA, Aug. 20-26, 1995.
- Lapointe, M., 1992. Burst-like sediment suspension events in a sand bed river. *Earth Surface Processes and Landforms* 17: 253-270.
- Laronne, J.B. and Carson, M.A., 1976. Interrelationships between bed morphology and bed material transport for a small, gravel-bed channel. *Sedimentology* 23:76-85.
- Laronne, J.B., D.N. Outhet, J.L. Duckham and T.J. McCabe, 1992. Determining event bedload volumes for evaluation of potential degradation sites due to gravel extraction, N.S.W., Australia. In: *Erosion and Sediment Transport Monitoring in River Basins*. IAHS Publ. no. 210: 87-94.
- Laronne, J.B., I. Reid, Y. Yitshak and L.E. Frostick, 1992. Recording bedload discharge in a semiarid channel, Nahal Yatir, Israel. In: *Erosion and Sediment Transport Monitoring in River Basins*. IAHS Publ. no. 210: 79-86.
- Laursen, E.M., 1963. An analysis of relief bridge scour. *Journal of the Hydraulics Division of the ASCE*, 89(HY3):93-118.
- Lawrence, W.H. and G.G. Ice, 1986. Understanding forest (environmental research) opportunities. In: Papers presented at the American Geophysical Union Meeting on cumulative effects. *NCASI Technical Bulletin* 490: 30-37.
- Lehre, A.K., R.D. Klein and W. Trush, 1993. Gravel mining, bed lowering, and bed material transport in the Mad River, Humboldt Co., California. *EOS, Transactions, American Geophysical Union*, Supplement to Vol. 74(43), p. 321.
- Lenzi, M.A., L. Marchi and G.R. Scussel, 1990. Measurement of coarse sediment transport in a small Alpine stream. In: *Hydrology in Mountainous Regions, 1*, IAHS Publ. no. 193: 223-230.
- Leopold, L.B. and W.W. Emmett, 1976. Bedload measurements, East Fork River, Wyoming. *Proceedings of the National Academy of Sciences, USA* 73(4): 1000-1004.
- Leopold, L. B. and W.W. Emmett, 1977. 1976 bedload measurements, East Fork River, Wyoming. *Proceedings of the National Academy of Sciences, USA*, 74(7): 2644-2648.
- Leopold, L. B. and D.C. Rosgen, 1991. Movement of bedmaterial clasts in mountain streams. In: *Proceedings of the Fifth Federal Interagency Sedimentation Conference*, March 18-21, 1991, Las Vegas, Nev., Subcommittee on Sedimentation of the Interagency Advisory Committee on Water Data, p. 4.183-4.188.
- Leopold, L.B., W.W. Emmett and R.M. Myrick, 1966. Channel and hillslope processes in a semiarid area, New Mexico. *U.S. Geological Survey Professional Paper* 352-G: 193-253.
- Lewis, J., 1991. An improved bedload sampler. In: *Proceedings of the Fifth Federal Interagency Sedimentation Conference*, March 18-21, 1991, Las Vegas, Nev., Subcommittee of the Interagency Advisory Committee on Water Data, p. 6.1- 6.8.
- Lisle, T.E., 1979. A sorting mechanism for a riffle-pool sequence: summary. *Geological Society of America Bulletin*, Part. 1, 90: 616-617.
- Lisle, T.E., 1989. Sediment transport and resulting deposition in spawning gravels, north coastal California. *Water Resources Research* 25(6): 1303-1319.
- Lisle, T.E. and S. Hilton, 1992. The volume of fine sediment in pools: an index of sediment supply in gravel-bed streams. *Water Resources Bulletin* 28(2): 371-383.
- Lisle, T.E. and M.A. Madej, 1992. Spatial variation in armouring in a channel with high sediment supply. In: *Dynamics of Gravel Bed Rivers*. P. Billi, R.D. Hey, C.R. Thorne and P. Tacconi (eds.), John Wiley and Sons, Chichester, p. 277-293.
- Lopez, V.L. and P.F. Ffolliott, 1993. Sediment rating curves for a clearcut Ponderosa pine watershed in northern Arizona. *Water Resources Bulletin* 29(3): 369-382.

- MacDonald, A. and E.A. Keller, 1987. Stream channel response to the removal of large woody debris, Larry Damm Creek, northwestern California. In: *Erosion and Sedimentation in the Pacific Rim*. IAHS Publ. no. 165: 405-406.
- MacDonald, L.H., 1989. Cumulative watershed effects: the implication of scale. Paper presented at the 1989 fall meeting of the American Geophysical Union, San Francisco, CA.
- Madej, M.A., 1987. Residence time of channel-stored sediment in Redwood Creek, northwestern California. In: *Erosion and Sedimentation in the Pacific Rim*. IAHS Publ. no. 165: 429-438.
- Madson, S.W., 1994. Channel response associated with predicted increases in water and sediment yield in Northwest Montana. Thesis submitted as partial requirement of the M.A. degree to the Dept. of Earth Resources, Colorado State University, Ft. Collins.
- Madson, S.W., L.H. MacDonald and E.E. Wohl, 1993. Step-pool channel response to predicted water and sediment yield increases in northwest Montana. *EOS, Transactions, American Geophysical Union*, Supplement to Vol. 74(43), p. 320.
- Mahmood, K. and M.H. Mehrdad, 1991. Prediction of bedload in sandbed channels. In: *Proceedings of the Fifth Federal Interagency Sedimentation Conference, March 18-21, 1991, Las Vegas, Nev.*, Subcommittee of the Interagency Advisory Committee on Water Data, p. 4.94 - 4.101.
- Maidment, (eds.) 1993. *Handbook of Hydrology*. McGraw-Hill, New York.
- Maner, S. B. and S.H. Barnes, 1953. Suggested criteria for estimating gross sheet erosion and sediment delivery rates for the Blackland Prairies problem area in soil conservation. U.S. Dept. of Agriculture, Soil Conservation Service, Ft. Worth.
- Maner, S.B. 1958. Factors affecting sediment delivery fates in the rice hills physiographic area. *Transactions, American Geophysical Union* 39 (4): 669-675.
- Mantz, P.A. and W.W. Emmett, 1986. Analyses of United States Geological Survey sediment transport data for some California streams. In: *Transport of Suspended Solids in Open Channels*. W. Bechteler (ed.), A.A. Balkema, Rotterdam, p. 177-182.
- Marchand, J.P., R.D. Jarrett and L.L. Jones, 1984. Velocity profile, water-surface slope, and bed material size for selected streams in Colorado. *U.S. Geological Survey Open-File Report 84-733*, 82pp.
- Martens, I., 1995. Die räumliche Verteilung von Schwebstoffkonzentrationsparametern im Querprofil vorapliner Fließgewässer. [Spatial distribution of suspended sediment concentration in a cross-section of a pre-alpine stream.] M.A. Thesis submitted to the Department of Geographical Sciences at the Freie Universität Berlin, Germany, 119 pp.
- Martin, C.W. and J.W. Hornbeck, 1993. Erosion, sediment, and turbidity in New England forests. In: *Proceedings of the Technical Workshop on Sediments, Feb. 3-7, 1992, Corvallis, Oregon*, sponsored by Terrene Institute, U.S. EPA and U.S. Forest Service. Terrene Institute, 1717 K Street, NW, Suite 801, Washington, DC.
- Martin, Y. and M. Church, 1995. Bed-material transport estimated from channel surveys: Vedder River, British Columbia. *Earth Surface Processes and Landforms* 20: 347-361.
- Matherne, A.M. and K.L. Prestegard, 1988. Hydrological characteristics as a determinant of sediment delivery in watersheds. In: *Sediment Budgets*. IAHS Publ. no. 174: 89-96.
- McLean, D.G., and B. Tassone, 1987. Discussion of "Bed Load Sampling and Analysis" by D.W. Hubbell. In: *Sediment Transport in Gravel-bed Rivers*. C.R. Thorne, J.C. Bathurst, and R.D. Hey (eds.), John Wiley, Chichester, p. 109-113.
- Meade, R.H., 1985. Wavelike movement of bedload sediment, East Fork River, Wyoming. *Environmental Geology and Water Sciences* 7(4): 215-225.
- Meade, R.H., T. Dunne, J.E. Richey, U.M. Santos, and E. Salati, 1985. Storage and remobilization of suspended sediment in the lower Amazon River of Brazil. *Science* 228: 488-490.
- Meade, R.H., W.W. Emmett, and R.M. Myrick, 1981. Movement and storage of bed material during 1979 in East Fork River, Wyoming, U.S.A. In: *Erosion and Sediment Transport in Pacific Rim Steeplands*. IAHS Publ. no. 132: 225-235.

- Meade, R.H., R.M. Myrick and W.W. Emmett, 1982. Field data describing the movement and storage of sediment in the East Fork River, Wyoming. Part IV. Bed Elevations, 1980. U.S. Geological Survey, Open-File Report 82-360, 197pp.
- Meade, R.H., T.R. Yuzyk and T.J. Day, 1990. Movement and storage of sediment in rivers of the United States and Canada. In: *The Geology of North America*, Vol.0-1, Surface Water Hydrology. M.G. Wolman and H.C. Griggs (eds.). The Geological Society of America, Boulder, Colorado, p.255-280.
- Megahan, W.F., 1982. Channel sediment storage behind obstructions in forested drainage basins draining the granitic bedrock of the Idaho Batholith. In: *U.S.D.A. Forest Service, Pacific Northwest Forest and Range Experiment Station, General Technical Report PNW-141: 114-121.*
- Megahan, W.F. and Nowlin, R.A., 1976. Sediment storage in channels draining small forested watersheds in the mountains of central Idaho. In: *Proceedings of the Third Federal Inter-Agency Sedimentation Conference, Denver, CO*, Sedimentation Committee of the Water Resources Council, p. 4.115-4.126.
- Megahan, W.F. and W.J. Kidd, 1972. Effects of logging and logging roads on erosion and sediment deposition from steep terrain. *Journal of Forestry* 70: 136-141.
- Megahan, W.F., S.B. Monsen, and M.D. Wilson, 1991. Probability of sediment yields from surface erosion on granitic roadfills in Idaho. *Journal of Environmental Quality* 20: 53-60.
- Megahan, W.F., K.A. Seyedbagheri, T.L. Mosko, and G.L. Ketcheson, 1986. Construction phase sediment budget for forest roads on granitic slopes in Idaho. In: *Drainage Basin Sediment Delivery*. IAHS Publ. no. 159: 31-39.
- Melville, M.D. and W. Erskine, 1986. Sediment remobilization and storage by discontinuous gullying in humid southeastern Australia. In: *Drainage Basin Sediment Delivery*. IAHS Publ. no. 159: 277-286.
- Miller, A.J. and L.L. Shoemaker, 1986. Channel storage of fine-grained sediment in the Potomac River. In: *Drainage Basin Sediment Delivery*. IAHS Publ. no. 159: 287-303.
- Miyamoto, K., J. Kurihara, T. Sawada and Y. Itakura, 1992. A study of field methods for measuring sediment discharge. In: *Erosion and Sediment Transport Monitoring in River Basins*. IAHS Publ. no. 210: 107-114.
- Montgomery, D.R. and J.M. Buffington, 1993. Channel classification, prediction of channel response, and assessment of channel condition. Report prepared for the SHAMW committee of the Washington State Timber/Fish/Wildlife Agreement, Report no. TFW-SH10-93-002, 83 pp.
- Montgomery, D.R. and J.M. Buffington, 1997. Channel-reach morphology in mountain drainage basins. *Geological Society of America Bulletin* 109 (5): 596-611.
- Montgomery, D.R. and W.E. Dietrich, 1994. Landscape dissection and drainage Area-slope thresholds. In: *Process Models and Theoretical Geomorphology*. M.J. Kirkby (ed.), John Wiley & Sons, New York, p. 221-246..
- Morgan, R.P.C., J.N. Quinton, and R.J. Rickson, 1992. *Eurosem Documentation Manual*. Silsoe College, Cranfield, GB, 31pp.
- Morisawa, M., 1968. *Streams. Their Dynamics and Morphology*. McGraw-Hill Book Company, New York, 175 pp.
- Mühlhofer, L., 1933. Untersuchung über die Schwebstoff- und Geschiebeführung des Inn nächst Kirchbichl. [Investigation of suspended load and bedload in the river Inn near Kirchbichl]. *Die Wasserwirtschaft*: 1-6, 43pp.
- Murphy, P. and M.I. Amin., 1979. Compartmented sediment trap. *Journal of the Hydraulics Division* 105 (HY5): 489-500.
- Naden, P., 1987a. An erosion criterion for gravel-bed rivers. *Earth Surface Processes and Landforms* 12: 83-93.
- Naden, P., 1987b. Modeling gravel-bed topography from sediment transport. *Earth Surface Processes and Landforms* 12: 353-367.

- Naden, P., 1988. Models of sediment transport in natural streams. In: *Modelling Geomorphological Systems*. M.G. Anderson (ed.), John Wiley, Chichester, p. 217-258.
- Nakamura, F. and F. J. Swanson, 1993. Effects of coarse woody debris on morphology and sediment storage of a mountain stream system in western Oregon. *Earth Surface Processes and Landforms* 18:43-61.
- Nakamura, F., T.Araya and S. Higashi, 1987. Influence of river channel morphology and sediment production on residence time and transport distance. In: *Erosion and Sedimentation in the Pacific Rim*. IAHS Publ. no. 165: 355-364.
- Nanson, G.C., 1974. Bedload and suspended-load transport in a small, steep, mountain stream. *American Journal of Science* 274: 471-486.
- Nearing, M.A., G.R. Foster, L.J. Lane, and S.C. Finkner, 1989. A process-based soil erosion model for USDA-Water Erosion Prediction Project Technology. *Transactions of the American Society of Agricultural Engineers* 32: 1587-1593.
- Neill, C.R. and J.D. Mollard, 1982. Erosional processes and sediment yield in the upper Oldman River basin, Alberta, Canada. In: *Recent Developments in the Explanation and Prediction of Erosion and Sediment Yield*. IAHS Publ. no. 137: 183-191.
- Nelson, J.M., 1993. Toolbox reference manual version 1.0, Nov. 1993, draft. U.S. Geological Survey, Water Resources Division, Lakewood, Colorado.
- Nelson, J.M., R.L. Shreve, S.R. McLean, S.R. Wolfe and T.G. Drake, 1993. Near bed turbulence structure and bedload transport: implications for bedform mechanics. *EOS, Transactions, American Geophysical Union*, Supplement to Vol. 74(43), p. 311.
- Nelson, J.M., W.W. Emmett and D.J. Smith, 1991. Flow and sediment transport in rough channels. In: *Proceedings of the Fifth Federal Interagency Sedimentation Conference*, March 18-21, 1991, Las Vegas, Nev., Subcommittee of the Interagency Advisory Committee on Water Data, p. 4.55 - 4.62.
- Nemenyi, P.F., 1946. Discussion of "Transportation of suspended sediment by water" by V.A. Vanoni. *Transactions of the American Society of Civil Engineers* 3: 116-124.
- Nezu, I. and H. Nakagawa, 1984. Cellular secondary currents in straight conduit. *Journal of Hydraulic Engineering* 110 (2): 173-193.
- Nolan, M.K. and R.J. Janda, 1981. Use of short-term water and suspended-sediment discharge observations to assess impacts of logging on stream-sediment discharge in the Redwood Creek basin, northwestern California, U.S.A. In: *Erosion and Sediment Transport in the Pacific Rim Steeplands*. IAHS Publ. no. 132: 415-437.
- Nordin, C.F. and G.R. Demster, 1963. Vertical distribution of velocity and suspended sediment, Middle Rio Grande, New Mexico. *Sediment Transport in Alluvial Channels. Geological Survey Professional Paper* 462-B, 20 pp.
- Nordin, C.F. and R.S. McQuivey, 1971. Suspended load. In: *River Mechanics, Vol. 1*. H.W. Shen (ed.), Colorado State University, Fort Collins, Colorado, 12.1-12.31.
- Nouh, M., 1988. Transport of suspended sediment in ephemeral channels. In: *Sediment Budgets*. IAHS Publ. no. 174: 97-106.
- Novotny, V., G.V. Simsiman, and G. Chesters, 1986. Delivery of pollutants from nonpoint sources. In: *Drainage Basin Sediment Delivery*. IAHS Publ. no. 159: 133-140.
- O'Leary, S.J. and R.L. Beschta, 1981. Bed load transport in an Oregon Coast Range stream. *Water Resources Bulletin* 17(5): 886-894.
- Olive, L.J. and W.A. Rieger, 1984. Sediment erosion and transport modelling in Australia. In: *Drainage Basin Erosion and Sedimentation: a Conference on Erosion, Transportation and Sedimentation in Australian Drainage Basins*. University of Newcastle and Soil Conservation Service of N.S.W., p. 81-93.
- Olive, L.J. and W.A. Rieger, 1985. Variation in suspended sediment concentration during storms in five small catchments in southeast New South Wales. *Australian Geographical Studies* 23: 38-51.
- Olive, L.J. and W.A. Rieger, 1986. Low Australian sediment yields - a question of inefficient sediment delivery? In: *Drainage Basin Sediment Delivery*. IAHS Publ. no. 159: 355-364.

- Olive, L.J. and W.A. Rieger, 1991. Assessing the impact of land use change on stream sediment transport in a variable environment. In: *Sediment and Stream Water Quality in a Changing Environment: Trends and Explanation*. IAHS Publ. no. 203: 73-81.
- Olley, J.M., A.S. Murray, D.H. Mackenzie and K. Edwards, 1993. Identifying sediment sources in a gullied catchment using natural and anthropogenic radioactivity. *Water Resources Research* 29(4): 1037-1043.
- Orme, A.R., 1990. Recurrence of debris production under coniferous forest, Cascade foothills, Northwest United States. In: *Vegetation and Erosion*. J.B. Thornes (ed.), John Wiley & Sons, p. 67-84.
- Parker, G., 1992. Some random notes on grain sorting. In: *Grain Sorting Seminar. Mitteilungen der Versuchsanstalt für Wasserbau, Hydrologie und Glaziologie der Eidgenössischen Technischen Hochschule Zürich*, 117: 19-76.
- Parker, G. and P.C. Klingeman, 1982. On why gravel bed streams are paved. *Water Resources Research* 18(5): 1409-1423.
- Parker, G., S. Dhamotharan and H. Stefan, 1982. Model experiments on mobile, paved gravel bed streams. *Water Resources Research* 18(5): 1395-1408.
- Parker, R.S. and B.M. Troutman, 1989. Frequency distribution for suspended sediment loads. *Water Resources Research* 25(7): 1567-1574.
- Pearce, A.J. and A. Watson, 1983. Medium-term effects of two landsliding episodes on channel storage of sediment. In: *Earth Surface Processes and Landforms* 8: 29-39.
- Peart, M.R. and D.E. Walling, 1982. Particle size characteristics of fluvial suspended sediment. In: *Recent Developments in the Explanation and Prediction of Erosion and Sediment Yield*. IAHS Publ. no. 137: 397-407.
- Peart, M.R. and D.E. Walling, 1986. Fingerprinting sediment sources: the example of a drainage basin in Devon, UK. In: *Drainage Basin Sediment Delivery*. IAHS Publ. no. 159: 41-55.
- Peart, M.R. and D.E. Walling, 1988. Techniques for establishing suspended sediment sources in the two drainage basins in Devon, UK: a comparative assessment. In: *Sediment Budgets*. IAHS Publ. no. 174: 269-279.
- Petts, G., 1987. Discussion of "Conceptual models of sediment transport in streams" by R.L. Beschta. In: *Sediment Transport in Gravel-bed Rivers*. C.R. Thorne, J.C. Bathurst, and R.D. Hey (eds.), John Wiley, Chichester, p. 408.
- Pfankuch, D.J., 1978. Stream reach inventory and channel stability evaluation. A watershed management procedure. U.S.D.A., Forest Service, Northern Region, Missoula, MT, 26p.
- Phillips, J.D., 1987. Sediment budget stability in the Tar River basin, North Carolina. *American Journal of Science* 287: 780-794.
- Phillips, J.D., 1989. Hillslope and channel sediment delivery and impact of soil erosion on water resources. In: *Sediment and the Environment*. IAHS Publ. no. 184: 183-190.
- Phillips, J.D., 1991. Fluvial sediment delivery to a coastal plain estuary in the Atlantic drainage of the United States. *Marine Geology* 98: 121-134.
- Phillips, J.D., 1992. Delivery of upper-basin sediment to the lower Neuse River, North Carolina, USA. *Earth Surface Processes and Landforms* 17: 699-709.
- Phillips, J.D., 1993. Pre- and post-colonial sediment sources and storage in the lower Neuse basin, North Carolina. *Physical Geography* 14(3): 272-284.
- Pickup, G., R.J. Higgins and I. Grant, 1983. Modelling sediment transport as a moving wave - the transfer and deposition of mining waste. *Journal of Hydrology* 60: 281-301.
- Pickup, G., 1988. Hydrology and Sediment Models. In: *Modelling Geomorphological Systems*. M.G. Anderson (ed.), John Wiley, Chichester, p. 153-215.
- Piest, R.F., L.A. Kramer and H.G. Heinemann, 1975. Sediment movement from loessial watersheds. In: *Present and Prospective Technology for Predicting Sediment Yields and Sources*. U.S. Dept. of Agriculture, Agricultural Research Service, Report ARS-S-40: 130-141.

- Pitlick, J.C., 1987. Discussion of "Bed load sampling and analysis" by D.W. Hubbell. In: *Sediment Transport in Gravel-bed Rivers*. C.R. Thorne, J.C. Bathurst, and R.D. Hey (eds.), John Wiley, Chichester, p. 106-108.
- Pitlick, J.C. and C.R. Thorne, 1987. Sediment supply, movement and storage in an unstable gravel-bed river. In: *Sediment Transport in Gravel-Bed Rivers*. C.R. Thorne, J.C. Bathurst, and R.D. Hey (eds.), John Wiley, Chichester, p. 156-187.
- Potyondy, J.P. and T. Hardy, 1994. Use of pebble counts to evaluate fine sediment increase in stream channels. *Water Resources Bulletin* 30 (3): 509-520.
- Potyondy, J.P., G.F. Cole and W.F. Megahan, 1991. A procedure for estimating sediment yields from forested watersheds. *Fifth Federal Interagency Sedimentation Conference, Las Vegas, Nev.*, Interagency Advisory Committee on Water Data, Subcommittee on Sedimentation, p. 12.46-1212-54.
- Powell, D.M., I. Reid, J.B. Laronne and L.E. Frostick, 1995. Cross stream variability of bedload flux in narrow and wider ephemeral channels during desert flash floods. Paper presented at the Gravel-Bed Rivers IV Workshop -- *Gravel-Bed Rivers in the Environment* --, held at Gold Bar, WA, Aug. 20-26, 1995.
- Proceedings of the Technical Workshop on Sediments*, Febr. 3-7, 1992, Corvallis, Oregon. Terrene Institute, Washington DC.
- Racotch, A. and R. Sagi, 1977. Bed load samplers for streams with sandy bed. *Journal of Hydraulics Division, ASCE*, 103 (HY8): 923-928.
- Rákóczi, L., 1977. The significance of infrequent, high suspended sediment concentrations in the estimation of annual sediment transport. In: *Erosion and Solid Matter Transport in Inland Waters*. IAHS Publ. no. 122: 19-25.
- Rakoczi, L., 1992. Field tracer investigations of grain sorting in gravel bed rivers. In: *Grain Sorting Seminar. Mitteilungen der Versuchsanstalt für Wasserbau, Hydrologie und Glaziologie der Eidgenössischen Technischen Hochschule Zürich*, 117: 77-92.
- Rathbun, R.E. and V.C. Kennedy, 1978. Transport and dispersion of fluorescent tracer particles for the dune-bed condition, Atrisco Feeder Canal near Bernalillo, New Mexico. *U.S. Geological Survey Professional Paper* 1037, 95 pp.
- Raudkivi, A.J., 1976. *Loose Boundary Hydraulics*. Pergamon Press, New York, 397 pp.
- Raudkivi, A.J., 1986. Functional trends of scour at bridge piers. *Journal of Hydraulic Engineering*, 112(1): 1-13.
- Reid, I. and L.E. Frostick, 1986a. Dynamics of bedload transport in Turkey Brook, a coarse grained alluvial channel. *Earth Surface Processes and Landforms* 11: 143-155.
- Reid, I. and L.E. Frostick, 1986b. Turkey Brook bedload data-base. Birkbeck College, University of London, Malet St., London WC1E 7HX, UK.
- Reid, I., A.C. Brayshaw and L.E. Frostick, 1984. An electromagnetic device for automatic detection of bedload motion and its field application. *Sedimentology* 31: 269-276.
- Reid, I., L.E. Frostick, and J.T. Layman, 1985. The incidence and nature of bedload transport during flood flows in coarse-grained alluvial channels. *Earth Surface Processes and Landforms* 10: 33-44.
- Reid, L.M., T. Dunne and C.J. Cederholm, 1981. Application of sediment budget studies to the evaluation of logging road impact. *New Zealand Journal of Hydrology* 20(1): 49-62.
- Reid, L.M. and T. Dunne, 1984. Sediment production from forest road surfaces. *Water Resources Research* 20(11): 1753-1761.
- Renfro, G., 1975. Use of equations and sediment delivery ration fro predicting sediment yield. In: *Present and Prospective Technology for Predicting Sediment Yields and Sources*. U.S. Dept. of Agriculture, Agricultural Research Service, Report ARS-S-40: 33-45.
- Rice, R.M. and R.B. Thomas, 1986. Cumulative sedimentation effects of forest management activities: How might they occur?. In: Papers presented at the American Geophysical Union Meeting on cumulative effects. *NCASI Technical Bulletin* 490: 1-11.

- Rice, R.M., F.B. Tilley and P.A. Datzman, 1979. A watershed's response to logging and roads: South Fork of Caspar Creek, California, 1967 - 1976. Forest Service, U.S Dept. of Agriculture, Pacific Southwest Forest and Range Experiment Station, Research Paper PSW 146, 12pp.
- Rickenmann, D., 1994. Bedload transport and discharge in the Erlenbach stream. In: *Dynamics and Geomorphology of Mountain Rivers*. P. Ergenzinger and K.-H. Schmidt (eds.). Lecture Notes in Earth Sciences 52: 53-66, Springer Verlag, Berlin.
- Rieffenberger, E. and D. Baird, 1991. Dump Creek: a man made ecological disaster. *Fifth Federal Interagency Sedimentation Conference, Las Vegas, Nev.*, Interagency Advisory Committee on Water Data, Subcommittee on Sedimentation, p.10.57-10.60.
- Rieger, W.A., and L.J. Olive, 1986. Sediment responses during storm events in small forested watersheds. In: *Statistical Aspects of Water Quality Monitoring*, A.H. El-Shaarawi and R.E. Kwiatkowski (eds.), Elsevier, Oxford, p. 490-498.
- Roberts, R.G. and M. Church, 1986. The sediment budget in severely disturbed watersheds, Queen Charlotte Ranges, British Columbia. *Canadian Journal of Forest Research* 19: 1092-1106.
- Roehl, J.W., 1962. Sediment source areas, delivery ratios and influencing morphological factors. In: *Proc. of the Bari Symposium 1962*. IASH Publ. no. 59: 202-213.
- Rosgen, D.L., 1976. The use of color infrared photography for the determination of suspended sediment concentrations and source areas. In: *Proceedings of the Third Federal Inter-Agency Sedimentation Conference*, Denver, CO., Sedimentation Committee of the Water Resources Council, p. 7.30-7.42.
- Rosgen, D.L., 1994. A classification of natural rivers. *Catena* 21: 169-199.
- Rosgen, D.L., 1996. *Applied River Morphology*. Wildland Hydrology, Pagosa Springs, Colorado,
- Rouse, H., 1937. Modern conceptions of the mechanics of turbulence. *Transactions, ACSE* 102: 463-543.
- Rouse, H.L., 1994. Measurement of bedload gravel transport: the calibration of a self-generated noise system. *Earth Surface Processes and Landforms* 19: 789-800.
- Ruby, E.C., 1976. Evaluation of an extensive sediment control effort in the Los Angeles river basin. In: *Proceedings of the Third Federal Inter-Agency Sedimentation Conference, Denver, CO*, Sedimentation Committee of the Water Resources Council, p. 2.91-2.102.
- Sayre, W.W. and D.W. Hubbell, 1965. Transport and dispersion of labeled bed material, North Loup River, Nebraska. *Geological Survey Professional Paper* 433-C, 48pp.
- Schick, A.P., J. Lekach and M.A. Hassan, 1987a. Vertical exchange of coarse bedload in desert streams. In: *Desert Sediments: Ancient and Modern*. L. Frostick and I. Reid (eds.), Geological Society Special Publication 35: 7-16.
- Schick, A.P., J. Lekach and M.A. Hassan, 1987b. Bed load transport in desert floods: observations in the Negev. In: *Sediment Transport in Gravel-Bed Rivers*. C.R. Thorne, J.C. Bathurst, and R.D. Hey (eds.), John Wiley, Chichester, p. 617-642.
- Schlatte, H., 1984. Anwendung einer akustischen Geschiebemeßmethode an der Möll. [Application of an acoustic method to measure bedload transport at the river Möll]. In: *Beitrag zur XII. Konferenz der Donauländer über hydrologische Vorhersagen*, Bratislava, p. 4-5.1 - 4-5.9.
- Schleyer, R., 1987. The goodness-of-fit to ideal Gauss and Rosin Distributions: a new grain-size parameter. *Journal of Sedimentary Petrology* 57(5): 871-880.
- Schmidt, J., 1993. Modelling long-term soil loss and landform change. In: *Overland Flow. Hydraulics and Erosion Mechanics*. A.J. Parsons and A.D. Abrahams (eds.), Chapman & Hall, New York.
- Schmidt, K.-H., 1994. River channel adjustment and sediment budget in response to a catastrophic flood event (Lainbach catchment, Southern Bavaria). In: *Dynamics and Geomorphology of Mountain Rivers*. P. Ergenzinger and K.-H. Schmidt (eds.). Lecture Notes in Earth Sciences, Springer Verlag, Berlin, 109-127.

- Schmidt, K. -H., and P. Ergenzinger, 1990. Radiotracer und Magnettracer. Die Leistungen neuer Meßsysteme für die fluviale Dynamik. [Radio tracer and magnetic tracer: the accomplishments of new measuring systems in analysing fluvial dynamics]. *Die Geowissenschaften* 8(4): 96-102.
- Schmidt, K. -H, and P. Ergenzinger, 1992. Bedload entrainment, travel lengths, step lengths, rest periods, studied with passive (iron, magnetic) and active (radio) tracer techniques. *Earth Surface Processes and Landforms* 17: 147-165.
- Schmidt, K.-H. and D. Gintz, 1995. Results of bedload tracer experiments in a mountain river. In: *River Geomorphology*. E.J. Hickins (ed.), John Wiley and Sons, Chichester, p.37-54.
- Schmidt, K.-H., D. Bley, R. Busskamp, and D. Gintz, 1989. Die Verwendung von Trübungsmessung, Eisentracern und Radiogeeschieben bei der Erfassung des Feststofftransportes im Lainbach, Oberbayern. [Applying turbidity measurements, iron tracers and radio tracer to measure sediment transport at the Lainbach river in upper Bavaria]. *Göttinger Geographische Abhandlungen* 86: 123-135.
- Schmidt, K.-H., D. Bley, R. Busskamp, P. Ergenzinger and D. Gintz, 1992. Feststofftransport und Flußbettdynamik in Wildbachsystemen. Das Beispiel des Lainbachs in Oberbayern. [Sediment transport and channel dynamics in mountain torrents. The example of the Lainbach in upper Bavaria]. *Die Erde* 123: 17-28.
- Schumm, S.A. 1956. Evolution of drainage systems and slopes in badlands at Perth Amboy, New Jersey. *Geological Society of America Bulletin*, 67: 597-646.
- Sedell, J.R., P.A. Bisson, F.J. Swanson, and S.V. Gregory, 1988. What we know about large trees that fall into streams and rivers. In: *From the forest to the sea: a story of fallen trees*. C. Maser et al. (eds.). U.S.D.A. Forest Service, General Technical Report, PNW-GTR 229, 153pp.
- Shields, A., 1936. Anwendung der Ähnlichkeitsmechanik und der Turbulenzforschung auf die Geschiebebewegung. [Application of similarity principles and turbulence research to bedload movement]. *Mitteilungen der Preußischen Versuchsanstalt für Wasser-, Erd- und Schiffbau, Berlin*, 26, 26 pp.
- Shih, S.-M. and P.D. Komar, 1990a. Hydraulic controls of grain-size distributions of gravels in Oak Creek, Oregon, USA. *Sedimentology* 37: 367-376.
- Shih, S.-M. and P.D. Komar, 1990b. Differential bedload transport rates in a gravel-bed stream: a grain-size distribution approach. *Earth Surface Processes and Landforms* 15: 539-552.
- Shuyou, C., F. Duo and Z. Chuanyi, 1988. Stochastic characteristics of cobble-gravel bed load transport. *Proceedings of the National Conference, sponsored by the Hydraulics Division of the ASCE*, S.R. Abt and J. Gessler (eds.), ASCE, New York, p. 322-327.
- Sidle, R.C., 1988. Bedload transport regime of a small forest stream. *Water Resources Research* 24(2): 207-218.
- Sidle, R.C., 1991. A conceptual model of changes in root cohesion in response to vegetation management. *Journal of Environmental Quality* 20: 43-52.
- Sidle, R.C. and J.W. Hornbeck, 1991. Cumulative effects: a broader approach to water quality research. *Journal of Soil and Water Conservation* 46(4): 268-271.
- Silverston, E. and E.M. Laursen, 1976. Patterns of scour and fill in pool-rapid rivers. In: *Proceedings of the Third Federal Inter-Agency Sedimentation Conference*, Sedimentation Committee of the Water Resources Council, p. 5.125-5.136.
- Simon, A. and C.R. Hupp, 1990. The recovery of alluvial systems in response to imposed channel modifications, west Tennessee, USA. In: *Vegetation and Erosion*. J.B. Thornes (ed.), John Wiley & Sons, p.145-160.
- Simons, D.B. and F. Sentürk, 1992. *Sediment Transport Technology. Water and Sediment Dynamics*. Water Resources Publications, Littleton, Colorado.
- Slaymaker, O., 1990. Climate change and erosion processes in mountain regions of western Canada. *Mountain Research and Development* 10 (2): 171-182.

- Sneed, E.D and R.L. Folk, 1958. Pebbles in the lower Colorado River. A study on particle morphogenesis. *Journal of Geology* 66: 114-150.
- Sobocinski, R.W., T.E. Cerling, S.J. Morrison and I.L. Larson, 1990. Sediment transport in a small stream based on <sup>137</sup>Cs inventories of the bed load fraction. *Water Resources Research* 26(6): 1177-1187.
- Spieker, R. and P. Ergenzinger, 1990. New developments in measuring bedload by the magnetic tracer technique. In: *Erosion, Transport and Deposition Processes*, IAHS Publ. no. 189: 171-180.
- Stott, T.A., R.I. Ferguson, R.C. Johnson, and M.D. Newson., 1986. Sediment budgets in forested and unforested basins in upland Scotland. In: *Drainage Basin Sediment Delivery*. IAHS Publ. no. 159: 57-68.
- Stow, D.A. and H.H. Chang, 1987. Coarse sediment delivery by coastal streams to the oceanside littoral cell, California. *Shore and Beach* 55(1): 30-40.
- Sullivan, K., S.H. Duncan, P.A. Bisson, J.T. Heffner, J.W. Ward, R.E. Bilby and J.L. Nielsen, 1987. A summary Report of the Deschutes River Basin: Sediment, flow, temperature and fish habitat. Weyerhaeuser Company Technology Center, Tacoma, Research Report, Paper No. 044-5002/87/1, 129 pp.
- Swanson, F.J., 1986. Comments from a panel discussion at the symposium on cumulative effects -- the UFO's of hydrology. Paper presented at the American Geophysical Union Meeting on cumulative effects. In: *NCASI Tech. Bulletin* No. 490: 66-69.
- Swanson F.J., M.M. Swanson and C. Woods, 1981. Analysis of debris-avalanche erosion in steep forest lands: an example from Mapleton, Oregon, USA. *Erosion and Sediment Transport in the Pacific Rim Steeplands*, IAHS Publ. no. 132: 67-75.
- Swanston, D.M., 1979. Landslide prediction and assessment - interpreting stability problems for the land manager. In: *Proceedings of the Workshop on Scheduling Timber Harvest for Hydrologic Concerns*, U.S. Dept. of Agriculture, Forest Service, Pacific Northwest Region, Pacific Northwest Forests and Range Experiment Station, 37pp.
- Swanston, D.N., 1981. Creep and Earthflow erosion from undisturbed and management impacted slopes in the Coast and Cascade Ranges of the Pacific Northwest. *Erosion and Sediment Transport in the Pacific Rim Steeplands*, IAHS Publ. no. 132: 76-94.
- Swanston, D.N. and D.A. Marion, 1991. Landslide response to timber harvest in southeast Alaska. *Fifth Federal Interagency Sedimentation Conference, Las Vegas, Nev.*, Interagency Advisory Committee on Water Data, Subcommittee on Sedimentation, p.10.49-10.56.
- Swanston, D.N. and F.J. Swanson, 1976. Timber harvest, mass erosion, and steepland forest geomorphology in the Pacific Northwest. In: *Geomorphology and Engineering*, D.R. Coates (ed.), Dowden, Hutchinson & Ross, Inc., Stroudsburg, PA, p. 199-221.
- Swift, L.W.Jr., 1988. Forest access roads: design, maintenance and soil loss. In: *Ecological Studies, Vol. 66: Forest Hydrology and Ecology in Coweeta*, W.T. Swank and D.A. Crossley (eds.). Springer-Verlag, New York, p. 313-324.
- Symader, W., 1988. Zur Problematic der Frachtermittlung. [The problem of estimating loads.] *Vom Wasser* (VCH Verlagsgesellschaft, Weinheim, Germany) 71:145-161.
- Symader, W., R. Bierl and R. Hierlmeier, 1989. Temporal variations of suspended particle characteristics in flowing waters and its significance to water quality. In: *Proceedings of the Fourth International Symposium on River Sedimentation, Beijing, China*, 1254-1259.
- Tacconi, P. and P. Billi, 1987. Bed load transport measurement by a vortex-tube trap on Virginio Creek, Italy. In: *Sediment Transport in Gravel-Bed Rivers*. C.R. Thorne, J.C. Bathurst, and R.D. Hey (eds.), John Wiley, Chichester, p. 583-616.
- Tang, Y., 1991. A study on the measuring method of bedload. *Proceedings of the Fifth Federal Interagency Sedimentation Conference*, March 18-21, 1991, Las Vegas, Nev., Subcommittee on Sedimentation of the Interagency Advisory Committee on Water Data, p. 2.89-2.96.
- Tang, Y., 1990. A study on the measuring method of bedload. *Journal of Sedimentary Research* 1: 1-11.

- Taniguchi, S., Y. Itakura, K. Miyamoto and J. Kurihara, 1992. A new acoustic sensor for sediment discharge measurement. In: *Erosion and Sediment Transport Monitoring in River Basins*. IAHS Publ. no. 210: 135-142.
- Tassone, B.L., 1988. Sediment loads from 1973 to 1984 08HB048 Carnation Creek at the mouth, British Columbia. In: *Proceedings of the Workshop: Applying 15 Years of Carnation Creek Results*. T.W. Chamberlin (ed.), Carnation Creek Steering Committee, Pacific Biological Station, Nanaimo, B.C., Can., p. 46-58.
- Tazioli, G.S., 1981. Nuclear techniques for measuring sediment transport in natural streams - examples from instrumented basins. *Erosion and Sediment Transport Measurement*. IAHS Publ. no. 133: 63-81.
- Thomas, R.B., 1985. Measuring suspended sediment in small mountain streams. *U.S.D.A., Forest Service, Pacific Southwest Forest and Range Experiment Station, General Technical Report PSW-83*, 9pp.
- Thomas, R.B., 1988. Measuring sediment yields of storms using PSALT. In: *Sediment Budgets*. IAHS Publ. no. 174: 315-324.
- Thomas, R.B., 1991. Systematic sampling for suspended sediment. In: *Proceedings of the Fifth Federal Interagency Sedimentation Conference, Las Vegas, Nev.*, Interagency Advisory Committee on Water Data, Subcommittee on Sedimentation, p. 2.17-2.24.
- Thomas, R.B. and J. Lewis, 1993. A comparison of selection at list time and time-stratified sampling for estimating suspended sediment loads. *Water Resources Research* 29(4): 1247-1256.
- Thompson, D., 1994. Hydraulics and sediment transport processes in a pool-riffle Rocky Mountain stream. Thesis submitted as partial requirement of the M.A. degree to the Dept. of Earth Resources, Colorado State University, Ft. Collins.
- Thomsen, T., 1980. The application of radioactive tracers for determination of bed-load transport in alluvial rivers. *Nordic Hydrology* 11: 133-144.
- Thorne, C.R., 1981. Field measurements of rates of bank erosion and bank material strength. In: *Erosion and Sediment Transport Measurement*. IAHS Publ. no. 133: 503-512.
- Thorne, C.R., 1988. Riverbank instability due to bed degradation. In: *Hydraulic Engineering. Proceedings of the 1988 National Conference*, sponsored by the Hydraulics Division of the ASCE, S.R. Abt and J. Gessler (eds.), ASCE, New York., p. 132-137.
- Thorne, C.R., 1991. Analysis of channel instability due to catchment land-use change. In: *Sediment and Stream Water Quality in a Changing Environment: Trends and Explanation*. IAHS Publ. no. 203: 111-122.
- Thorne, P.D., J.J. Williams, and A.D. Heathershaw, 1989. In situ acoustic measurements of marine gravel threshold transport. *Sedimentology* 36: 61-74.
- Trimble, G.R. and S. Weitzman, 1953. Soil erosion on logging roads. *Soil Science Society of America Proceedings* 17(11): 152-154.
- Trimble, S.W., 1975. Denudation studies: can we assume stream steady state? *Science* 188:1207-1208.
- Trimble, S.W., 1976. Sedimentation in Coon Creek Valley, Wisconsin. In: *Proceedings of the Third Federal Inter-Agency Sedimentation Conference, Sedimentation Committee of the Water Resources Council*. p. 5.100-5.111.
- Trimble, S.W., 1977. The fallacy of stream equilibrium in contemporary denudation studies. *American Journal of Science* 277:876-887.
- Trimble, S.W., 1981. Changes in sediment storage in the Coon Creek basin, Driftless Area, Wisconsin, 1853 to 1975. *Science* 214: 181-183.
- Trimble, S.W., 1983. A sediment budget for Coon Creek basin in the driftless area, Wisconsin, 1953-1977. *American Journal of Science* 283: 454-474.
- Trimble, S.W., 1993. The distributed sediment budget model and watershed management in the Paleozoic Plateau of the upper midwestern United States. *Physical Geography* 14(3): 285-303.

- Troendle, C.A., 1993. Sediment transport for instream flow/channel maintenance. Proceedings of the Technical Workshop on Sediments, Febr. 3-7, 1992, Corvallis, Oregon. Terrene Institute, Washington DC.
- Troendle, C.A. and R.M. King, 1985. The effect of timber harvest on the Fool Creek watershed, 30 years later. *Water Resources Research* 21(12): 1915-1922.
- U.S. Forest Service, 1980. An approach to water resources evaluation of non-point silvicultural sources (WRENSS), (a procedural handbook). U.S. Environmental Protection Agency, Athens, Georgia, EPA-6000/8-80-012.
- U.S. Forest Service, 1981. Guide for predicting sediment yields from forested watersheds. U.S.D.A. Forest Service, Northern Region (R1) and Intermountain Region (R4).
- U.S. Forest Service, 1992. R1-Watsed-PC Handbook. U.S.D.A. Forest Service Region 1, Missoula, MT.
- U.S.D.A., Soil Conservation Service, 1983. National Engineering Handbook. Section 3, Sedimentation; chapter 6, Sediment Sources, Yields, and Delivery Ratios, p. 6.1-6.13.
- VanSickle, J., 1981. Long-term distribution of annual sediment yields from small watersheds. *Water Resources Research* 17(3): 659-663.
- VanSickle, J. and R.L. Beschta, 1983. Supply-based models of suspended sediment transport in streams. *Water Resources Research* 19(3): 768-778.
- Walling, D.E., 1977a. Limitations of the rating curve technique for estimating suspended sediment loads, with particular reference to British rivers. In: *Erosion and Solid Matter Transport in Inland Waters*. IAHS Publ. no. 122: 34-48.
- Walling, D.E., 1977b. Assessing the accuracy of suspended sediment rating curves for a small basin. *Water Resources Research* 13(3): 531-538.
- Walling, D.E., 1977c. Natural sheet and channel erosion of unconsolidated source material (Geomorphic control, magnitude and frequency of transfer mechanisms). In: *Proceedings of a Workshop on the Fluvial Transport of Sediment-Associated Nutrients and Contaminants*. H. Shear and A.E.P. Watson (eds.), held in Kitchener, Ontario, October 20-22, 1976, p. 11-36.
- Walling, D.E., 1983. The sediment delivery problem. *Journal of Hydrology* 65: 209-237.
- Walling, D.E. and S.B. Bradley, 1988. The use of caesium-137 measurements to investigate sediment delivery from cultivated areas in Devon, UK. In: *Sediment Budgets*. IAHS Publ. no. 174: 325-335.
- Walling, D.E. and S.B. Bradley, 1990. Some application of caesium-137 measurements in the study of erosion, transport and deposition. In: *Erosion, Transport and Deposition Processes*. IAHS Publ. no. 189: 179-203.
- Walling, D.E., S.B. Bradley, and C.J. Wilkinsons, 1986. A caesium-137 budget approach to the investigation of sediment delivery from a small agricultural drainage in Devon, UK. In: *Drainage Basin Sediment Delivery*. IAHS Publ. no. 159: 423-435.
- Walling, D.E. and P.W. Moorehead, 1989. The particle size characteristics of fluvial suspended sediment: an overview. *Hydrobiologia* 176/177: 125-149.
- Walling, D.E. and T.A. Quine, 1991. Recent rates of soil loss from areas of arable cultivation in the UK. In: *Sediment and Stream Water Quality in a Changing Environment: Trends and Explanation*. IAHS Publ. no. 203: 123-131.
- Walling, D.E. and B.W. Webb, 1981. The reliability of suspended sediment load data. In: *Erosion and Sediment Transport Measurement*. IAHS Publ. no. 133: 177-194.
- Walling, D.E. and B.W. Webb, 1982. Sediment availability and the prediction of storm period sediment yield. In: *Recent Developments in the Explanation and Prediction of Erosion and Sediment Yield*. IAHS Publ. no. 137: 327-337.
- Walling, D.E. and B.W. Webb, 1987. Suspended load in gravel-bed rivers: UK experience. In: *Sediment Transport in Gravel-Bed Rivers*. C.R. Thorne, J.C. Bathurst, and R.D. Hey (eds.), John Wiley, Chichester, p. 691-732.
- Walling, D.E. and B.W. Webb, 1988. The reliability of rating-curve estimates of suspended sediment load: some further comments. In: *Sediment Budgets*. IAHS Publ. no. 174: 337-350.

- Walling, D.E., B.W. Webb and J.C. Woodward, 1992. Some sampling considerations in the design of effective strategies for monitoring sediment-associated transport. In: *Erosion and Sediment Transport Monitoring in River Basins*. IAHS Publ. 210: 279-288.
- Wang, S.S.Y. (ed.), 1989. An overview of computer stream sedimentation models. In: *Sediment Transport Modeling*. American Society of Civil Engineers, New York, 829pp.
- Washington Forest Practices Board, 1992. Standard methodology for conducting watershed analysis. Version 2.1, Dept. of Natural Resources, Olympia, WA., Approx. 465 pp.
- Wathen, S.J., T.B. Hoey and A. Werritty, 1995. Unequal mobility of gravel and sand in weakly bimodal river sediments. *Water Resources Research* 31 (8): 2087-2096.
- Watson, C.C., M.D. Harvey, and J. Garbrecht, 1986. Geomorphic - hydraulic simulation of channel evolution. In: *Proceedings of the Fourth Federal Interagency Sedimentation Conference*, Las Vegas, Nevada. Subcommittee on Sedimentation of the Interagency Advisory Committee on Water Data, p. 5.21-5.30.
- Watson, C.C., M.D. Harvey, D.S. Biedenharn and P. Combs, 1988. Geotechnical and hydraulic stability numbers for channel rehabilitation: Part I, the approach. In: *Hydraulic Engineering*. Proceedings of the National Conference, S.R. Abt and J. Gessler (eds.), p. 120-124.
- Weaver, W.E. and M.A. Madej, 1981. Erosion control techniques used in Redwood National Park, Northern California, 1978-1979. In: *Erosion and Sediment Transport in Pacific Rim Steeplands*. IAHS Publ. no. 132: 640-654.
- Weaver, W.E., D. Hagans, and M.A. Madej, 1987. Managing forest roads to control cumulative erosion and sedimentation effects. In: *Proceedings of the California Watershed Management Conference*, Wildland Resources Center, University of California, Report no. 11: 119-124.
- Whiting, P.J., W.E. Dietrich, L.B. Leopold, T.G. Drake, and R.L. Shreve, 1988. Bedload sheets in heterogeneous sediment. *Geology* 16: 105-108.
- Whiting, P.J. and J.B. Bradley, 1993. A process-based classification system for headwater streams. *Earth Surface Processes and Landforms* 18: 603-612.
- Wilcox, M.S., C.A. Troendle and J.M. Nankervis, 1996. Bedload transported in gravelbed streams in Wyoming. *Proceedings of the Sixth Federal Interagency Sedimentation Conference*, March 10-14, Las Vegas, Nevada. Interagency Advisory on Water Data, Subcommittee on Sedimentation, Vol. 2: VI.28-VI.33.
- Williams, G.P., 1989. Sediment concentration versus water discharge during single hydrologic events in rivers. *Journal of Hydrology* 111: 89-106.
- Williams, J.J., P.D. Thorne, and A.D. Heathershaw, 1989a. Measurements of turbulence in a benthic boundary layer over a gravel bed. *Sedimentology* 36: 959-971.
- Williams, J.J., P.D. Thorne, and A.D. Heathershaw, 1989b. Comparison between acoustic measurements and predictions of the bedload transport of marine gravels. *Sedimentology* 36: 973-979.
- Willis, J.C., 1991. Sand transport in Goodwin Creek. *Proceedings of the Fifth Federal Interagency Sedimentation Conference*. Las Vegas, Nevada. Subcommittee on Sedimentation of the Interagency Advisory Committee on Water Data, p. 4.131-4.138. Wyoming. *Proceedings of the National Academy of Sciences, USA* 73(4): 1000-1004.
- Wischmeier, W.H. and D.D. Smith, 1978. Predicting rainfall erosion losses - a guide to conservation planning. *U.S. Dept. of Agriculture, Agriculture Handbook* No. 537.
- Witter, J.V. and G.W.A.M. Waajen, 1992. Separate in-situ entrapment of sand and silt in river systems. In: *Erosion and Sediment Transport Monitoring in River Basins*. IAHS Publ. no. 210: 165-174.
- Wolman, G.M., 1977. Changing needs and opportunities in the sediment field. *Water Resources Research* 13(1): 50-54.
- Wolman, M.G., 1987. Sediment movement and knickpoint behavior in a small Piedmont drainage basin. *Geografiska Annaler* 69 A (1): 5-14.

- Xiang, Z. and G. Zhu, 1992. Measuring techniques of bed load in the Yangtze River. In: *Erosion and Sediment Transport Monitoring in River Basins*. IAHS Publ. no. 210: 175-180.
- Yanmaz, A.M. and H.D. Altmbilek, H.D., 1991. Study of time dependent local scour around bridge piers, *Journal of Hydraulic Engineering.*, 117 (10), 1247-1268.
- Ziemer, R.R., 1981. Roots and the stability of forested slopes. In: *Erosion and Sediment Transport in Pacific Rim Steeplands*. IAHS Publ. no. 132: 343-361.
- Ziemer, R.R., J. Lewis, T.E. Lisle, and R.M. Rice, 1991a. Long-term effects of different patterns of timber harvesting. In: *Sediment and Stream Water Quality in a Changing Environment: Trends and Explanation*. IAHS Publ. no. 203: 143-150.
- Ziemer, R.R., J. Lewis, R.M. Rice, and T.E. Lisle, 1991b. Modeling the cumulative watershed effects of forest management strategies. *Journal of Environmental Quality* 20: 36-42.

